THE STRENGTH AND DEFORMATIONAL BEHAVIOUR OF A COHESIONLESS SOIL UNDER GENERALISED STRESS CONDITIONS

a thesis presented by

Stuart Dyson

for the degree of

Doctor of Philosophy

Department of Civil Engineering
University of Aston in Birmingham

October 1970

VOLUME TWO

SYNOPSIS

Predictions of the stresses and displacements induced within a soil mass by interaction with an engineering structure are made, at present, with only a limited knowledge of the deformational behaviour of soils under generalised stress conditions. The majority of routine testing and laboratory research investigations are performed on cylindrical soil specimens in the conventional triaxial apparatus, which is limited to imposing axially-symmetrical stress conditions. In very few field problems are such conditions strictly relevant. Many problems approximate more closely to plane strain, and recent progress has been made in investigating the behaviour of cuboidal specimens constrained from deformation in one of the principal directions. However, the experimental difficulties are increased, and controversies remain regarding the influence exerted by the apparatus on the soil behaviour.

The general field condition is one in which the stresses and strains are different in each of their three principal directions at a point. Very few satisfactory attempts have been made to overcome the complex problem of testing elements of soil under similar conditions.

The design and development of a new apparatus is described which allows generalised stress or strain conditions to be applied to cuboidal specimens. The methods used to apply the three boundary principal stresses ensure a high degree of stress uniformity, and suitable lubrication encourages uniform strains. Comparisons between the results of tests carried out under simple stress conditions, on specimens of the same sand, in this and in more conventional apparatus, indicate negligible apparatus interference. A further series of tests in plane strain shows that the deformational behaviour of loose specimens is similar to that observed in triaxial compression. For dense specimens, however, considerable strength increases result from the restriction imposed on strains. The results of generalised stress tests suggest that the intermediate principal stress is of most significance when its magnitude is less than that observed at failure in plane strain.

LIST OF CONTENTS

VOLUME ONE

CHAPTER FOUR - ASTON TRIAXIAL APPARATUS - DESIGN DEVELOPMENT AND TESTING TECHNIQUE

CHAPTER SIX - ASTON TRIAXIAL APPARATUS TESTS - RESULTS AND DISCUSSION

CHAPTER TWO

FIGURES

(a)
Simple cubic

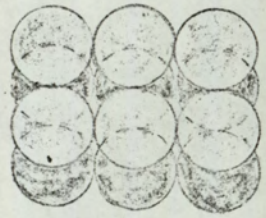

(b)
Orthorhombic

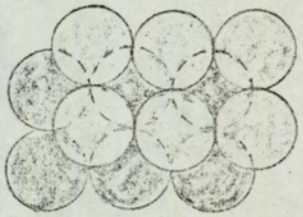

(c)
Pyramidal
(Face-centered cubic)

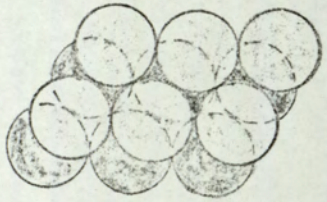

(d)
Tetragonal-sphenoidal

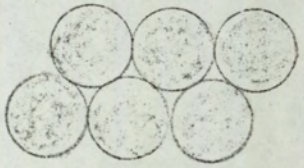

(e)
Cubic-tetragonal

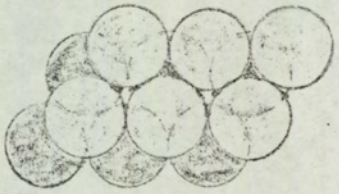

(f)
Tetrahedral
(Rhombic)

	Coordination Number (N)	Porosity (n)
(a)	6	0.4764
(b)	8	0.3954
(c)	12	0.2595
(d)	10	0.3019
(e)	8	0.3954
(f)	12	0.2595

FIG. 2.1
PACKING OF EQUAL SPHERES
(After Graton & Fraser)

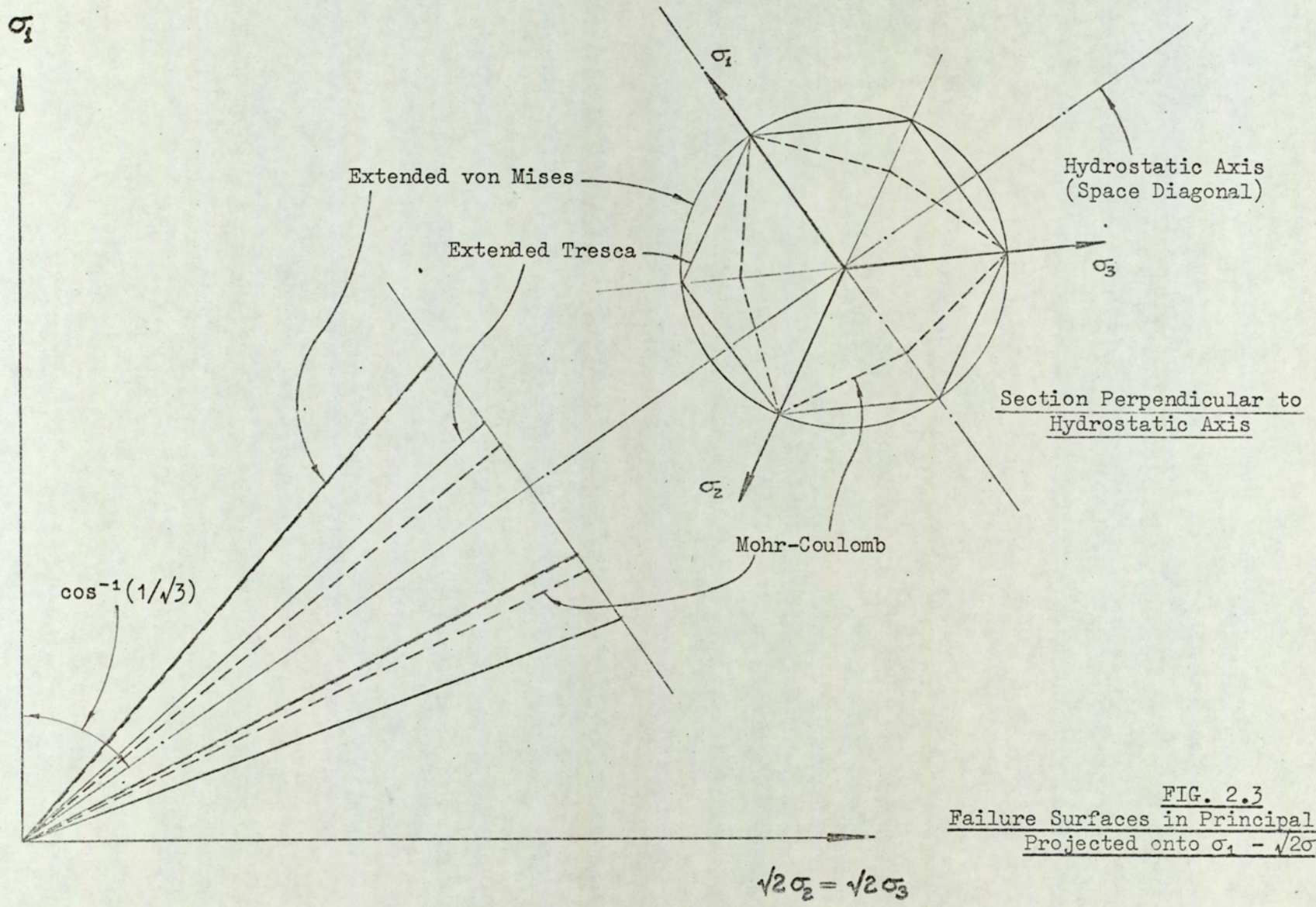

FIG. 2.3
Failure Surfaces in Principal Stress Space
Projected onto $\sigma_1 - \sqrt{2}\sigma_3$ Plane

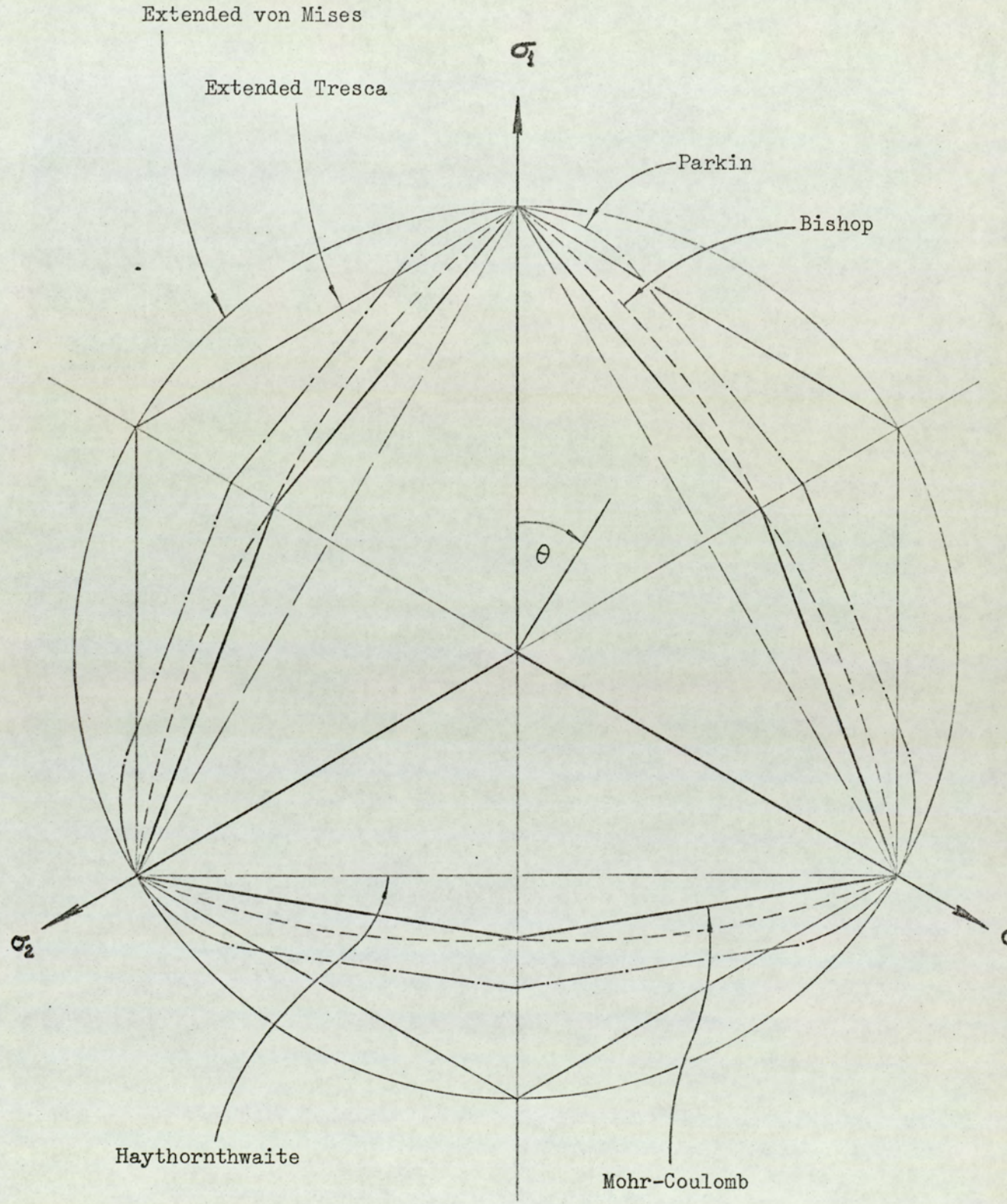

FIG. 2.4
Failure Criteria in Principal Stress Space
Section Perpendicular to Hydrostatic Axis

CHAPTER THREE

FIGURES

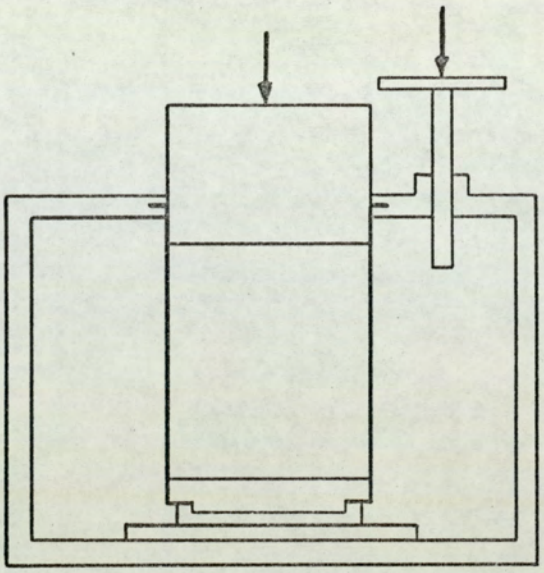

FIG. 3.1 (a)
HOUSEL'S STABILOMETER

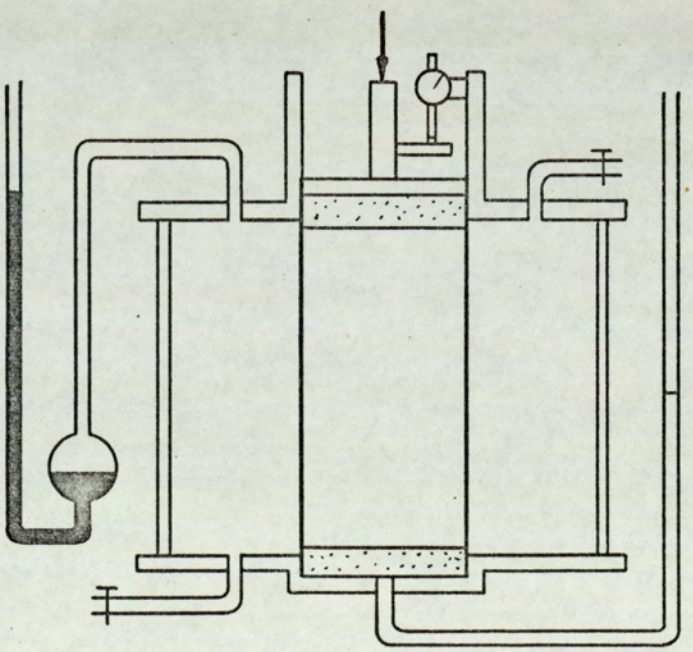

FIG. 3.1 (b)
CELL TEST APPARATUS

FIG. 3.2 (a)
VACUUM TRIAXIAL
- GEUZE

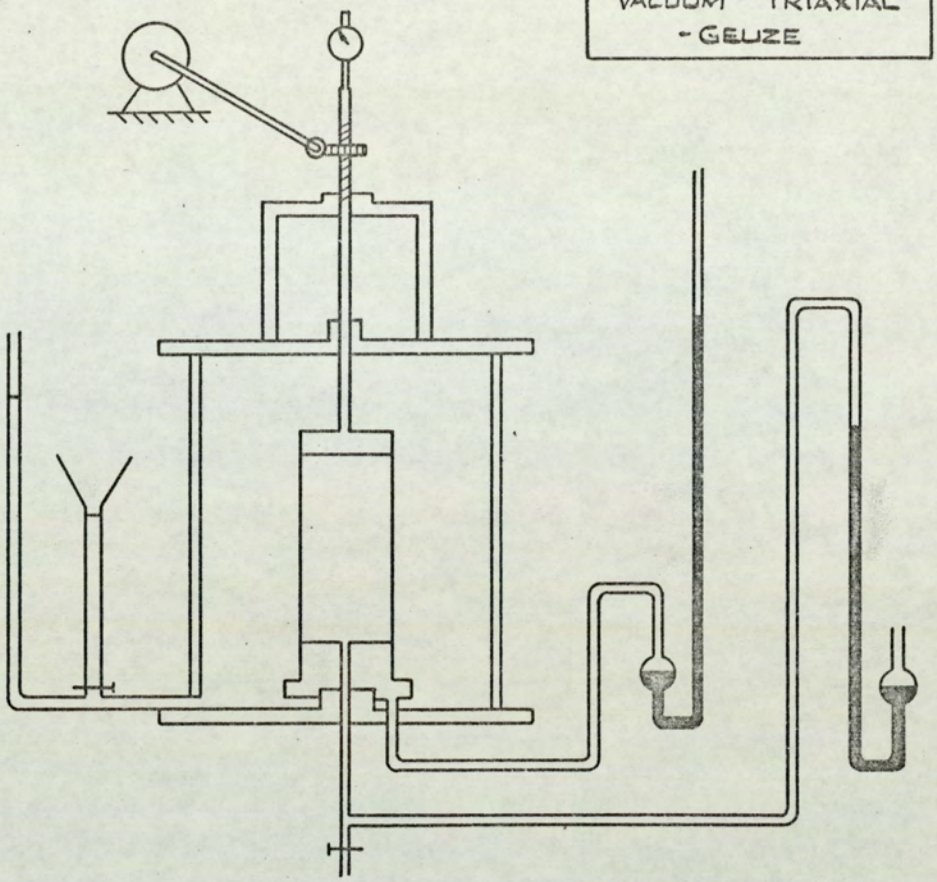

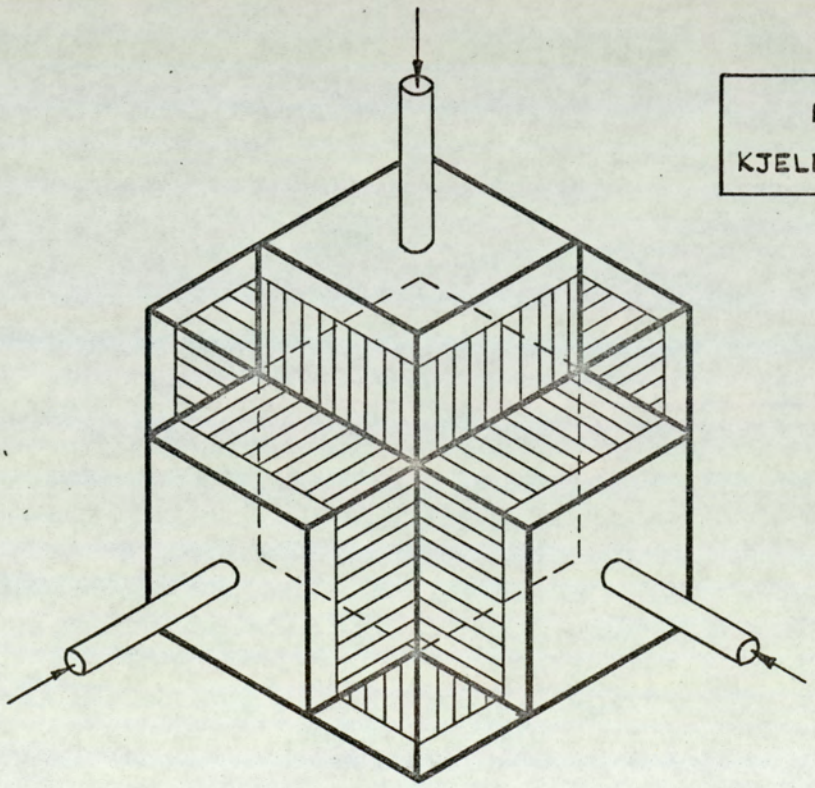

FIG. 3.2 (b)
KJELLMAN'S APPARATUS

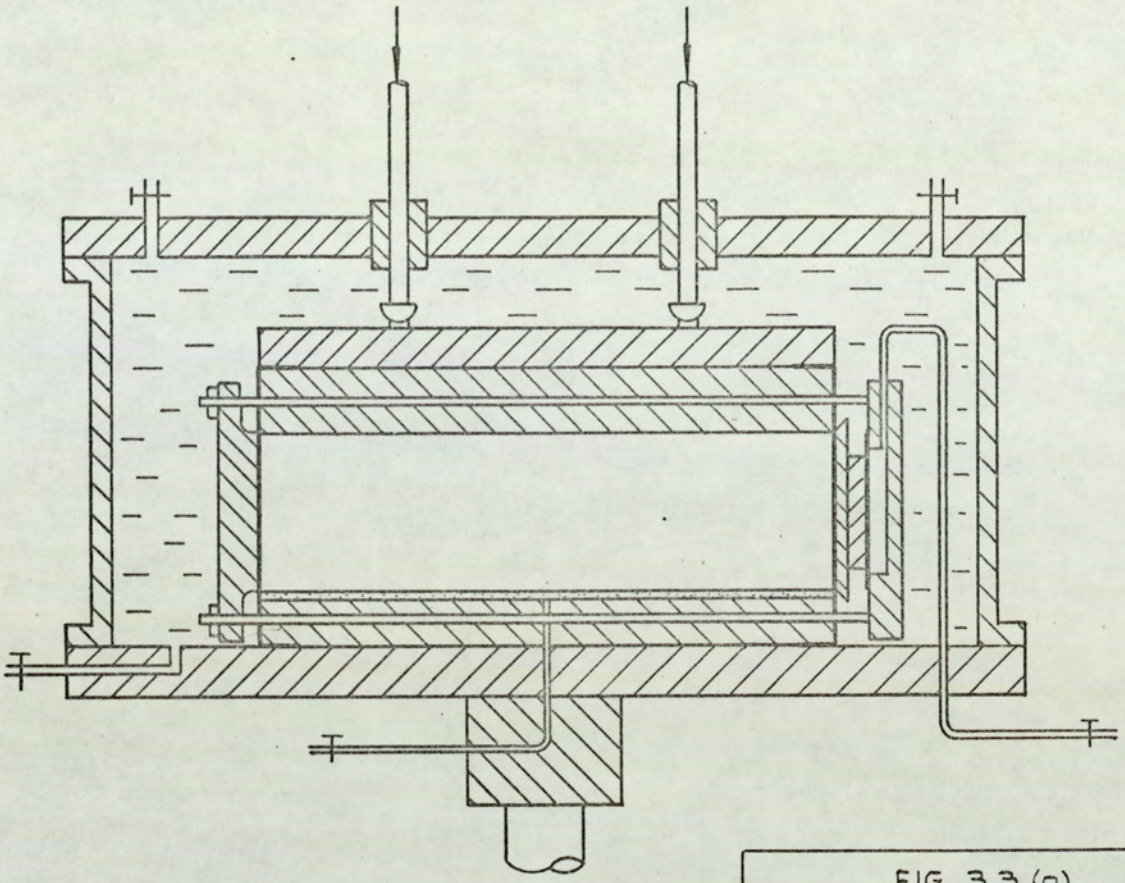

FIG. 3.3.(a)
PLANE STRAIN APPARATUS
- WOOD

FIG. 3.3.(b)
PLANE STRAIN APPARATUS
- HAMBLY
SCHEMATIC PLAN

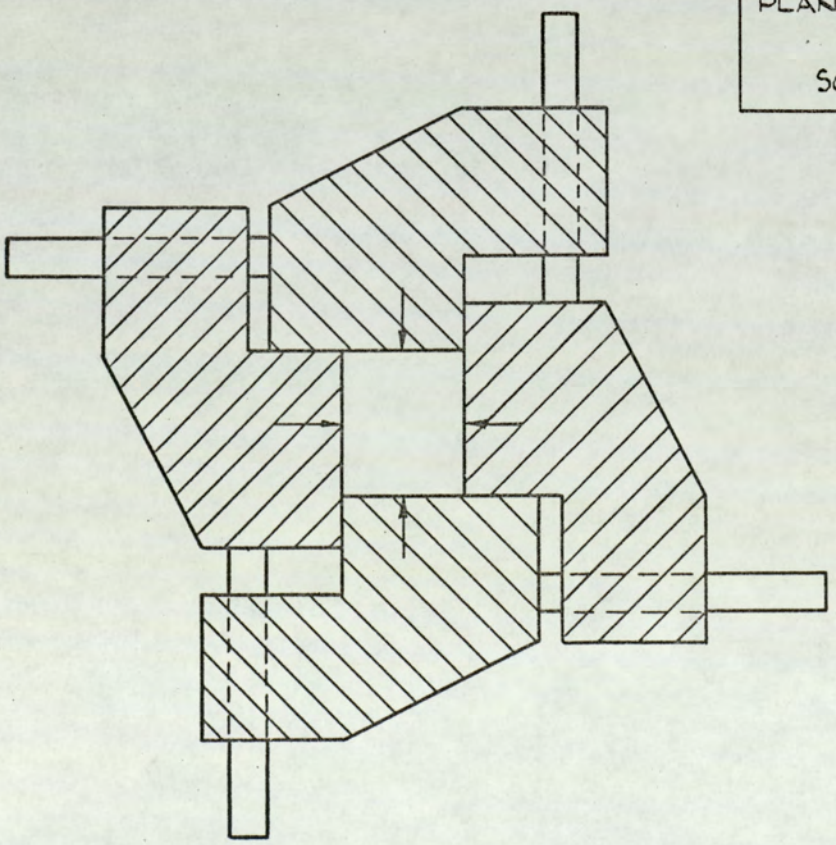

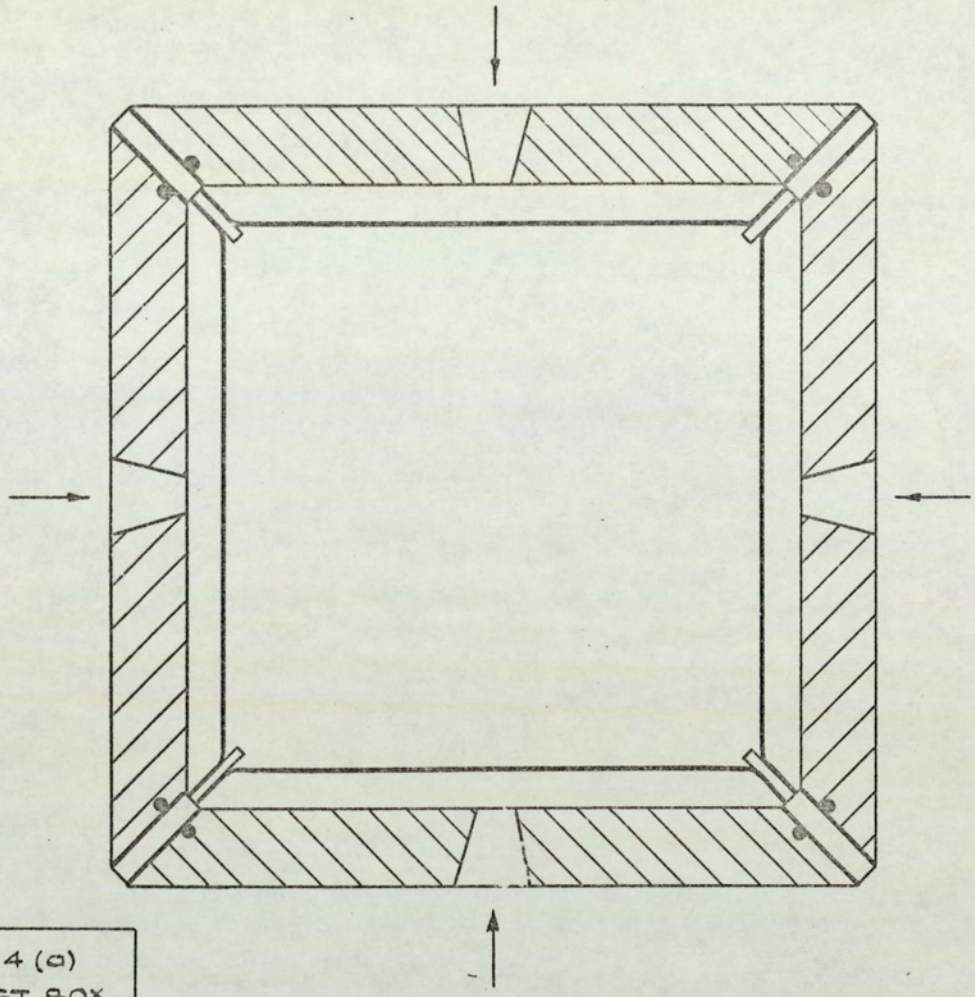

FIG. 3.4 (a)
SOIL TEST BOX
- KO & SCOTT

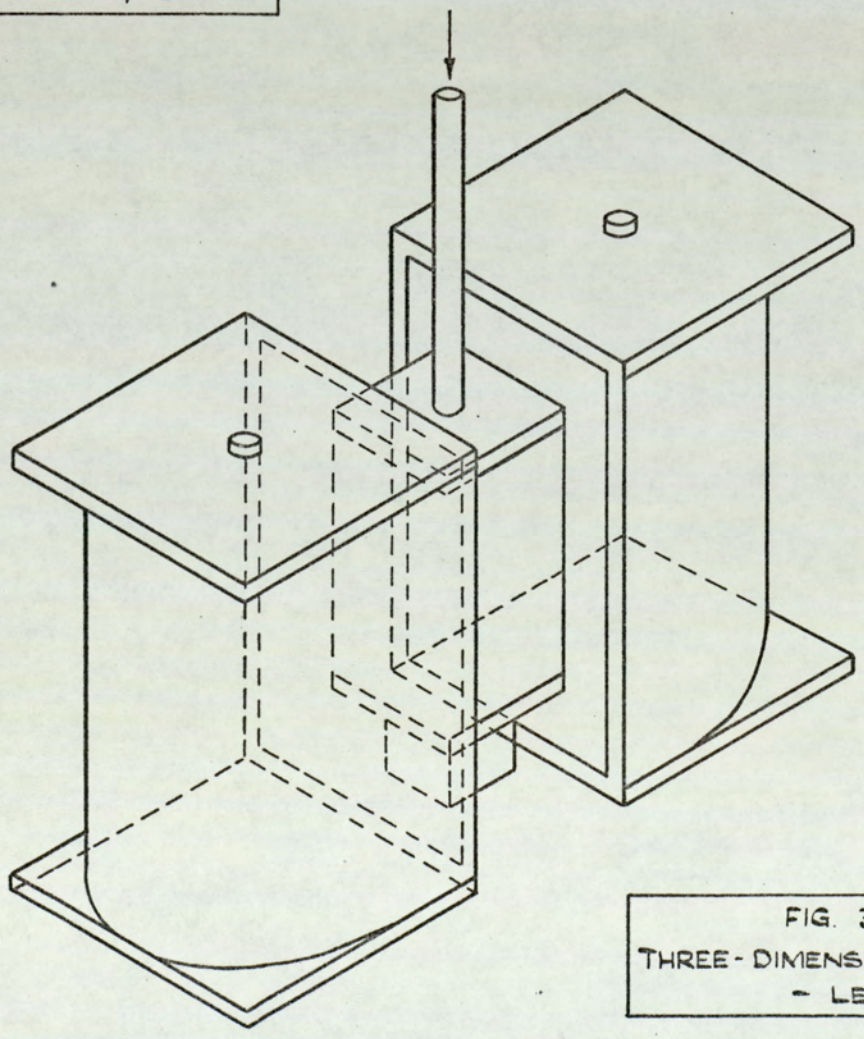

FIG. 3.4 (b)
THREE-DIMENSIONAL APPARATUS
- LENOE

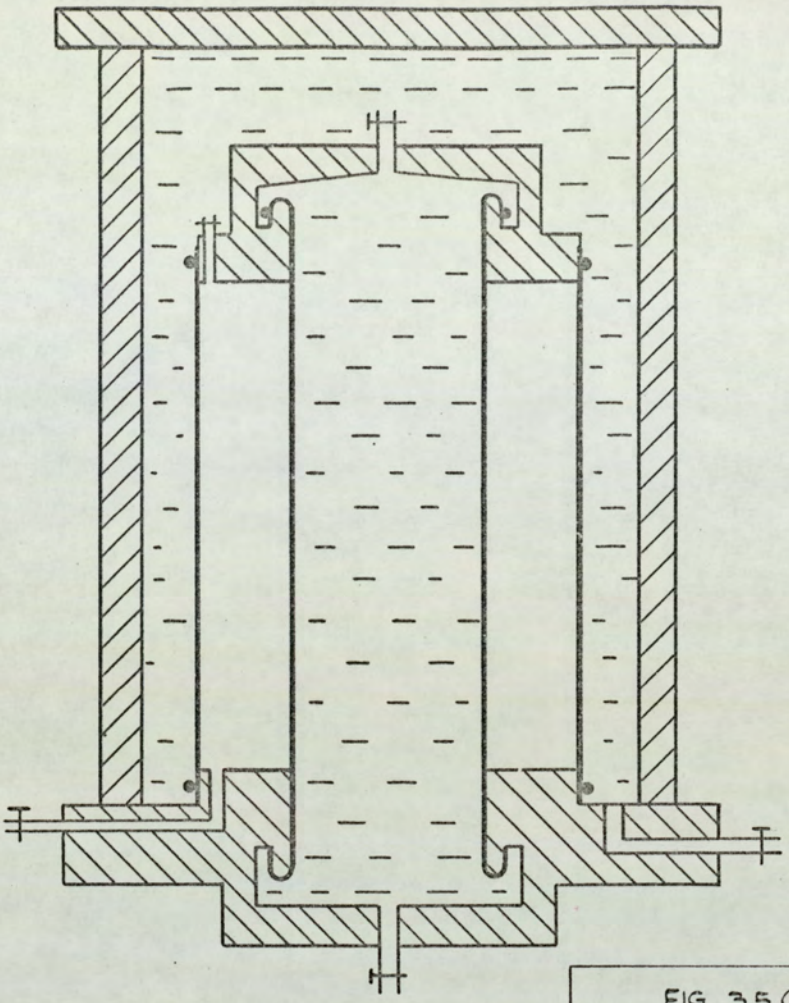

FIG. 3.5 (a)
HOLLOW CYLINDER TEST
- KIRKPATRICK

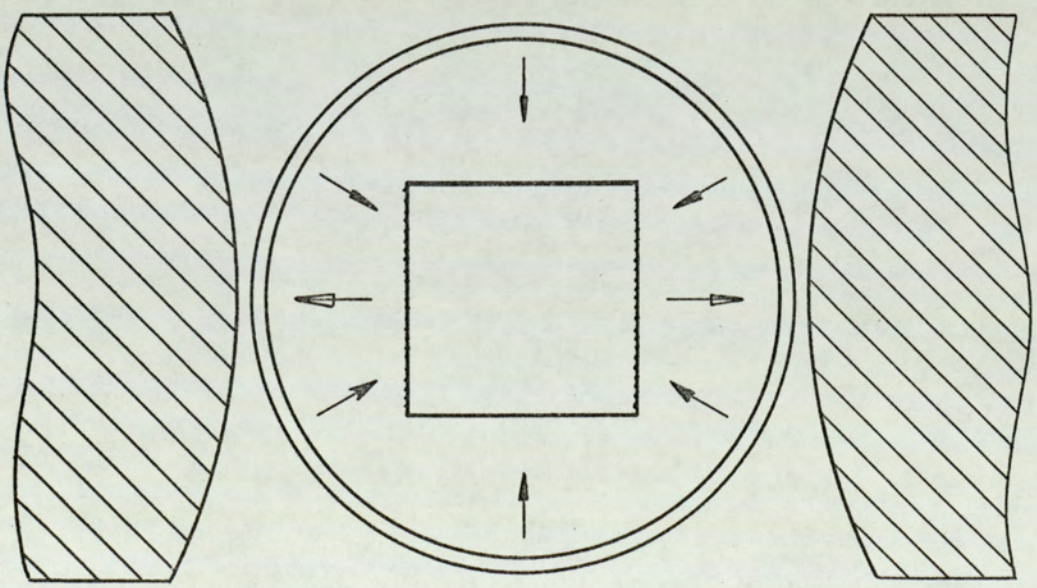

FIG. 3.5 (b)
MAGNETIC TRIAXIAL APPARATUS
- ESCARIO
SCHEMATIC PLANE

CHAPTER FOUR

FIGURES

FIG. 4.1/A.1
MEMBRANE FORMERS
Scale - Half Size

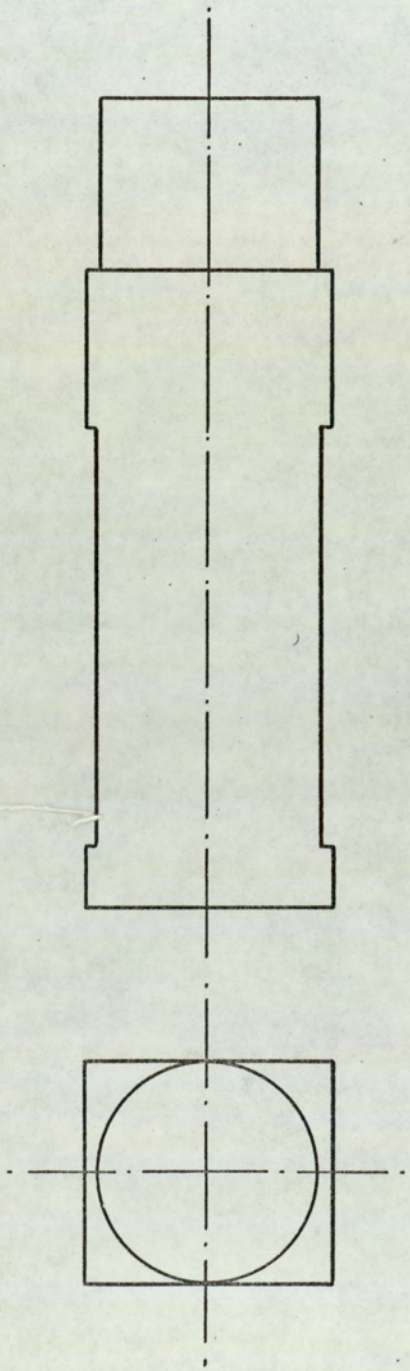

(a) CUBOIDAL SPECIMEN MEMBRANES

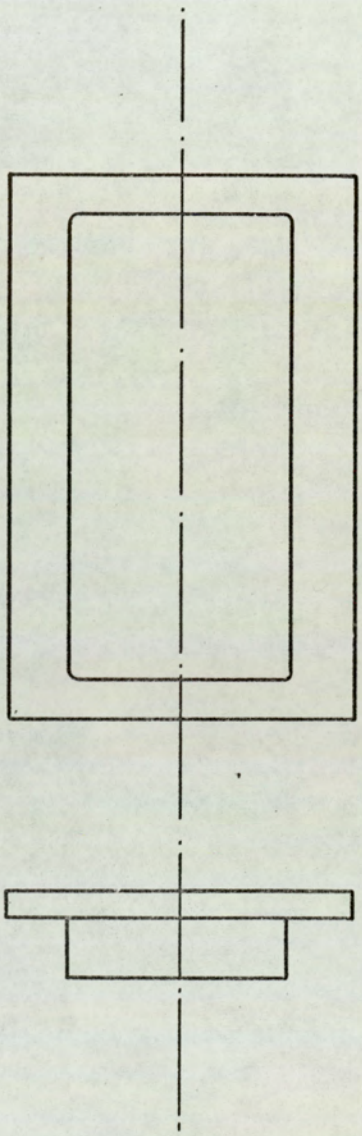

(b) SIDE STRESS - CELL MEMBRANES

FIG.4.2(b)
TOP STRESS-CELL

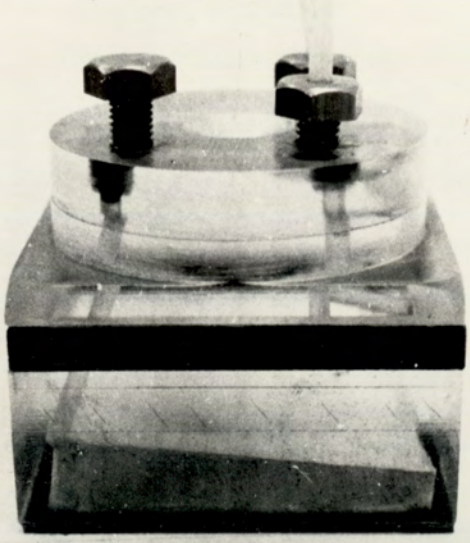

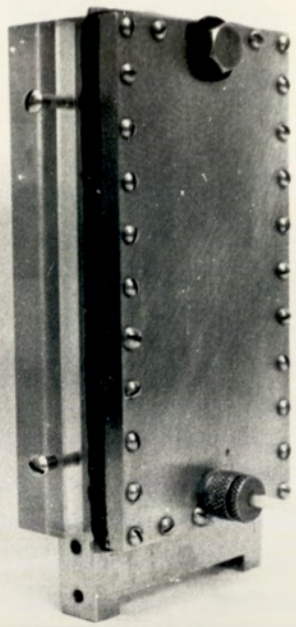

FIG.4.2(a)
SIDE STRESS-CELLS

FIG.4.2(c)
BOTTOM STRESS-CELL
UPPER AND LOWER SECTIONS

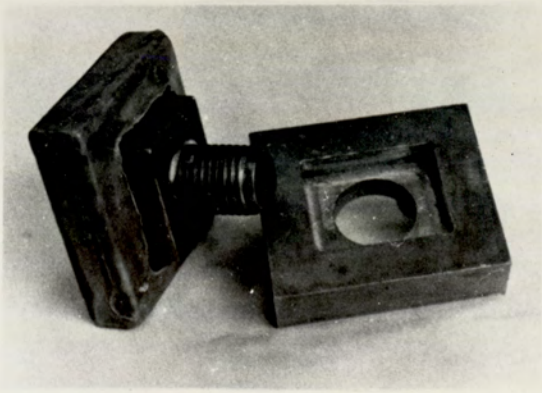

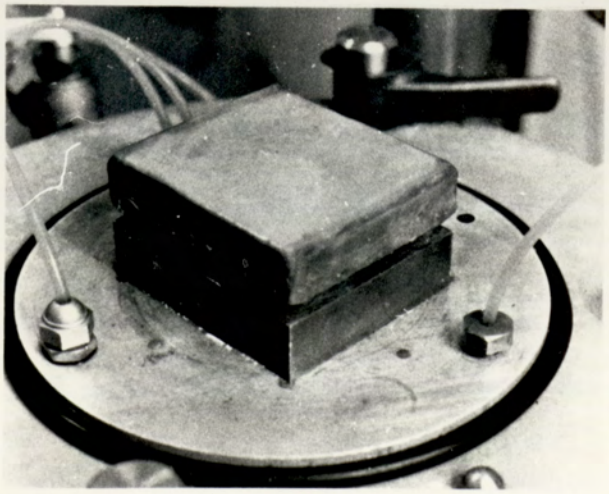

FIG.4.2(d)
BOTTOM STRESS-CELL
ASSEMBLED WITHOUT
SPECIMEN MEMBRANE

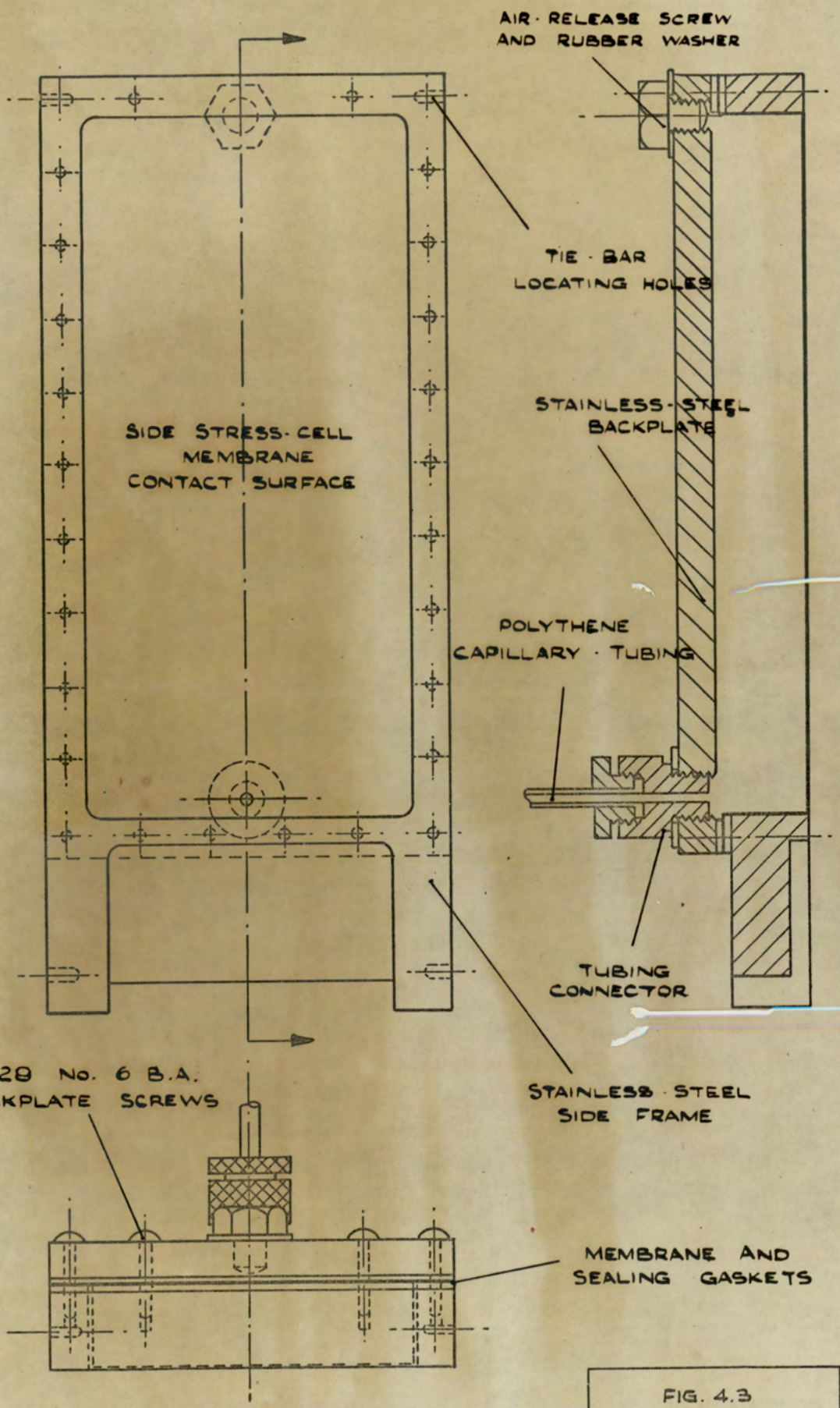

FIG. 4.3
ATA MK I & II
SIDE STRESS · CELLS
Scale - Full Size

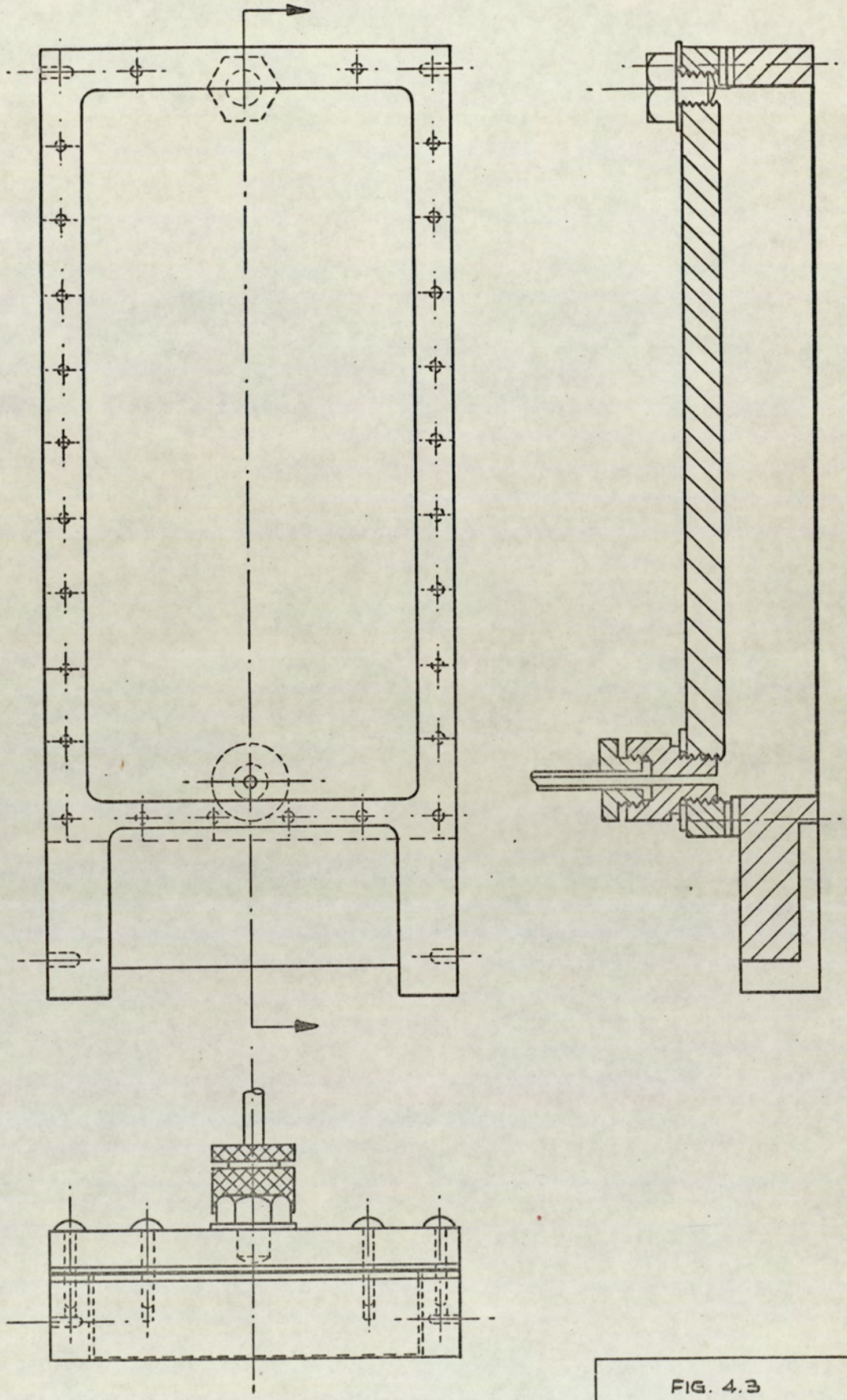

FIG. 4.3
ATA MK I & II
SIDE STRESS-CELLS
Scale - Full Size

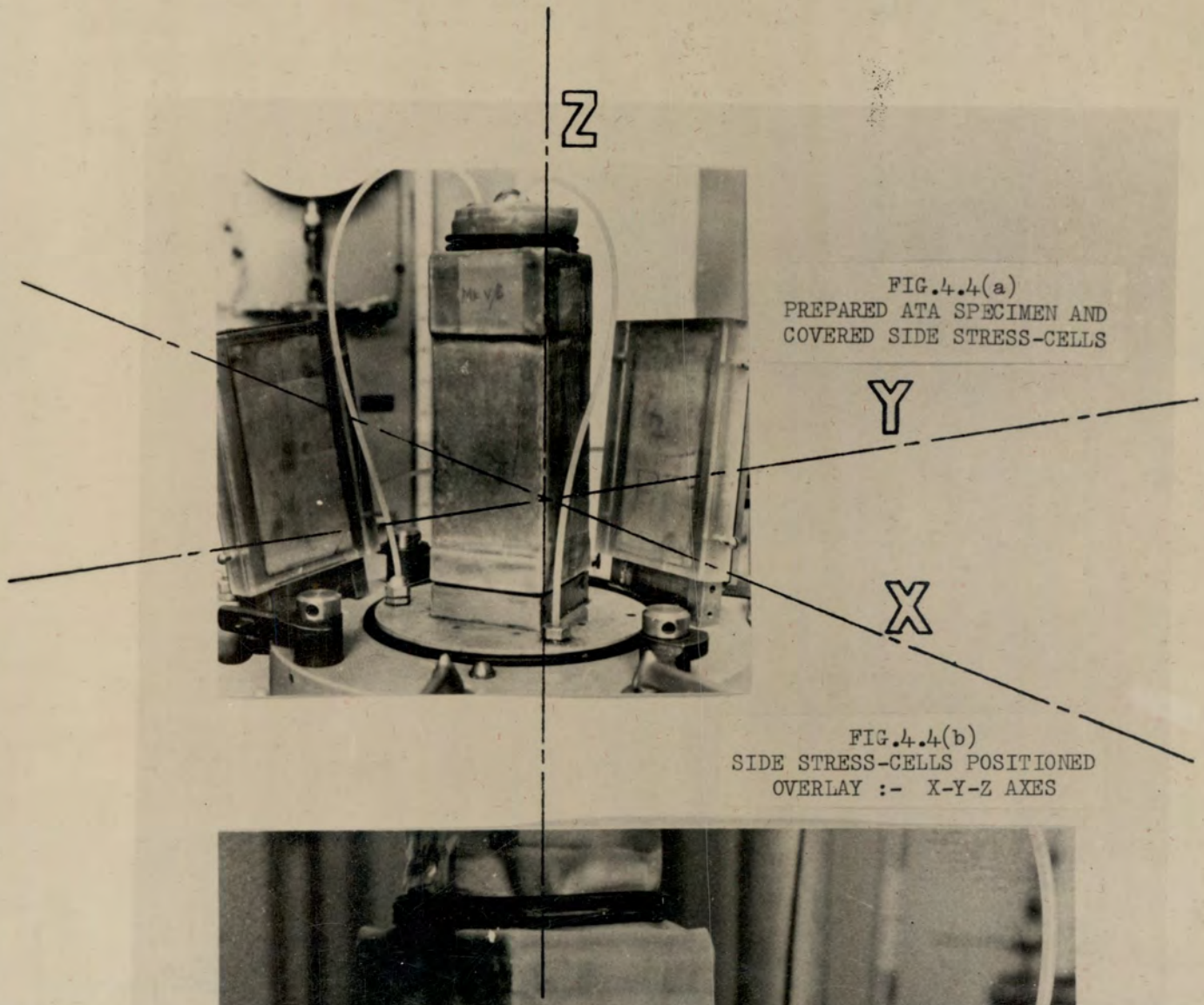

FIG.4.4(a)
PREPARED ATA SPECIMEN AND
COVERED SIDE STRESS-CELLS

FIG.4.4(b)
SIDE STRESS-CELLS POSITIONED
OVERLAY :- X-Y-Z AXES

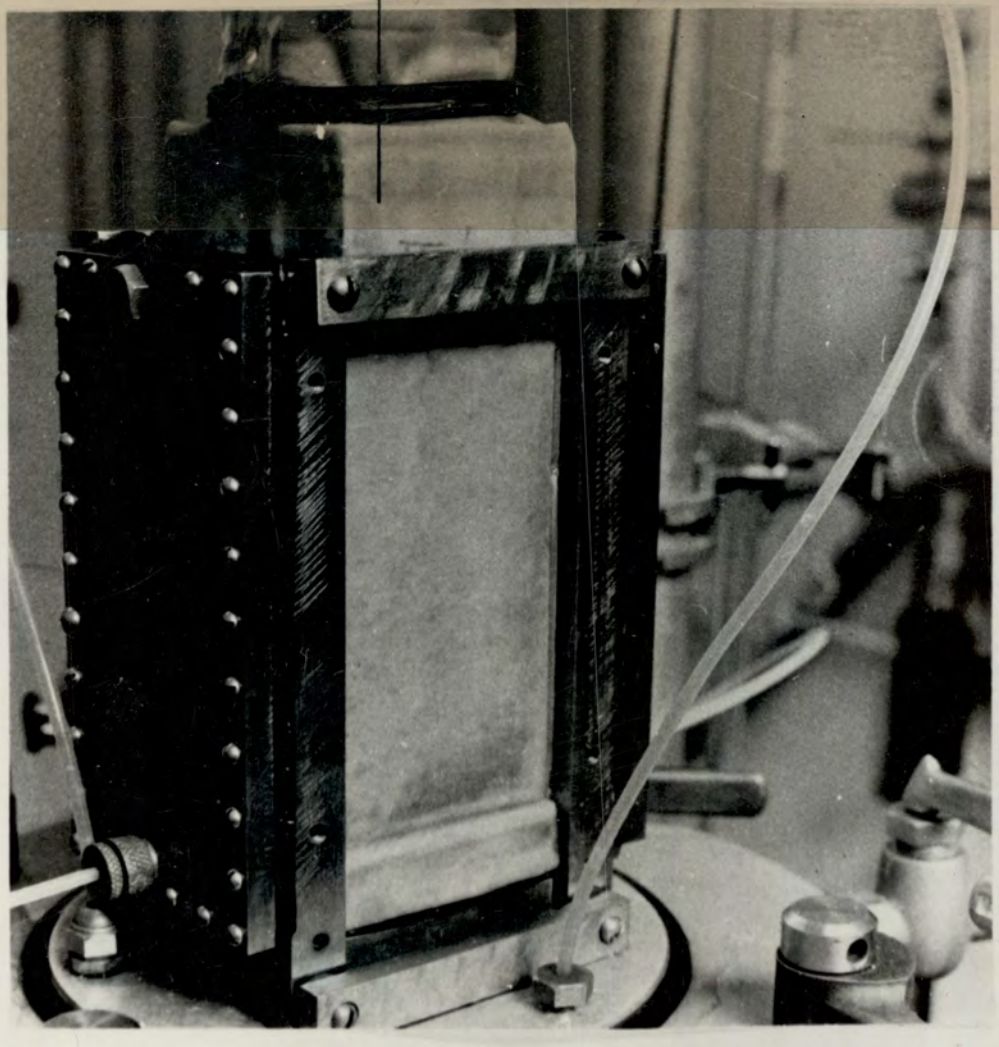

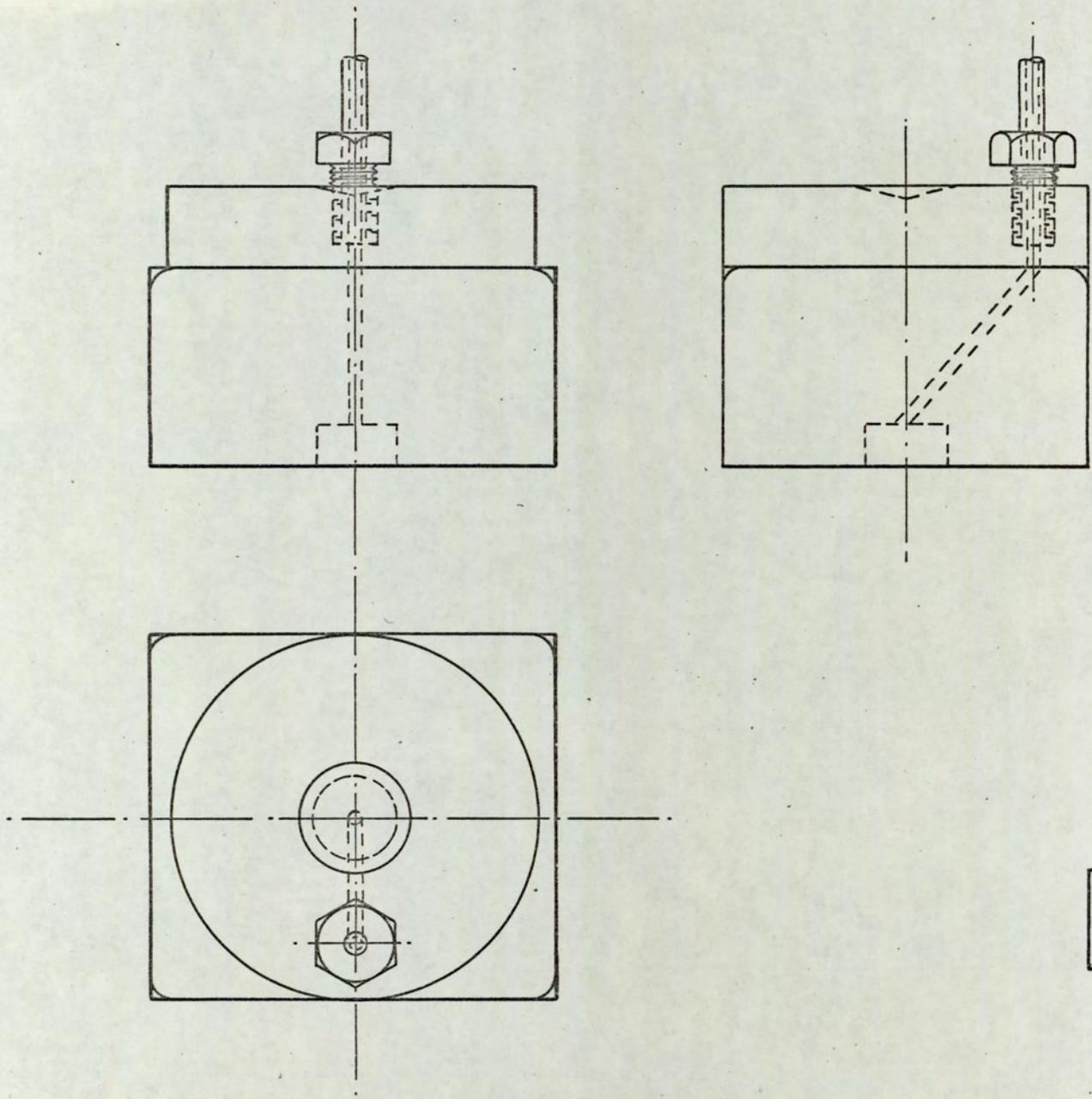

FIG. 4.5
ATA MK I TOP PLATTEN
Scale - Full Size

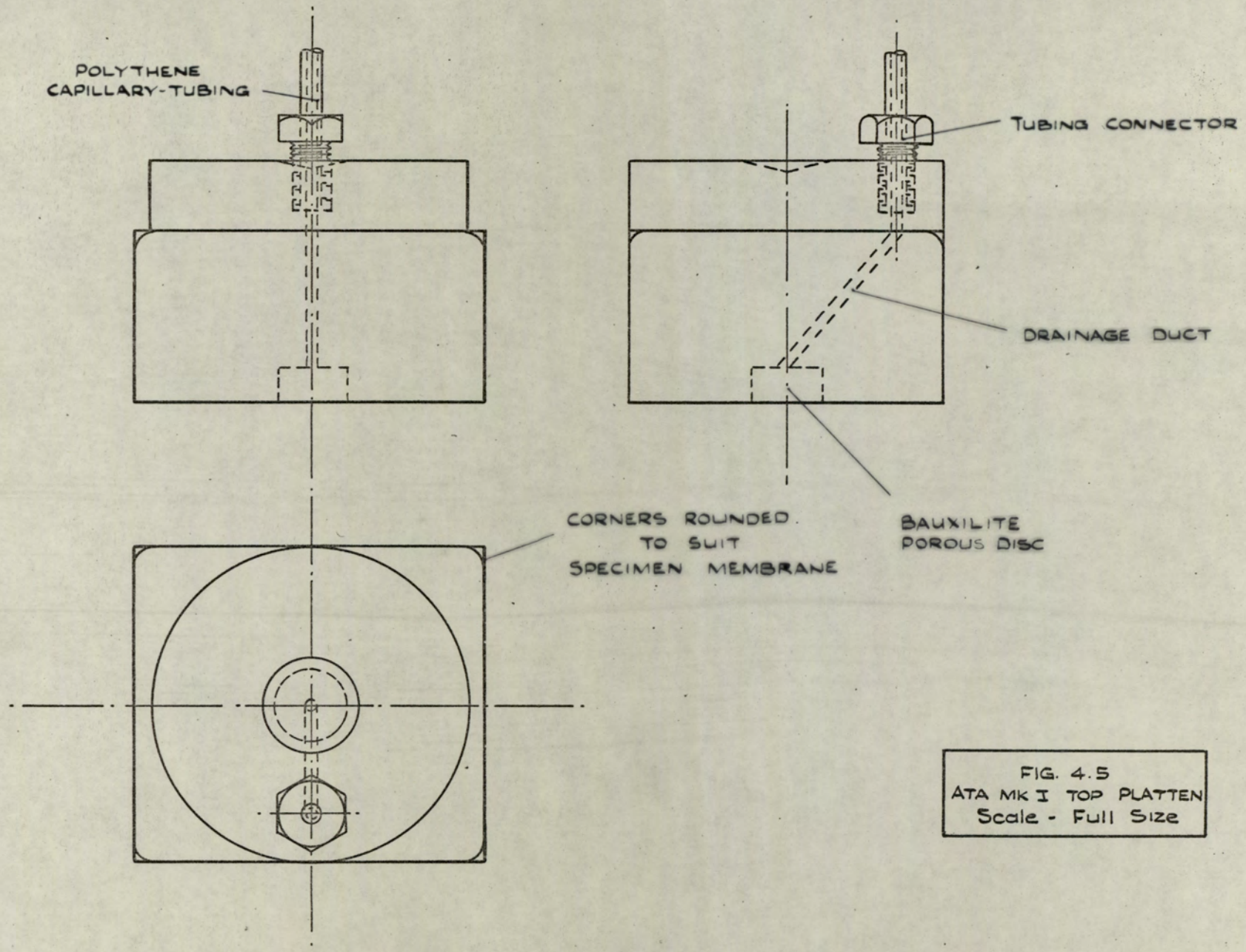

FIG. 4.5
ATA MK I TOP PLATTEN
Scale - Full Size

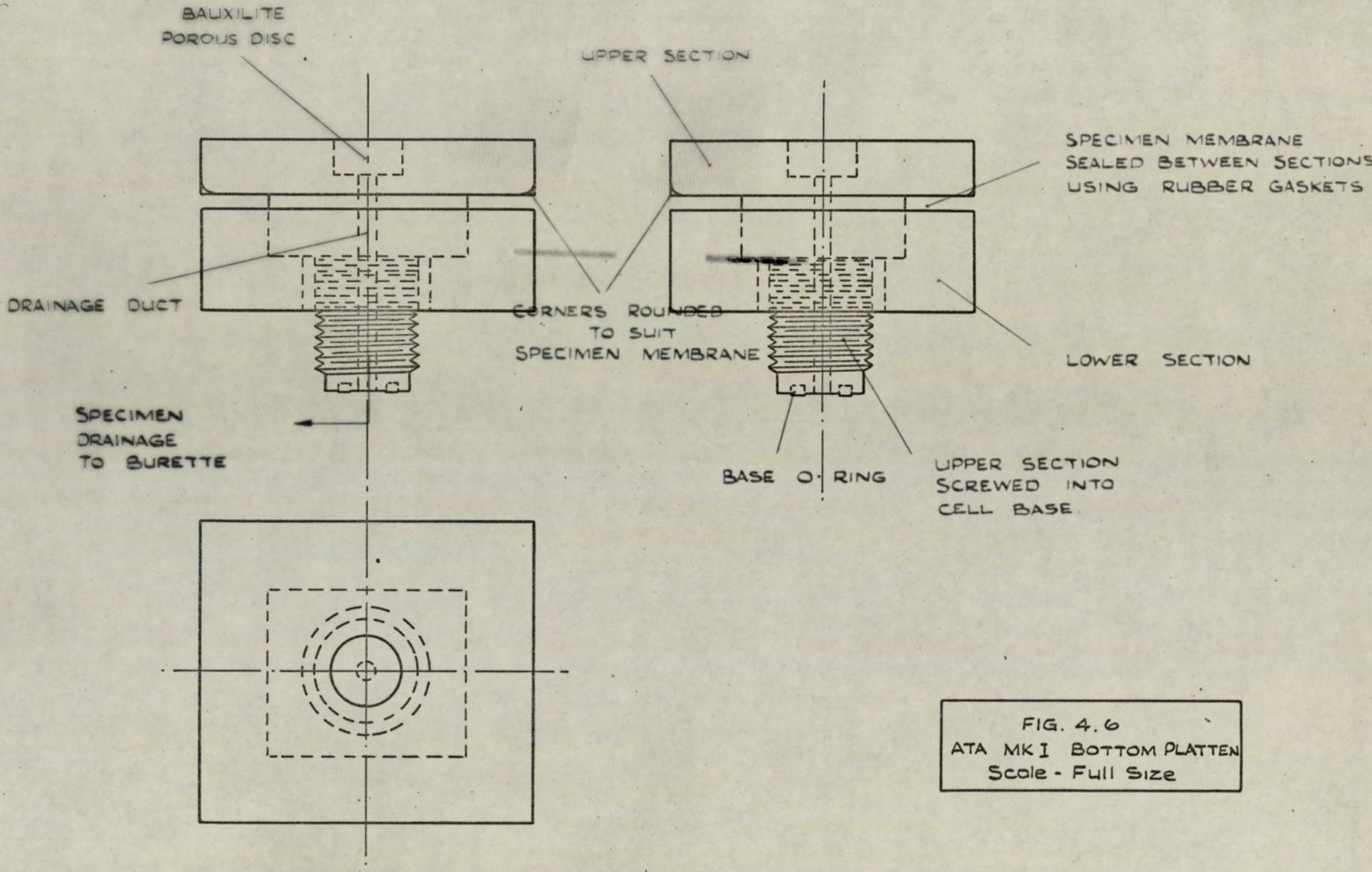

FIG. 4.6
ATA MK I BOTTOM PLATTEN
Scale - Full Size

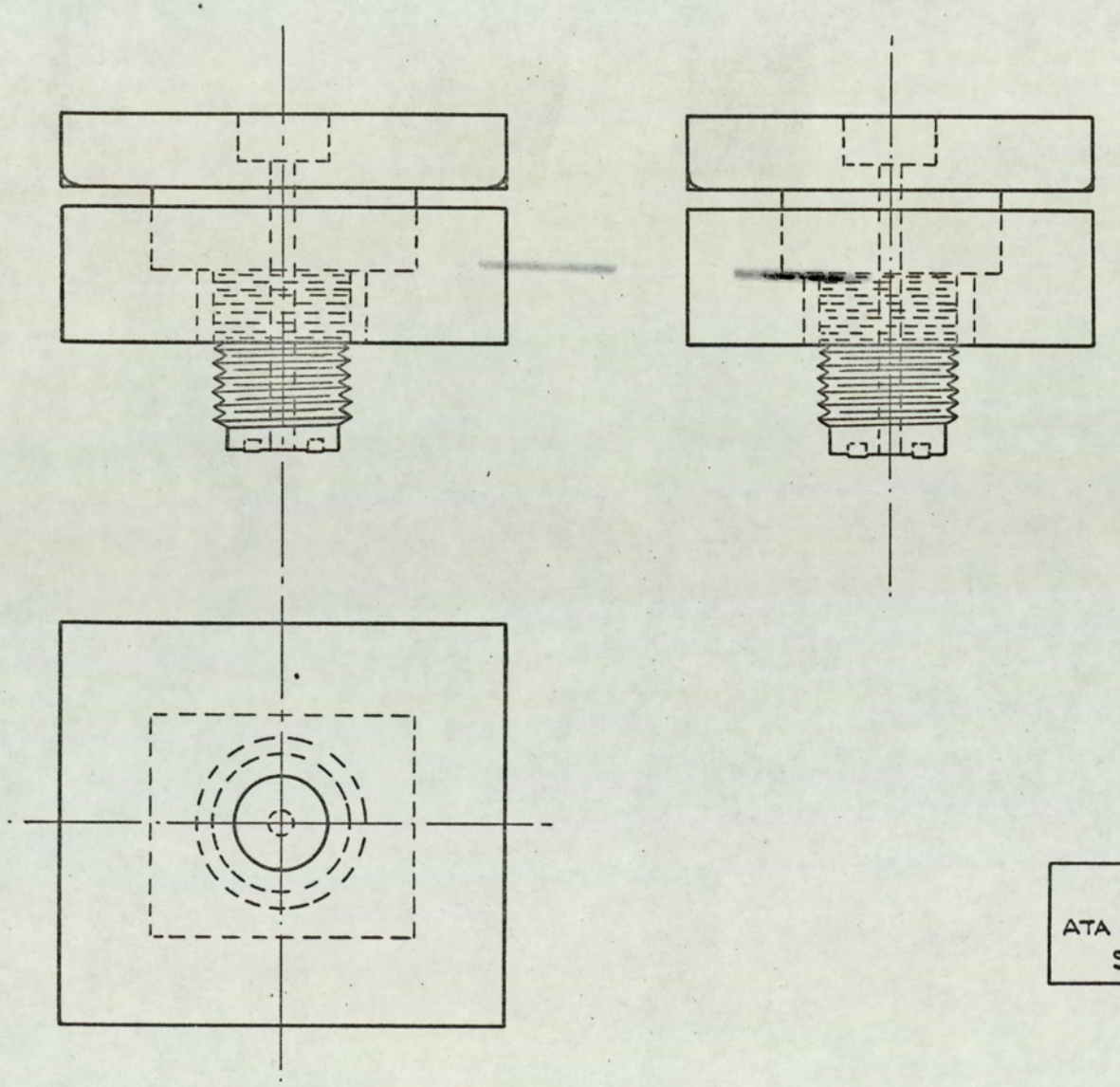

FIG. 4.6
ATA MK I BOTTOM PLATTEN
Scale - Full Size

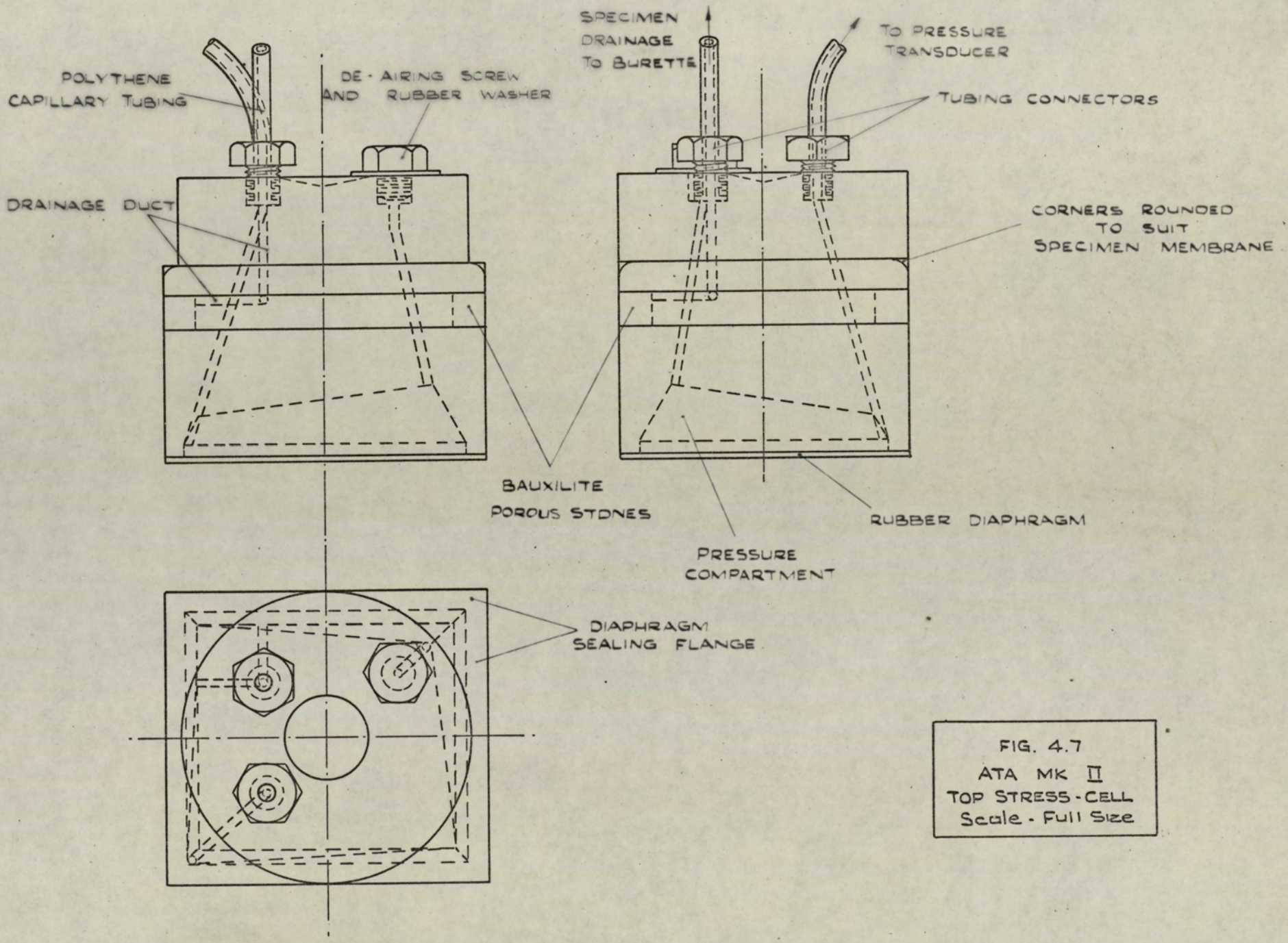

FIG. 4.7
ATA MK II
TOP STRESS-CELL
Scale - Full Size

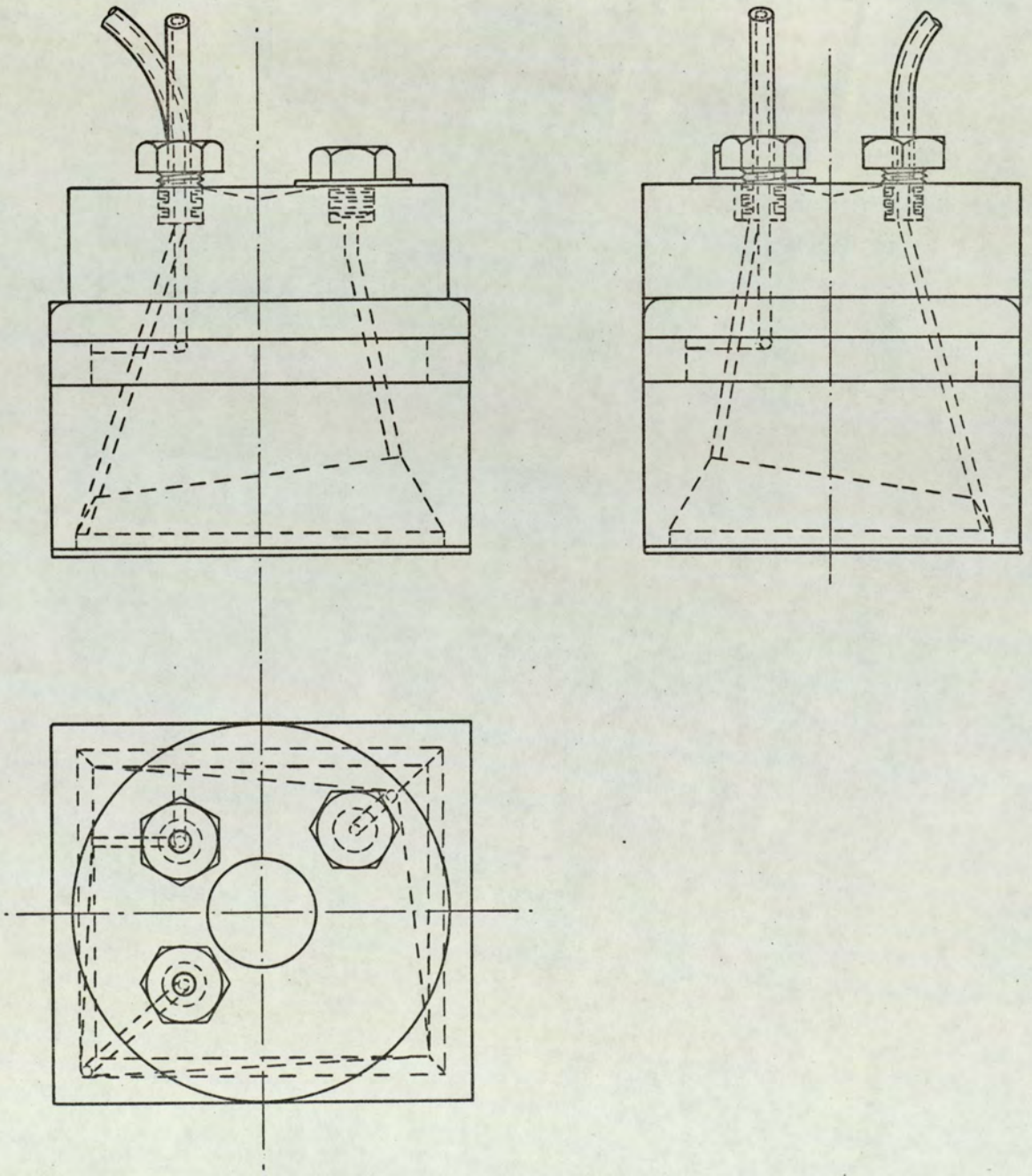

FIG. 4.7
ATA MK II
TOP STRESS-CELL
Scale - Full Size

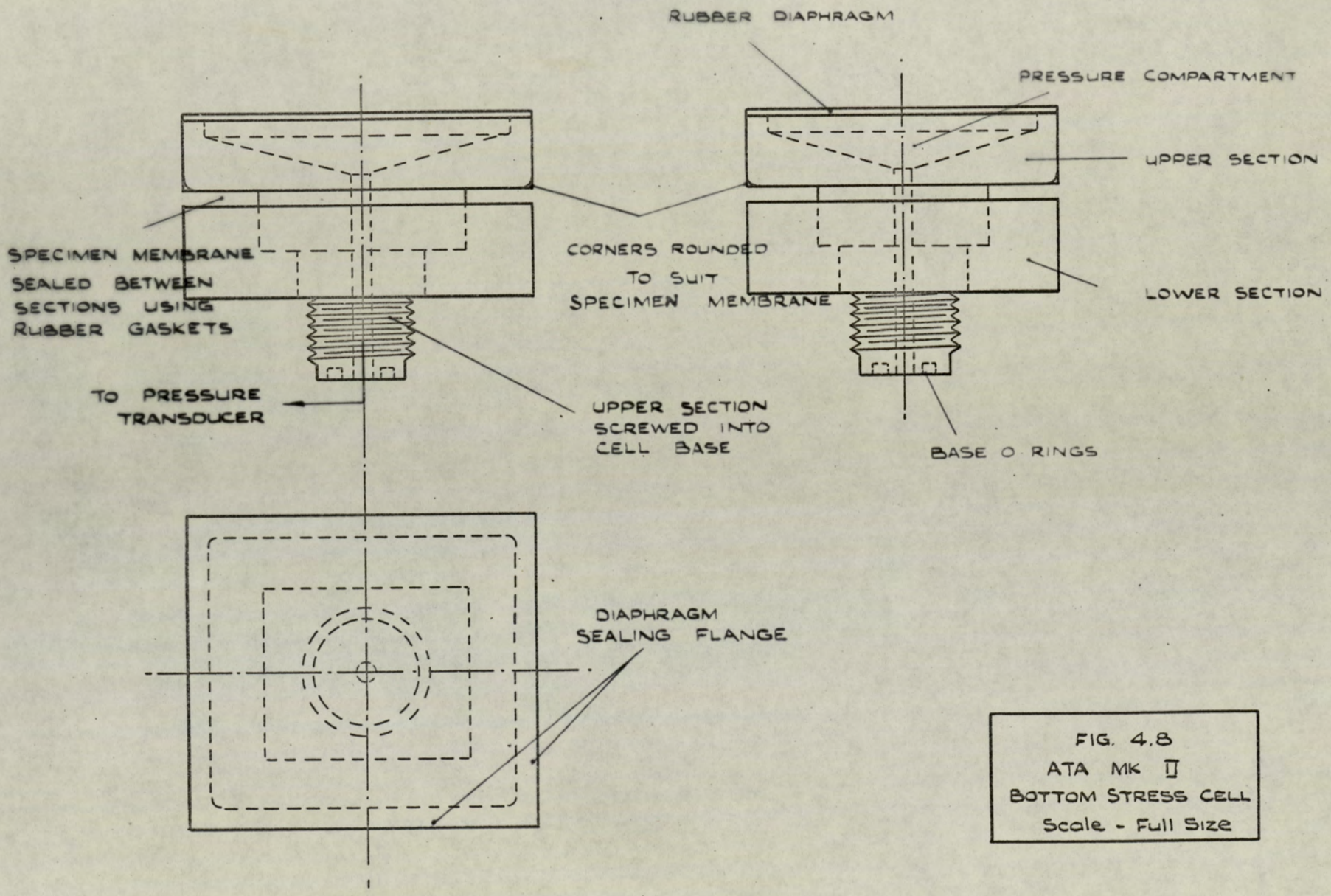

FIG. 4.8
ATA MK II
BOTTOM STRESS CELL
Scale - Full Size

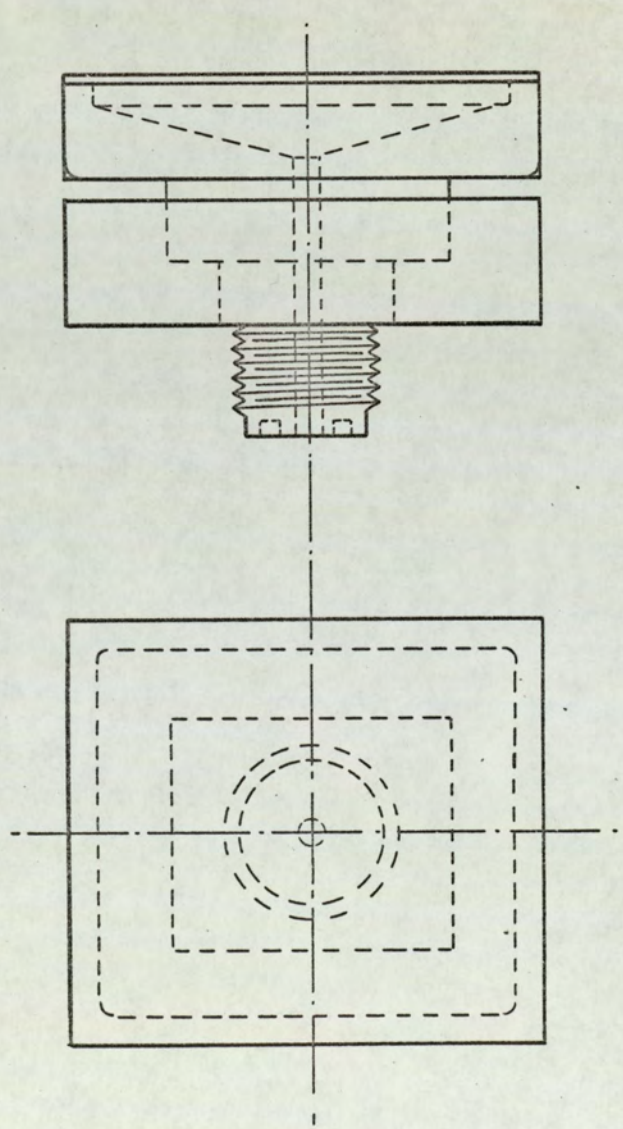

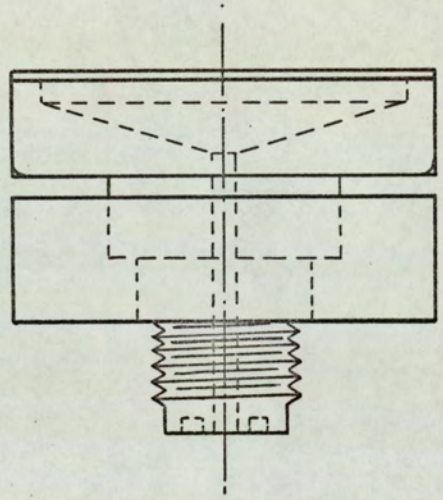

FIG. 4.8
ATA MK II
BOTTOM STRESS CELL
Scale - Full Size

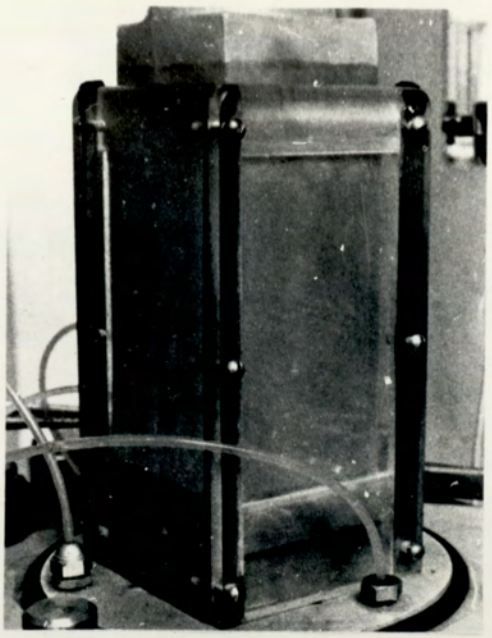

FIG.4.9(a)
SPECIMEN MEMBRANE
AND PERSPEX FORMER

FIG.4.9(d)
PREPARED ATA SPECIMEN

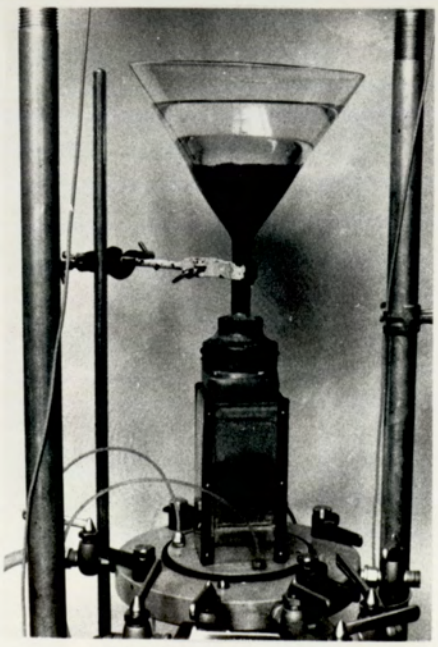

FIG.4.9(b)
METHOD OF DEPOSITION

FIG.4.9(c)
PLACEMENT OF
TOP STRESS-CELL

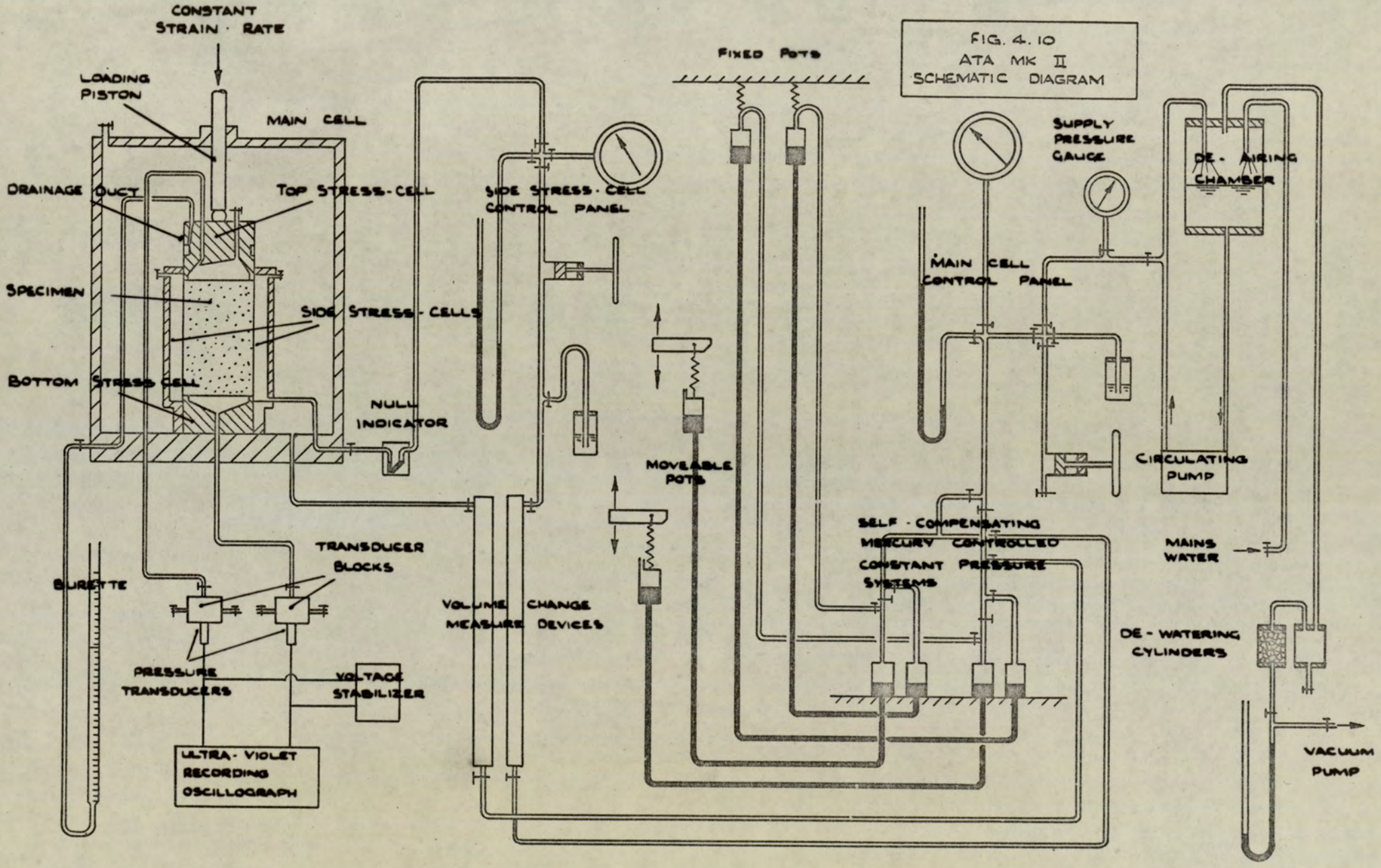

FIG. 4.10
ATA MK II
SCHEMATIC DIAGRAM

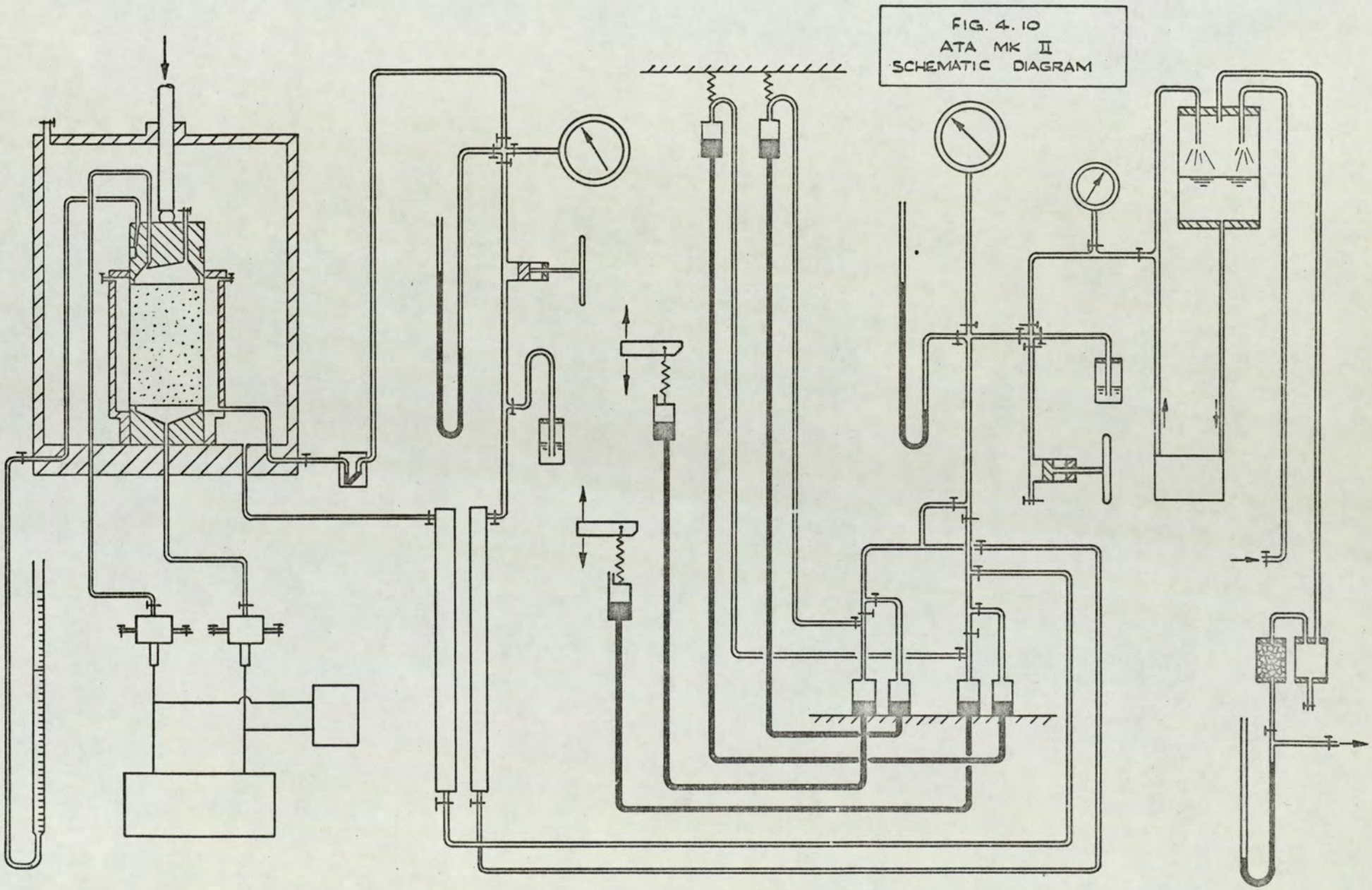

FIG. 4.10
ATA MK II
SCHEMATIC DIAGRAM

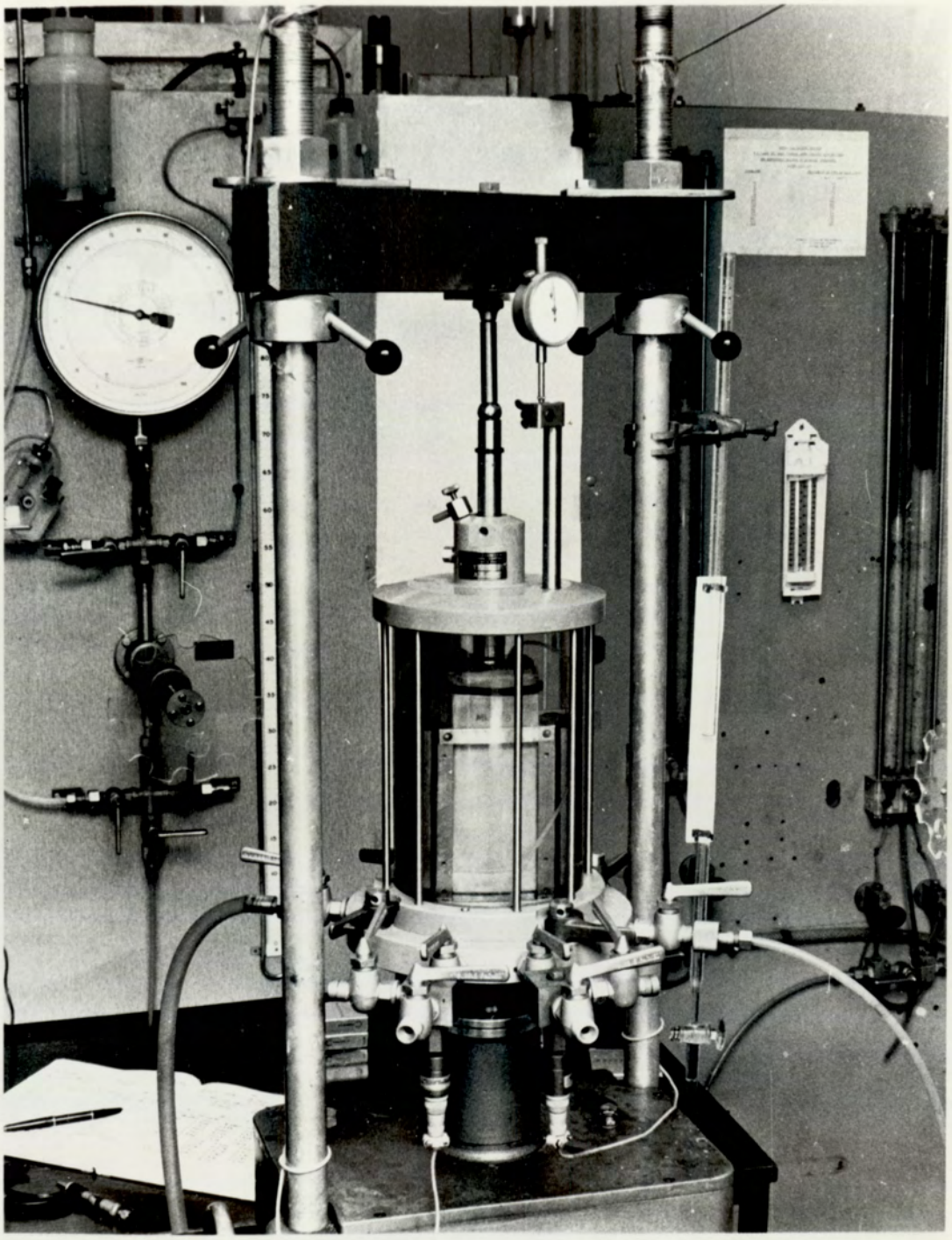

FIG.4.11
THE ATA TEST
BASIC LAYOUT OF APPARATUS

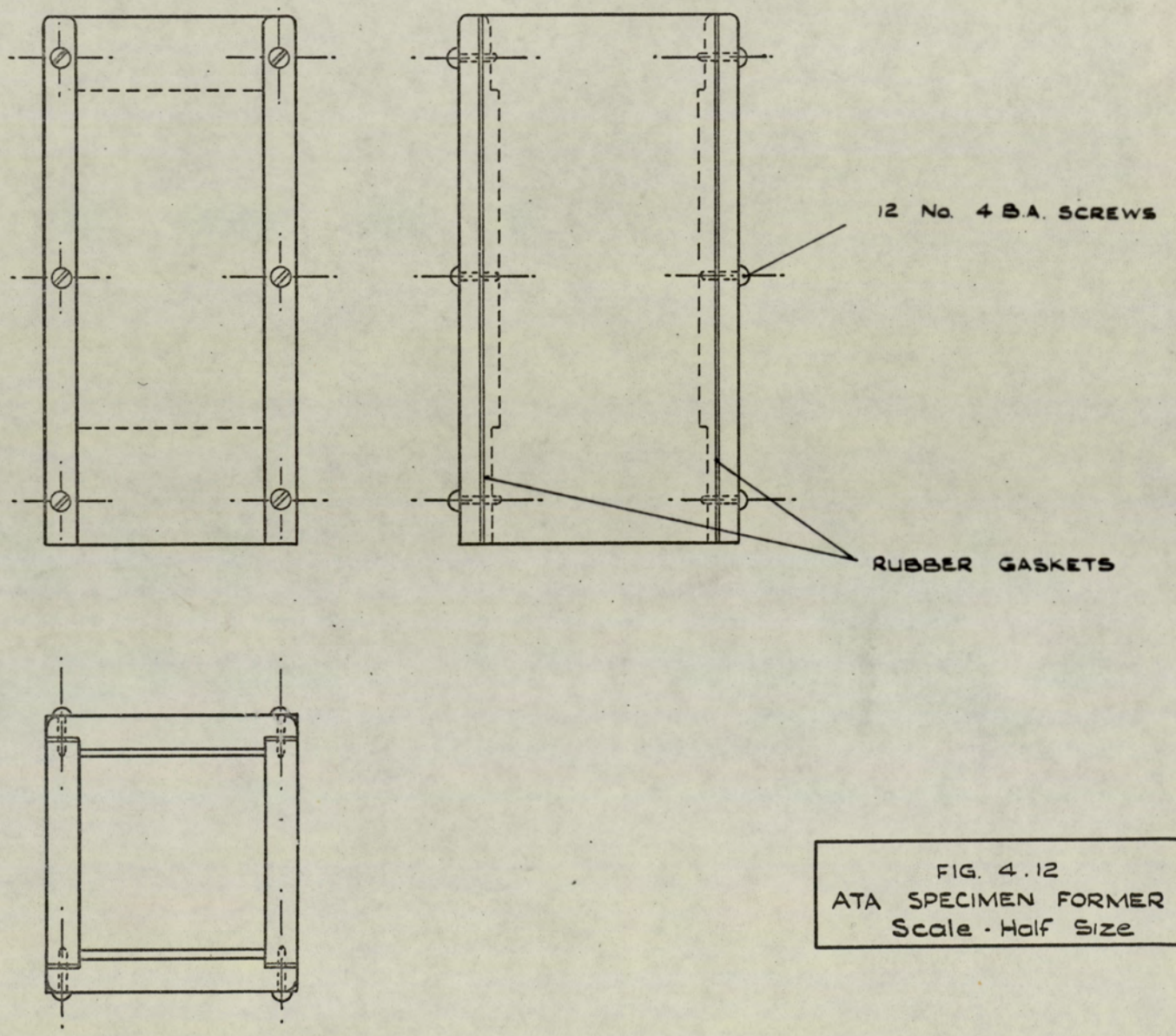

FIG. 4.12
ATA SPECIMEN FORMER
Scale - Half Size

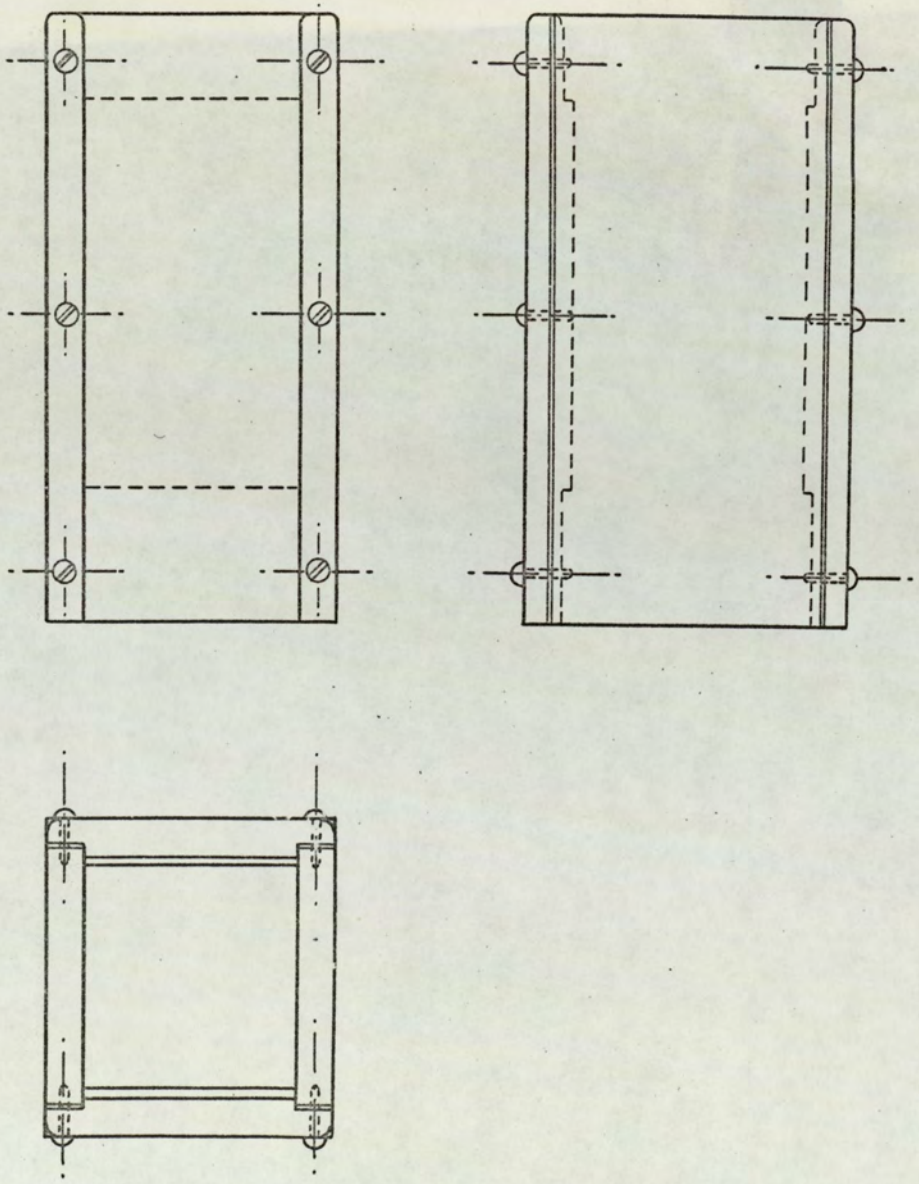

FIG. 4.12
ATA SPECIMEN FORMER
Scale - Half Size

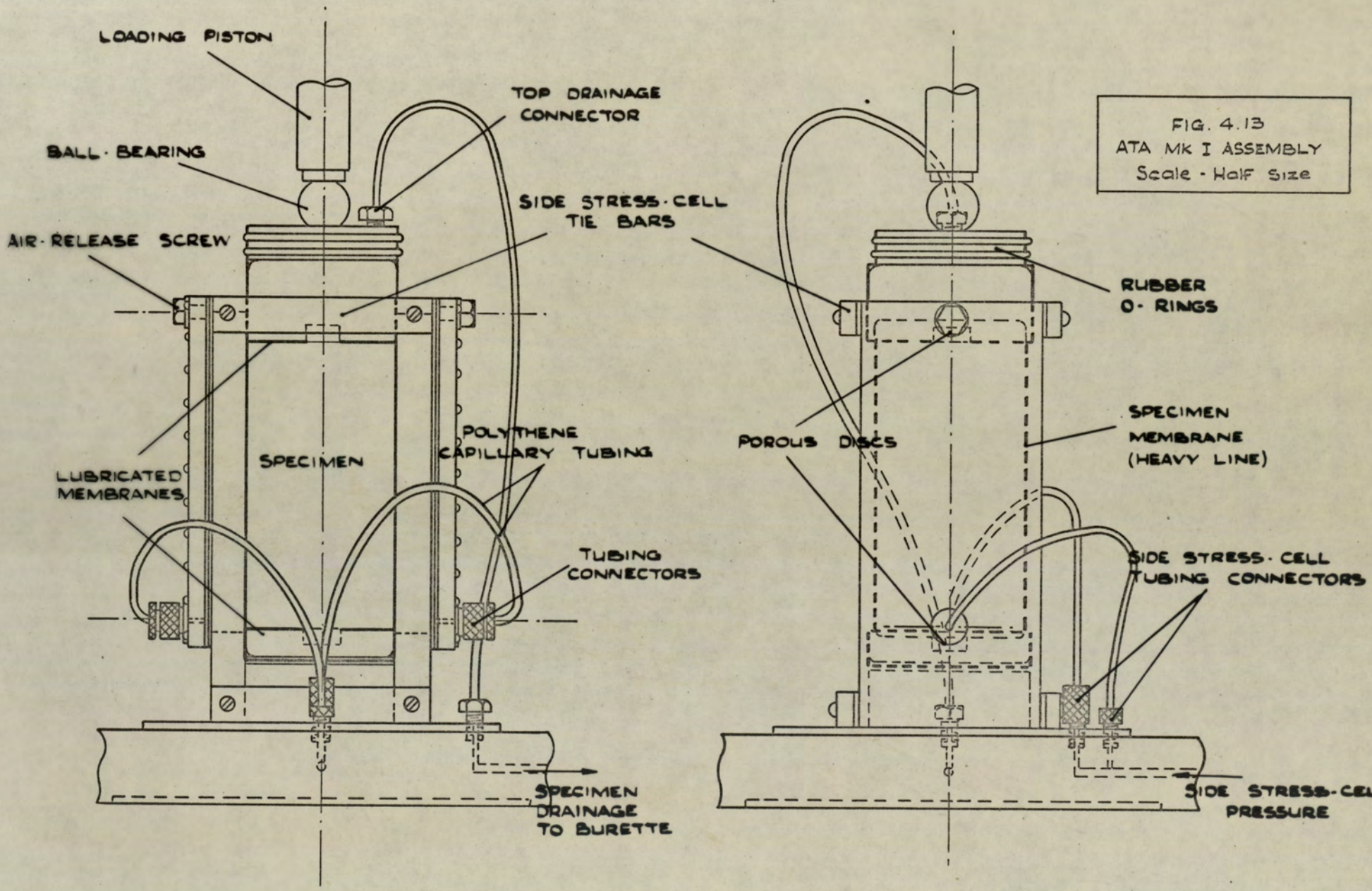

FIG. 4.13
ATA Mk I ASSEMBLY
Scale - Half Size

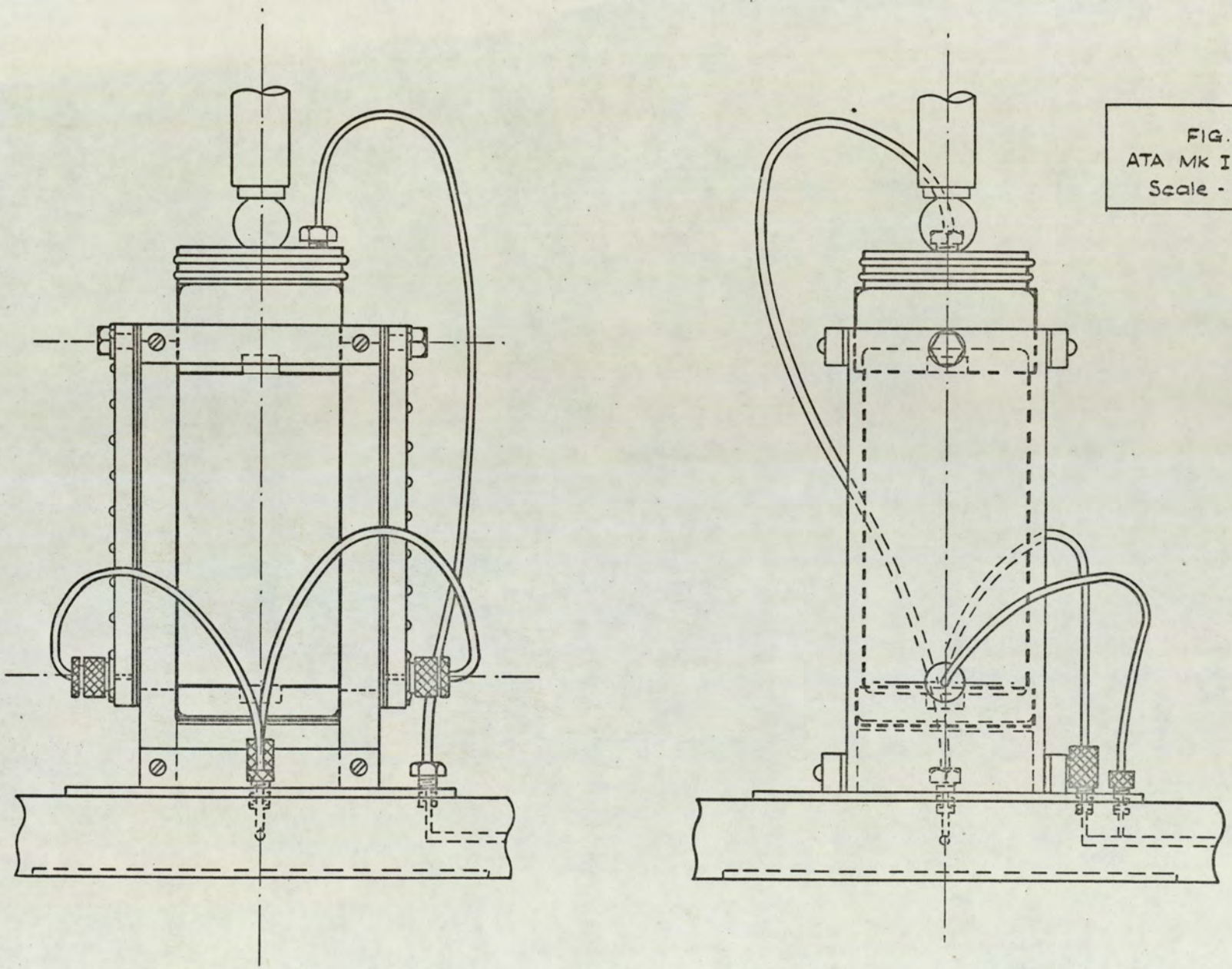

FIG. 4.13
ATA MK I ASSEMBLY
Scale - Half Size

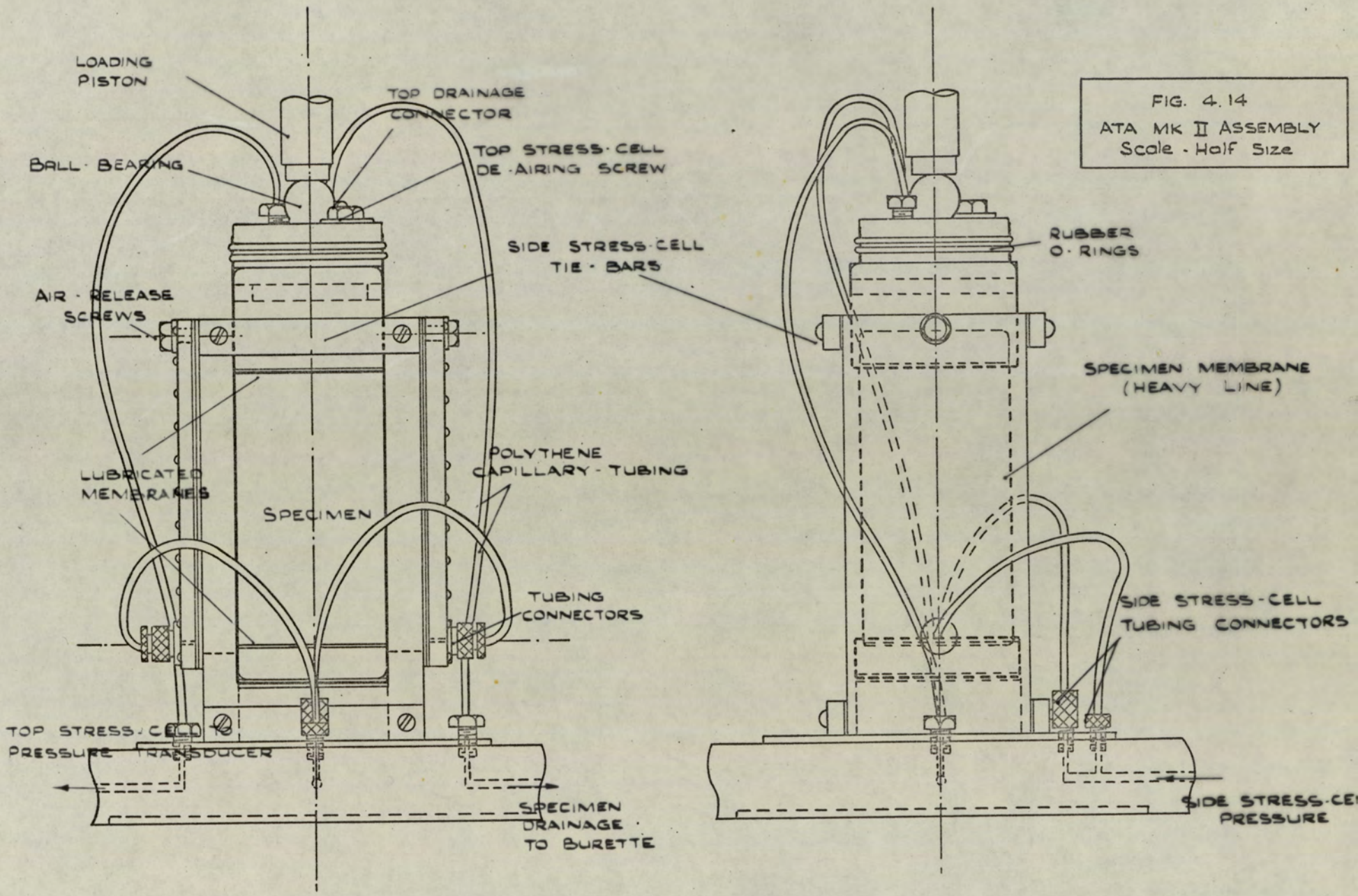

FIG. 4.14
ATA MK II ASSEMBLY
Scale - Half Size

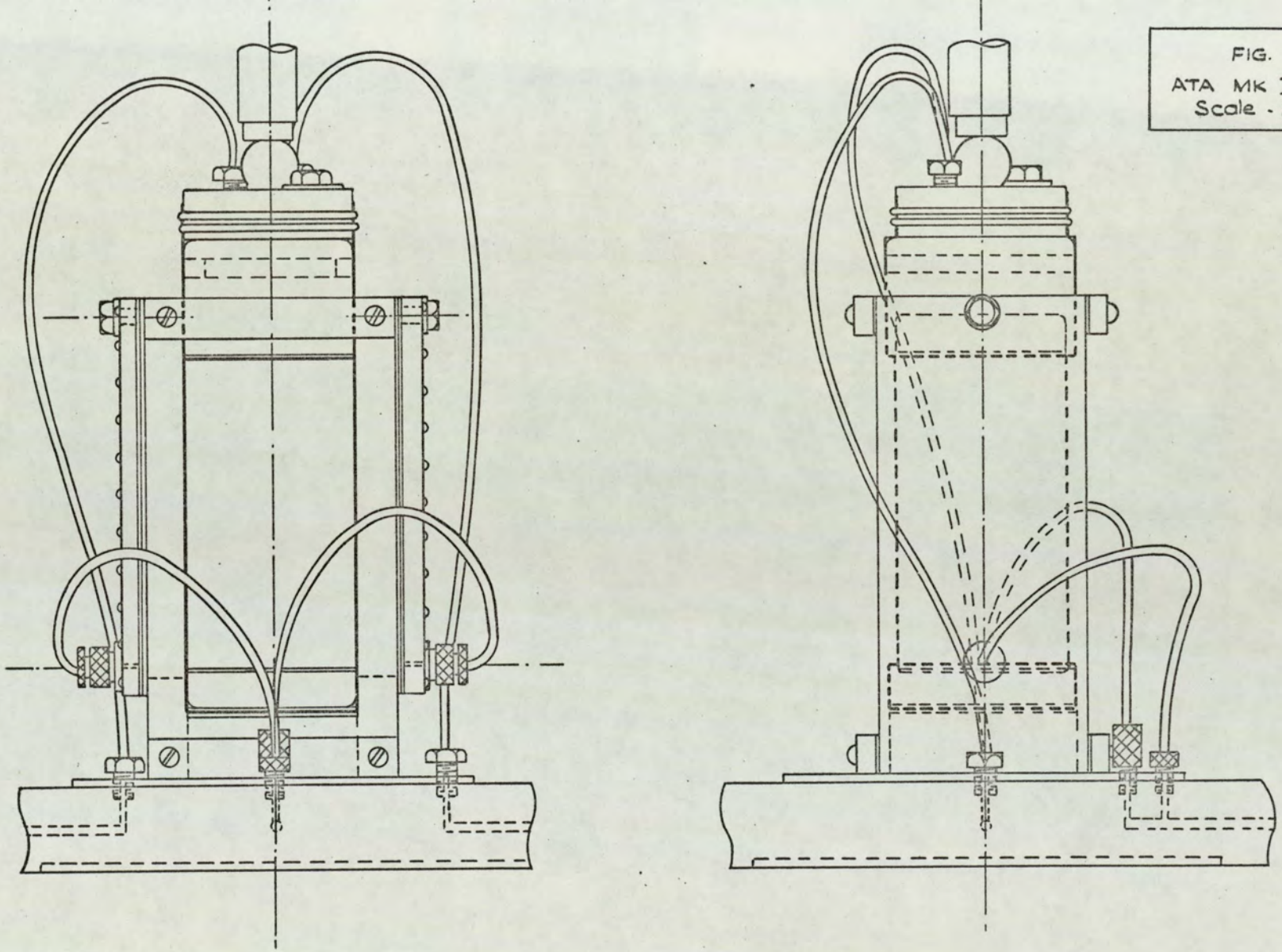

FIG. 4.14
ATA MK II ASSEMBLY
Scale - Half Size

CHAPTER FIVE

FIGURES

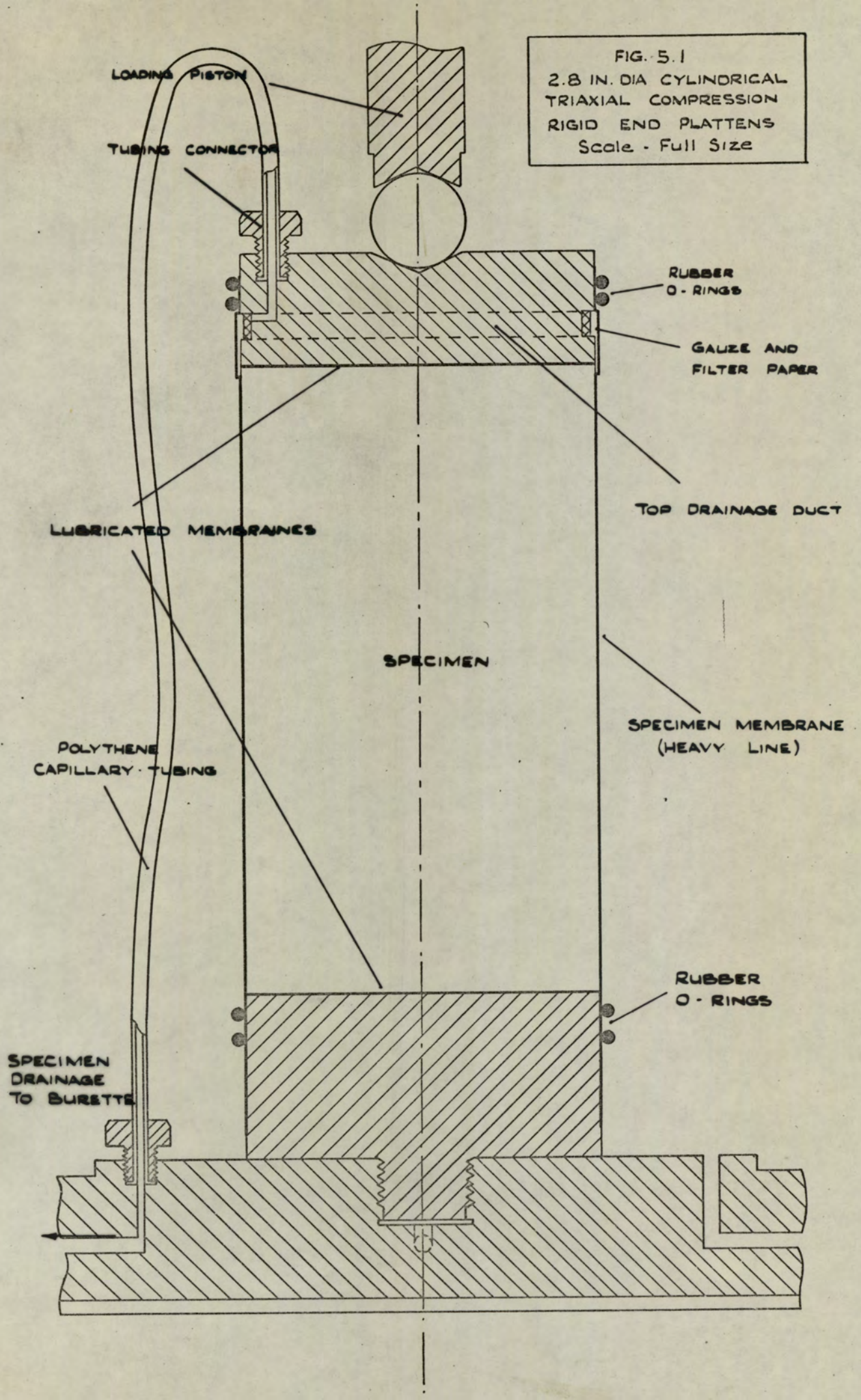
FIG. 5.1
2.8 IN. DIA CYLINDRICAL
TRIAXIAL COMPRESSION
RIGID END PLATTENS
Scale - Full Size
LOADING PISTON
TUBING CONNECTOR
RUBBER
O - RINGS
GAUZE AND
FILTER PAPER
TOP DRAINAGE DUCT
LUBRICATED MEMBRANES
SPECIMEN
SPECIMEN MEMBRANE
(HEAVY LINE)
POLYTHENE
CAPILLARY TUBING
RUBBER
O - RINGS
SPECIMEN
DRAINAGE
TO BURETTE

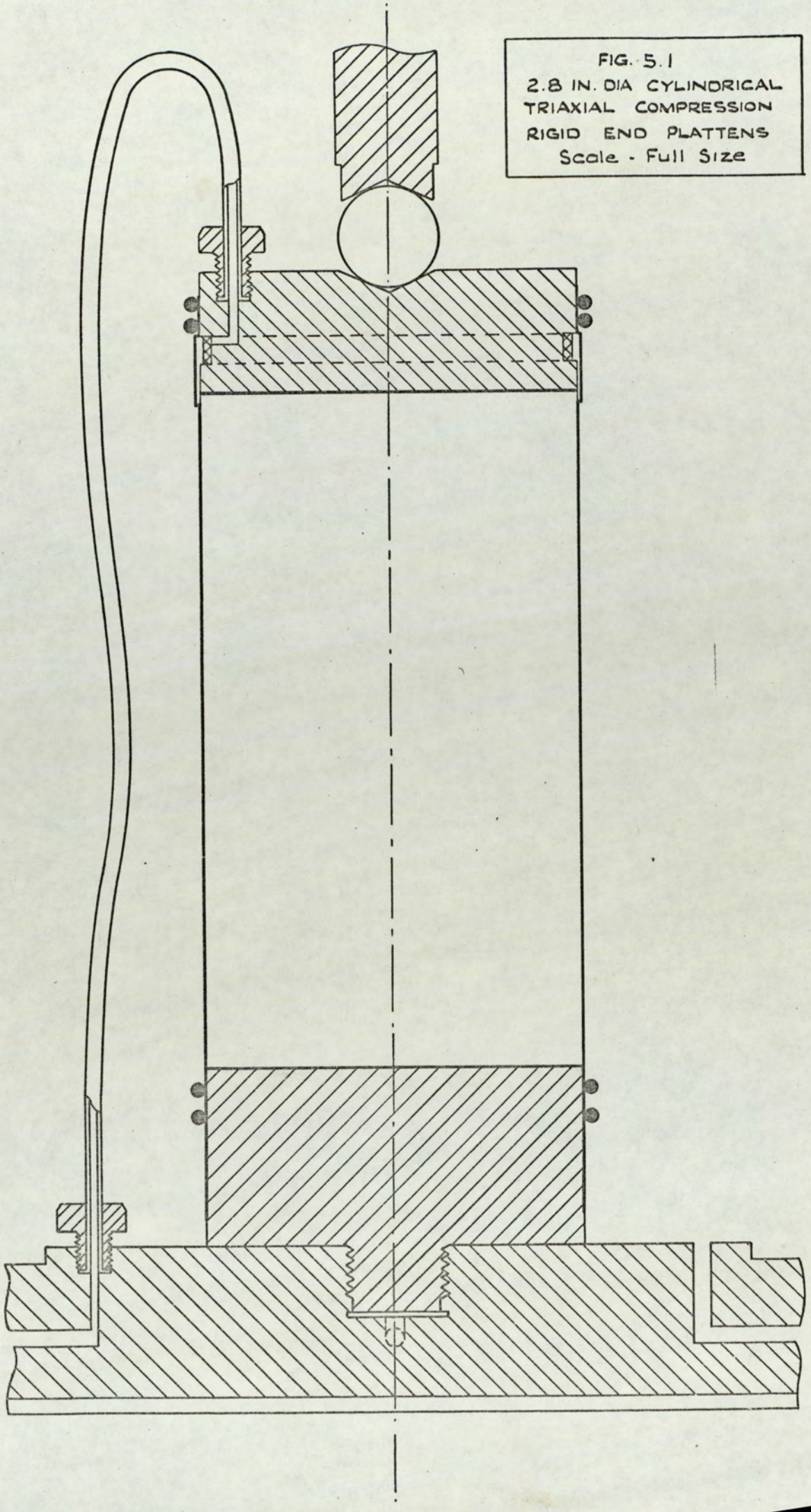

FIG. 5.1
2.8 IN. DIA CYLINDRICAL
TRIAXIAL COMPRESSION
RIGID END PLATTENS
Scale - Full Size

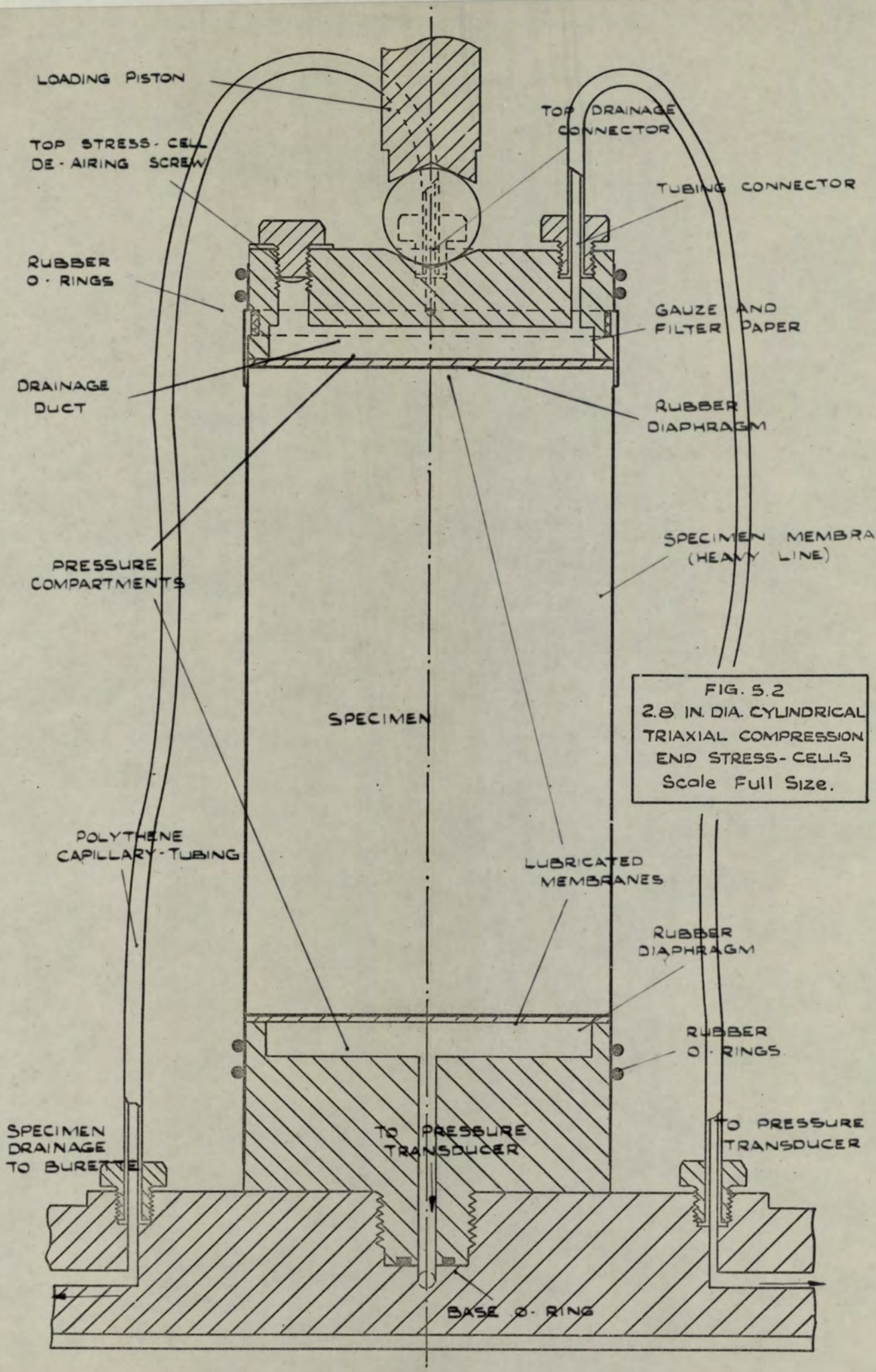

FIG. 5.2
2.8 IN. DIA. CYLINDRICAL TRIAXIAL COMPRESSION END STRESS-CELLS
Scale Full Size.

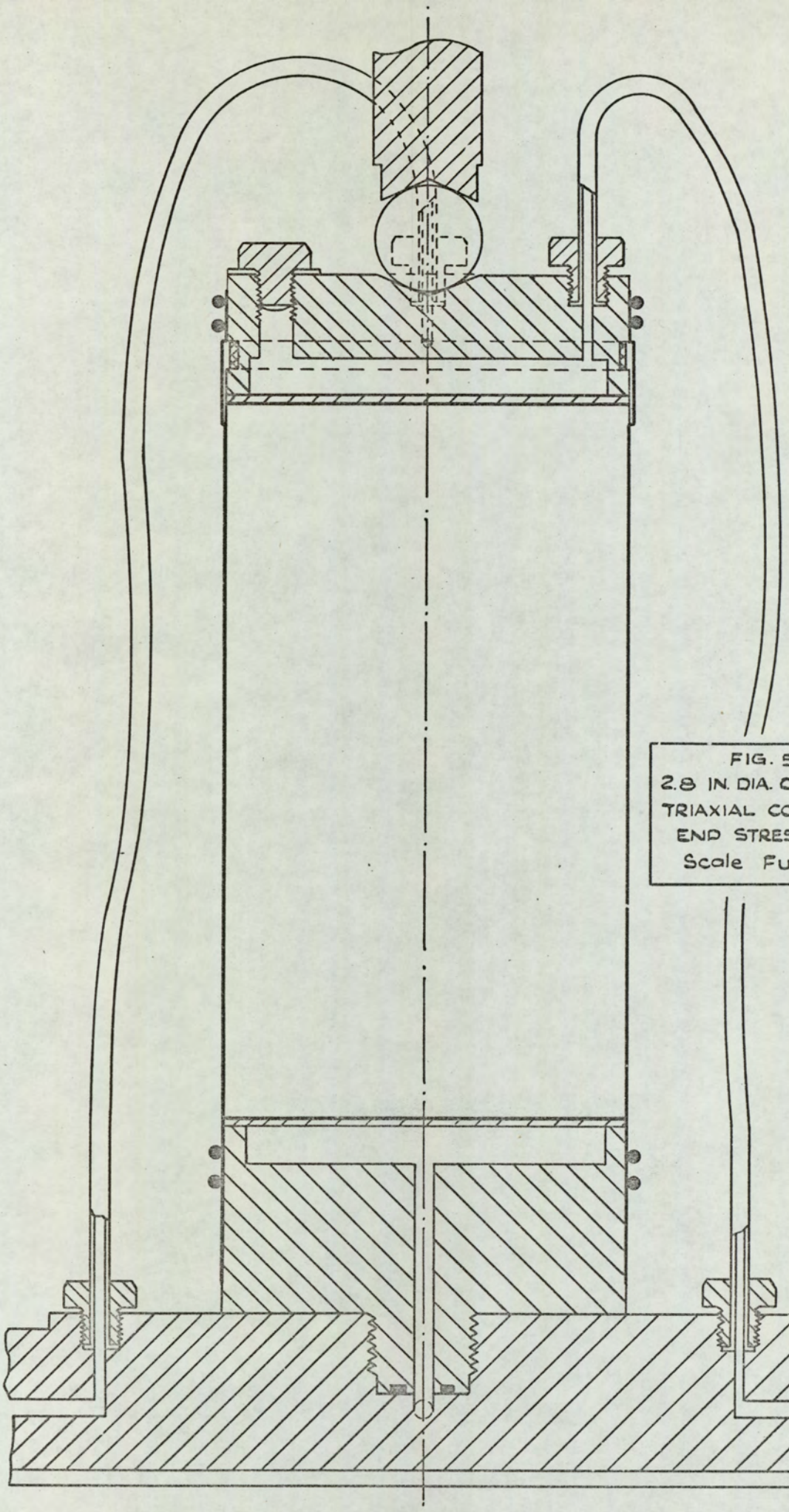

FIG. 5.2
2.8 IN. DIA. CYLINDRICAL
TRIAXIAL COMPRESSION
END STRESS-CELLS
Scale Full Size.

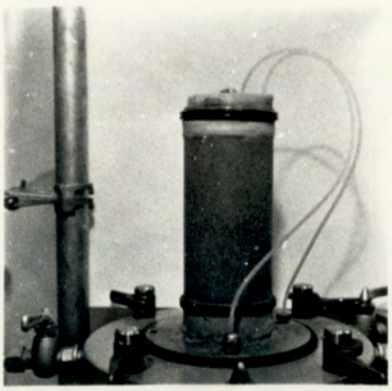

FIG.5.3(a)
PREPARED SPECIMEN
CYLINDRICAL TRIAXIAL COMPRESSION

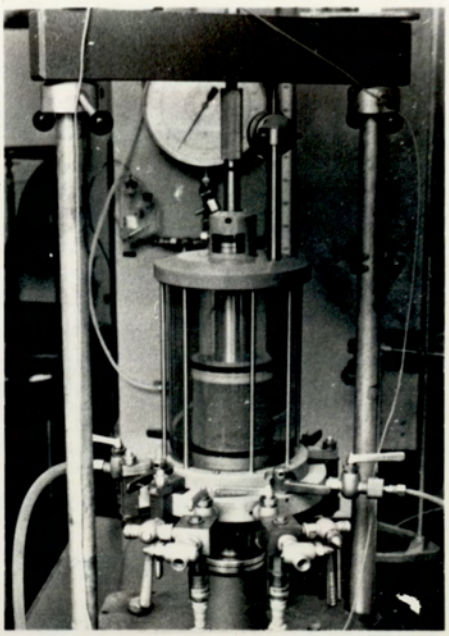

FIG.5.3(b)
CYLINDRICAL TRIAXIAL EXTENSION
LAYOUT OF APPARATUS

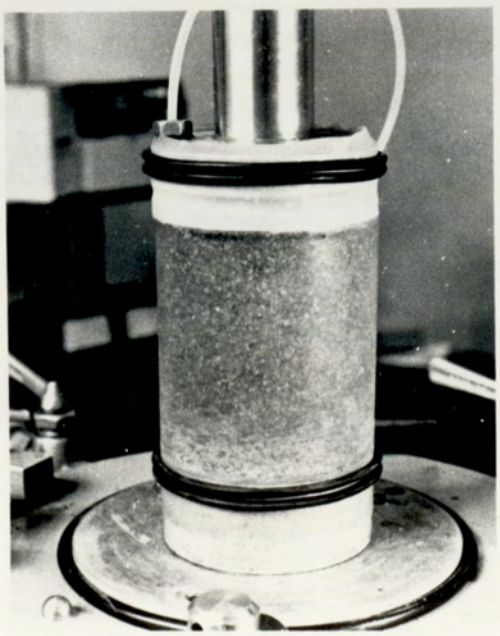

FIG.5.3(c)
PREPARED SPECIMEN
CYLINDRICAL TRIAXIAL EXTENSION
RIGID TOP PLATTEN
BOTTOM STRESS-CELL

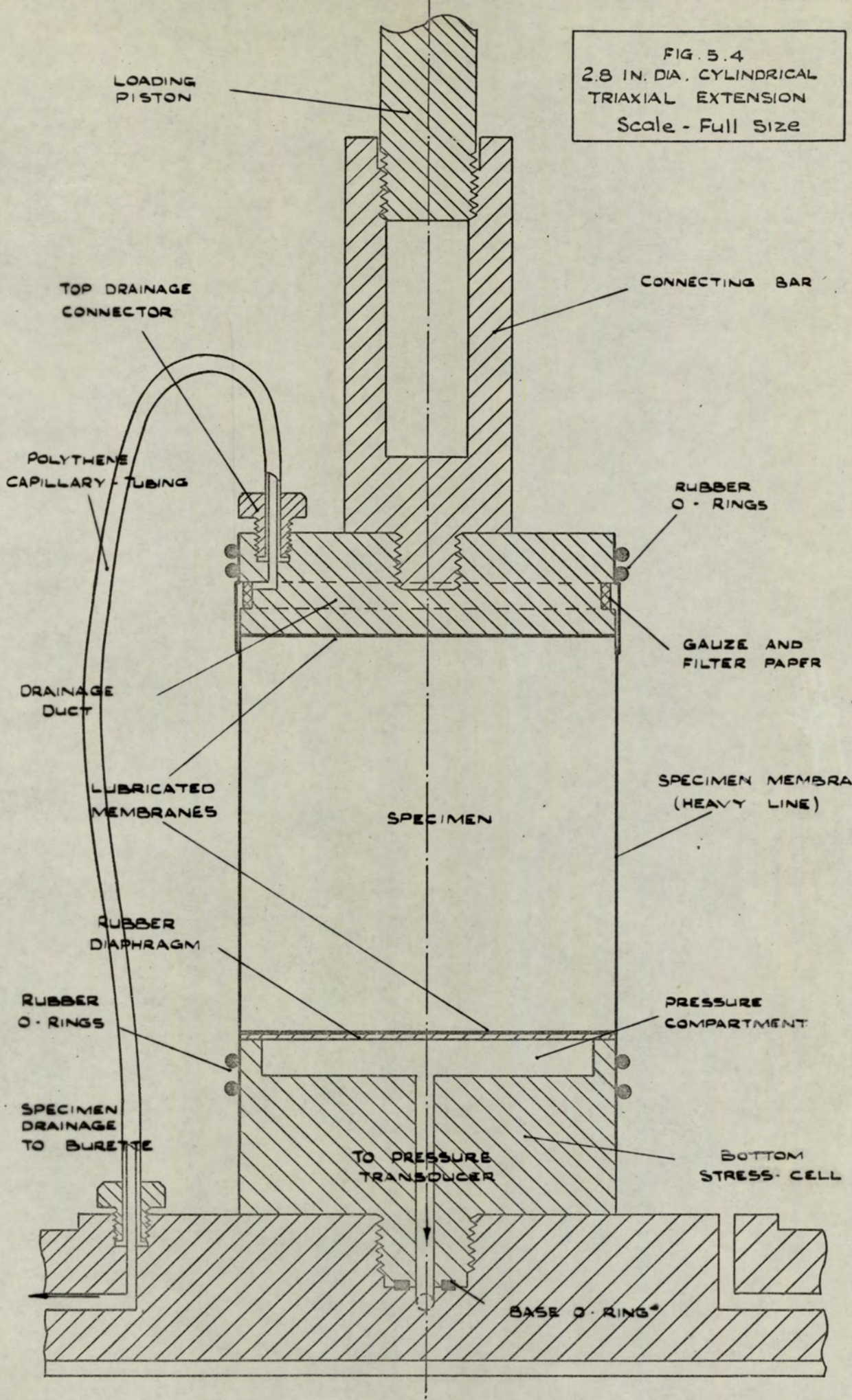
FIG. 5.4
2.8 IN. DIA. CYLINDRICAL
TRIAXIAL EXTENSION
Scale - Full Size
LOADING PISTON
TOP DRAINAGE CONNECTOR
CONNECTING BAR
POLYTHENE CAPILLARY - TUBING
RUBBER O - RINGS
GAUZE AND FILTER PAPER
DRAINAGE DUCT
LUBRICATED MEMBRANES
SPECIMEN
SPECIMEN MEMBRANE (HEAVY LINE)
RUBBER DIAPHRAGM
RUBBER O - RINGS
PRESSURE COMPARTMENT
SPECIMEN DRAINAGE TO BURETTE
TO PRESSURE TRANSDUCER
BOTTOM STRESS - CELL
BASE O - RING

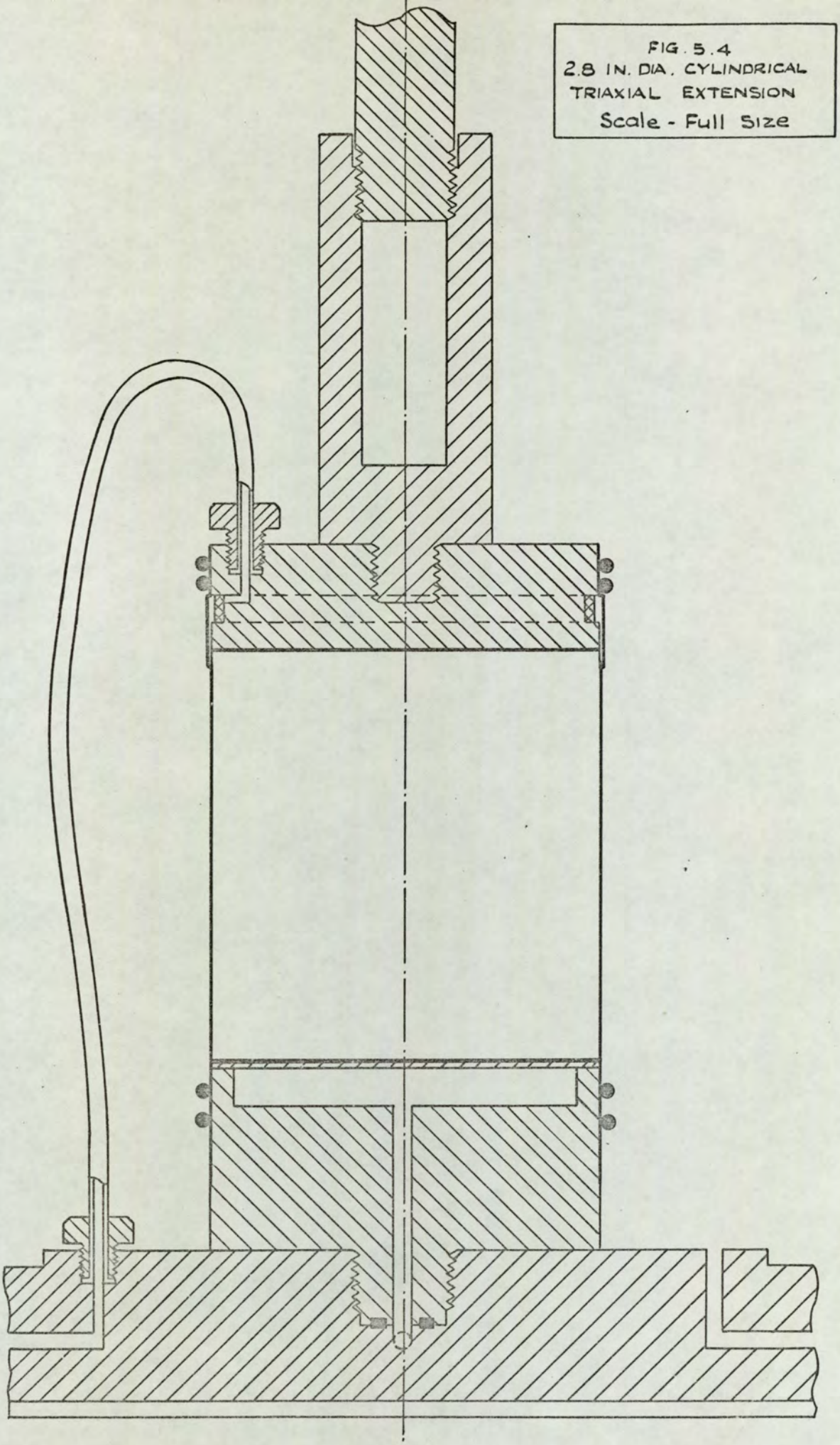

FIG. 5.4
2.8 IN. DIA. CYLINDRICAL
TRIAXIAL EXTENSION
Scale - Full Size

CHAPTER SIX

FIGURES

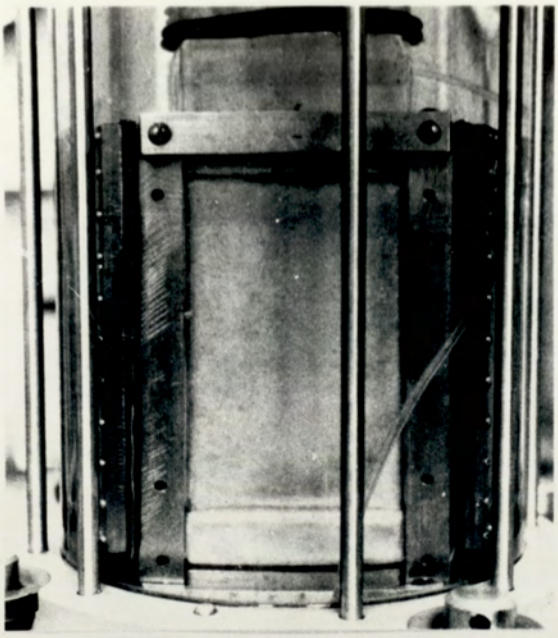

FIG.6.1(a)
ATA PLANE STRAIN TEST
PS 11, e_i = 0.610, ε_3 = 0.0

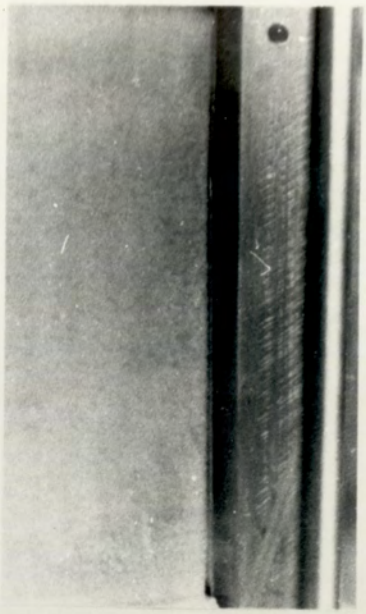

FIG.6.1(b)
ATA PLANE STRAIN TEST
PS 11, K_o STAGE, ε_3 = 1.06 %

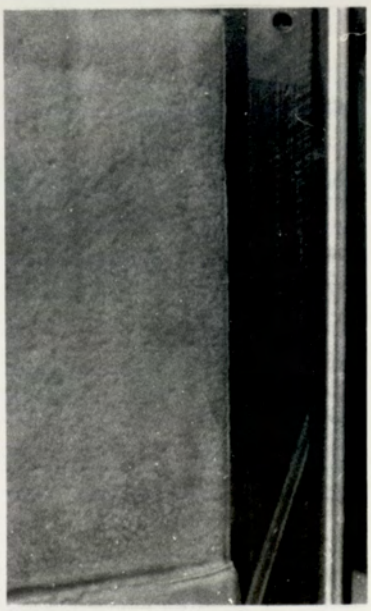

FIG.6.1(c)
ATA PLANE STRAIN TEST
PS 11, DECREASING σ_r, ε_3 = 3.37 %

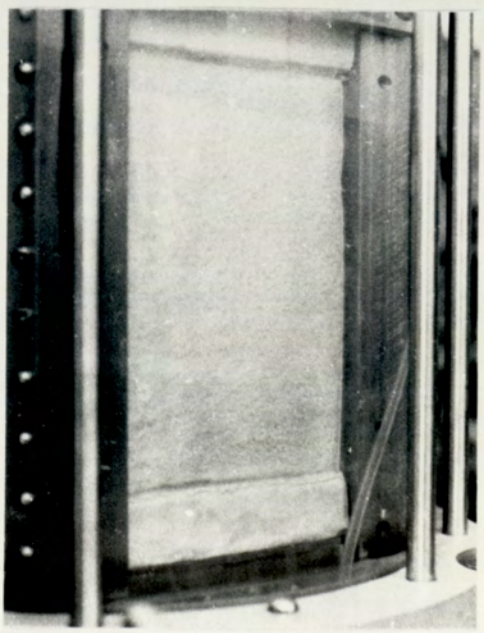

FIG.6.1(d)
ATA PLANE STRAIN TEST
PS 11, DECREASING σ_r, ε_3 = 4.86 %

FIG.6.2(a)
ATA PLANE STRAIN TEST
PS 25, e_i = 0.621
DECREASING σ_r, ε_3 = 5.51 %

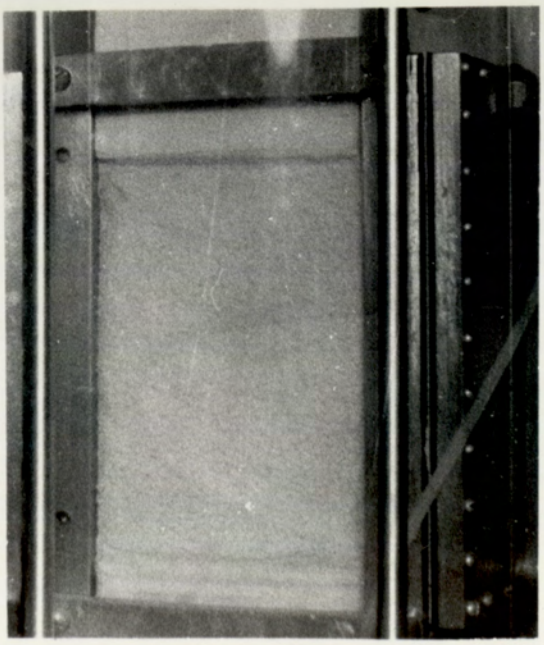

FIG.6.2(b)
ATA PLANE STRAIN TEST
PS 17, e_i = 0.549
INCREASING σ_r, ε_3 = 5.27 %

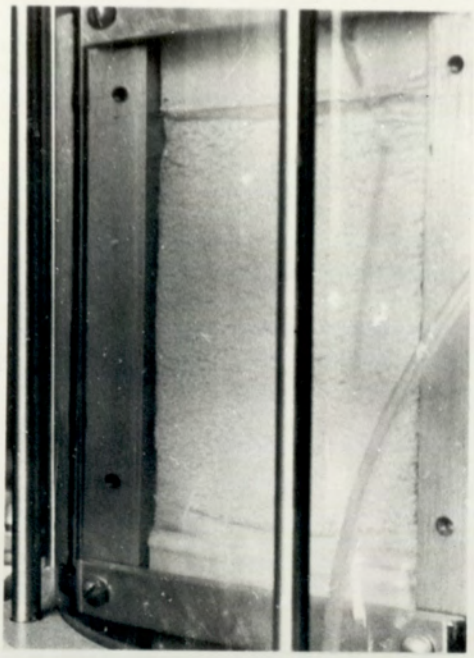

FIG.6.3(a)
ATA PLANE STRAIN TEST
POST-FAILURE CONDITION
PS 15, INCREASING σ_x, ε_3 = 8.37 %

FIG.6.3(b)
PS 15 POST-FAILURE CONDITION
SPECIMEN DISCONTINUITY
AND MEMBRANE PENETRATION EFFECT

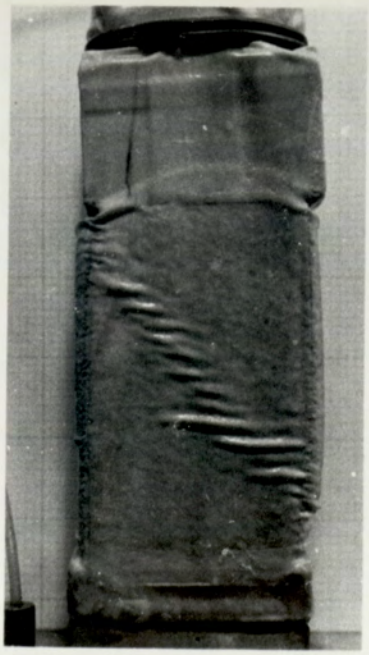

FIG.6.3(c)
PS 15, σ_y FACE
AFTER REMOVAL OF
SIDE STRESS-CELLS

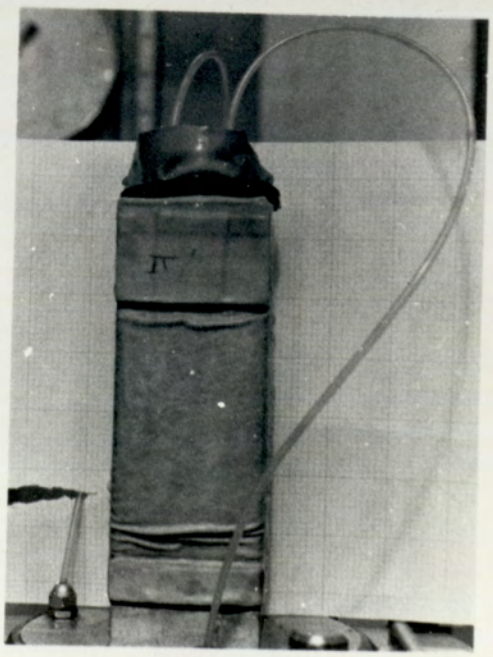

FIG.6.3(d)
PS 15, σ_x FACE
AFTER REMOVAL OF
SIDE STRESS-CELLS

FIG.6.4(a)
ATA INTERMEDIATE-STRESS TEST
TEST STOPPED AT FAILURE
INT 2, e_i = 0.530, ε_3 = 7.86 %

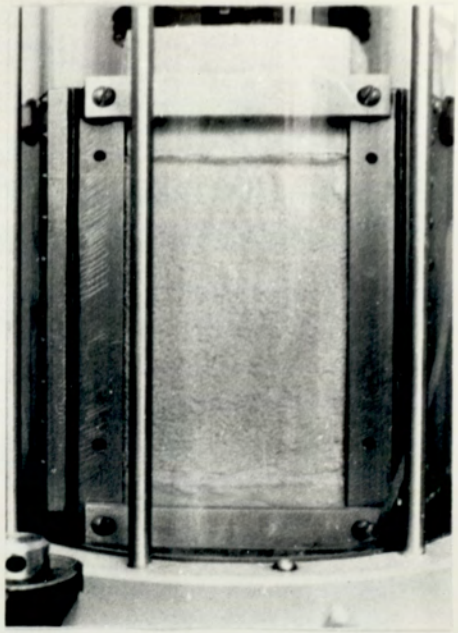

FIG.6.4(b)
INT 2, σ_x AND σ_y FACES
AFTER REMOVAL OF
SIDE STRESS-CELLS

FIG.6.4(c)
INT 2, σ_y FACE
AFTER REMOVAL OF
SIDE STRESS-CELLS

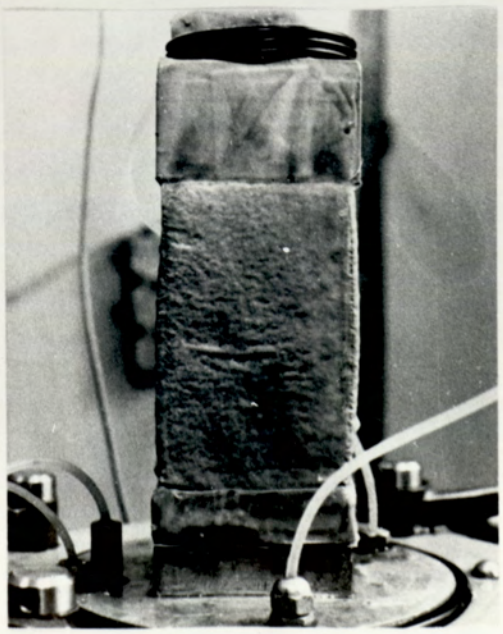

FIG.6.5(a)
ATA TRIAXIAL EXTENSION TEST
TEST STOPPED AT FAILURE
ATA TE 1
e_i = 0.548, ε_3 = -5.75 %

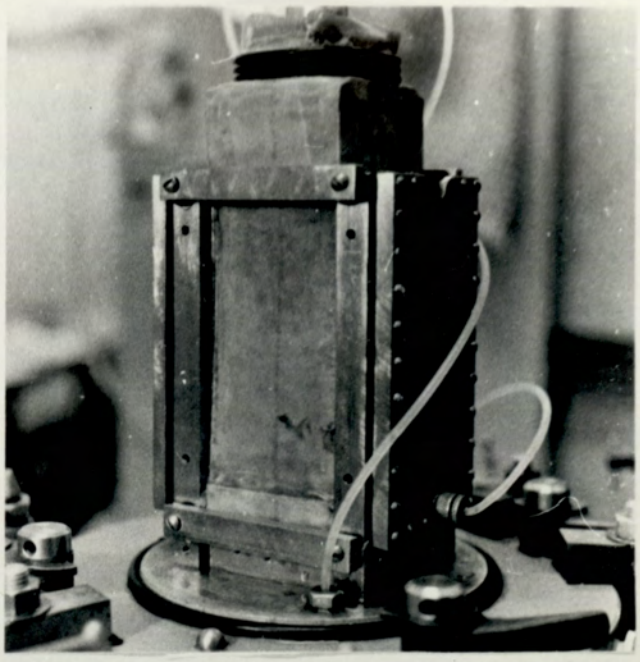

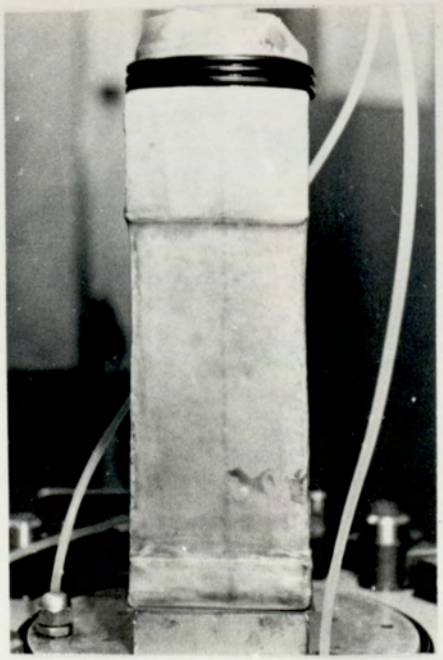

FIG.6.5(b)
ATA TE 1, σ_x FACE
AFTER REMOVAL OF
SIDE STRESS-CELLS

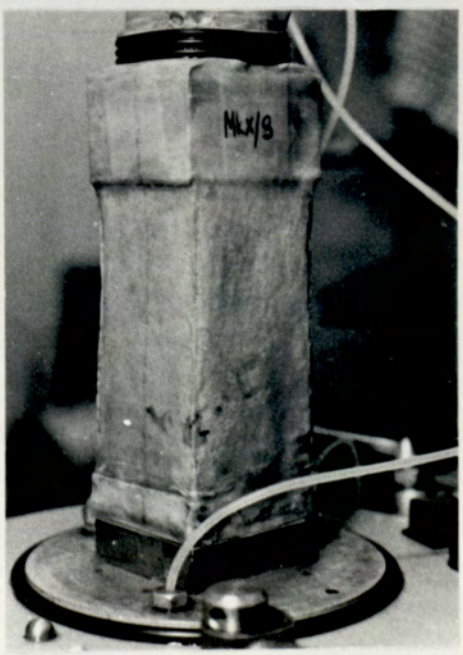

FIG.6.5(c)
ATA TE 1, σ_x AND σ_y FACES
AFTER REMOVAL OF
SIDE STRESS-CELLS

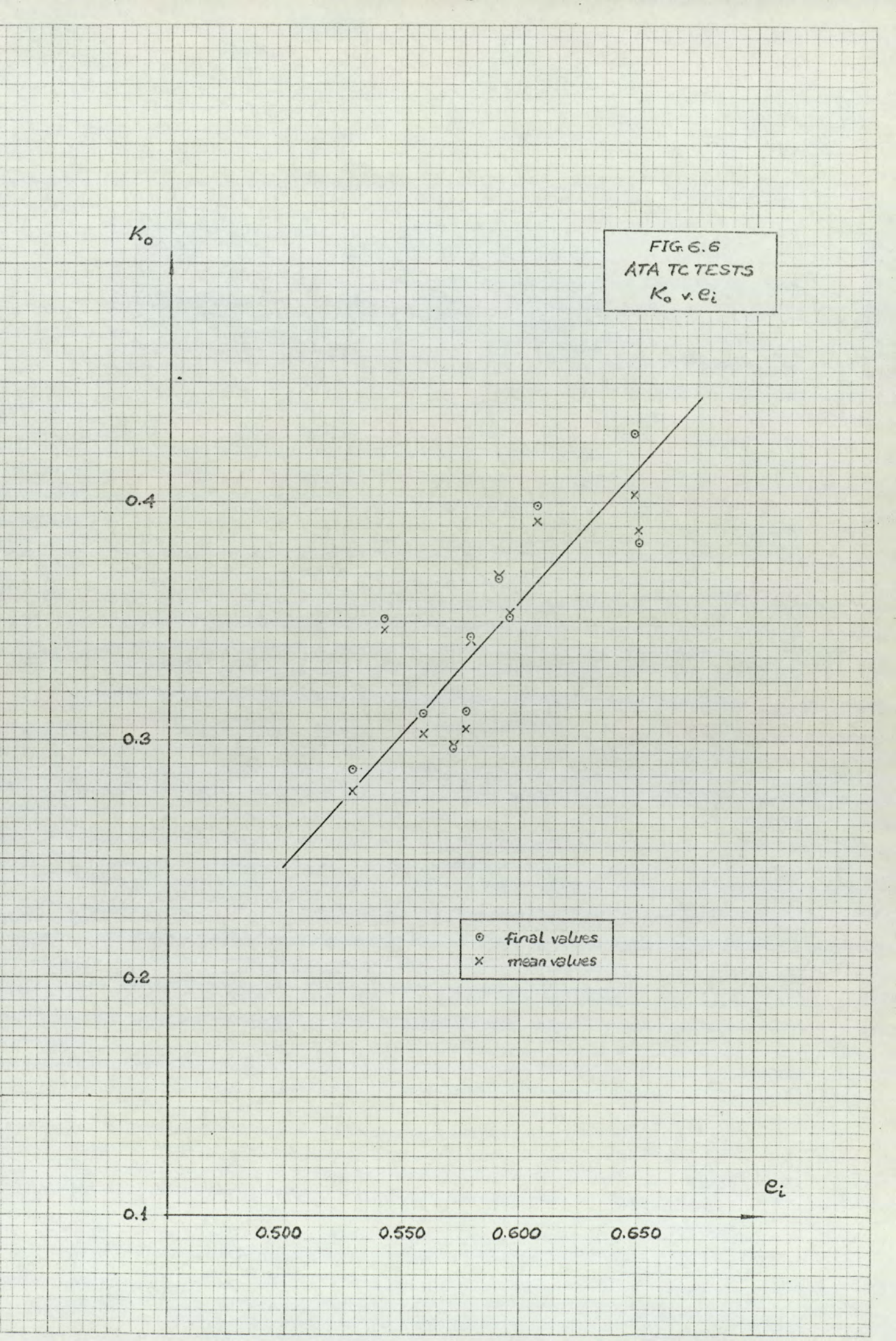
FIG. 6.6
ATA TC TESTS
K_o v. e_i
K_o
0.4
0.3
0.2
0.1
0.500
0.550
0.600
0.650
e_i
final values
mean values

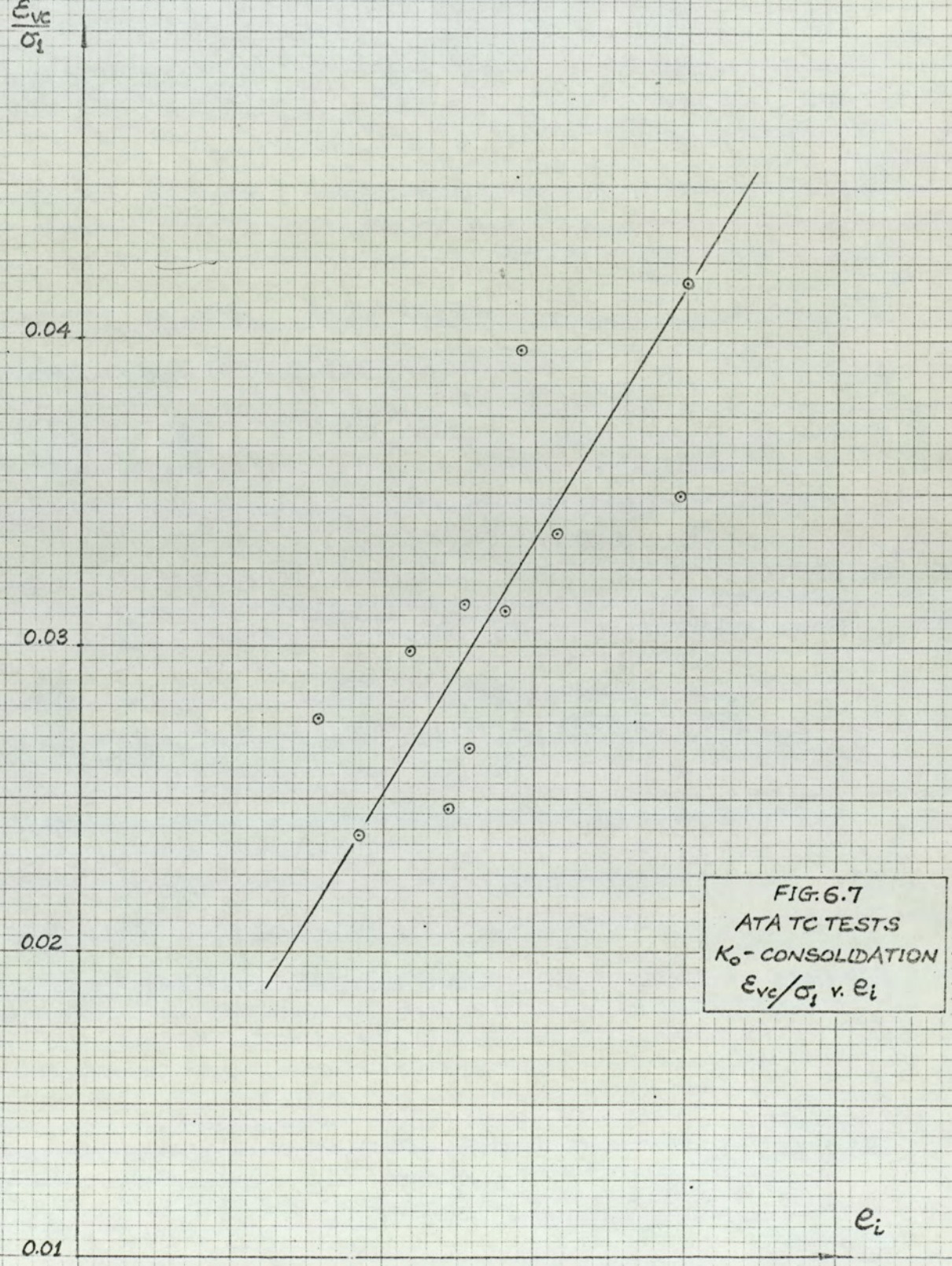

FIG. 6.7
ATA TC TESTS
K_o - CONSOLIDATION
$\varepsilon_{vc}/\sigma_1$ v. e_i

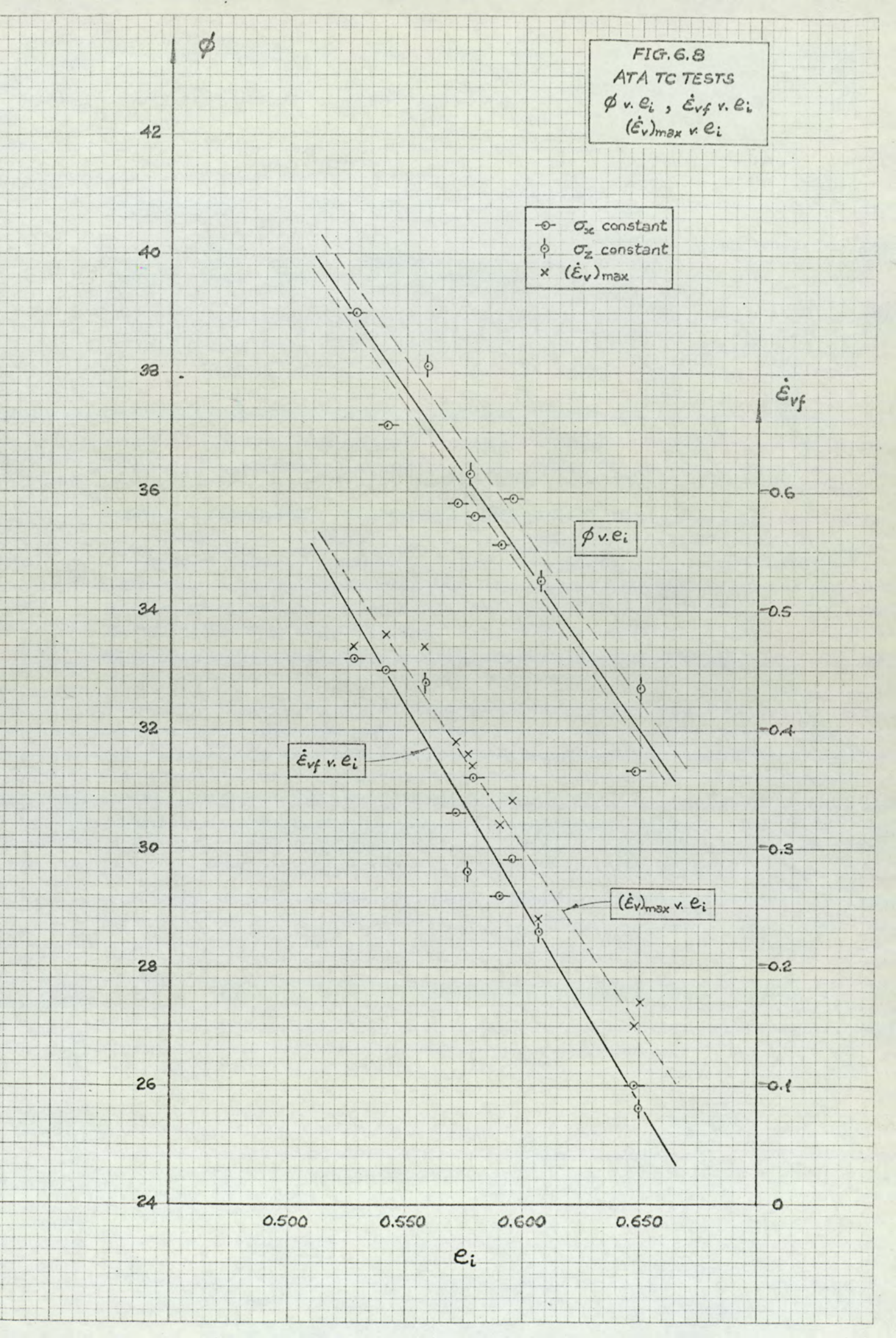
FIG. 6.8
ATA TC TESTS
ϕ v. e_i , $\dot{\varepsilon}_{vf}$ v. e_i
$(\dot{\varepsilon}_v)_{max}$ v. e_i
σ_{3c} constant
σ_z constant
$(\dot{\varepsilon}_v)_{max}$
ϕ v. e_i
$\dot{\varepsilon}_{vf}$ v. e_i
$(\dot{\varepsilon}_v)_{max}$ v. e_i
ϕ
$\dot{\varepsilon}_{vf}$
42
40
38
36
34
32
30
28
26
24
0.6
0.5
0.4
0.3
0.2
0.1
0
0.500
0.550
0.600
0.650
e_i

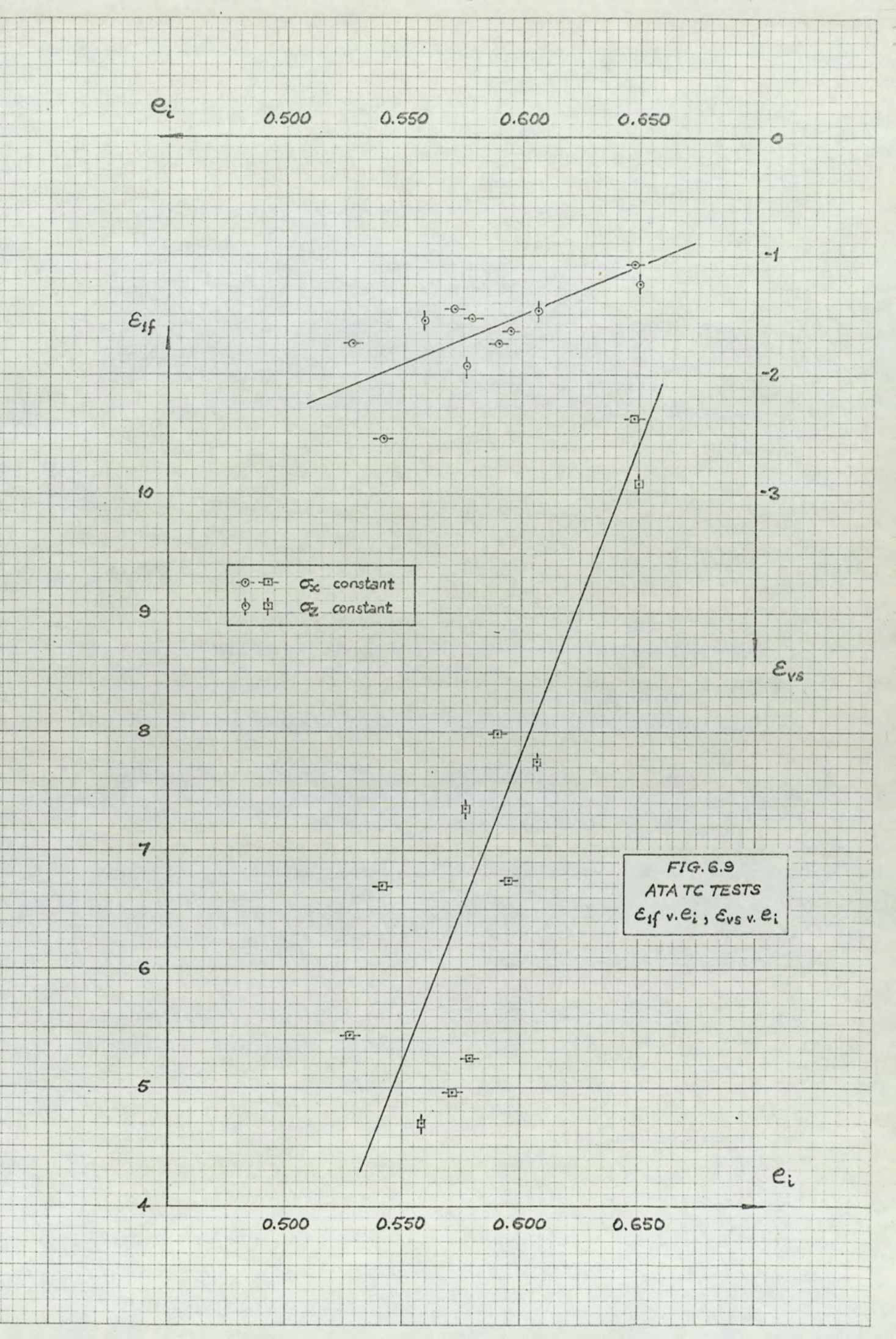

FIG. 6.9
ATA TC TESTS
ε_{1f} v. e_i , ε_{vs} v. e_i

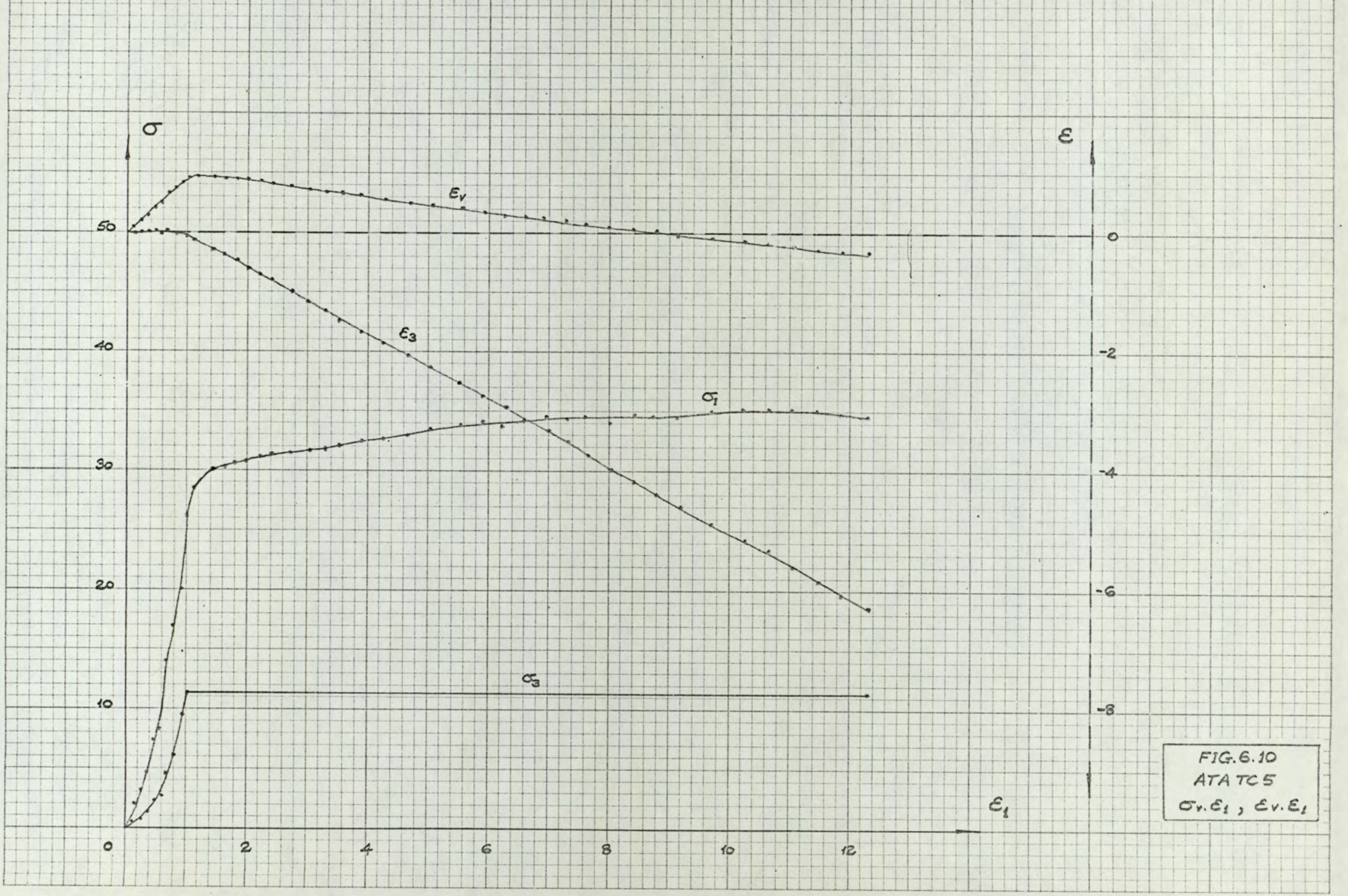

FIG. 6.10
ATA TC 5
$\sigma_v . \varepsilon_1$, $\varepsilon_v . \varepsilon_1$

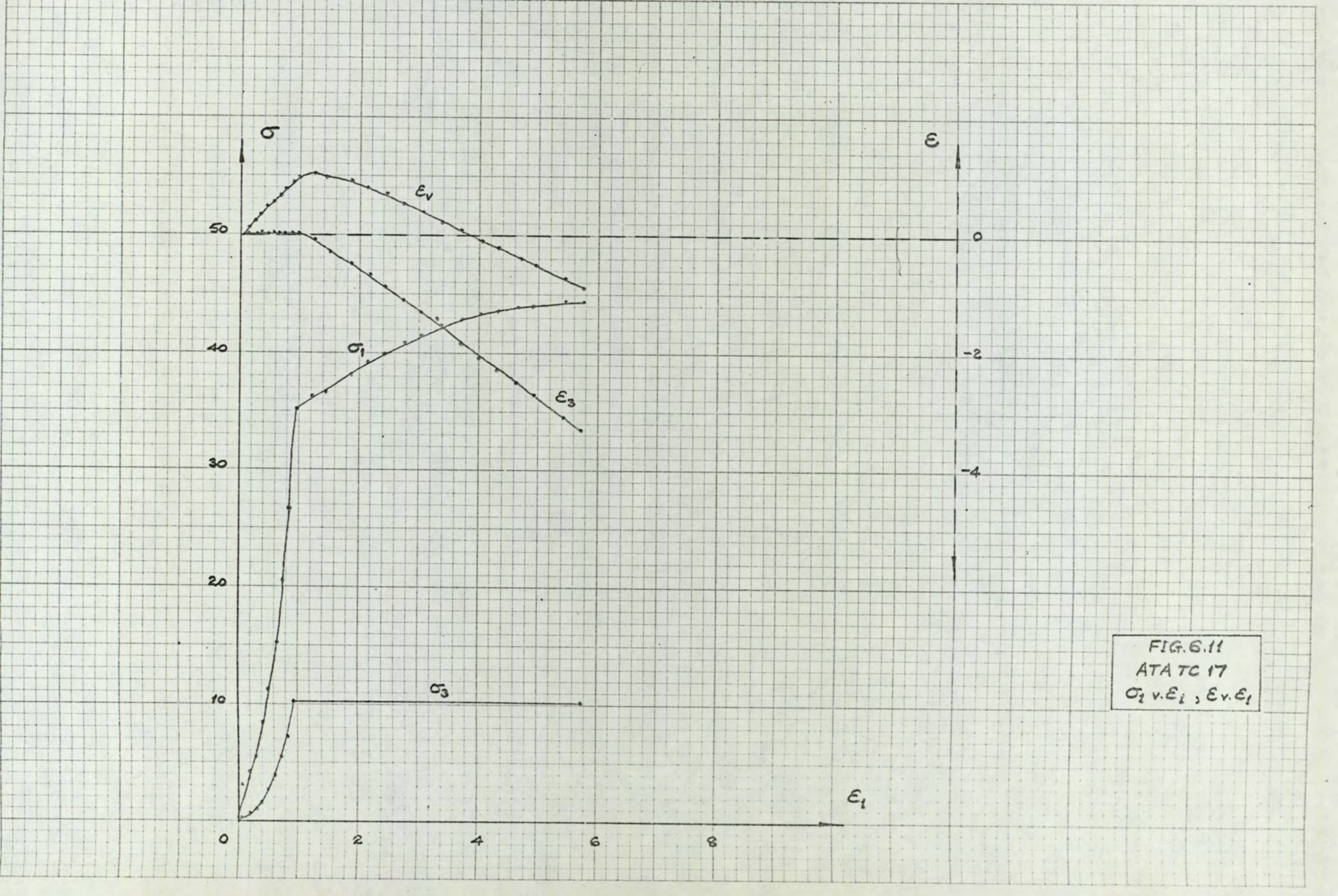

FIG. 6.11
ATA TC 17
σ_1 v. ε_1 , ε_v v. ε_1

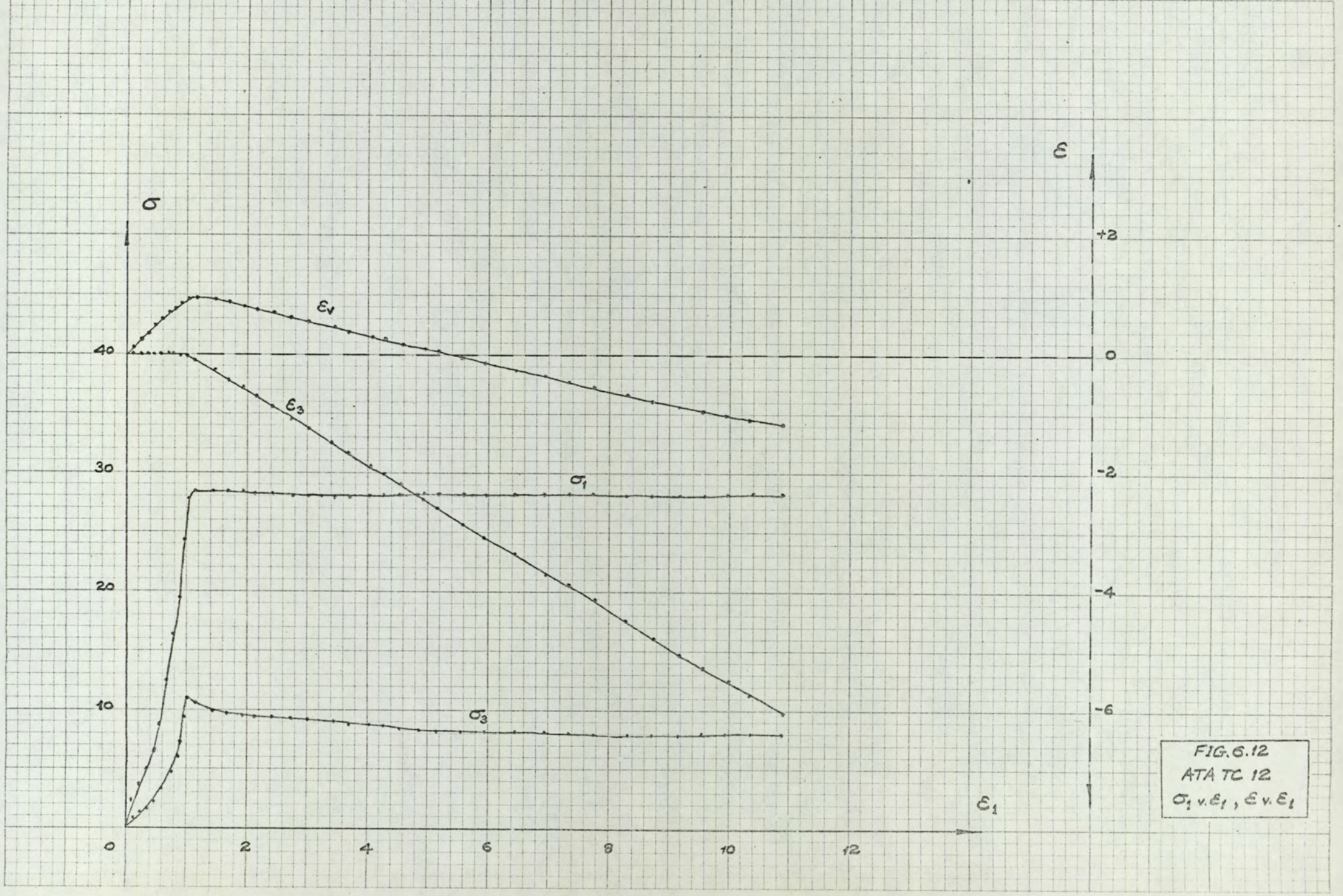

FIG. 6.12
ATA TC 12
σ_1 v. ε_1 , ε v. ε_1

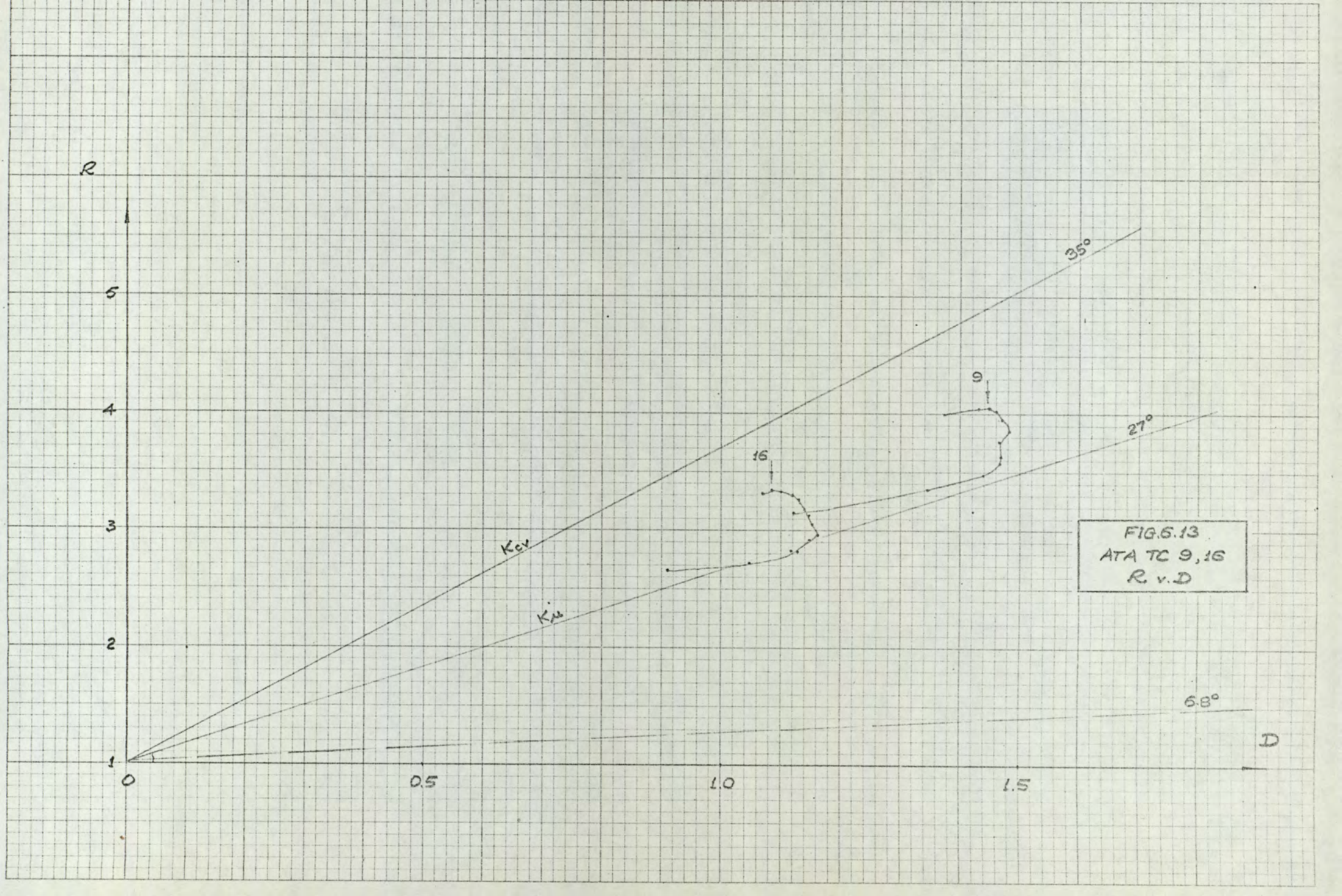

FIG.6.13
ATA TC 9, 16
R v. D

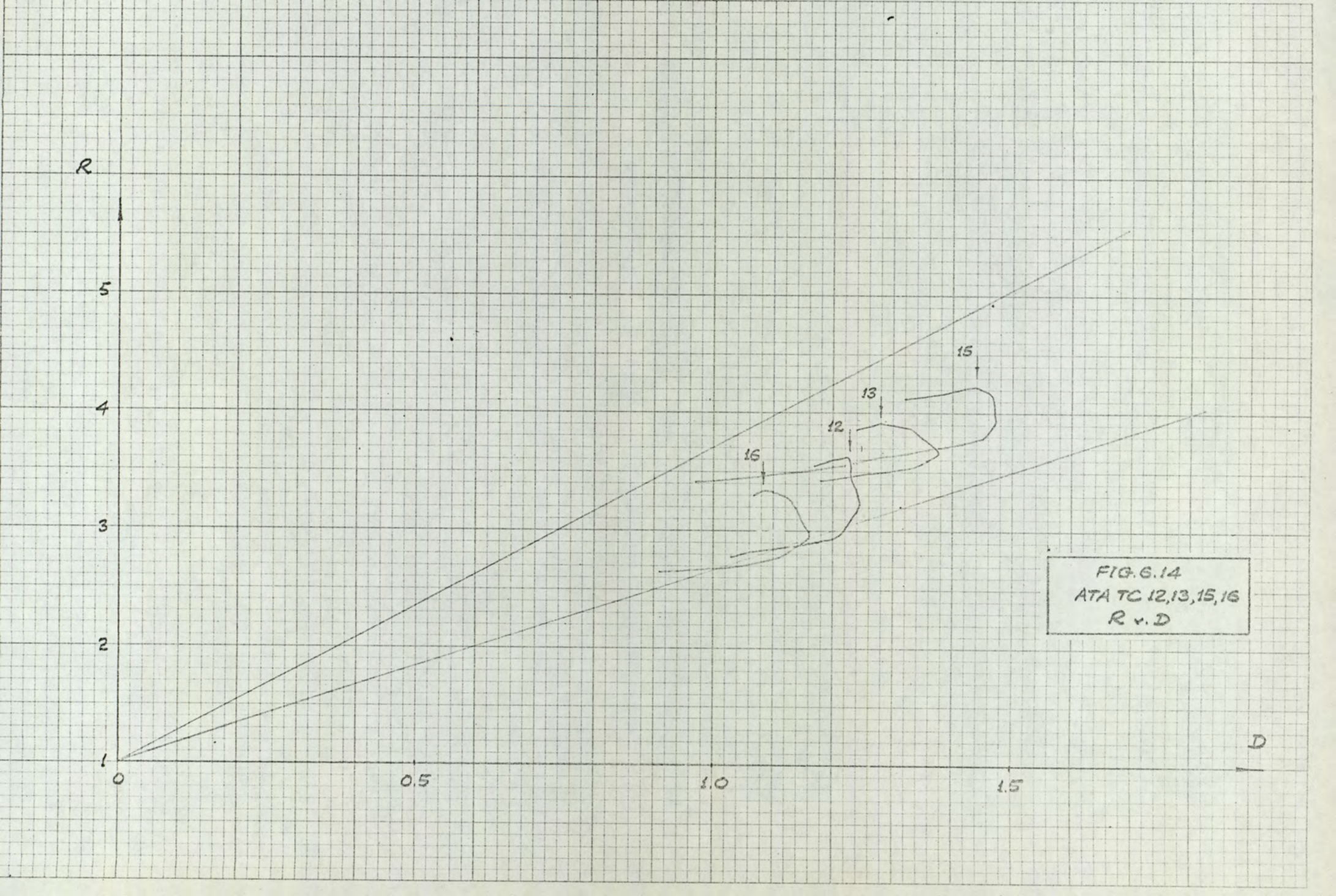

FIG. 6.14
ATA TC 12,13,15,16
R v. D

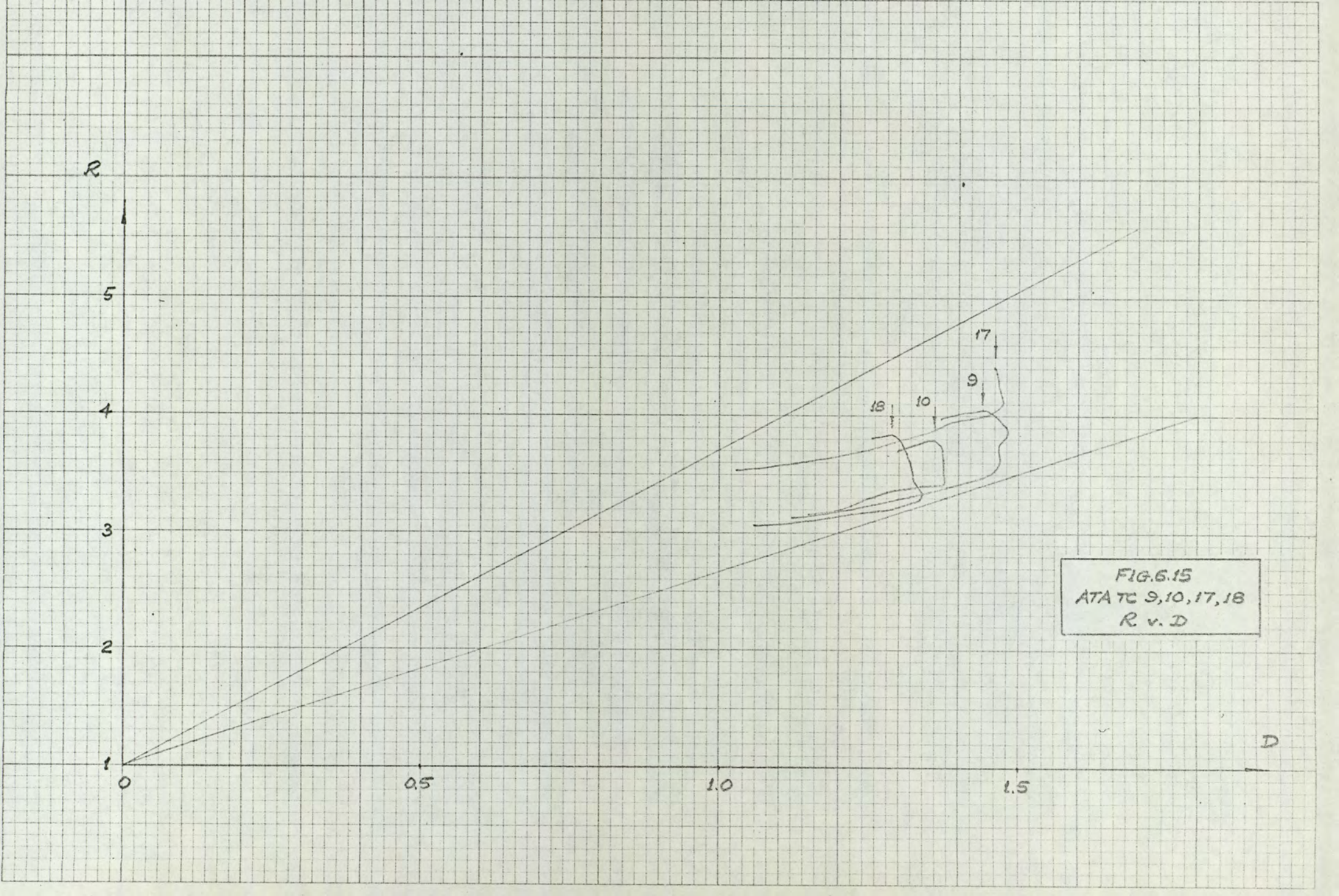

FIG. 6.15
ATA TC 9, 10, 17, 18
R v. D

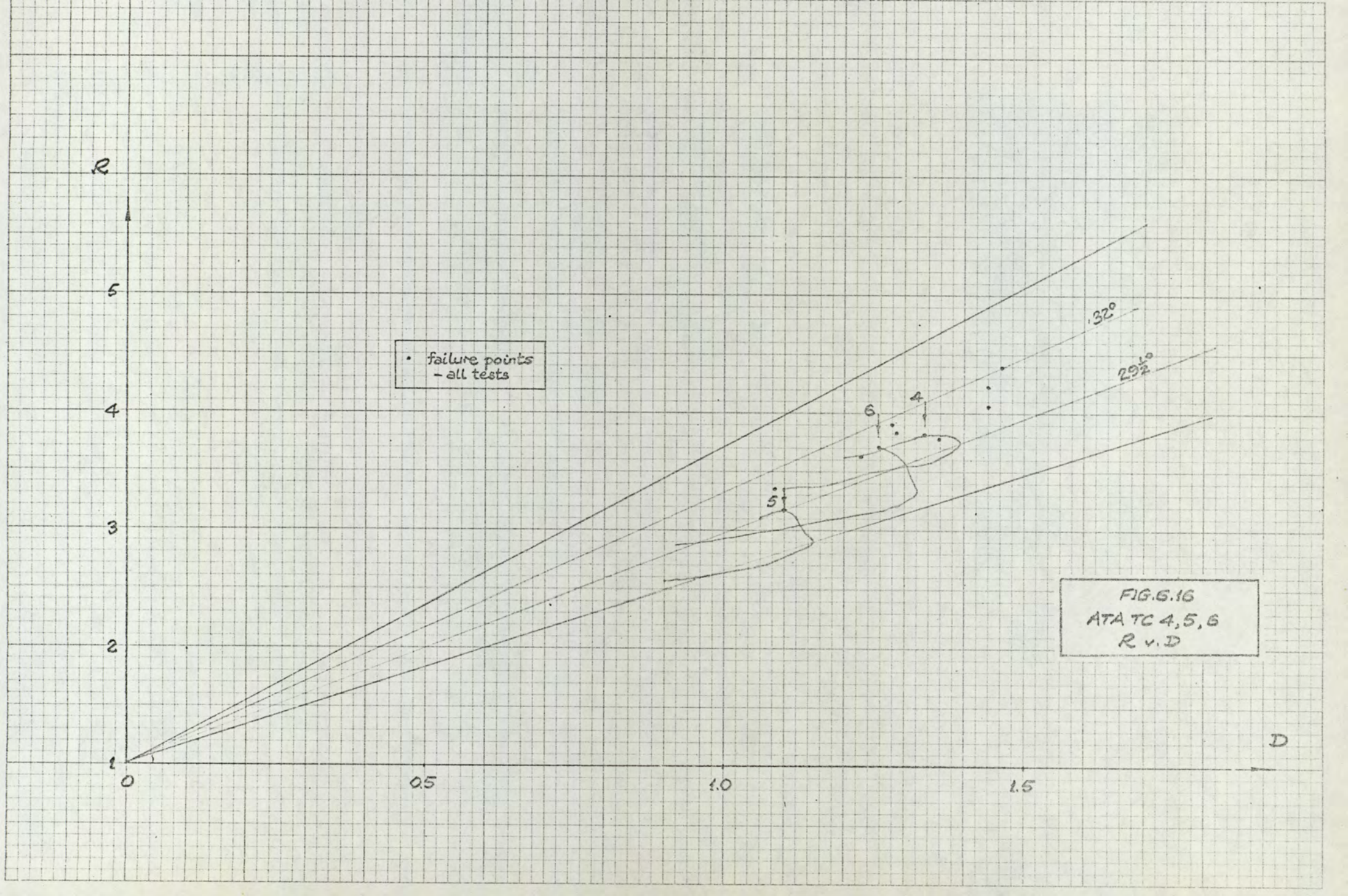

FIG.6.16
ATA TC 4,5,6
R v. D

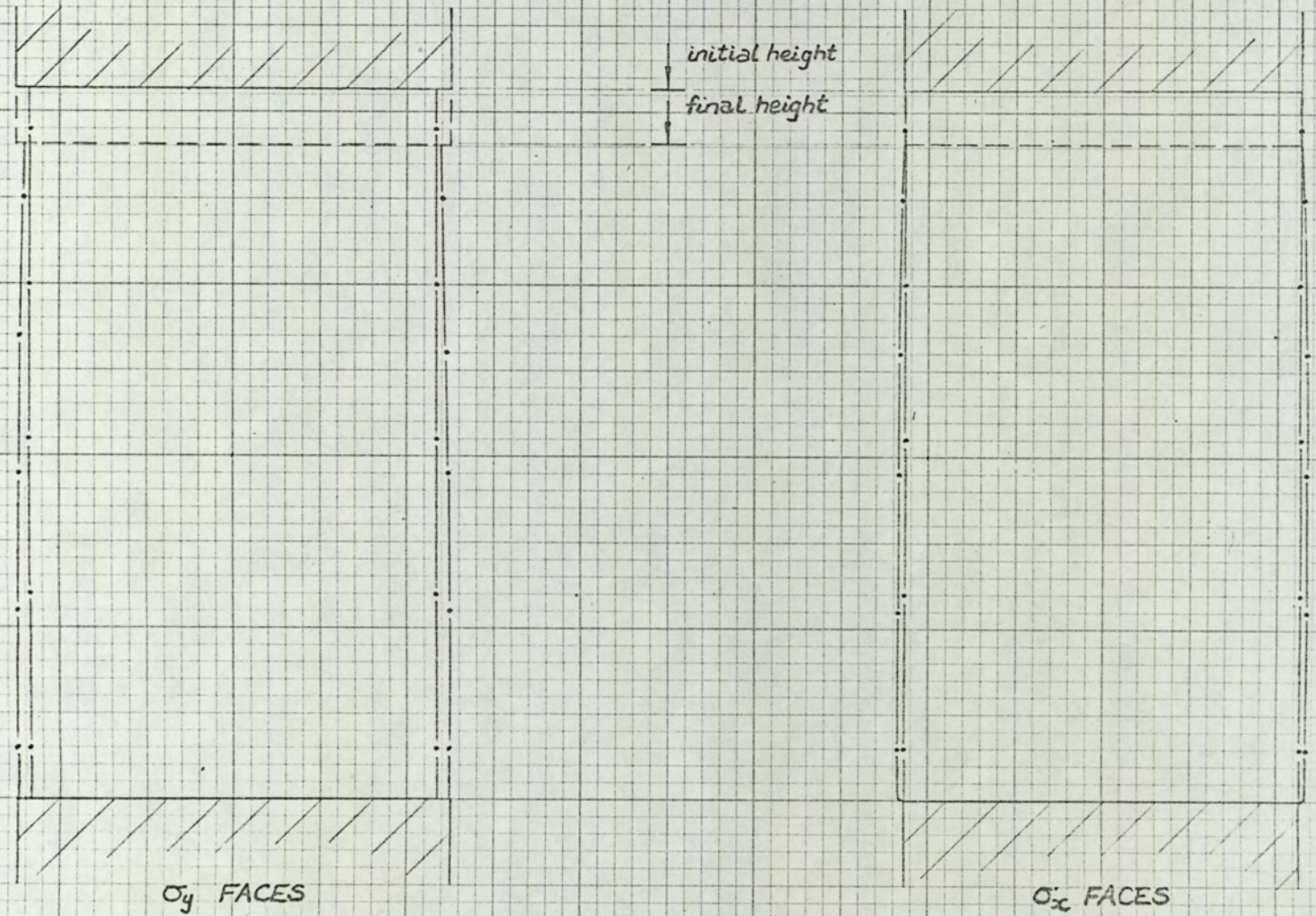

SCALE :-
full size

FIG. 6.17
ATA TC 6
MODE OF DEFORMATION

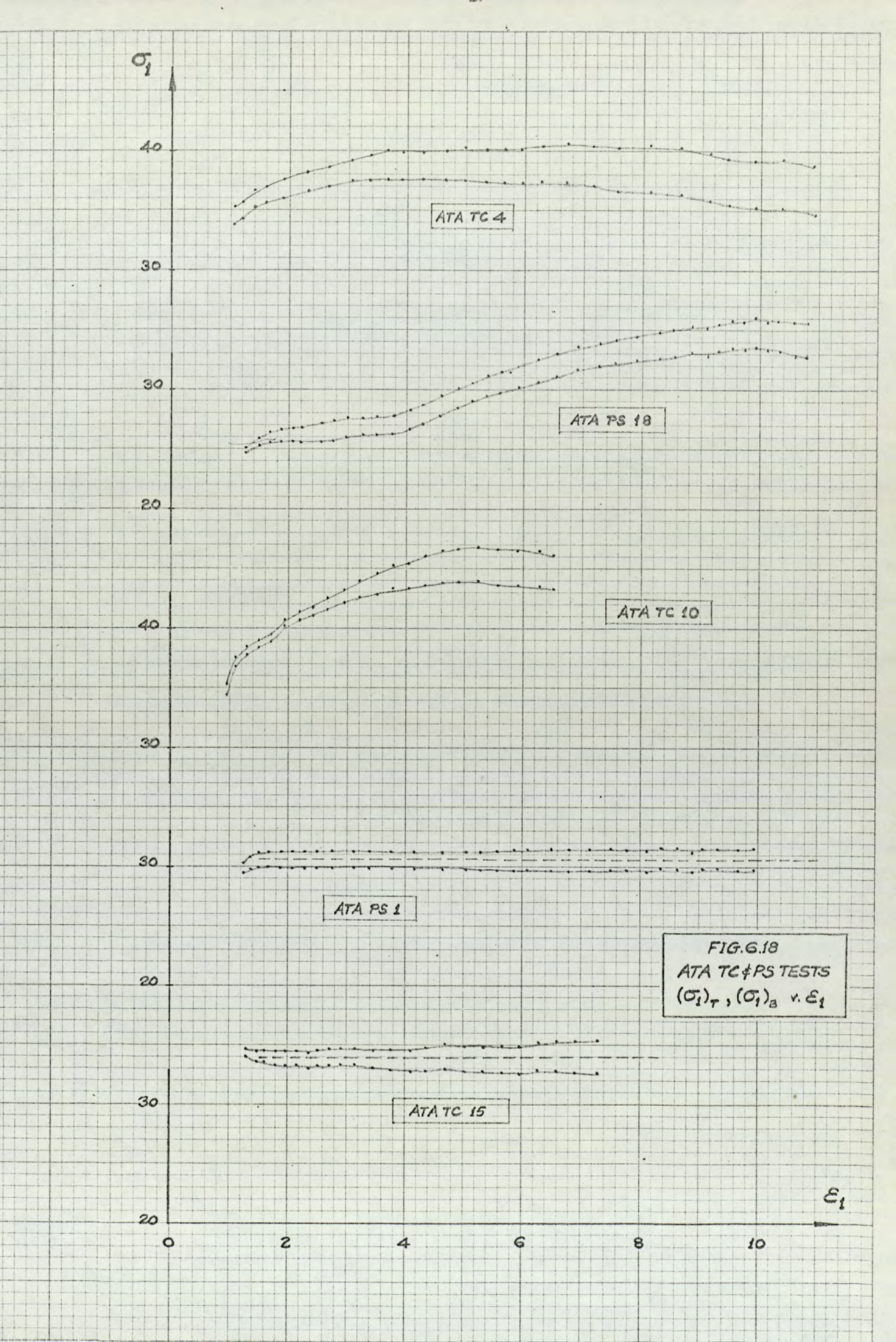

FIG. 6.18
ATA TC & PS TESTS
$(\sigma_1)_T$, $(\sigma_1)_B$ v. ε_1

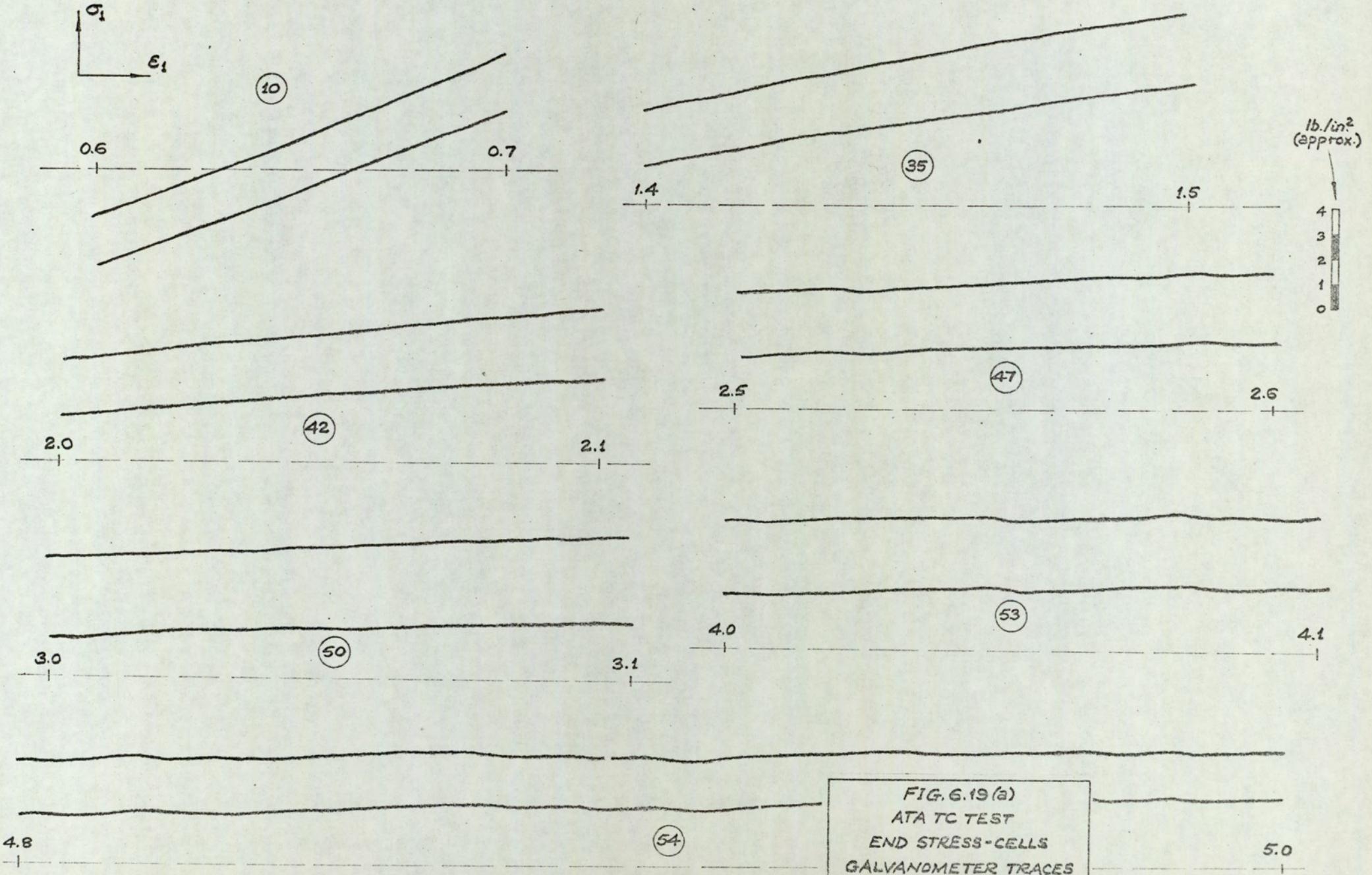

FIG. 6.19 (a)
ATA TC TEST
END STRESS-CELLS
GALVANOMETER TRACES

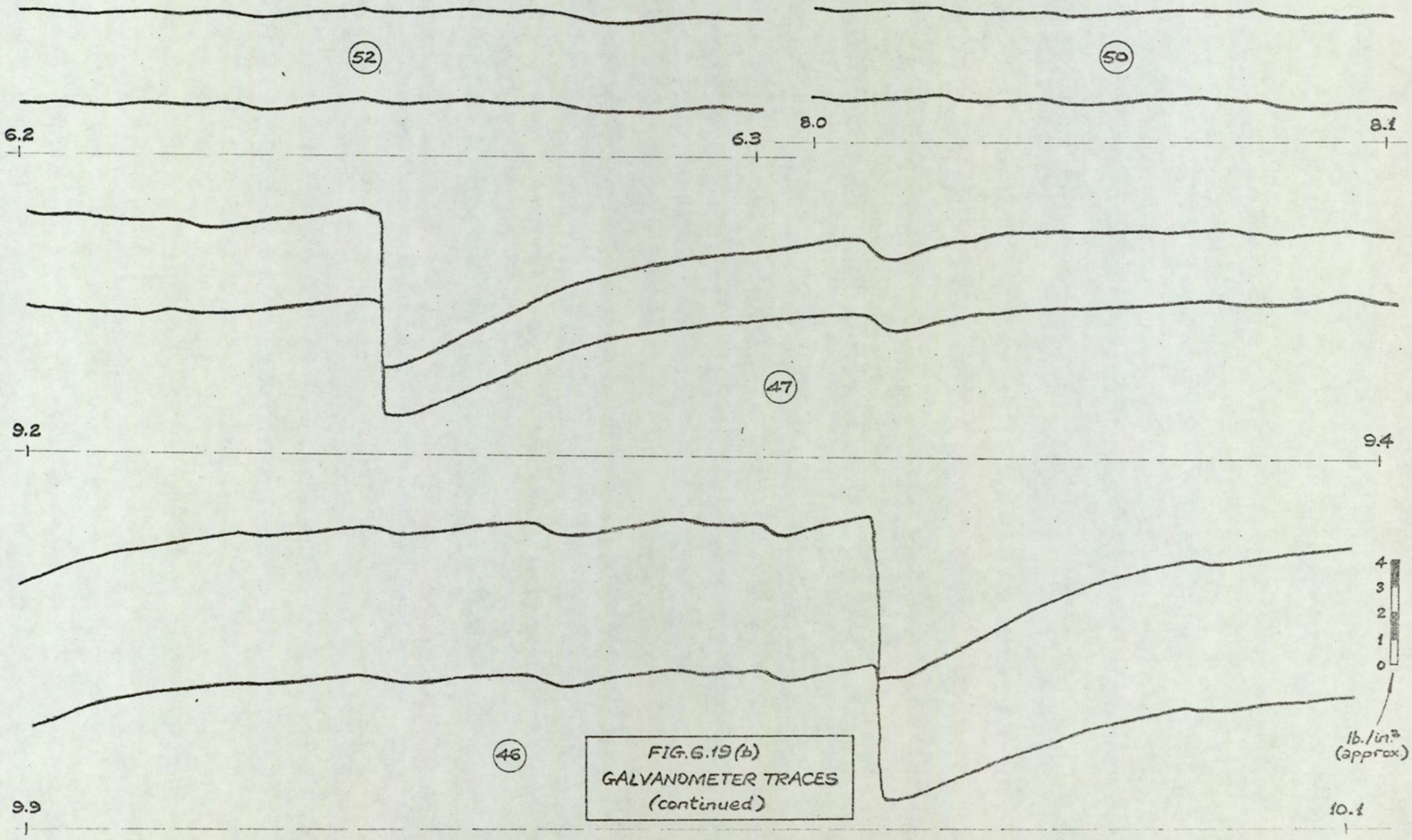

FIG. 6.19 (b)
GALVANOMETER TRACES
(continued)

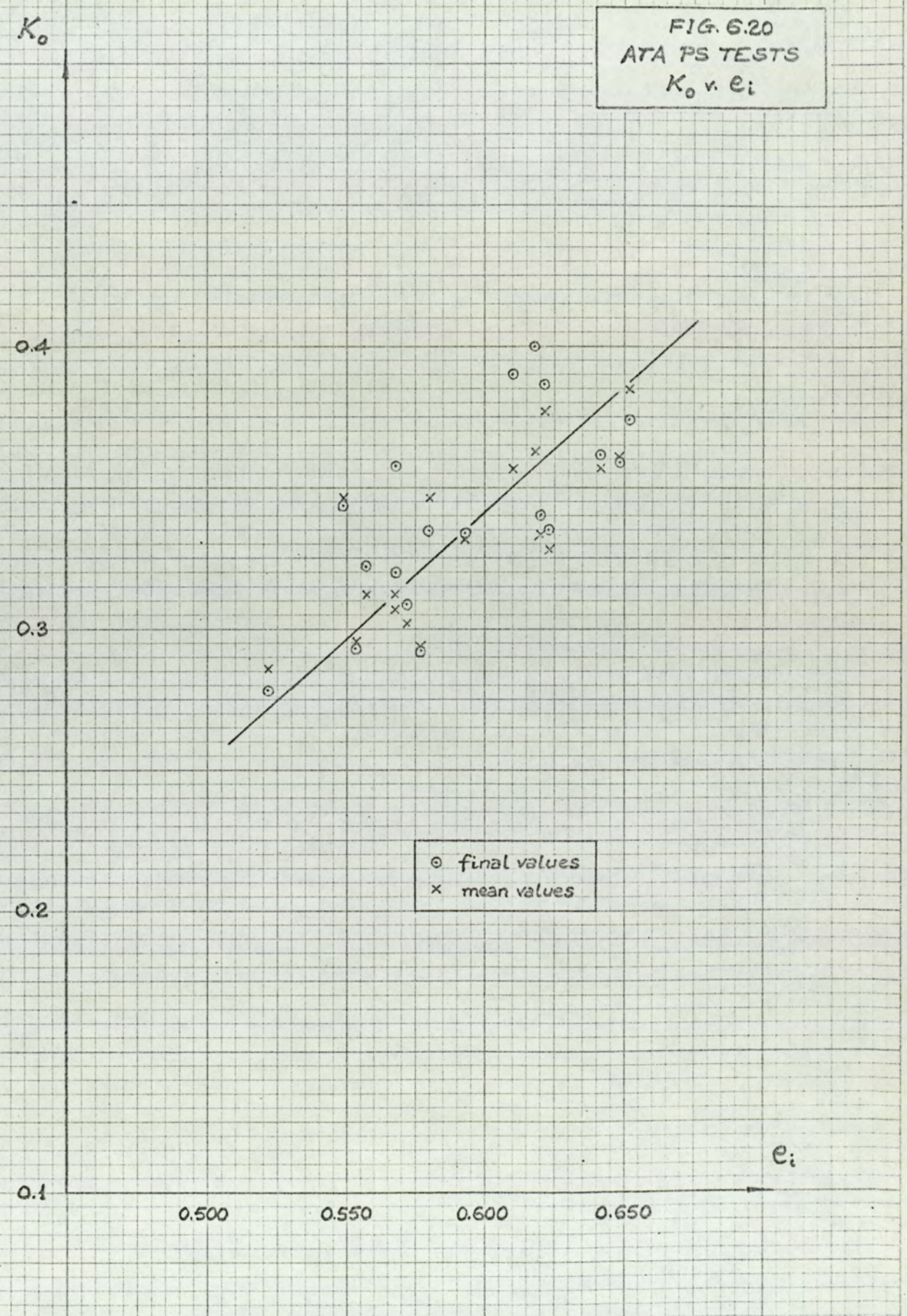
FIG. 6.20
ATA PS TESTS
K_o v. e_i
K_o
0.4
0.3
0.2
0.1
e_i
0.500
0.550
0.600
0.650
final values
mean values

FIG. 6.21
ATA TC & PS TESTS
K_o v. e_i

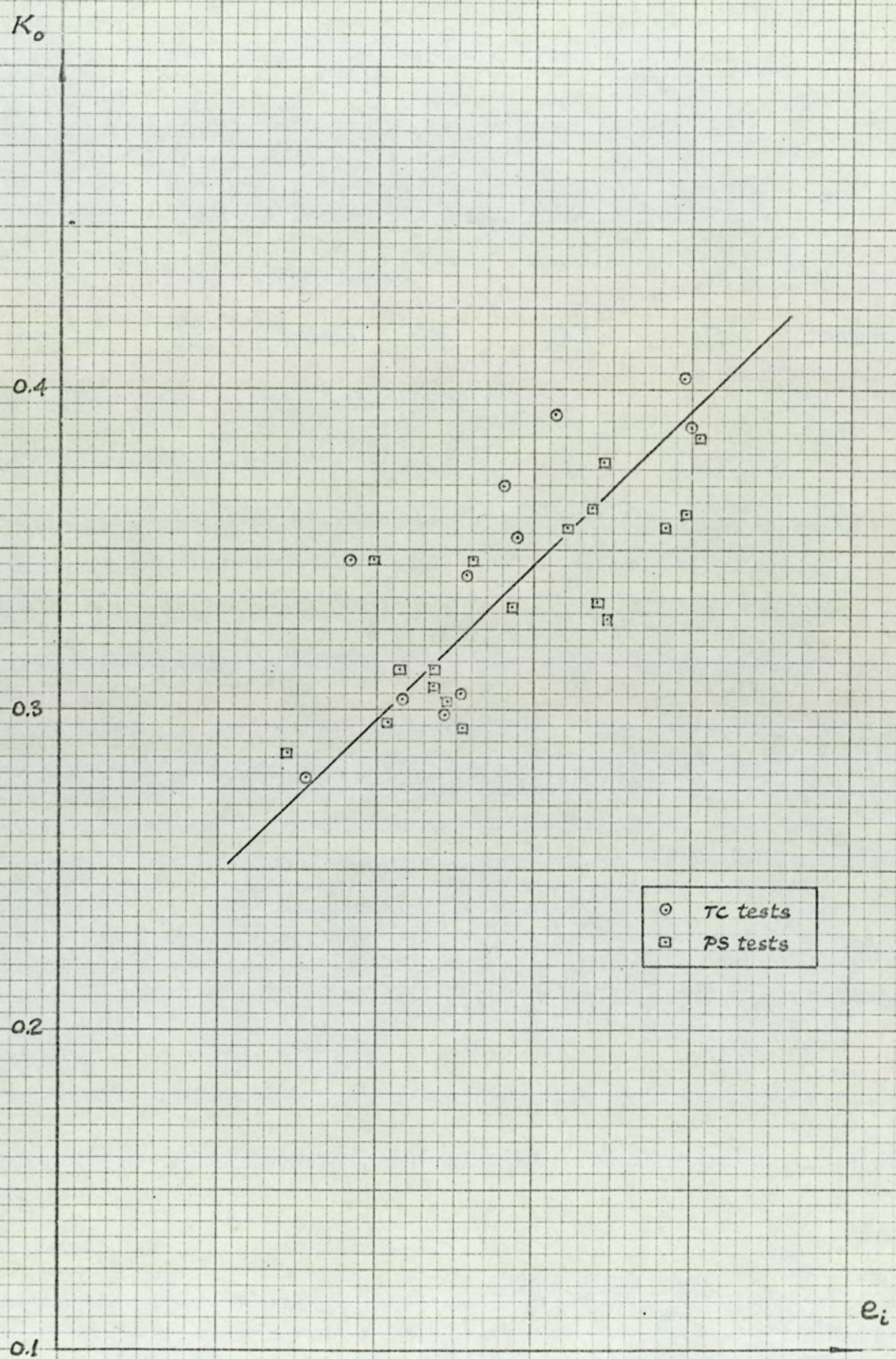

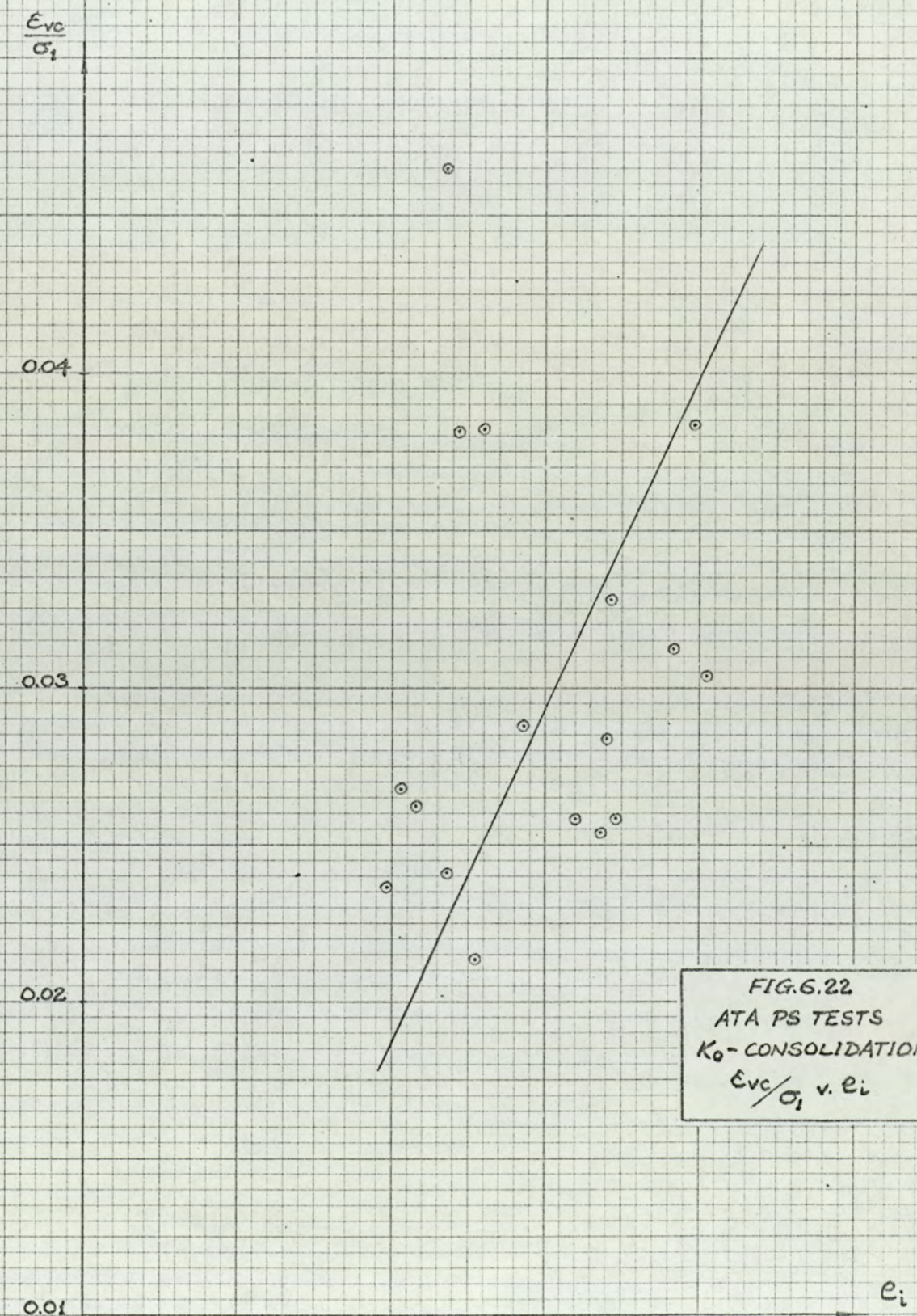

FIG. 6.22
ATA PS TESTS
K_o - CONSOLIDATION
$\varepsilon_{vc}/\sigma_1$ v. e_i

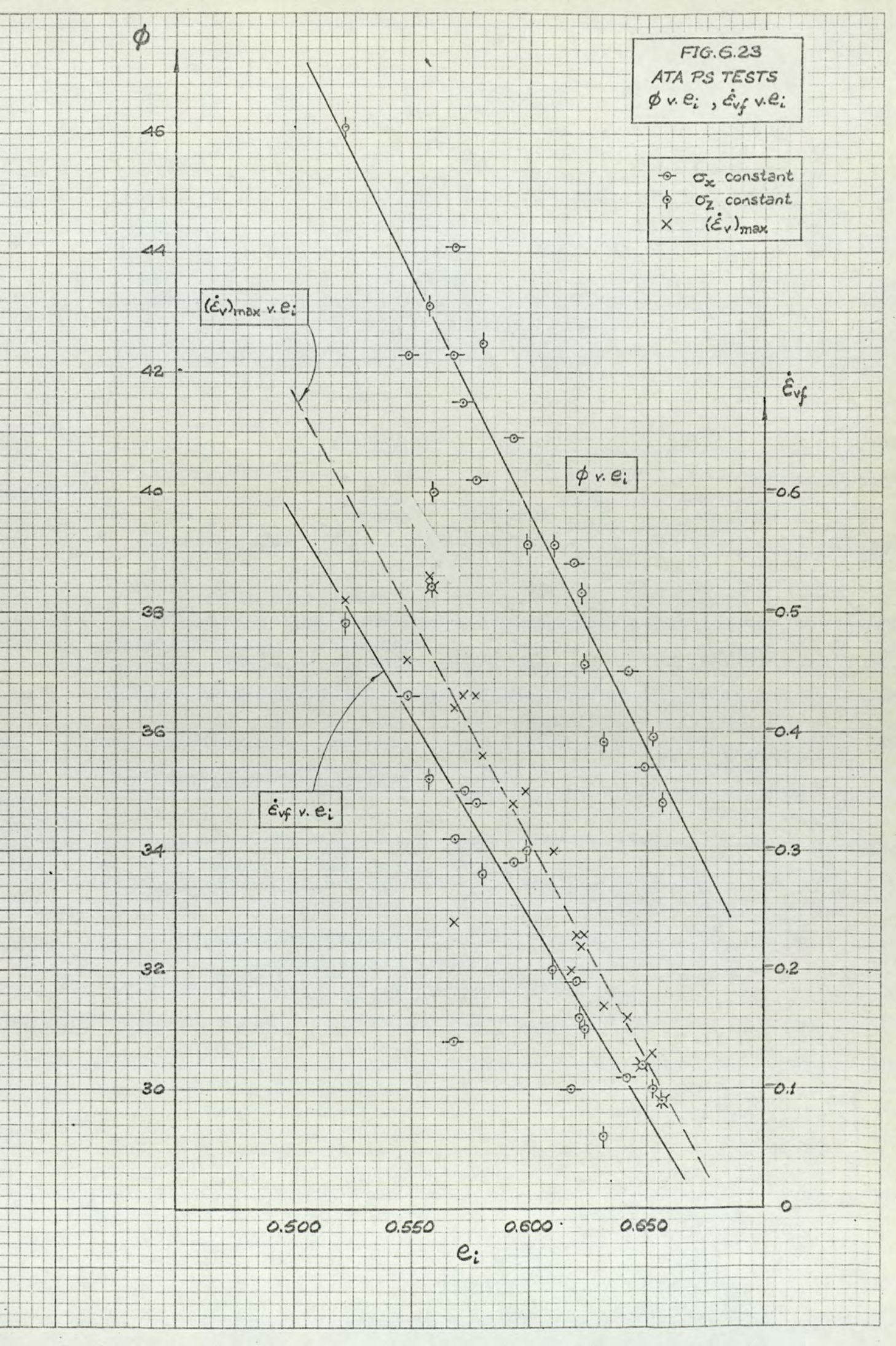
FIG. 6.23
ATA PS TESTS
ϕ v. e_i , $\dot{\varepsilon}_{vf}$ v. e_i
σ_x constant
σ_z constant
$(\dot{\varepsilon}_v)_{max}$
$(\dot{\varepsilon}_v)_{max}$ v. e_i
$\dot{\varepsilon}_{vf}$ v. e_i
ϕ v. e_i
ϕ
$\dot{\varepsilon}_{vf}$
46
44
42
40
38
36
34
32
30
0.6
0.5
0.4
0.3
0.2
0.1
0
0.500
0.550
0.600
0.650
e_i

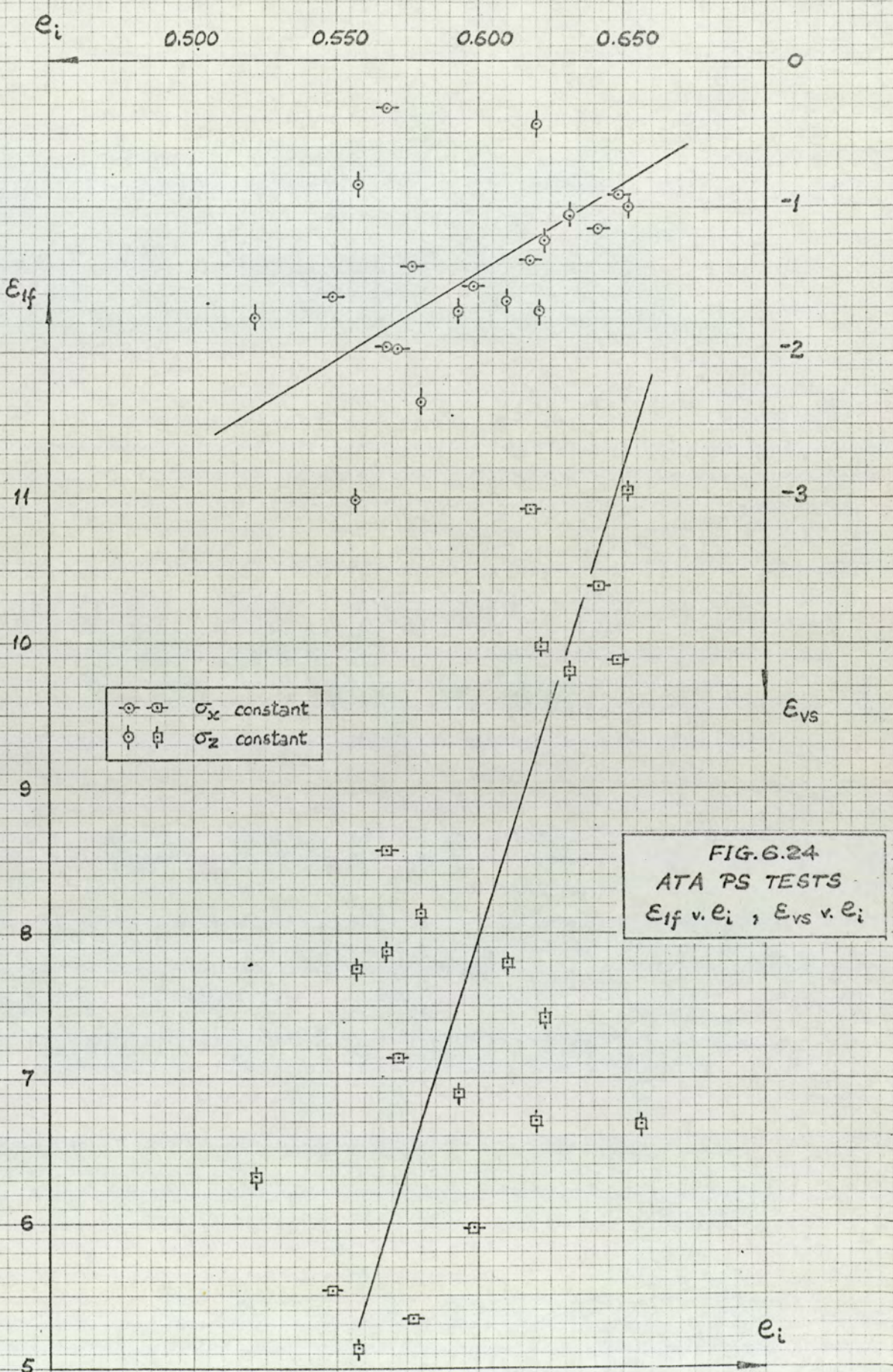

FIG. 6.24
ATA PS TESTS
ε_{1f} v. e_i , ε_{vs} v. e_i

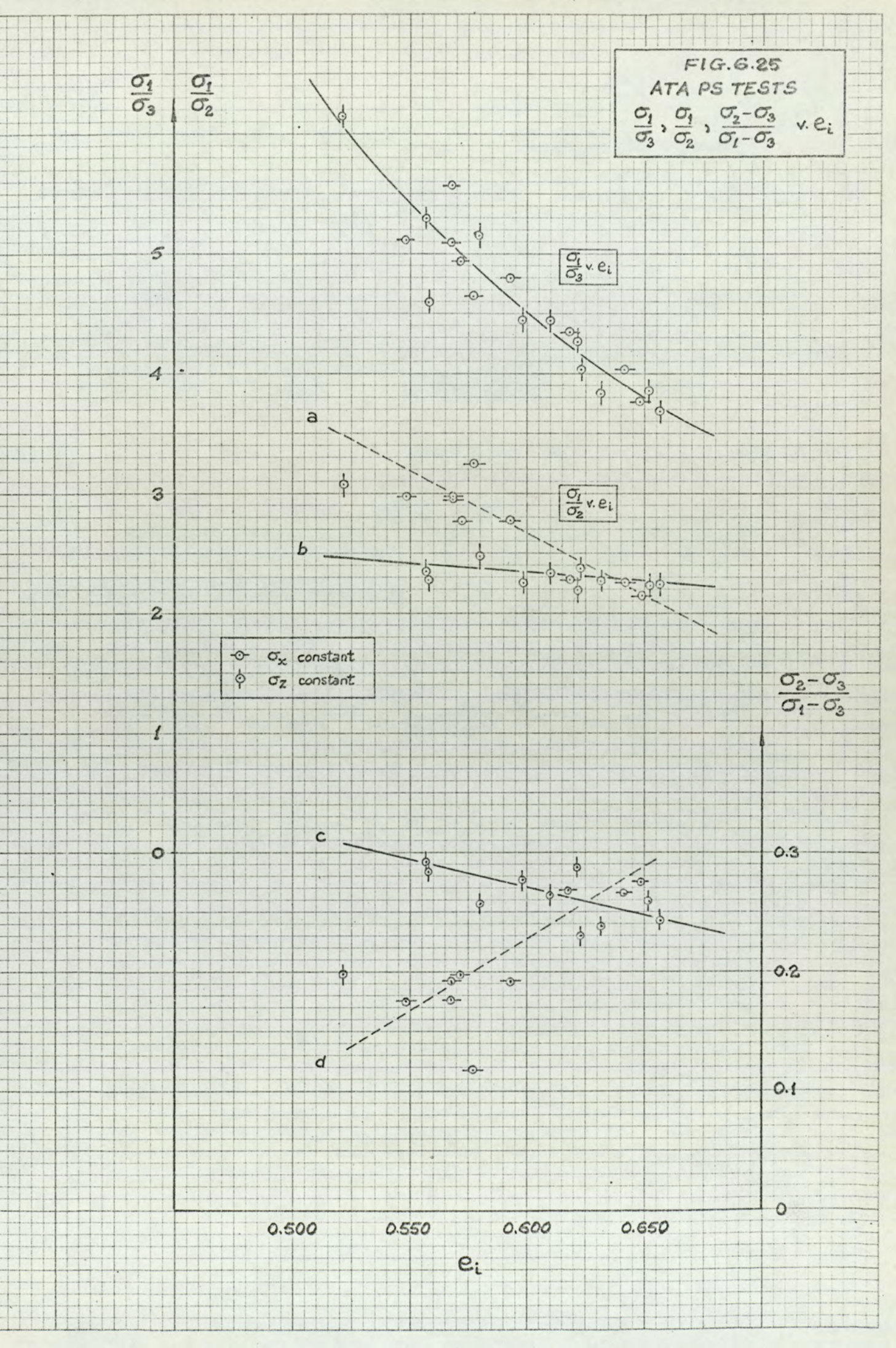
FIG. 6.25
ATA PS TESTS
$\frac{\sigma_1}{\sigma_3}$, $\frac{\sigma_1}{\sigma_2}$, $\frac{\sigma_2-\sigma_3}{\sigma_1-\sigma_3}$ v. e_i
$\frac{\sigma_1}{\sigma_3}$ $\frac{\sigma_1}{\sigma_2}$
$\frac{\sigma_1}{\sigma_3}$ v. e_i
$\frac{\sigma_1}{\sigma_2}$ v. e_i
a
b
c
d
σ_x constant
σ_z constant
$\frac{\sigma_2-\sigma_3}{\sigma_1-\sigma_3}$
5
4
3
2
1
0
0.3
0.2
0.1
0
0.500
0.550
0.600
0.650
e_i

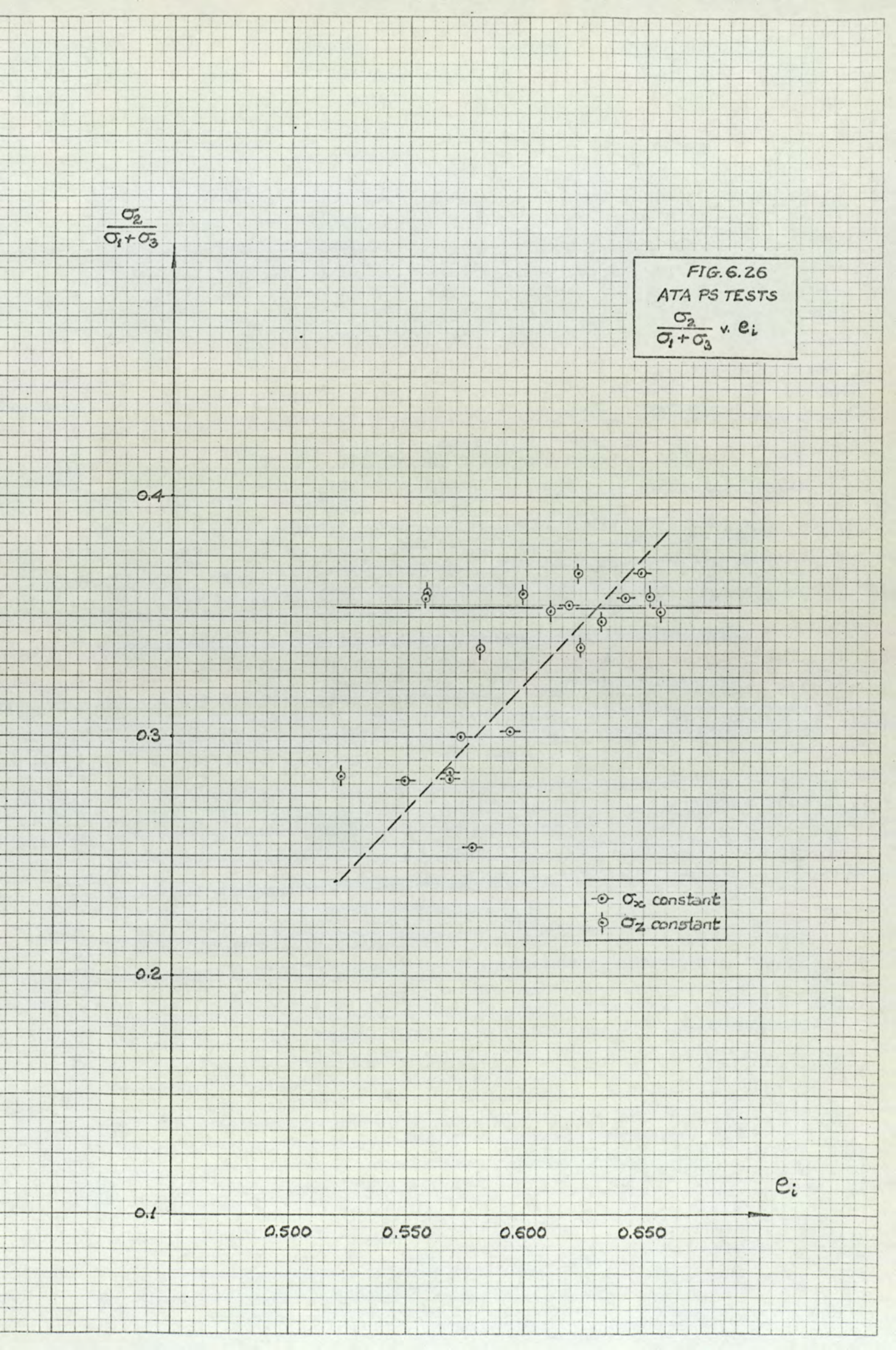
$\frac{\sigma_2}{\sigma_1+\sigma_3}$
FIG. 6.26
ATA PS TESTS
$\frac{\sigma_2}{\sigma_1+\sigma_3}$ v. e_i
0.4
0.3
0.2
0.1
σ_x constant
σ_z constant
e_i
0.500
0.550
0.600
0.650

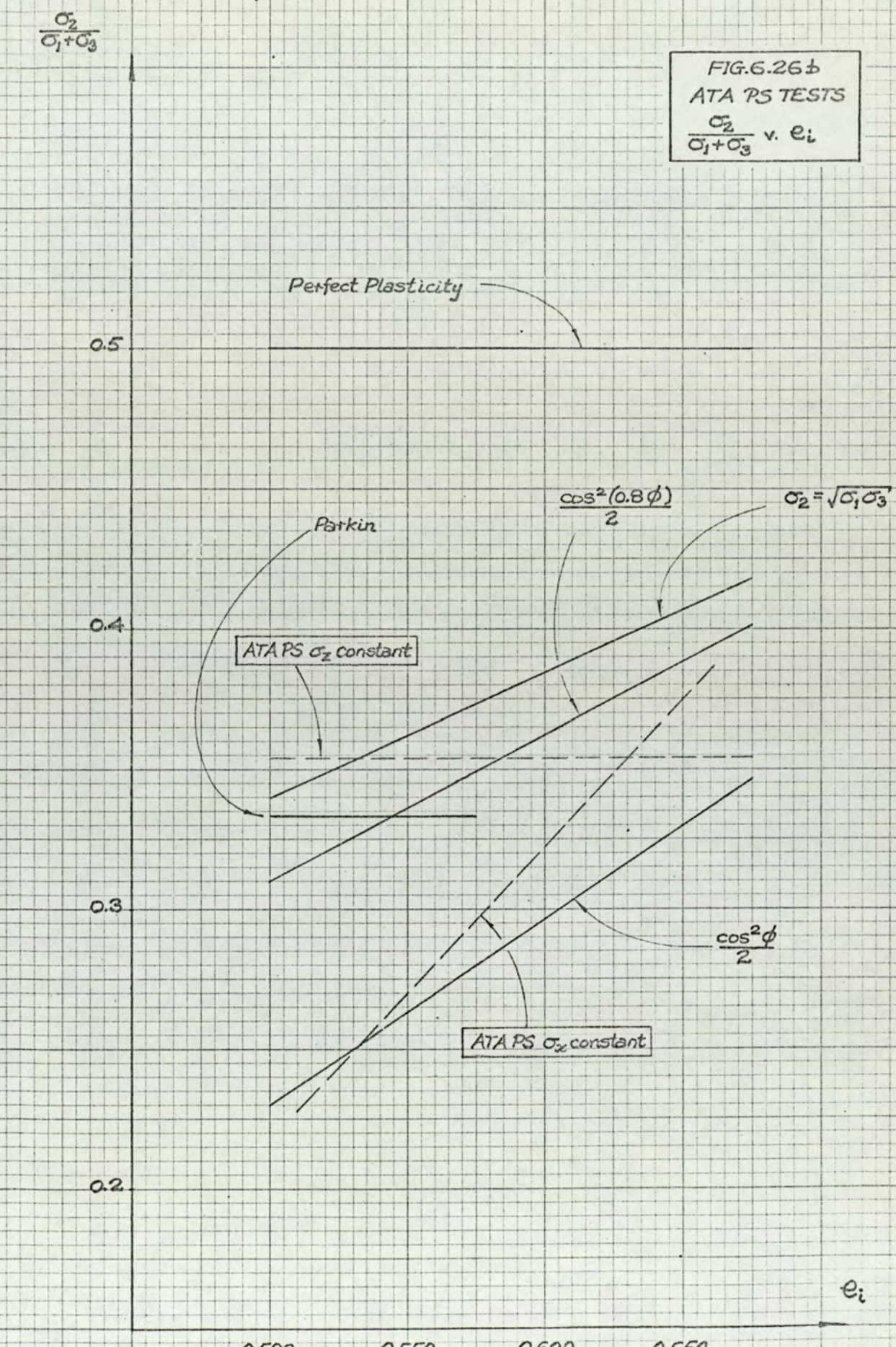
$\frac{\sigma_2}{\sigma_1+\sigma_3}$
FIG.6.26b
ATA PS TESTS
$\frac{\sigma_2}{\sigma_1+\sigma_3}$ v. e_i
Perfect Plasticity
0.5
$\frac{\cos^2(0.8\phi)}{2}$
$\sigma_2=\sqrt{\sigma_1\sigma_3}$
Parkin
0.4
ATA PS σ_z constant
0.3
$\frac{\cos^2\phi}{2}$
ATA PS σ_x constant
0.2
e_i
0.500
0.550
0.600
0.650

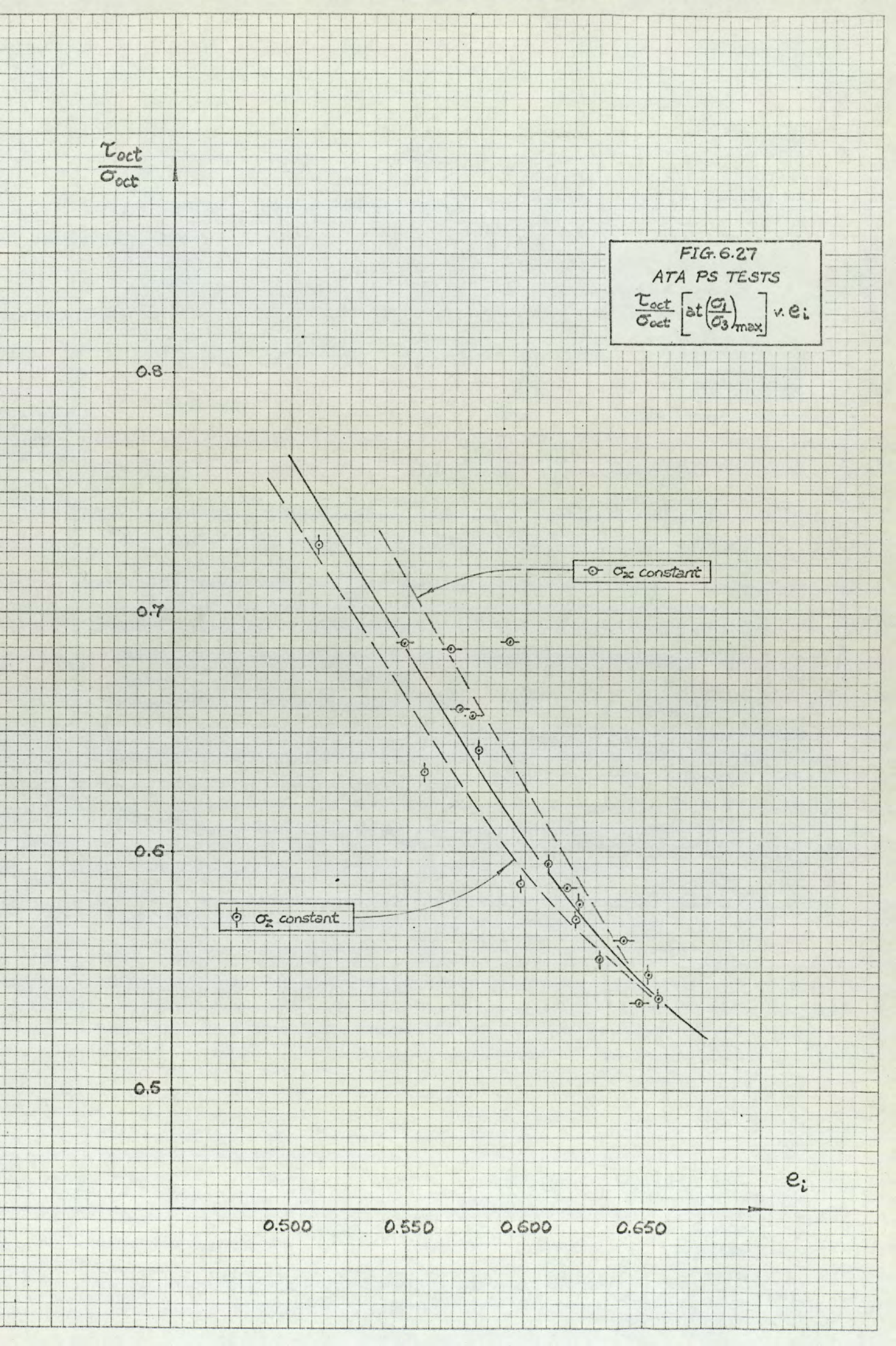

FIG. 6.27
ATA PS TESTS
$\frac{\tau_{oct}}{\sigma_{oct}}$ at $\left(\frac{\sigma_1}{\sigma_3}\right)_{max}$ v. e_i

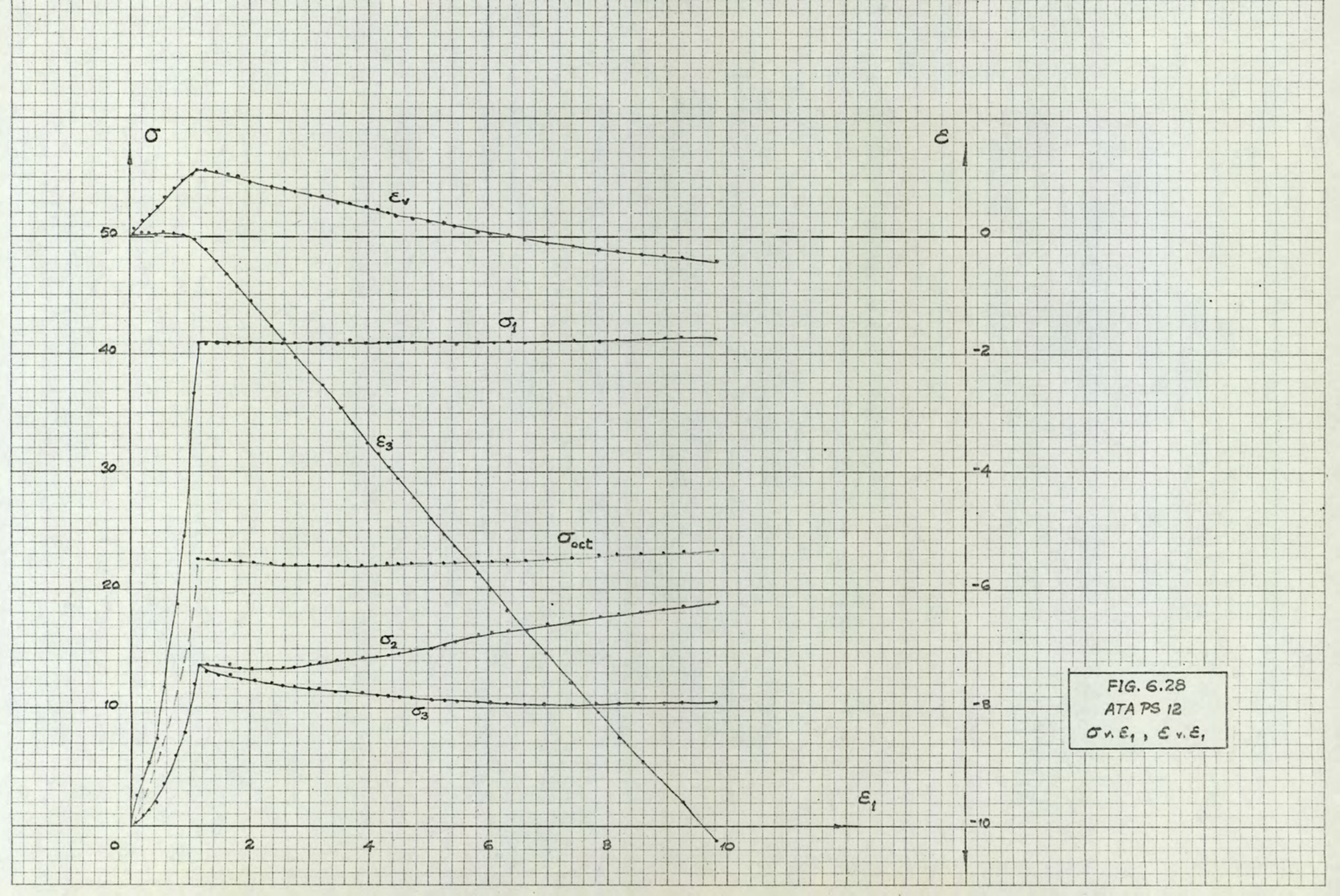

FIG. 6.28
ATA PS 12
σ v. ε_1 , ε v. ε_1

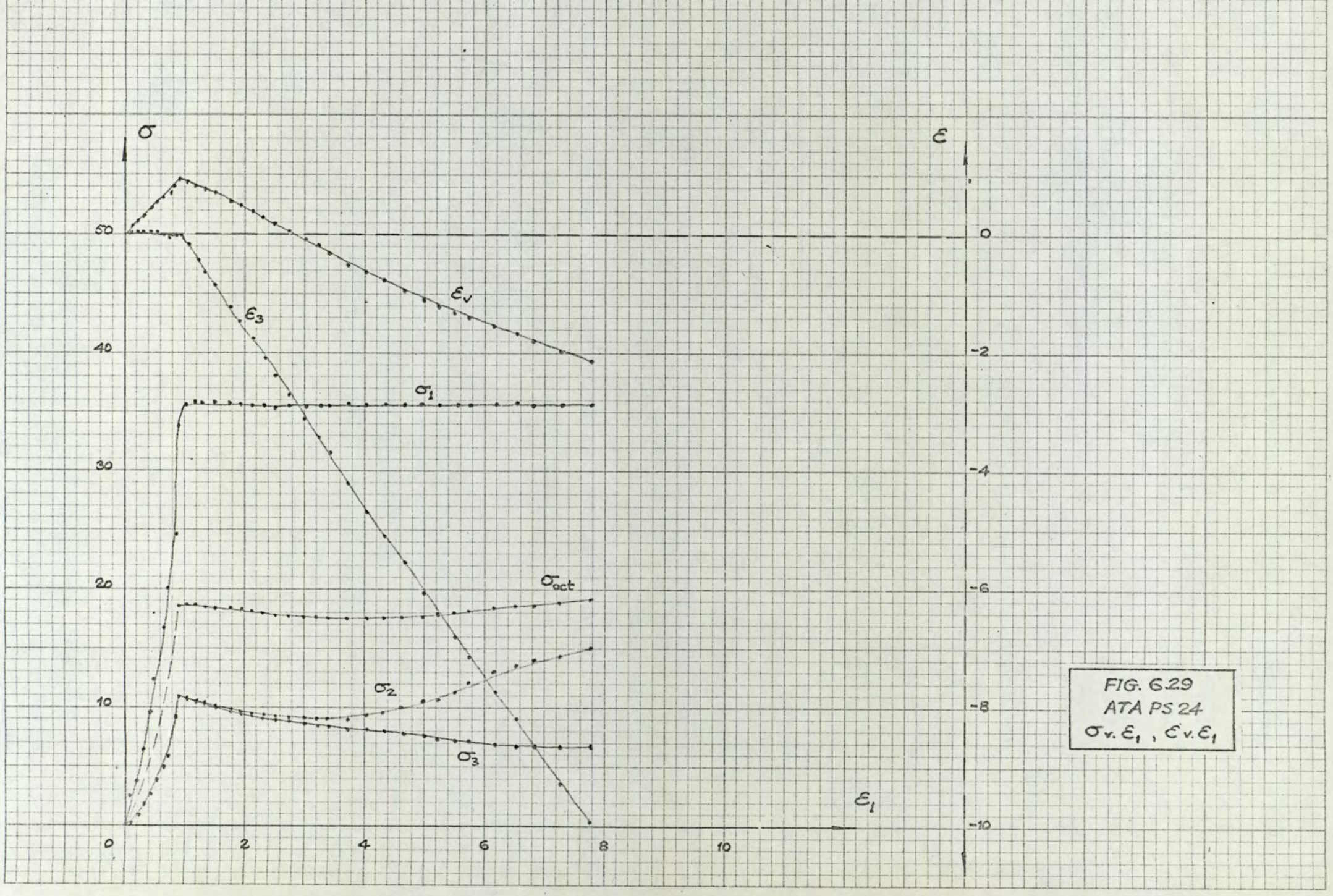

FIG. 6.29
ATA PS 24
σ v. ε_1 , ε v. ε_1

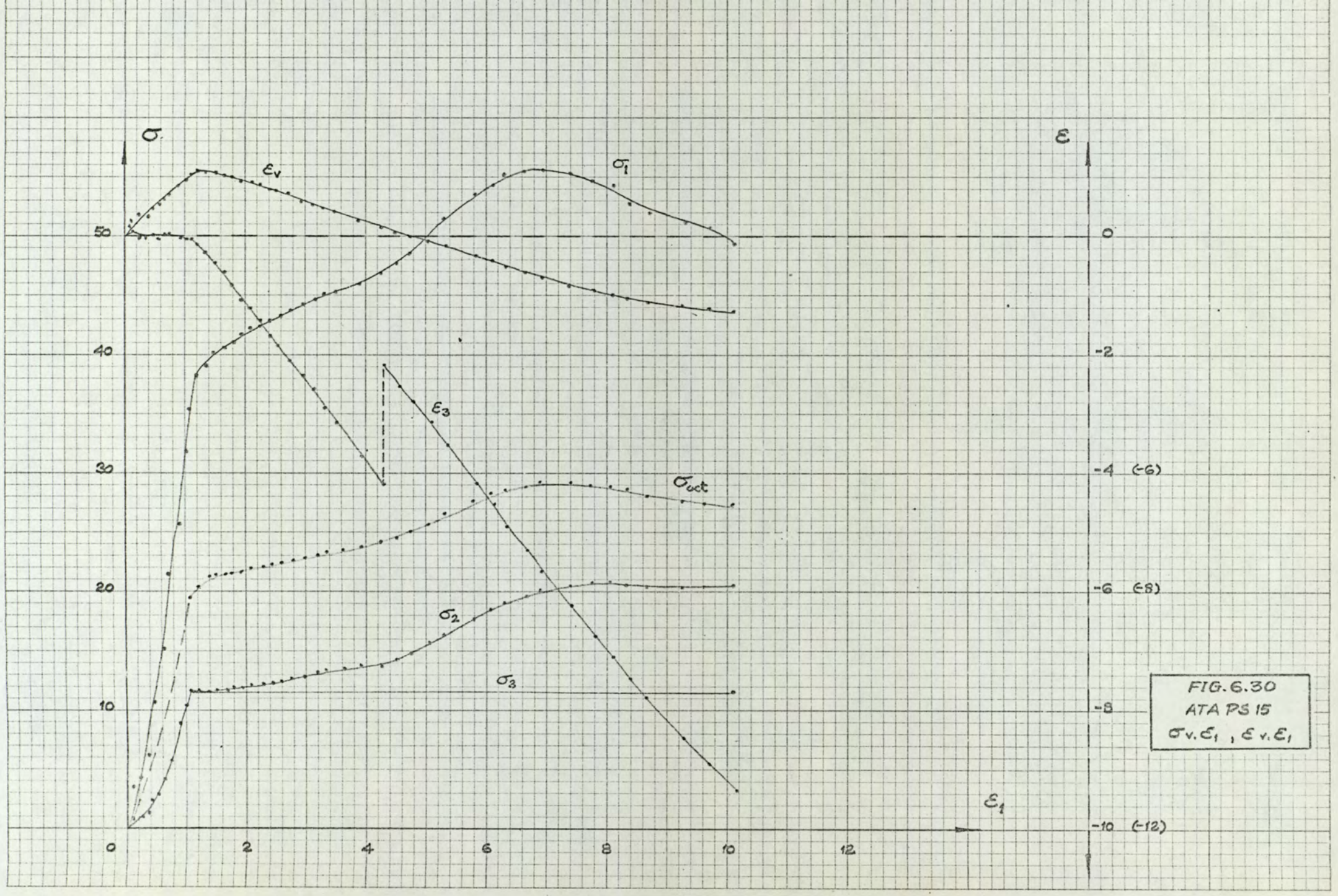

FIG. 6.30
ATA PS 15
$\sigma_v . \varepsilon_1$, $\varepsilon_v . \varepsilon_1$

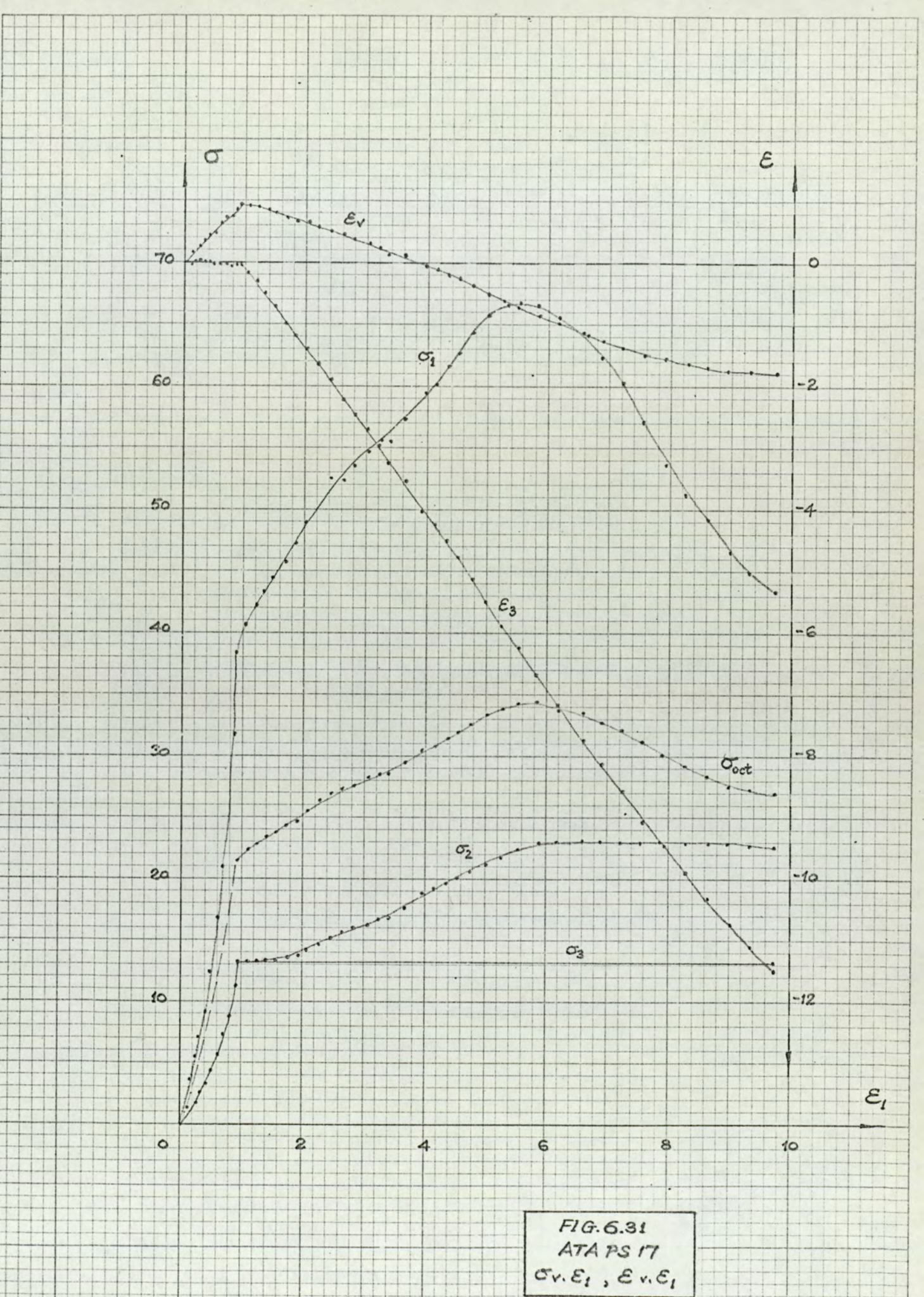

FIG. 6.31
ATA PS 17
σ_v. ε_1 , ε_v. ε_1

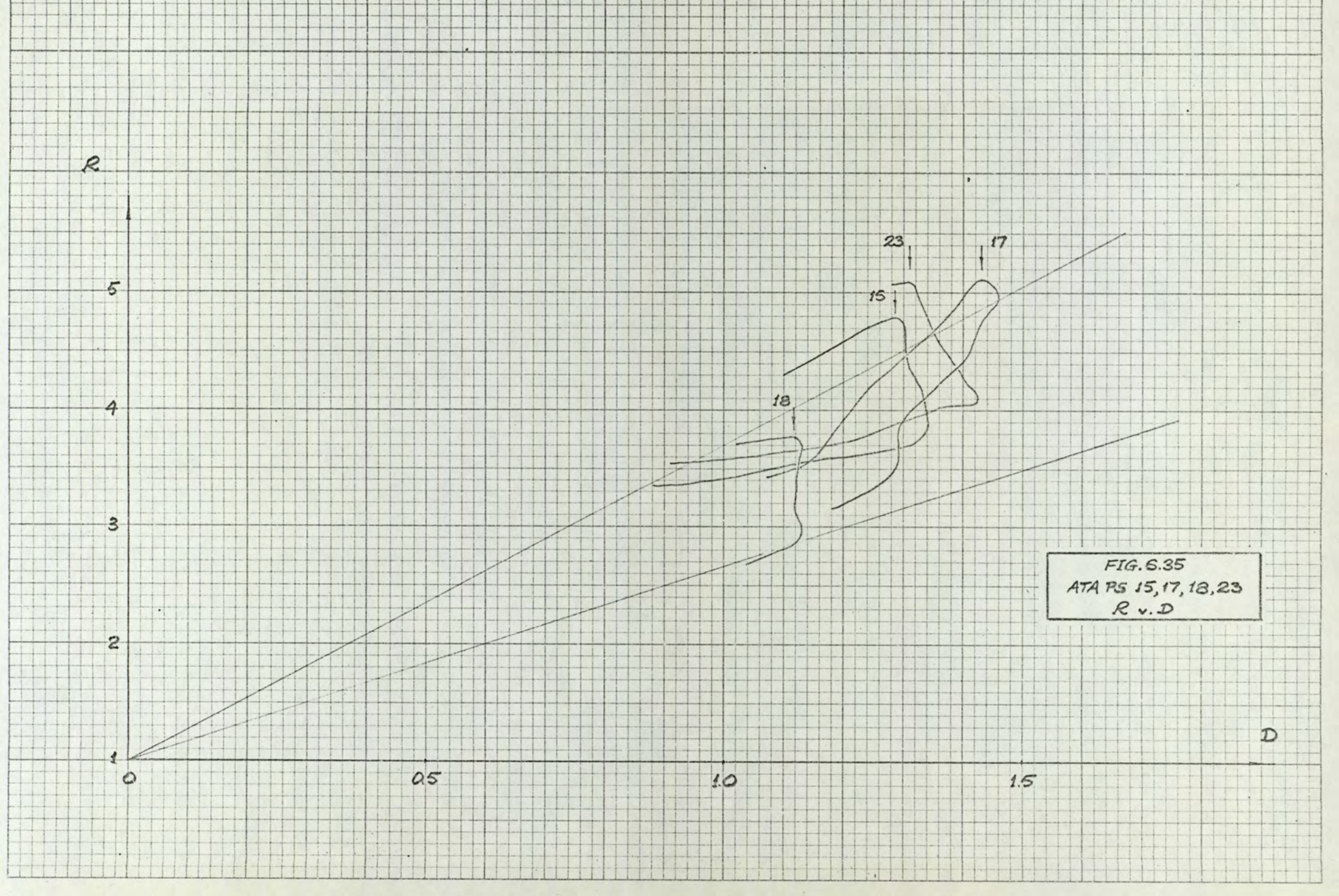

FIG. 6.35
ATA PS 15, 17, 18, 23
R v. D

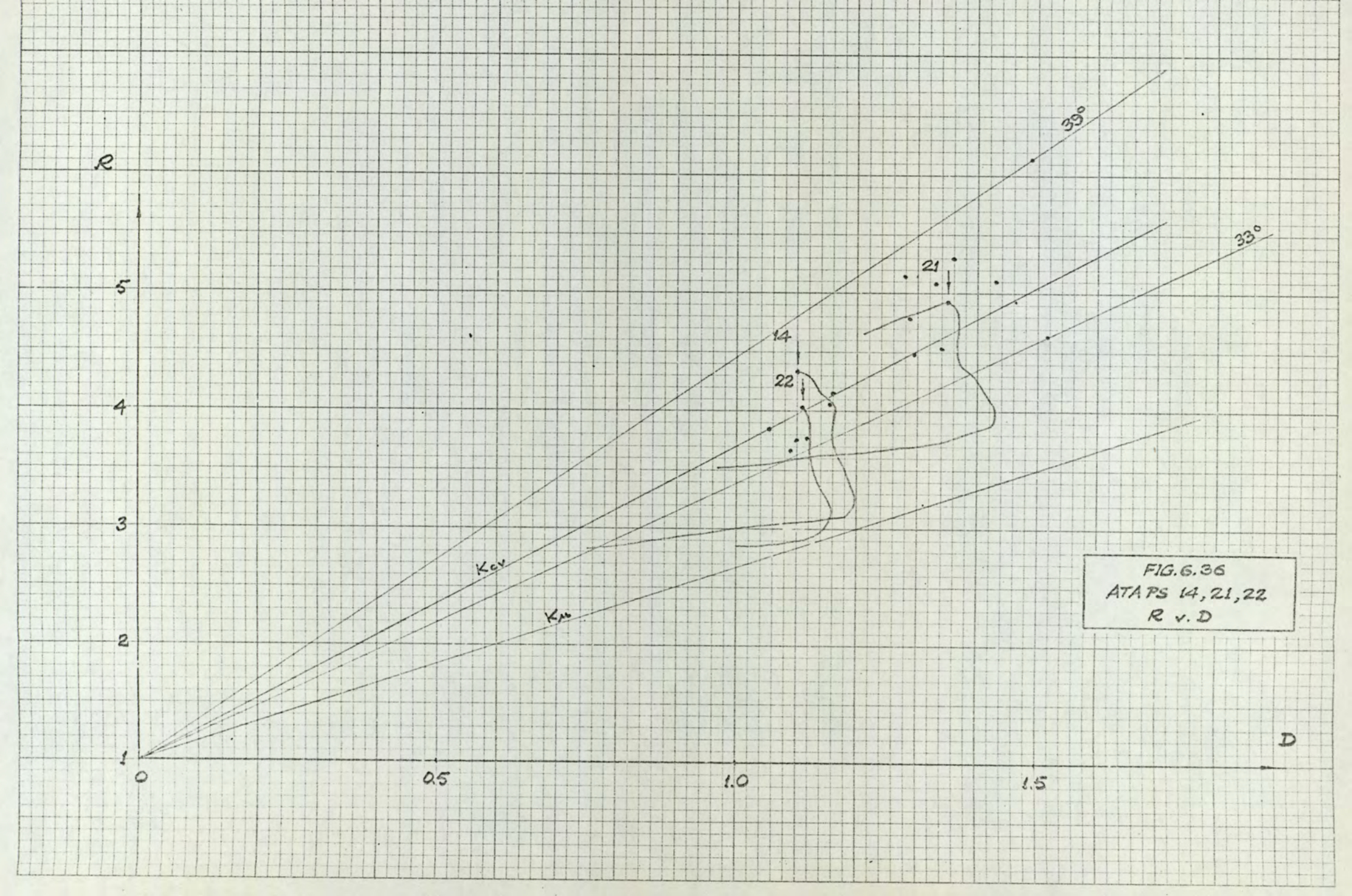

FIG. 6.36
ATAPS 14, 21, 22
R v. D

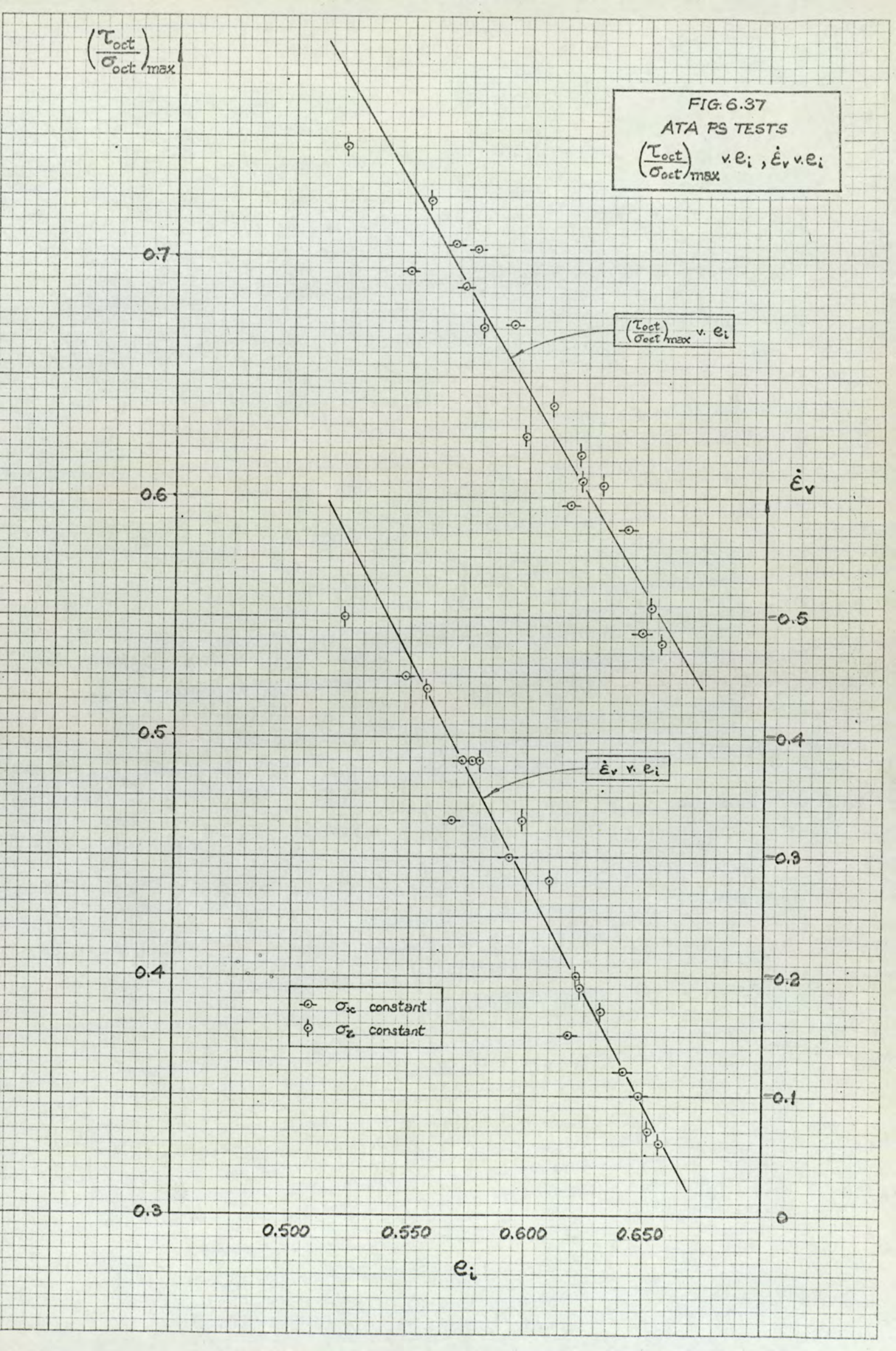
$\left(\frac{\tau_{oct}}{\sigma_{oct}}\right)_{max}$
FIG. 6.37
ATA PS TESTS
$\left(\frac{\tau_{oct}}{\sigma_{oct}}\right)_{max}$ v. e_i , $\dot{\varepsilon}_v$ v. e_i
0.7
0.6
0.5
0.4
0.3
$\left(\frac{\tau_{oct}}{\sigma_{oct}}\right)_{max}$ v. e_i
$\dot{\varepsilon}_v$
0.5
0.4
0.3
0.2
0.1
0
$\dot{\varepsilon}_v$ v. e_i
σ_x constant
σ_z constant
0.500
0.550
0.600
0.650
e_i

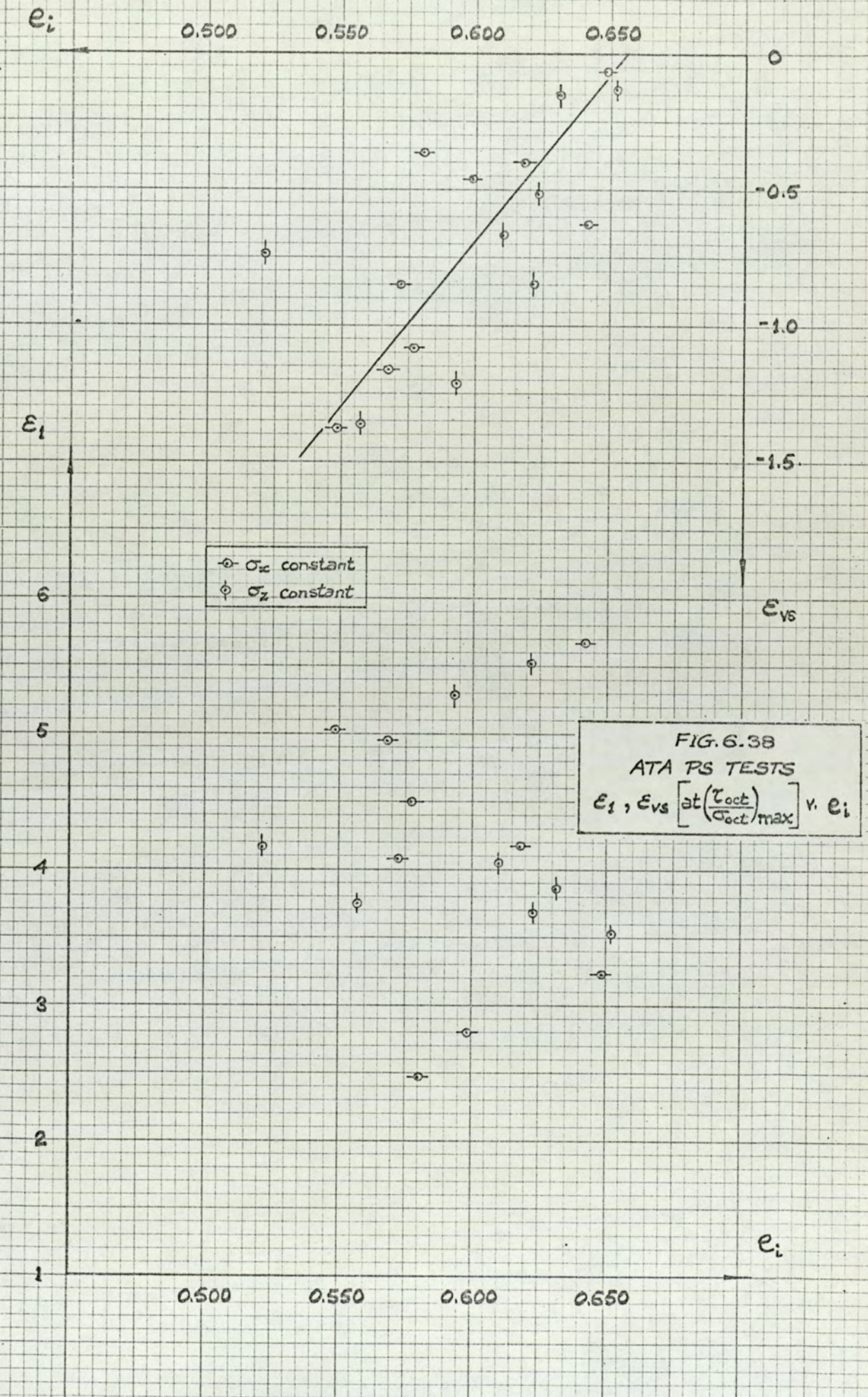

FIG. 6.38
ATA PS TESTS
ε_1, ε_{vs} $\left[\text{at}\left(\frac{\tau_{oct}}{\sigma_{oct}}\right)_{max}\right]$ v. e_i

FIG. 6.39

ATA PS TESTS

$\frac{\sigma_2}{\sigma_1+\sigma_3}$, $\frac{\sigma_2-\sigma_3}{\sigma_1-\sigma_3}$ at $\left(\frac{\tau_{oct}}{\sigma_{oct}}\right)_{max}$ v. e_i

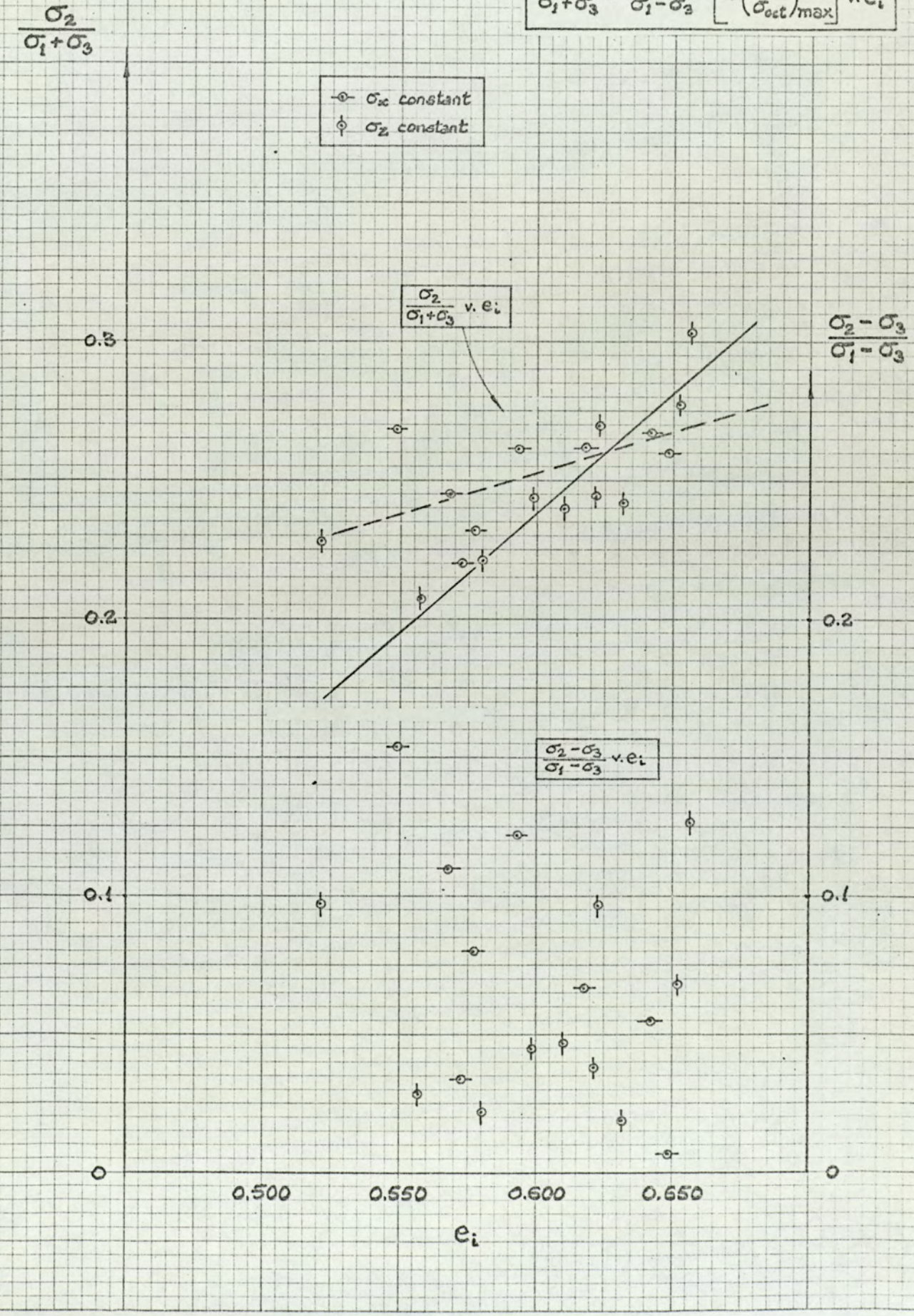

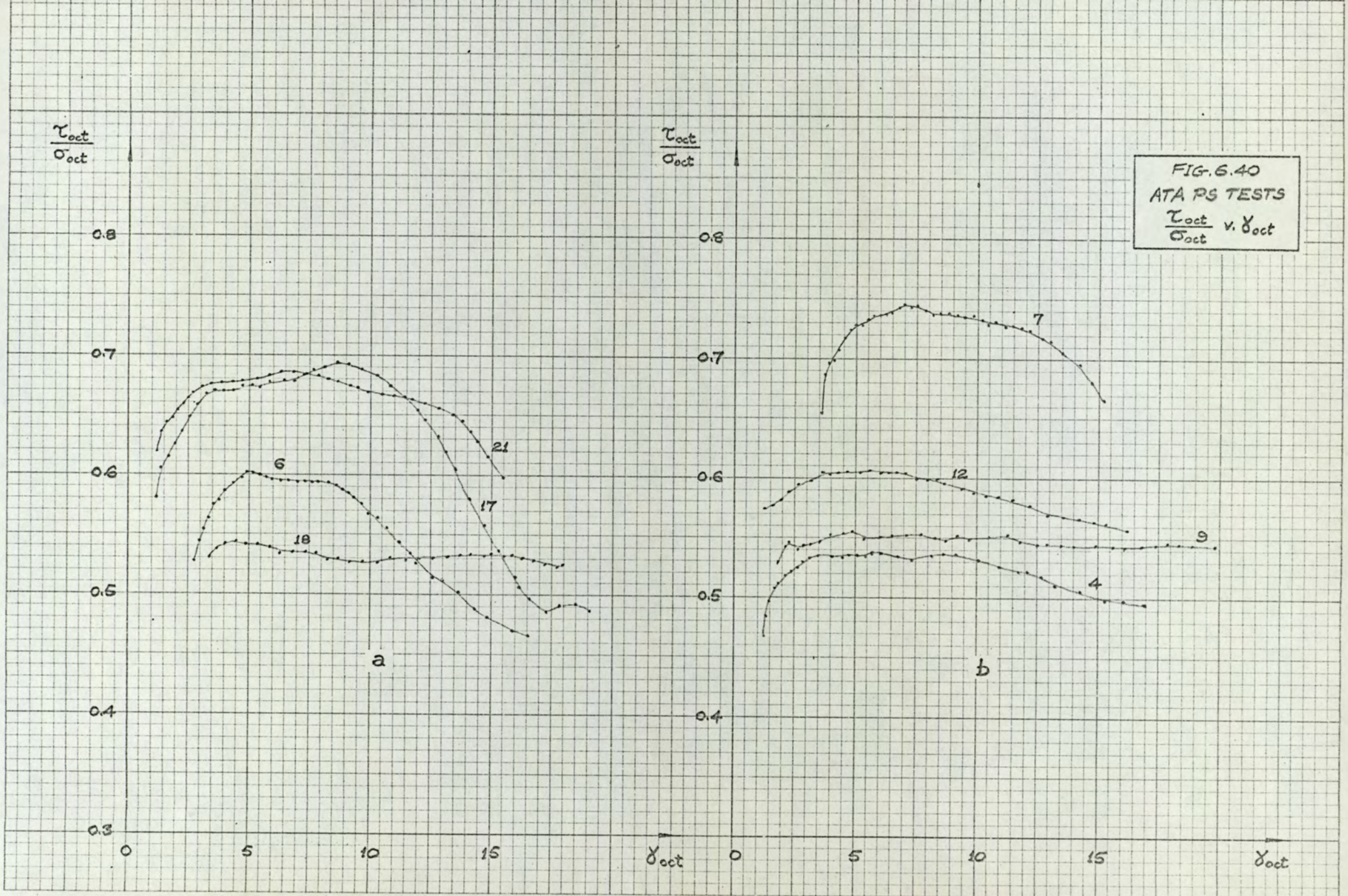

FIG. 6.40
ATA PS TESTS
$\frac{\tau_{oct}}{\sigma_{oct}}$ v. γ_{oct}

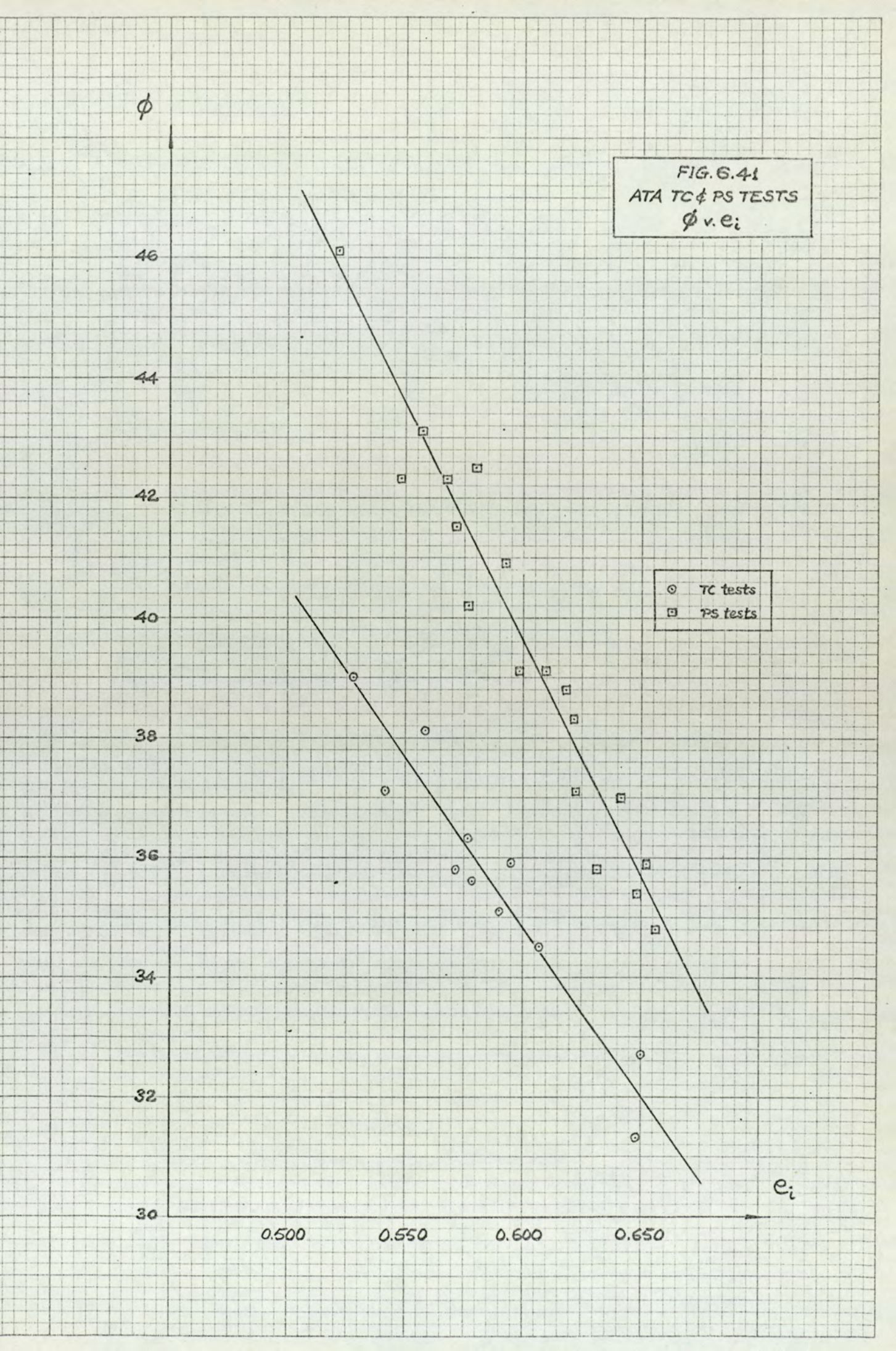
FIG. 6.41
ATA TC & PS TESTS
φ v. e_i
φ
46
44
42
40
38
36
34
32
30
TC tests
PS tests
0.500
0.550
0.600
0.650
e_i

FIG. 6.42
ATA TC & PS TESTS
$\dot{\varepsilon}_{vf}$ v. e_i

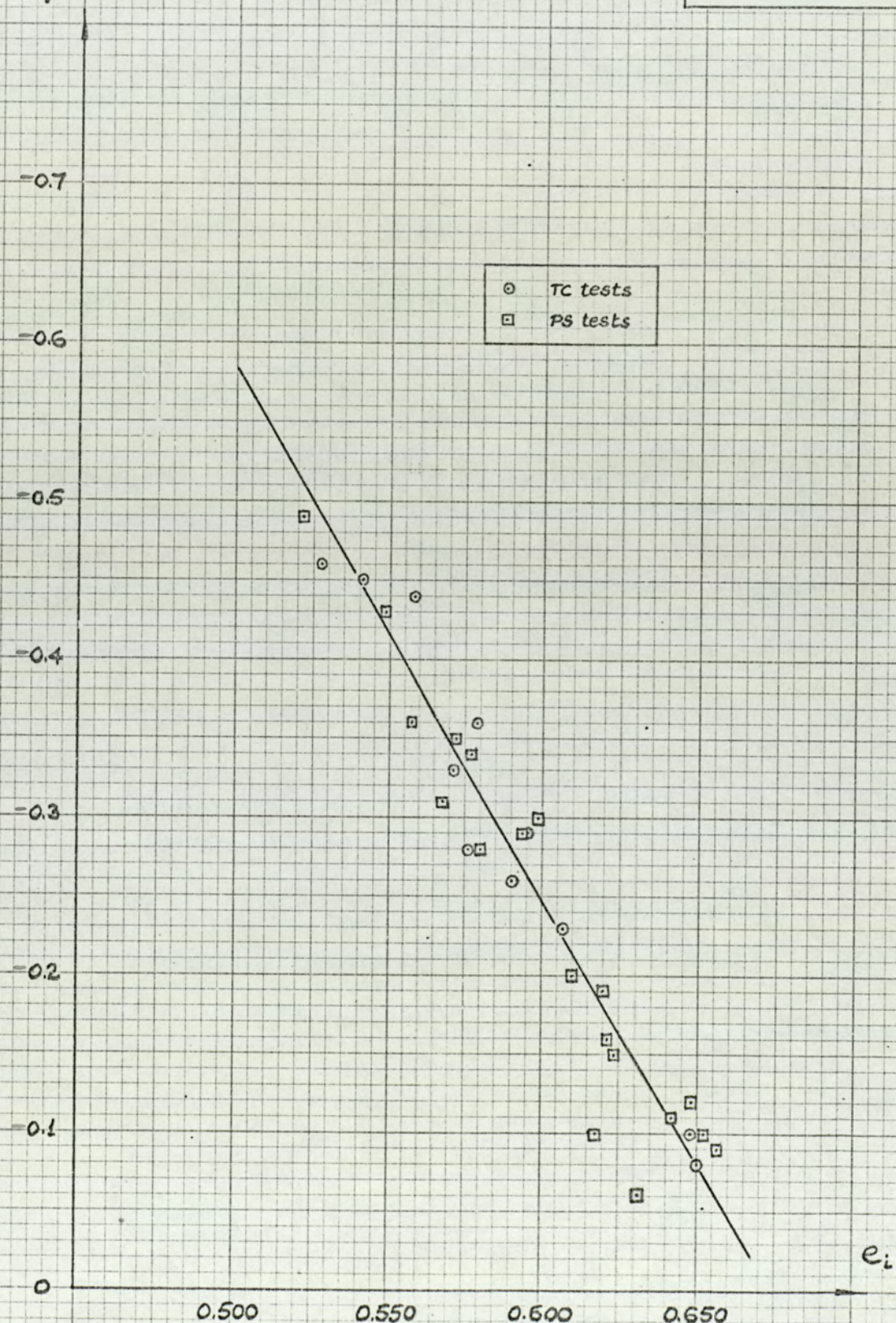

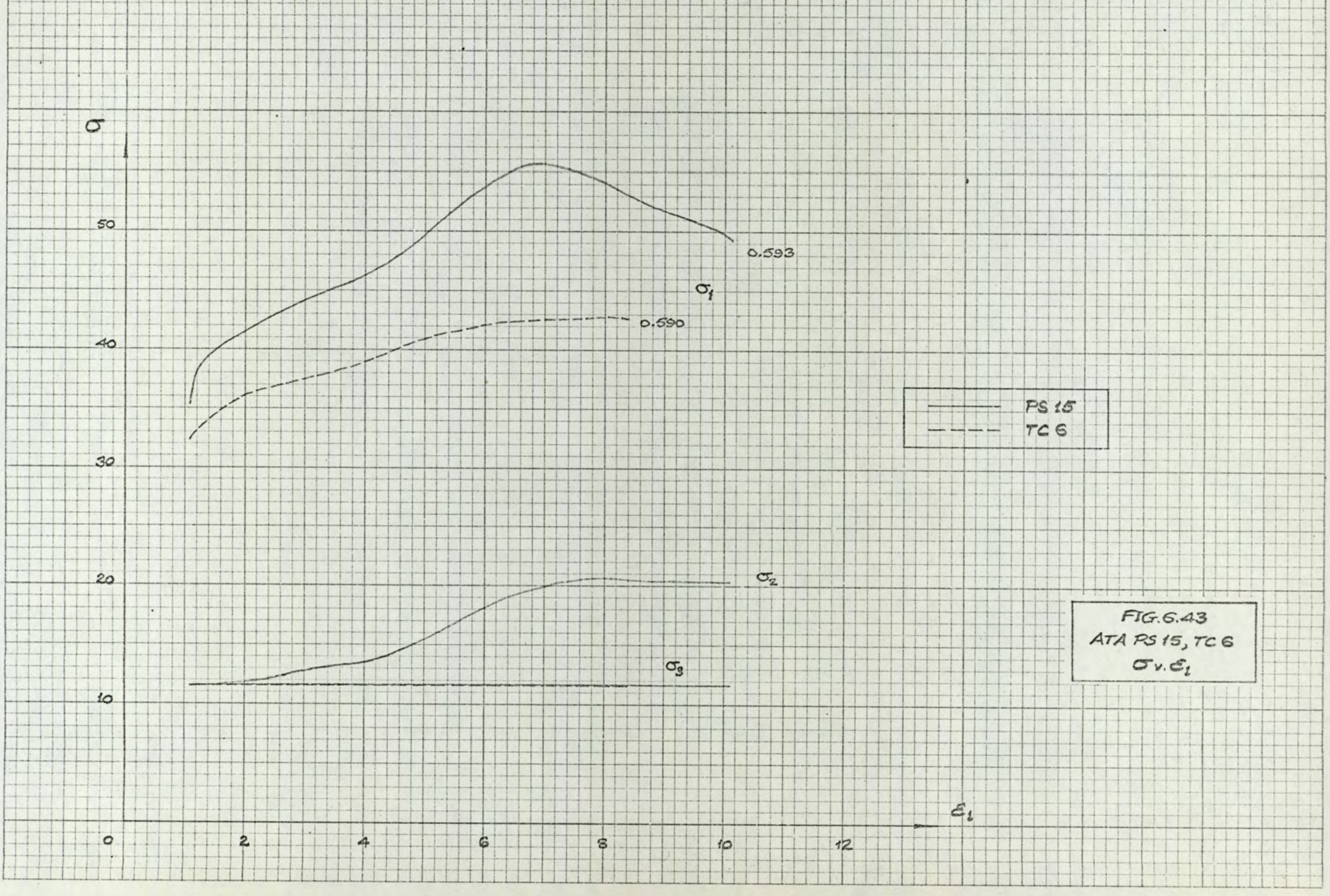

FIG. 6.43
ATA PS 15, TC 6
σ v. ε_1

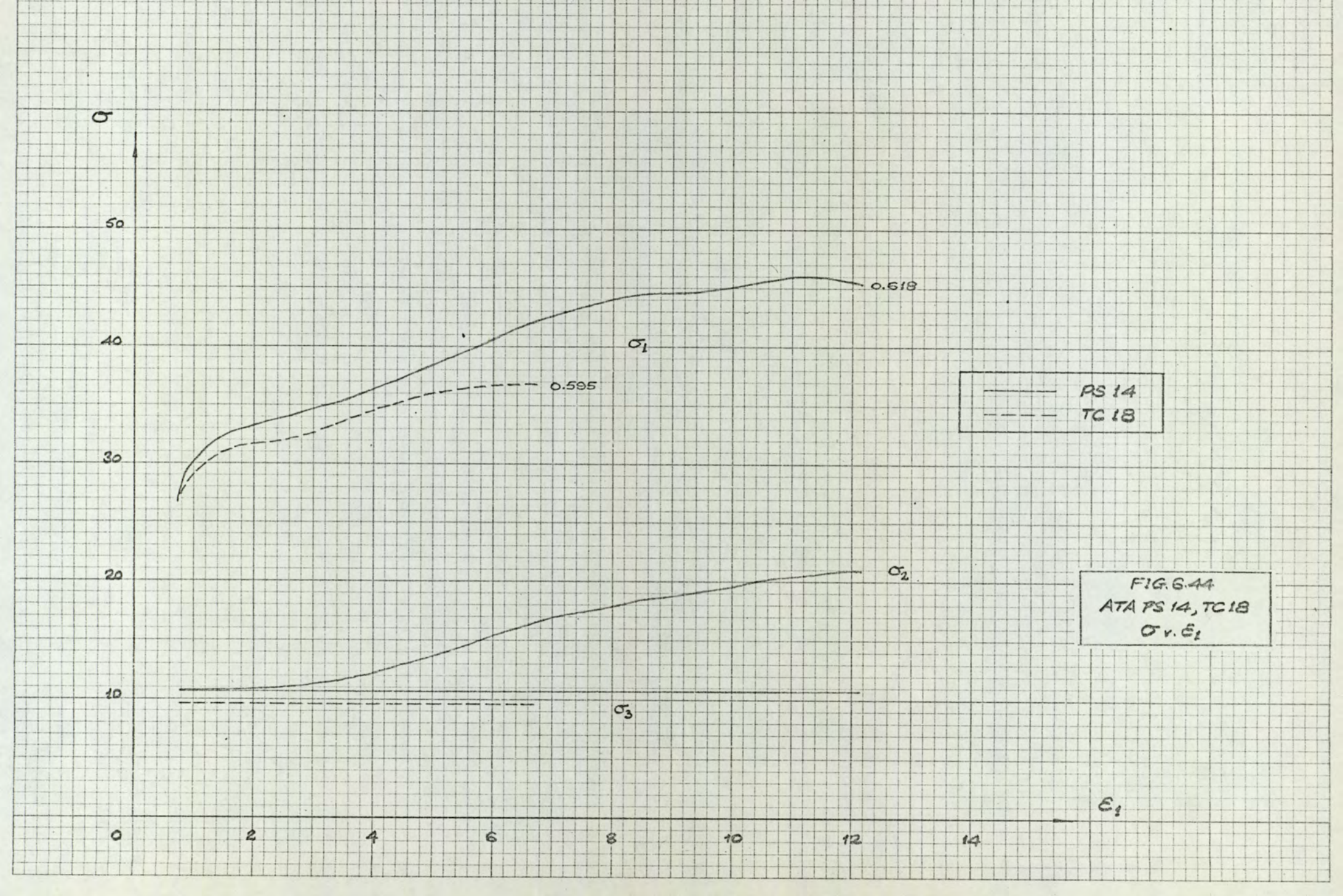

FIG. 6.44
ATA PS 14, TC 18
σ v. ε1

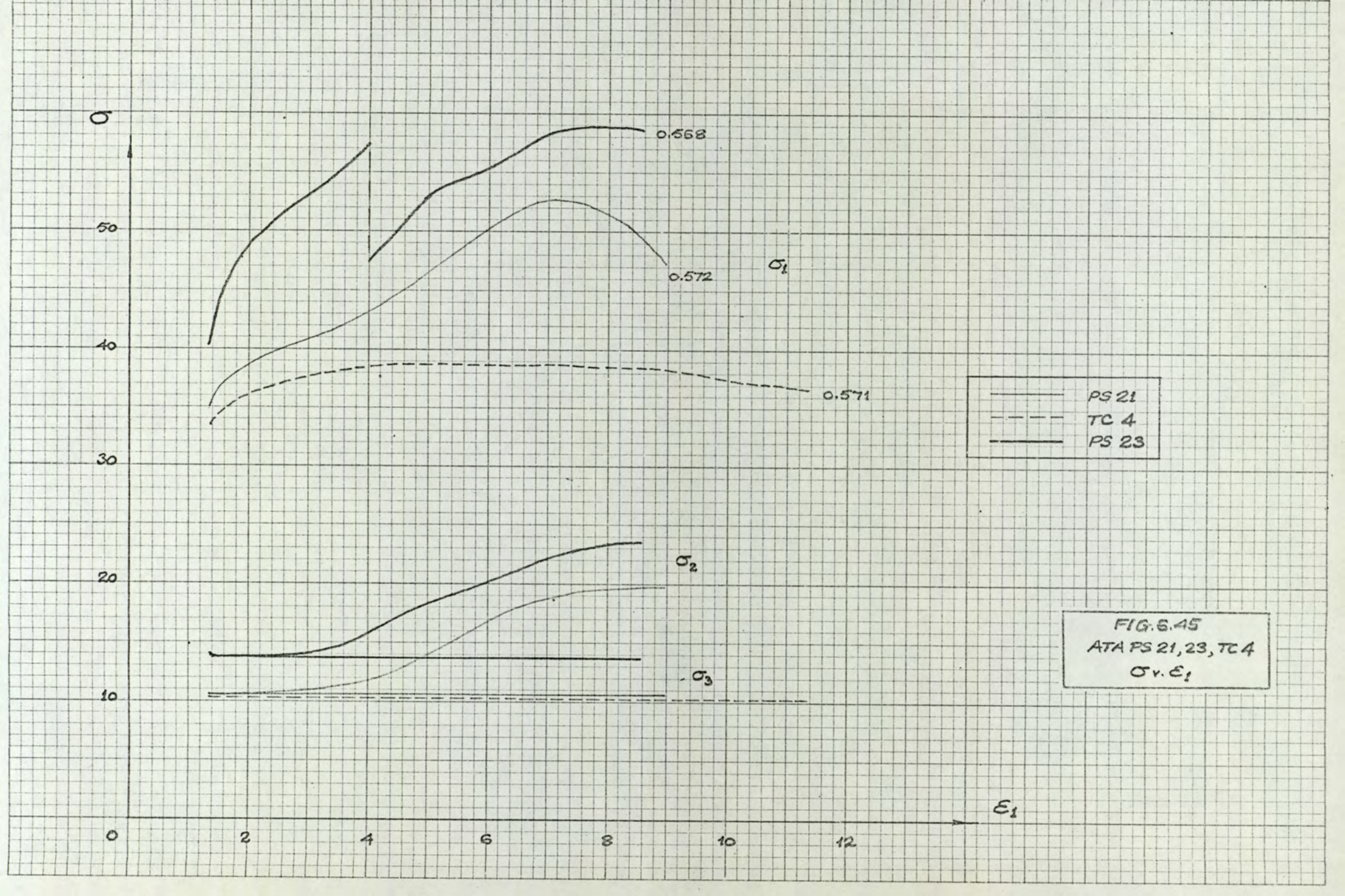

FIG. 6.45
ATA PS 21, 23, TC 4
σ v. ε1

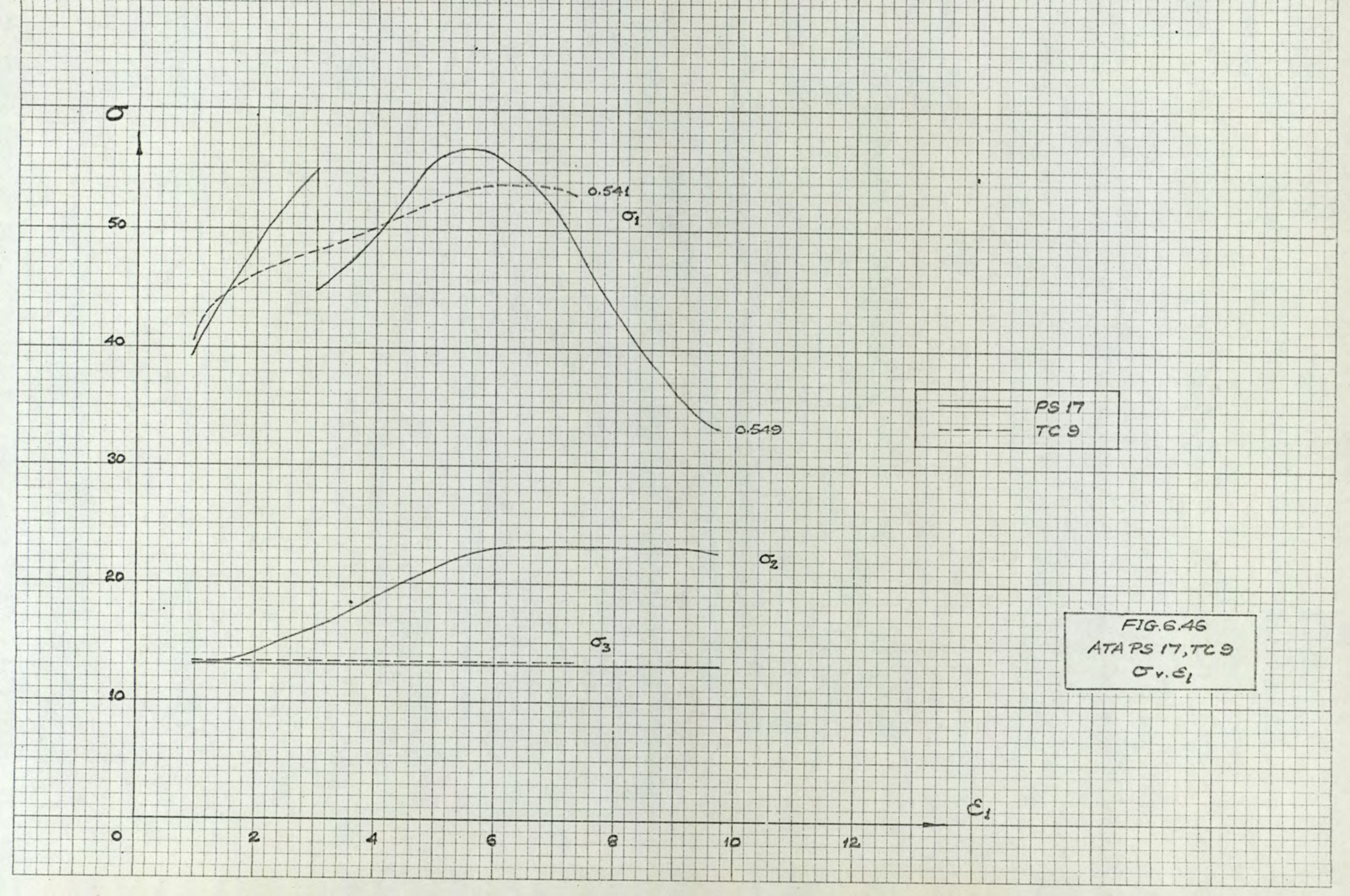

FIG. 6.46
ATA PS 17, TC 9
σ v. ε1

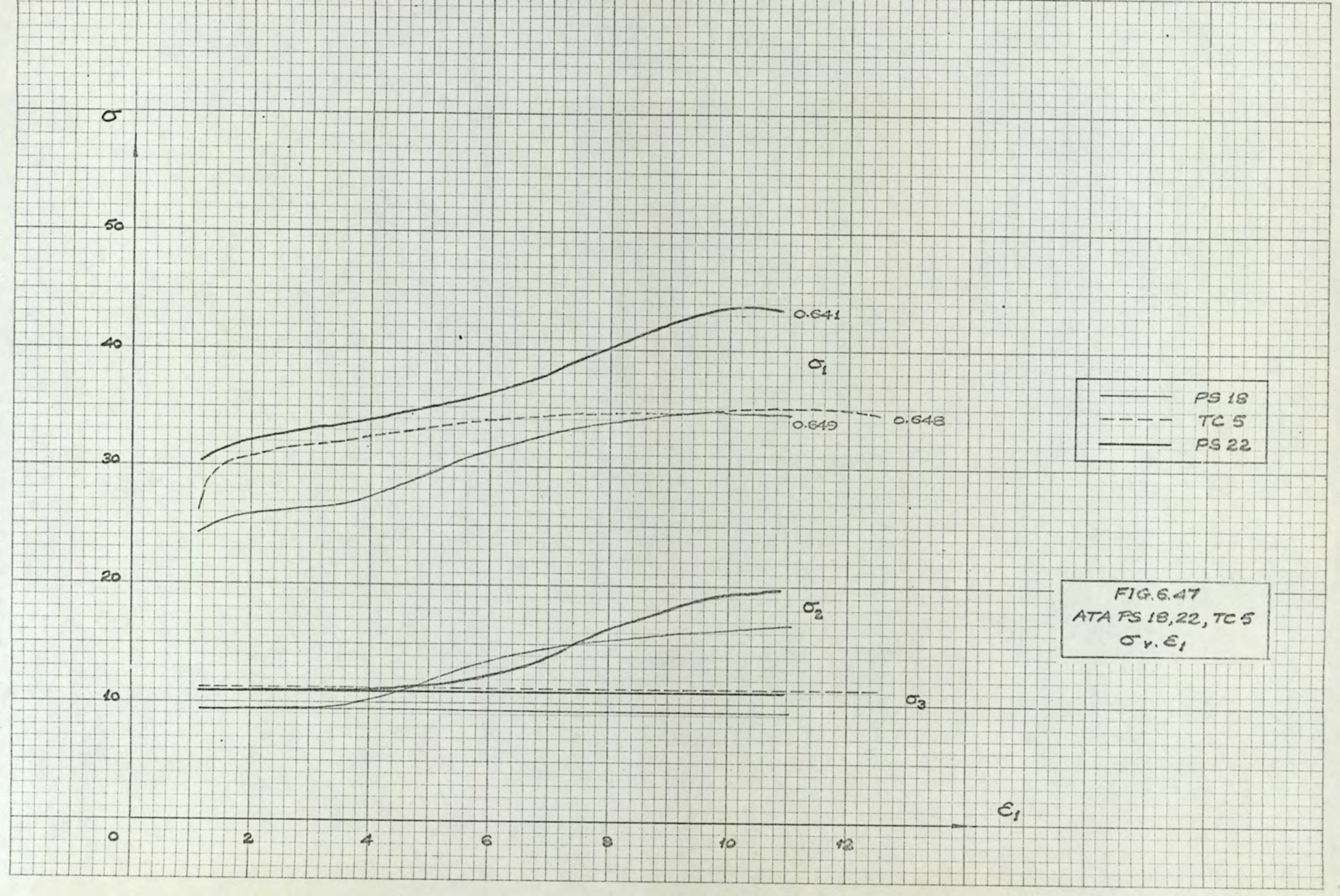

FIG. 6.47
ATA PS 18, 22, TC 5
σ v. ε_1

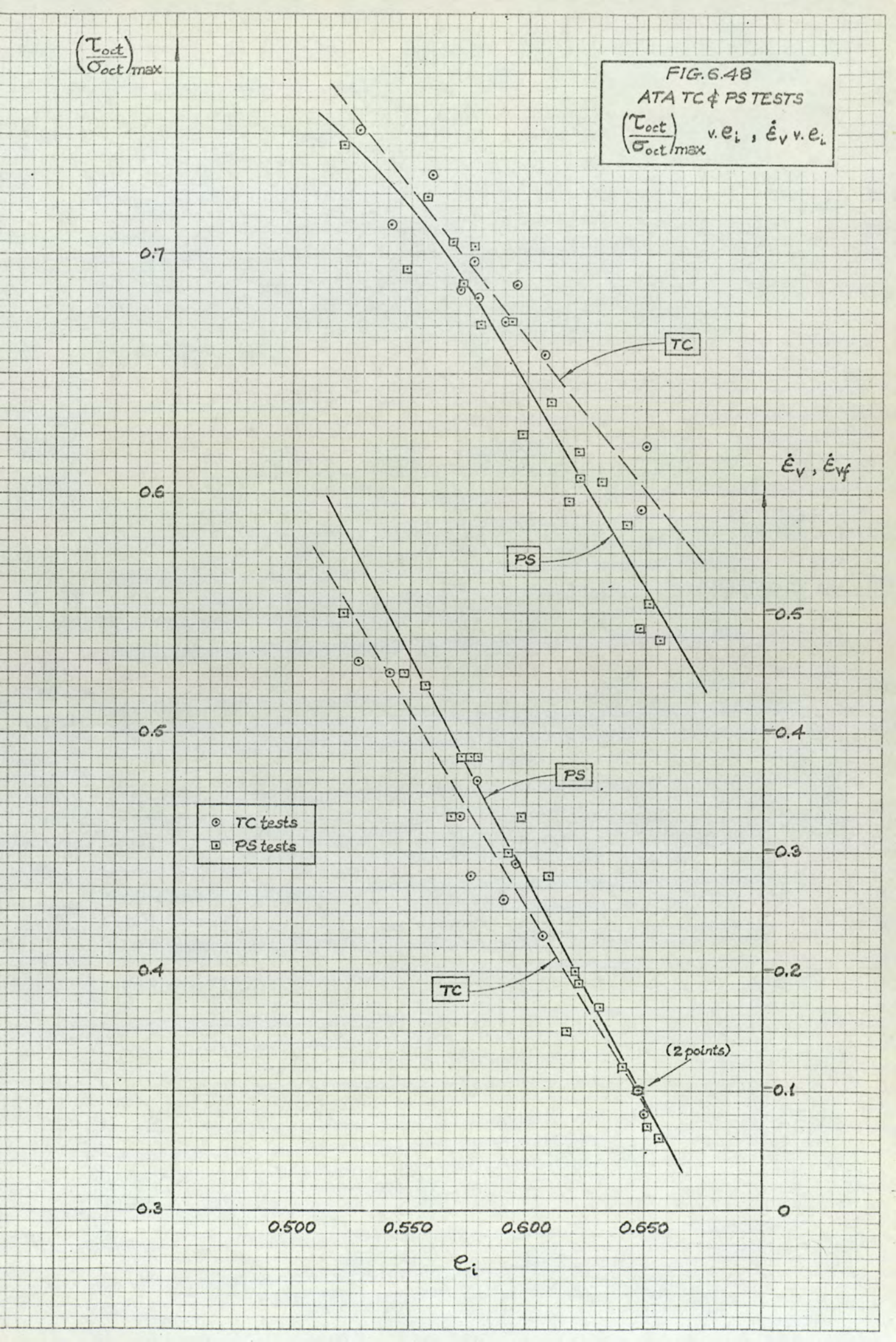
FIG. 6.48
ATA TC & PS TESTS
$\left(\frac{\tau_{oct}}{\sigma_{oct}}\right)_{max}$ v. e_i , $\dot{\varepsilon}_v$ v. e_i
$\left(\frac{\tau_{oct}}{\sigma_{oct}}\right)_{max}$
0.7
0.6
0.5
0.4
0.3
TC
PS
PS
TC
TC tests
PS tests
(2 points)
$\dot{\varepsilon}_v$, $\dot{\varepsilon}_{vf}$
0.5
0.4
0.3
0.2
0.1
0
0.500
0.550
0.600
0.650
e_i

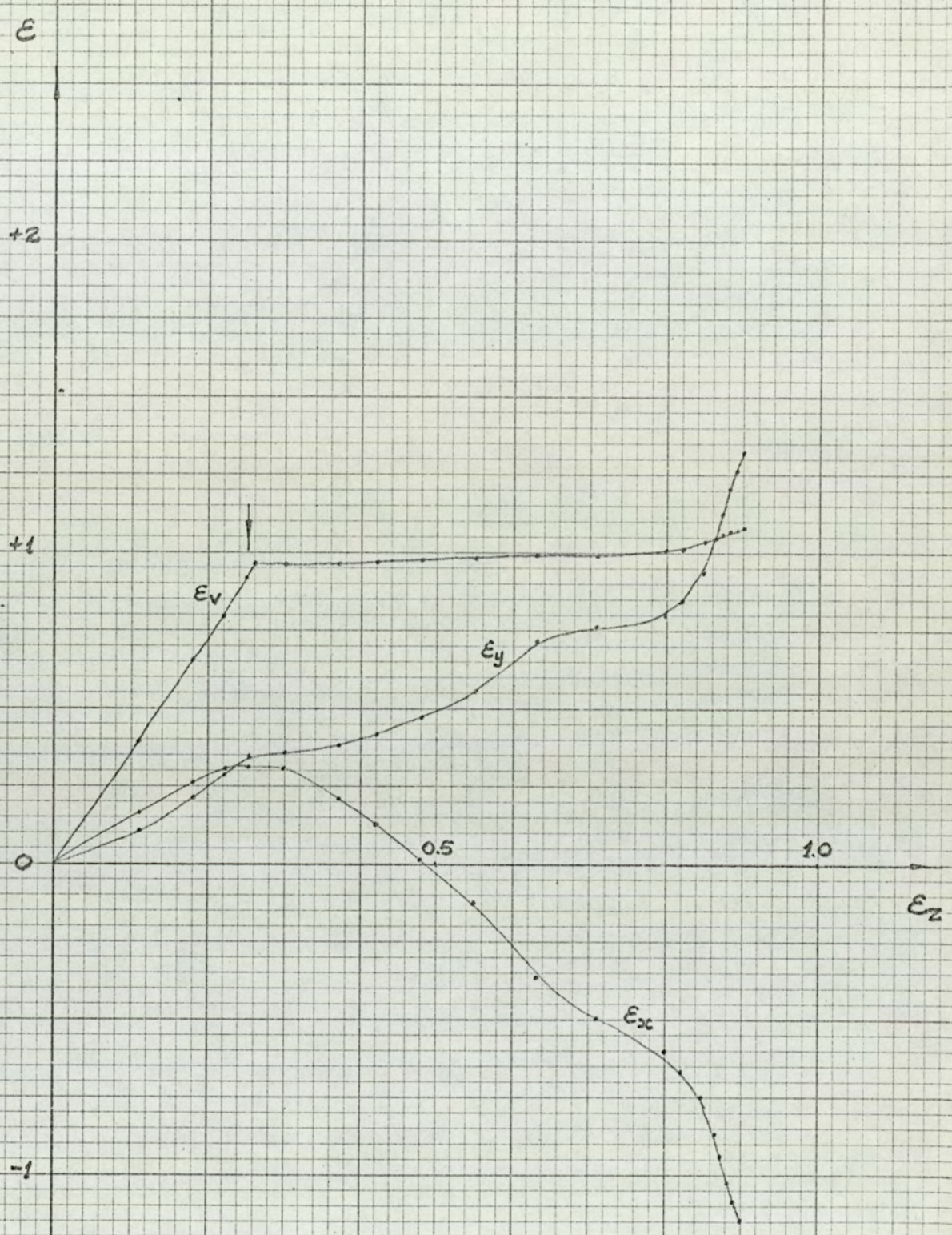

FIG. 6.49
ATA INT 2
CONSOLIDATION
ε v. ε_z

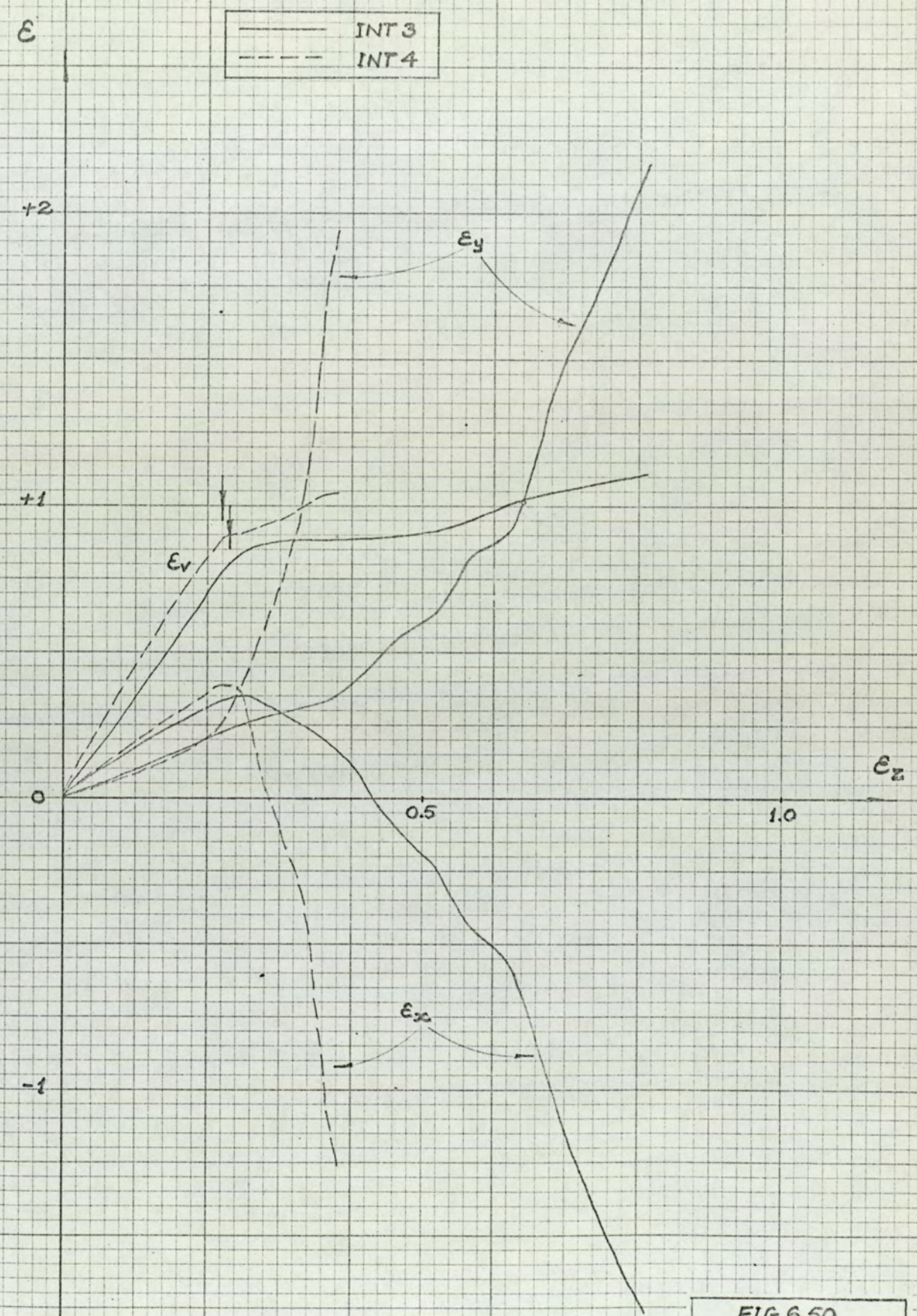

FIG. 6.50
ATA INT 3, 4
CONSOLIDATION
ε v. ε_z

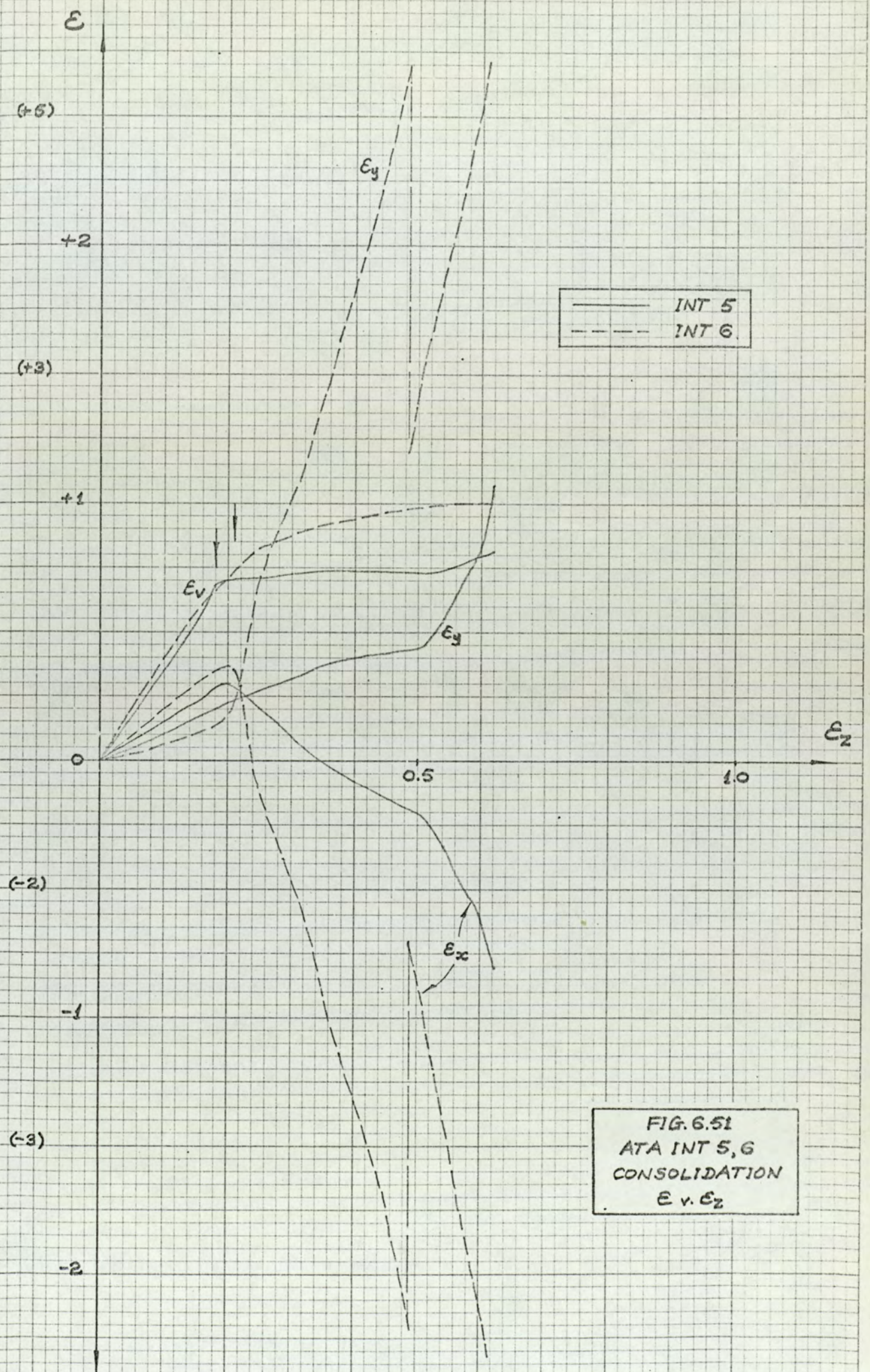

FIG. 6.51
ATA INT 5, 6
CONSOLIDATION
ε v. ε_z

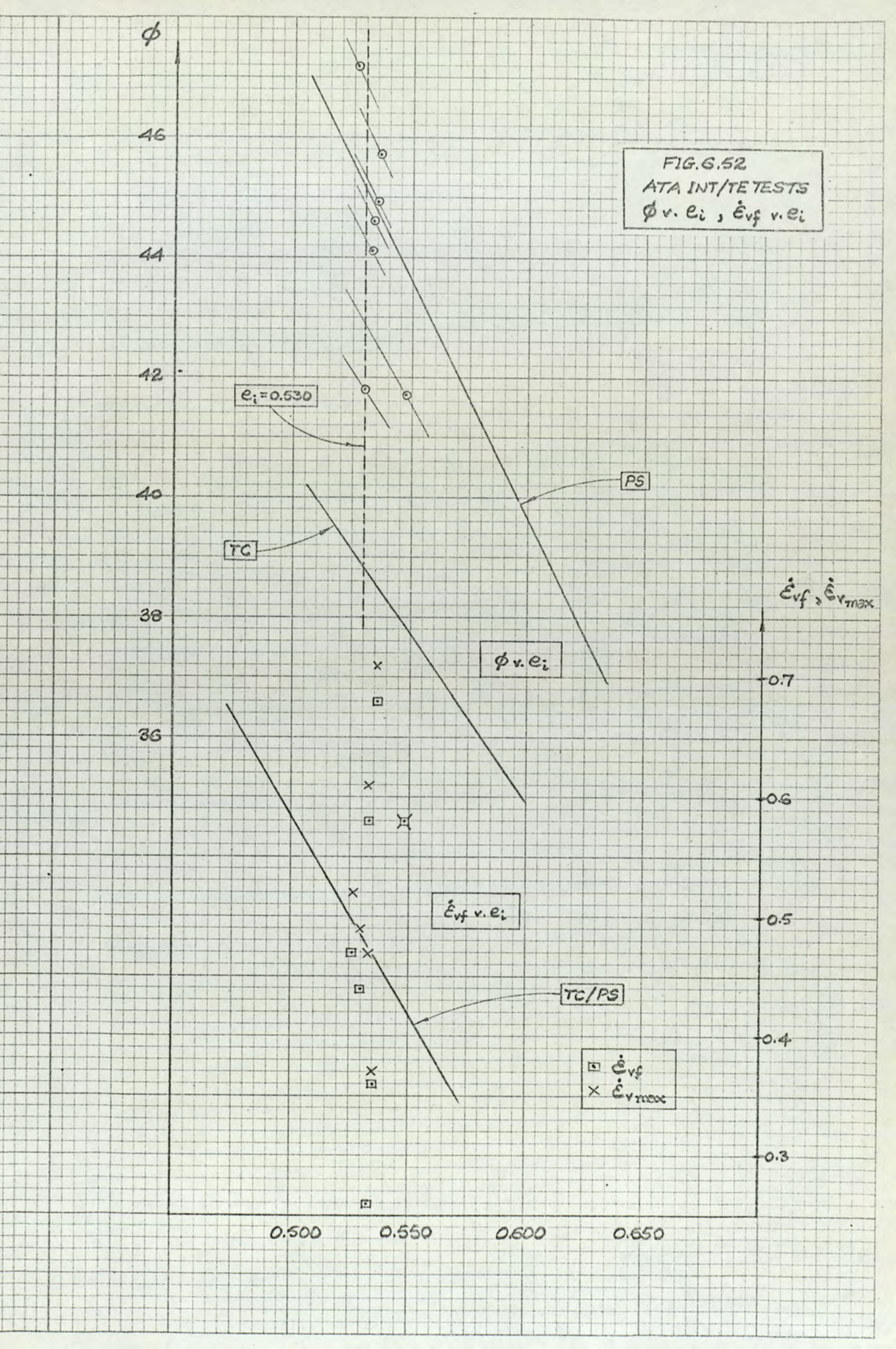
FIG. 6.52
ATA INT/TE TESTS
ϕ v. e_i , $\dot{\varepsilon}_{vf}$ v. e_i
ϕ
46
44
42
40
38
36
$e_i = 0.530$
PS
TC
ϕ v. e_i
$\dot{\varepsilon}_{vf}$ v. e_i
TC/PS
$\dot{\varepsilon}_{vf}$
$\dot{\varepsilon}_{v\,max}$
$\dot{\varepsilon}_{vf}$, $\dot{\varepsilon}_{v\,max}$
0.7
0.6
0.5
0.4
0.3
0.500
0.550
0.600
0.650

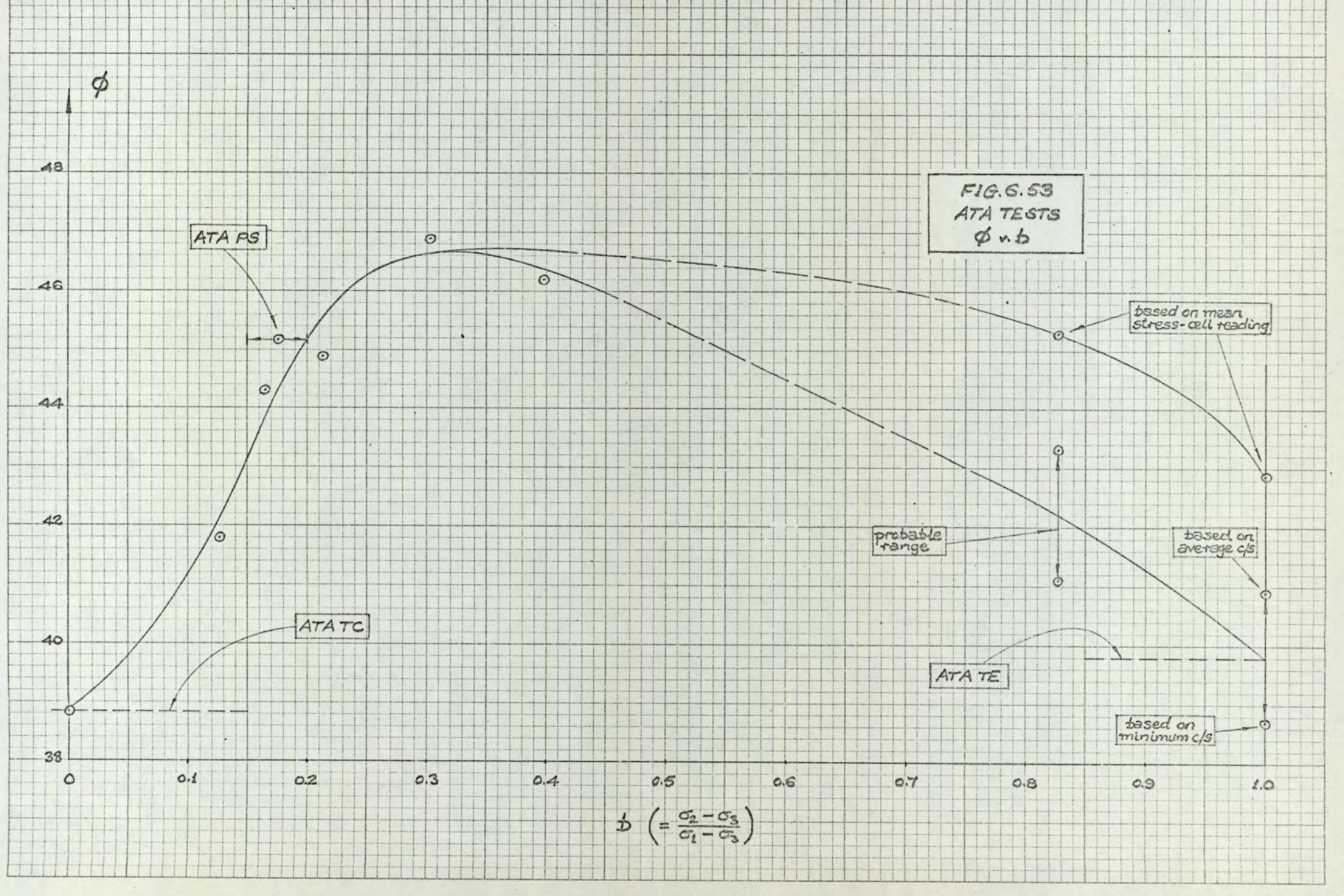
φ
48
46
44
42
40
38
0
0.1
0.2
0.3
0.4
0.5
0.6
0.7
0.8
0.9
1.0
b (= σ2 − σ3 / σ1 − σ3)
FIG. 6.53
ATA TESTS
φ v. b
ATA PS
ATA TC
ATA TE
based on mean stress-cell reading
probable range
based on average c/s
based on minimum c/s

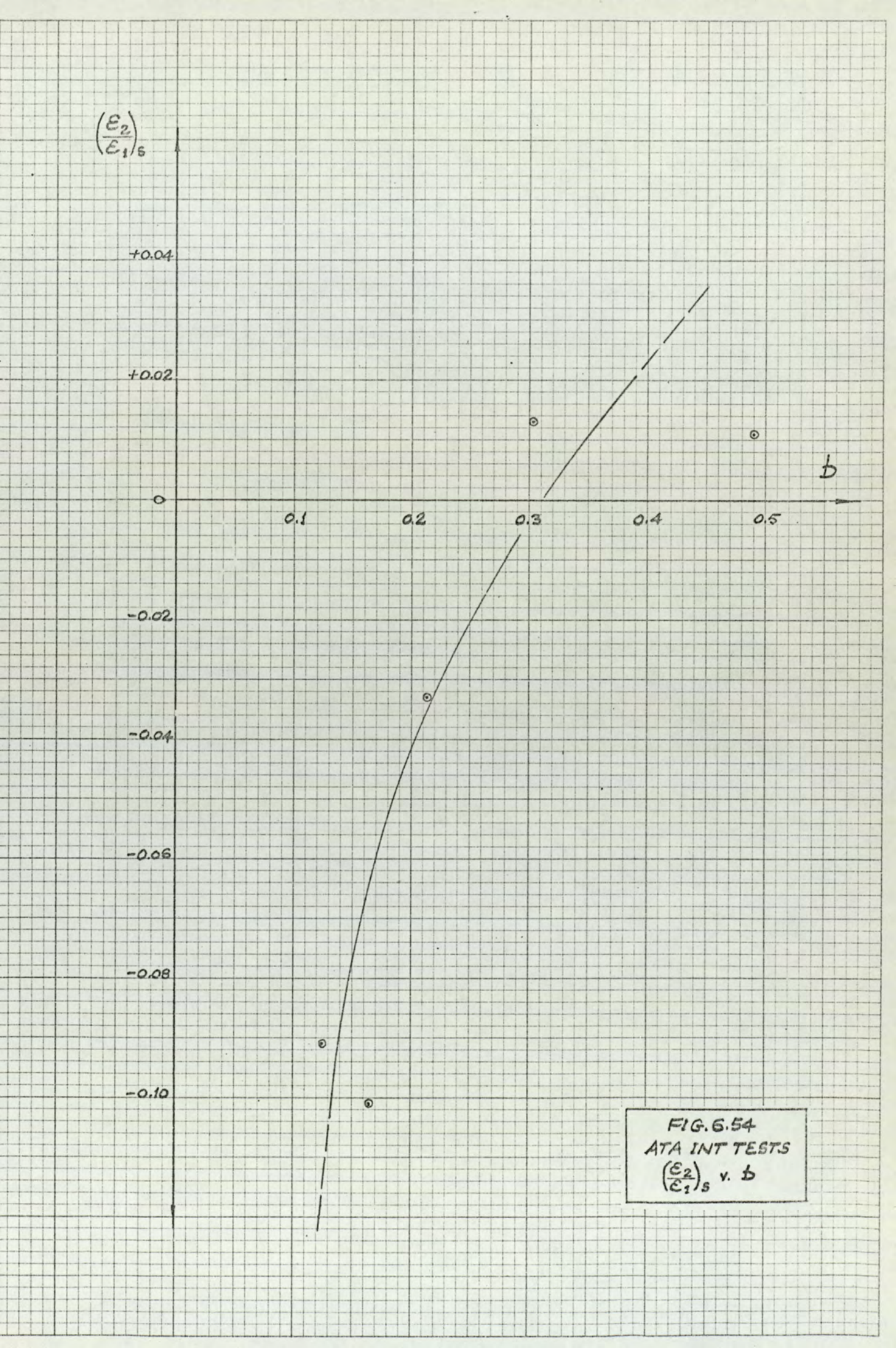

FIG. 6.54
ATA INT TESTS
$\left(\frac{\varepsilon_2}{\varepsilon_1}\right)_s$ v. b

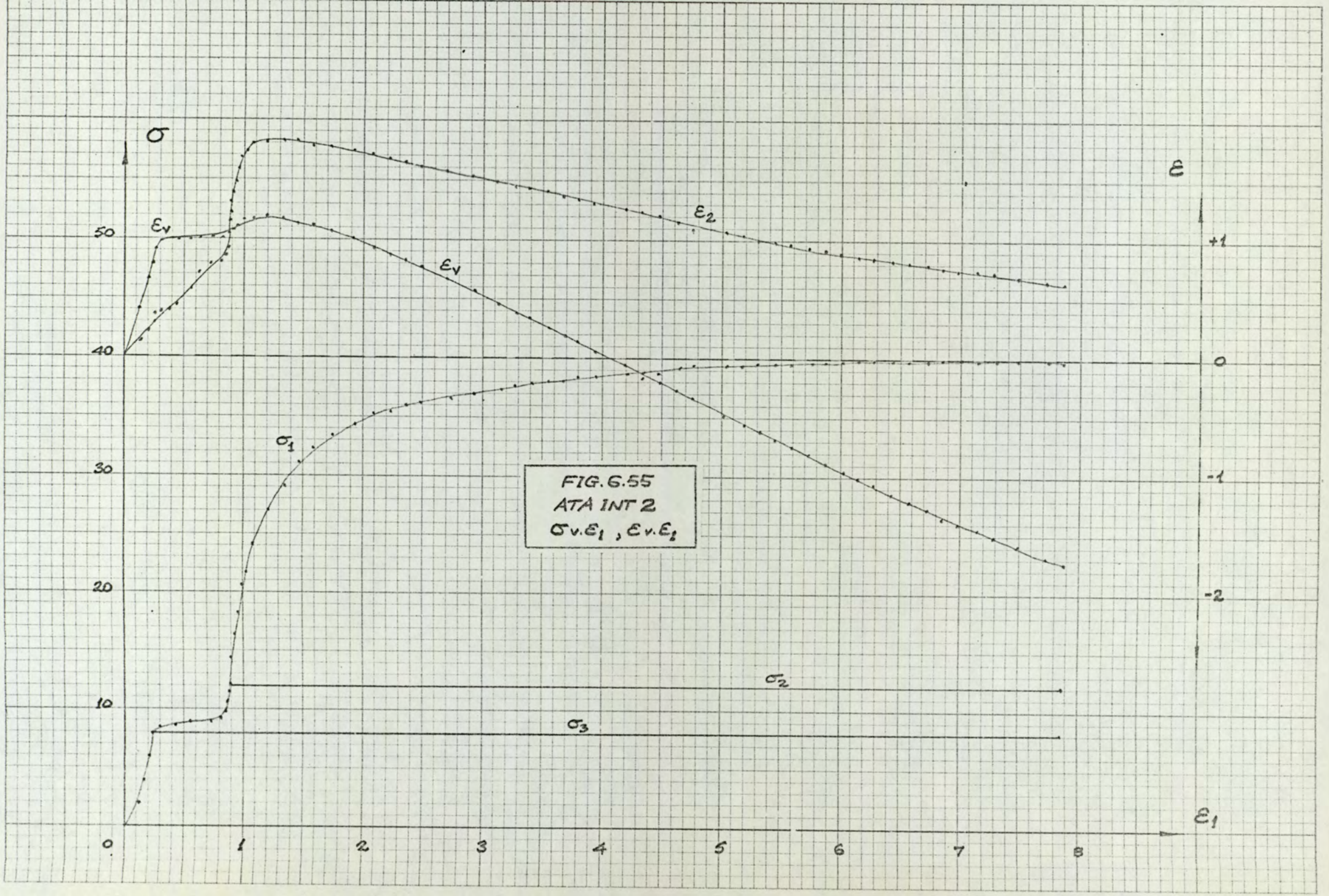

FIG. 6.55
ATA INT 2
$\sigma_v \cdot \varepsilon_1$, $\varepsilon_v \cdot \varepsilon_1$

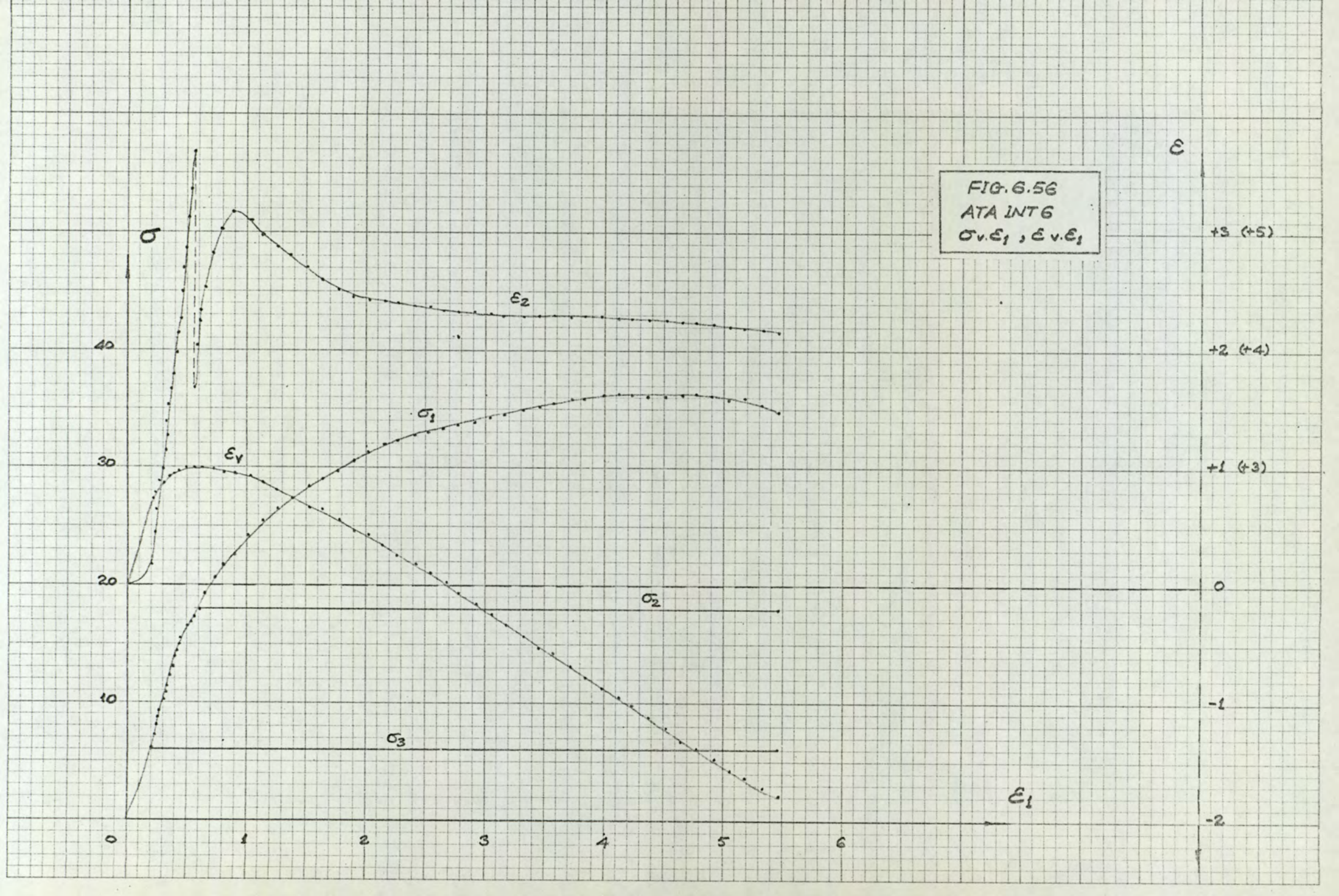
FIG. 6.56
ATA INT 6
σ v. ε1 , ε v. ε1
σ
ε
ε2
σ1
ε1
σ2
σ3
40
30
20
10
0
1
2
3
4
5
6
+3 (+5)
+2 (+4)
+1 (+3)
0
-1
-2
ε1

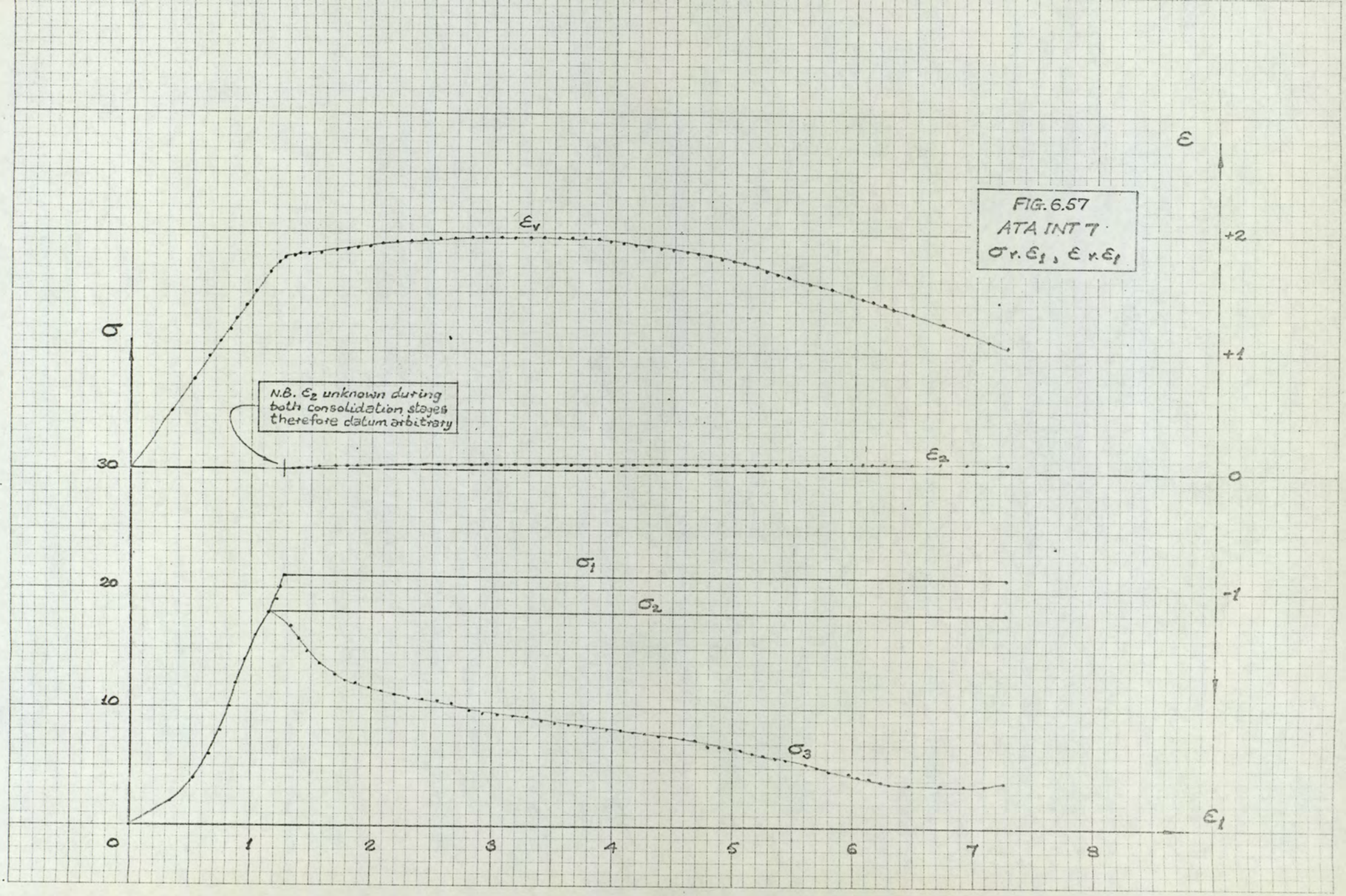
FIG. 6.57
ATA INT 7
σv. ε1 , ε v. ε1
σ
ε
εv
ε2
ε1
σ1
σ2
σ3
N.B. ε2 unknown during both consolidation stages therefore datum arbitrary
30
20
10
0
+2
+1
0
-1
1
2
3
4
5
6
7
8

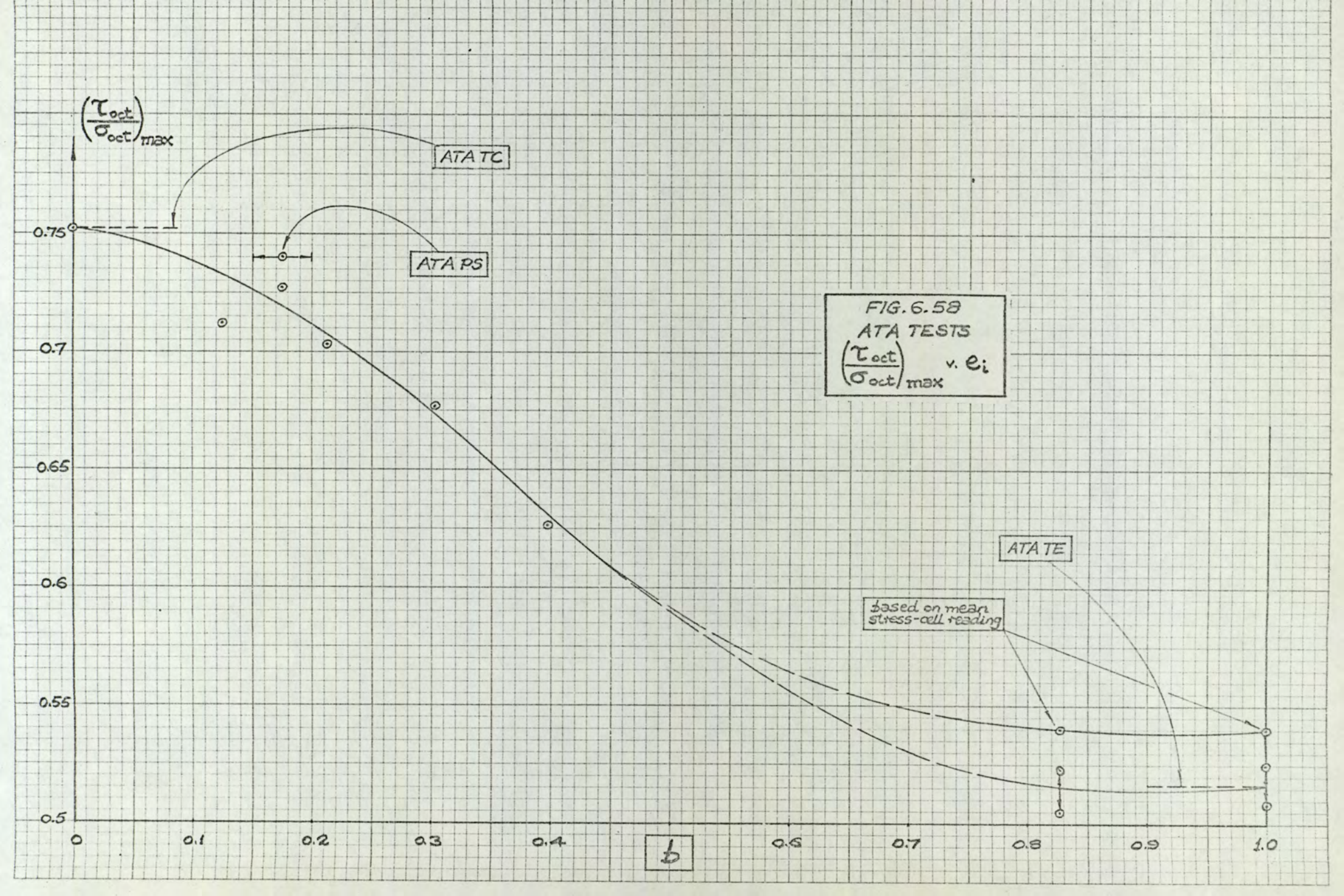

FIG. 6.58
ATA TESTS
$\left(\frac{\tau_{oct}}{\sigma_{oct}}\right)_{max}$ v. e_i

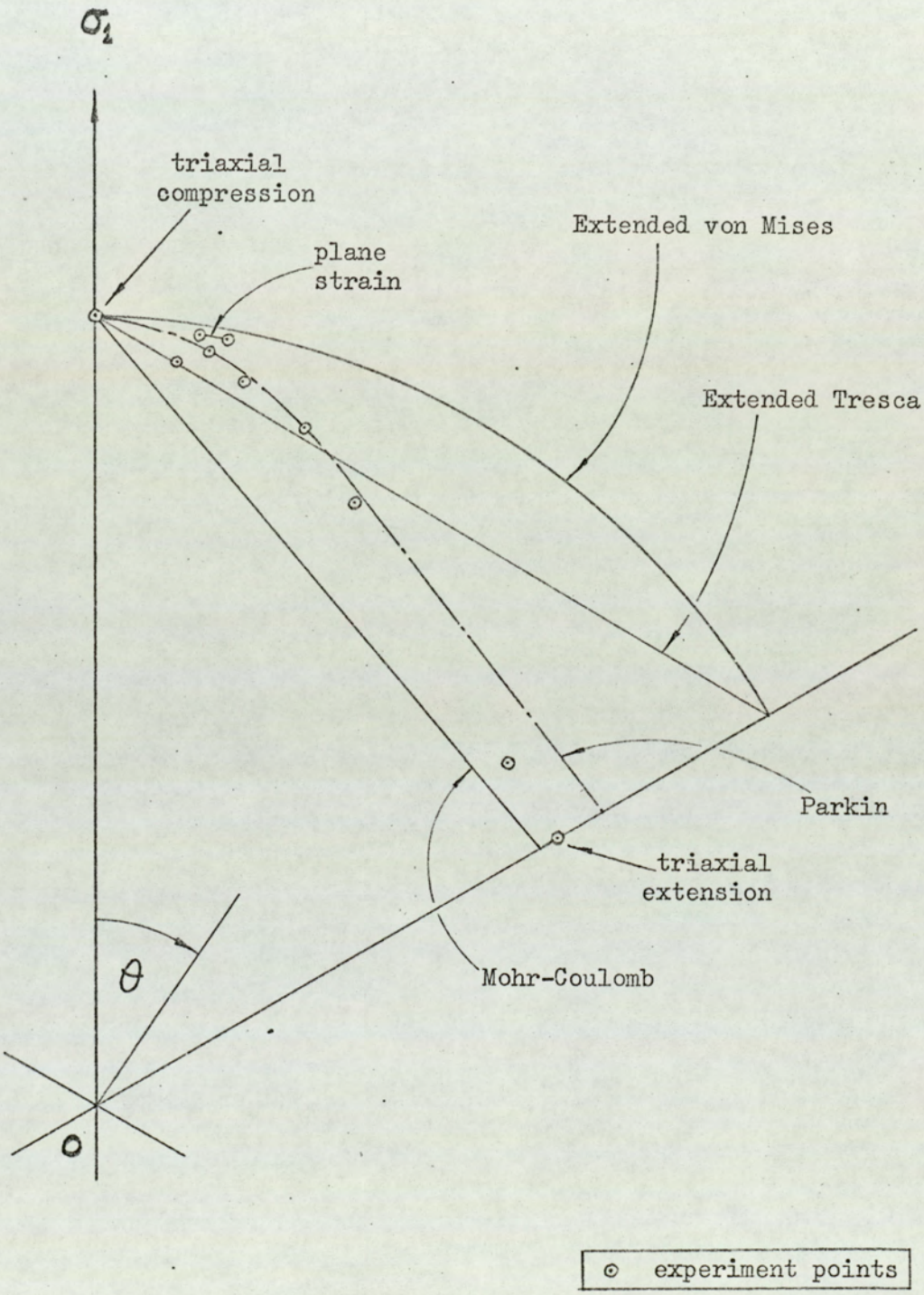

FIG.6.59
Failure Criteria

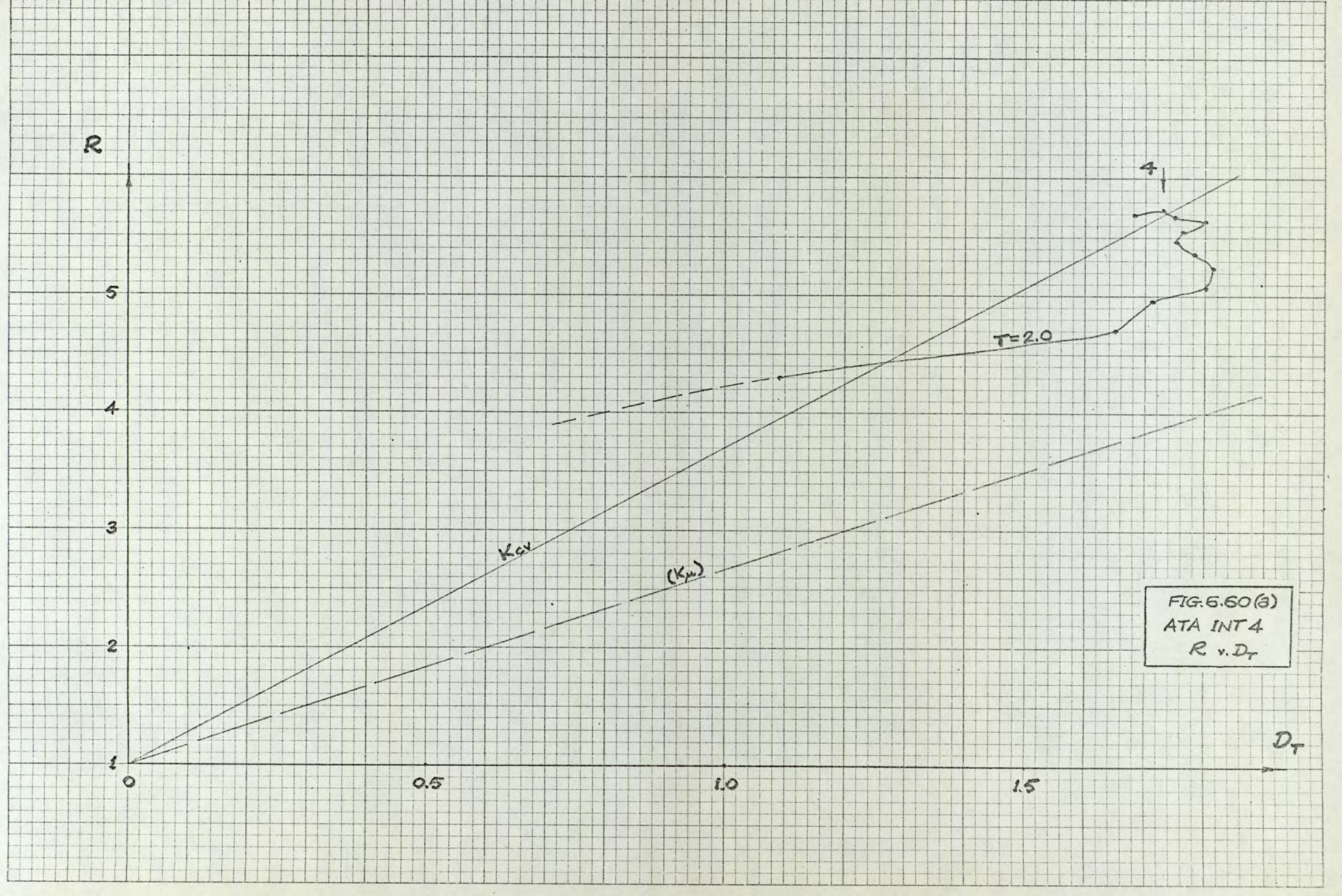

FIG. 6.60(8)
ATA INT 4
R v. D_T

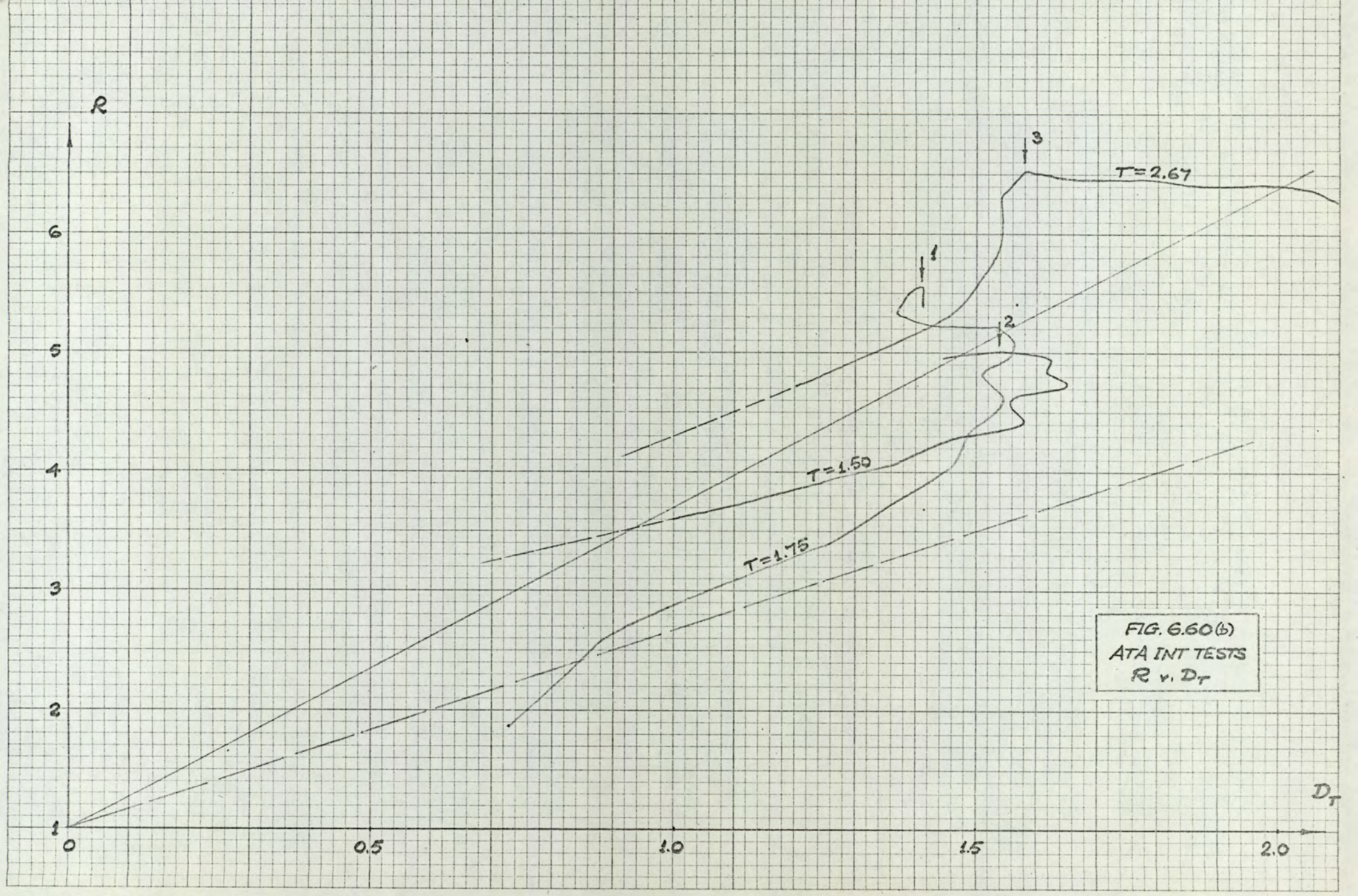

FIG. 6.60(b)
ATA INT TESTS
R v. D_T

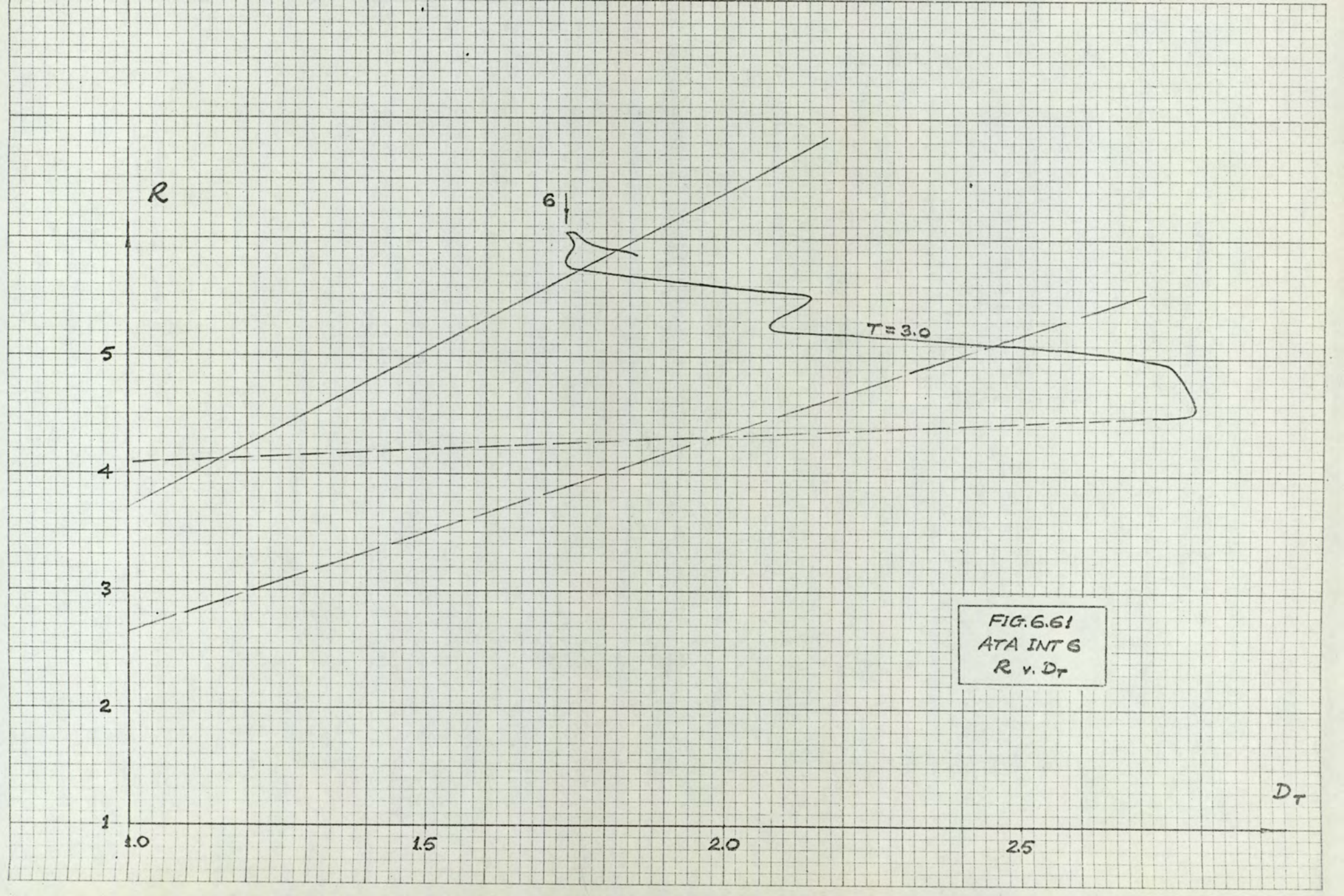

FIG. 6.61
ATA INT 6
R v. D_T

CHAPTER SEVEN

FIGURES

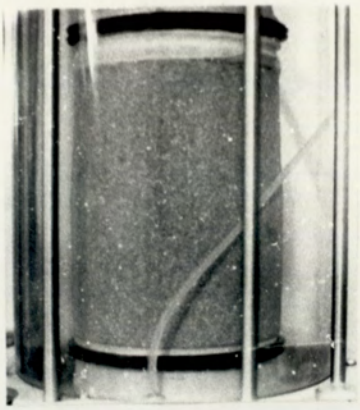

(a) ε_a = 3.14 %

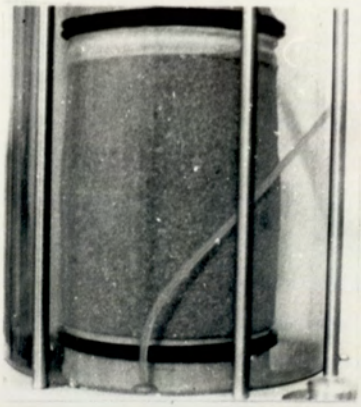

(b) ε_a = 8.57 %

(c) ε_a = 13.26 %

FIG.7.1
CYLINDRICAL TRIAXIAL COMPRESSION TEST
CYL TC 21, e_i = 0.560, $(\varepsilon_a)_f$ = 8.11 %

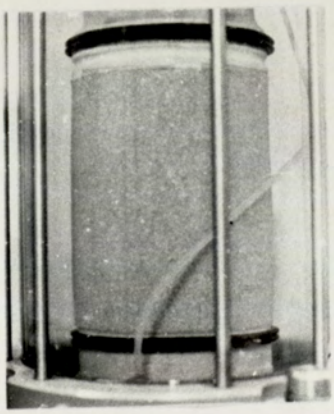

(a) ε_a = 3.31 %

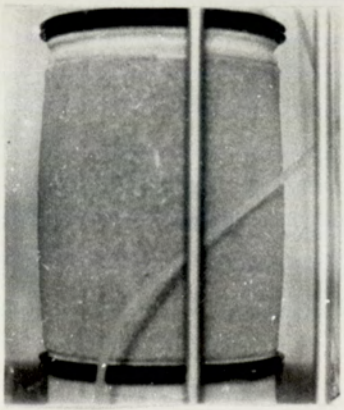

(b) ε_a = 9.12 %

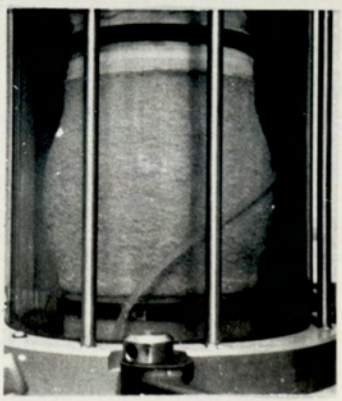

(c) ε_a = 22.01 %

FIG.7.2
CYLINDRICAL TRIAXIAL COMPRESSION TEST
CYL TC 17, e_i = 0.543, $(\varepsilon_a)_f$ = 8.66 %

(a) ε_a = -1.86 %

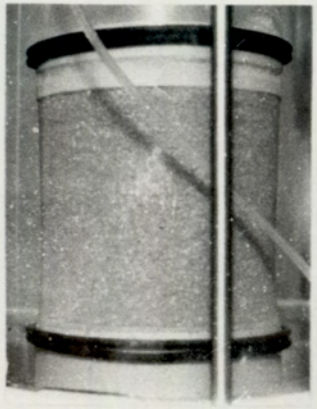

(b) ε_a = -2.64 %

(c) ε_a = -4.00 %

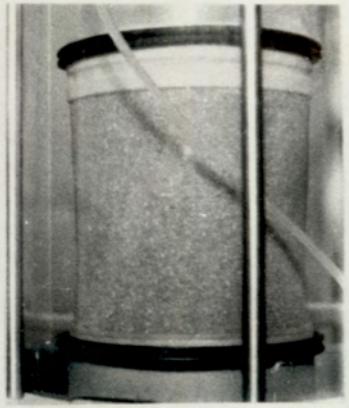

(d) ε_a = -5.62 %

(e) ε_a = -7.04 %

FIG.7.3
CYLINDRICAL TRIAXIAL EXTENSION TEST
CYL TE 6, e_i = 0.649, $(\varepsilon_a)_f$ = -8.01 %

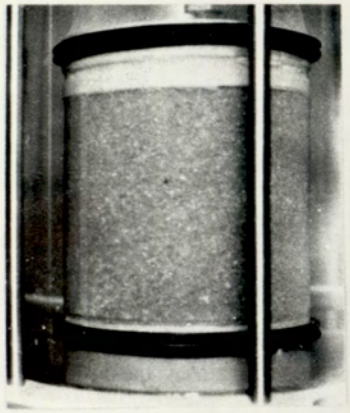

(a) ε_a = 0.0 %

(b) ε_a = -2.05 %

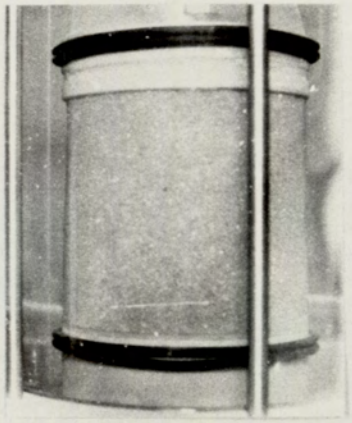

(c) ε_a = -3.54 %

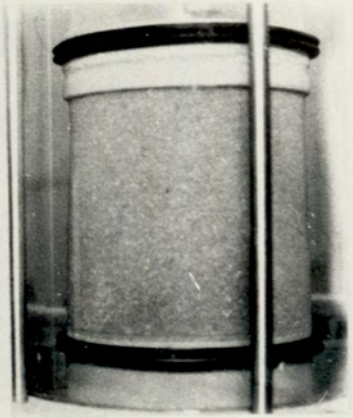

(d) ε_a = -4.98 %

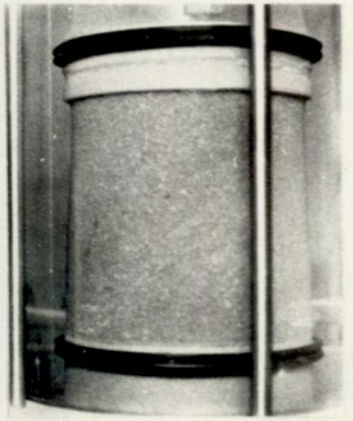

(e) ε_a = -6.39 %

FIG.7.4
CYLINDRICAL TRIAXIAL EXTENSION TEST
CYL TE 7, e_i = 0.624, $(\varepsilon_a)_f$ = -5.41 %

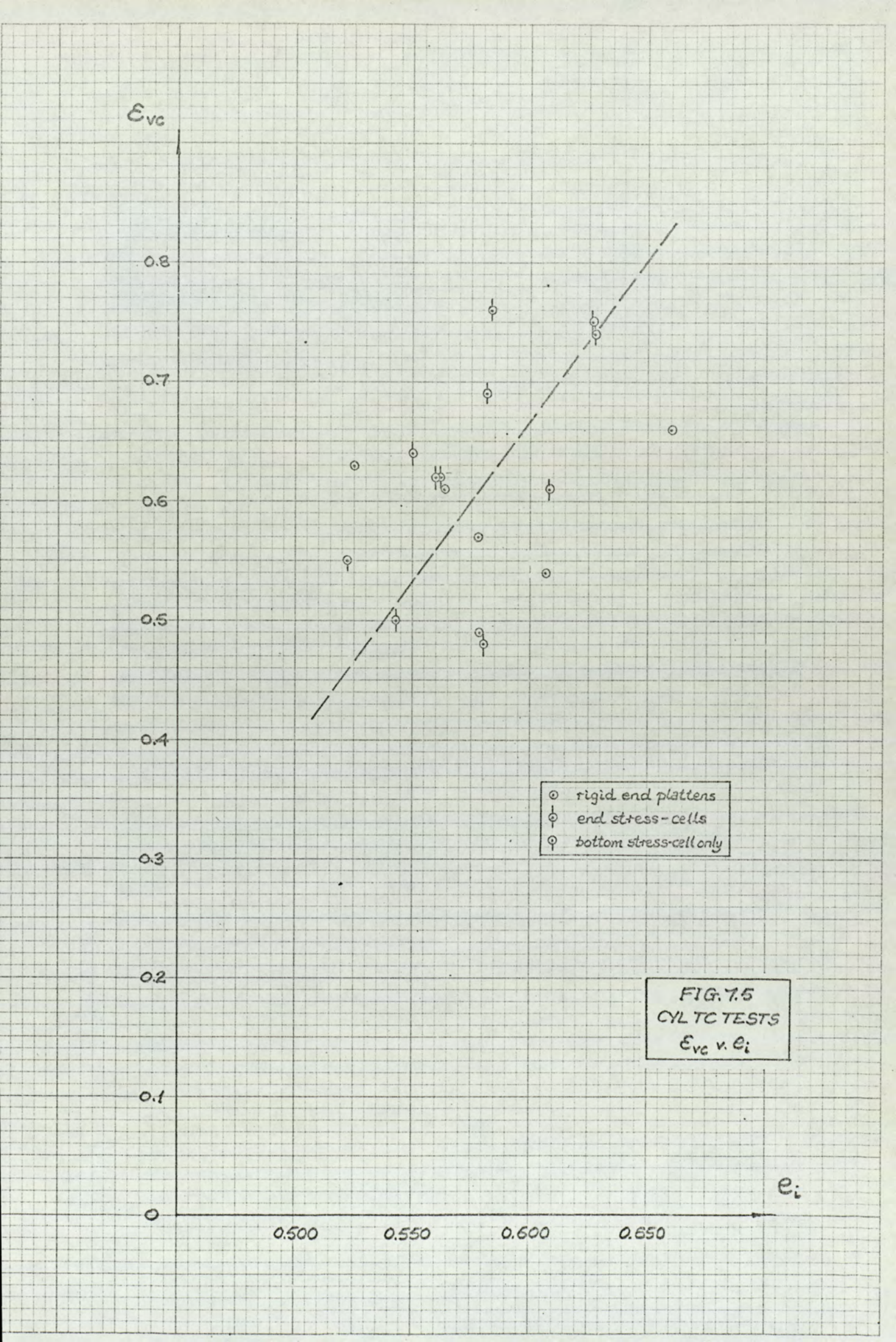

FIG. 7.5
CYL TC TESTS
ε_{vc} v. e_i

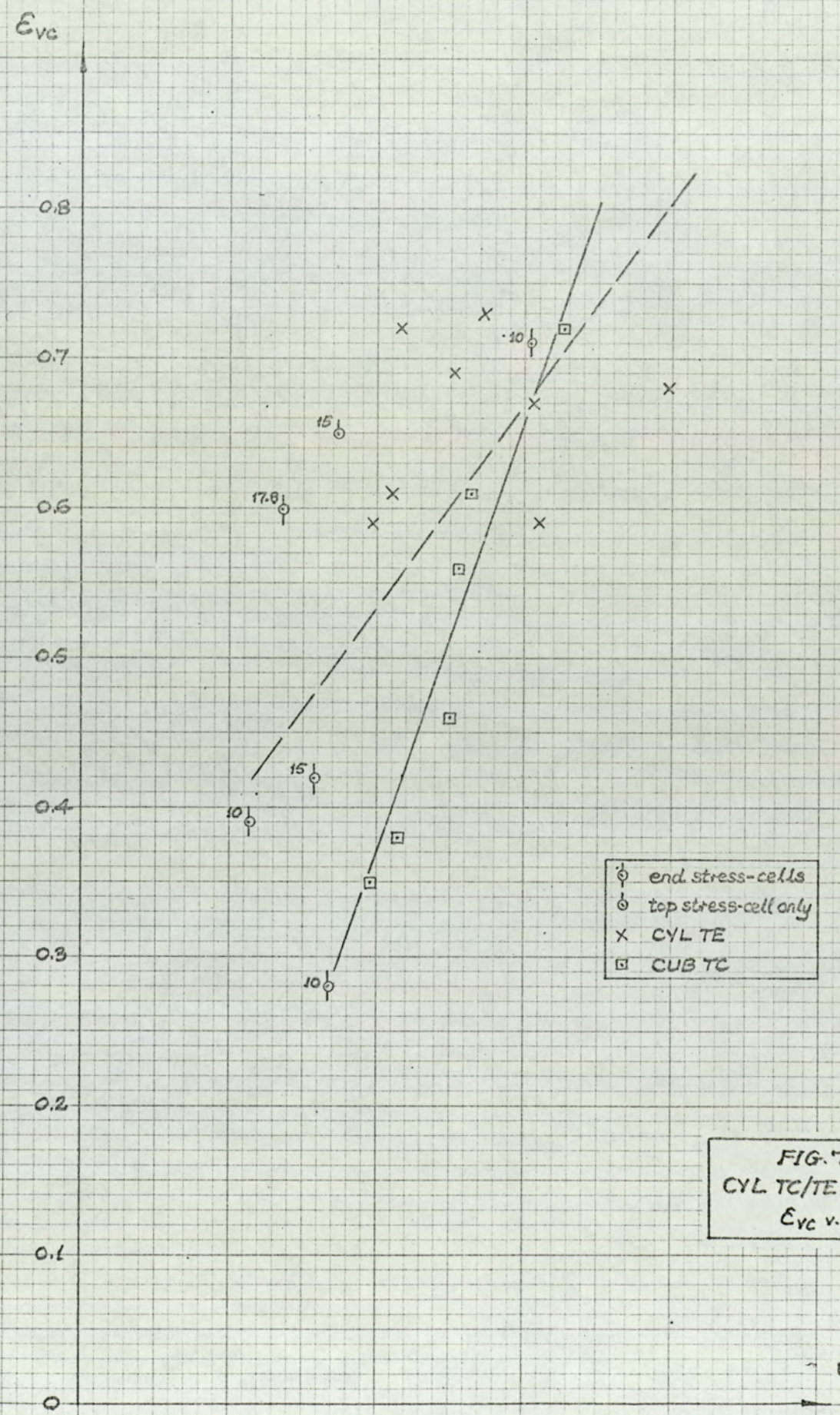

FIG. 7.6
CYL TC/TE, CUB TC
ε_{vc} v. e_i

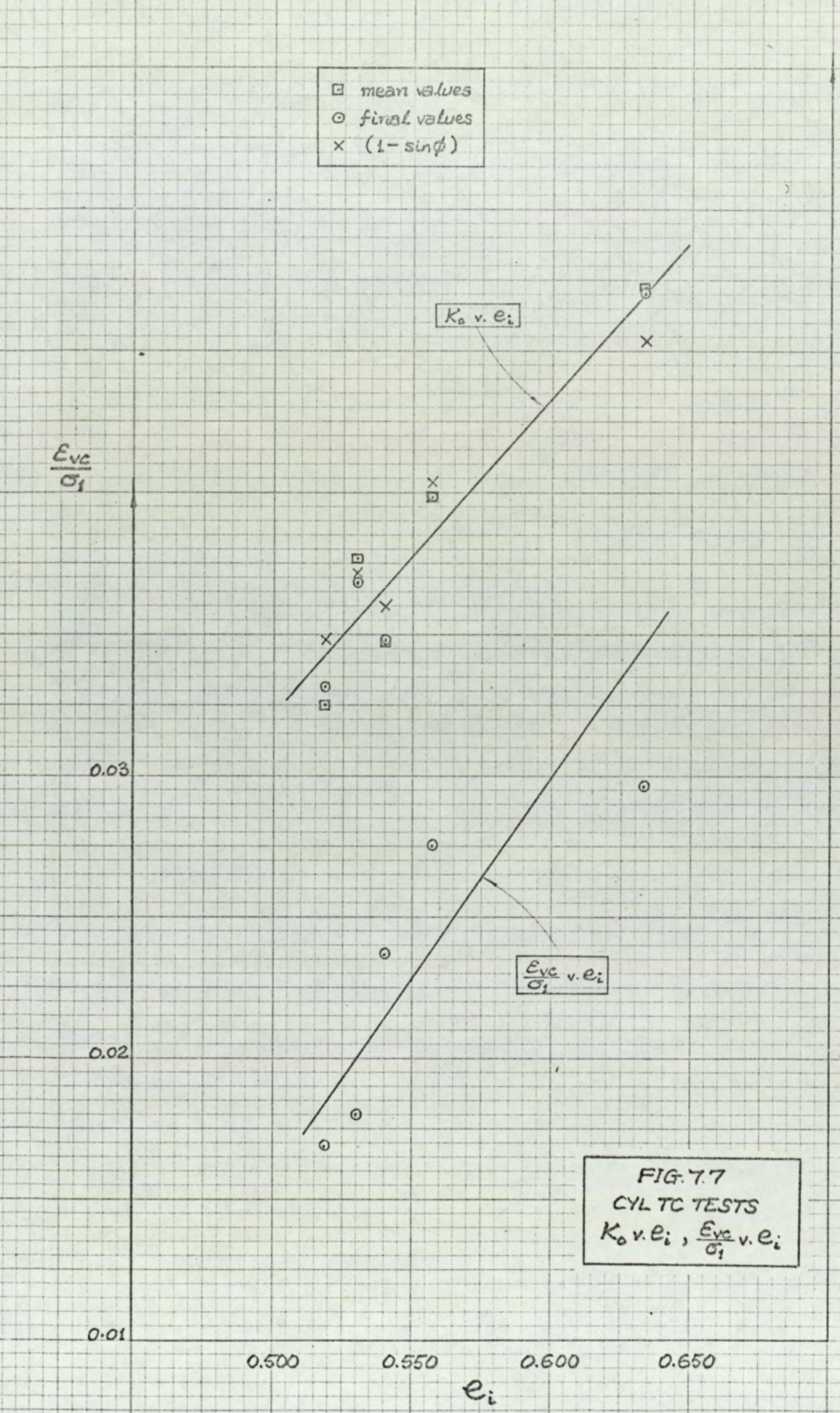

FIG. 7.7
CYL TC TESTS
K_o v. e_i , $\frac{\varepsilon_{vc}}{\sigma_1}$ v. e_i

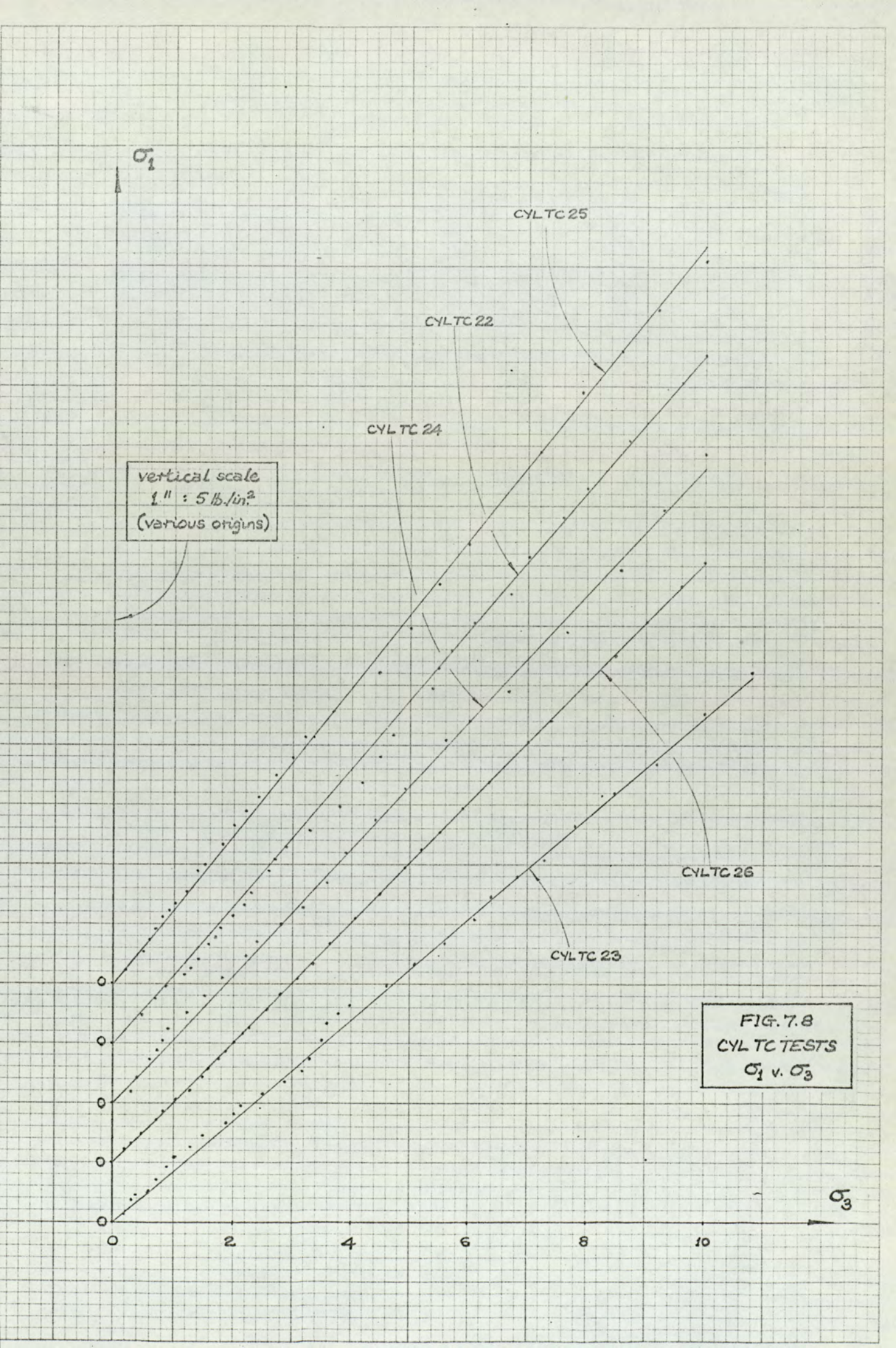

FIG. 7.8
CYL TC TESTS
σ_1 v. σ_3

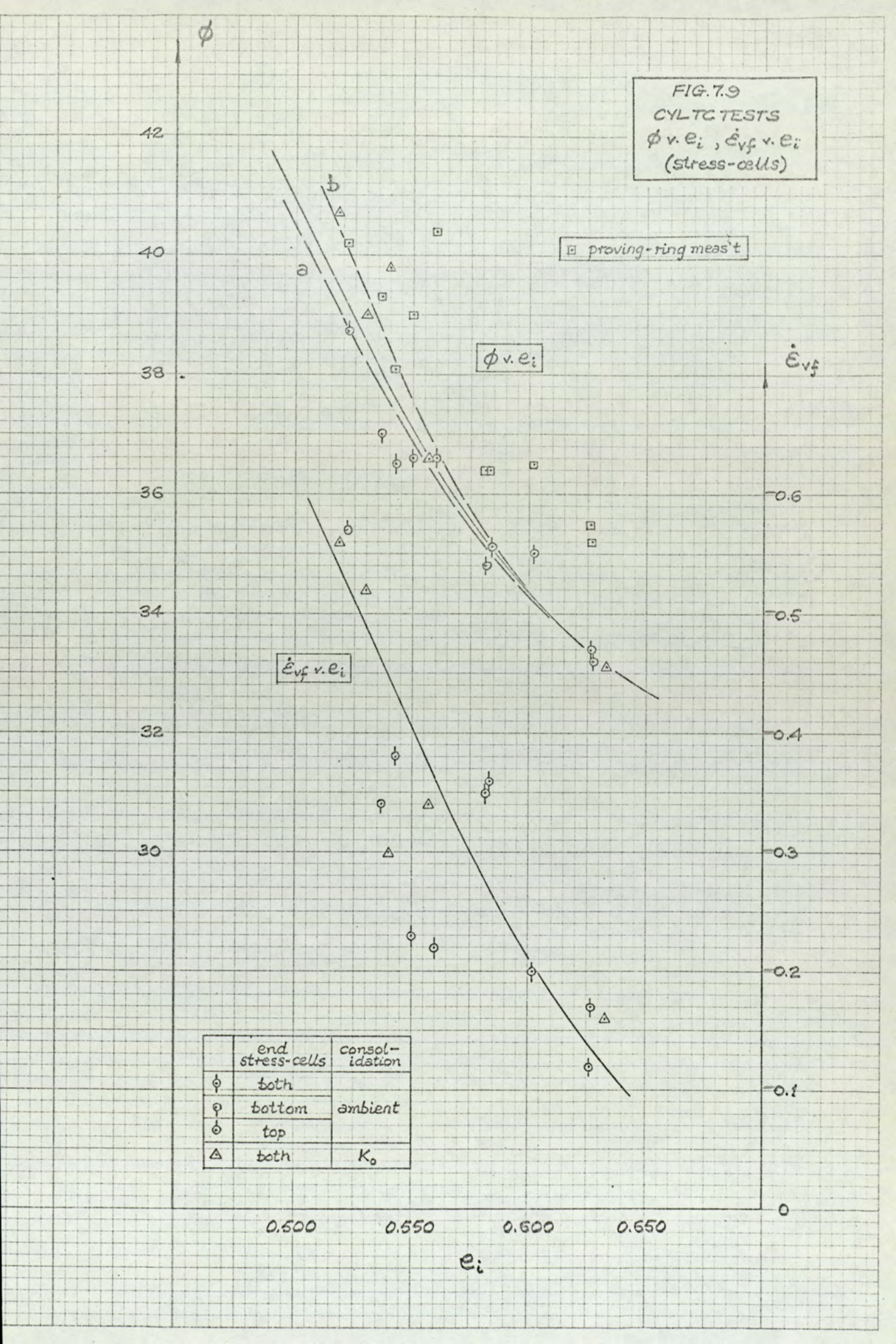
FIG. 7.9
CYL TC TESTS
ϕ v. e_i , $\dot{\varepsilon}_{vf}$ v. e_i
(stress-cells)
ϕ
42
40
38
36
34
32
30
b
a
proving-ring meas't
ϕ v. e_i
$\dot{\varepsilon}_{vf}$ v. e_i
$\dot{\varepsilon}_{vf}$
0.6
0.5
0.4
0.3
0.2
0.1
0
0.500
0.550
0.600
0.650
e_i
end stress-cells
consol-idation
both
bottom
top
ambient
both
K_o

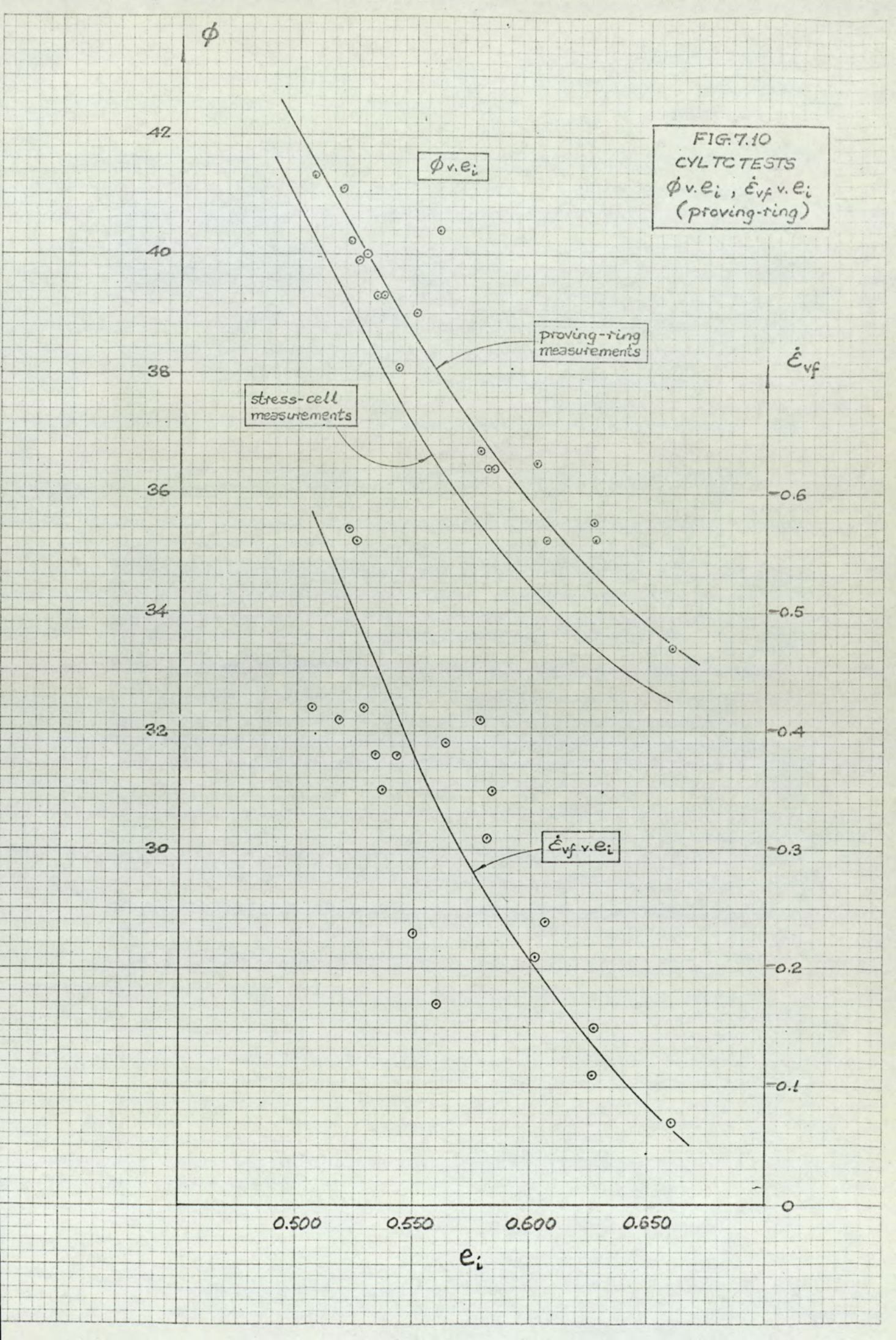

FIG. 7.10
CYL TC TESTS
ϕ v. e_i , $\dot{\varepsilon}_{vf}$ v. e_i
(proving-ring)

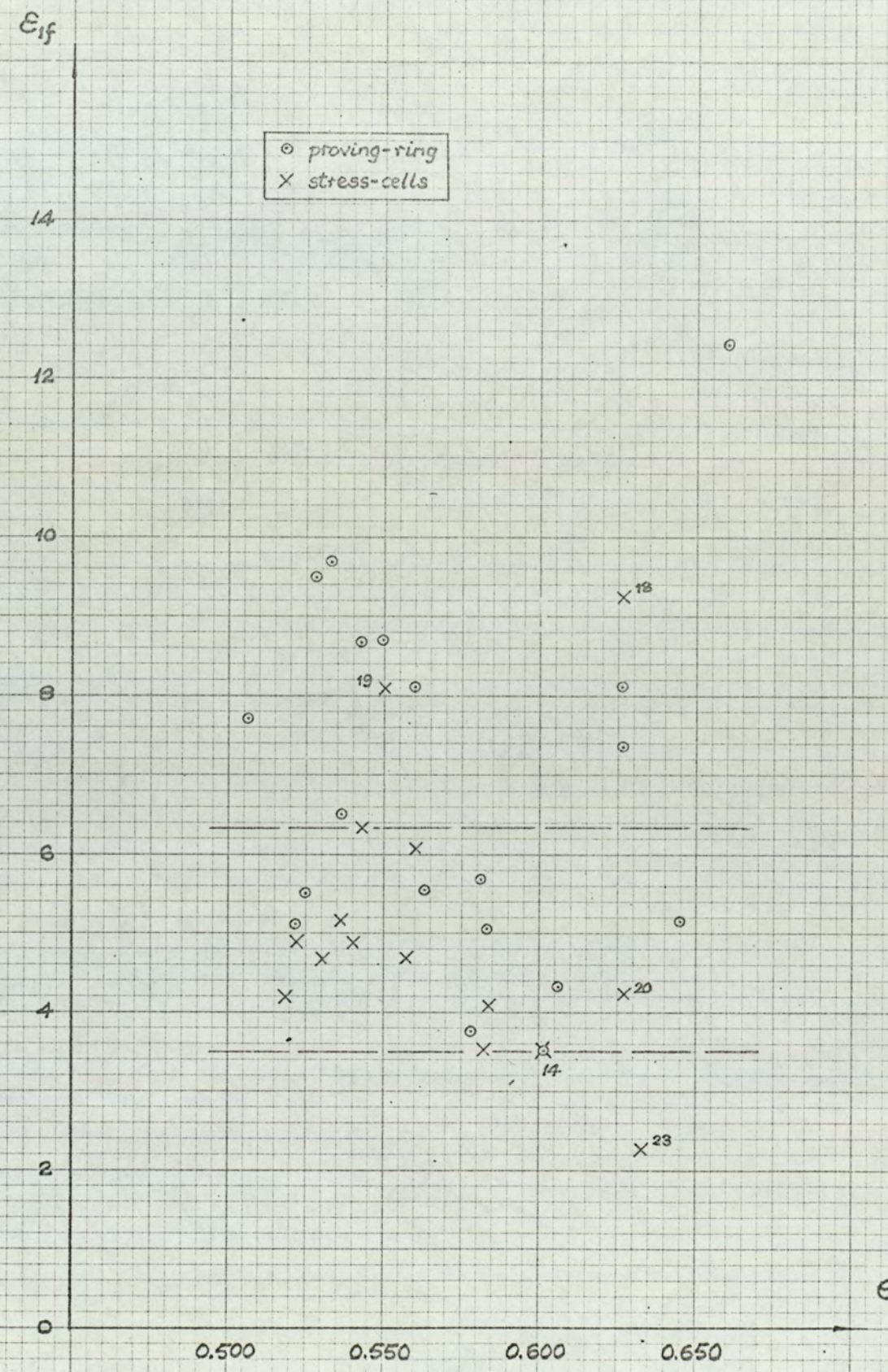

FIG. 7.11
CYL TC TESTS
ε_{1f} v. e_i

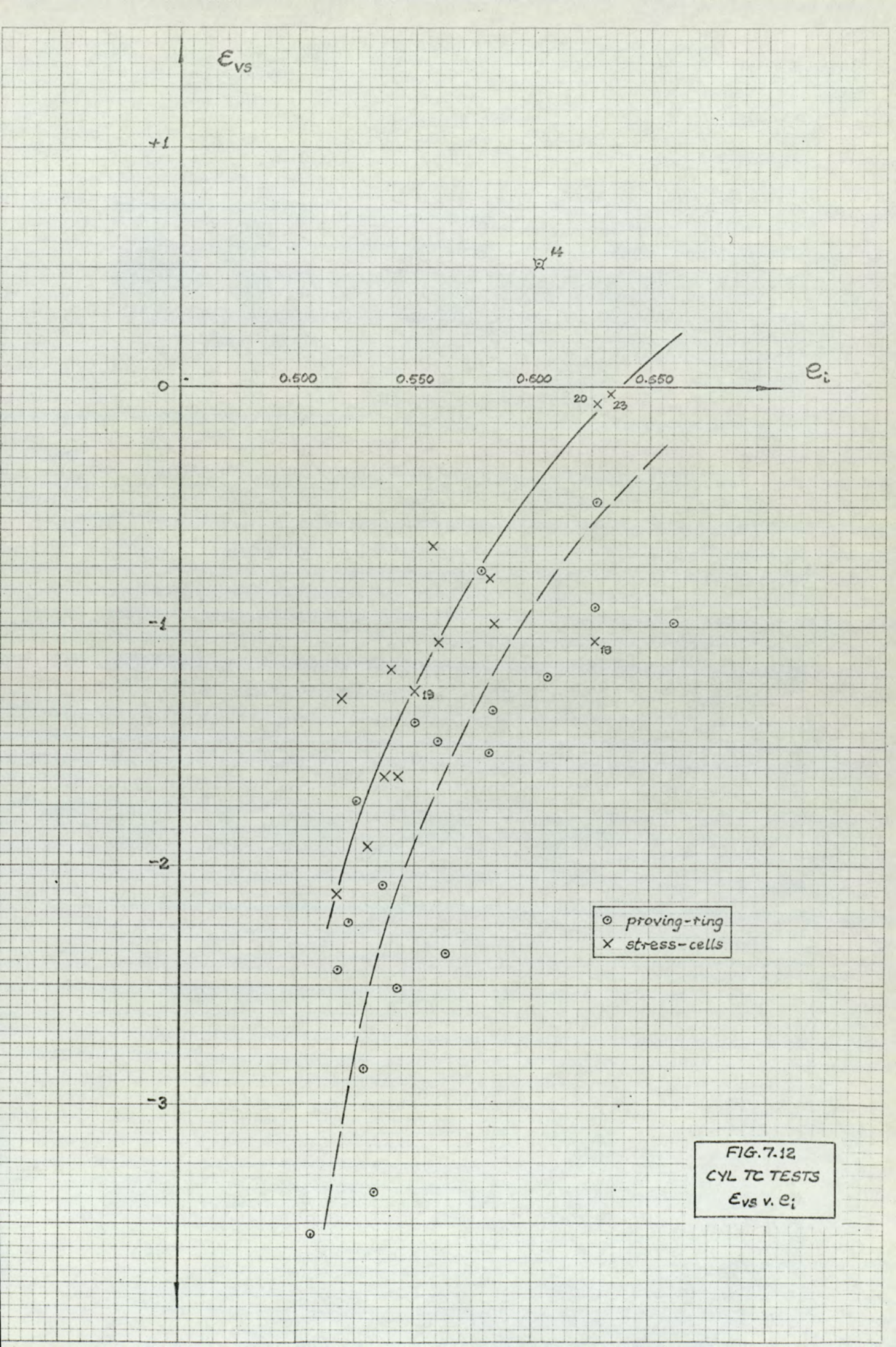

FIG. 7.12
CYL TC TESTS
ε_{vs} v. e_i

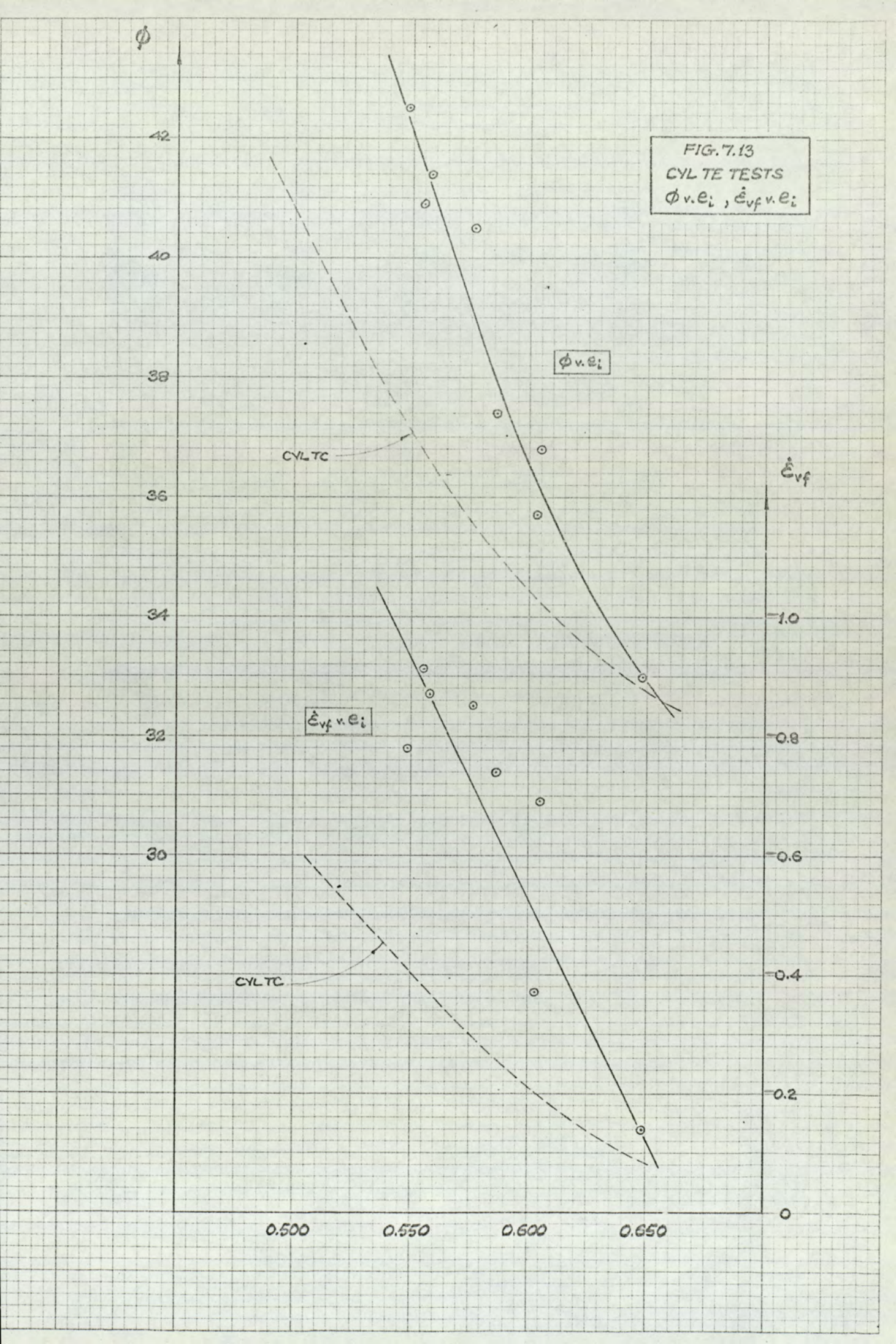
FIG. 7.13
CYL TE TESTS
ϕ v. e_i , $\dot{\varepsilon}_{vf}$ v. e_i
ϕ
42
40
38
36
34
32
30
ϕ v. e_i
CYL TC
$\dot{\varepsilon}_{vf}$
1.0
0.8
0.6
0.4
0.2
0
$\dot{\varepsilon}_{vf}$ v. e_i
CYL TC
0.500
0.550
0.600
0.650

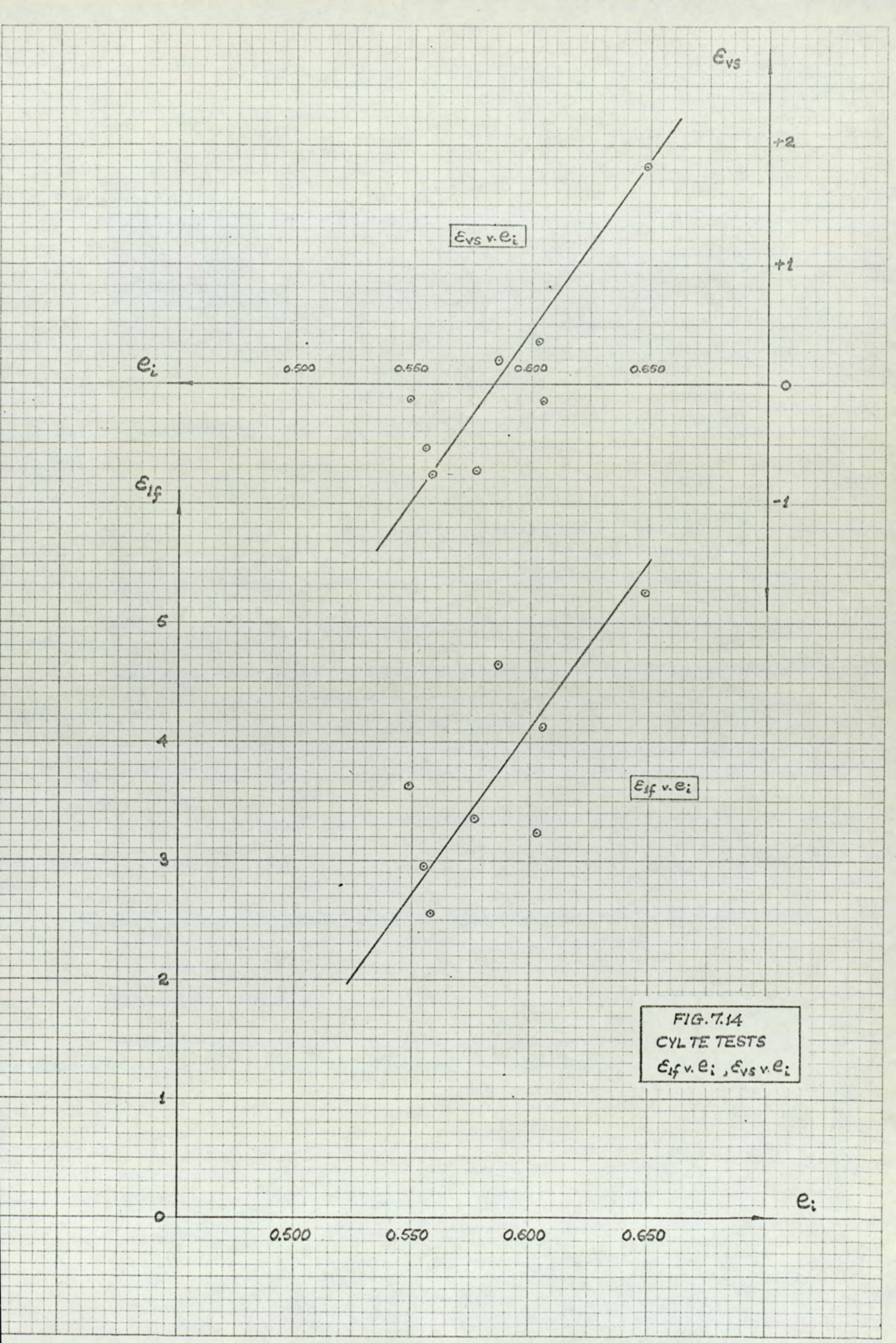

FIG. 7.14
CYL TE TESTS
ε_{1f} v. e_i , ε_{vs} v. e_i

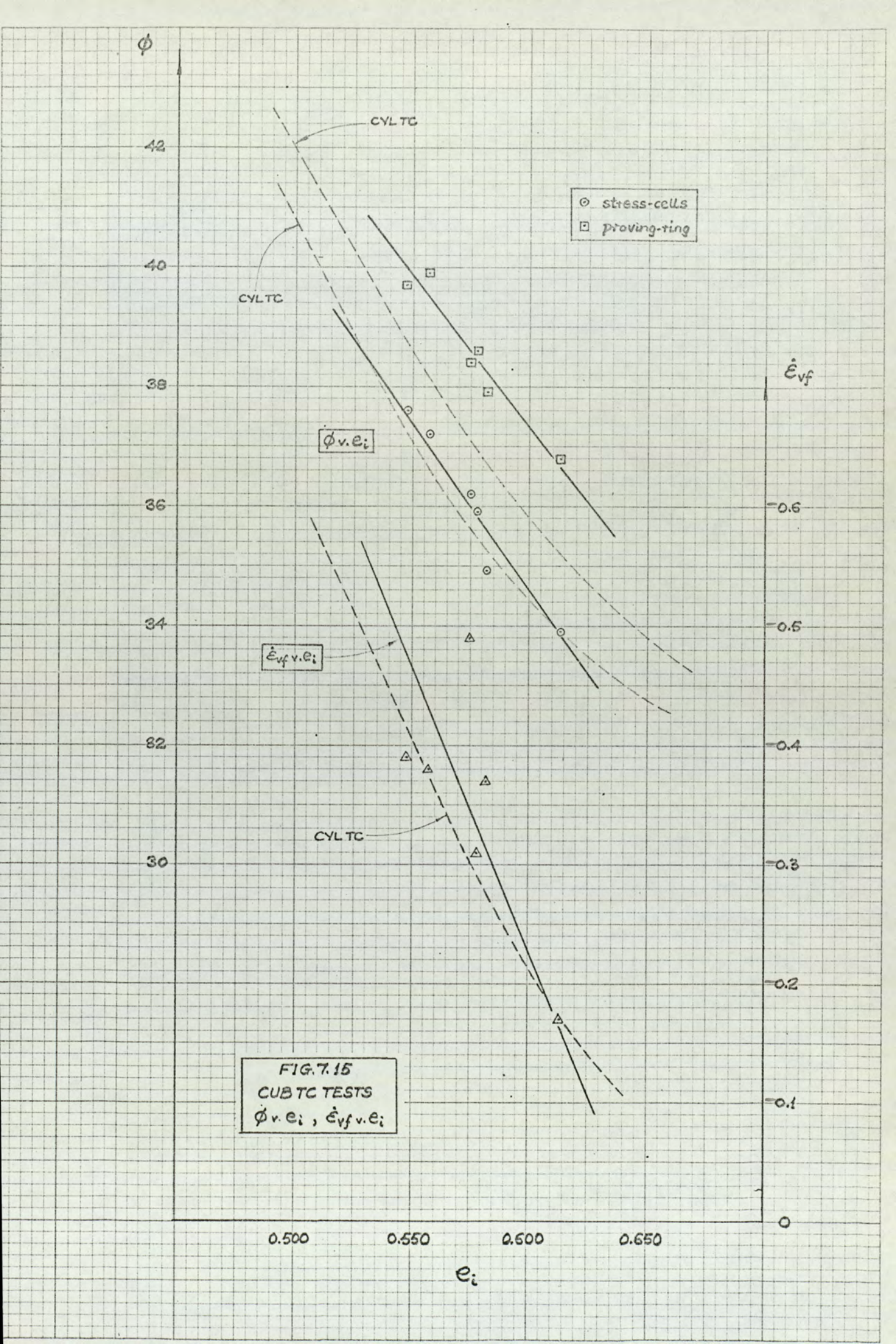

FIG. 7.15
CUB TC TESTS
ϕ v. e_i , $\dot{\varepsilon}_{vf}$ v. e_i

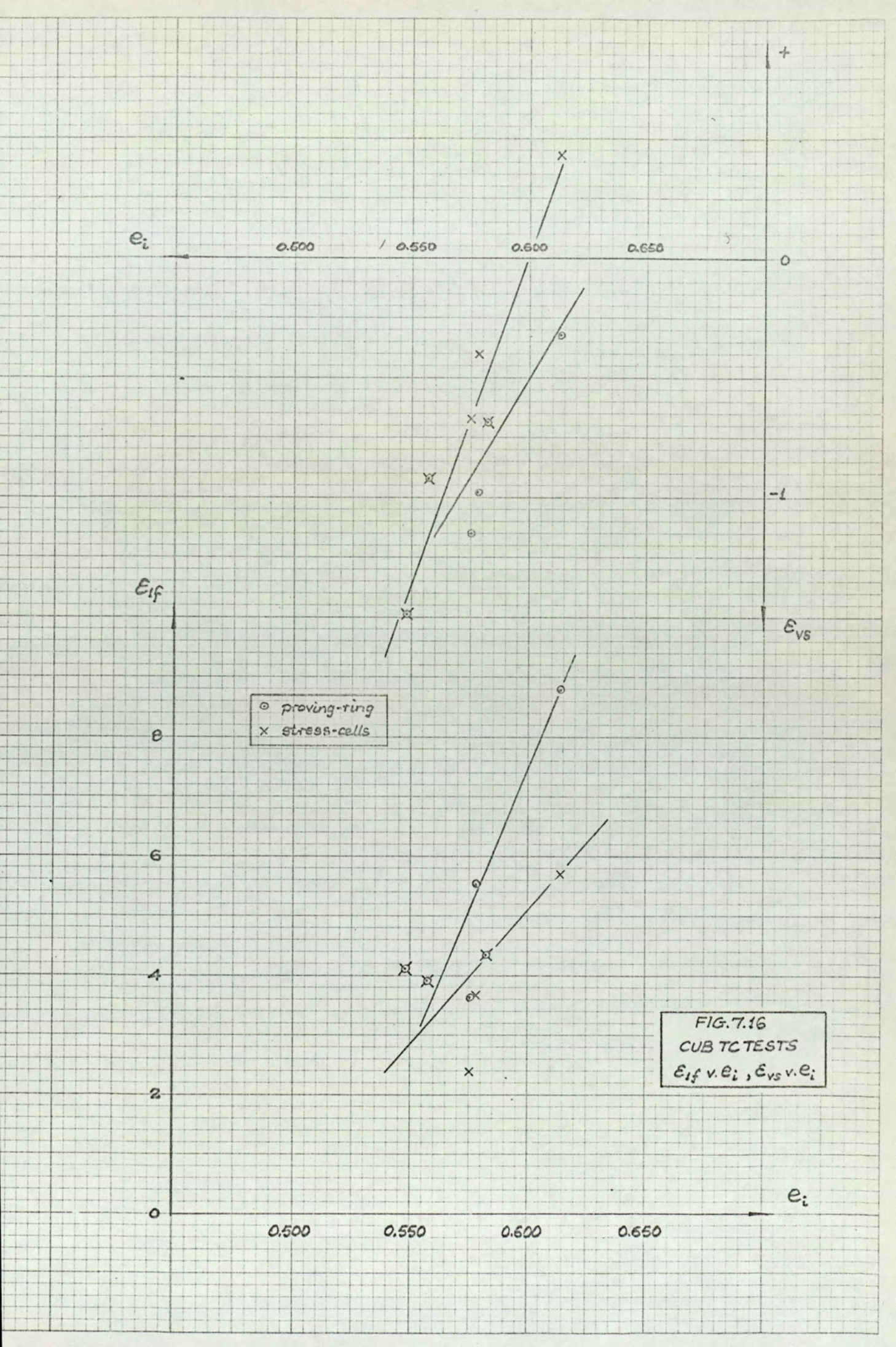

FIG. 7.16
CUB TC TESTS
ε_{1f} v. e_i , ε_{vs} v. e_i

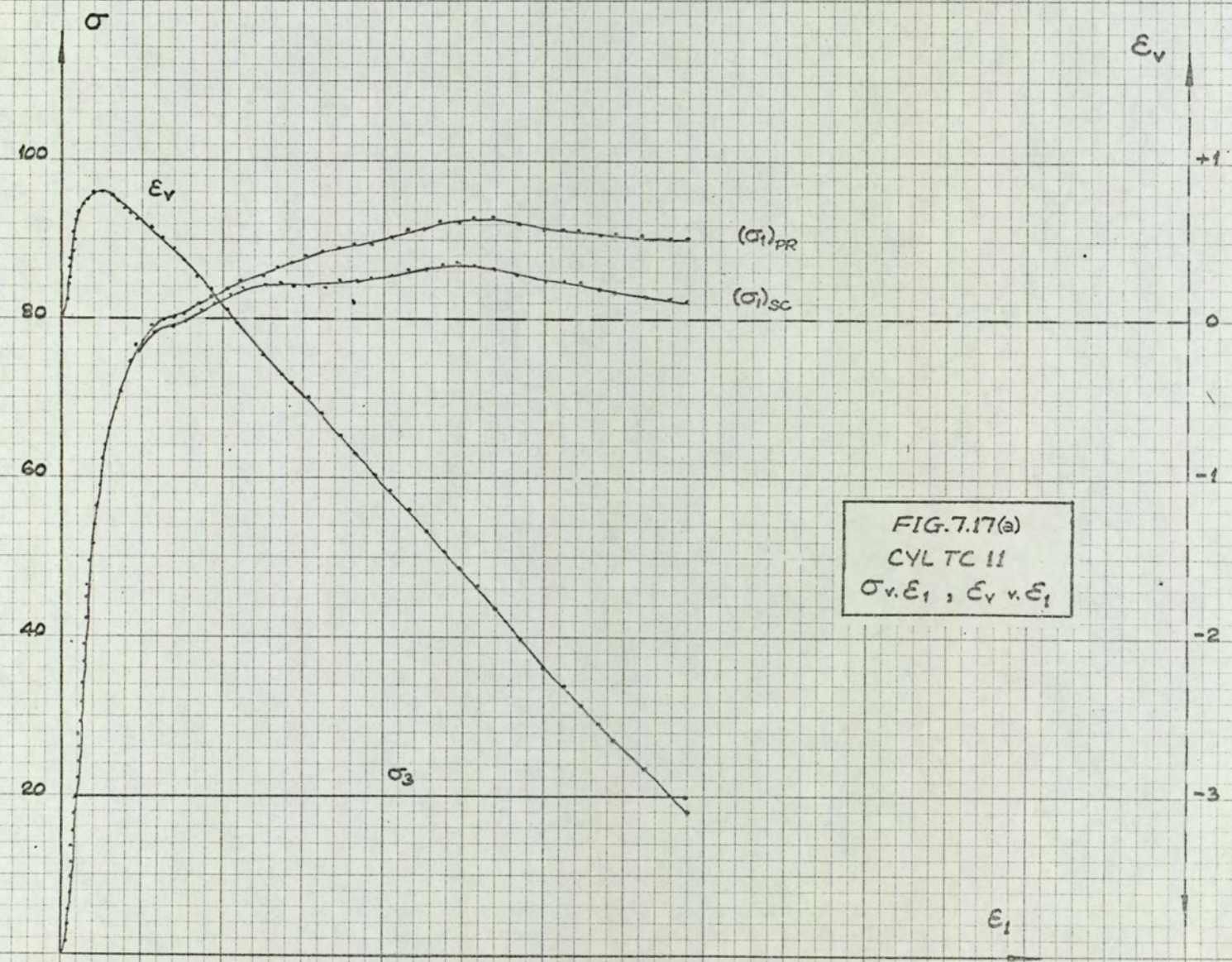

FIG. 7.17(a)
CYL TC 11
σ_v. ε_1 , ε_v v. ε_1

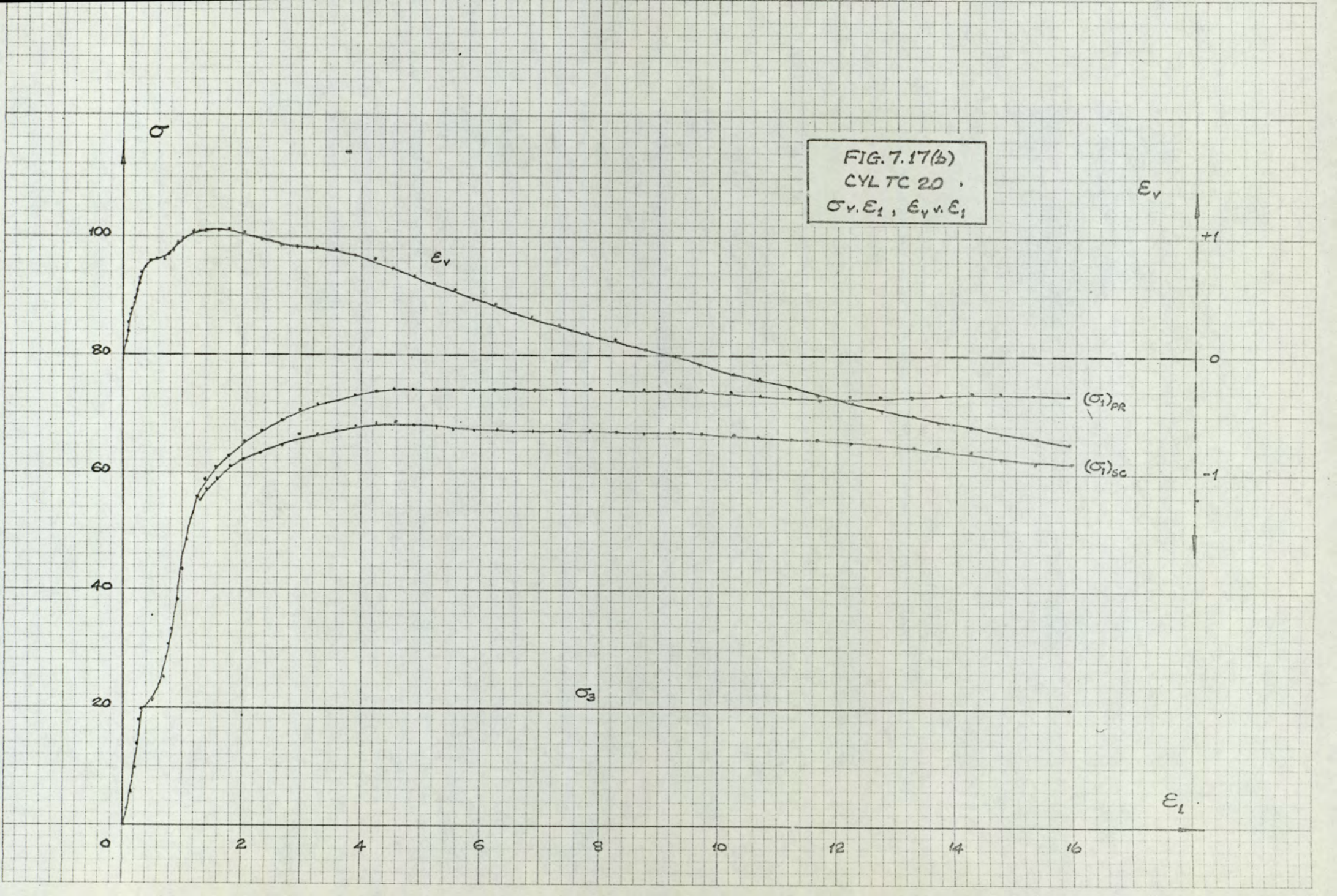
FIG. 7.17(b)
CYL TC 20 .
σv. ε1 , εv v. ε1
σ
εv
100
80
60
40
20
0
2
4
6
8
10
12
14
16
+1
0
-1
(σ1)PR
(σ1)SC
σ3
ε1

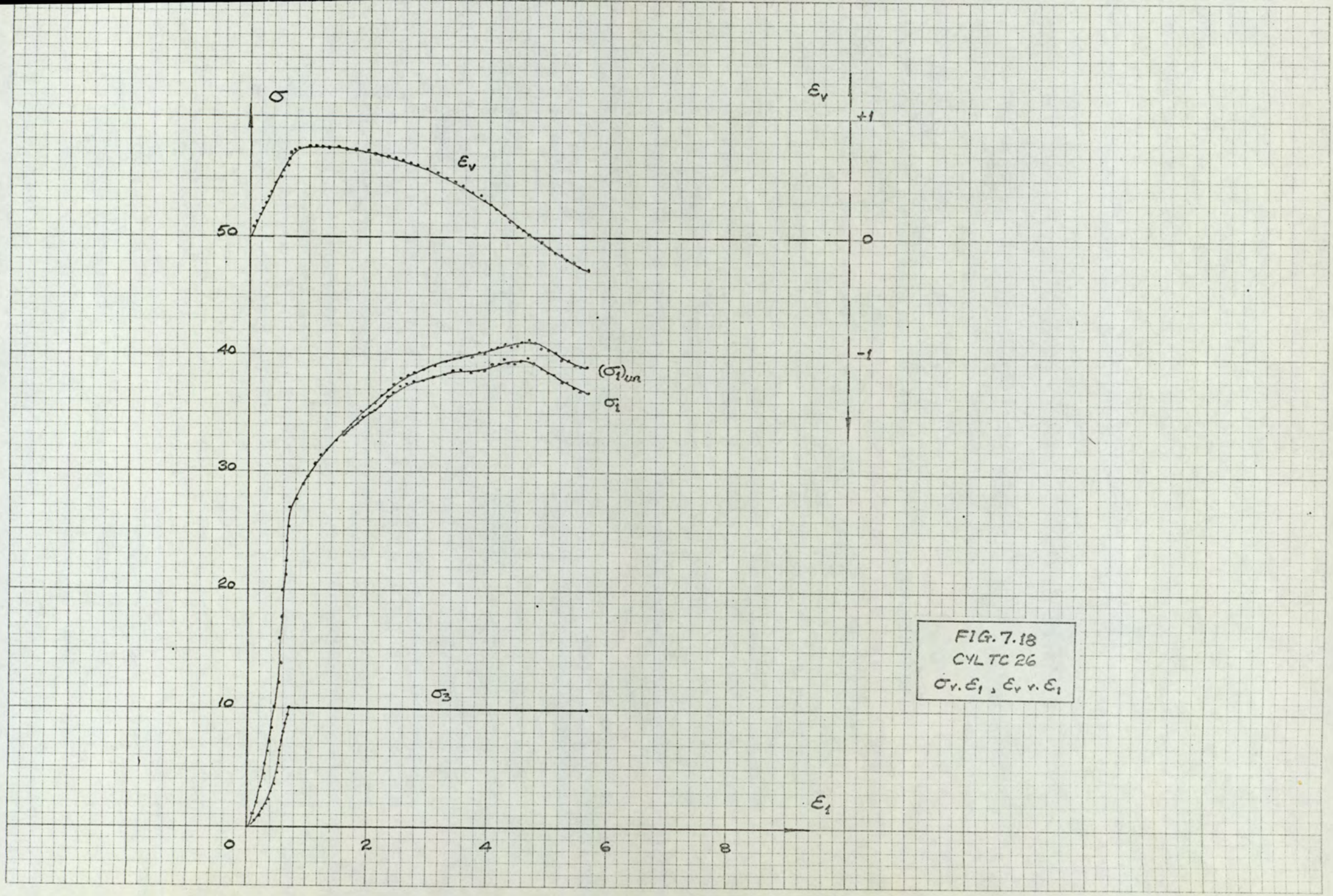

FIG. 7.18
CYL TC 26
σ_v. ε_1 , ε_v v. ε_1

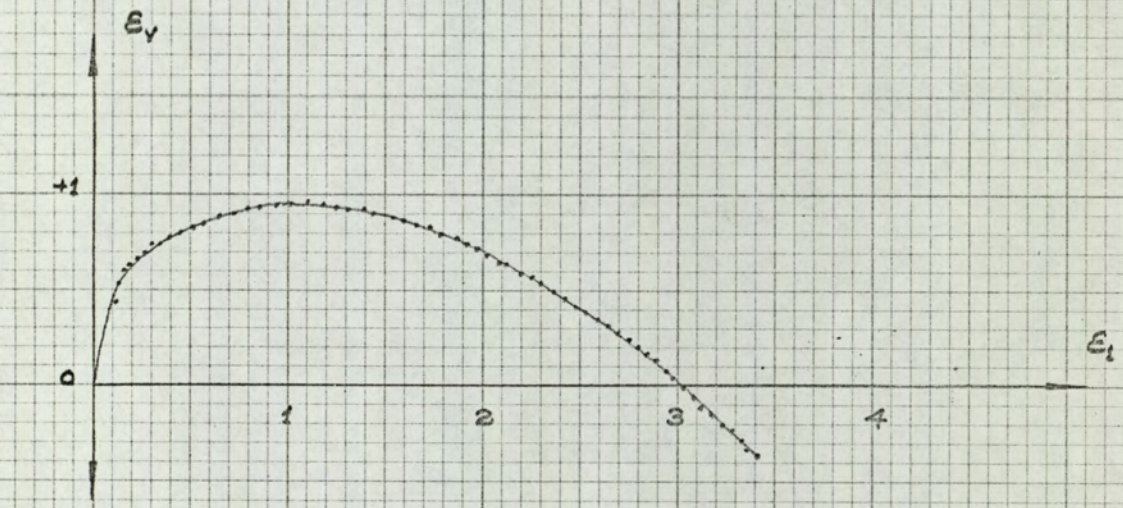

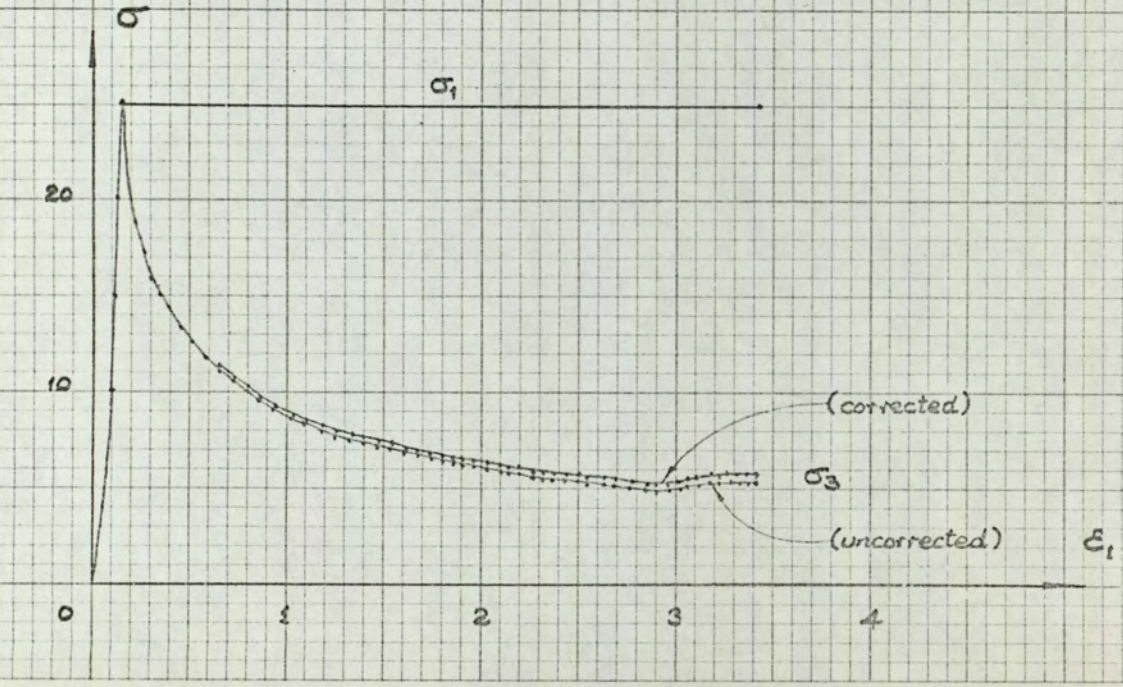

FIG. 7.19
CYLTE4
σ v. ε_1 , ε_v v. ε_1

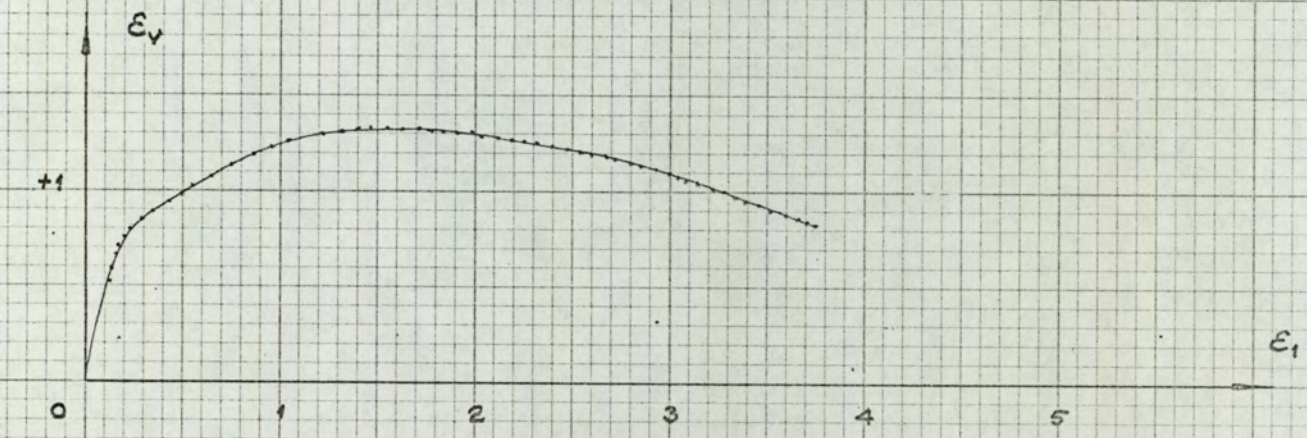

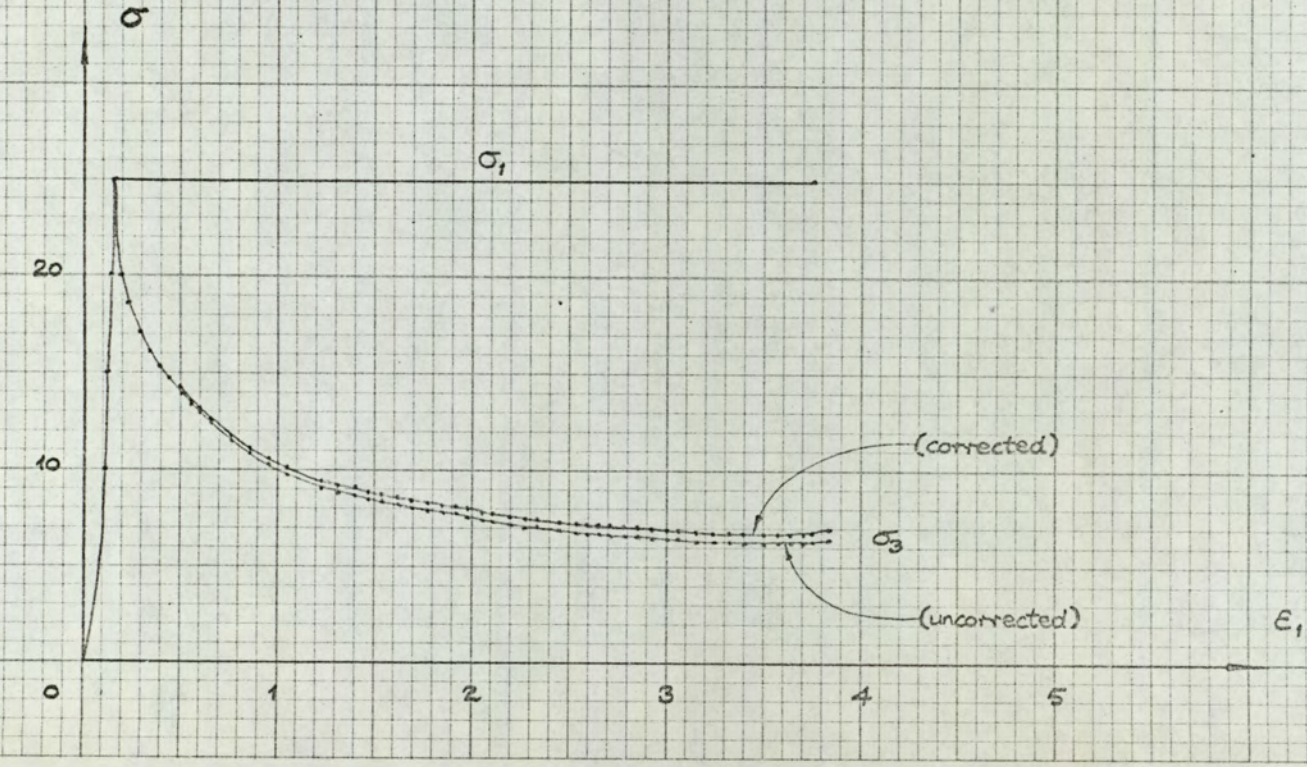

FIG. 7.20
CYLTE 7
$\sigma_v . \varepsilon_1$, ε_v v. ε_1

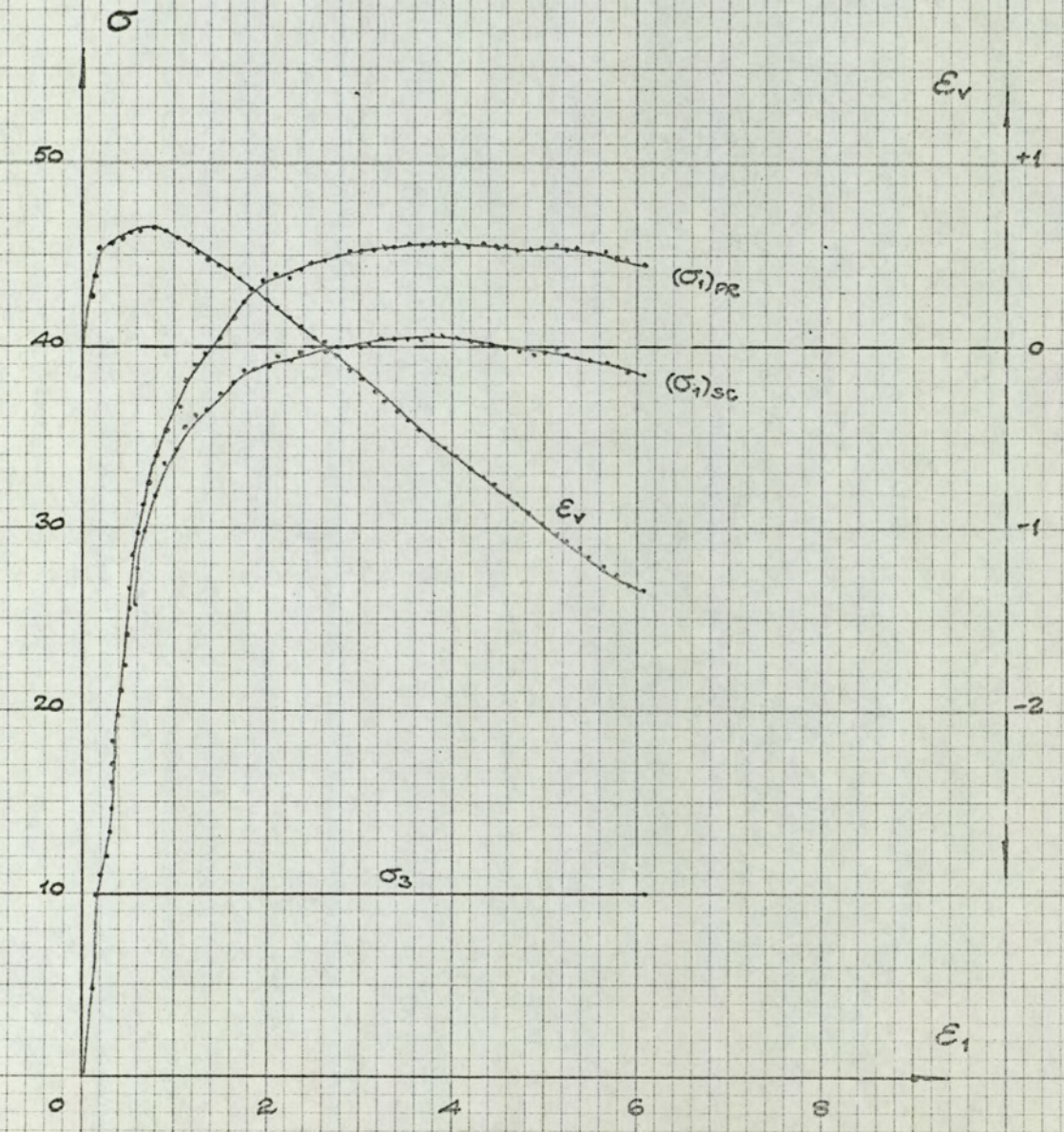

FIG. 7.21
CUBTC 5
σ_v v. ε_1 , ε_v v. ε_1

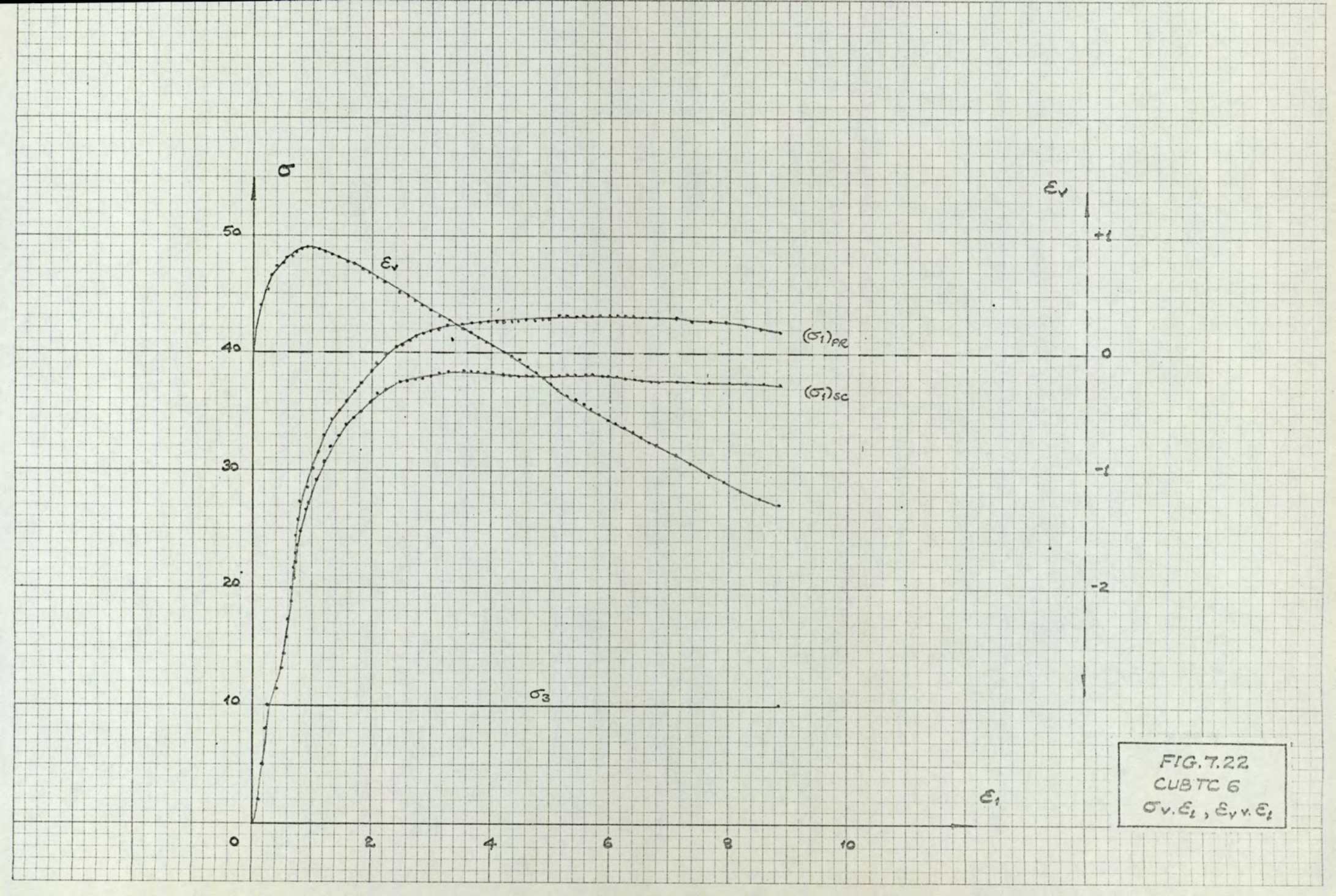

FIG. 7.22
CUBTC 6
σ_v v. ε_1 , ε_v v. ε_1

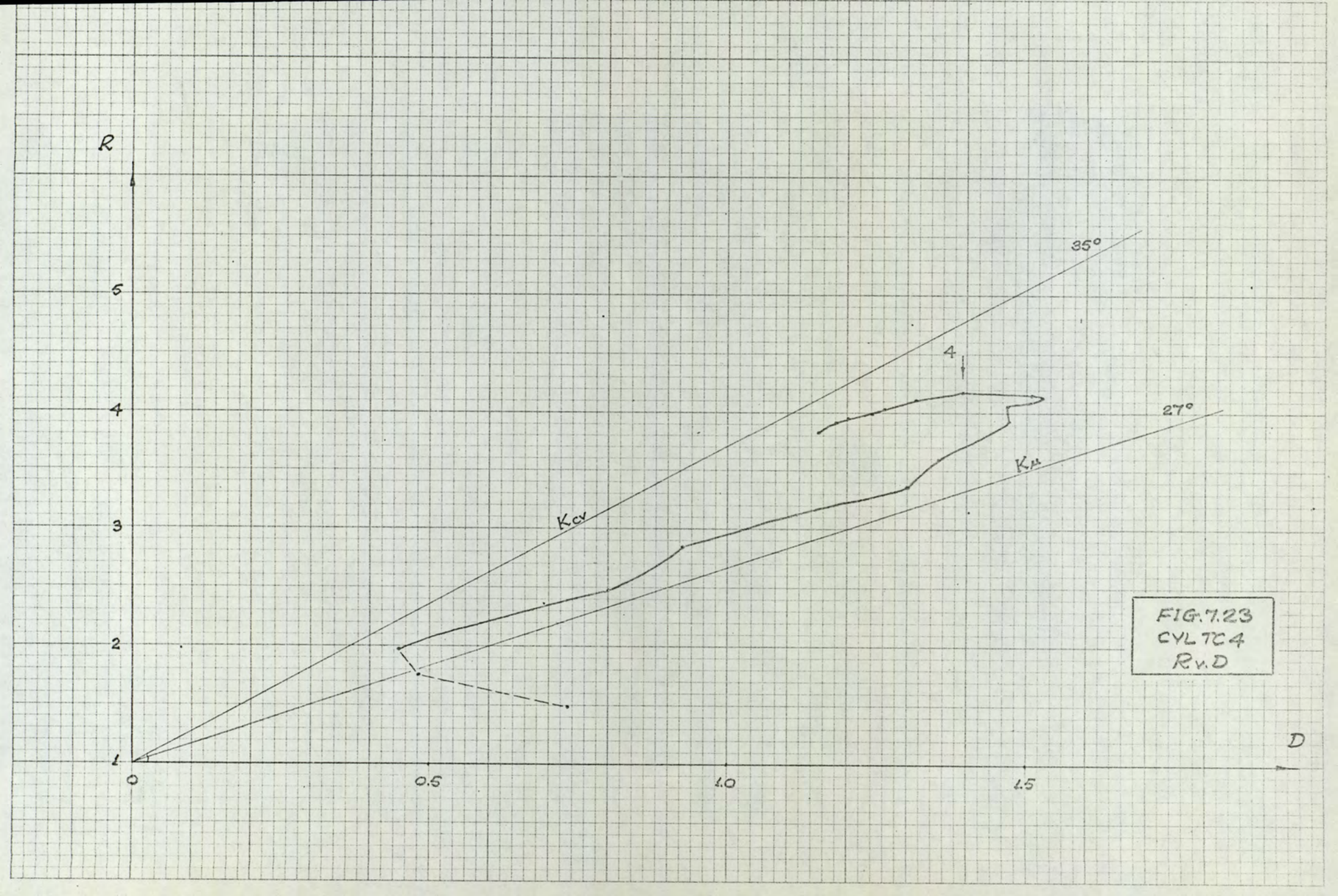

FIG. 7.23
CYL TC 4
Rv. D

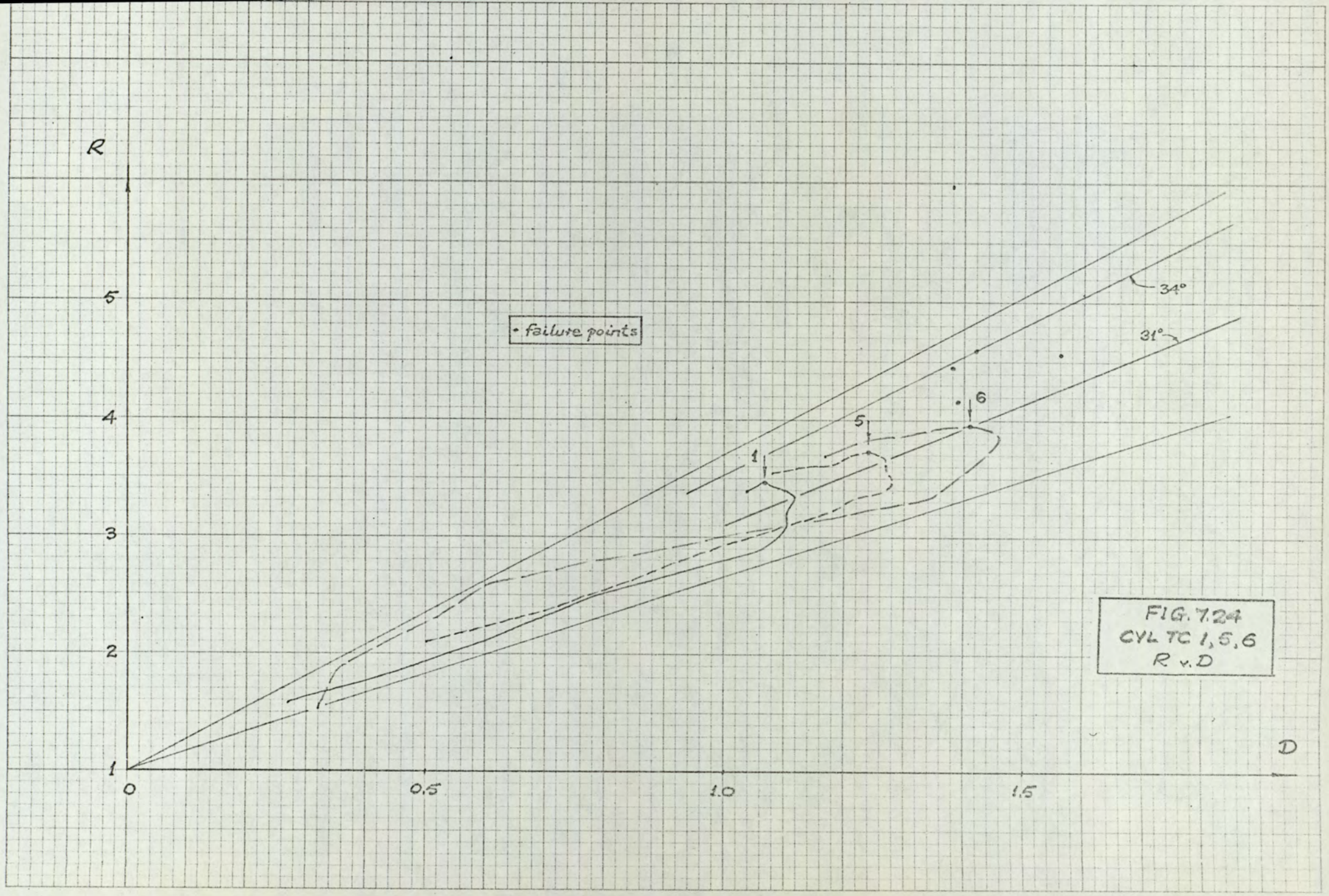

FIG. 7.24
CYL TC 1, 5, 6
R v. D

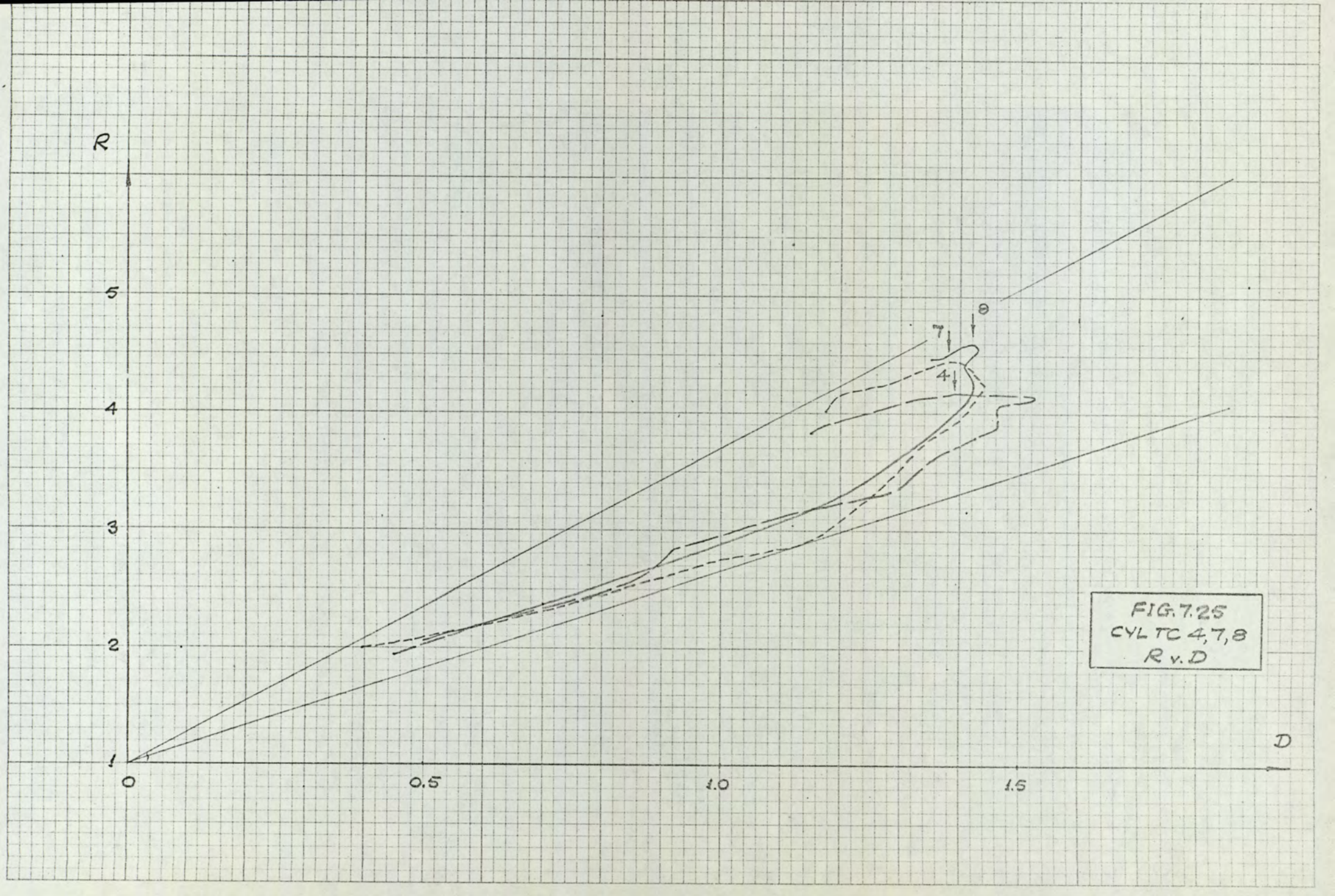

FIG. 7.25
CYL TC 4, 7, 8
R v. D

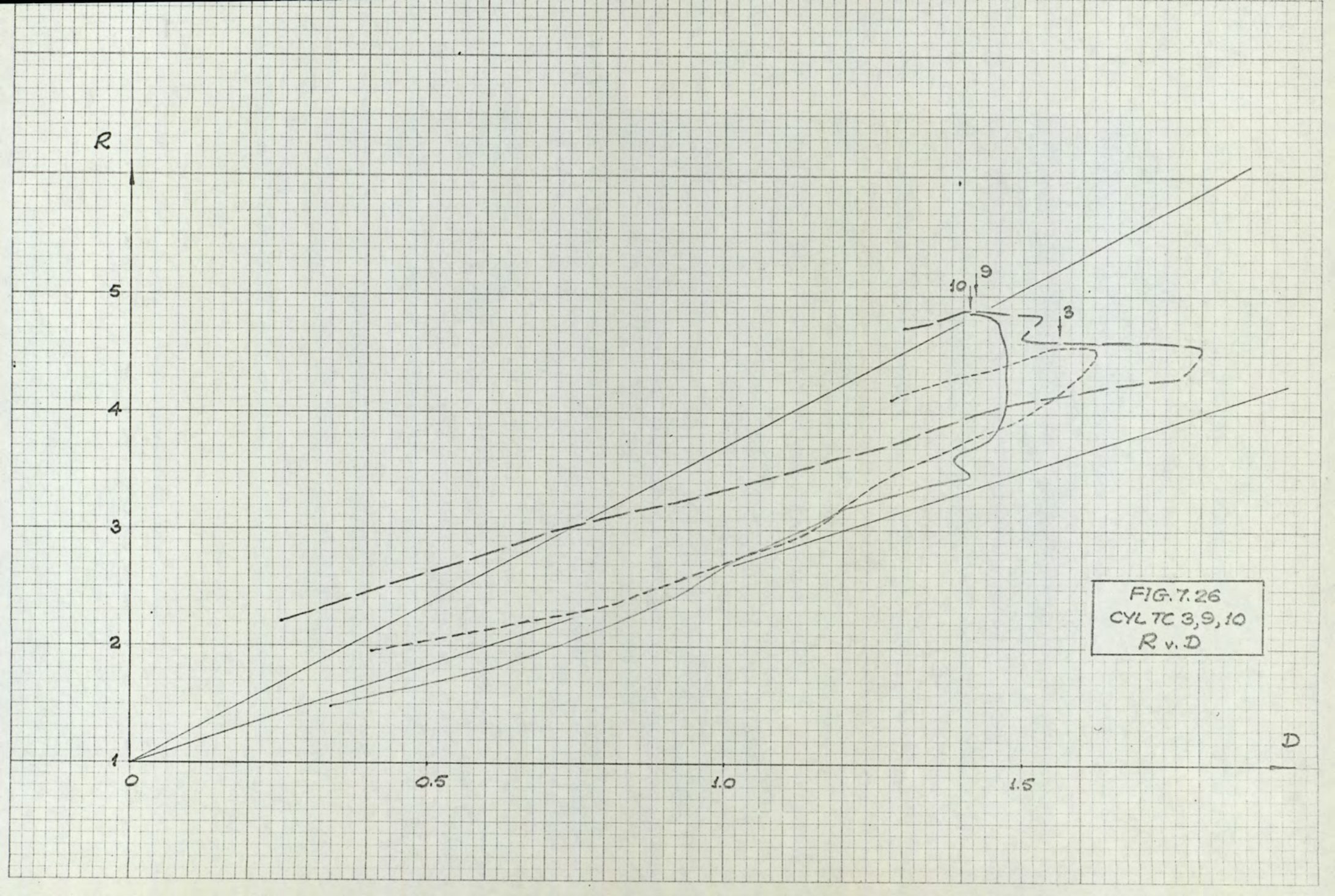

FIG. 7.26
CYL TC 3, 9, 10
R v. D

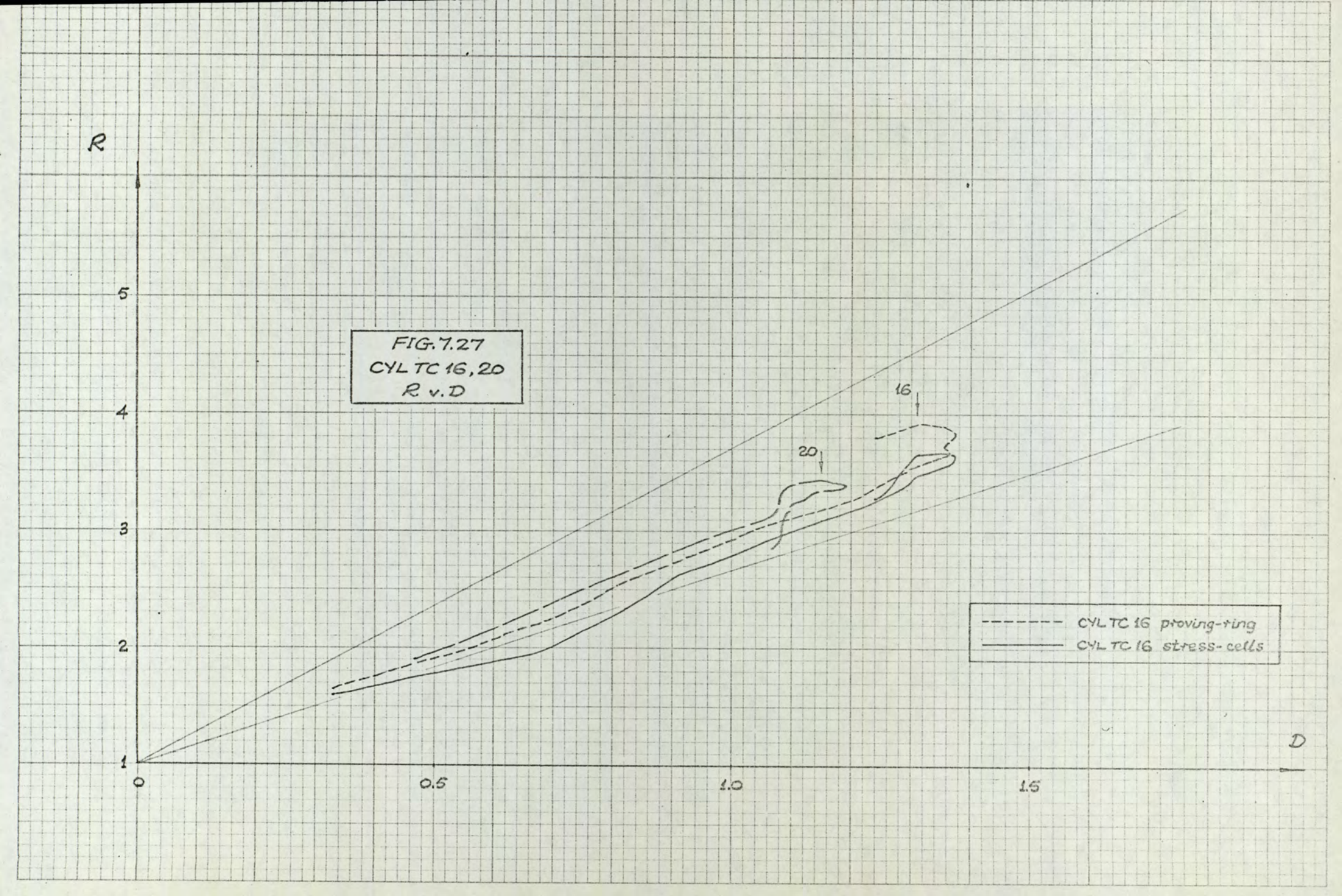

FIG. 7.27
CYL TC 16, 20
R v. D

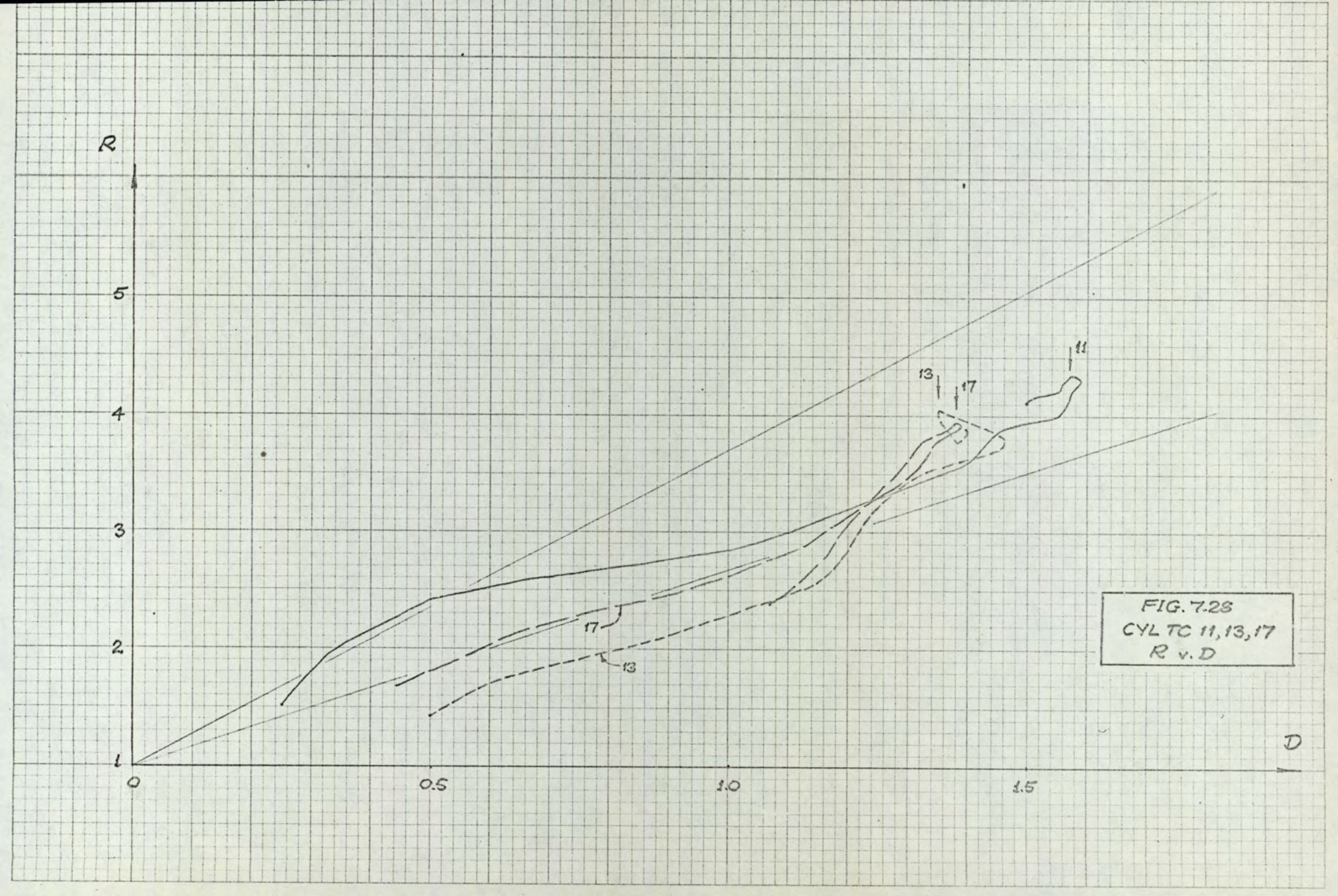

FIG. 7.28
CYL TC 11, 13, 17
R v. D

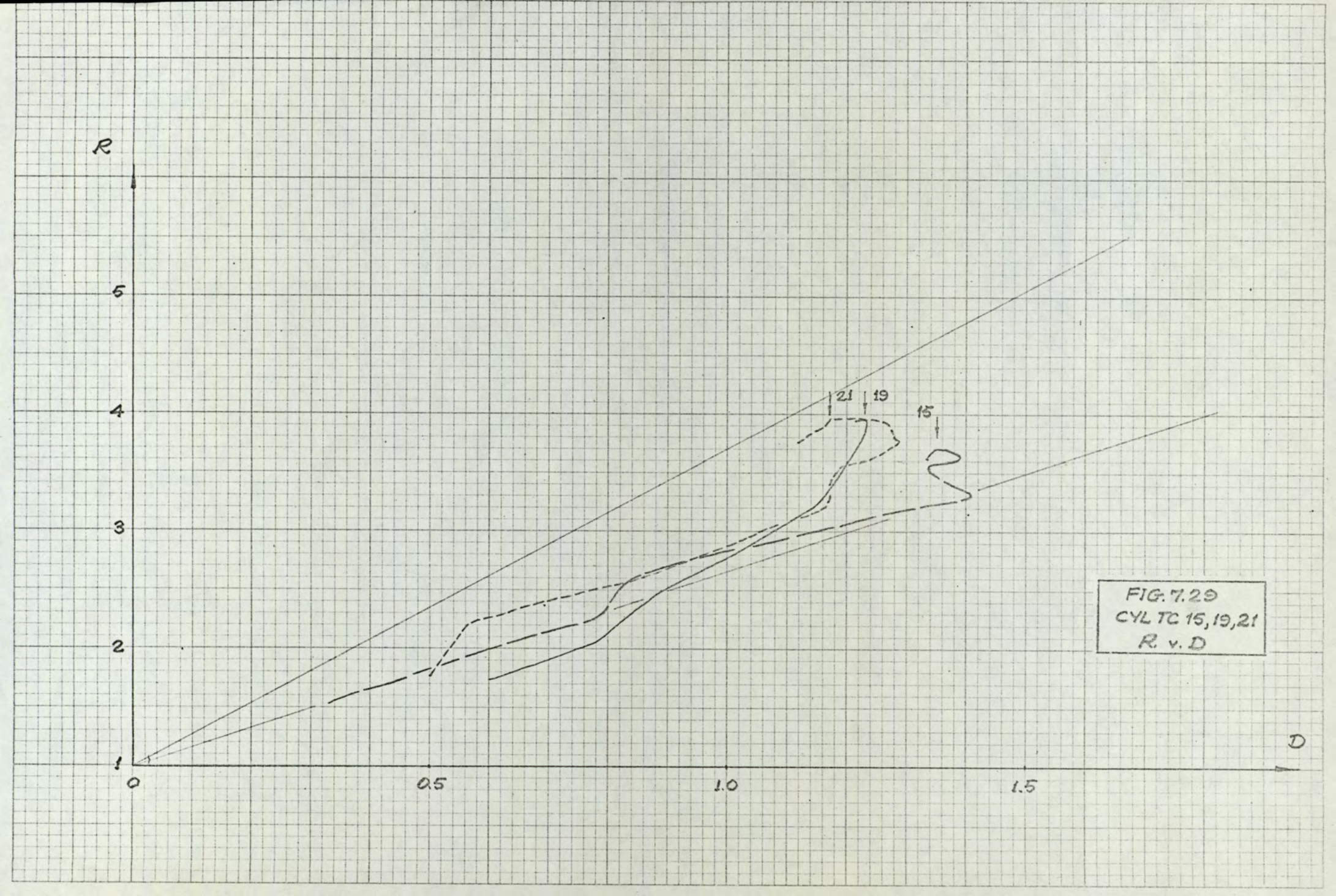

FIG. 7.29
CYL TC 15, 19, 21
R v. D

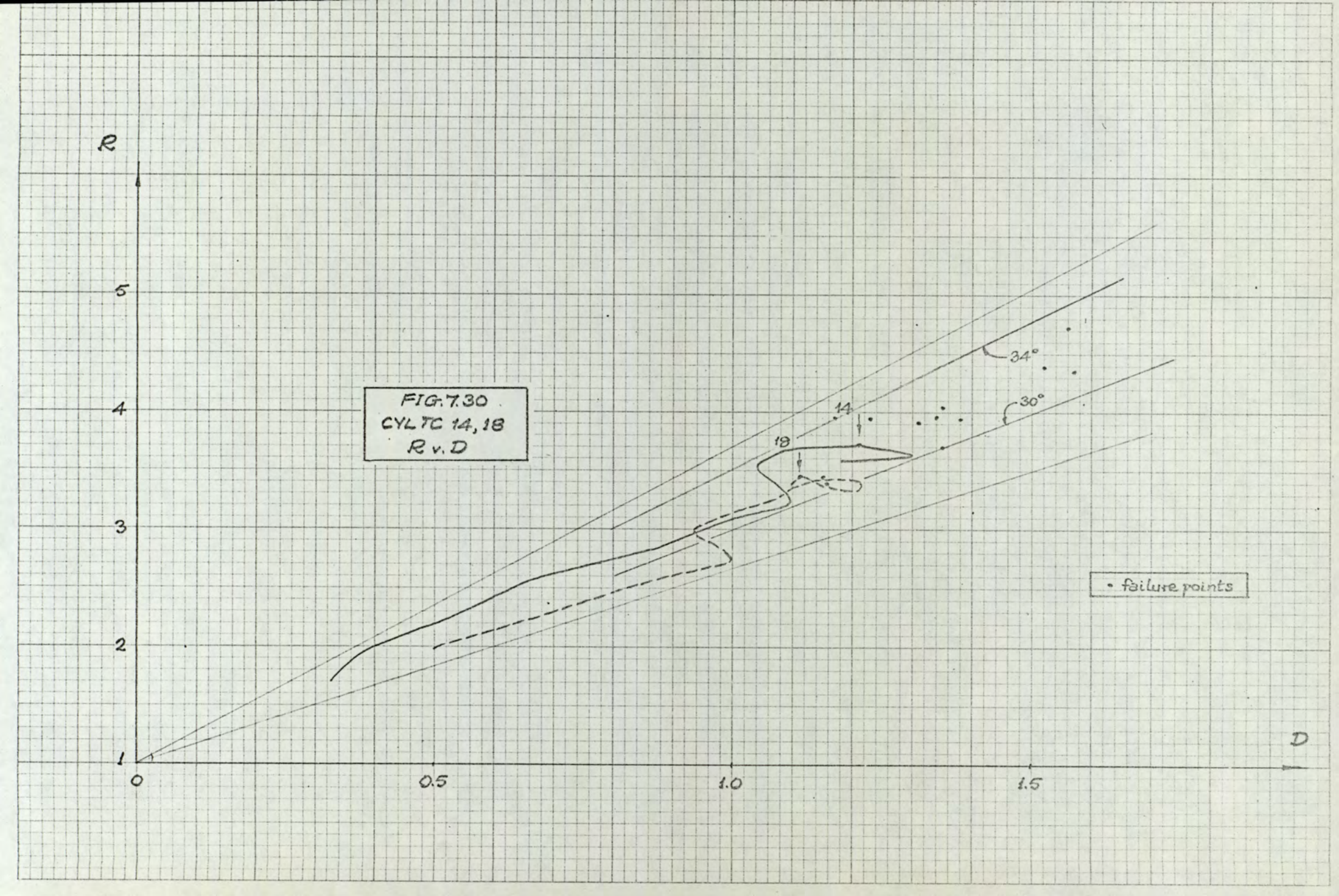

FIG. 7.30
CYL TC 14, 18
R v. D

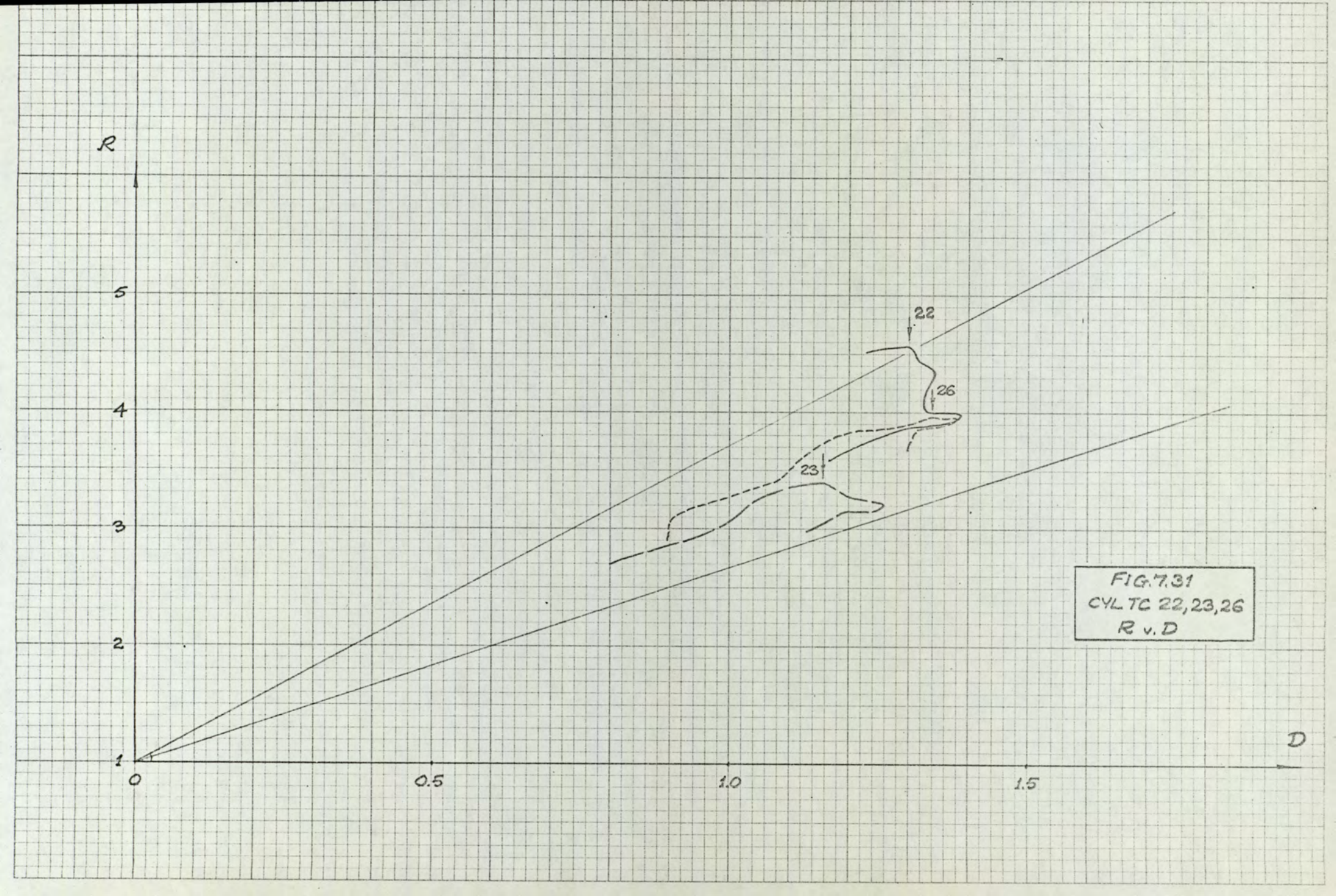

FIG. 7.31
CYL TC 22,23,26
R v. D

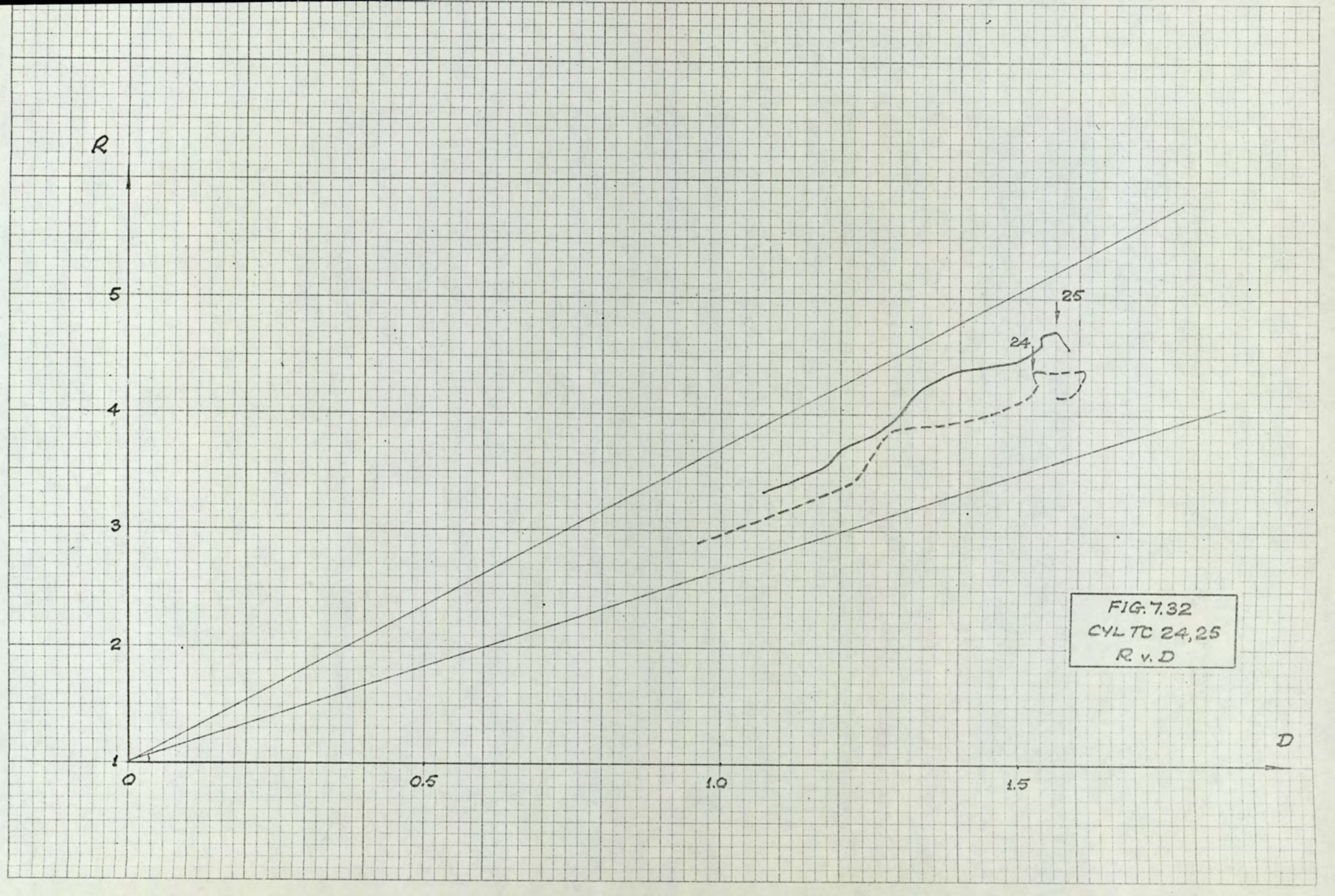

FIG. 7.32
CYL TC 24, 25
R v. D

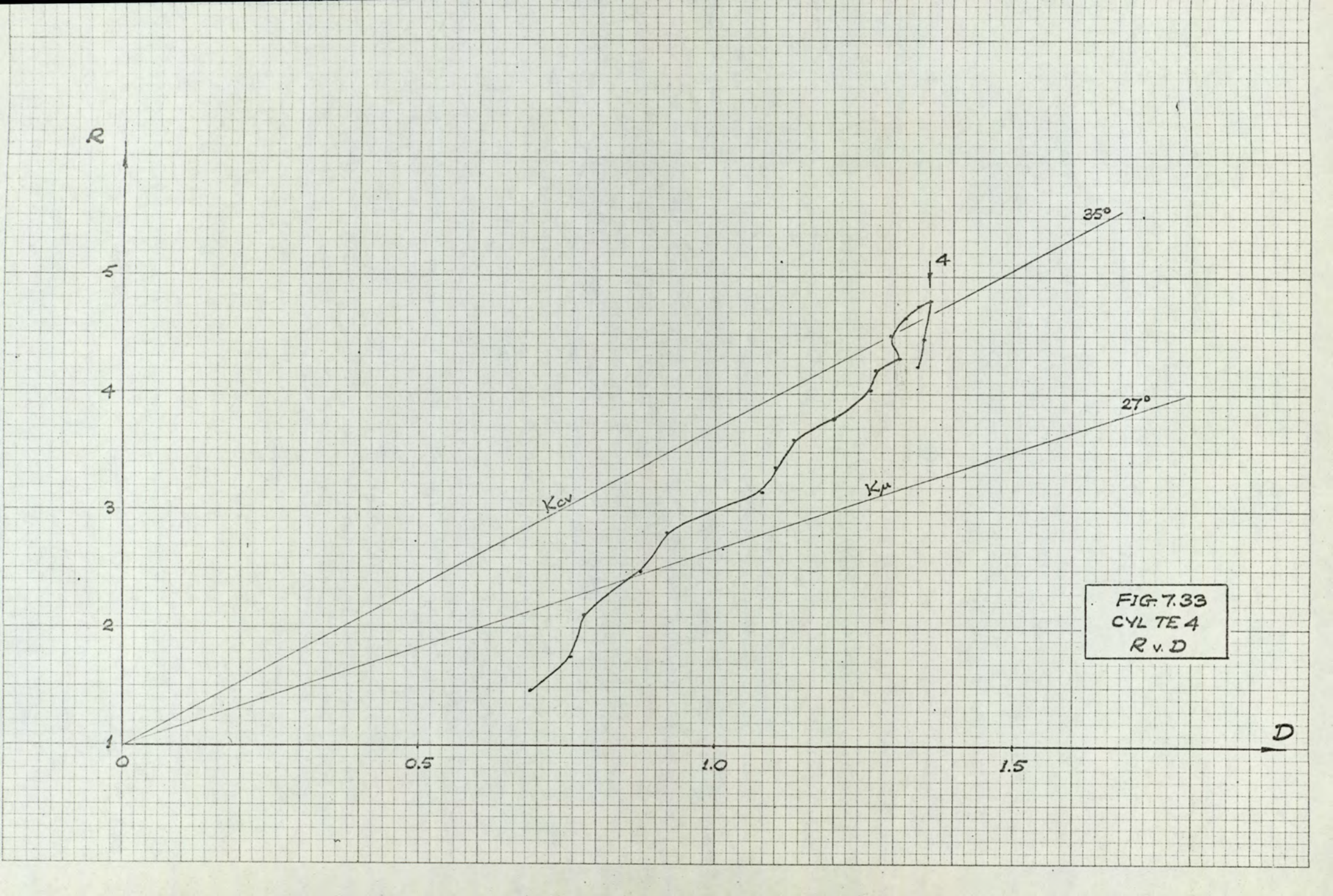

FIG. 7.33
CYL TE 4
R v. D

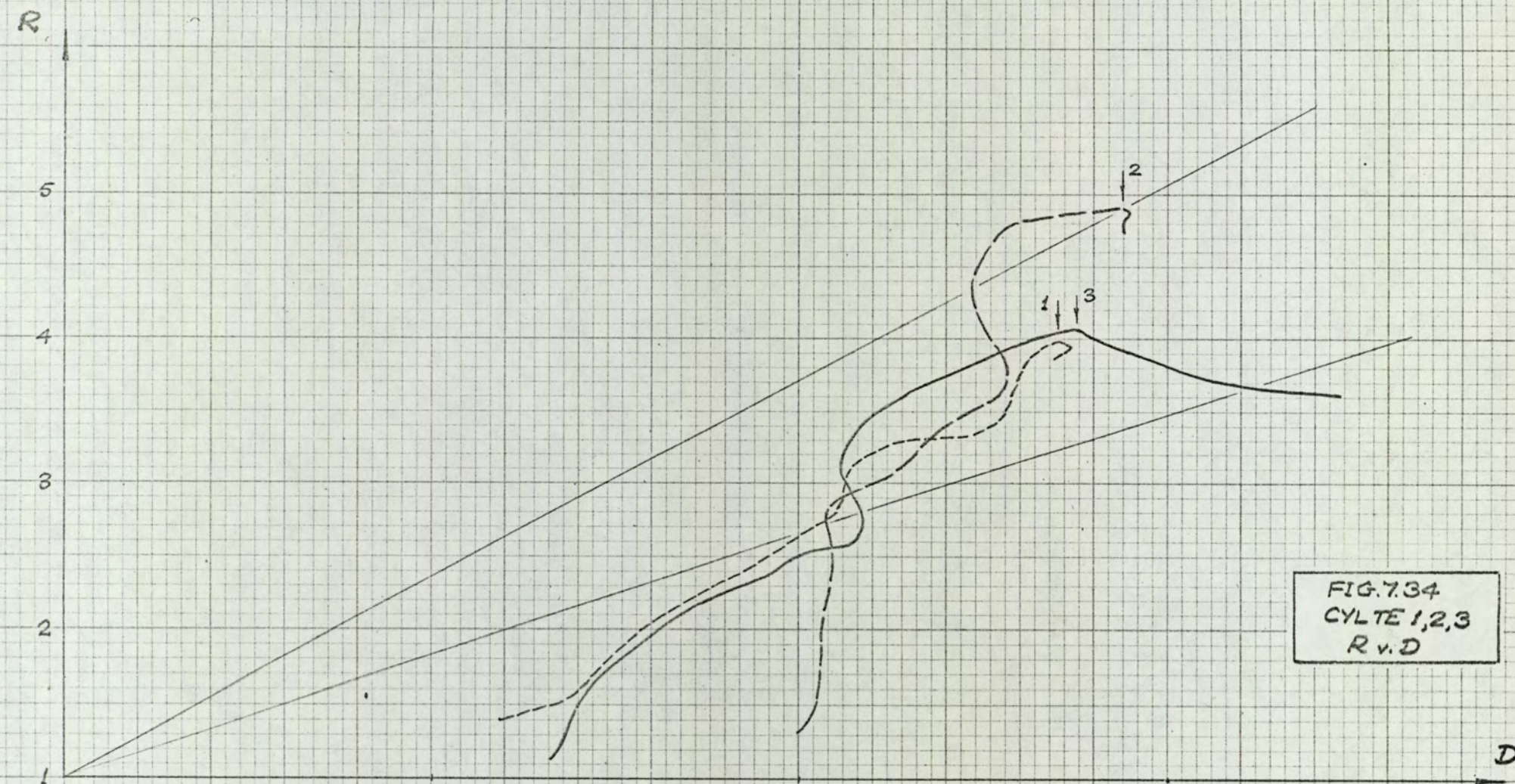

FIG. 7.34
CYL TE 1,2,3
R v. D

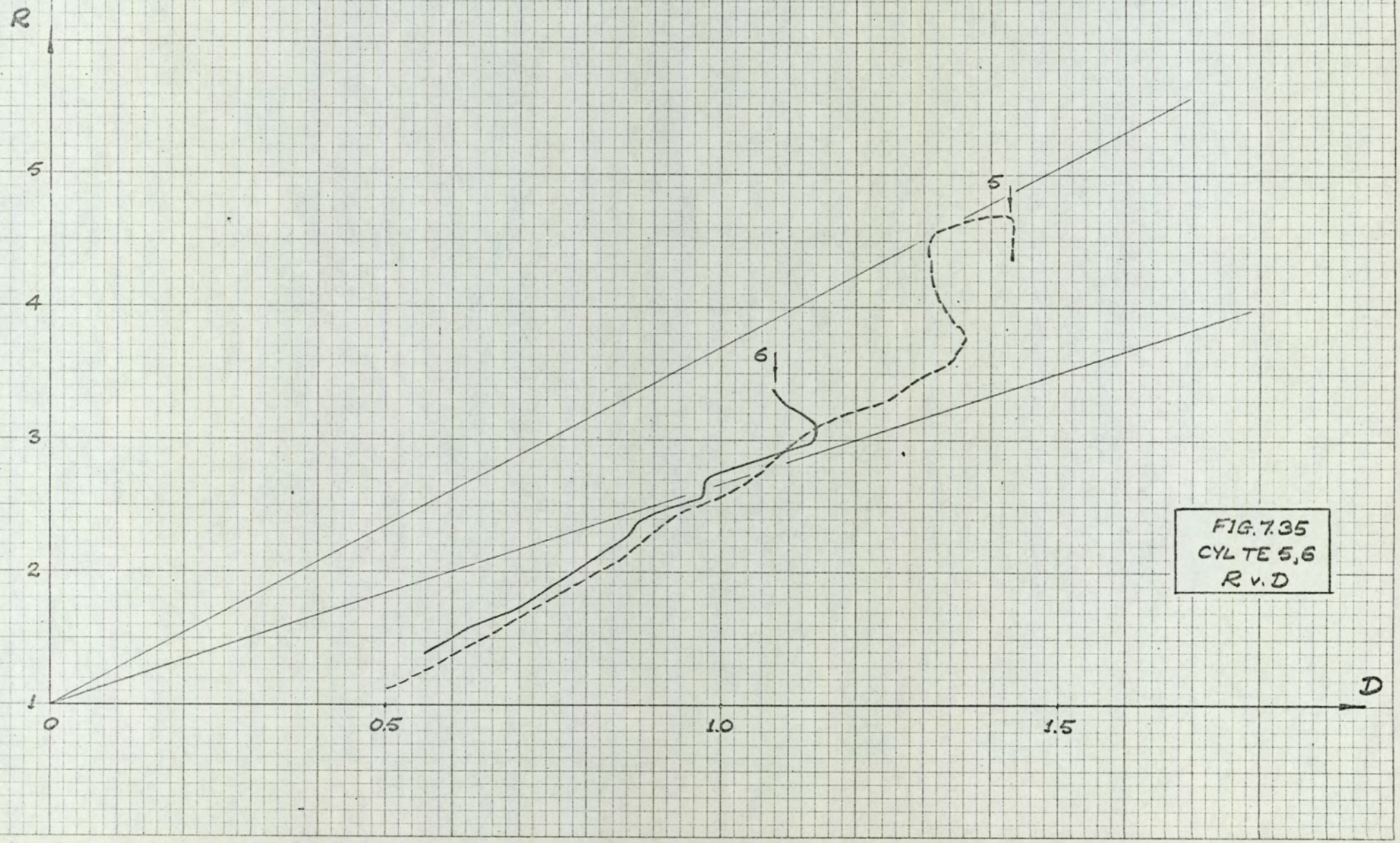

FIG. 7.35
CYL TE 5,6
R v. D

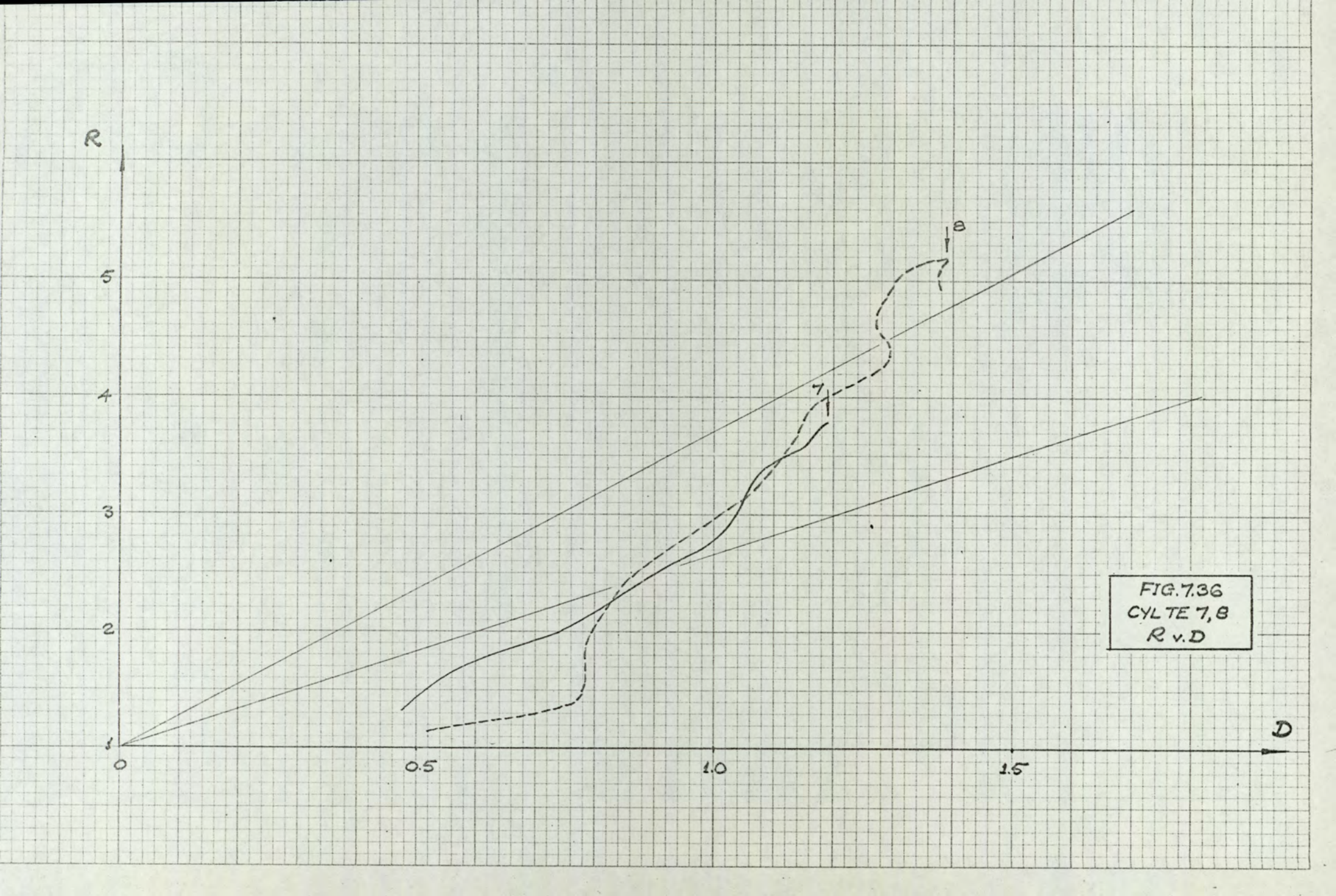

FIG. 7.36
CYL TE 7, 8
R v. D

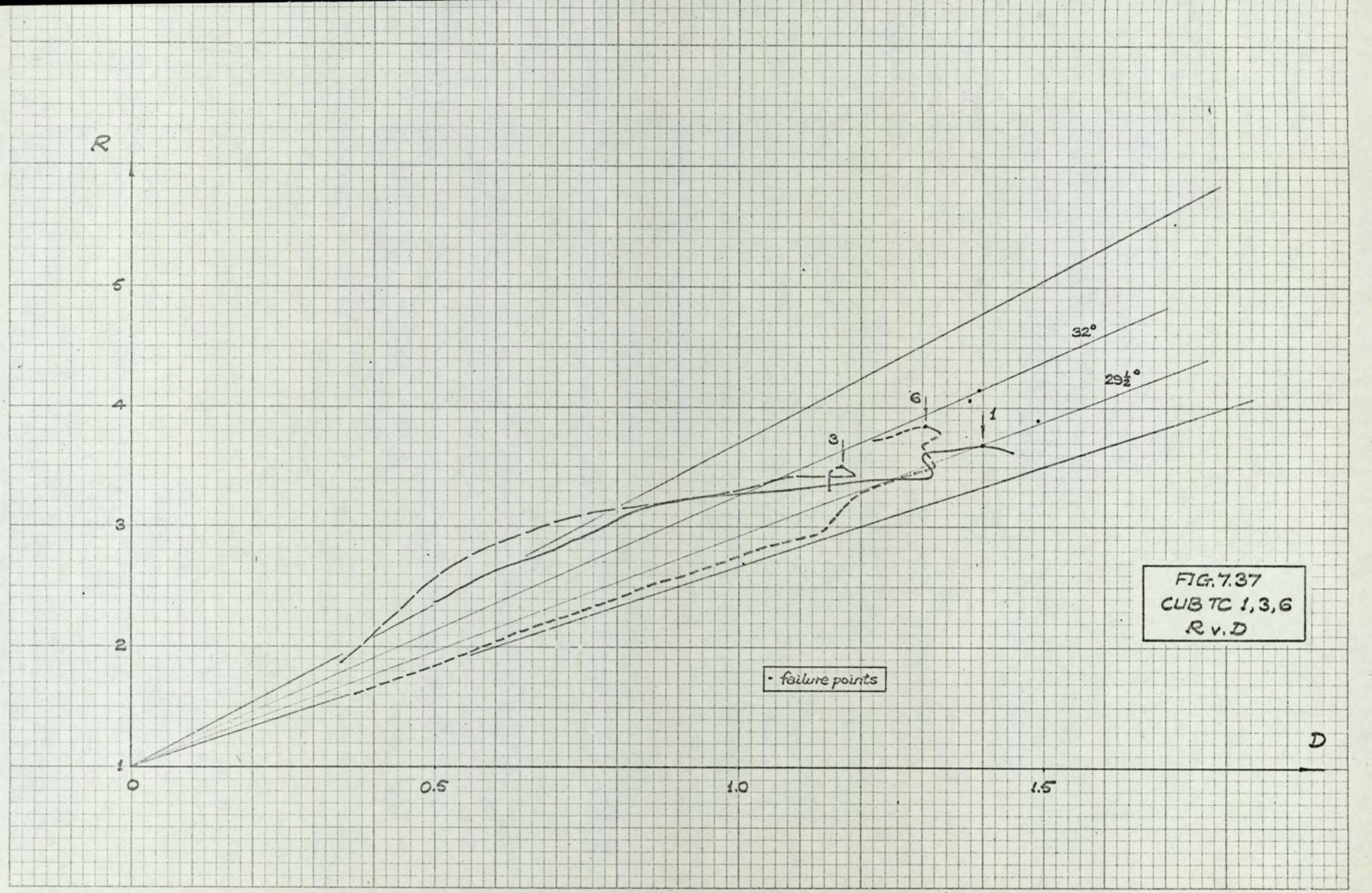

FIG. 7.37
CUBTC 1, 3, 6
R v. D

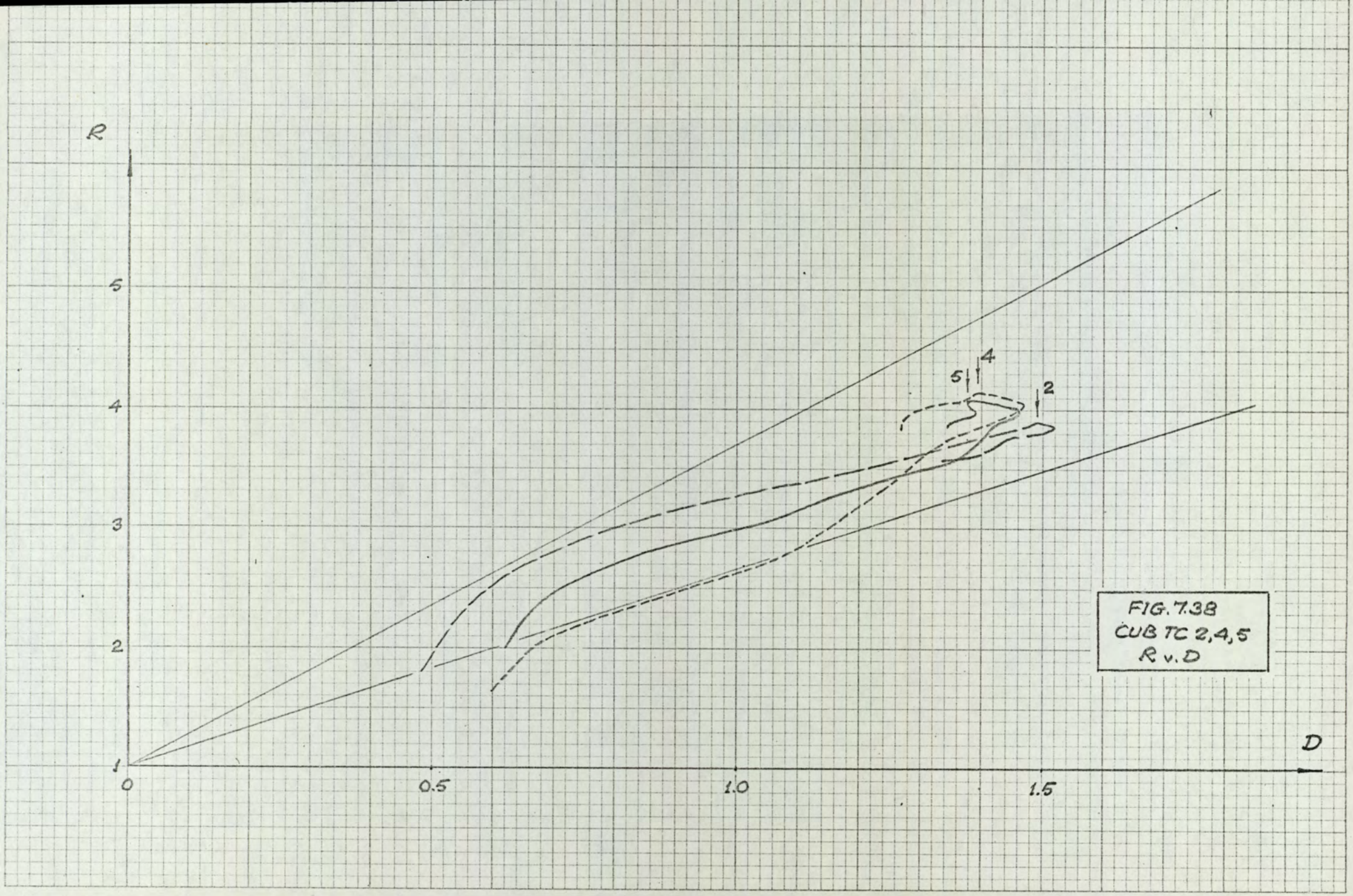

FIG. 7.38
CUB TC 2,4,5
R v. D

FIG. 7.39
CYL TC TESTS
MODE OF DEFORMATION

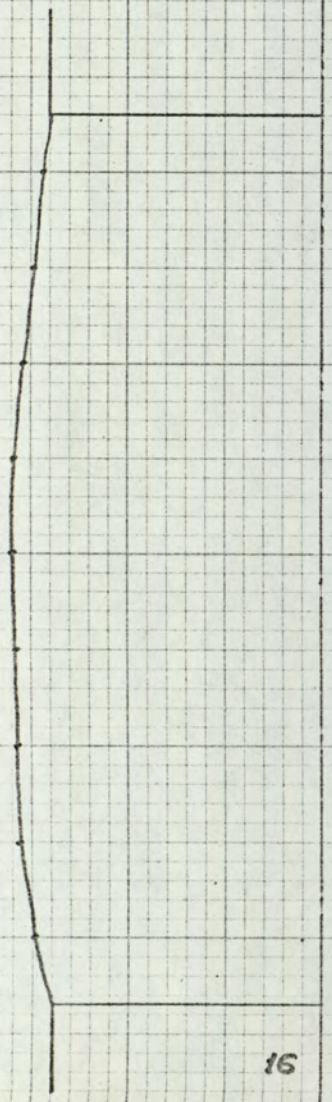

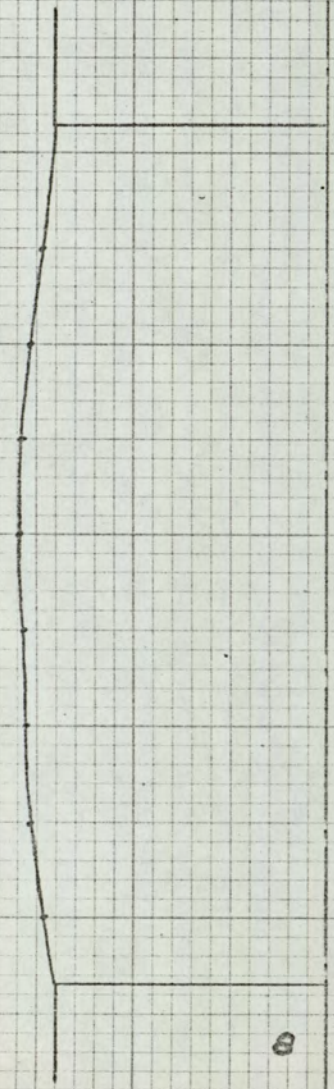

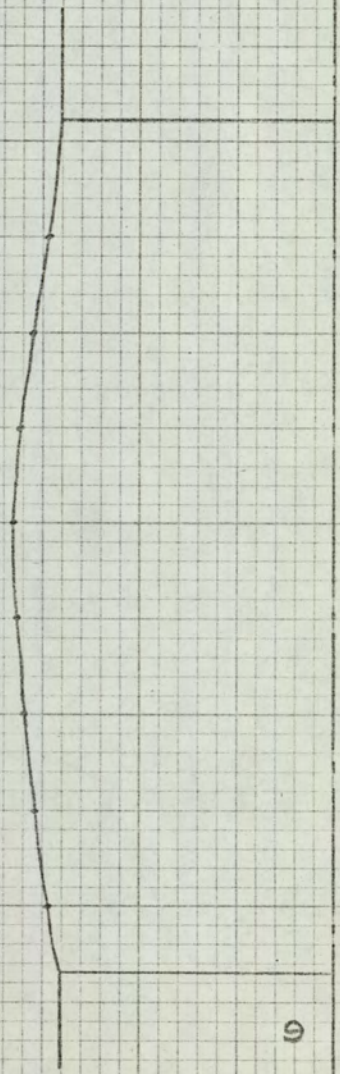

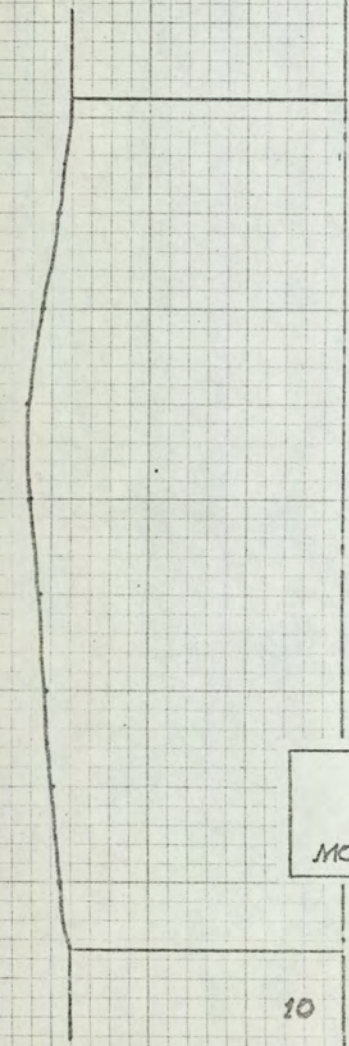

FIG. 7.40
CYL TC TESTS
MODE OF DEFORMATION

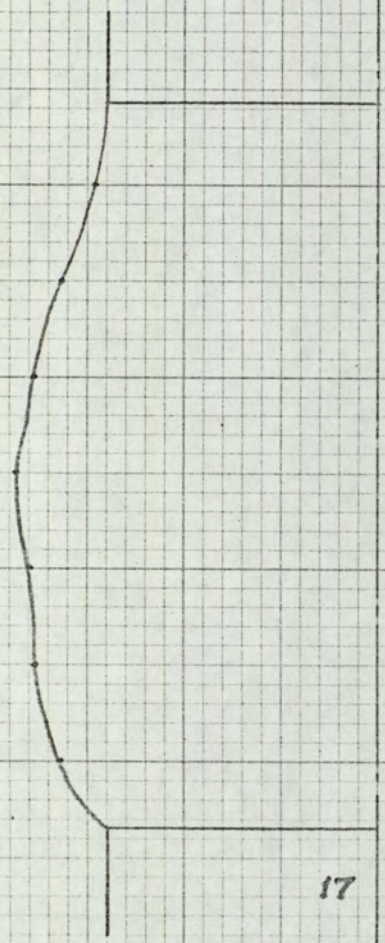

FIG. 7.41
CYL TC TESTS
MODE OF DEFORMATION

FIG. 7.42
CYL TE TESTS
MODE OF DEFORMATION

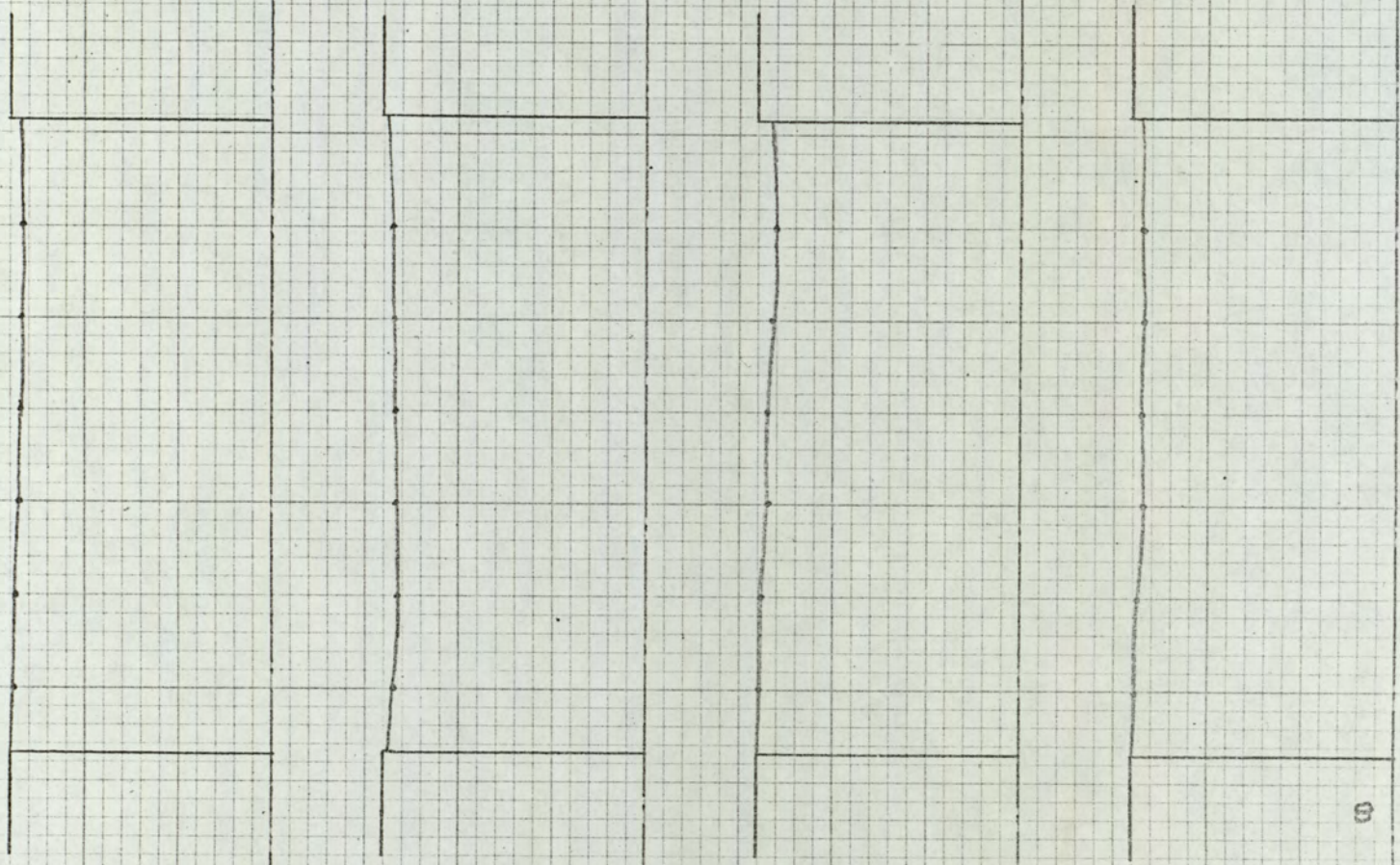

FIG. 7.43
CYL TE TESTS
MODE OF DEFORMATION

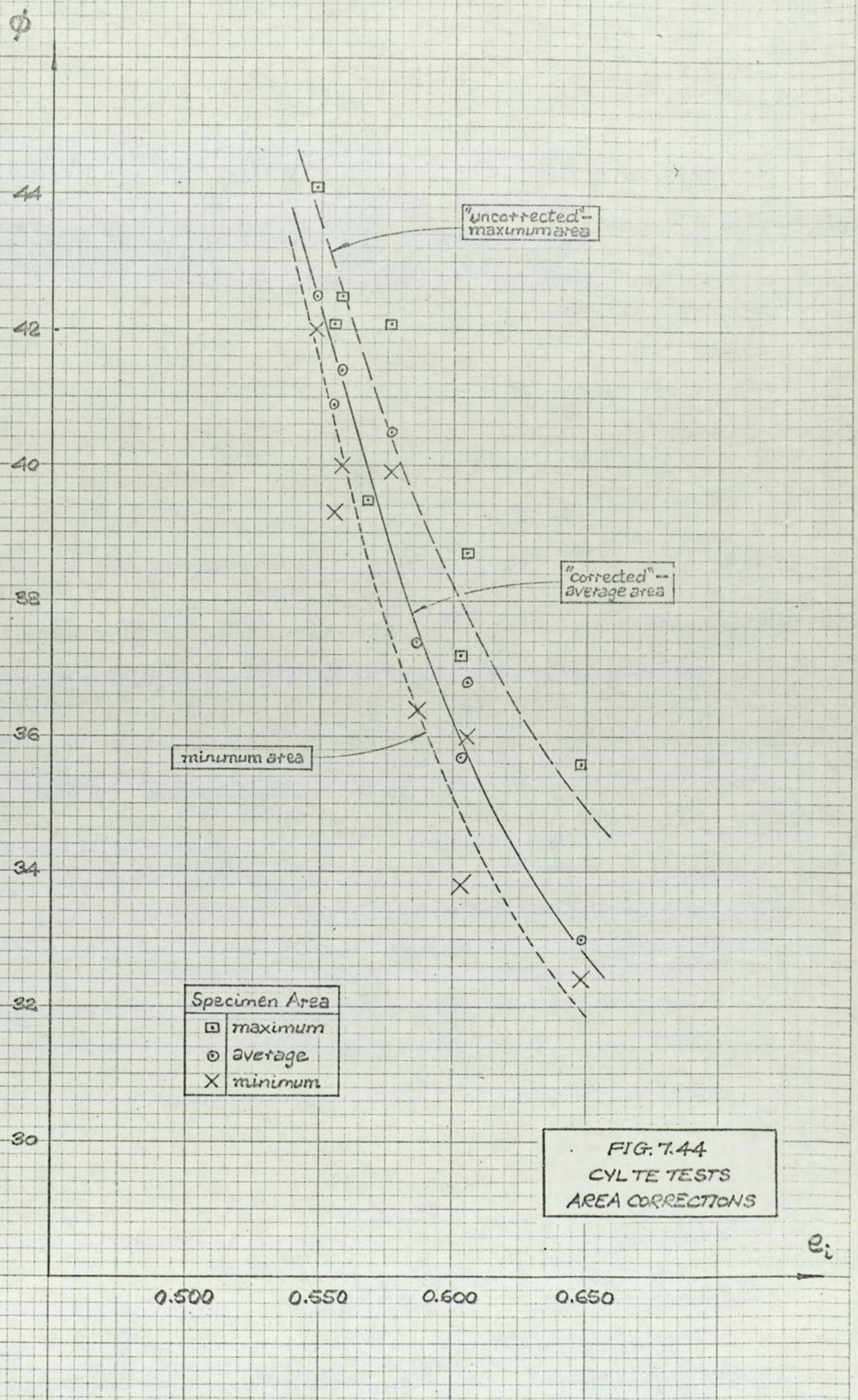

FIG. 7.44
CYL TE TESTS
AREA CORRECTIONS

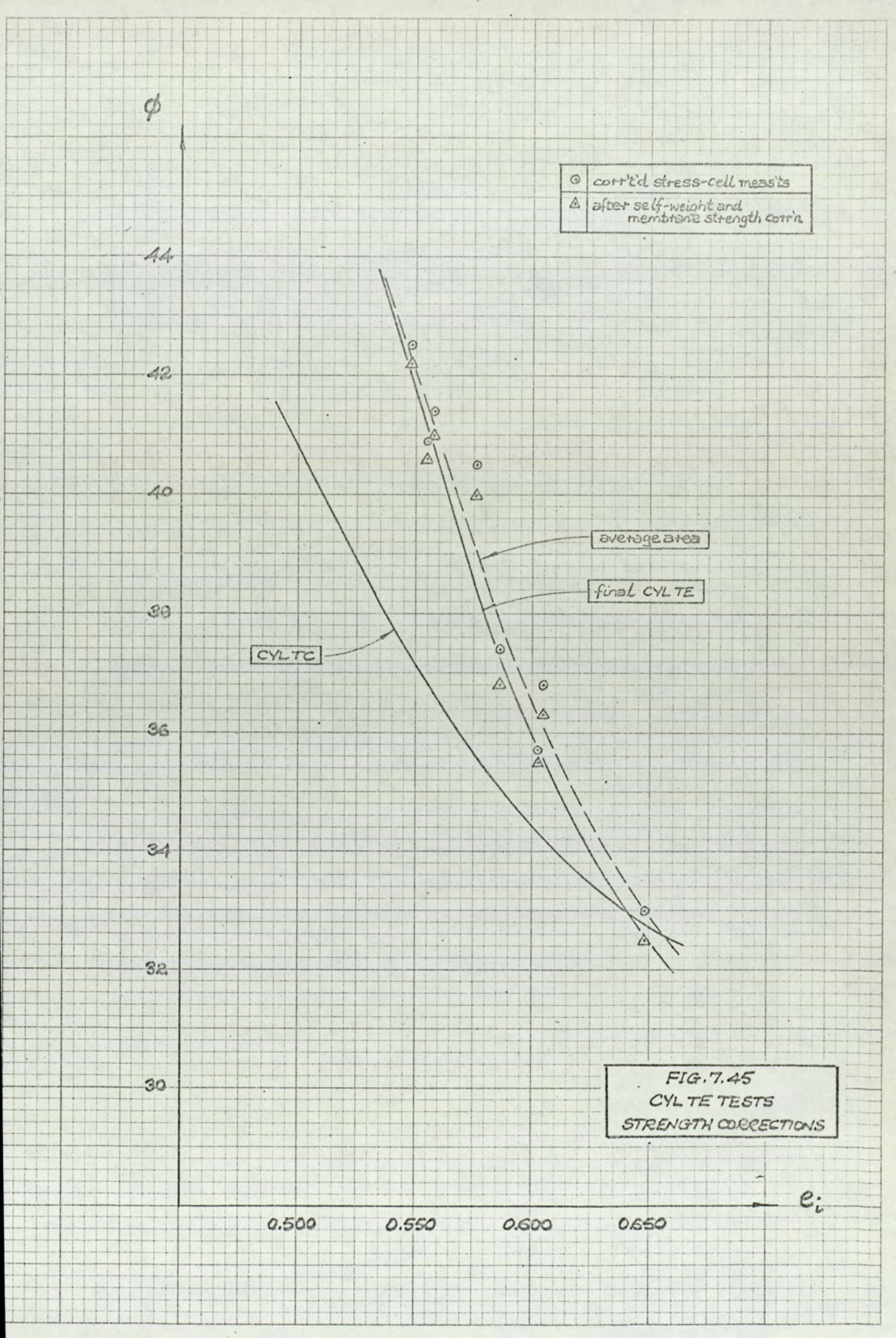

FIG. 7.45
CYL TE TESTS
STRENGTH CORRECTIONS

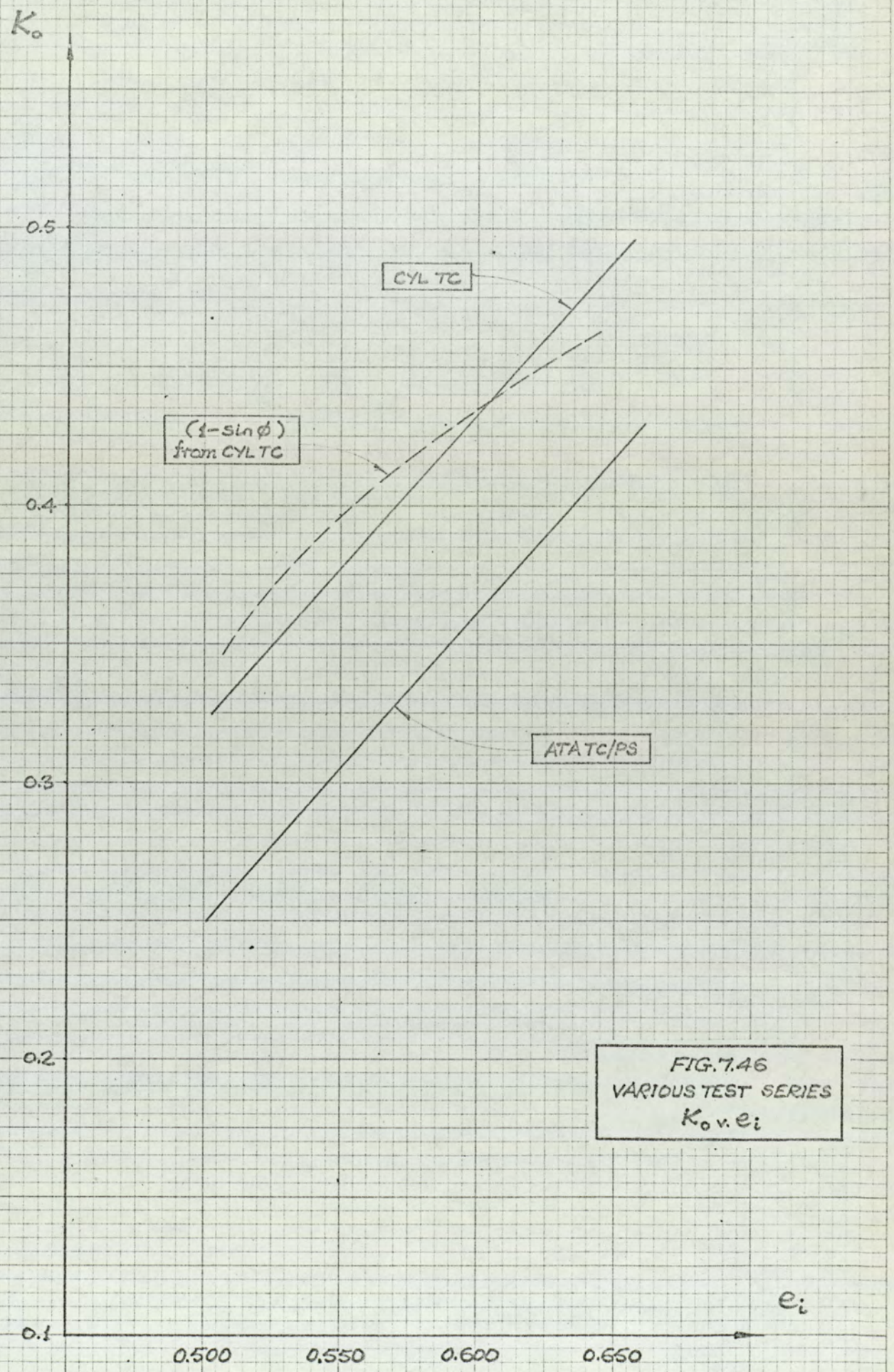

FIG. 7.46
VARIOUS TEST SERIES
K_o v. e_i

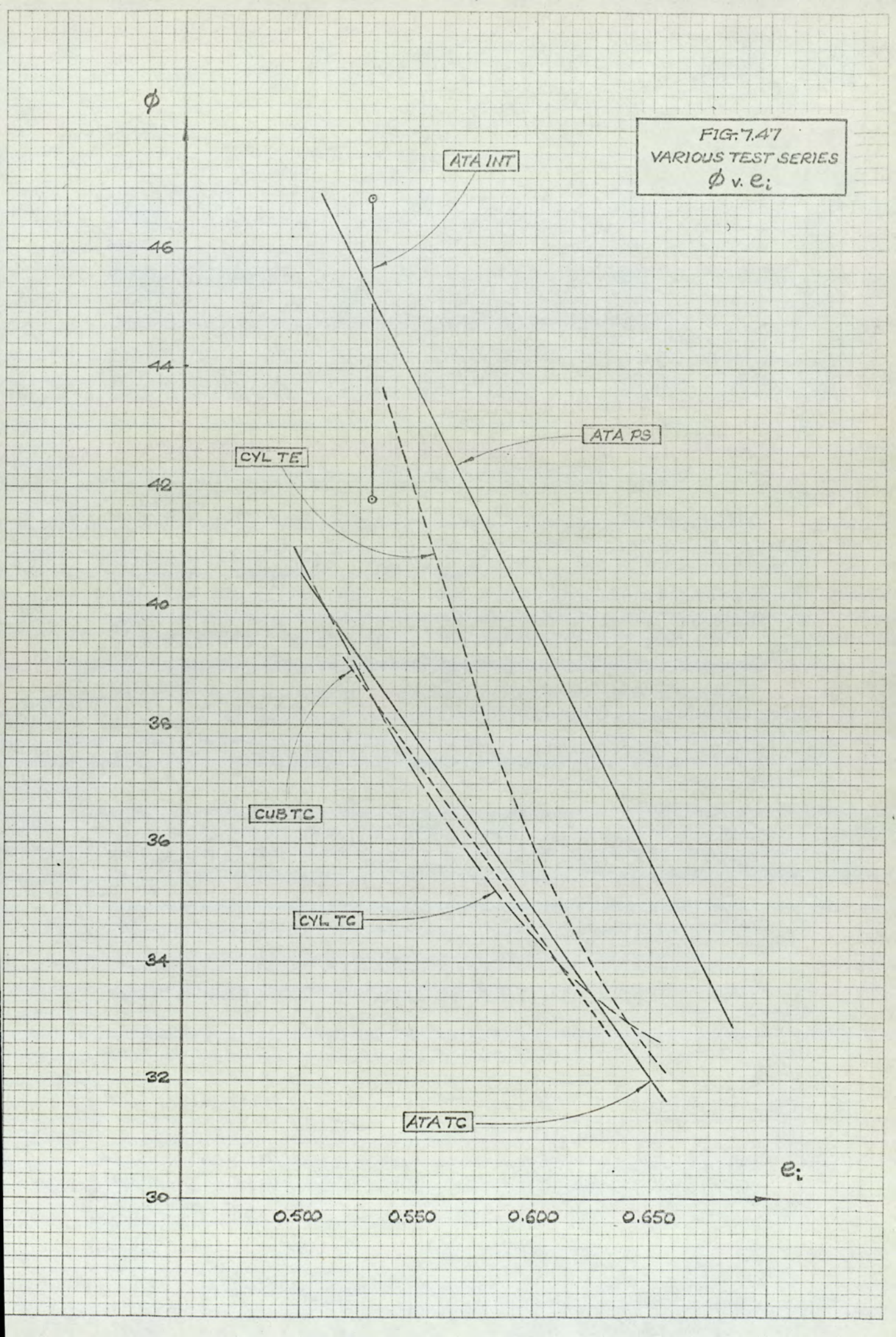
FIG: 7.47
VARIOUS TEST SERIES
φ v. e_i
φ
ATA INT
ATA PS
CYL TE
CUB TC
CYL TC
ATA TC
46
44
42
40
38
36
34
32
30
e_i
0.500
0.550
0.600
0.650

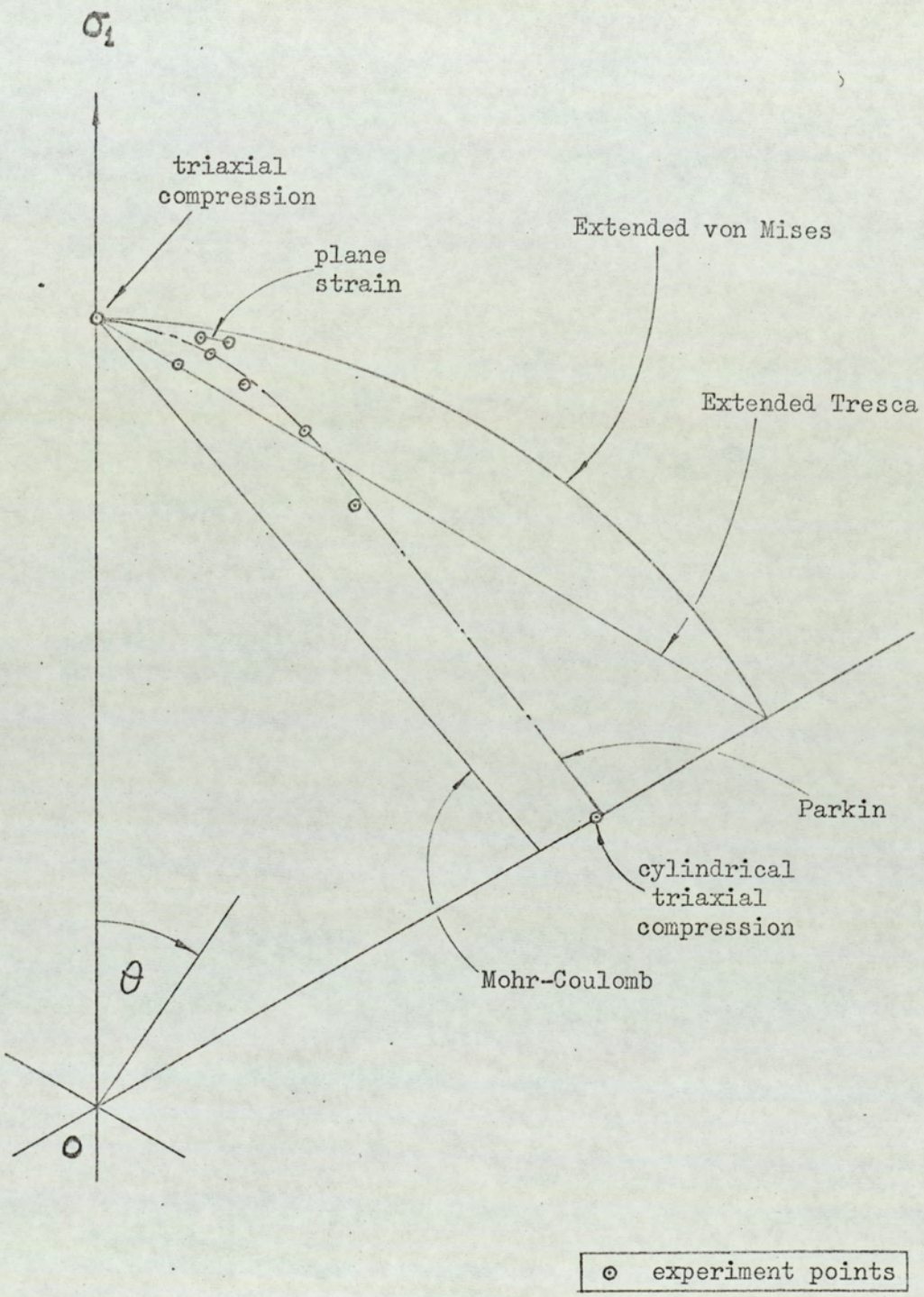

FIG.7.48
Failure Criteria

FIG. 7.49
VARIOUS TEST SERIES
$\dot{\varepsilon}_{vf}$ v. e_i

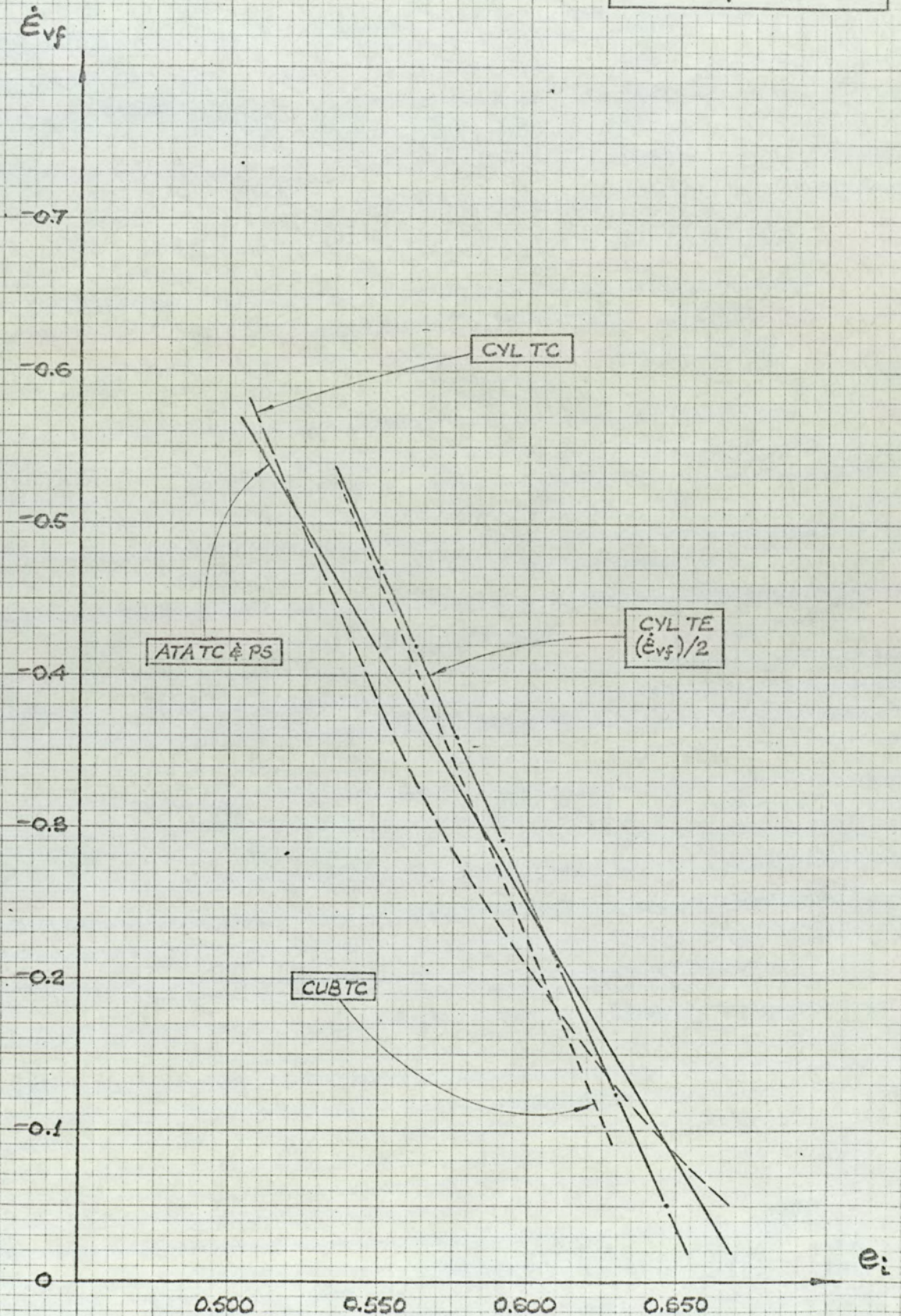

APPENDICES

APPENDIX A

LABORATORY MANUFACTURE OF LATEX-RUBBER MEMBRANES

The specially designed side stress-cell membranes and cuboidal specimen membranes were manufactured in the laboratory from a pre-vulcanised, ammonia-stabilised latex.

The process is essentially simple. A perspex former is dipped into a tank of the latex. When withdrawn the former is coated with a thin latex film which upon drying takes the same shape as the former. However, an allowance must be made for shrinkage of the film when deciding the dimensions of the former.

Control of the membrane thickness is facilitated by the use of a coagulent which also improves membrane uniformity. Prior immersion of the former into the coagulent causes a gelling of the latex during the subsequent dip, the strength of the coagulent solution being one of the factors determining thickness. If necessary several dips can be used to build up sufficient thickness.

From these basic principles, the following process has evolved as the most suitable for the manufacture of membranes in the laboratory:-

(i) Clean former and immerse in coagulent (20% solution of calcium nitrate in I.M.S.).

(ii) Withdraw slowly and allow a few seconds for excess coagulent to run off.

(iii) Lower former steadily into latex, at approximately 1 in./sec.; keep immersed for about 5 seconds; withdraw at same rate.

(iv) Invert and slowly rotate to prevent any excess latex from forming globules.

(v) Inspect surfaces carefully, if necessary "dabbing on" latex to complete coverage.

(vi) Dry under lamp for a few minutes, then place in oven at 70-80°C.

(vii) Remove when transparent (2 to 3 hours is usually sufficient) and leave to cool naturally to ambient temperature.

(viii) Dust membrane with talc and strip from former, simultaneously dusting inside surface.

(ix) Wash off talc, dry membrane and inspect for perforations or weaknesses by stretching against a bright light. (Water-filling may be used as a further check).

(x) Trim with scissors as required.

(xi) Dust with talc and store in a closed container.

Before dipping, it is important to ensure that air bubbles have been removed from the latex. This is done most easily by allowing the tank to stand uncovered for several hours, periodically skimming off the latex skin which forms on the surface.

After oven-drying, by allowing the membrane to cool while still on the former, shrinkage was reduced to about 6% on average. However, since the magnitude of shrinkage varied from point to point, the best method of obtaining the desired membrane size was found to be one of trial and error, with continual adjustment of the former dimensions.

When manufacturing both the cuboidal specimen membranes and the side stress-cell membranes, it proved beneficial to increase the thickness of rubber in certain areas not on the "working-surface". This increase was desirable at the top and bottom of the specimen membranes for more efficient sealing with the end stress-cells, and to reduce the vulnerability of the membrane to puncture around the relatively sharp edges. Similarly the thickness around the flange of side stress-cell membranes was increased to improve the seal between back-plate and side-frame. In such cases the second dipping-cycle may be performed

a few minutes after the first, without the necessity of oven-drying during the interim period.

During inspection of the stripped membrane any perforations or weaknesses may be repaired by "dabbing on" latex followed by oven-drying to transparency. However, repairs should be restricted to areas not on the working-surface.

The side stress-cell membranes were replaced as necessary and, in general, each cuboidal specimen membrane was used for one, or occasionally two, tests. Therefore membranes with even slight imperfections on the working-surface were discarded before use.

The formers used are shown in Fig. A1 together with the dimensions of the finished membranes.

Thickness uniformity of several membranes manufactured in the laboratory was studied. Using a micrometer gauge, 36 measurements of thickness were taken on the working-surfaces of each of four specimen membranes. In addition the thickness of each of two side stress-cell membranes was measured in six positions distributed evenly over the surface, and further measurements were taken of the thickness of membranes subjected to two dipping-cycles. The results are shown in Table A.1.

TABLE A.1.

Membrane Type	Average thickness (in.)	Standard deviation (in.)
Cuboidal specimen membranes	0.0127	0.0015
Side stress-cell membranes	0.0129	0.0014
Twice-dipped surfaces	0.0210	-

The average thicknesses of all working-surfaces were assumed in all calculations.

FIG. 4.1/A.1
MEMBRANE FORMERS
Scale - Half Size

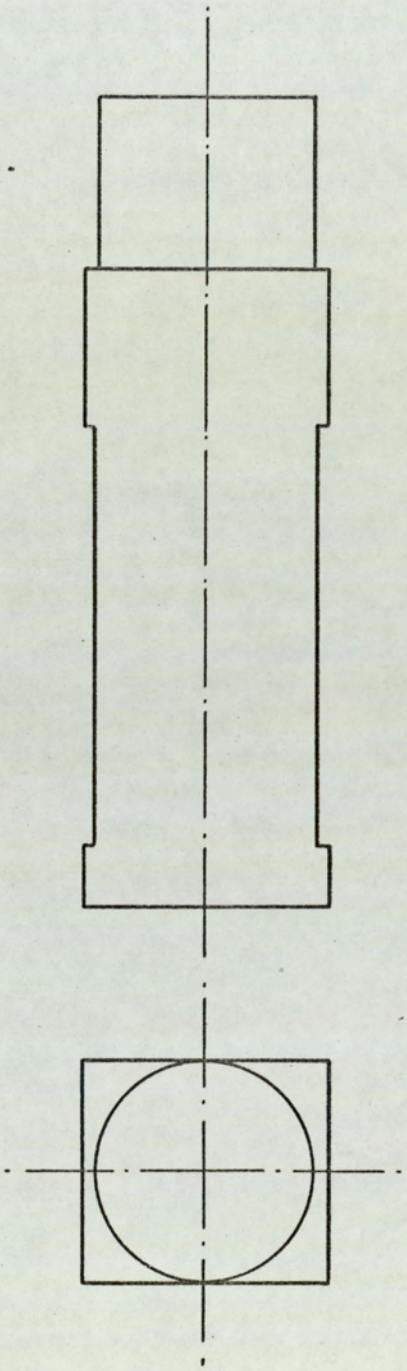

(a) CUBOIDAL SPECIMEN MEMBRANES

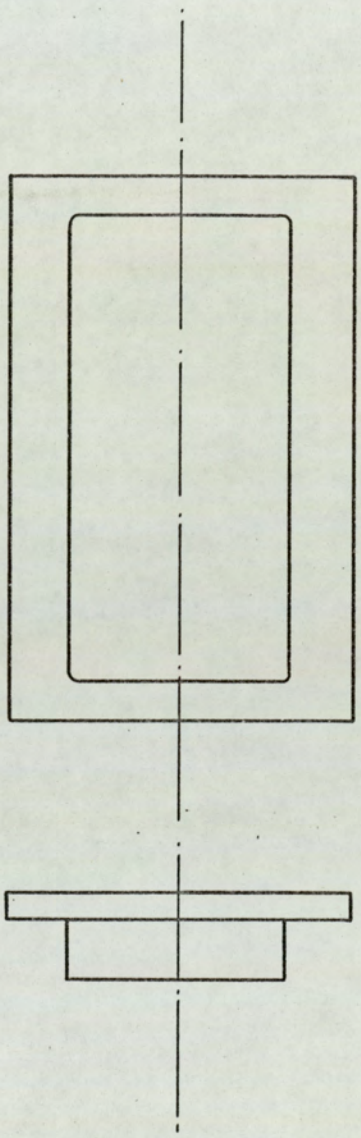

(b) SIDE STRESS - CELL MEMBRANES

APPENDIX B

MEMBRANE PENETRATION TESTS

The measurement of volumetric deformation of cohesionless soils, if based on the volume of pore-fluid entering or leaving the specimen, is susceptible to errors resulting from penetration of the rubber membrane into the voids under pressure (4.4.2). All of the experiments in this research program, including triaxial compression of cylindrical and cuboidal specimens, triaxial extension of cylindrical specimens, and tests under a variety of stress conditions in the ATA, were carried out on specimens of coarse sand. Therefore it was essential to correct the volumetric deformations for membrane penetration.

It was decided to use a method similar to that described by Roscoe et al (1963) in which cylindrical annular specimens of sand, with rigid coaxial cylindrical rods, were tested under ambient stress conditions. Although the authors expressed doubts regarding the accuracy of corrections obtained in this way, these were based apparently on a comparison between this method and another which would appear inferior (4.4.2).

B.1 SPECIMEN PREPARATION AND MEASUREMENT

The specimen density, or porosity, is an important factor in determining the magnitude of the membrane penetration effect. Triaxial compression and extension tests, and those in the ATA, were carried out over a range of initial density. Therefore in order to make membrane penetration corrections for any one test, it was necessary to investigate this effect over a similar density range, and attempts were made to prepare specimens at four relative densities.

At each density four specimens, nominally 5 in. long and 2.8 in. O.D., were formed around coaxial cylindrical perspex rods, 0.75, 1.25, 1.75 and 2.25 in. in diameter respectively, and also 5 in. long. Each specimen was subjected to ambient stress, and the apparent volume change determined for each stress increment between 0 and 80 lbf/in^2.

Formation of the specimen was difficult, since the presence of the rods, placed in position prior to sand deposition, precluded the use of one of the more conventional methods of preparation, such as settlement through water. In addition the height of the required specimen was fixed at 5 in., and in each case it was hoped to produce a uniform specimen of a predetermined initial density.

The following technique was found to be the most suitable:-

The mass of sand needed to form the specimen was calculated from the approximate initial volume and required initial density. A mass slightly in excess of this was submerged in water and boiled. Having placed a lubricated end membrane in position covering the bottom platten, the specimen membrane was sealed with rubber O-rings and the specimen former set up as described in 5.5.1.

The membrane was then partially filled with de-aired water, to an extent dependent upon the rod diameter, and similar precautions were

taken against trapping air during the filling process. The rod was lowered into position in the centre of the bottom platten, displacing water upwards so that the membrane, supported several inches above the top of the former, was filled almost to its brim.

Sand was transferred from the container into the membrane by spooning, the rod being held firmly in position during this and subsequent processes. For each volume of sand transferred, a little water was siphoned off to maintain an approximately constant level above the rod. Spilling over could have resulted in a loss of particles. Except for the loosest specimens, vibration was applied to the former, the degree depending on the required density. When preparing the densest specimens, the cell base also was vibrated.

Under the effect of a small pore-suction, conventional solid cylindrical sand specimens consolidate, reducing in both height and diameter. Unless the top platten is free to move in the former, a "neck" results at the top of the specimen. In the membrane penetration specimens, top platten movement is prohibited, except for a very small compression of the lubricated membranes, by the presence of the rod. Therefore, if the sand were to be finished level with the top of the rod, necking would undoubtedly occur when the pore-suction was applied. This happened in early attempts to form specimens.

The difficulty was overcome by "banking" the sand surface outwards from the rod towards the specimen circumference, the gradient of the slope for each density and rod diameter being determined by experience.

Having banked the top of the sand in this way, the top platten, with its lubricated end membrane and circumferential filter paper (5.5.1), was placed in position, and de-aired water passed through the drainage connection to remove trapped air-bubbles. The specimen membrane was

then sealed with rubber O-rings and a small pore-suction, 0.4 lb./in^2, applied.

If, upon removing the former, a significant neck had formed or the specimen was greater than 5.020 in. long, the specimen was rejected and preparation begun again. The latter fault results from excessive banking of the sand prior to placing the top platten. Although the specimen profile may appear uniform, there is a clear possibility that sand particles have become trapped between the perspex rod and the top platten causing the initial length of the specimen to be greater than that of the perspex rod and the thickness of two lubricated membranes. The effect of overlooking this fault is likely to be much greater than the effect of accepting slight necking at the top of the specimen due to insufficient banking of sand. However, after initial experimentation with this type of preparation, few specimens had to be rejected because of either fault.

The height and mean diameter of each specimen were determined in the manner described for cylindrical triaxial compression tests. The triaxial cell was then clamped to the base and the plunger, which is not used actively in this type of test, was vertically restrained in its bushing before filling the cell.

With the burette at specimen mid-height, the cell pressure was raised in increments from zero to 5, 10, 20, 30, 50 and 80 lbf/in^2 and the discharged volume of water measured. For brevity this will be described as the "volume change". However, it is meant to imply only that this volume of pore-fluid has been discharged, and not that the sand specimen has compressed by this amount. Each increment of ambient stress was maintained for a period long enough to ensure that full consolidation had occurred. Normally about 15 minutes was sufficient for each stage.

It was expected that the resulting strains would be reasonably

uniform since lubricated end membranes were used. Although they compress slightly under pressure, the magnitude of compression for a given ambient stress should be the same in all tests, and therefore have negligible effect on the extrapolated membrane penetration correction (B.2). Moreover, their inclusion meant that the tests were carried out under the conditions of minimal end friction appertaining to all stress-deformation tests in this research program.

B.2 RESULTS AND DISCUSSION

The volume changes resulting from the initial stress increment, 0 to 5 lbf/in^2, in each of the sixteen tests were found to be inconsistent with those occuring during subsequent increments. In addition, inconsistencies in volume change among specimens prepared at different densities were apparent for the initial increment only. Probably this was caused by slight differences in the preparation of the specimen, end-membrane compression, bedding at each end of the perspex rod, sealing of the specimen membrane and associated effects which are variable. Clearly these are likely to be insignificant at higher stress levels.

Therefore it was decided to ignore the first stress increment and to use the specimen volume at 5 lbf/in^2 as the datum from which to measure volume change. The results are shown in Figs. B.1, B.2, B.3 and B.4, as graphs of total volume change, ΔV (ml), against applied ambient stress, σ_r (lbf/in^2) for each diameter rod, D_r (in.). As expected, the volume change decreases with increase in rod diameter and initial density of the specimen, γ_d(lbf/ft^3).

Figs. B.5, B.6, B.7 and B.8 show that for each stress level, the decrease in volume change is approximately linear with initial dry density for all four rod diameters. By interpolating values of ΔV for three convenient densities, 100, 103 and 106 lbf/in^2, and plotting against the rod diameter, the effect of the latter at each stress level was determined. Figs. B.9, B.10 and B.11 show that the relationship is again linear.

These curves were extrapolated to D_r = 2.8 in. in order to determine the volume change that would occur in the hypothetical case of a fully rigid specimen having surface properties identical with those of a solid, cylindrical specimen. The extrapolated values of ΔV were

plotted against σ_{3c}, for each value of γ_d, to a natural scale, Fig. B.12, and to a semi-logarithmic scale, Fig. B.13.

For all three densities, the graphs of ΔV against log σ_{3c} approximate very closely to straight lines passing through $\sigma_{3c} = 5.0$, the stress at which the datum for ΔV was chosen. Therefore that part of the membrane penetration correction associated with ambient stress above 5.0 lbf/in^2 may be written in the form:-

$$\Delta V = k.\log(\sigma_{3c}/5), \qquad (1)$$

where k, the gradient, is dependent only upon density. By interpolation from the curves for the various densities, k may be expressed in terms of initial porosity, a more convenient parameter, as:-

$$k = (17.02n - 5.25), \qquad (2)$$

giving

$$\Delta V = (17.02n - 5.25).\log(\sigma_{3c}/5). \qquad (3)$$

Below $\sigma_{3c} = 5.0$, for the reasons discussed, the results of these membrane penetration tests are less conclusive, being more widely scattered. However, at low stress levels the effects are likely to be less significant, and it was decided to take the overall average behaviour of the 16 specimens tested, irrespective of initial density, to complete the membrane penetration correction, ΔV_p, as follows:-

$$\text{for } \sigma_{3c} \leq 5.0, \quad \Delta V_p = 0.10\sigma_{3c}; \qquad (4a)$$

$$\text{for } \sigma_{3c} > 5.0, \quad \Delta V_p = 0.50 + (17.02n - 5.25).\log(\sigma_{3c}/5). \qquad (4b)$$

This is the basic form of correction incorporated in the computer programs used to process results of stress-deformation tests on this soil.

The true volumetric strain of the membrane penetration specimens was very small, not greater than about $\frac{1}{2}\%$ even for loose specimens stressed to 80 lbf/in^2. Therefore it was assumed, in deriving the correction equations, that the initial porosity applied throughout the range of stress. During stress-deformation testing of cohesionless soils, the application of deviatoric stresses usually causes considerable

volumetric strains, particularly in dense dilating assemblies. The effect of such porosity changes on membrane penetration is assumed to be given by equation (4b), the implication being that this equation describes the effect of any changes in porosity, regardless of whether they result from ambient or deviatoric stresses.

A further assumption, that the measured overall average porosity is representative of the soil properties at surfaces subject to membrane penetration, was necessary in the absence of information on specimen homogeneity (4.5.1). Nevertheless the corrections obtained from these tests, given by equation (4), were thought to be sufficiently reliable for the accuracy of corrected volumetric strain to be compatible with that of corrected stress.

The membrane penetration tests described were carried out on cylindrical specimens, almost exactly 5 in. long and 2.8 in. in diameter. Because it is a condition associated with the specimen surface, the effect of membrane penetration will decrease with decrease in surface area, providing other factors are constant. All cylindrical tests, whether in triaxial compression or extension, were carried out on nominally 2.8 in. dia. specimens. However, their lengths were various. In particular, those of compression and extension specimens were widely different. Therefore a factor was incorporated in the membrane penetration correction, based on direct proportionality between surface area and penetration, and hence between specimen length and penetration.

The corrections applied to the volumetric deformations during cuboidal triaxial compression tests were also based on specimen surface area. The perimeter of the cuboidal specimens and circumference of the cylindrical specimens were very similar, and therefore length was again the dominant factor. However, the difference in curvature

of the surfaces, particularly at the corners of the cuboidal specimens, may have some slight influence on membrane penetration. It was assumed that this was negligible.

ATA specimens were treated in a similar manner, the correction being based on the surface area exposed to main-cell pressure, i.e. the σ_x faces of the specimen. It was assumed that the combination of membranes and silicone grease on the σ_y faces, on which the side stress-cells operate, and that of the rubber diaphragm and lubricated end-membranes on the σ_3 faces, on which the end stress-cells operate, would minimize membrane penetration on these surfaces.

The various forms of membrane penetration correction were included in the respective computer programs for each type of test along with any other necessary corrections, such as those to be applied to axial deformations (Appendix C.).

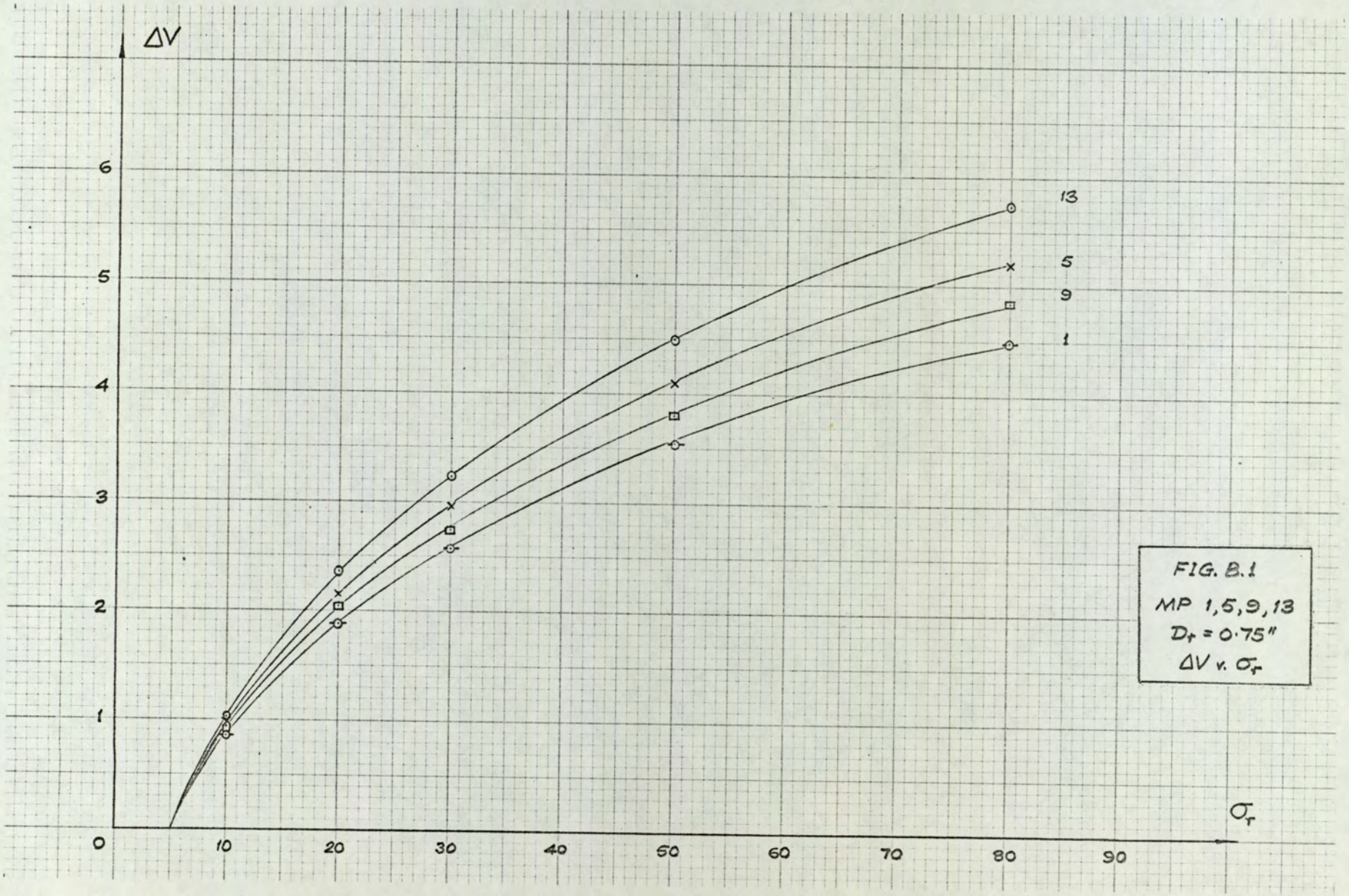
ΔV
6
5
4
3
2
1
0
10
20
30
40
50
60
70
80
90
σ_r
13
5
9
1
FIG. B.1
MP 1,5,9,13
$D_r = 0.75''$
ΔV v. σ_r

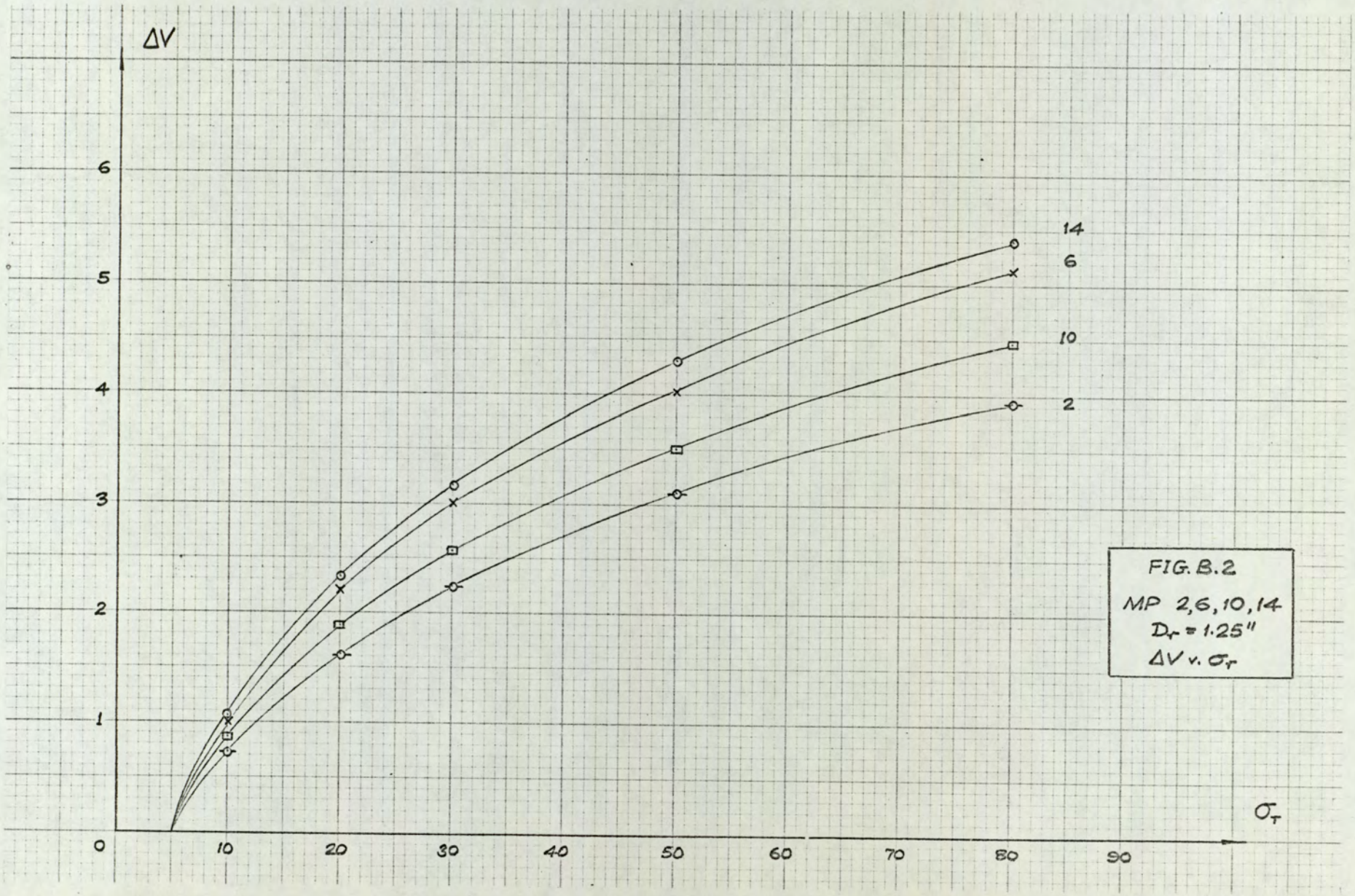

FIG. B.2
MP 2,6,10,14
$D_r = 1.25''$
ΔV v. σ_T

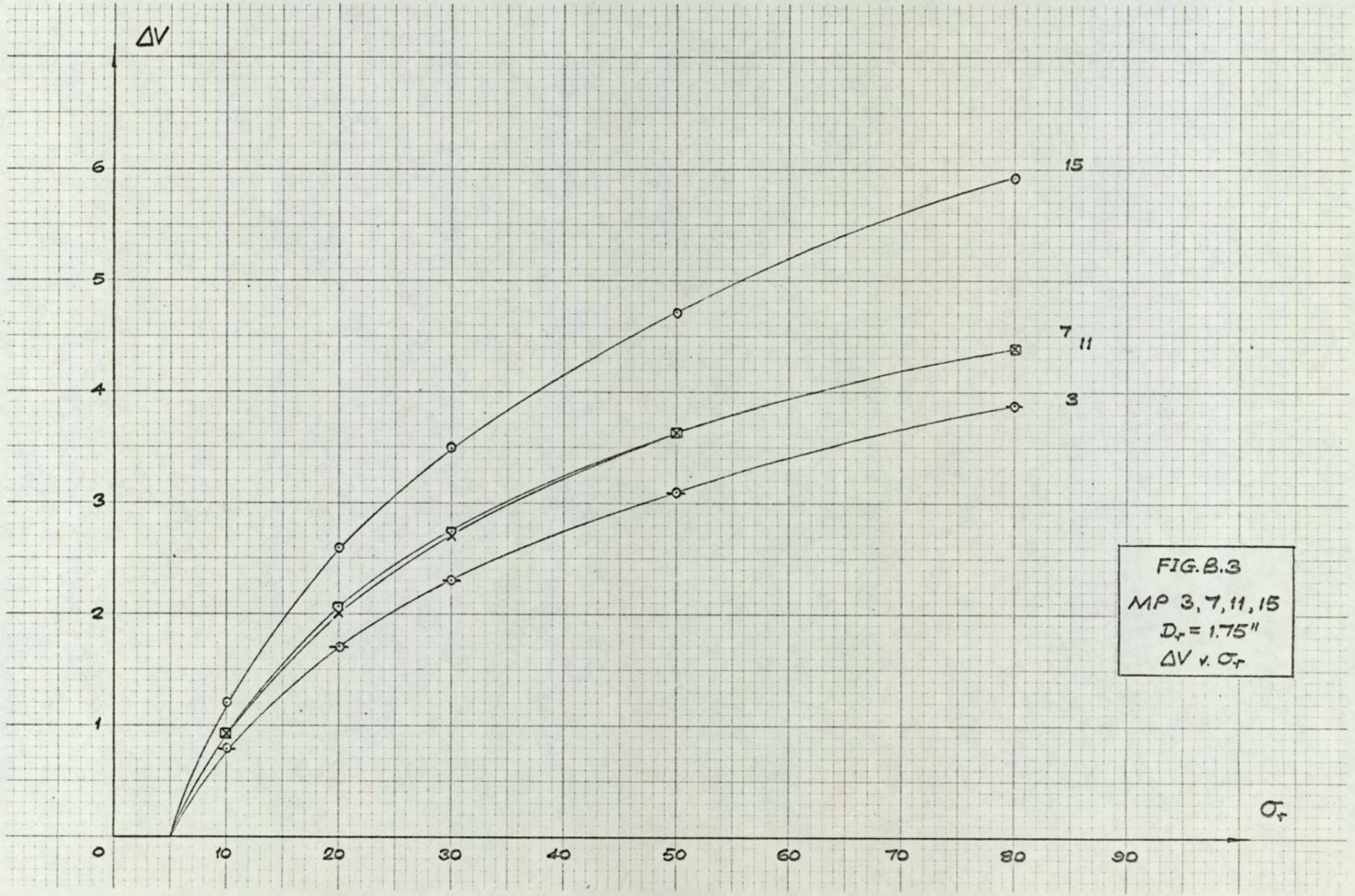

FIG. B.3
MP 3, 7, 11, 15
D_r = 1.75"
ΔV v. σ_r

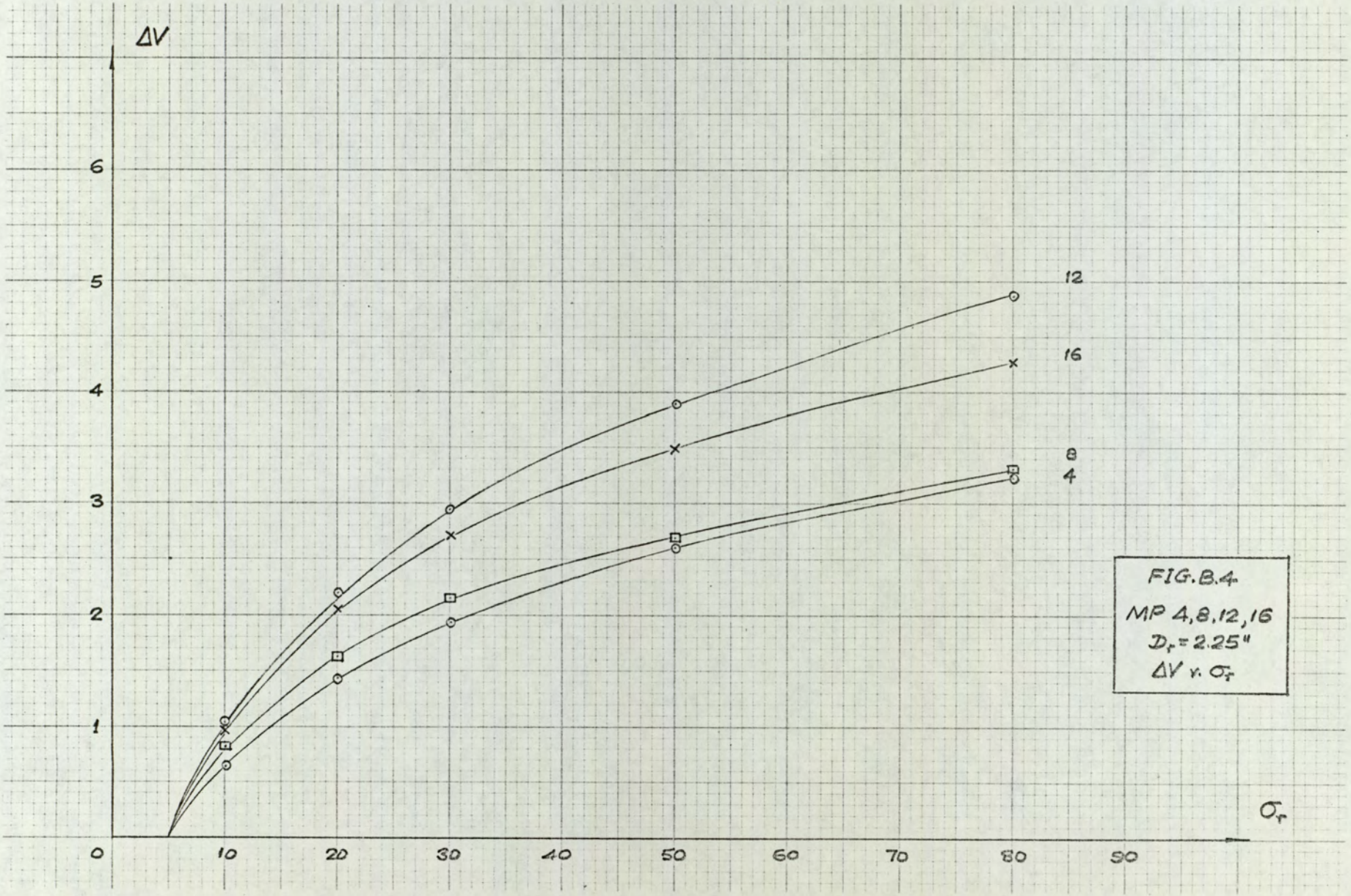

FIG. B.4
MP 4, 8, 12, 16
$D_r = 2.25"$
ΔV v. σ_r

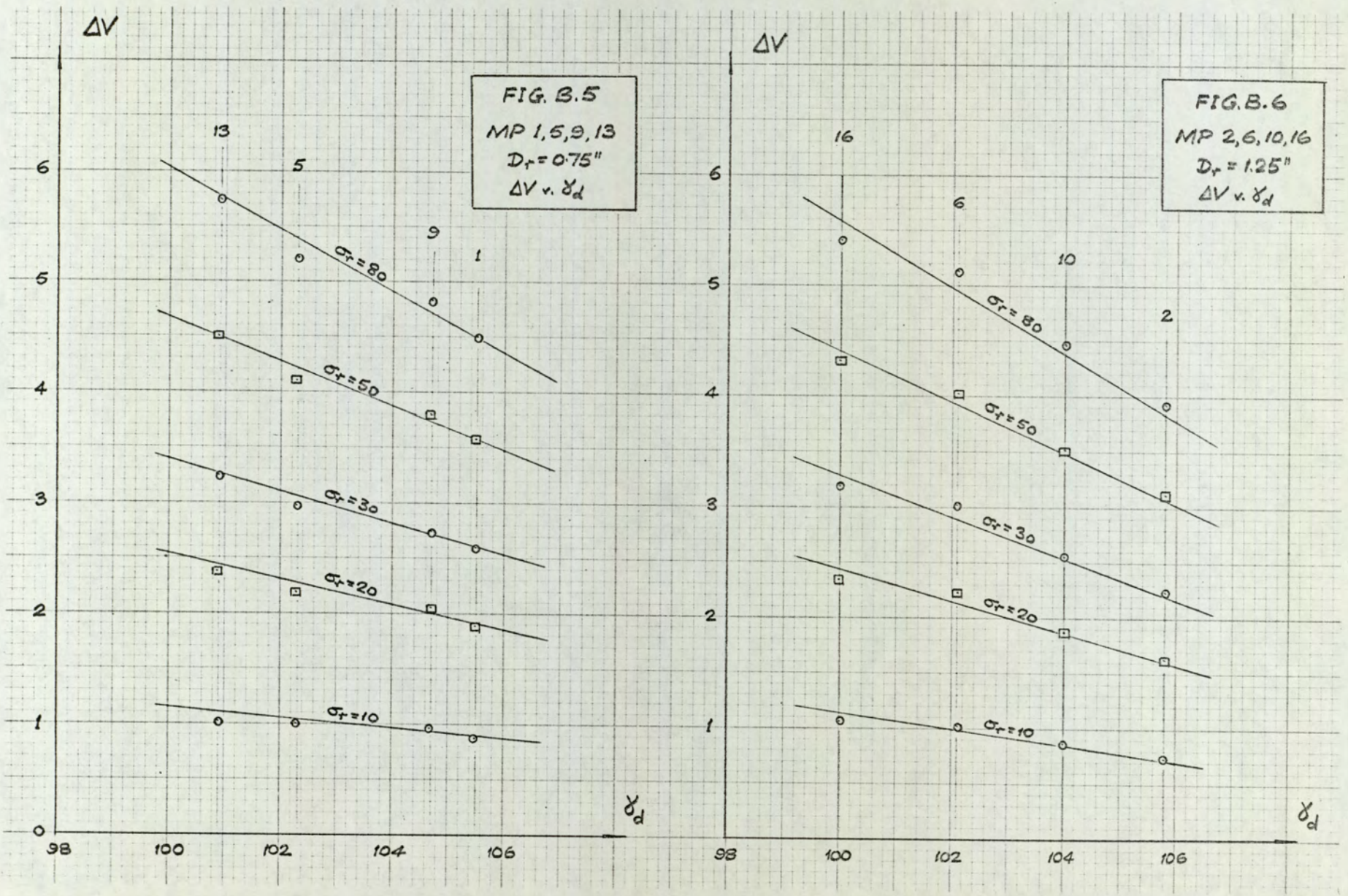
ΔV
FIG. B.5
MP 1,5,9,13
D_r = 0.75"
ΔV v. γ_d
13
5
9
1
σ_r = 80
σ_r = 50
σ_r = 30
σ_r = 20
σ_r = 10
0
1
2
3
4
5
6
98
100
102
104
106
γ_d
ΔV
FIG. B.6
MP 2,6,10,16
D_r = 1.25"
ΔV v. γ_d
16
6
10
2
σ_r = 80
σ_r = 50
σ_r = 30
σ_r = 20
σ_r = 10
1
2
3
4
5
6
98
100
102
104
106
γ_d

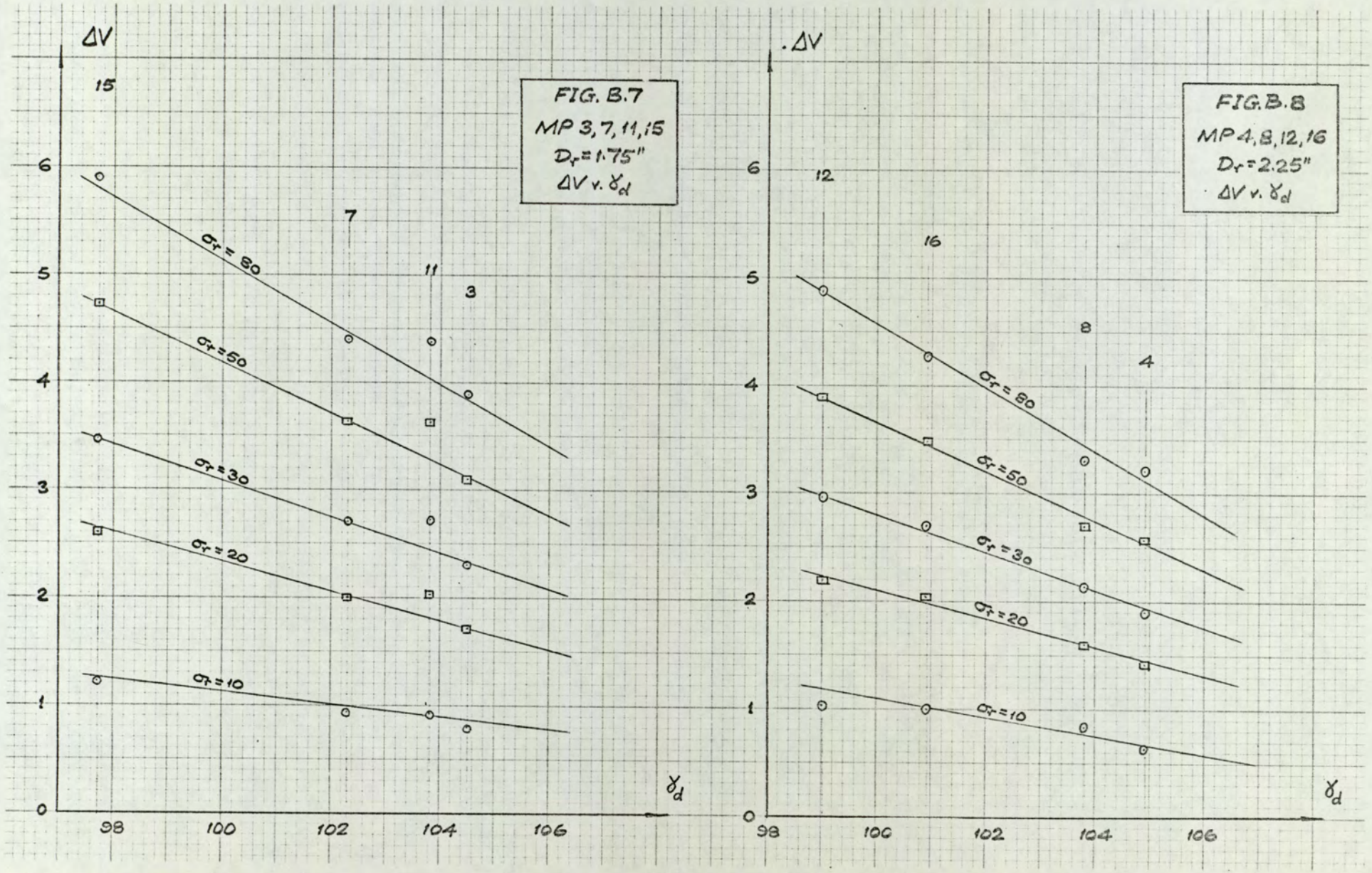
ΔV
15
6
5
4
3
2
1
0
98
100
102
104
106
γ_d
$\sigma_r = 80$
$\sigma_r = 50$
$\sigma_r = 30$
$\sigma_r = 20$
$\sigma_r = 10$
7
11
3
0
FIG. B.7
MP 3, 7, 11, 15
$D_r = 1.75"$
ΔV v. γ_d
ΔV
12
6
5
4
3
2
1
0
98
100
102
104
106
γ_d
$\sigma_r = 80$
$\sigma_r = 50$
$\sigma_r = 30$
$\sigma_r = 20$
$\sigma_r = 10$
16
8
4
0
FIG. B.8
MP 4, 8, 12, 16
$D_r = 2.25"$
ΔV v. γ_d

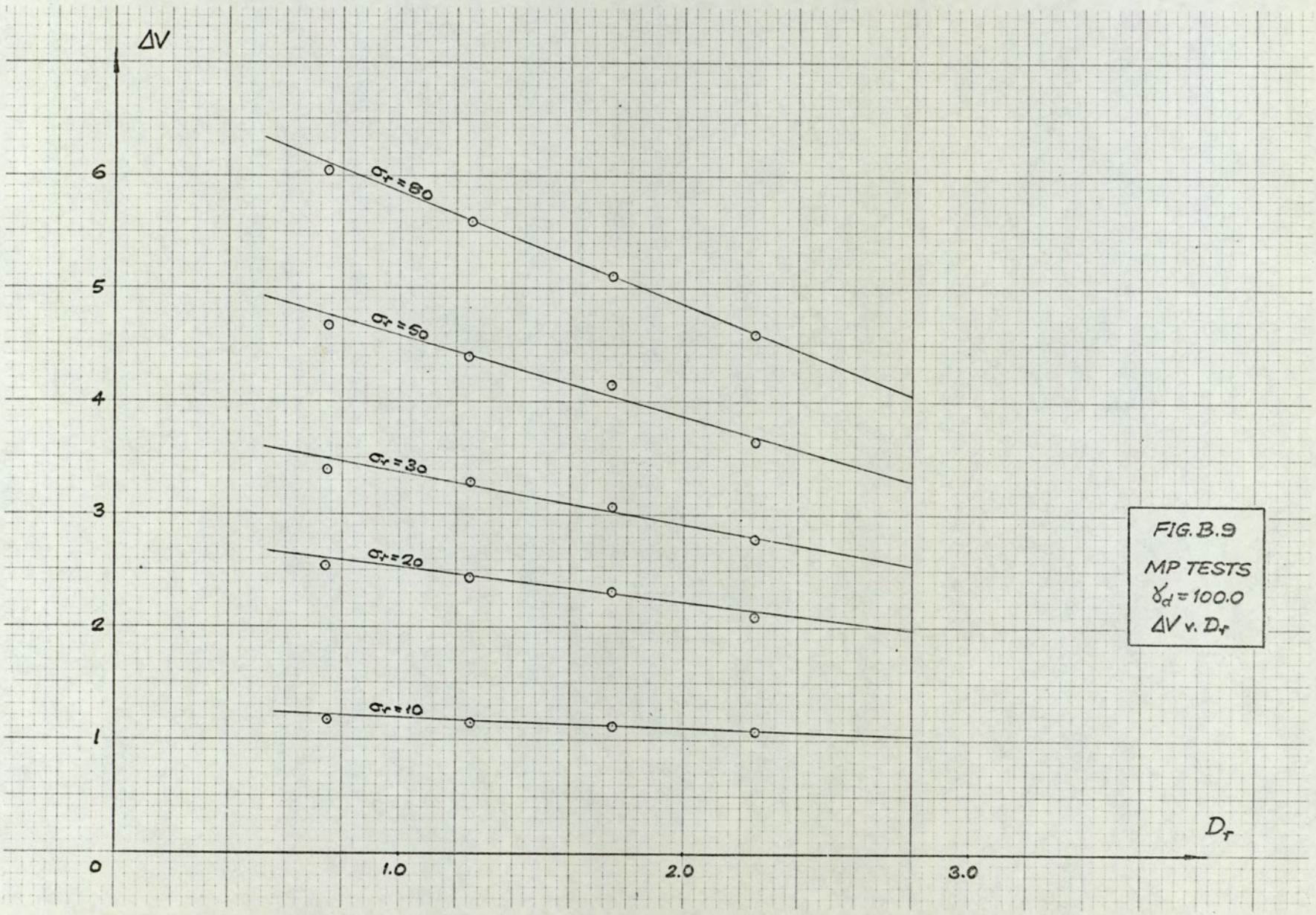

FIG. B.9
MP TESTS
$\gamma_d = 100.0$
ΔV v. D_r

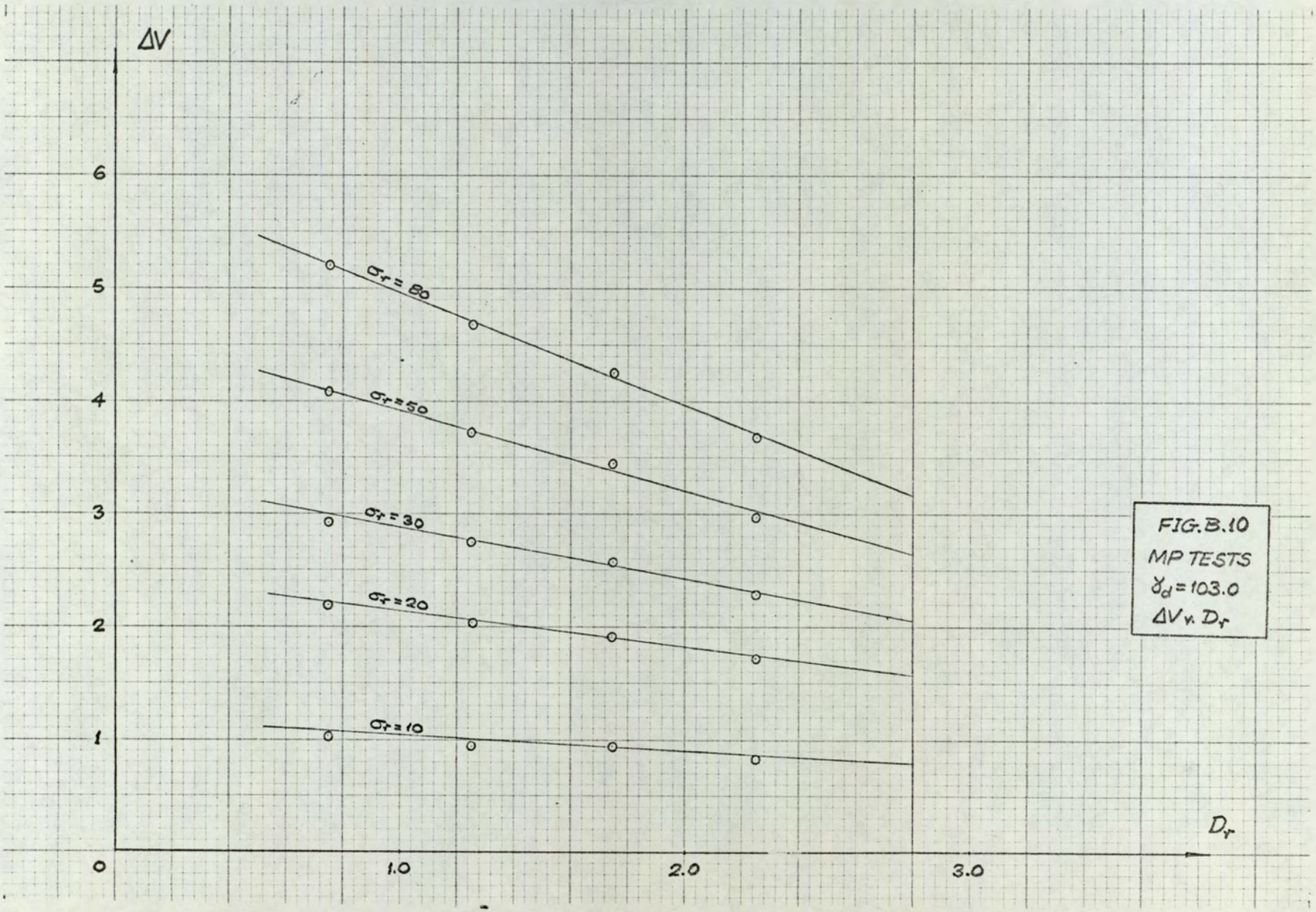

FIG. B.10
MP TESTS
$\gamma_d = 103.0$
ΔV v. D_r

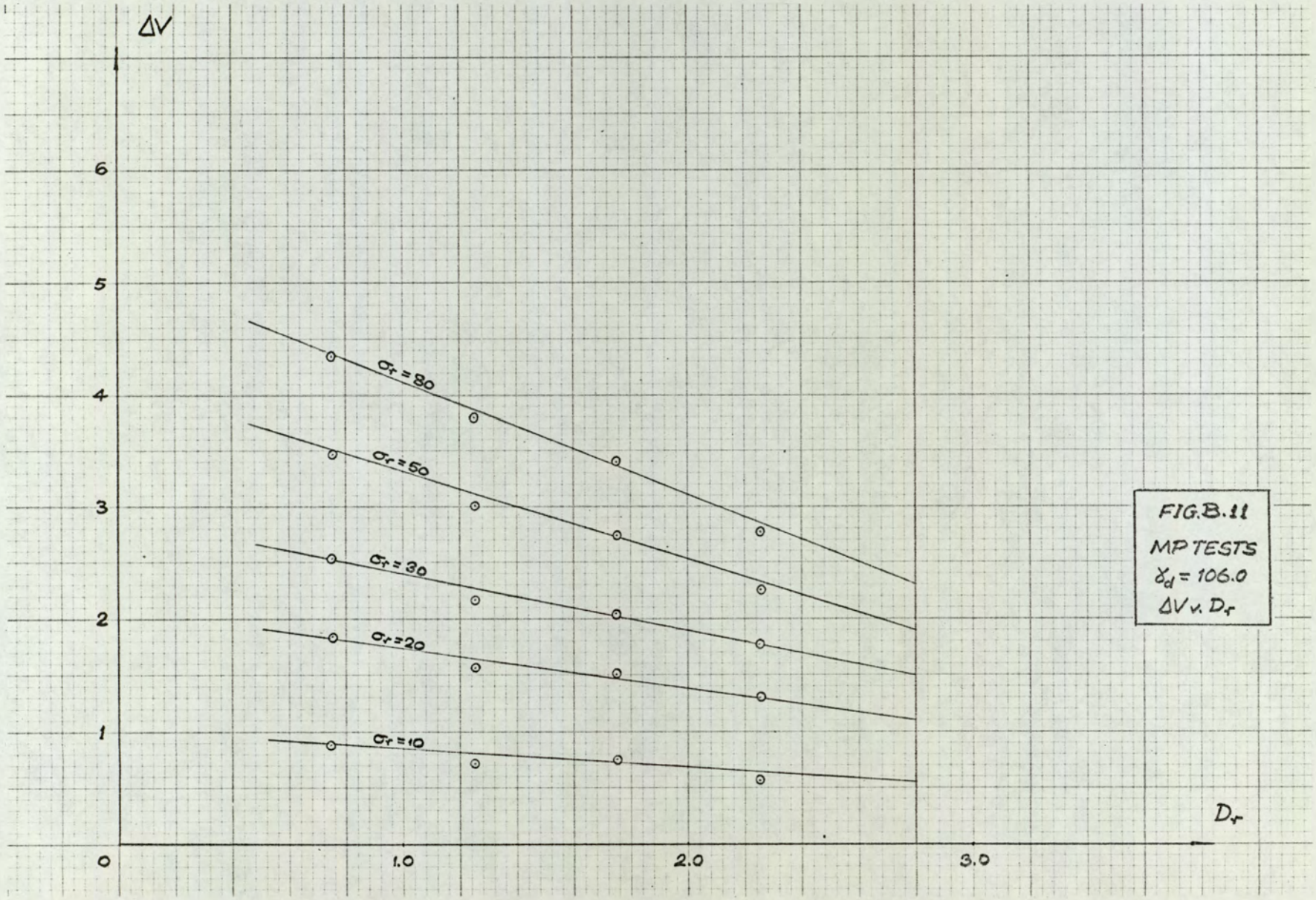

FIG. B.11
MP TESTS
$\gamma_d = 106.0$
ΔV v. D_r

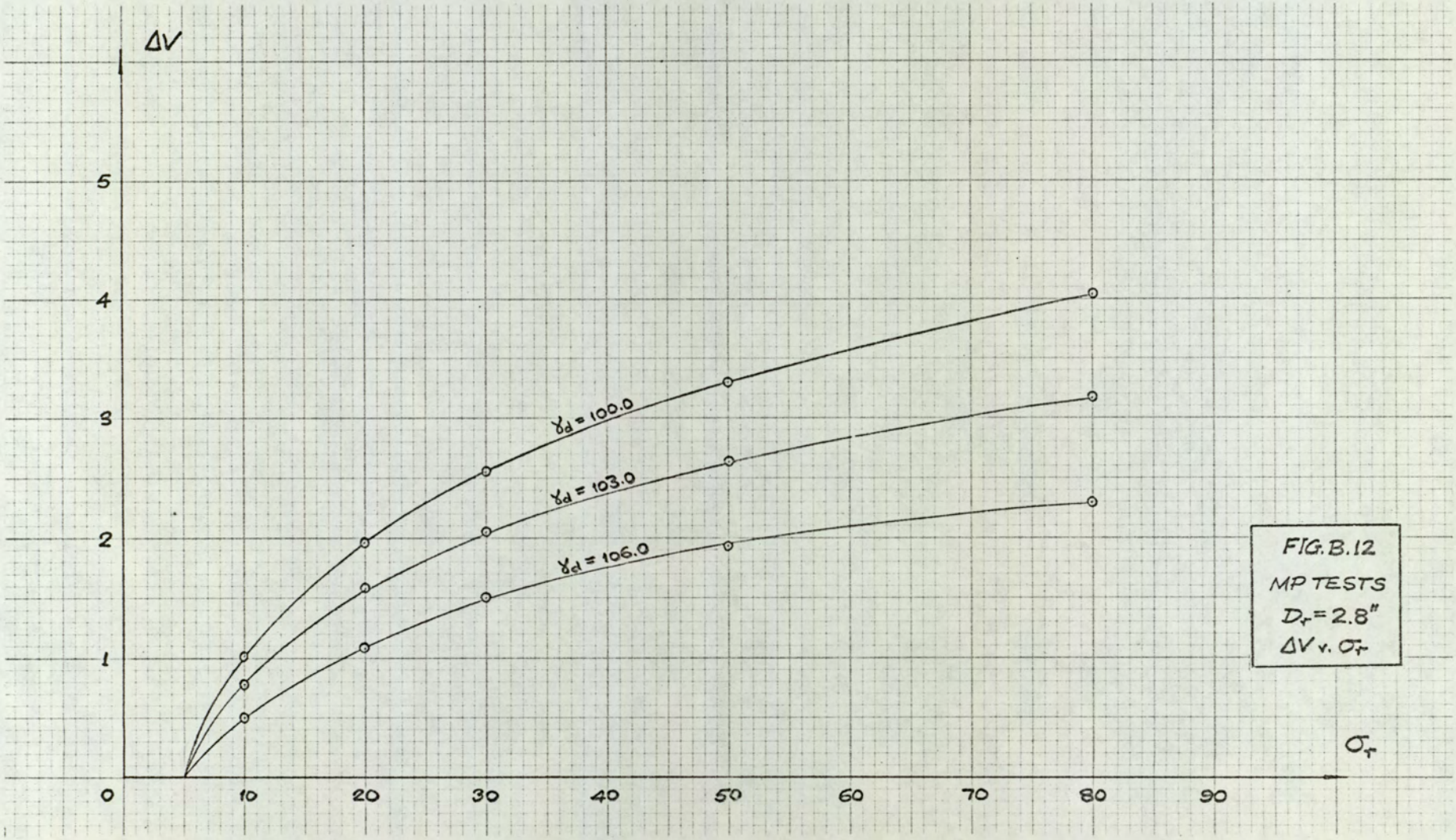

FIG. B.12
MP TESTS
D_r = 2.8"
ΔV v. σ_r

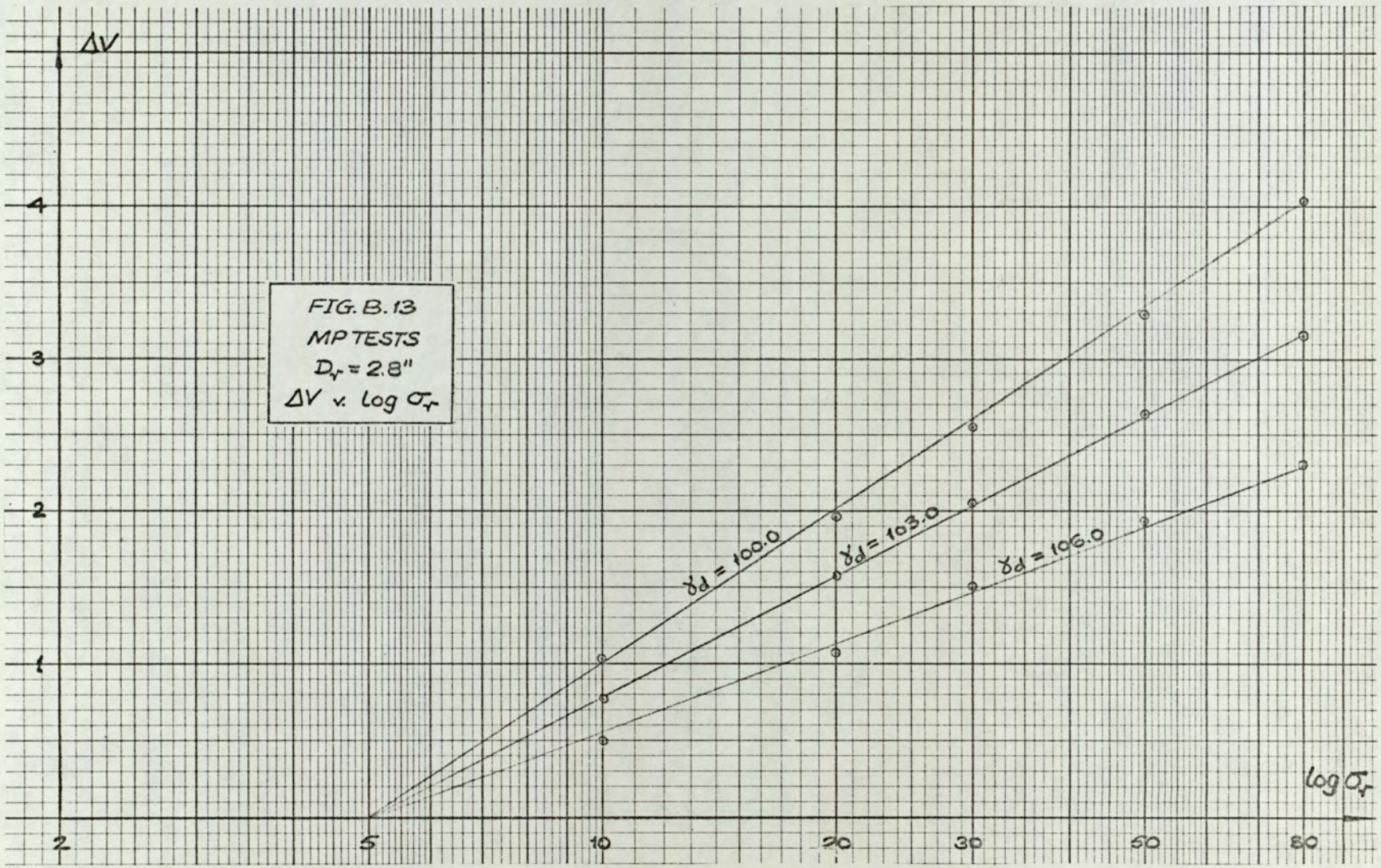
ΔV
4
3
2
1
FIG. B.13
MP TESTS
D_r = 2.8"
ΔV v. log σ_r
γ_d = 100.0
γ_d = 103.0
γ_d = 106.0
log σ_r
2
5
10
20
30
50
80

APPENDIX C

APPARATUS CALIBRATION TESTS

The methods used to measure the direct strains of ATA specimens were described in 4.4.1. Similar systems were used in all the other stress-deformation tests carried out, reliance being placed on accurate correction of observed deflections.

In ATA tests only two of the three direct strains are measured, the third being calculated from knowledge of volumetric deformation corrected for membrane penetration (Appendix B). Therefore calibration of measuring instruments to allow for strain of the apparatus, and bedding of the specimens at boundaries where measurements are made, is essential. Moreover, the accuracy of the instruments themselves must be known.

Measurements of stress in the x- and y-directions were made using two Budenberg pressure gauges. In the z-direction, pressure induced in the top and bottom stress cells, and transmitted to pressure transducers, was recorded using an ultra-violet recorder, (Consolidated Electrodynamics 5-127 Recording Oscillograph). Similar arrangements were used for testing cylindrical and cuboidal triaxial specimens, except that in the majority of tests a proving ring was used to measure axial stress in addition to the end stress-cells, so that a comparison between these systems could be made. This was also the case in a few ATA tests.

C.1 AXIAL STRAIN

Calibration tests were carried out in order to determine the corrections to be applied to measurements of strain in the axial-direction in cylindrical triaxial compression tests. The results of these tests were then used as the basis for correcting axial strains measured in the various other tests, including those in the ATA. Fig. C.1 shows the layout of the apparatus in diagrammatical form.

A mild-steel cylindrical dummy specimen, 5 in. long and 2.8 in. dia., was used in order to eliminate the soil specimen deformation as a factor in the calibration. In all other respects the apparatus was identical with that used for cylindrical triaxial compression tests with top and bottom stress-cells. In a second series of tests, the stress-cells were replaced with rigid end plattens so that their relative deflections under stress could be studied.

The deflection dial gauge mounting used in the majority of tests was that shown in Fig. C.1. The disadvantages of this system, relative to internal methods of axial deformation measurement, were discussed in 4.4.1. However, the size of the main-cell relative to that of the specimen was such that internal measurement was precluded.

The following are the major sources of error in determining axial strains (see Fig. C.1):-

(a) seating of the proving-ring at the loading crosshead;

(b_1) seating of the proving-ring onto the plunger;

(b_2) seating of the ball-bearing between the plunger and the top stress-cell;

(b_3) compression of the lubricated end-membrane, squeezing out of the silicone grease layer, compression of the stress-cell and rubber diaphragm, and bedding of the specimen;

(b_4) a similar condition at the bottom of the specimen;

(c) seating of the cell onto its base and the associated O-ring compression;

(d_1) seating of the cell base onto the brass spacer;

(d_2) seating of the spacer onto the loading pedestal;

(e) expansion of the loading frame;

(f) distortion of the cell.

In most ATA tests the proving-ring was replaced with a brass rod and ball-bearing. Although this permitted the application of a genuinely constant rate of deformation, since proving-ring compression was eliminated, the seating errors are likely to be similar. Errors due to compression of the body of the stress-cells are probably negligible compared with that of the rubber diaphragms and membrane-silicone grease sandwich.

Bedding of the specimen onto loading plattens is a problem common to the majority of stress-deformation testing, and tests in the ATA are no exception. However, the provision of flexible surfaces at each end of the specimen may, in addition to increasing the degree of stress homogeneity, improve the intimacy of contact.

In 4.4.1, Barden and Khayatt's (1966) experiments on axial strain measurement were discussed, with particular reference to their comments regarding reliability of calibration for cell distortion, and its dependence upon the clamping of the cell to its base. During the ATA test program, no difficulty was experienced with this process, Clockhouse "quick release" clamps being used. It was expected that the clamping force was very similar in each case, and therefore that the error due to cell distortion was not variable. However, the seating of the cell onto the cell-base O-ring must be regarded as another possible source of error.

A Clockhouse Universal Triaxial Cell was used as one of the basic

components in the development of the ATA, and also served for triaxial compression and extenstion tests. The testing program was, however, carried out using a Wykeham Farrance 5 ton capacity compression testing machine. Therefore the diameter of the loading pedestal was different from that of the recess in the cell-base, and a brass spacer had to be inserted to ensure that the cell remained centrally-positioned during testing. Although machined plane, the seating of the spacer represents another source of error.

In order to investigate the relative magnitudes of the errors described, a "triaxial compression test" was carried out on the dummy specimen at a "rate of strain" of 0.004 in./min. The cell pressure was zero during this stage of the test, but was later raised in increments to about 80 lbf/in^2 in order to determine cell distortion. Deflections were measured (Fig. C.1) using a dial gauge fixed to the loading machine to measure the upward movement of the pedestal (PDG), a dial gauge mounted on the base of the proving-ring, in the conventional manner, (DDG), and the proving-ring dial gauge (PRDG).

Taking all apparatus deformations as positive in compression, and assuming that the dummy specimen is incompressible, it can be shown that the three dial gauges measure the following compressions:-

$$DDG = (b - c - f), \tag{1}$$

$$PRDG = PDG - (a + b + d), \tag{2}$$

$$PDG - (DDG + PRDG) = (a + c + d + f), \tag{3}$$

assuming that distortion of the loading frame is negligible for the loads considered, i.e. e = 0. Since the initial tests were carried out with zero cell pressure, cell distortion was insignificant and therefore equation (1) becomes:-

$$DDG = (b - c) \tag{4}$$

Fig. C.2 shows the results of seven tests in which this quantity

was measured.

In three tests, the end conditions were similar to those in tests using end stress-cells; in a further two tests rigid end-platten conditions were simulated. Finally two tests were carried out with rigid end-plattens in direct contact with the dummy specimen, in order to determine compressions other than those due to the lubricated end-membranes and diaphragms.

Not surprisingly the use of end stress-cells in place of rigid end-plattens increases the overall compressibility of the system. However, the increase is little above 50% in the extreme case, despite the far greater thickness of rubber, the reason being that the stress-cell diaphragms are glued around a peripheral flange and therefore restrained from lateral movement.

The tests carried out on the dummy specimen only were inconclusive in separating the various components of compression, since bedding onto the end-plattens introduced a further unknown. Nevertheless, the results do show that the majority of end compression must be due to the membranes and diaphragms. Again, in equation (3), $f = 0$ and therefore, by elimination between deflection readings, the combined effect of the compression of components a, c and d was shown to be negligible (Fig. C.2).

In Figs. C.3 and C.4 the mean values of (b - c) are plotted against the square root of axial stress $\sqrt{\sigma_a}$. Because (a + c + d) is negligible, neglecting the possibility of significant compensating errors, c must be negligible, and therefore these curves represent the compression of the components listed in Fig. C.2. Each has been idealized as a straight line, passing through $\sigma_a = 1$ lbf/in^2., in order to formulate the correction to axial deformation of the specimen.

Two experiments were carried out to determine the effect of cell

distortion under pressure. The dummy specimen was set up as before, with lubricated end membranes, and the plunger brought into contact with the ball-bearing and the proving-ring. No further movement of the pedestal was allowed, and hence the PDG reading remained constant, while the cell pressure was raised to 75 lbf/in^2 in increments of 5 lbf/in^2.

From the previous compression tests, (a + c + d) was shown to be negligible relative to the compressibility of the remaining system. If this quantity is assumed to be zero, the vertical component of cell expansion, -f, under pressure, is given by:-

$$-f = (DDG + PRDG). \qquad (5)$$

The curves of expansion against cell pressure for the two experiments were of similar form, and the discrepancy between them at no point exceeded 10%. Fig. C.5 shows the mean curve of vertical expansion (in. $\times 10^{-3}$) against σ_3 (lbf/in^2), and the relationship assumed in formulating the necessary correction, idealized into two linear portions above and below 20 lbf/in^2.

The measured axial deflections, DDG, of a soil specimen in this apparatus, were corrected by subtracting the errors due to compression of the various components and expansion of the cell, the corrected axial deflection, ΔL, being given by:-

$$\Delta L = DDG - (b - f), \qquad (6)$$

where b and f are both positive in compression.

$$\text{For } \sigma_a \leq 1.0,\ b = 0;$$

$$\text{for } \sigma_a > 1.0,\ b = k\sqrt{\sigma_a} - k,$$

where k is a constant dependent upon the end conditions.

$$\text{For } \sigma_3 \leq 20.0,\ -f = 0.03\sigma_3;$$

$$\text{for } \sigma_3 > 20.0,\ -f = \{0.60 + 0.079(\sigma_3 - 20)\}.$$

These corrections, together with those for membrane penetration,

were incorporated in computer programs for the respective tests. The constant k, defining the slope of the compression correction curve, Figs. C.3 and C.4, could be varied according to whether rigid end-plattens or end stress-cells were used or the end lubrication system was changed.

The combined results of the experiments described were used to determine axial strains in both cylindrical and cuboidal specimens, including those in the ATA. Although both the shape and end surface area of the cuboidal and cylindrical specimens were different, the compressibility of the various components was expected to be very similar. The most significant compression errors in cylindrical tests were shown to be those concerned with the stress-cell diaphragms and lubricated end membranes. A vertical section through these components would be identical with that for a cuboidal specimen. It is conceivable that shape may have a slight effect on the total compression, but this was expected to be negligible.

One important proviso regarding the reliability of the applied corrections is that they take no account of specimen bedding. This is a problem common to most stress-deformation tests. Apart from the errors which may be incurred in measuring specimen deformations, particularly at small strains, it seems likely that differences in the nature of specimen bedding at the top and bottom are responsible for the characteristic displacement of the lateral "bulge" below the mid-height of the specimen in triaxial and other tests (Bishop and Green, 1965).

It is suggested that the use of the top stress-cell in place of a rigid end-platten, improves the nature of initial specimen contact, since local flexing of the diaphragm may compensate for non-planarity of the prepared sand surface. If this is so, the errors in deflection

measurements, at low axial stress, resulting from specimen bedding will also be reduced.

C.2 LATERAL STRAIN

The difficulties associated with the measurement of lateral strains in stress-deformation tests were discussed in 4.4.3. In triaxial testing of cylindrical specimens, it is common practice to calculate the average radial strain from measurements of axial and volumetric strain.

This procedure was used in the analysis of all axially-symmetrical tests, cylindrical and cuboidal, carried out in this research program. The accuracy of the average lateral strains, so determined, depends entirely upon the accuracy with which axial and volumetric deformations are measured and, if necessary, corrected. Therefore, the calibration tests described in C.1 and those for membrane penetration in Appendix B are indirectly relevant to lateral deformation measurements in these tests.

In the ATA, strain in the y-direction is calculated from the volume of de-aired water entering or leaving the side stress-cell compartments. This strain, together with the axial and volumetric strains, is then used to determine the x-direction strain. Again there is no redundancy of measured quantities, and hence no means of checking the strains.

The majority of ATA tests were carried out to investigate soil behaviour under plane strain conditions or under axially-symmetrical stress conditions. In the former case, the y-direction strain was monitored using a "null-indicator" system and, in the latter, equality of the two lateral strains was normally assumed. Only in intermediate-stress tests was the volume change in the side stress-cell compartments consistently measured with an apparatus of suitable sensitivity.

In order to determine the magnitude of any necessary correction to this volume, calibration tests were carried out using a cuboidal

mild-steel dummy specimen, 4.05 in. × 2.33 in. × 2.26 in., the approximate dimensions of the average ATA specimen. The dummy was placed in position between the end stress-cells, lubricated membranes being used at top and bottom in the usual way. The side stress-cells were filled and, after greasing the working-surfaces, connected together on opposite faces of the dummy. Finally, a small pressure was applied and a small volume volume of water bled from the de-airing screw to ensure that no air-bubbles were trapped. Pressure increments of 2 lbf/in^2, from 0 to 10 lbf/in^2, were applied, and the corresponding volume change was measured. It was anticipated that 10 lbf/in^2 would be the maximum difference between main-cell and side-cell pressures used in the research program. This was exceeded slightly in a few tests.

The observed volume changes, particularly those for the first pressure increment, were of a more erratic nature than the compressions measured during axial deformation calibrations. However, in none of the three tests did the volume of water entering the side stress-cell system exceed 1.3 ml for the full pressure range, which is equivalent to approximately 0.008 in. compression in the y-direction, or about 0.35% error in the strain measurement.

Probably a large proportion of this error is due to compression of the membrane surfaces and expansion of the compartment. These may well be constant at moderate pressures. That part of the error which can be attributed to extension of the tie-bars or, more importantly, movement at their anchorage, is unknown and likely to be different for each test.

The size of the dummy specimen was such that the side-cell membranes were fully covered and in full contact with the two vertical faces. These conditions are not exactly the same as those in the

genuine ATA test, where slight initial exposure of the side-cell membranes is a common feature of tests over a wide range of stress paths (4.2.3). It is probable this exposure leads to further small errors in strain measurement, which are also liable to vary from test to test, especially at small strains.

In view of the uncertainty regarding the errors associated with the y-direction strains, their probable variability, and difficulty of devising a calibration test to allow not only for changes in stress but also for changes in specimen size and shape, it was decided not to correct the measured strains. However, it is suggested, in the light of the calibration tests that were carried out, that the errors are small, and result in slight overestimation of the true strains. Subsequent calculation of strains in the x-direction are therefore likely to be slight underestimates.

C.3 AXIAL STRESS

In the Mk. I ATA, axial stress was computed from external proving-ring measurements of axial load. During the remainder of the research program, with the exception of a few tests in cylindrical triaxial compression, stress-cells were used in place of rigid end-plattens to measure axial stress directly at the specimen surface. The proving-ring was retained in some of these tests so that the effect of bushing friction could be observed. The Works figures for proving-ring calibration were accepted.

Calibration of the end stress-cells was carried out as follows:- The two stress-cells, having been de-aired in the usual manner (4.3.2), were positioned inside the main-cell which was then filled with water. The pressure was raised in increments of 5 lbf/in^2, up to a maximum value appropriate to test requirements, and the resulting galvanometer mirror deflections recorded. Galvanometer sensitivity could be varied by adjustment of the stabilized voltage supply, so that maximum sensitivity was obtained. In this way a stress range of 0 to 70 lbf/in^2, measured using one of the Budenberg pressure gauges, was recorded over an effective paper width of about 18 in., or two and a half full-scale deflections, the galvanometer traces being re-set when they reached the edge of the 7 in. paper. Each 0.1 in. scale graduation therefore represented a stress difference of approximately 0.4 lbf/in^2. The graduations were further sub-divided to obtain an accuracy of at least 0.1 lbf/in^2, which with careful calibration could be improved upon, particularly at low stress levels.

Having calibrated the stress-cells at a given constant voltage, it is essential that this voltage should not change. Therefore the stabilized voltage supply was kept in continuous operation between calibrations, even when tests were not in progress.

In general, calibration curves were linear, or could be separated into linear sections, depending on the galvanometers used and the voltage supplied. Whenever the galvanometers or the operating conditions were changed, the stress-cells were re-calibrated. Otherwise checks were made at regular intervals to ensure that the calibration had not changed.

By applying pressure directly to the transducer blocks, with the stress-cell connections closed off, calibration curves were obtained which were identical with those from the above method. This facilitated quick and accurate spot checks without the necessity for setting-up the stress-cells inside the main-cell, though the latter method was also used at regular intervals as a primary check.

No significant hysteresis effect was observed during end stress-cell calibration using either of the methods described.

C.4 LATERAL STRESSES

In all tests the lateral stresses, applied through flexible membrane surfaces, were measured using Budenberg pressure gauges. Generally, during tests under axially-symmetrical stress conditions only the main-panel system was used. However, in ATA tests it was essential that measurements of stress in both x- and y-directions were both accurate and compatible.

Each gauge was calibrated against a mercury manometer for pressures up to 10 lbf/in^2. After suitable adjustments for datum head, in relation to specimen mid-height, the maximum discrepancy between their respective measurements was found to be 0.2 lbf/in^2. The main-panel gauge, used for measurement of σ_x in ATA tests, was found to be the more reliable during this calibration, and was therefore used as the standard against which to calibrate the other stress systems, including the end stress-cells (C.3), over the full pressure range. In the absence of an absolute standard against which to check measured stresses, it is conceivable that slight errors were incurred at the higher stress levels. However, it is very improbable that this would in any way invalidate the conclusions drawn from the test results, since such errors are likely to be constant.

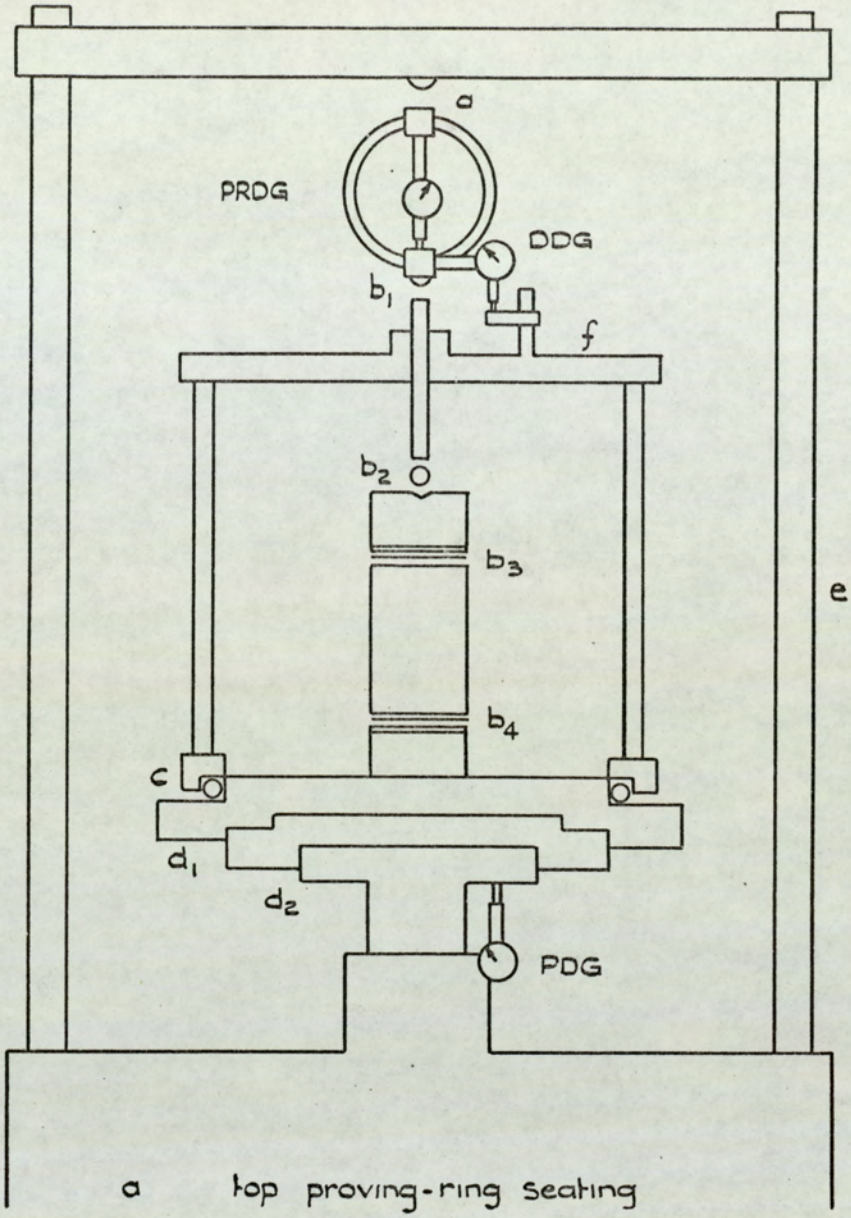

a	top proving-ring seating
b_1	bottom proving-ring seating
b_2	ball-bearing seating
b_3, b_4	compression of membranes, grease stress-cells, and specimen bedding
c	seating of cell on base O-ring
d_1	seating of cell-base on spacer
d_2	seating of spacer on pedestal
e	expansion of loading frame
f	cell distortion.

DDG	deflection dial gauge
PRDG	proving-ring dial gauge
PDG	pedestal dial gauge

FIG. C.1
APPARATUS CALIBRATION
SCHEMATIC DIAGRAM

FIG. C.2
COMPRESSION v. AXIAL STRESS
VARIOUS COMPONENTS
(see FIG. C.1)

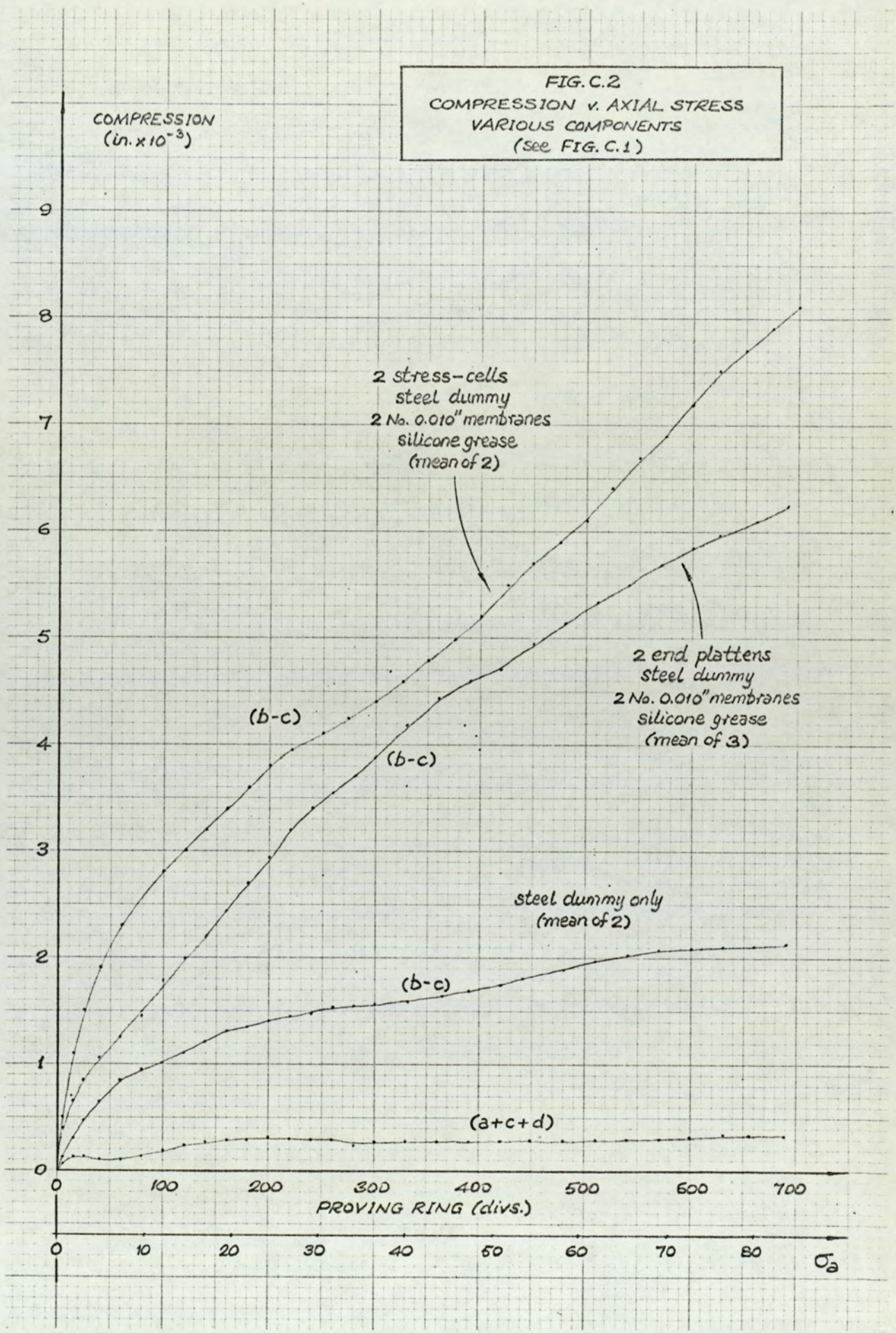

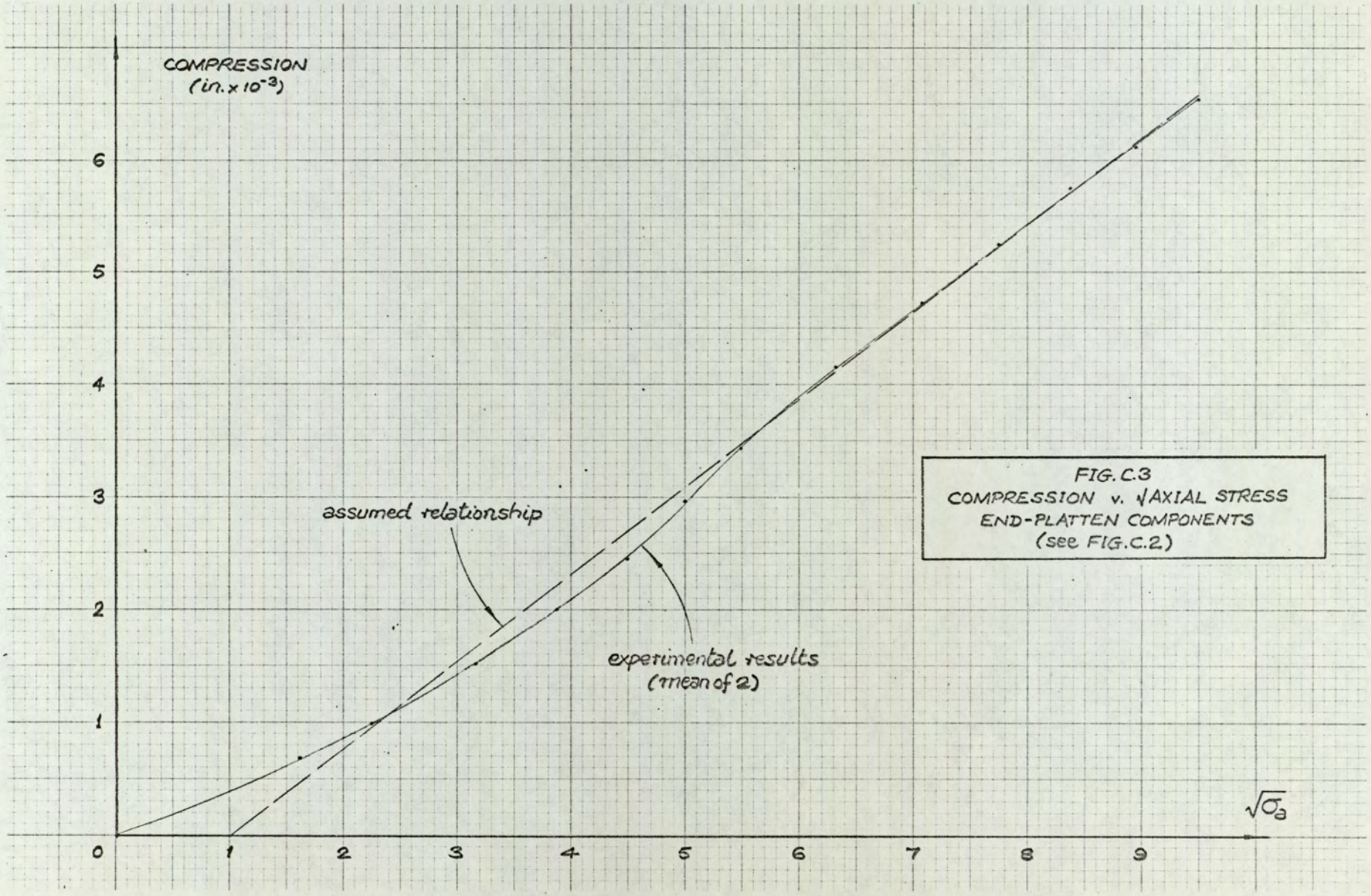

FIG. C.3
COMPRESSION v. √AXIAL STRESS
END-PLATTEN COMPONENTS
(see FIG. C.2)

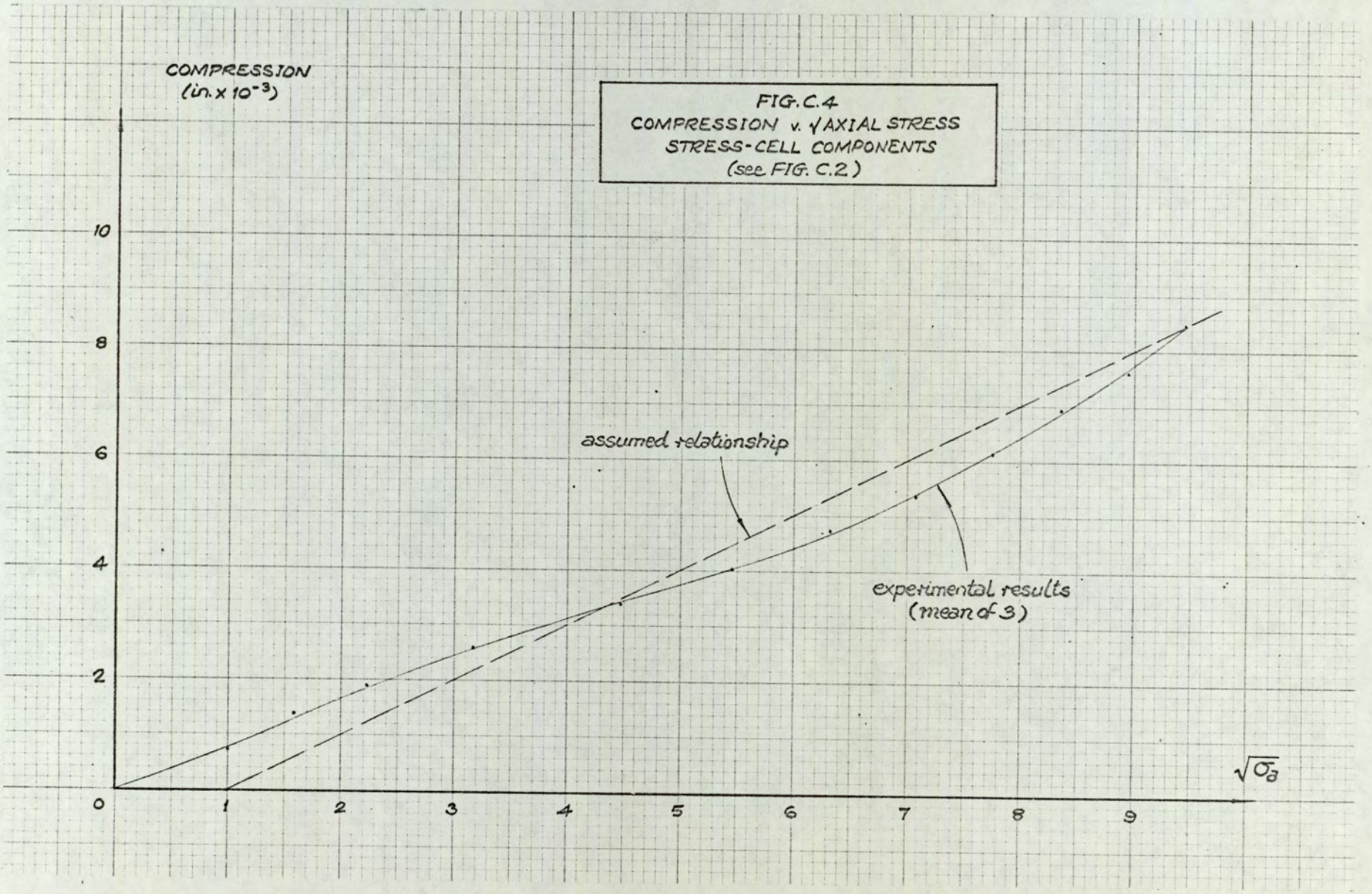
COMPRESSION
(in. x 10⁻³)
FIG. C.4
COMPRESSION v. √AXIAL STRESS
STRESS-CELL COMPONENTS
(see FIG. C.2)
10
8
6
4
2
0
1
2
3
4
5
6
7
8
9
assumed relationship
experimental results
(mean of 3)
√σ₃

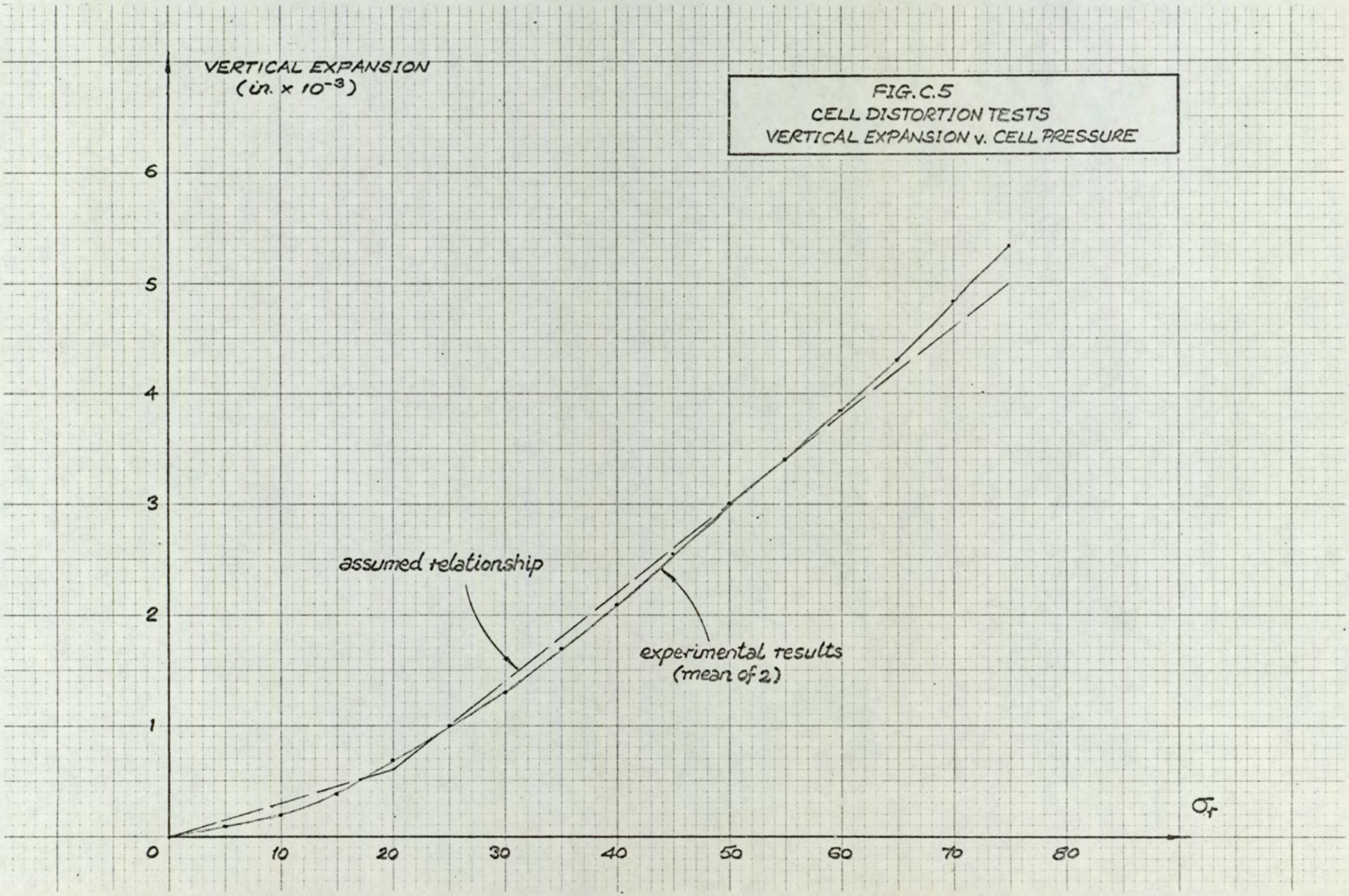
VERTICAL EXPANSION
(in. x 10⁻³)
FIG. C.5
CELL DISTORTION TESTS
VERTICAL EXPANSION v. CELL PRESSURE
6
5
4
3
2
1
0
10
20
30
40
50
60
70
80
σr
assumed relationship
experimental results
(mean of 2)

APPENDIX D

MEMBRANE STRENGTH TESTS

The majority of stress-deformation tests on soils require the specimen to be enclosed within an impermeable rubber membrane in order to isolate the pore-fluid from the confining fluid. The membrane is usually sealed firmly to top and bottom plattens, or their equivalent, and hence acts as a thin shell, in compression or extension, as the specimen deforms.

By assuming that the specimen, and therefore the membrane, deformed as a right cylinder, and that the cell pressure prevented membrane buckling, Henkel and Gilbert (1952) derived a simple expression for correcting the deviator stress in undrained triaxial compression tests. Their experiments on $1\frac{1}{2}$ in. dia. specimens, with and without membranes, verified the correction.

In drained tests on sand ν, Poisson's ratio, is different from that of the membrane, for which $\nu = \frac{1}{2}$, and therefore hoop stresses are induced in the membrane. However, their magnitudes do not, in normal circumstances, justify the use of a lateral stress correction. The form of deviator stress correction suggested by Henkel and Gilbert has been extended for use in testing cuboidal specimens, e.g. Wood (1958). A simple substitution of specimen circumference by specimen perimeter yields a deviator stress correction, $(\sigma_1 - \sigma_3)ms$, given by

$$(\sigma_1 - \sigma_3)ms = L.M.\varepsilon_a/A, \qquad (1)$$

where L is the length of perimeter of the cross-section,

M is the compression modulus of the rubber per unit width, and

A is the specimen cross-sectional area.

The extension moduli of the cylindrical and cuboidal specimen

membranes used in the author's research program were determined using the method suggested by Bishop and Henkel (1957). It was assumed that the extension and compression moduli were similar.

Three 1 in. circumferential strips were cut from three different 2.8 in. dia. cylindrical specimen membranes, and the average thickness of each was determined. In each case this value approximated closely to 0.010 in., the manufacturer's specification. The load was increased from 0 to 200 lb. in increments of 50 lb. and the corresponding strain increments were measured using a vernier microscope. The resulting average total strain for the three tests was about 6%.

Incremental values of the extension modulus, M(lb./in.), are plotted against the load per inch, P(lb.), in Fig. D.1. Although M appears to decrease with increasing P, and hence increasing strain, the changes are erratic and a mean value of 2.24 lb./in., calculated from all three tests over the full range, was considered appropriate.

It was anticipated that the extension modulus of laboratory-manufactured cuboidal membranes would be more variable, since the standard deviation from overall average thickness was greater (Appendix A). In addition, the shape of the membrane does itself lead to a wider variation of local thickness, particularly in the region of the "corners".

The majority of cuboidal membranes were used within a few days of manufacture; in some cases the time period was much less. Occasionally some were used in more than one test. In order to investigate the effect of age on the extension modulus, a 1 in. strip was cut from each of five cuboidal specimen membranes, two of which had been used in tests and were several months old, the remaining three having been freshly manufactured.

After measuring the average thickness, each strip was set up and tested in the manner described for cylindrical membrane strips. However,

unlike the latter which appear uniform, each cuboidal membrane strip has four discernible ridges, the four corners of the original membrane section, running across its surface. When stretched against a bright light, the corners appear more transparent than the remainder of the membrane, indicative of smaller thickness. Therefore when setting up, the strips were always suspended from a membrane face rather than a membrane corner, so that two corners were always visible from each side.

In addition to measuring the total elongation of the strip for each load increment, local elongations in the regions of the two visible corners were also determined. Two thin horizontal lines were drawn on the membrane approximately $2\frac{1}{2}$ mm above and below each of the corners, thus spanning the weaker zones. In the initial unloaded condition, and for each subsequent load increment, vernier micrometer readings of the positions of these lines were taken, enabling the local strains to be calculated.

Fig. D.2 shows the extension modulus, M(lb./in.), based on overall strain, plotted against load increment per inch, P(lb.), for the five strips tested. Once more the points are widely scattered, though the tendency for M to decrease with increasing P is noticeable. The horizontal lines on the graph represent the arithmetic mean values of M for individual strips. The age of the membrane does not appear to be a relevant factor, and the differences cannot be accounted for by the thicknesses of the membranes, which were all very close to 0.013 in. The average of the five mean values of M was 2.35 lb./in., only slightly greater than that of the three cylindrical membrane strips.

Consideration of the local deformation in the region of the cuboidal membrane corners showed, as would be expected, that elongation was much greater. The mean strain from the two visible 5 mm zones was used to calculate a local extension modulus for each load increment.

Assuming that the two corner regions on the remote side of the strip behaved similarly to those on which measurements were taken, which was qualitatively confirmed, the mean value of M was calculated for the membrane faces. Fig. D.3 shows the results for the one-day old strip, which are typical.

The average values of M for all the membranes tested are summarized in Table D.1.

TABLE D.1

Membrane Type	Average thickness (in.)	Extension Modulus (lb./in.)		
		Overall	Faces	Corners
Cylindrical	0.010	2.24	-	-
Cuboidal	0.013	2.35	2.52	0.88

From equation (1), using the average extension modulus of the faces of cuboidal specimen membranes, the deviator stress corrections are:-

$(\sigma_1 - \sigma_3)ms = 2.24\, L\varepsilon_a/A$ for cylindrical specimens, and

$(\sigma_1 - \sigma_3)ms = 2.52\, L\varepsilon_a/A$ for cuboidal specimens.

These corrections must be subtracted from the measured deviator stress in triaxial compression and therefore are given as negative quantities in Table D.2, which shows the resulting effect on the peak strength for both cylindrical and cuboidal specimens over a range of initial voids ratio.

The corrections applicable to ϕ are quoted to the nearest 0.1°. Clearly the effect is negligible except for loose specimens at low stress levels, which reach failure at greater values of axial strain. Beyond the failure condition it is probable that membrane strains may be less uniform, especially if specimen discontinuities occur. However,

it would appear unlikely that significant errors would result from using the method of correction described.

TABLE D.2

Test Number	Initial voids ratio e_i	Axial strain at failure ε_{af} (%)	Uncorrtd ϕ	Deviator stress correction $(\sigma_1-\sigma_3)_{ms}$ (lbf/in²)	Correction to be applied to ϕ
CYL TC 11	0.522	4.89	38.7	-0.15	0.0
CYL TC 16	0.581	3.58	34.8	-0.11	0.0
CYL TC 18	0.626	9.25	33.4	-0.27	-0.1
CUB TC 3	0.614	5.69	33.9	-0.24	0.0
CUB TC 4	0.548	4.12	37.6	-0.17	0.0
ATA TC 13	0.576	7.34	36.3	-0.29	-0.2
ATA TC 16	0.650	10.09	32.7	-0.40	-0.3
ATA TC 17	0.528	5.43	39.0	-0.22	-0.1

In triaxial extension tests, the specimen membrane is stretched in the axial direction and therefore the membrane strength correction becomes additive with respect to the axial stress. However, since the latter is the minor principal stress, the correction must again be subtracted from the measured deviator stress. Table D.3 shows that although the magnitudes of the corrections are similar to those calculated for triaxial compression specimens, the effect on ϕ is much more pronounced.

The greater sensitivity of ϕ to correction for the strength of the specimen membrane results from the fact that corrections are always applied to the axial stress. A comparison may be drawn between the effect of a 0.2 lbf/in² correction on the results of a triaxial compression and a triaxial extension test, each reaching failure at a mean stress of 30 lbf/in². The changes in magnitude of the axial stress are

0.3% and 2% respectively, and consequently the peak stress ratios are affected in an approximately proportionate manner.

TABLE D.3

Test Number	Initial voids ratio e_i	Axial strain at failure ε_{af} (%)	Uncorrtd ϕ	Deviator stress correction $(\sigma_1-\sigma_3)ms$ (lbf/in²)	Correction to be applied to ϕ
CYL TE 1	0.605	-7.80	36.8	-0.27	-0.9
CYL TE 2	0.558	-5.15	41.4	-0.17	-0.8
CYL TE 3	0.586	-8.35	37.4	-0.29	-0.9
CYL TE 4	0.555	-5.81	40.9	-0.20	-0.7
CYL TE 5	0.576	-6.75	40.5	-0.23	-0.9
CYL TE 6	0.649	-8.00	33.0	-0.28	-0.9
CYL TE 7	0.603	-5.42	35.7	-0.19	-0.6
CYL TE 8	0.549	-6.82	42.5	-0.23	-0.8

In developing membrane strength corrections for axially-symmetrical tests, it was assumed that the strains were uniformly distributed. Therefore, providing the extension modulus was constant, uniform stresses would be induced in the membrane. Clearly this may not be so in ATA tests, even prior to the formation of slip planes, since the strains in the x- and y-directions are not normally equal. However, the corrections for membrane strength are again small, and the magnitude of errors resulting from the assumption of uniform behaviour is unlikely to justify the use of a more sophisticated method of correction.

Typical examples of the effect of corrections applied to the results of ATA plane strain tests are given in Table D.4.

The effect of corrections applied to tests under other stress or strain conditions in the ATA would be similar, except when the minor

principal stress acts in the z-direction. In this case, the conditions are similar to those prevailing in the triaxial extension test, and the necessary corrections may be of comparable magnitude.

TABLE D.4

Test Number	Initial voids ratio e_i	Axial strain at failure ε_{af} (%)	Uncorrtd ϕ	Deviator stress correction $(\sigma_1-\sigma_3)ms$ (lbf/in^2)	Correction to be applied to ϕ
ATA PS 7	0.521	6.31	46.1	-0.26	-0.1
ATA PS 10	0.599	5.98	39.1	-0.25	-0.1
ATA PS 17	0.549	5.53	42.3	-0.23	0.0
ATA PS 22	0.641	10.39	37.0	-0.41	-0.2

In general the effect of membrane strength on the results of stress-deformation tests is small enough to be ignored for most purposes. However, stresses may be conveniently corrected by assuming uniform deformation of the membrane and equality of compression and extension moduli. Corrections to peak strength data are marginally greater for loose specimens, since failure usually occurs at greater values of axial strain. The effect of membrane strength is more significant in triaxial extension tests and tests performed in the ATA under similar stress conditions. Nevertheless, the magnitudes of the corrections may be no greater than those of the errors resulting from uncertainty regarding specimen cross-sectional area. Similarly, non-uniform deformation of the membrane, resulting from the formation of post-failure slip surfaces, is likely to be insignificant compared with the difficulties of relating measured overall stresses and strains to the behaviour of the soil in this condition.

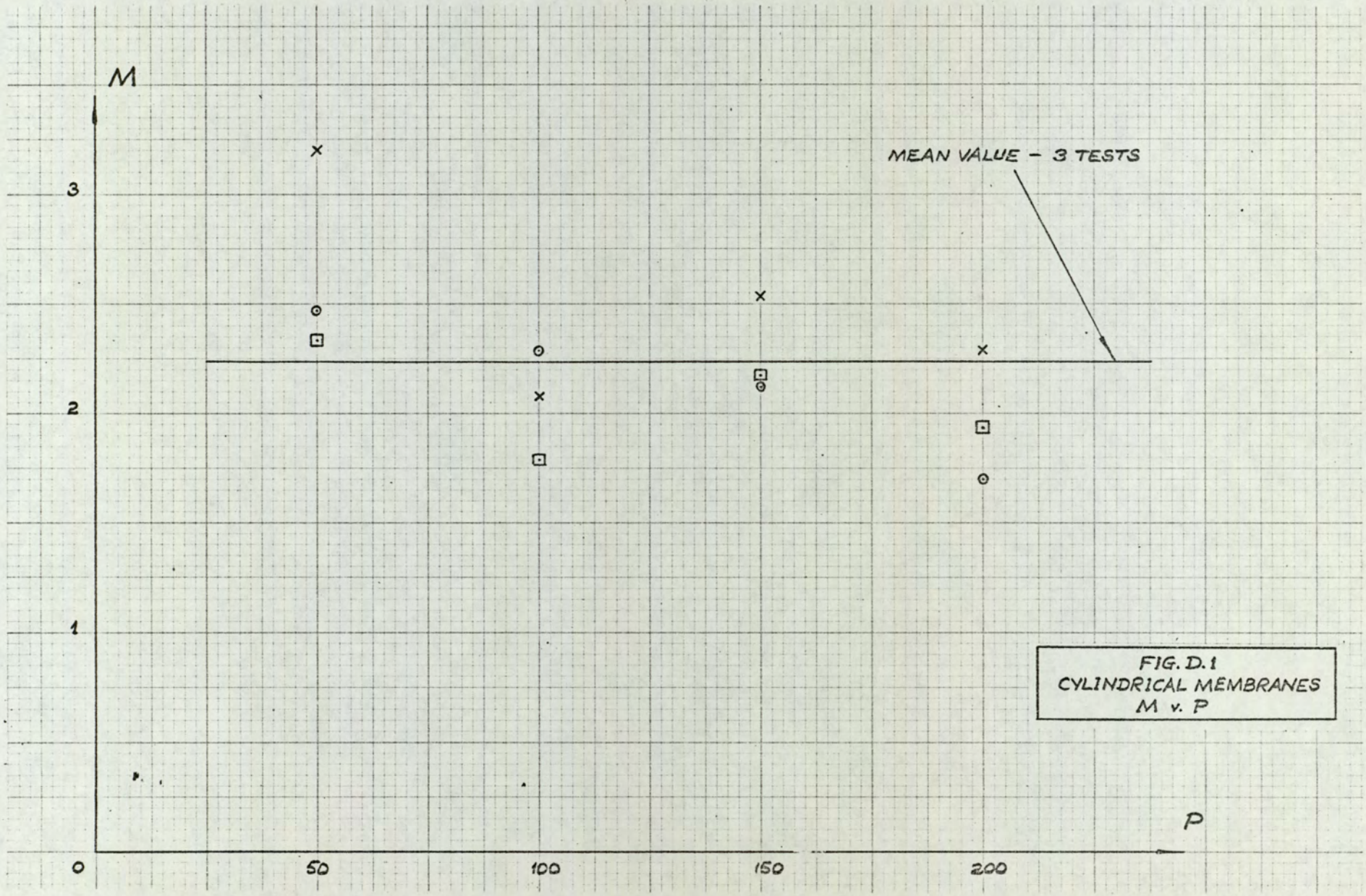

FIG. D.1
CYLINDRICAL MEMBRANES
M v. P

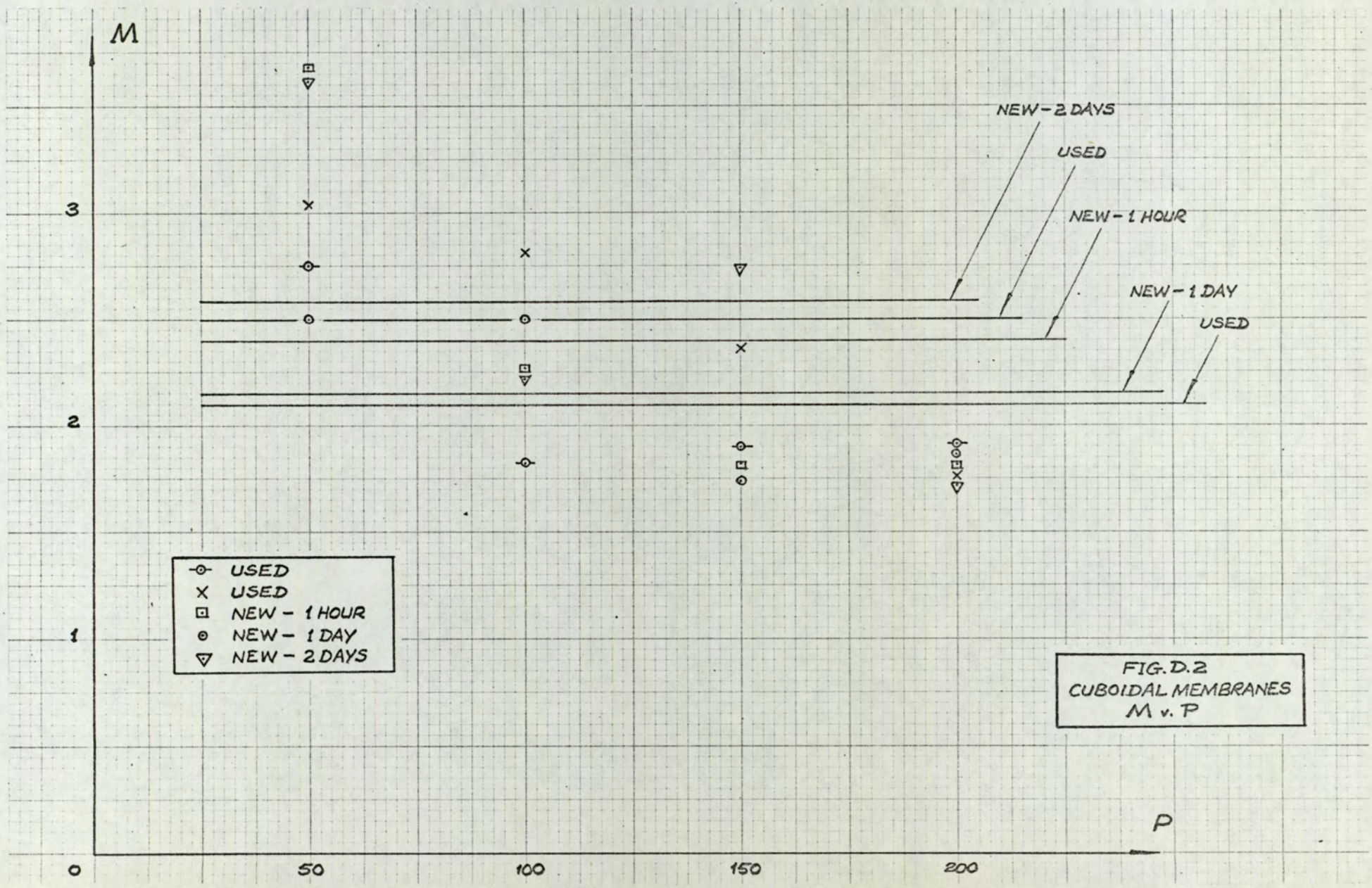

FIG. D.2
CUBOIDAL MEMBRANES
M v. P

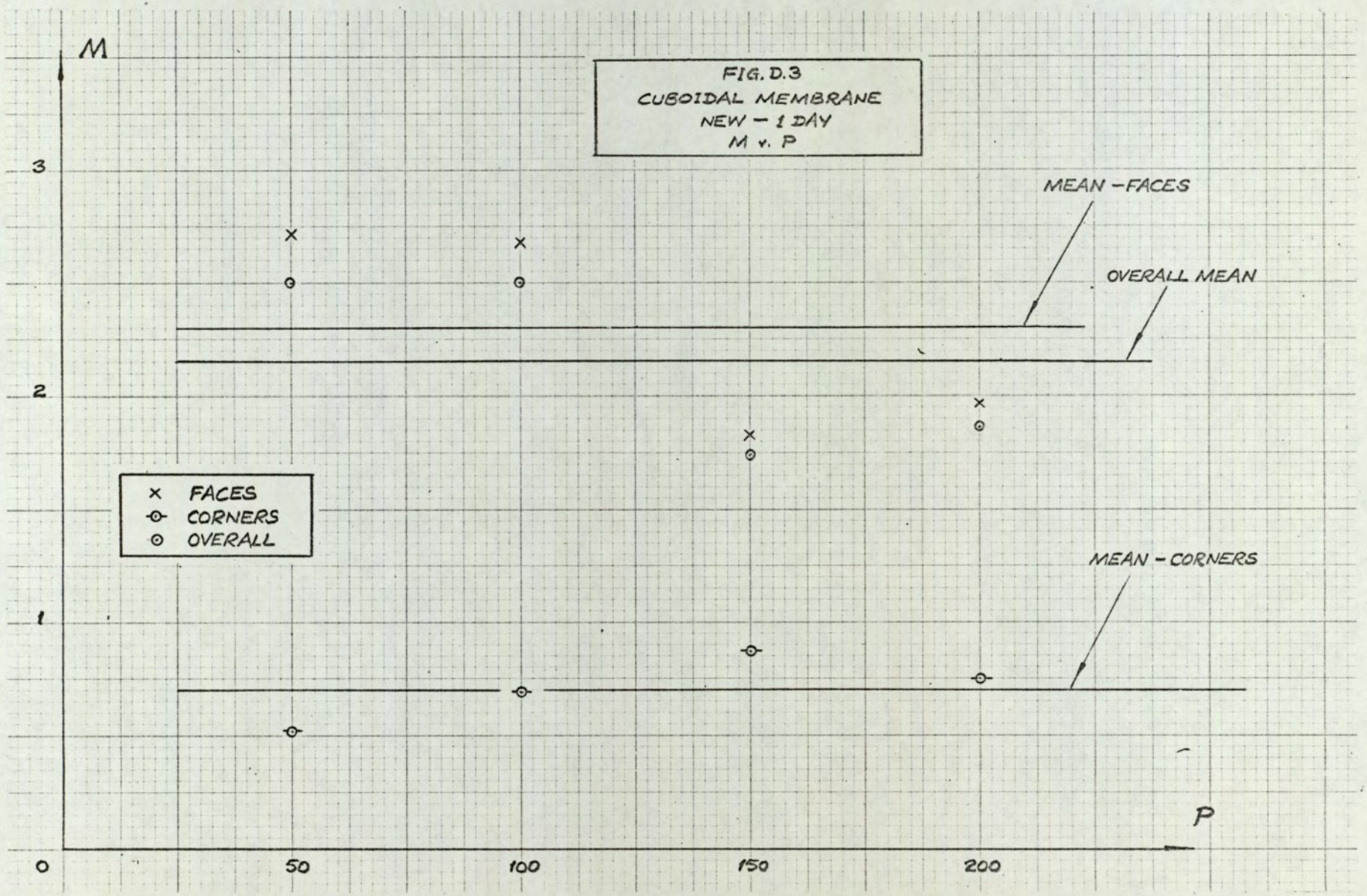
FIG. D.3
CUBOIDAL MEMBRANE
NEW – 1 DAY
M v. P
M
P
3
2
1
0
50
100
150
200
MEAN – FACES
OVERALL MEAN
MEAN – CORNERS
FACES
CORNERS
OVERALL

APPENDIX E

PROPERTIES OF SOIL TESTED

E.1 PARTICLE SIZE AND SHAPE

The uniform coarse sand, used in all of the tests carried out as part of this research program, was taken from a batch delivered to the Department several years ago by a local contractor no longer in business. Its exact origin could not be traced, but since the source was undoubtedly also local, the description "Birmingham Area sand" has been used.

The medium and fine fractions were removed by mechanical sieving, so that the remaining particles were retained on the No. 25 B.S.S., having passed the No. 14. Before usage, the sand was washed, and any extraneous material removed.

The shape of individual particles was observed at various magnifications using a binocular microscope, and a micrograph was taken at × 10 magnification (Fig. E.1). Corresponding sketches of several particles were made, and are shown in Fig. E.2. Clearly the particles rest horizontally with their longitudinal axis parallel to the plane of the paper. The group was large enough to be considered representative, and an estimation of the two-dimensional sphericity of the particles, using the method suggested by Rittenhouse (1943), gave a value of 0.81. Using more general terminology the particles could be described as "sub-rounded".

During stress-deformation testing, the crushing and fracture of particles has been shown to occur at high pressures (Bishop 1966). However, changes in particle size distribution of sands have been observed, by analysis before and after shearing tests, at much lower pressures, i.e. within the range of normal laboratory apparatus

(Cornforth 1961, Bishop and Green 1965).

Barden and Khayatt (1967) indicated that for cell pressures less than 50 lbf/in^2 the effect of crushing on stress-deformational behaviour was negligible. Therefore, although it would have been preferable to have used fresh samples, taken from the same batch, for each test, the consequences of not doing so were unlikely to significantly affect the test results, especially since the maximum stress level was considerably lower than that quoted above.

The batch of sand from which the specimens were formed was, however, replaced or replenished at regular intervals from the main batch.

E.2 SPECIFIC GRAVITY

The specific gravity of the particles was determined using the B.S. 1377 procedure for fine-grained soils, since the removal of trapped air using vacuum desiccation was found to be more efficient.

Three representative samples were tested in 50 ml density bottles, and the specific gravities obtained were 2.648, 2.650 and 2.645. In all test computations a value of 2.648 was assumed.

E.3 MAXIMUM AND MINIMUM POROSITIES

Kolbuszewski's (1948) "rapid tilt" method was used to determine the maximum porosity, five tests yielding an average value of 0.417, (voids ratio = 0.715).

To determine the minimum porosity, a B.S. Compaction Test cylinder was filled with the dry sand, and a normal load of 20 lb. was applied through a loosely-fitting rigid piston. The cylinder and piston were then mechanically vibrated at varying frequencies for several minutes.

The results of three such tests were very similar, giving an average value for the minimum porosity of 0.335, (voids ration = 0.503).

E.4 FRICTIONAL PROPERTIES

The mineral frictional properties of cohesionless soils are likely to have considerable influence on their stress-deformational behaviour. In several theories, the magnitude of the friction angle is regarded as sensibly constant, (2.2). In order to determine these properties for the quartz sand used in this research program, simple friction-slider tests were performed using a smooth quartz crystal and three sand particles. The arrangement is shown in Fig. E.3. Tests were carried out under both air-dry and submerged conditions.

The quartz crystal was set into a plaster block with its smoothest surface horizontal. Apart from ensuring that the surface was clean and, in the first series, dry, no further surface treatment was undertaken.

The slider, consisting of three sand particles positioned at the corners of an equilateral triangle and glued onto the surface of a square perspex block, was placed gently on the quartz crystal and the normal load applied. The frictional force was then increased in small increments, the loading system being supported during this process to prevent jarring of the slider. When sliding occurred, it was usually rapid.

Tests were carried out under submerged conditions by forming a water-bath with a rubber O-ring and plastercine, the slider being placed in position only after the quartz crystal was flooded. Results from each test series are shown in Table E.1

Previous investigators had observed variations in ϕ_μ with normal load, and therefore an estimate was made of the interparticle force appropriate to the stress-deformation test conditions, by consideration of the mean particle size. The stress levels in all tests were within the range from 0 to 100 lbf/in^2, and the corresponding friction-slider normal loads were between 0 and 500 g,

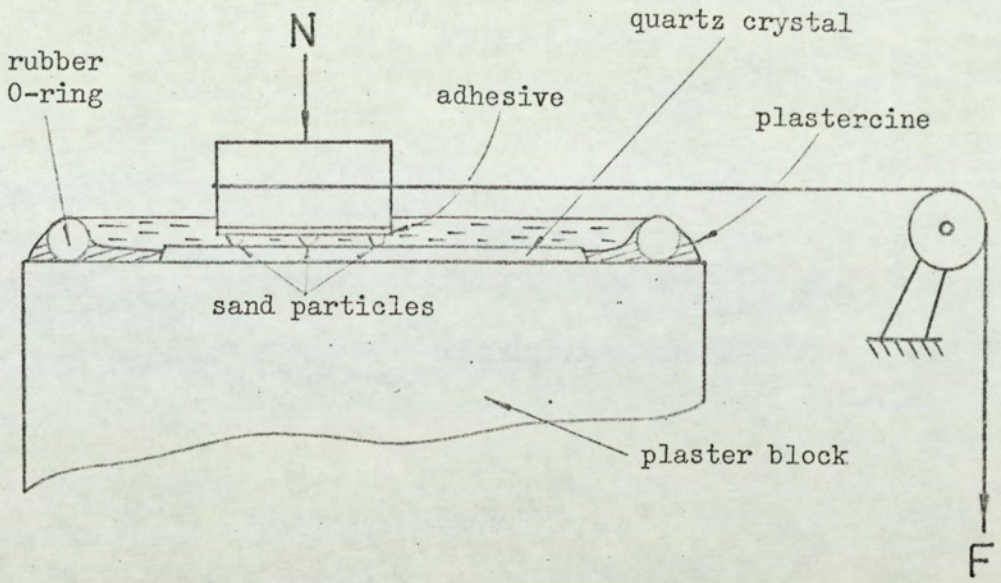

FIG. E.3

TABLE E.1

Test Conditions	Normal Load N (g)	Maximum Frictional Load F (g)	Frictional Coefficient μ	Angle of Friction ϕ_μ°
Air-dry	123.5	35.5	0.287	16.0
	223.5	64.5	0.289	16.1
	523.5	154.3	0.295	16.4
	1023.5	340.0	0.332	18.4
	3023.5	1090.0	0.360	19.8
	6023.5	2290.0	0.380	20.8
Submerged	123.5	14.8	0.120	6.8
	223.5	27.8	0.124	7.1
	523.5	59.2	0.113	6.5

The results show that within this range, the angles of friction for both the air-dry and submerged conditions are independent of normal load, having regard to the degree of accuracy attainable using this apparatus. Moreover, it is clear that the magnitude of the frictional coefficient in the air-dry condition is approximately $2\frac{1}{2}$ times greater than that observed when the surfaces are submerged.

A further series of tests was carried out at higher normal loads,

in the air-dry condition only, and the results (Table E.1) show a slight progressive increase in the angle of friction. However, at the highest normal load, particle crushing was considerable.

The results described may be compared with those of other workers in this field.

Penman (1953) obtained a value of ϕ_μ of about 31° for silt-sized quartz particles, and showed that its submerged value decreased with increasing normal load.

Horn and Deere (1962) studied the frictional characteristics of several minerals, observing that for massive-structured minerals, such as quartz, water had an anti-lubricating effect, but that this effect decreased rapidly as surface roughness increased. For very smooth quartz surfaces, friction angles of 6° and 27° were observed for oven-dry and saturated conditions respectively. The increase in frictional coefficient with ambient relative humidity was such that, for air-dry and submerged conditions, similar values of ϕ_μ were observed for rough quartz surfaces. It was also pointed out that the practice of polishing the sliding surfaces may cause the development of different surface structure.

Skinner (1969), using an unspecified "friction apparatus", obtained friction angles for dry glass ballotini which increased from about 2° to 5°, as the normal load increased from 5 to 50 gm. The corresponding values for the "flooded" condition were 27° and 39°.

Many investigators have used the "three-point" friction-slider. This has been criticized on the grounds that significant wear could be caused to smooth surfaces. Rowe (1962) used a mass of sand particles sliding over a quartz block, and demonstrated a decrease in ϕ_μ with load per particle, varying from 31° for silt-size to 22° for pebble-size.

However, it is difficult to substantiate the criticism of the three-

point slider, providing the test conditions are based on sensible magnitudes of load per particle. In particular, in the series of tests described as part of the author's research program, the initial values of ϕ_μ were determined with a previously unused smooth quartz block, and it was only later that high normal loads were applied.

The results are not easily explained in the light of some of the earlier work described, especially since the friction angles obtained were considerably lower than those frequently quoted for the same mineral. Slightly different values might reasonably have been expected due to the limited amount of surface preparation. Conversely, the possible adverse effect of surface polishing, suggested by Horn and Deere, may itself explain the discrepancies.

Particular care was taken to avoid shock loading, especially since initial tests had given friction angles lower than those expected, and therefore, because of the apparent repeatability of results, the values obtained were considered accurate for the test conditions described. Taken together with the results from previous similar studies, however, they reinforce the view that the angle of friction between the minerals which constitute soil material is extremely difficult to determine.

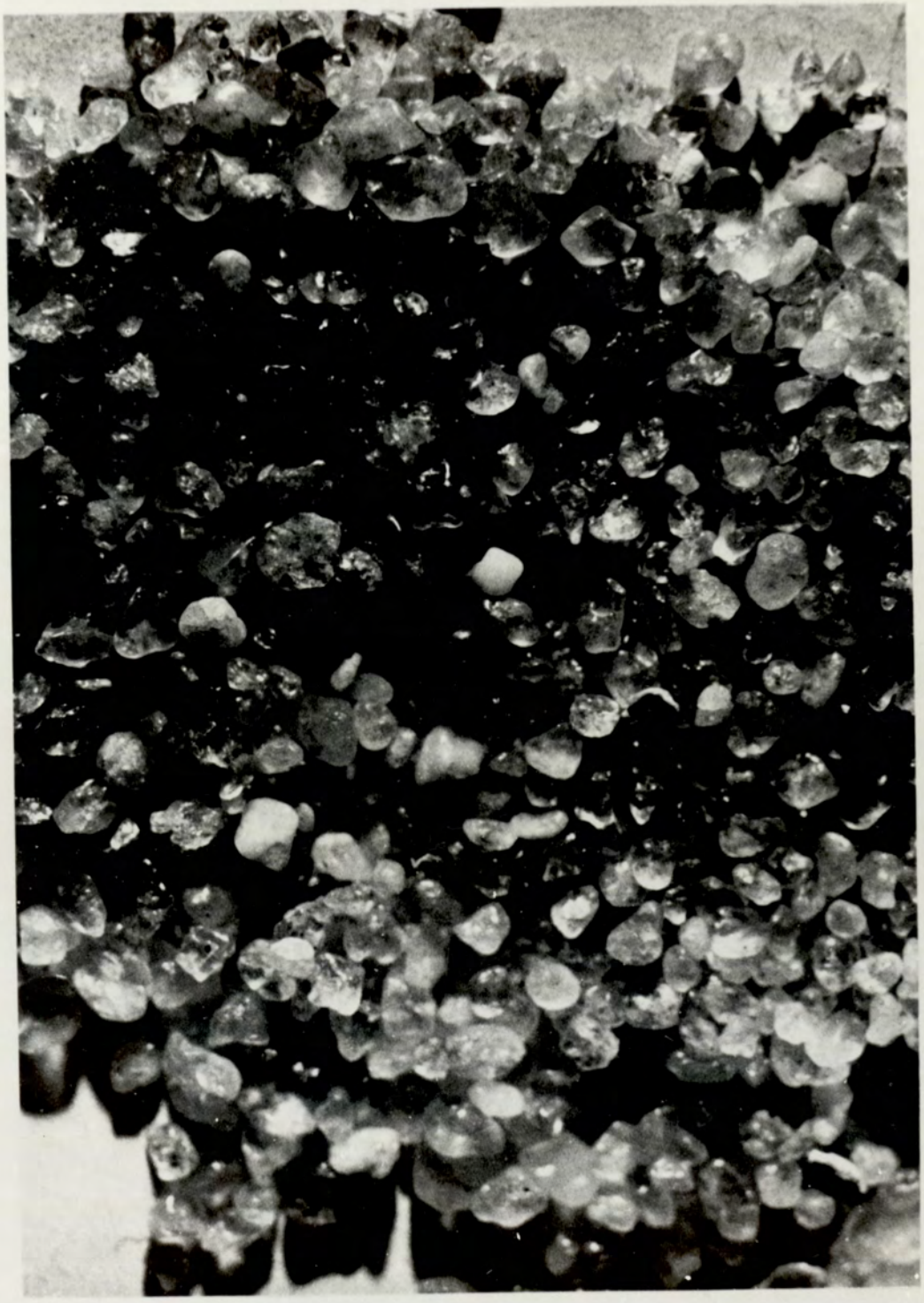

FIG. E.1
BIRMINGHAM AREA SAND
PASSING No.14 RETAINED ON No.25
B.S. SIEVES
MAGNIFICATION × 10 APPROX.

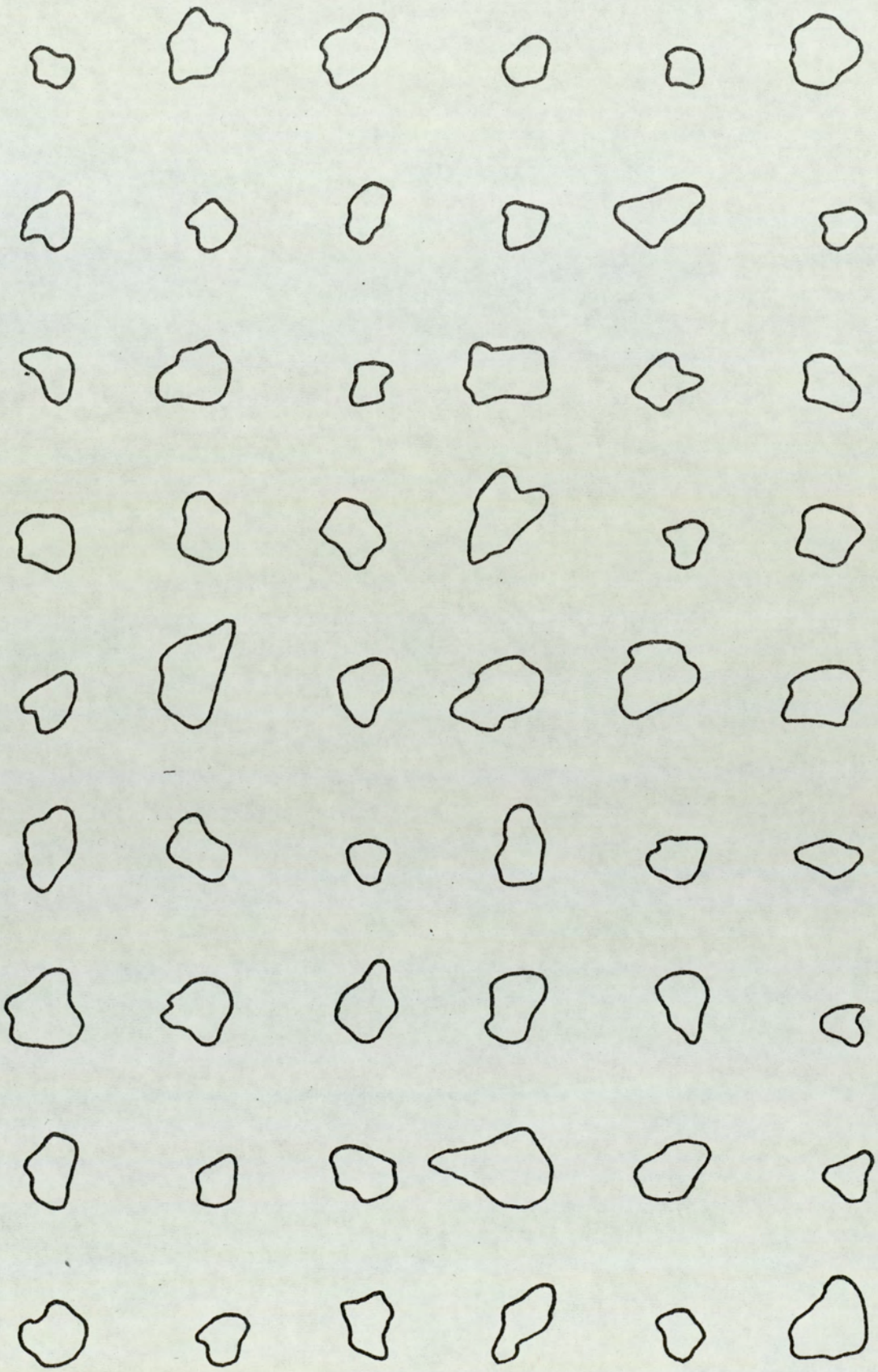

FIG. E.2
BIRMINGHAM AREA SAND
FROM BINOCULAR MICROSCOPE
MAGNIFICATION × 10 APPROX.

APPENDIX F

EFFICIENCY OF LUBRICATION METHODS

Laboratory investigations of the stress-deformational behaviour of soils usually involves the application of stresses or strains, or combinations of the two, to the boundaries of specimens either cylindrical or cuboidal in shape. Generally, it is highly desirable for the stresses and strains to be uniformly distributed throughout the specimen, since frequently measurements of its response are taken only at the boundaries. Consequently a complete analysis of the soil's behaviour is possible only if these measurements are assumed to be representative.

Some of the methods with which investigators have attempted to improve stress-strain homogeneity were discussed in Chapter 3, including the use of lubricants, usually separated from the soil with a flexible rubber membrane, at the specimen boundaries. The specific procedures used in this research program were described in Chapter 4.

In all of the tests carried out, both in the ATA and the more conventional triaxial apparatus, the top and bottom of the specimen was lubricated using one or more rubber membranes, 0.010 in. thick, coated with a thin layer of silicone grease (Releasil 7 - Midland Silicones Ltd.). In addition, the interfaces between ATA specimens and the side stress-cells were similarly lubricated.

Extensive research has been carried out concerning the effect of end restraint on soil strength and stress-deformational behaviour. Usually it was assumed that the lubricating effect of silicone grease was similar for different soils, and also that the coefficient of friction, μ, determined from a simple test was that appropriate to test conditions. However, Roscoe (1967) reports tests performed in the Mk. 6 "simple

shear apparatus", in which friction forces were induced along the rigid sides of the specimen container, consistent with a value of μ of approximately 0.25. The soil used was a coarse Leighton Buzzard sand, and the sides were lubricated using silicone grease and single rubber membrane.

F.1 APPARATUS AND TEST PROCEDURE

The first series of tests were performed during the development of the Mk.I ATA, and were aimed at determining the magnitude of μ for the lubrication system, under conditions similar to those at the Mk.I rigid end plattens and at the side stress-cells. The apparatus, a converted shear box, is shown in Fig. F.1a.

A "sandwich" consisting of two 0.010 in. thick membranes and a thin layer of grease was tested between 2.8 in. dia. cylindrical aluminium plattens and $2\frac{1}{4}$ in. square plattens in both perspex and brass. In some of the tests a $\frac{1}{2}$ in. diameter hole was cut in the middle of each membrane to represent the specimen drainage holes, but their effect was not discernible.

The top and bottom membranes were mutually displaced at a rate of 0.045 in./min. and the shear force was measured at regular intervals. The normal load was 172.5 lb. in each test, equivalent to initial normal stresses of 28 and 34 lbf/in^2 respectively, for the cylindrical and square plattens.

Seven tests were carried out for each end condition, and no noticeable differences were observed for the various combinations. In each case, the frictional force increased steadily to a maximum, which was reached at between 0.1 and 0.2 in. movement. The magnitudes of the coefficient of friction were randomly scattered between 0.01 and 0.03, with an average value of 0.02.

In a later series of tests, carried out using the apparatus shown in Fig. F.1b, this figure was confirmed for sliding between a single greased membrane and a smooth brass surface. A constant normal load was applied and the frictional force increased slowly until noticeable movement occurred. For the three normal stresses used, 2, 4 and 10 lbf/in^2 the value of μ was identical, being only slightly greater

than the 0.02 previously obtained.

By replacing the top brass block with a sand surface composed of particles from the batch used in the stress-deformation test program, it was hoped to simulate the rigid-end test conditions, and to observe any loss in efficiency of the lubrication system.

A mould, having a cross-section equal to that of an ATA specimen, was filled with rapid-hardening cement. Sand particles were then sprinkled over the surface and loaded through a flat plate, so that when the cement was set, the protruding particles were in a single plane. The results of these tests performed with this block were inconclusive, since although a coefficient of friction of 0.08 was recorded for normal loads of 2 and 4 lbf/in^2, it was found possible to increase the frictional force to several times this value without movement.

In ATA Mk.II tests, and in the majority of cylindrical and cuboidal triaxial tests, the end plattens were replaced with end stress-cells, having flexible diaphragm surfaces. To simulate these conditions, a strip of rubber, the same as that used to form the diaphragms, was laid over the lower brass block (Fig. F.2a). However, there was little improvement, and although the previous minimum μ was observed, it was again possible to obtain much greater values.

A final series of tests was performed using the arrangement shown in Fig. F.2b. The lubricated membrane was positioned on the brass block or rubber strip as before, and sand was poured into the bottom section of a shear box, supported freely on roller bearings. The sand was lightly tamped and the normal load applied through a rigid loading cap. Small increments of frictional force were applied until movement occurred.

The results of tests carried out at various magnitudes of normal load are shown in Fig. F.3, each curve being drawn through seven test points.

F.2 DISCUSSION OF RESULTS

Clearly there is little doubt that the degree of lubrication obtained using a silicone grease-membrane sandwich between rigid flat surfaces would be highly desirable in much soils testing. However, the effect of replacing one of the rigid surfaces with a surface having the irregularity of those at the ends of the normal test specimen is not clear. Some of the tests described may have indicated the likely effect, for the particular soil and lubrication system used.

It would seem reasonable to suppose that the greater the load, the greater is the possibility of the lubricant being squeezed out. Since coarse sands, such as that used in this research program, carry a greater load per particle, for a given normal stress, these are likely to be critical. Similarly, the thinner the membrane, the higher the stress concentration and the greater the possibility of puncture, leading to direct contact between the particles and the surface.

It was hoped that in the cement block tests the conditions would represent a plane of uniformly loaded particles moving, by translation only, over rigid platten or flexible stress-cell surfaces. However, the very erratic nature of the observed frictional coefficients would appear to suggest that this was not the case, and that certain particles carried loads far in excess of the average. Several particles were lost from the block after each usage. This, together with changes in positioning of the block for each test, would explain the wide variations in the results.

The final test series was more successful, the scatter being greatly reduced.

The test conditions did not preclude rolling of the particles, which might possibly have been exaggerated, since movement occurred in one direction only. (In triaxial testing, the particles move in radial

directions over the end plattens). The mechanism of movement, rolling or sliding, at the specimen ends in stress-deformation testing, must, however, be regarded as uncertain, since assumptions concerning the mechanism within the interior of the soil element are still controversial (2.2).

Despite the scatter of results shown in Fig. F.3, it was considered appropriate to draw linear curves through the tests points for each surface condition. The respective average μ values for the brass block and rubber strip conditions were 0.11 and 0.08, indicating an advantage in using a flexible surface. The lower average value was about the same as the minimum obtained using the cement block.

It is suggested that the greater flexibility of the specimen boundaries in the ATA tests, and some of the other tests described, would lead to a further reduction in μ. Certainly at the side stress-cells boundaries, where silicone grease is applied between the specimen membrane and the stress-cell membranes, the frictional coefficient may be expected to be little different from that observed for a membrane-grease sandwich between two rigid surfaces, (μ = 0.02). The flexibility of the end stress-cell diaphragms is less than that of the side stress-cell membranes, and therefore, under test conditions, the magnitude of μ will probably lie between 0.02 and 0.08. Unfortunately, it was not possible to simulate these conditions more precisely, due to the possibility of stress-cell damage. Moreover, it would seem unlikely that the true nature of the contact between the sand particles and the end surfaces could be represented experimentally with any great accuracy.

The results of this series of tests indicate that although the frictional coefficient under simulated test conditions is greater than that for silicone-grease-membrane sandwiches alone, the values are not excessive, and the lubrication system used may be regarded as effective.

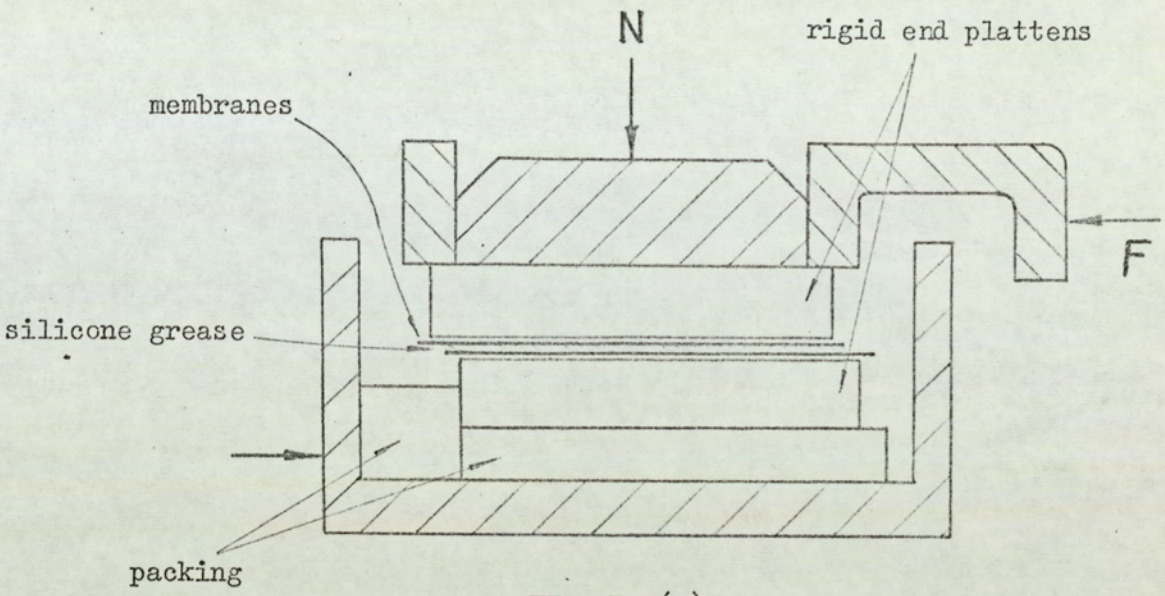

FIG. F.1(a)

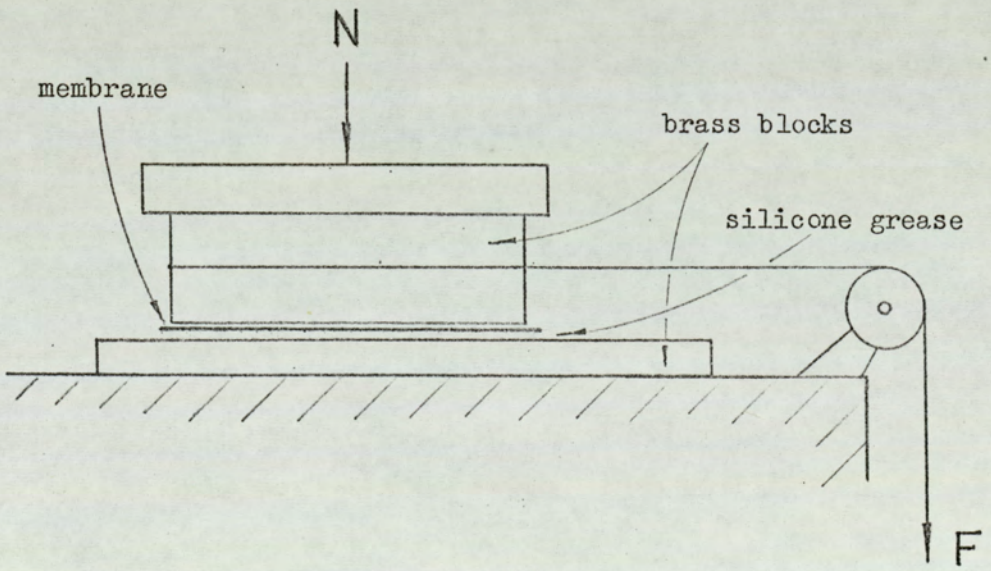

FIG. F.1(b)

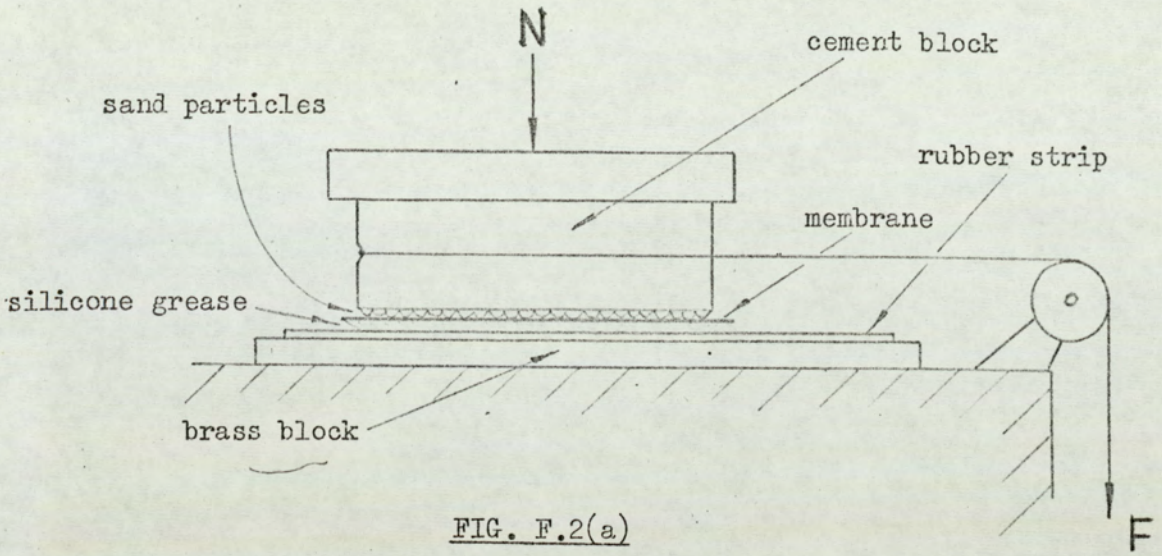

FIG. F.2(a)

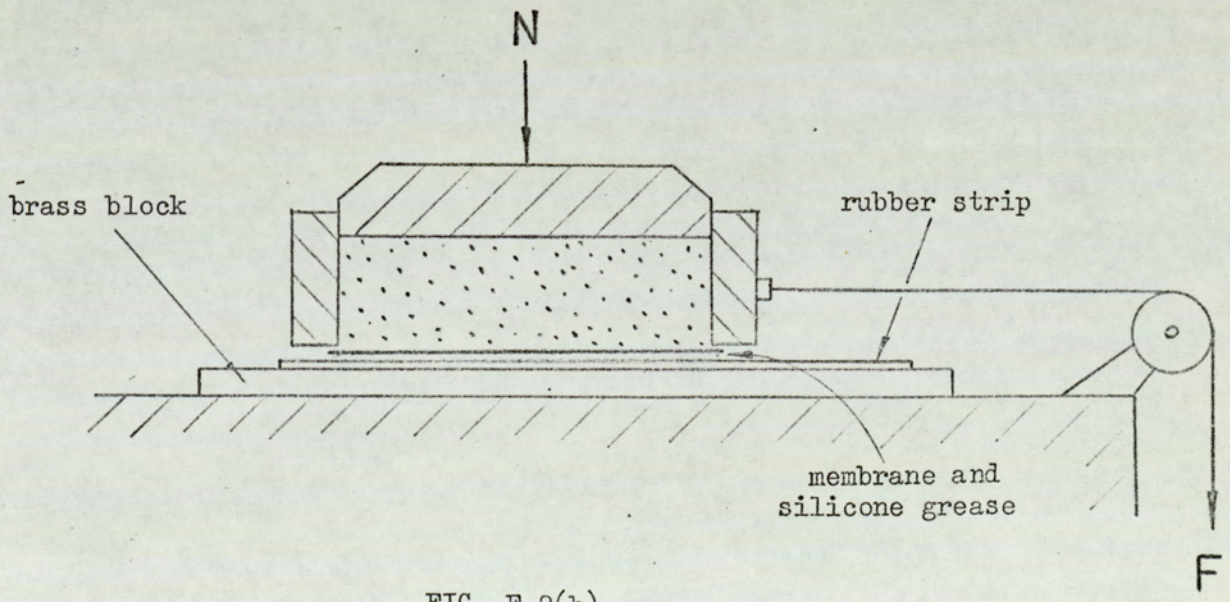

FIG. F.2(b)

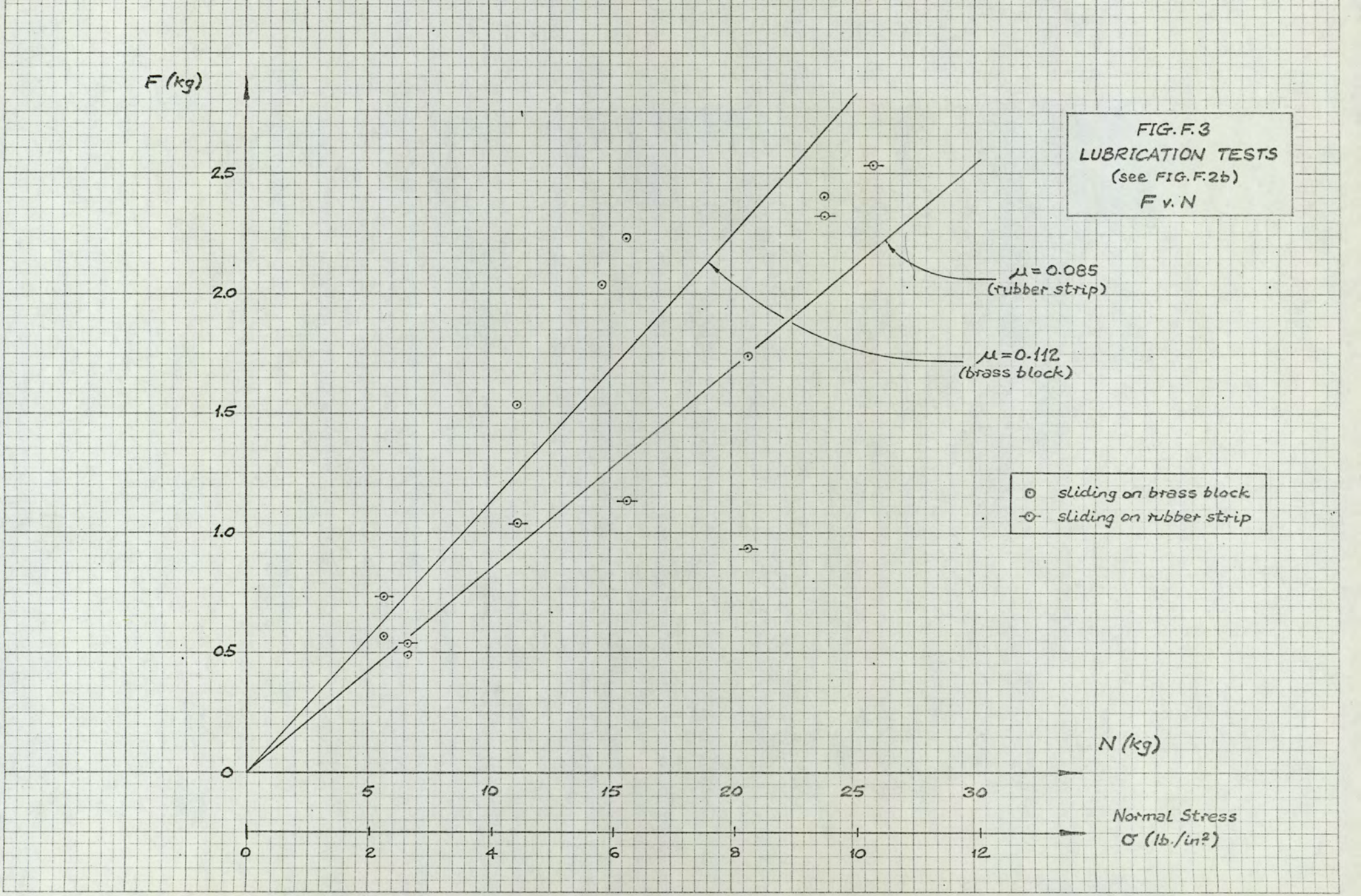
F (kg)
2.5
2.0
1.5
1.0
0.5
0
5
10
15
20
25
30
N (kg)
0
2
4
6
8
10
12
Normal Stress
σ (lb./in²)
μ = 0.085
(rubber strip)
μ = 0.112
(brass block)
sliding on brass block
sliding on rubber strip
FIG. F.3
LUBRICATION TESTS
(see FIG. F.2b)
F v. N

APPENDIX G

ASTON TRIAXIAL APPARATUS - MK.I TESTS

The design and development of the ATA was described in Chapter 4, and in particular the methods used to measure stress in the z-direction were discussed at length.

The external measurement of axial deviator stress in conventional triaxial testing gives rise to significant errors; in the ATA, where the sideways thrust on the loading piston is likely to be greater, the magnitude of these errors will be increased. In addition, knowledge of the stresses at both top and bottom of the specimen was considered desirable. However, before the Mk.II end stress-cells were developed to allow such measurements, plane strain tests were performed using the Mk.I apparatus. The results from these tests are reported briefly herein.

All specimens were consolidated under zero lateral strain, though deviations from this condition occurred to a greater extent than in the ATA Mk.II, since the testing procedure was less sophisticated. Clearly the erroneous σ_1 measurements affect the values of K_o and ϕ, as can be seen from Table G.1 and Figs. G.7 and G.8 where comparison is made with the results from ATA Mk.II tests.

Following consolidation, the minor principal stress was maintained constant as σ_3 and σ_y increased under plane strain conditions. After a further axial strain of about 1%, the cell pressure, σ_x, was adjusted to keep the axial stress, σ_3, constant, failure being reached at the minimum σ_x value. The majority of tests were continued into the post-peak region. Plane strain was maintained throughout by adjusting the magnitude of σ_y to balance a null-indicator, as described for Mk.II tests.

TABLE G.1

ATA Mk.I Test Number	Initial Voids Ratio e_i	Consolidation		Conditions at Failure			
		Minor Stress $\sigma_y=\sigma_x$	Stress Ratio $\frac{\sigma_3}{\sigma_1}$	Major Stress σ_3	Inter Stress σ_y	Minor Stress σ_x	Angle Sh'g Res ϕ
PS 1	0.548	12.0	0.275	53.4	18.8	9.0	45.3
PS 2	0.566	12.0	0.278	-	-	-	-
PS 3	0.557	12.0	0.264	53.4	17.5	8.2	47.1
PS 4	0.550	12.0	0.278	-	-	-	-
PS 5	0.570	12.0	0.264	53.4	17.7	10.6	42.0
PS 6	0.521	12.0	0.273	-	-	-	-
PS 7	0.612	12.0	0.278	48.0	17.6	11.1	38.6
PS 8	0.656	12.0	0.298	45.2	16.6	10.6	38.3
PS 9	0.640	12.0	0.304	46.2	16.6	11.0	38.0

A set of charts were drawn to enable the magnitude of the axial stress to be calculated at any stage of a test from the proving-ring reading, the measurements of axial and lateral deformation, and the cell pressure. However, since the error due to plunger friction was almost certainly increasing with specimen strain, the genuine value of the major principal stress was probably steadily decreasing. This would account for the smaller strains at failure recorded for these tests, when compared with those in the ATA Mk.II. The peak strengths, plotted in Fig. G.7 are widely scattered and, in general, considerably in excess of the corresponding Mk.II mean values.

The general trend of the variation in the intermediate principal stress is in keeping with that observed in the latter apparatus, although a direct comparison is not possible, because of the two-part shearing stage in tests carried out using the Mk.I apparatus. However,

apart from the sudden drop in σ_2 which occurred in the PS 1 test (Fig. G.1), and which was most probably caused by a fault in the apparatus or in the specimen sealing system, σ_2 increased during shearing to an extent determined largely by the initial porosity of the specimen.

Since it is unlikely that the frictional errors were similar in each test, detailed quantitative comparison with ATA Mk.II results would be unwarranted.

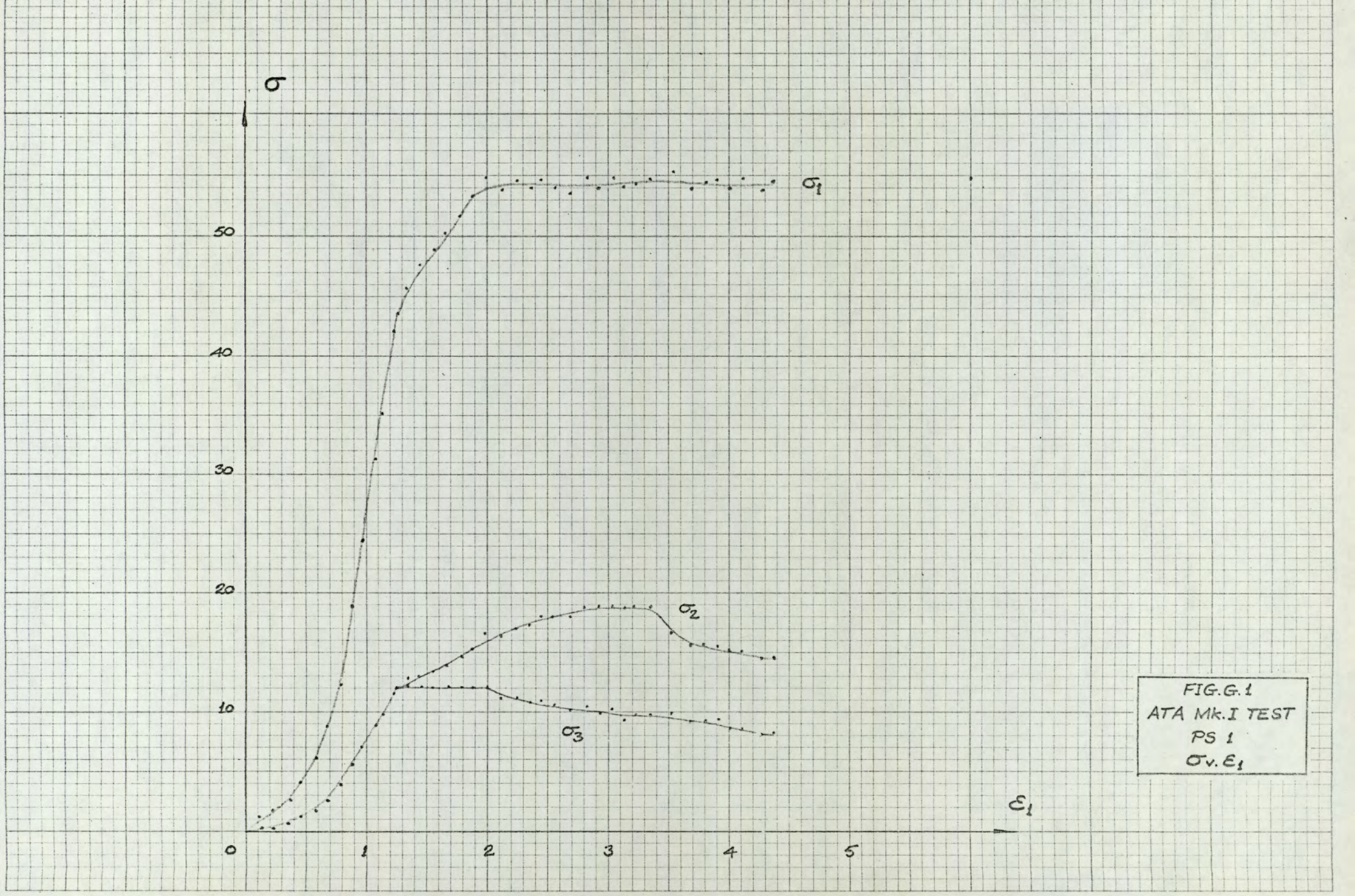

FIG. G. 1
ATA Mk. I TEST
PS 1
σv. ε1

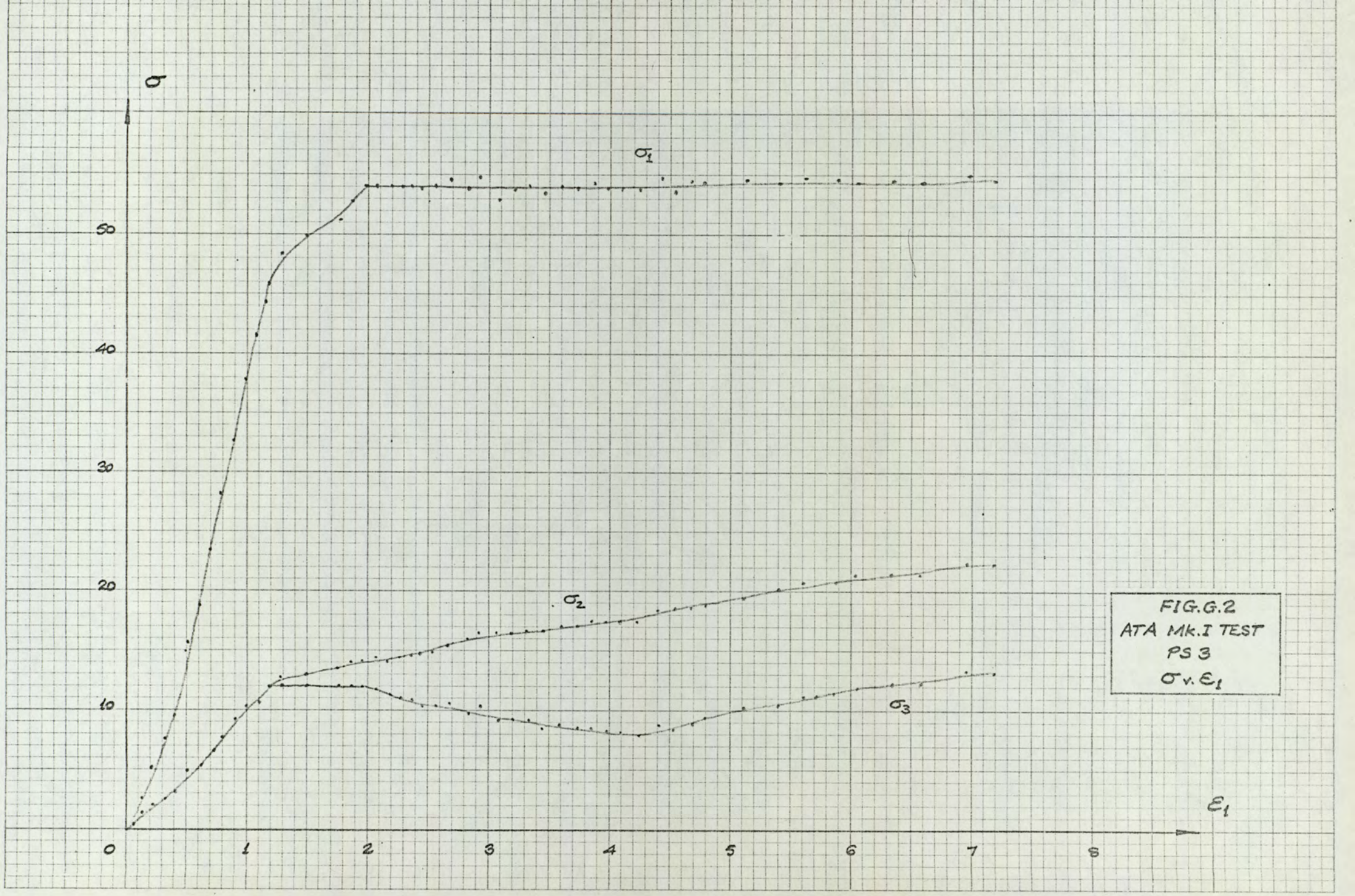

FIG. G.2
ATA Mk. I TEST
PS 3
σ v. ε_1

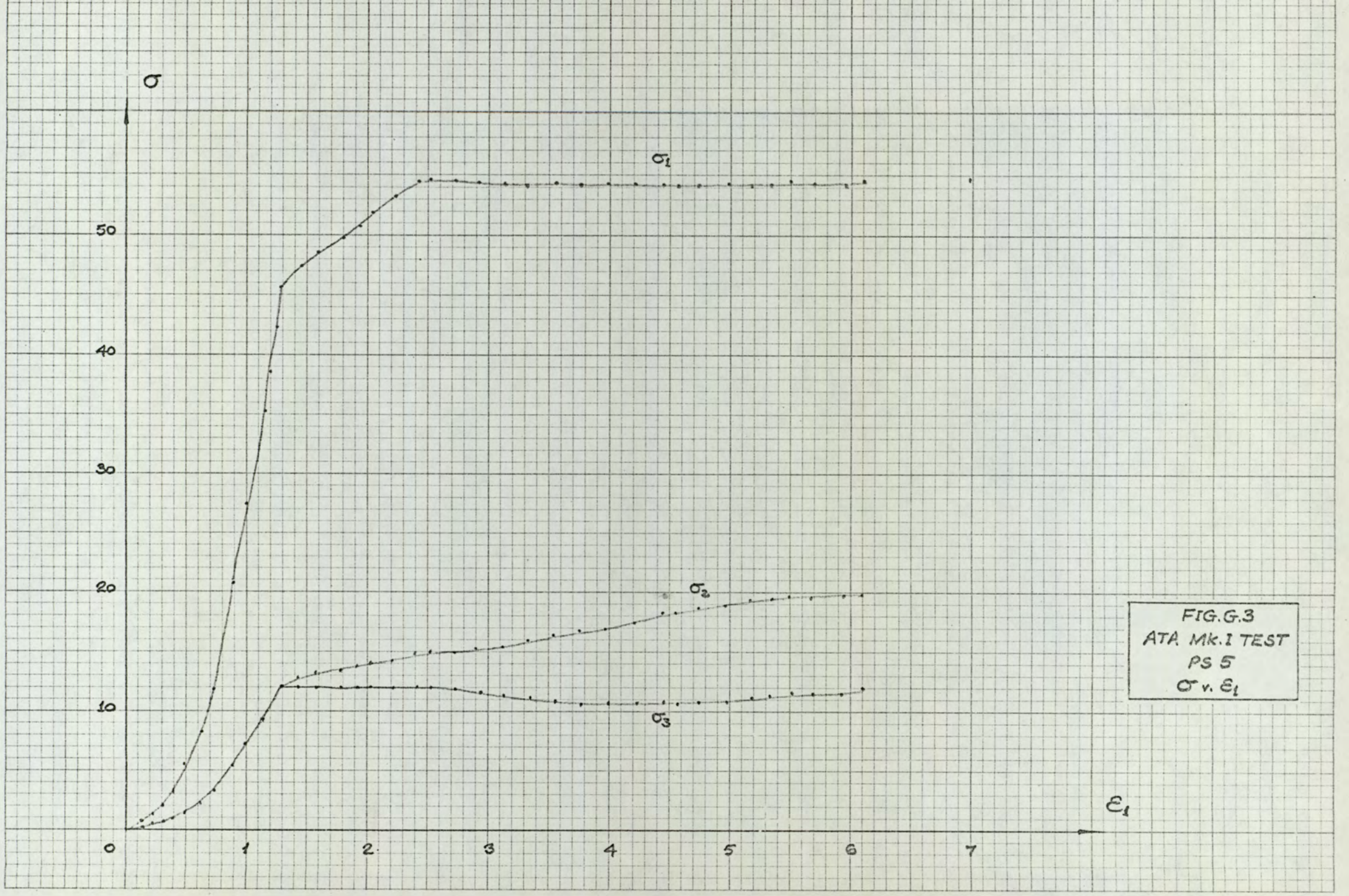

FIG. G.3
ATA Mk. I TEST
PS 5
σ v. ε_1

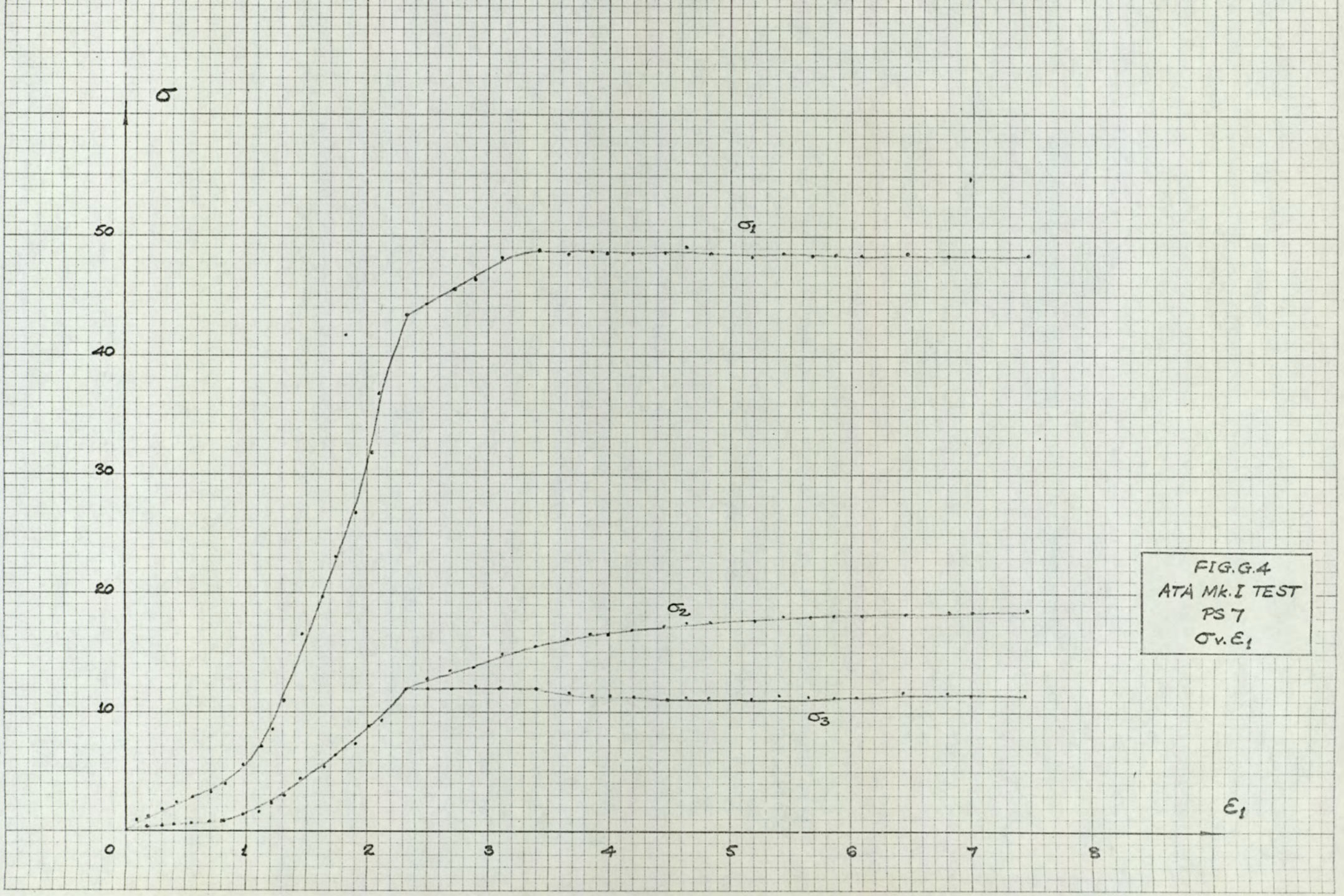

FIG. G.4
ATA Mk. I TEST
PS 7
σv. ε1

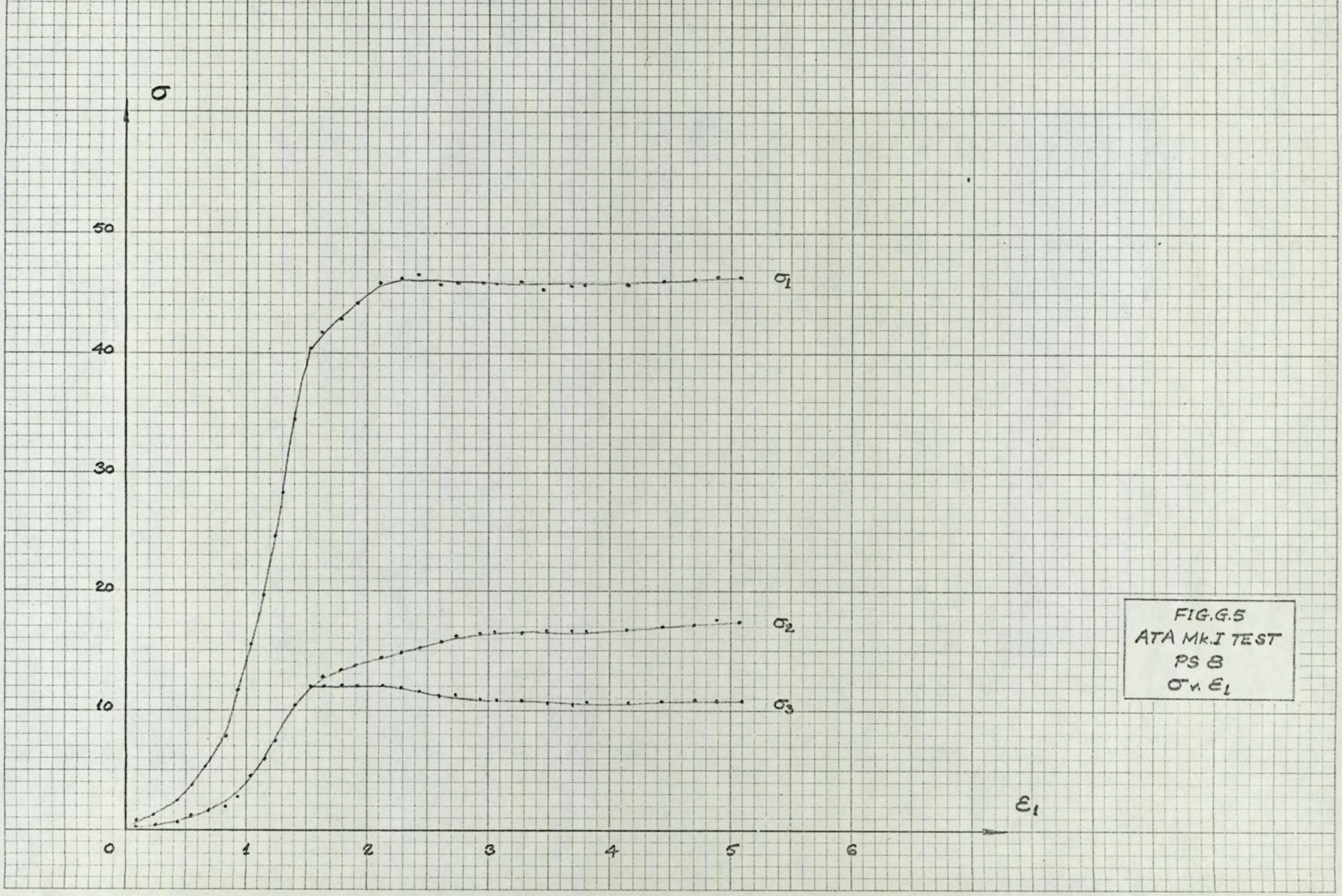

FIG.G.5
ATA Mk.I TEST
PS 8
σ v. ε_1

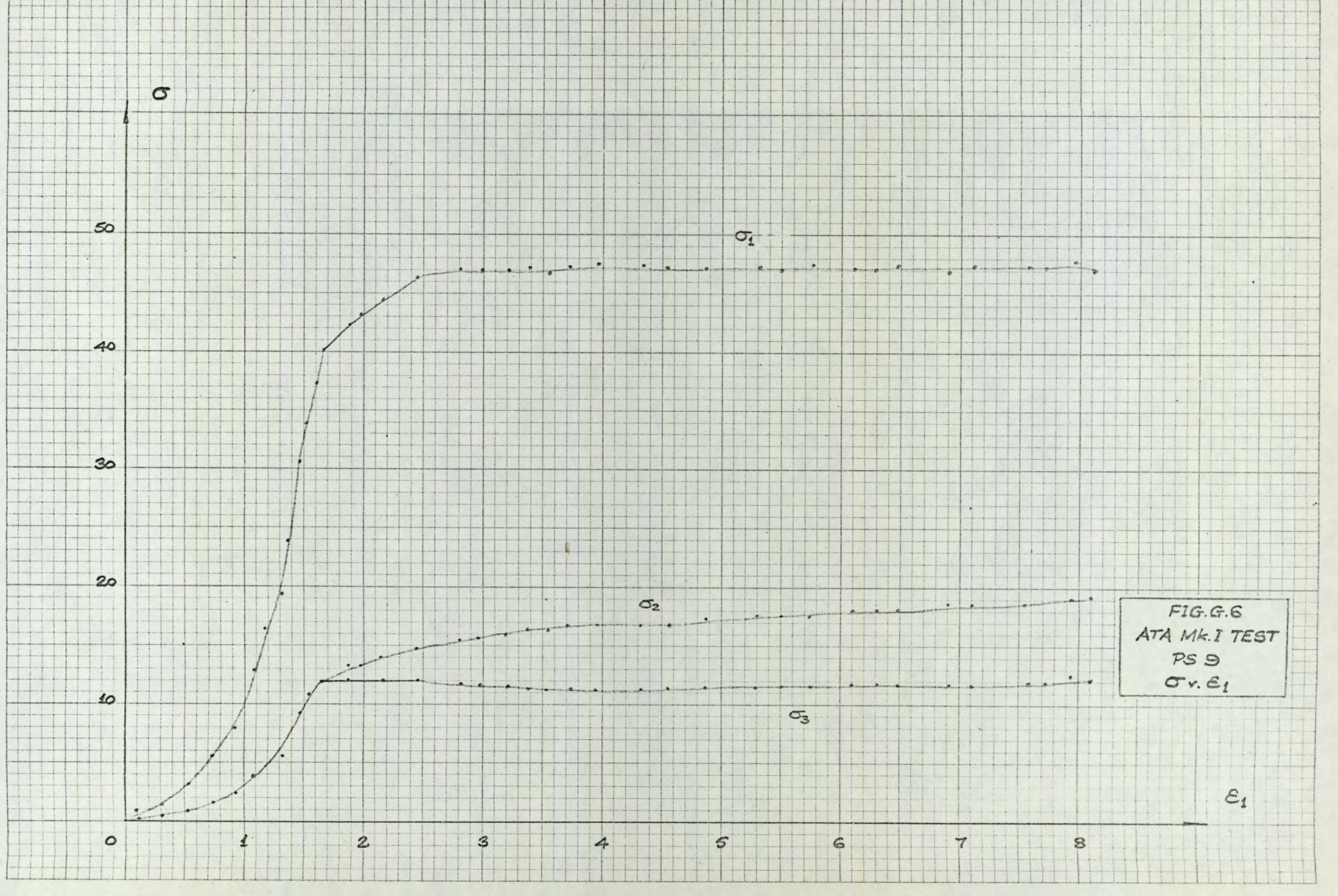

FIG. G.6
ATA Mk. I TEST
PS 9
σ v. ε1

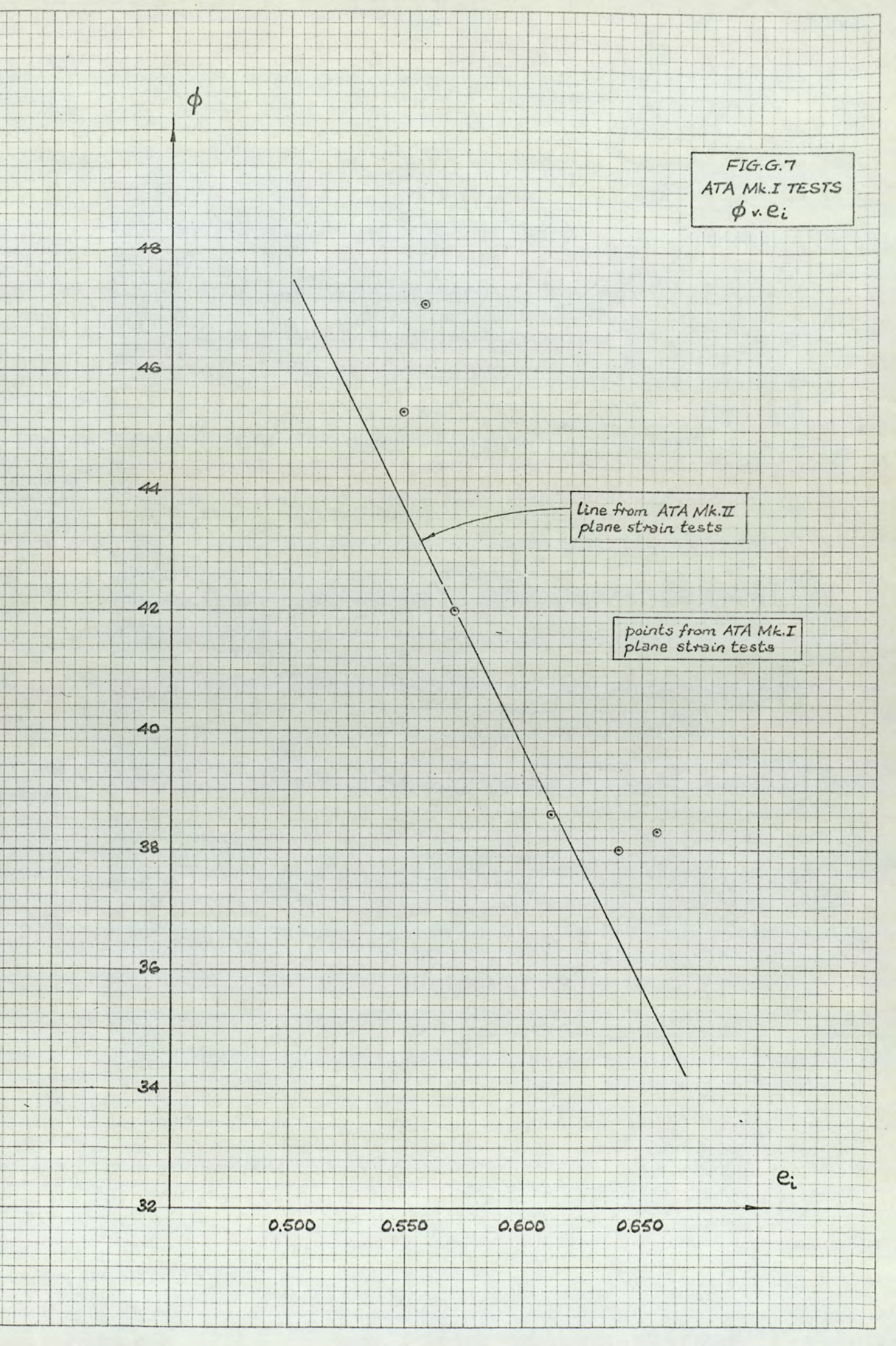
FIG.G.7
ATA Mk.I TESTS
ϕ v. e_i
ϕ
48
46
44
42
40
38
36
34
32
line from ATA Mk.II plane strain tests
points from ATA Mk.I plane strain tests
e_i
0.500
0.550
0.600
0.650

FIG. G.8
ATA Mk. I TESTS
K_o v. e_i

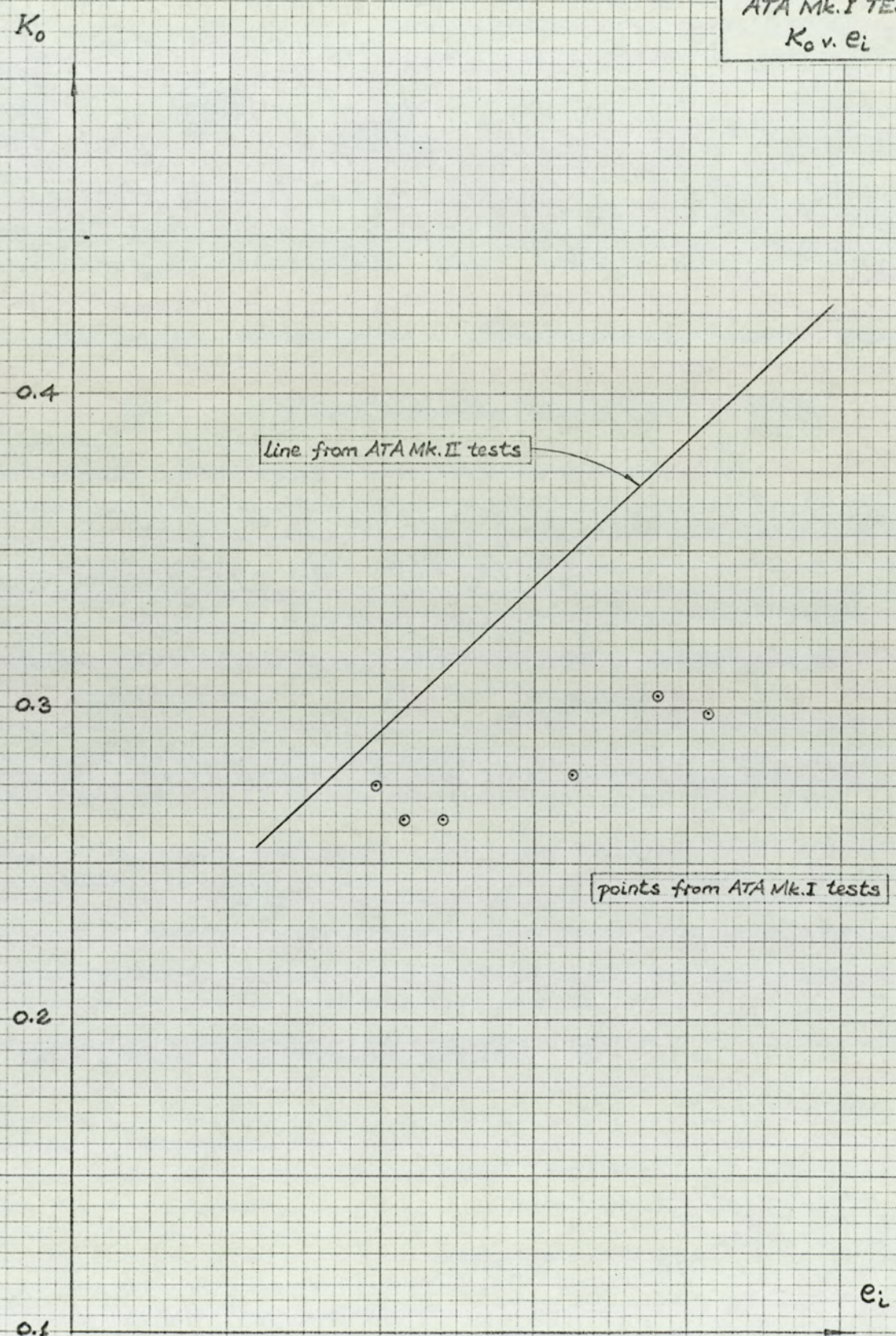

APPENDIX H

CLASSIFIED TEST RESULTS IN GRAPHICAL FORM

In Chapters 6 and 7, the results of stress-deformation tests performed on cuboidal and cylindrical sand specimens using either the ATA Mk.II, or modified forms of the conventional triaxial compression and extension apparatus, were discussed. The major implications of these investigations were presented by selecting a few specific test results to indicate typical behaviour, or by summarizing the results from a series of tests in tabular or graphical form.

To allow more detailed comparisons to be made between these findings and those of other workers using different apparatuses, this appendix includes graphs showing the relationships between the more important measured quantities, obtained from all tests which yielded valid experimental data up to or beyond the failure condition. The principal stresses are plotted against the major principal strain in each case, as is the volumetric strain. For tests carried out in the ATA, the remaining principal strains are also shown.

The order of presentation is as follows:-

(i) Figs. H.1 - H.24, CYL TC 1-26;

(ii) Figs. H.25 - H.30, CUB TC 25-30;

(iii) Figs. H.31 - H.38, CYL TE 31-38;

(iv) Figs. H.39 - H.49, ATA TC 4-18;

(v) Figs. H.50 - H.70, ATA PS 1-25;

(vi) Figs. H.71 - H.76, ATA INT 1-7;

(vii) Fig. H.77, ATA TE 1.

Figs. H.10-19 show both proving-ring and corrected end stress-cell readings of σ_1 for CYL TC tests, as do Figs. H.25-30 for the CUB TC tests. Corrected and uncorrected values of σ_1 are shown in Figs. H.20-24

for the CYL TC tests, in which a proving-ring was not used. Similarly, all graphs for CYL TE tests show two curves for σ_3, the upper of which represents its magnitude after end stress-cell correction.

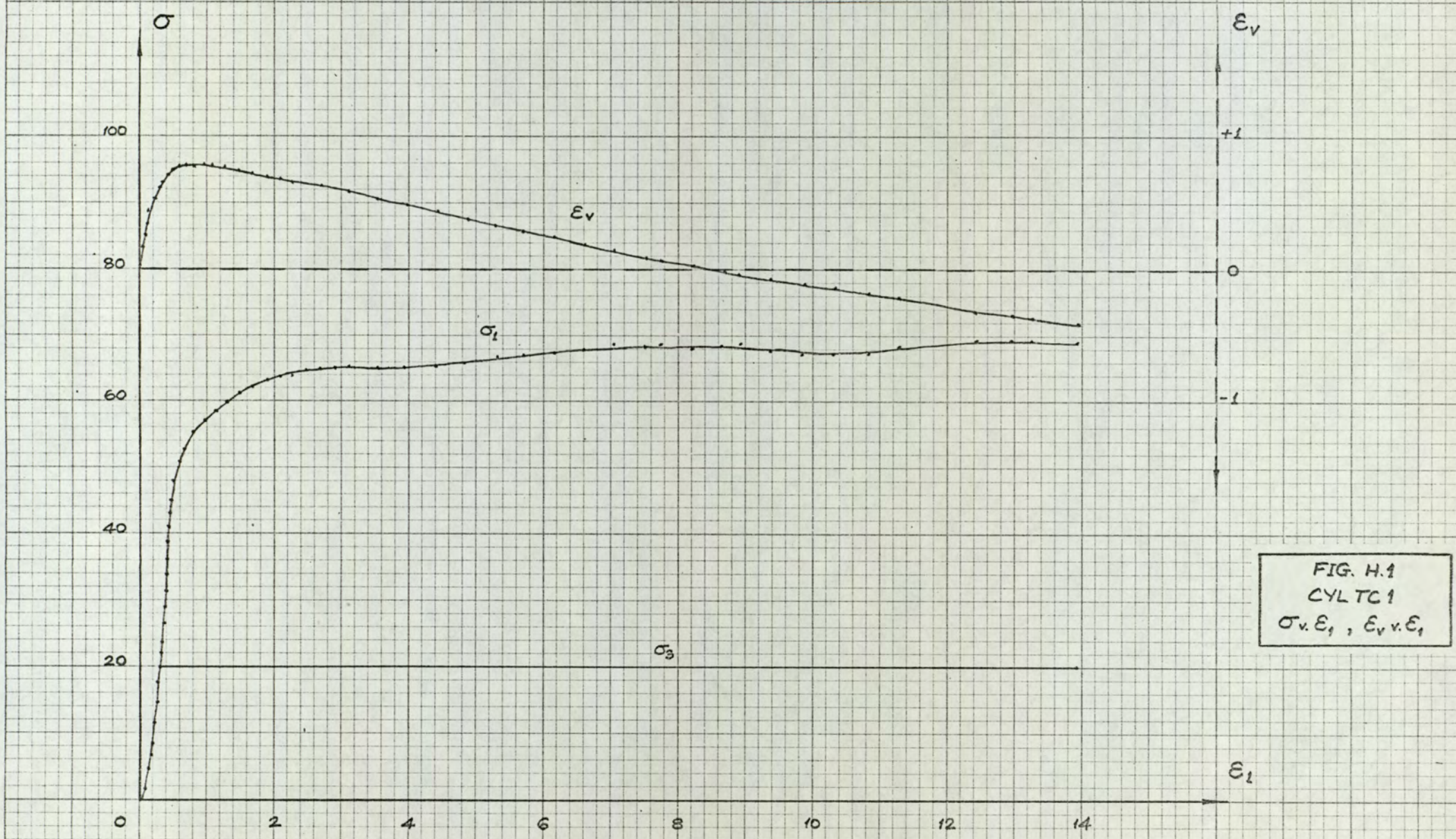

FIG. H.1
CYL TC 1
σ_v. ε_1 , ε_v v. ε_1

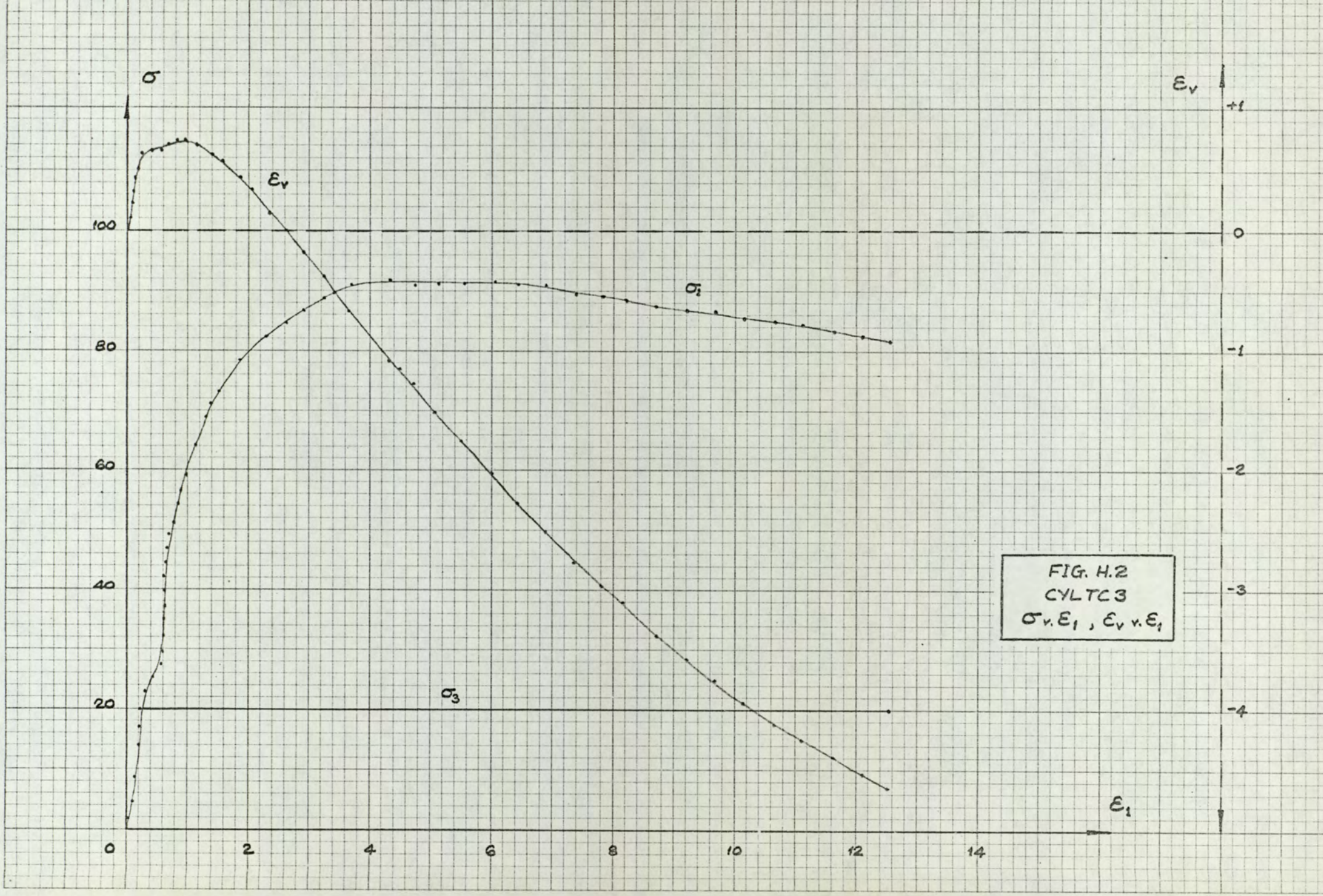

FIG. H.2
CYLTC3
σ_v v. ε_1 , ε_v v. ε_1

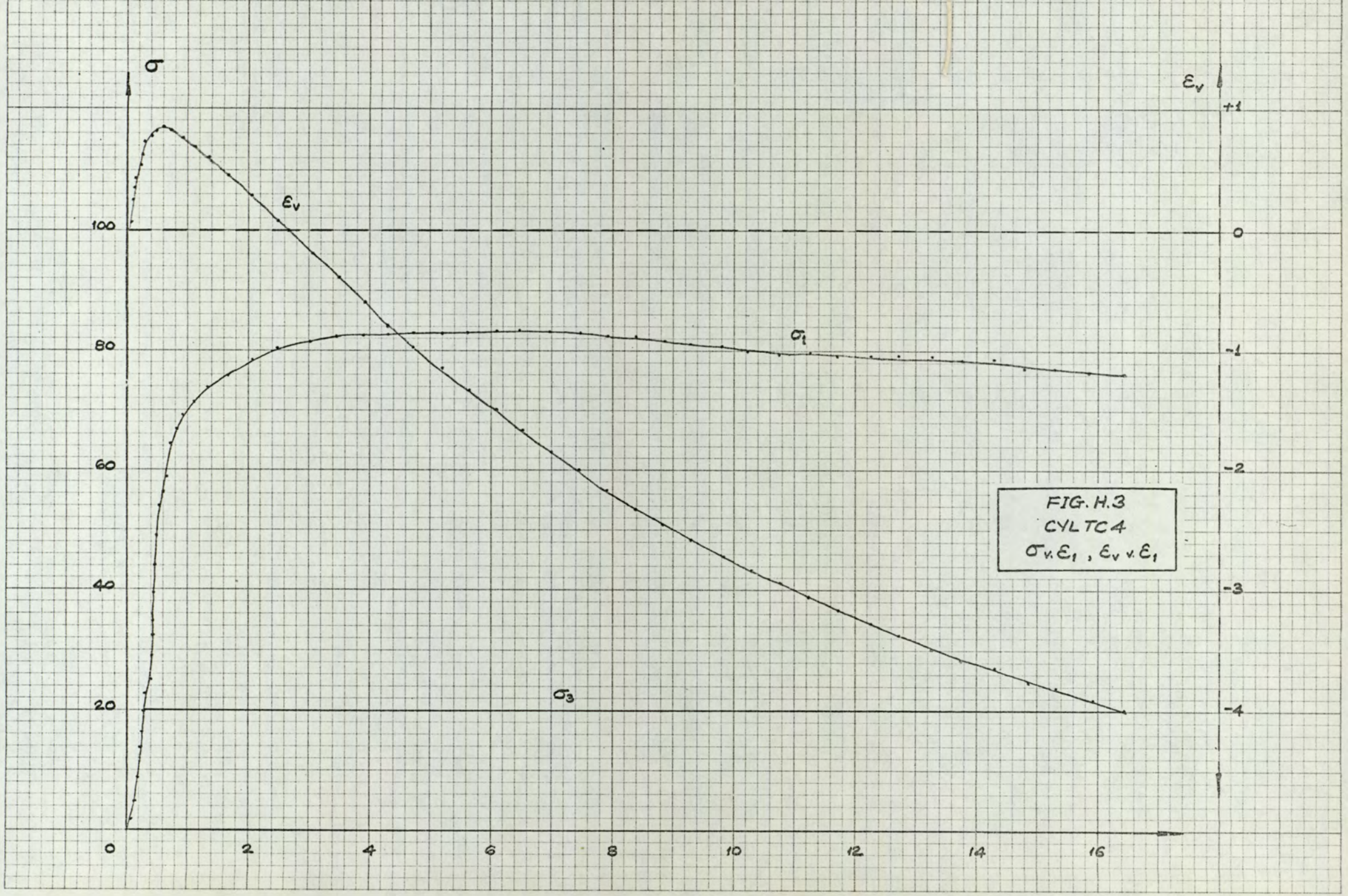
σ
ε_v
+1
0
-1
-2
-3
-4
100
80
60
40
20
0
2
4
6
8
10
12
14
16
ε_v
σ_1
σ_3
FIG. H.3
CYL TC 4
σ_v v. ε_1 , ε_v v. ε_1

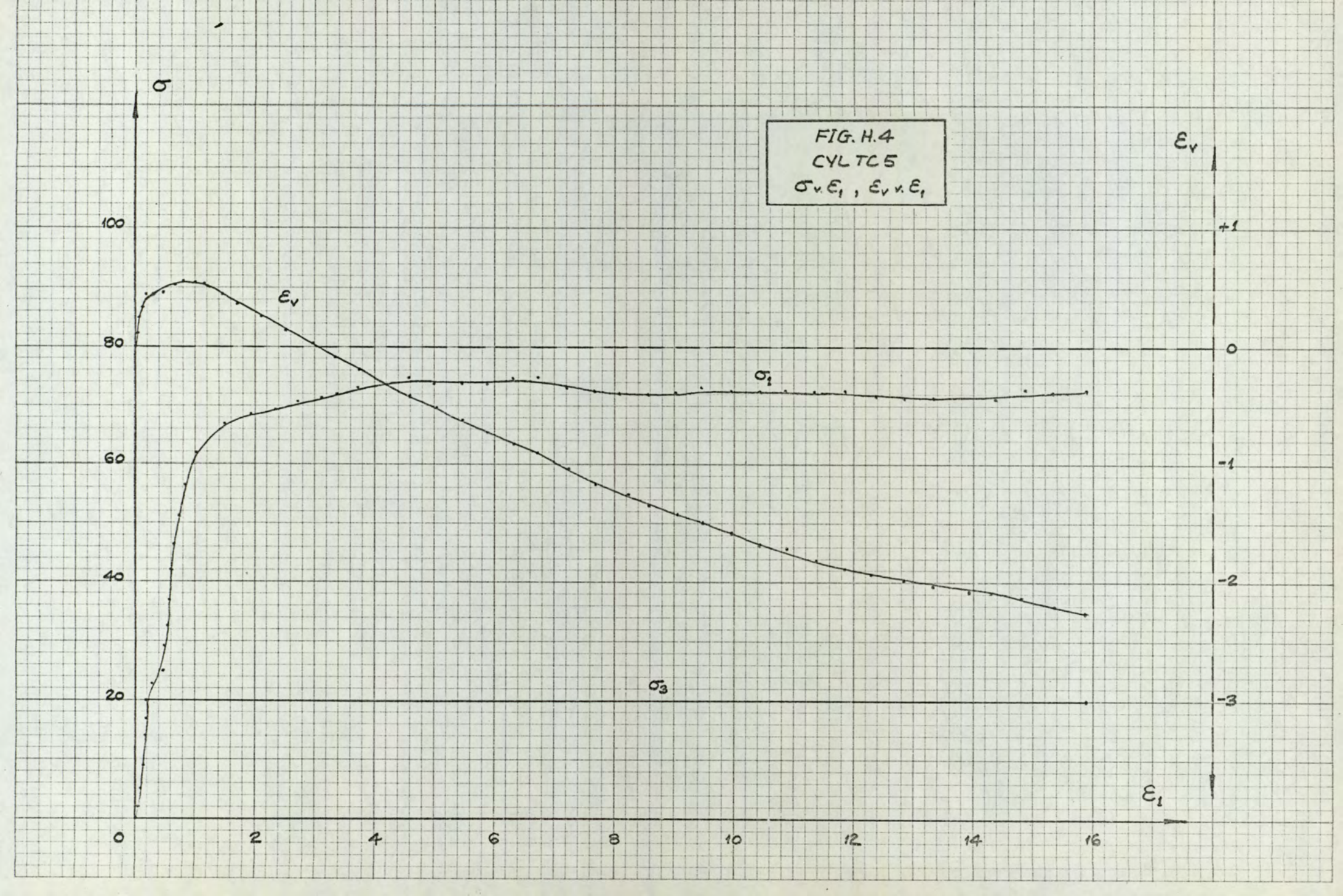
FIG. H.4
CYL TC 5
$\sigma_v \varepsilon_1$, ε_v v. ε_1
σ
ε_v
100
80
60
40
20
0
+1
0
-1
-2
-3
ε_v
σ_1
σ_3
ε_1
0
2
4
6
8
10
12
14
16

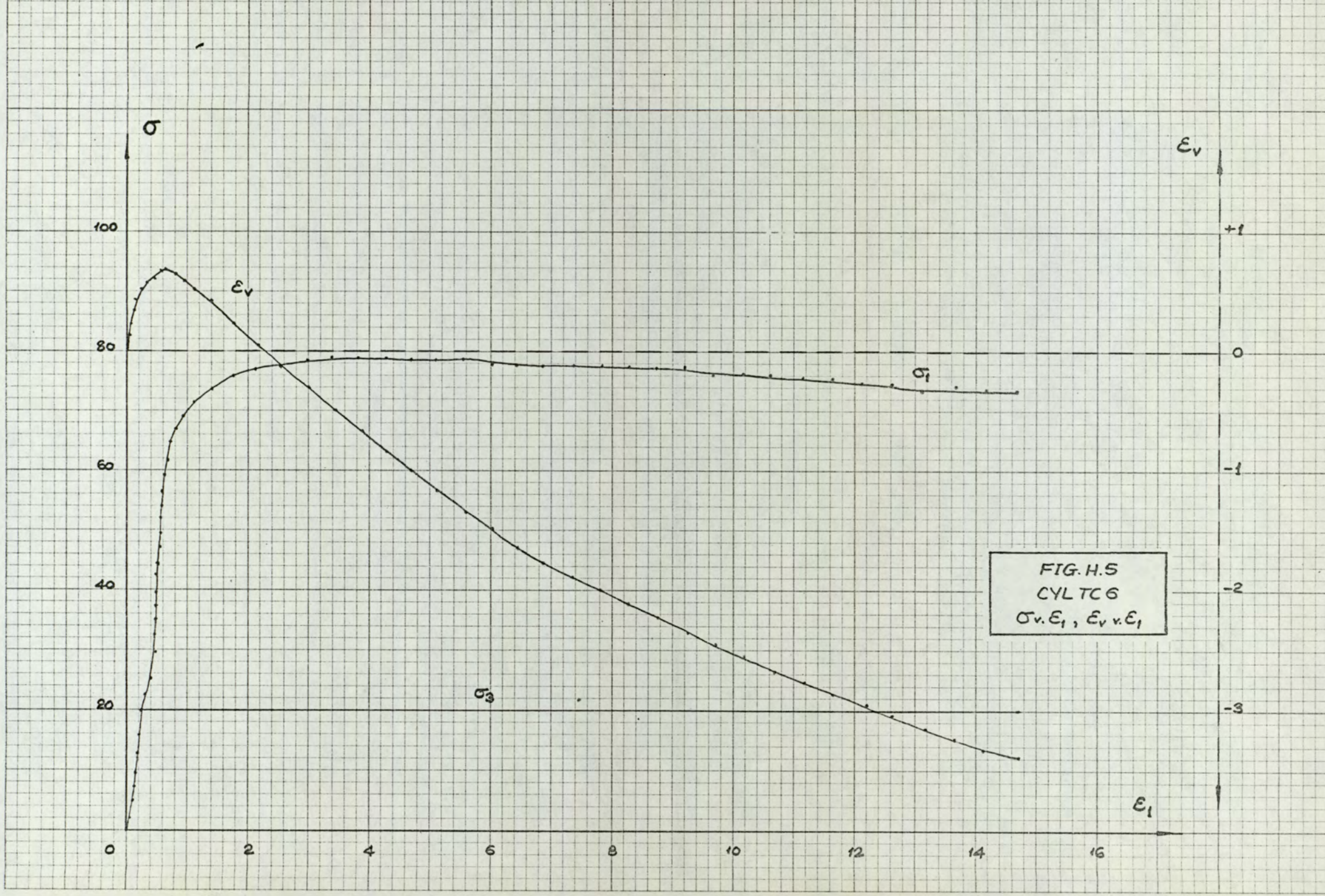

FIG. H.5
CYL TC 6
$\sigma_v . \varepsilon_1$, ε_v v. ε_1

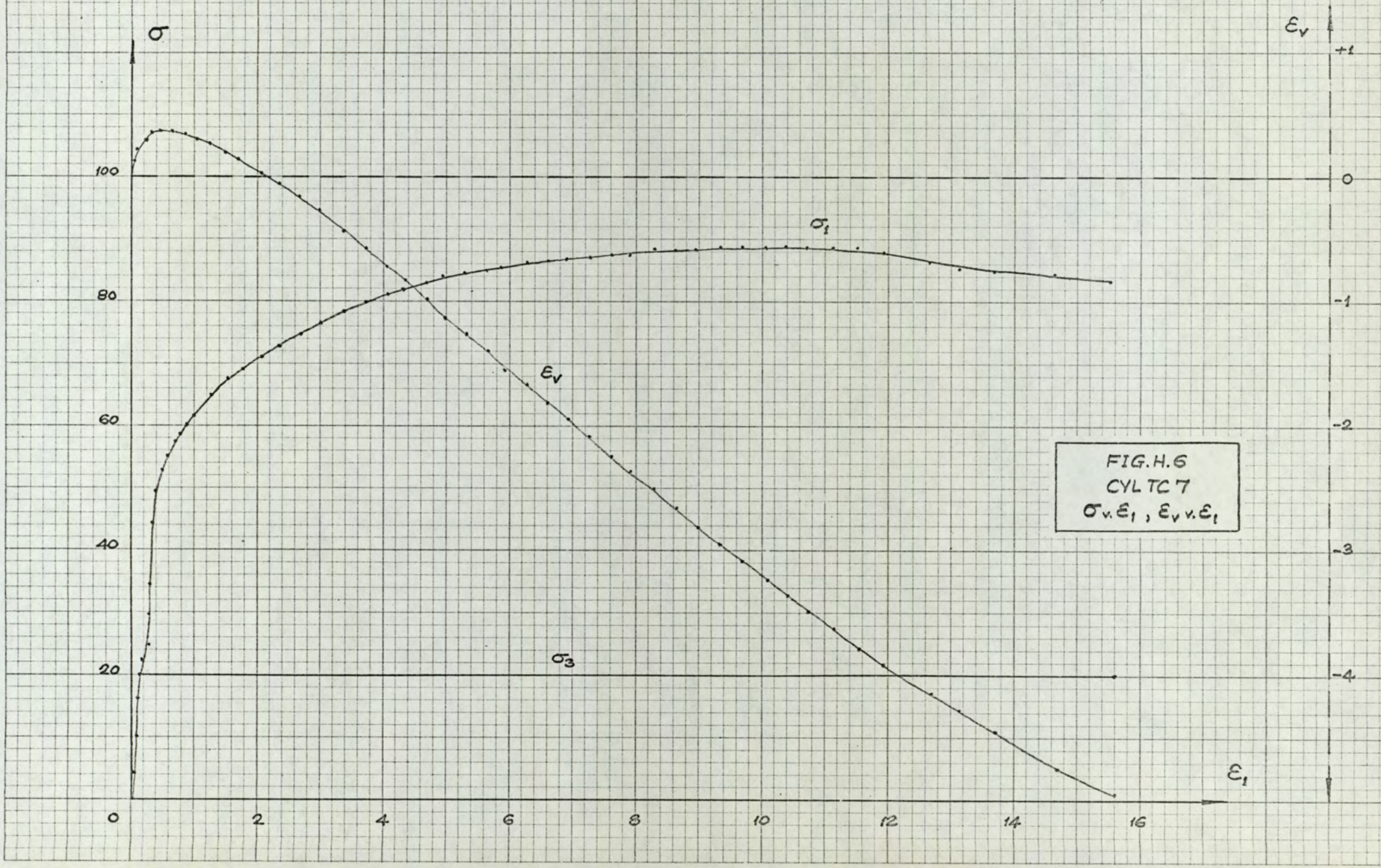

FIG. H.6
CYL TC 7
σ_1 v. ε_1 , ε_v v. ε_1

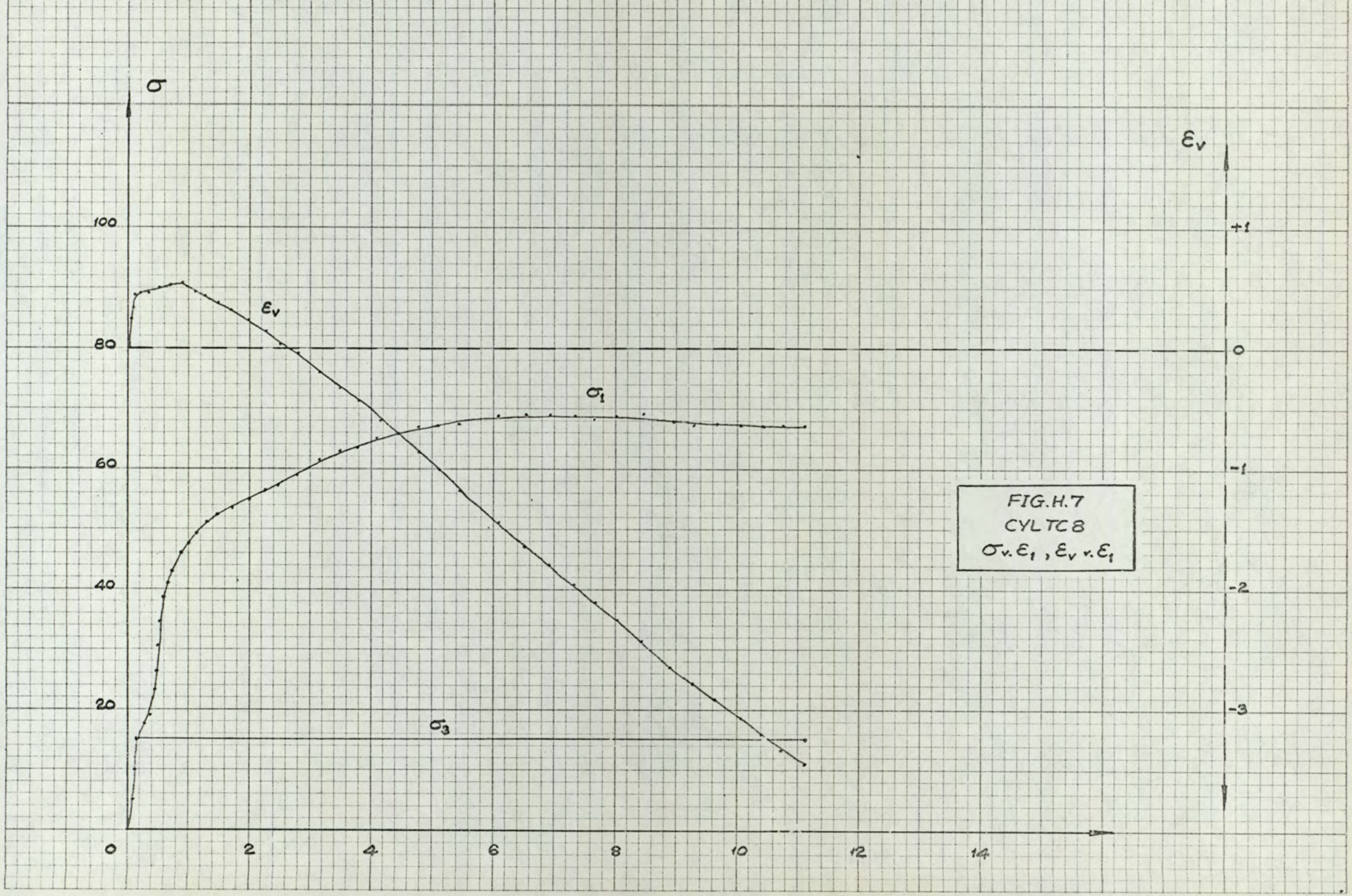

FIG. H.7
CYL TC 8
$\sigma_v . \varepsilon_1$, ε_v v. ε_1

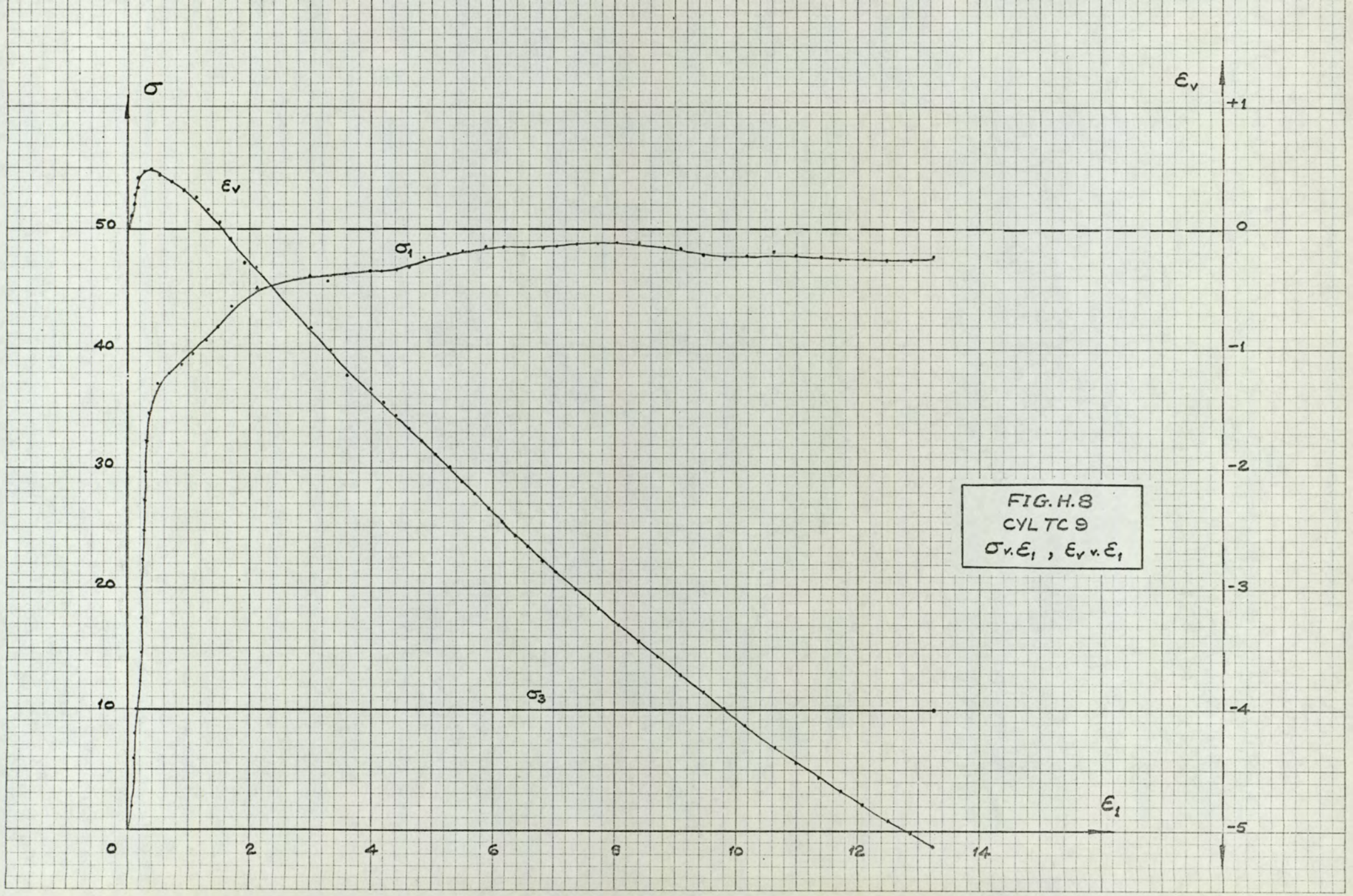

FIG. H.8
CYL TC 9
σ v. ε_1 , ε_v v. ε_1

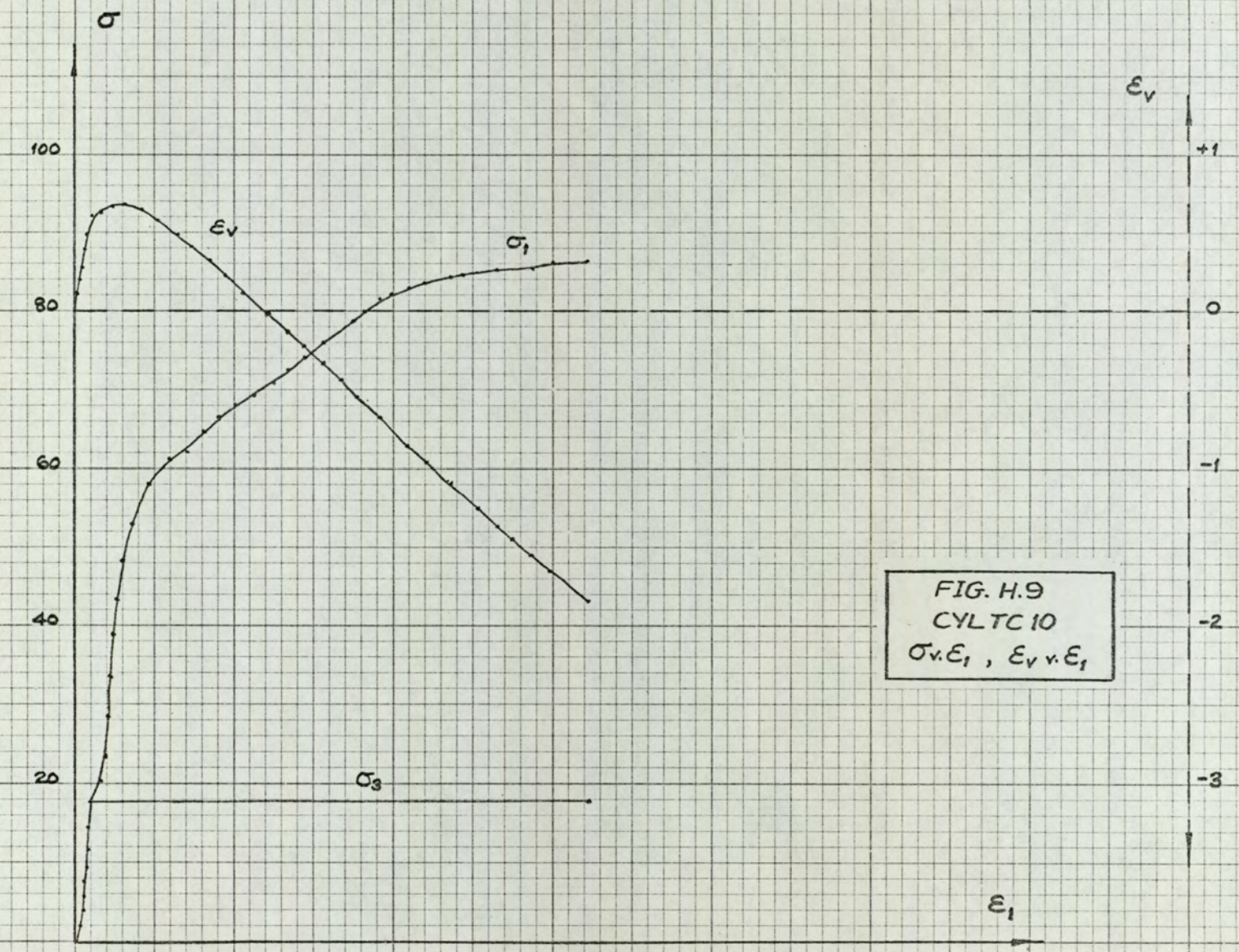

FIG. H.9
CYLTC 10
$\sigma_v . \varepsilon_1$, ε_v v. ε_1

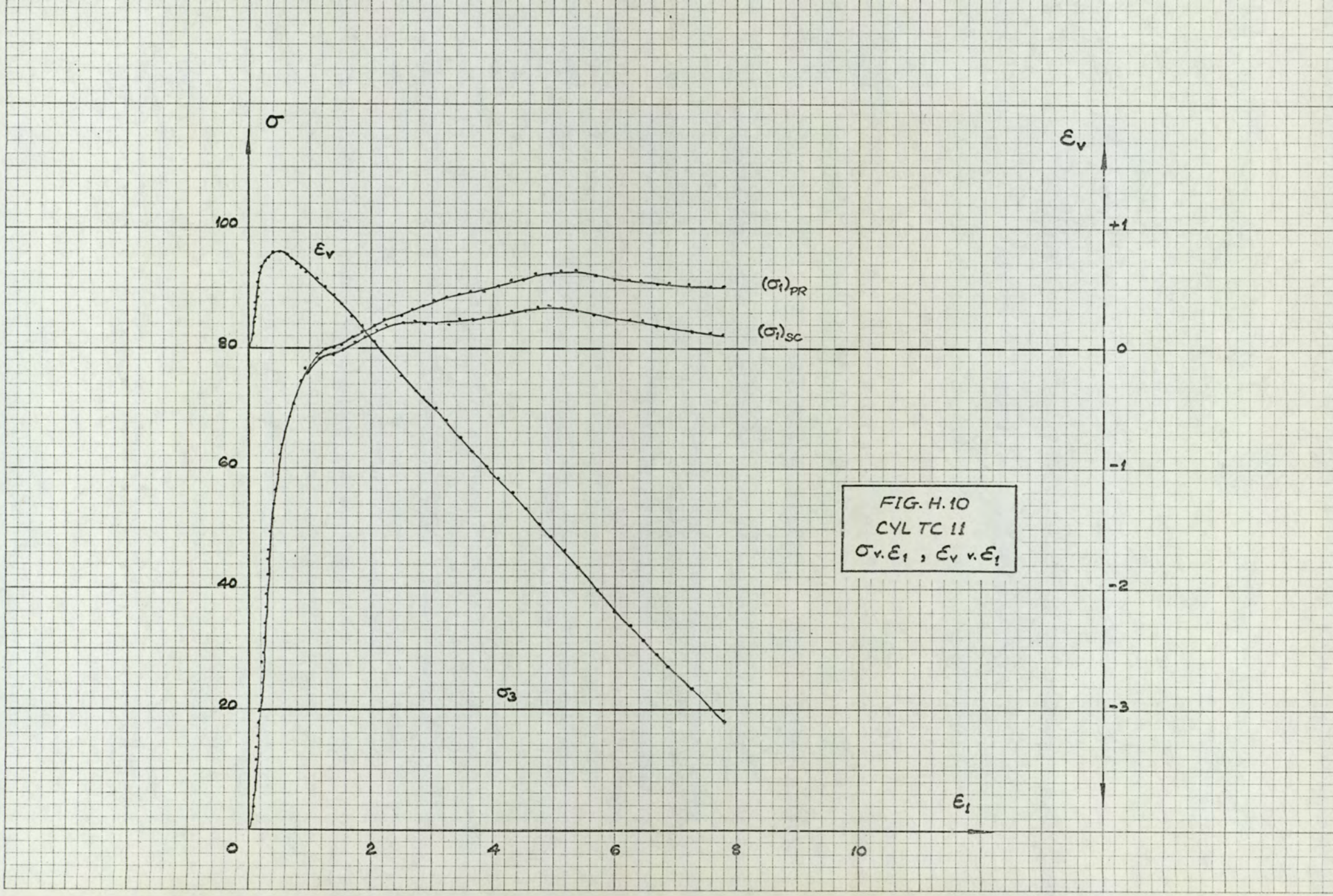

FIG. H.10
CYL TC 11
σ_v v. ε_1 , ε_v v. ε_1

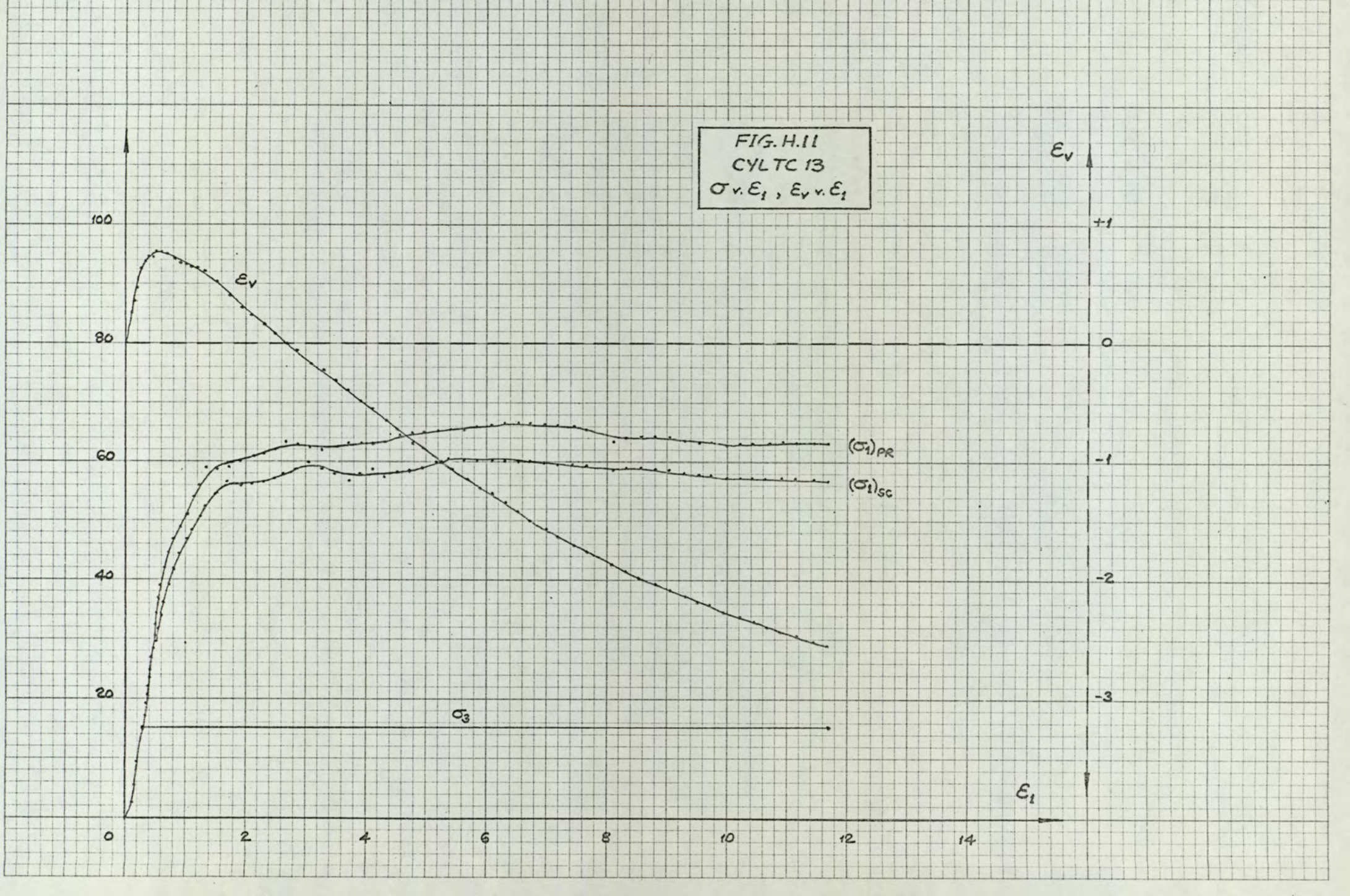
FIG. H.11
CYLTC 13
σ v. ε1 , εv v. ε1
εv
100
80
60
40
20
0
+1
0
-1
-2
-3
2
4
6
8
10
12
14
ε1
σ3
(σ1)PR
(σ1)SC

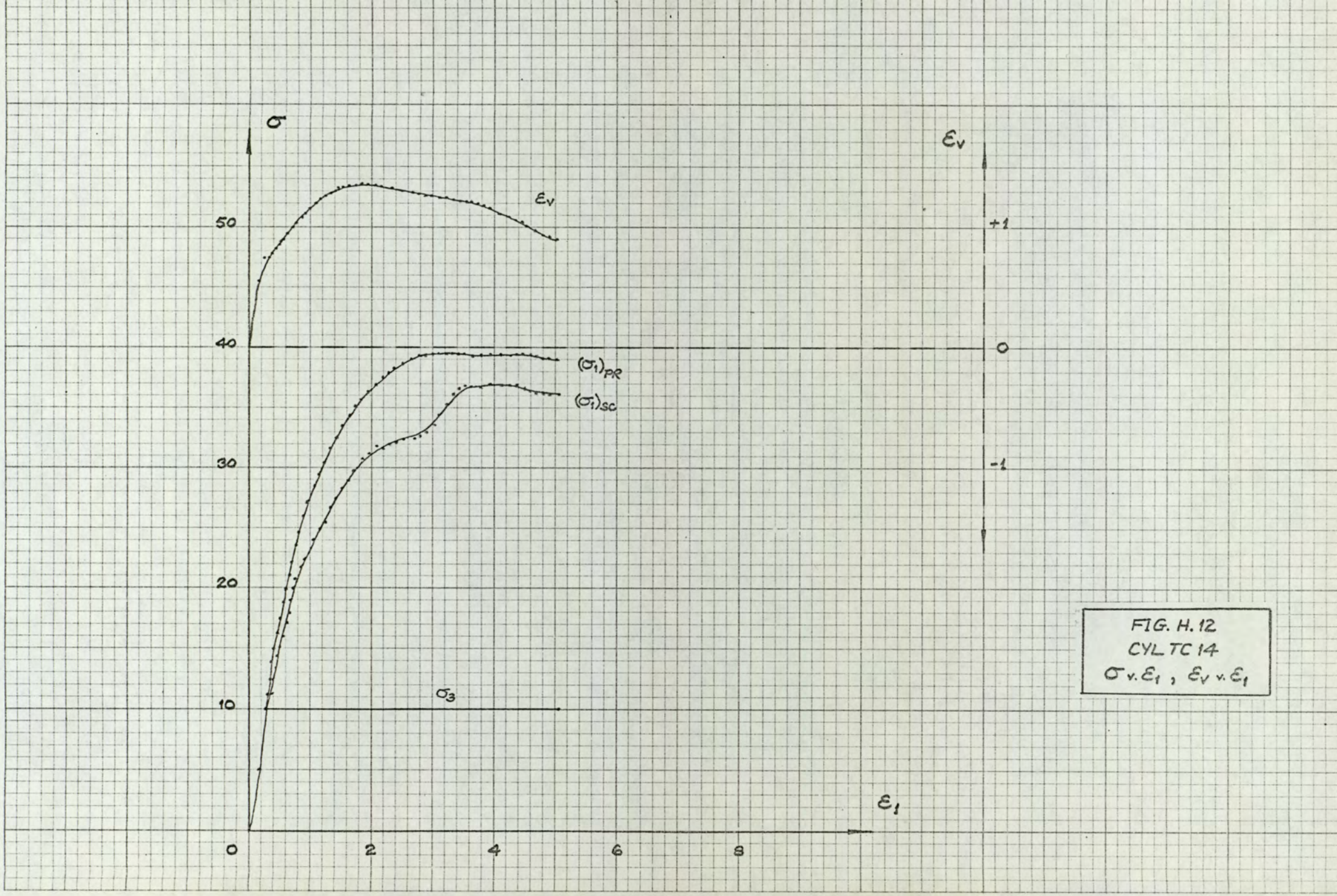

FIG. H.12
CYL TC 14
σ v. ε_1 , ε_v v. ε_1

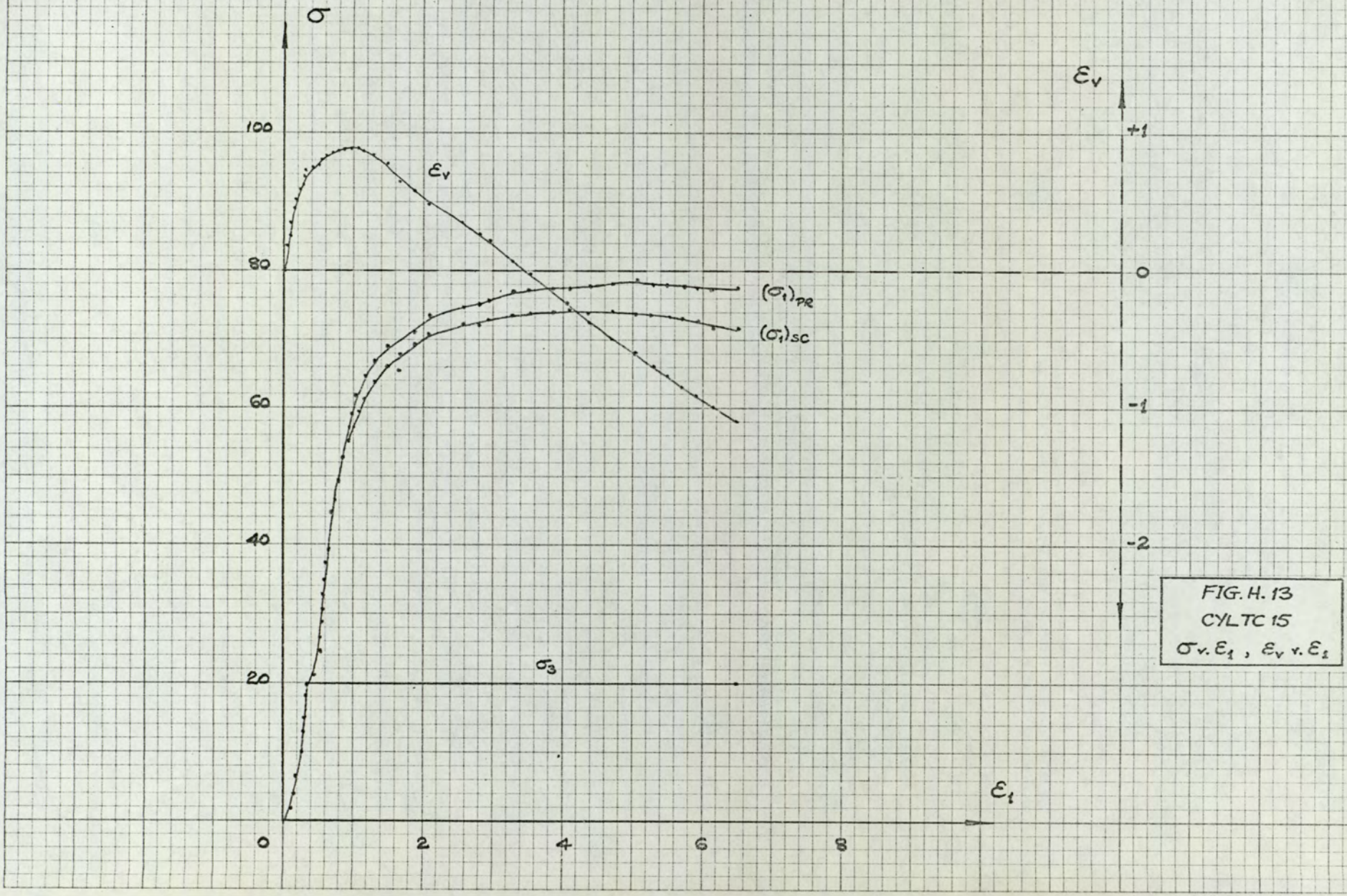

FIG. H. 13
CYLTC 15
σ v. ε_1 , ε_v v. ε_1

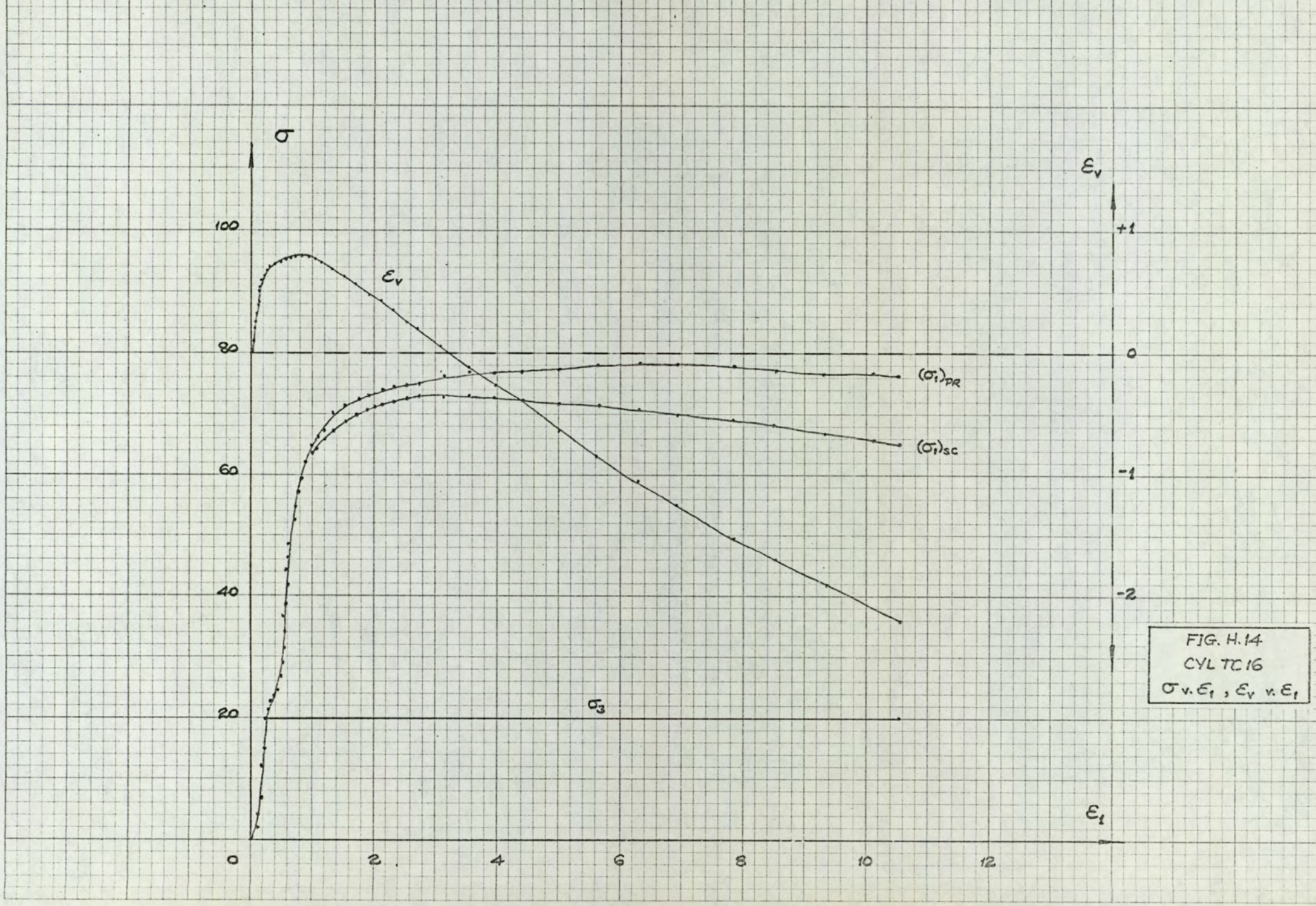

FIG. H.14
CYL TC 16
σ v. ε_1 , ε_v v. ε_1

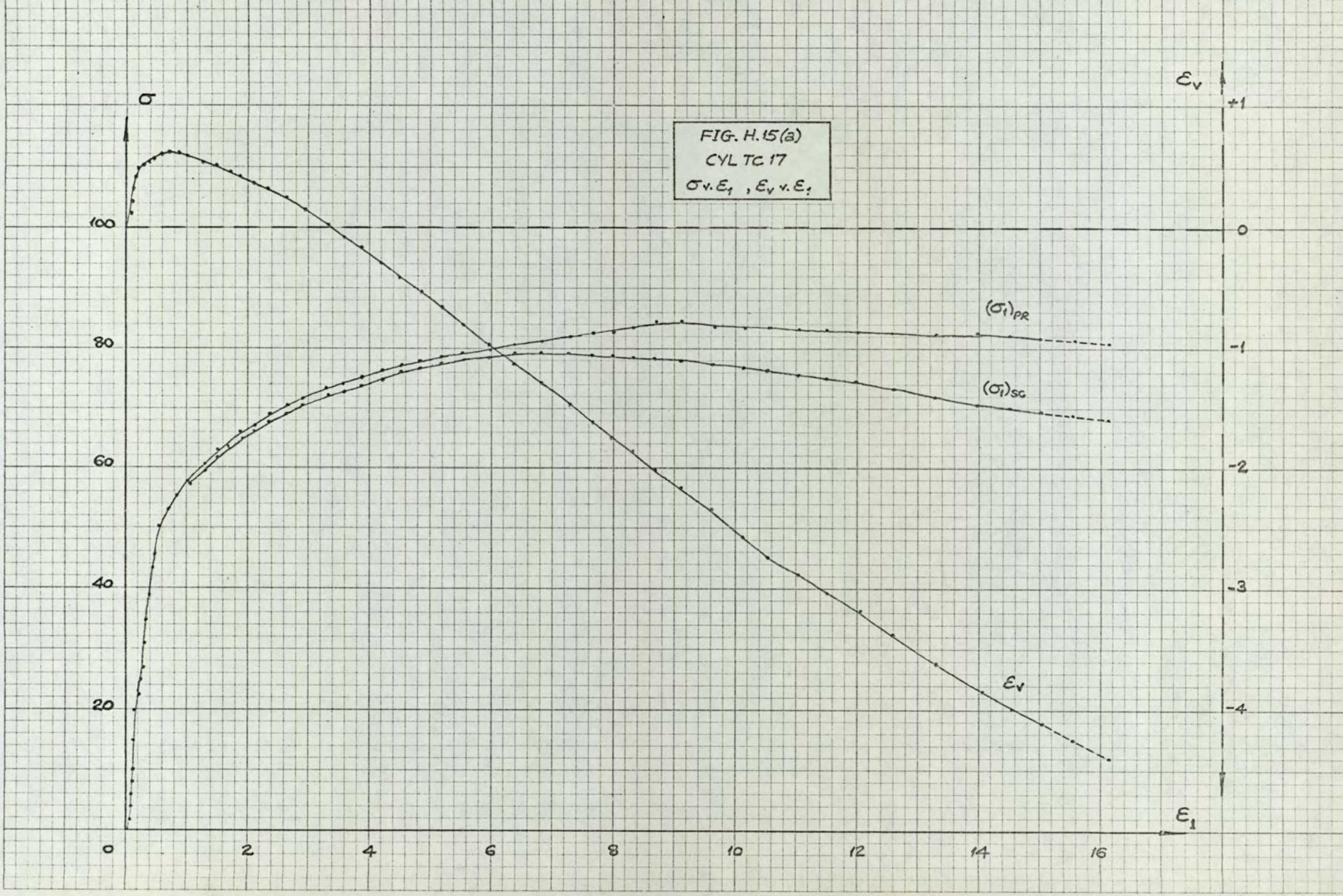
FIG. H.15(a)
CYL TC 17
σ v. ε1 , εv v. ε1
σ
εv
+1
0
-1
-2
-3
-4
100
80
60
40
20
0
2
4
6
8
10
12
14
16
ε1
(σ1)PR
(σ1)SC
εv

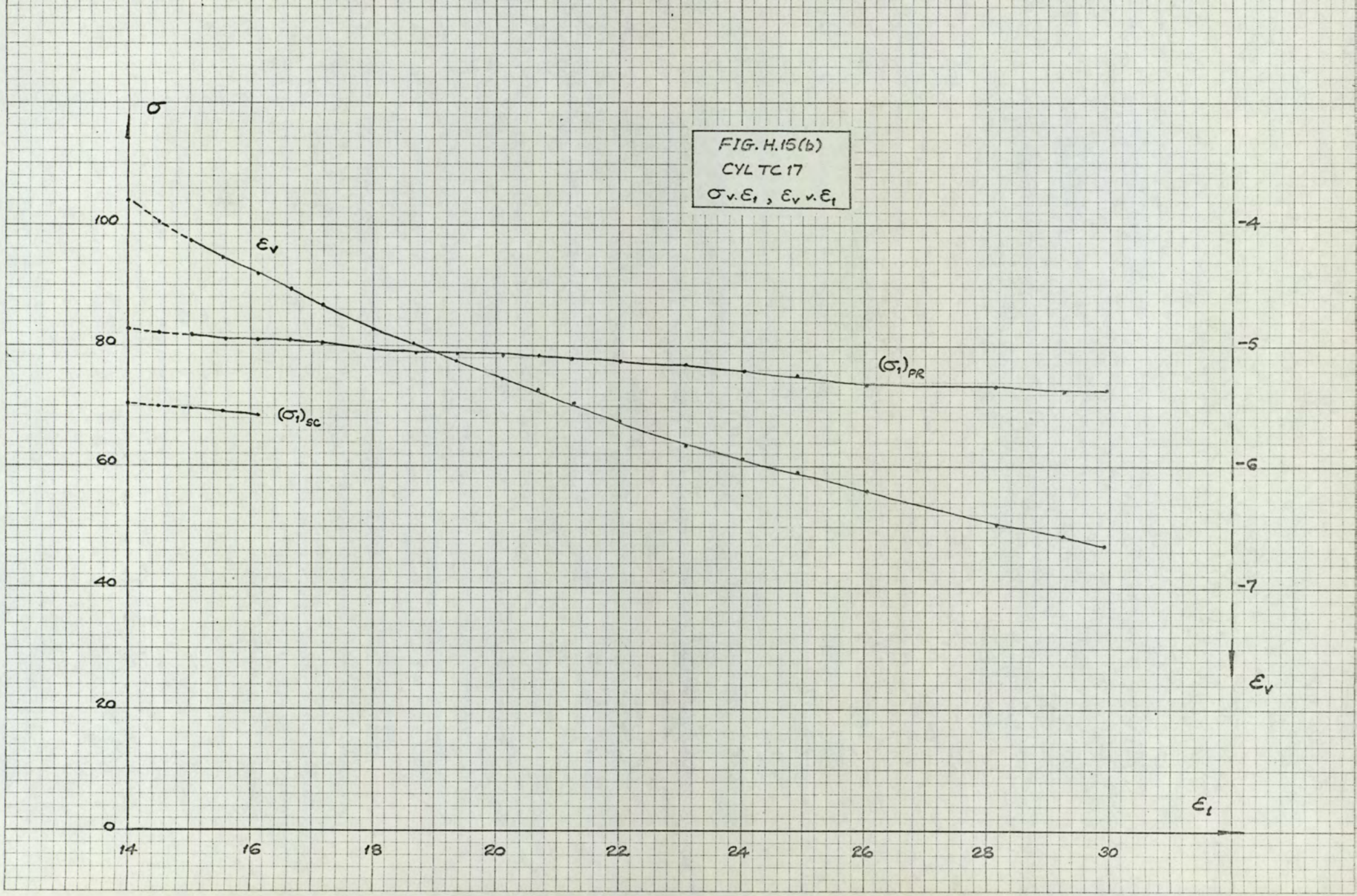
FIG. H.15(b)
CYL TC 17
σ v. ε1 , εv v. ε1
σ
100
80
60
40
20
0
εv
(σ1)PR
(σ1)SC
-4
-5
-6
-7
εv
ε1
14
16
18
20
22
24
26
28
30

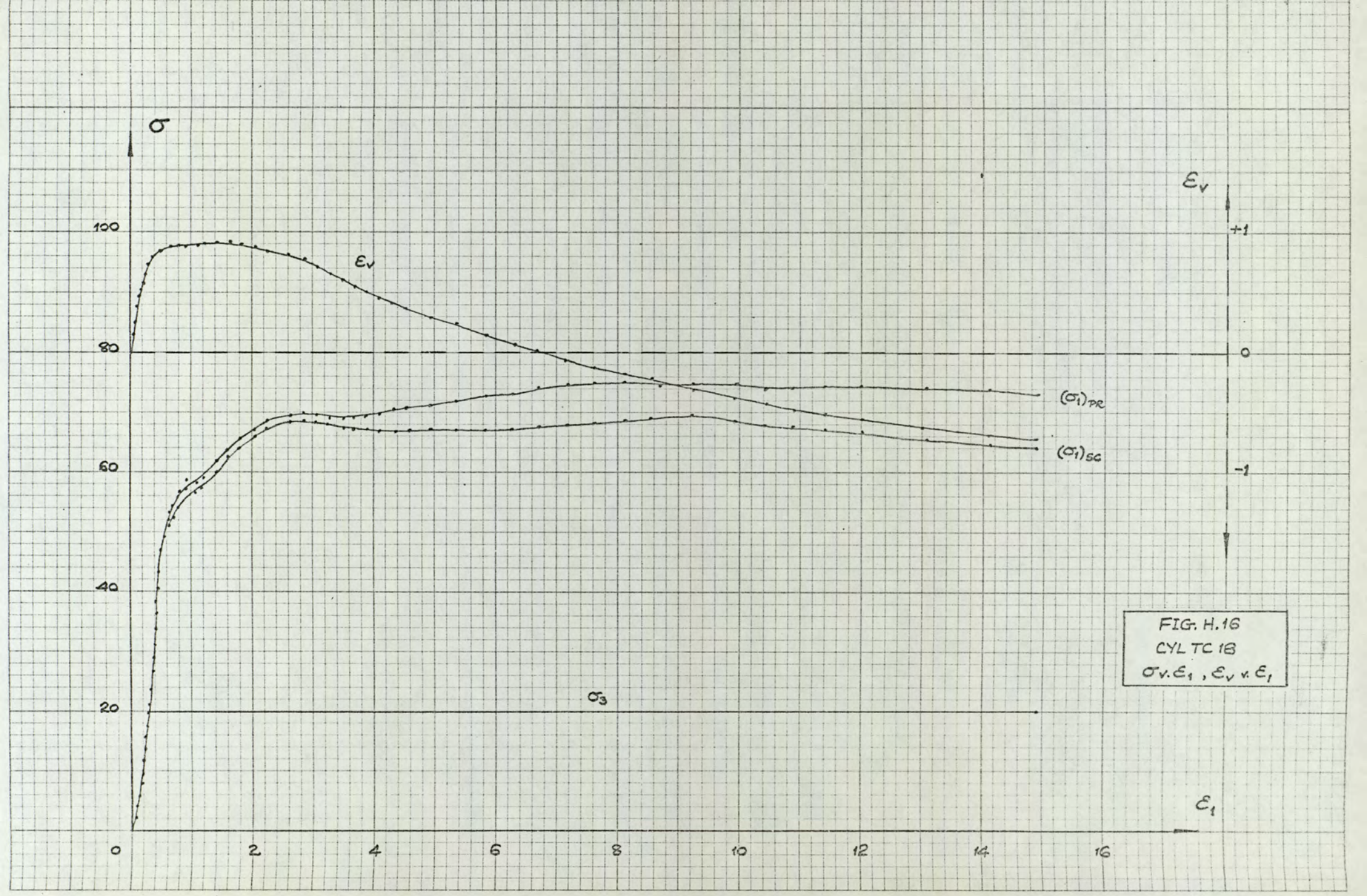

FIG. H.16
CYL TC 18
$\sigma_v . \varepsilon_1$, ε_v v. ε_1

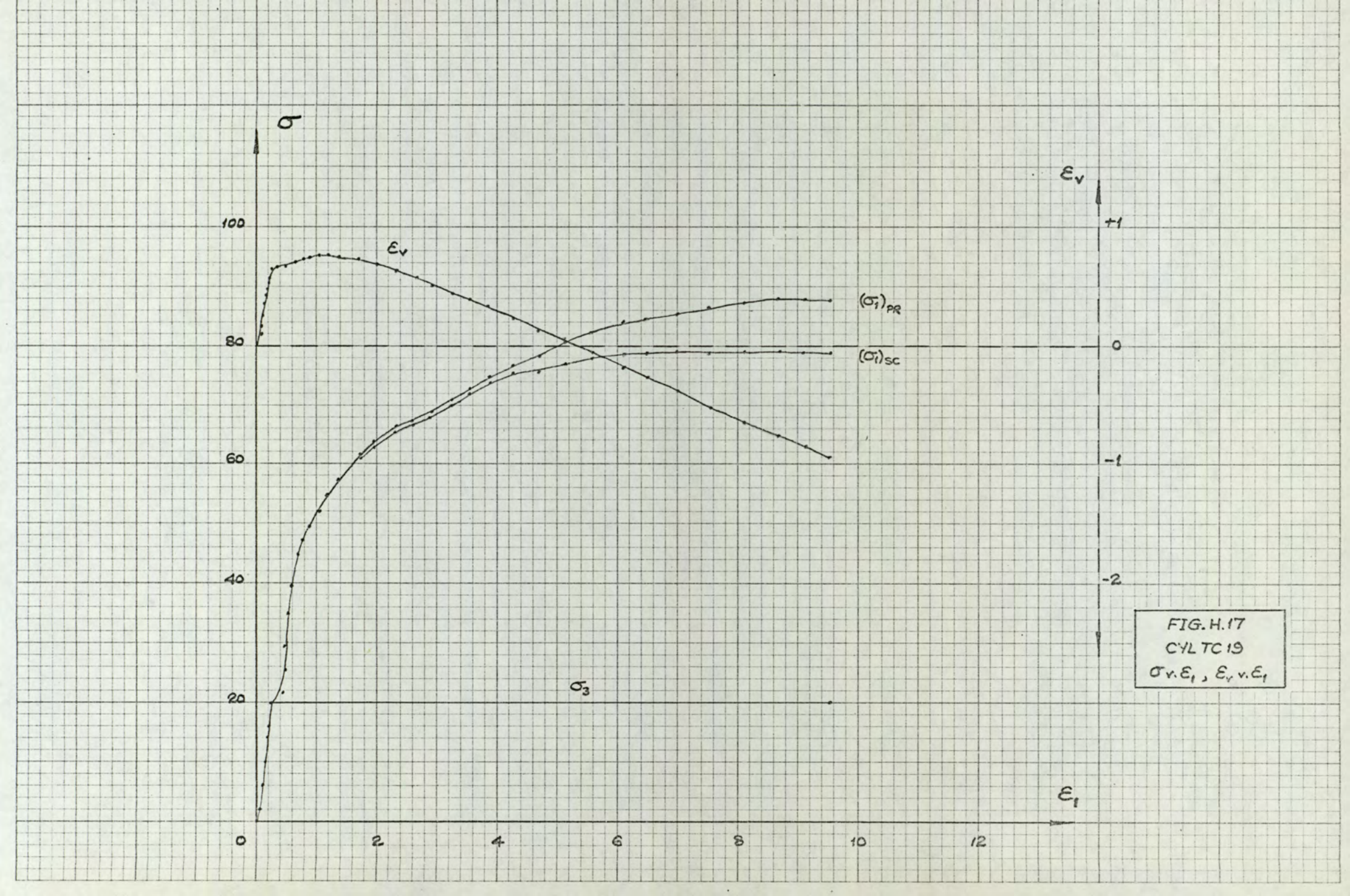

FIG. H.17
CYL TC 19
σ v. ε_1 , ε_v v. ε_1

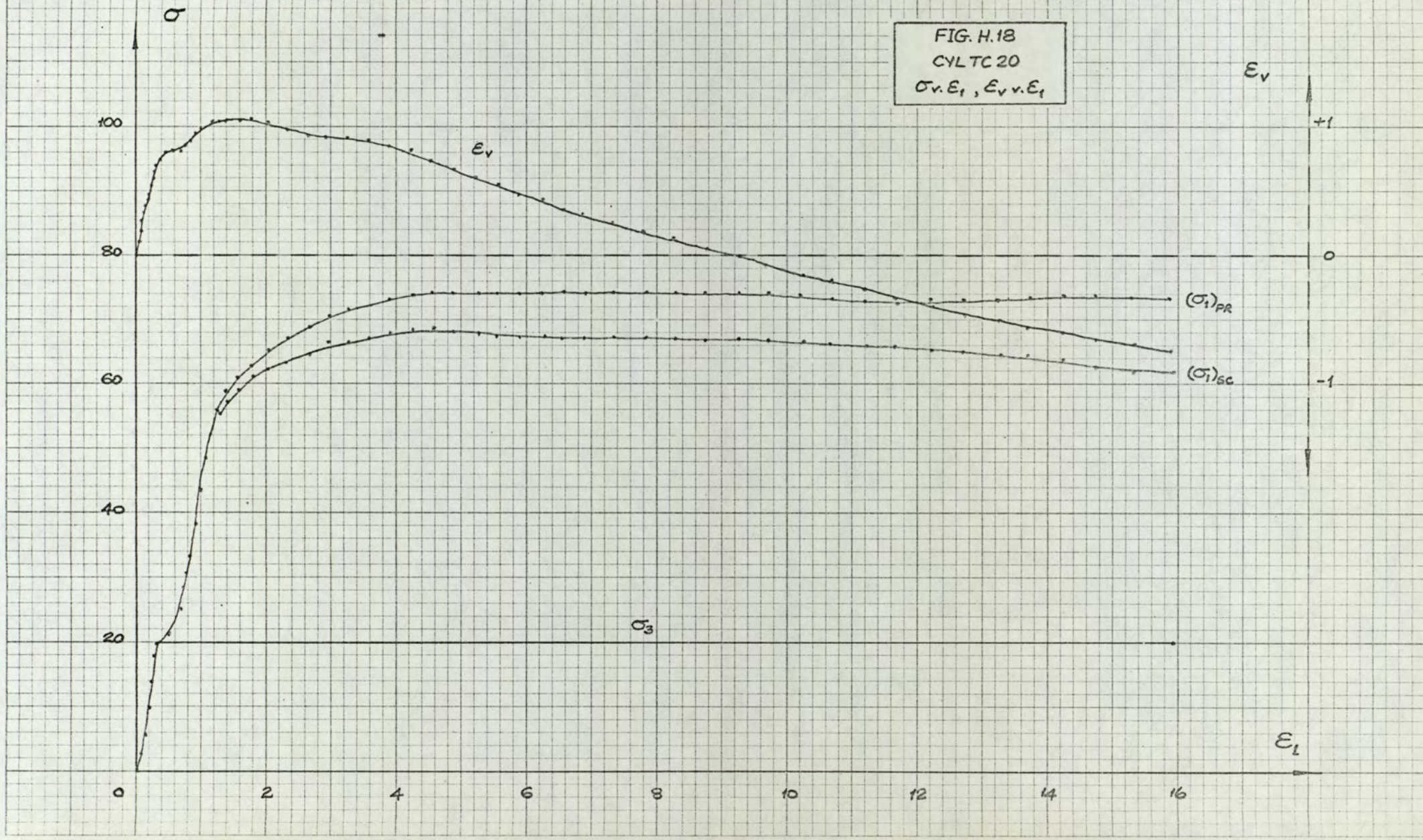
σ
FIG. H.18
CYL TC 20
σv. ε1 , εv v. ε1
εv
100
80
60
40
20
0
2
4
6
8
10
12
14
16
+1
0
-1
εv
(σ1)PR
(σ1)SC
σ3
ε1

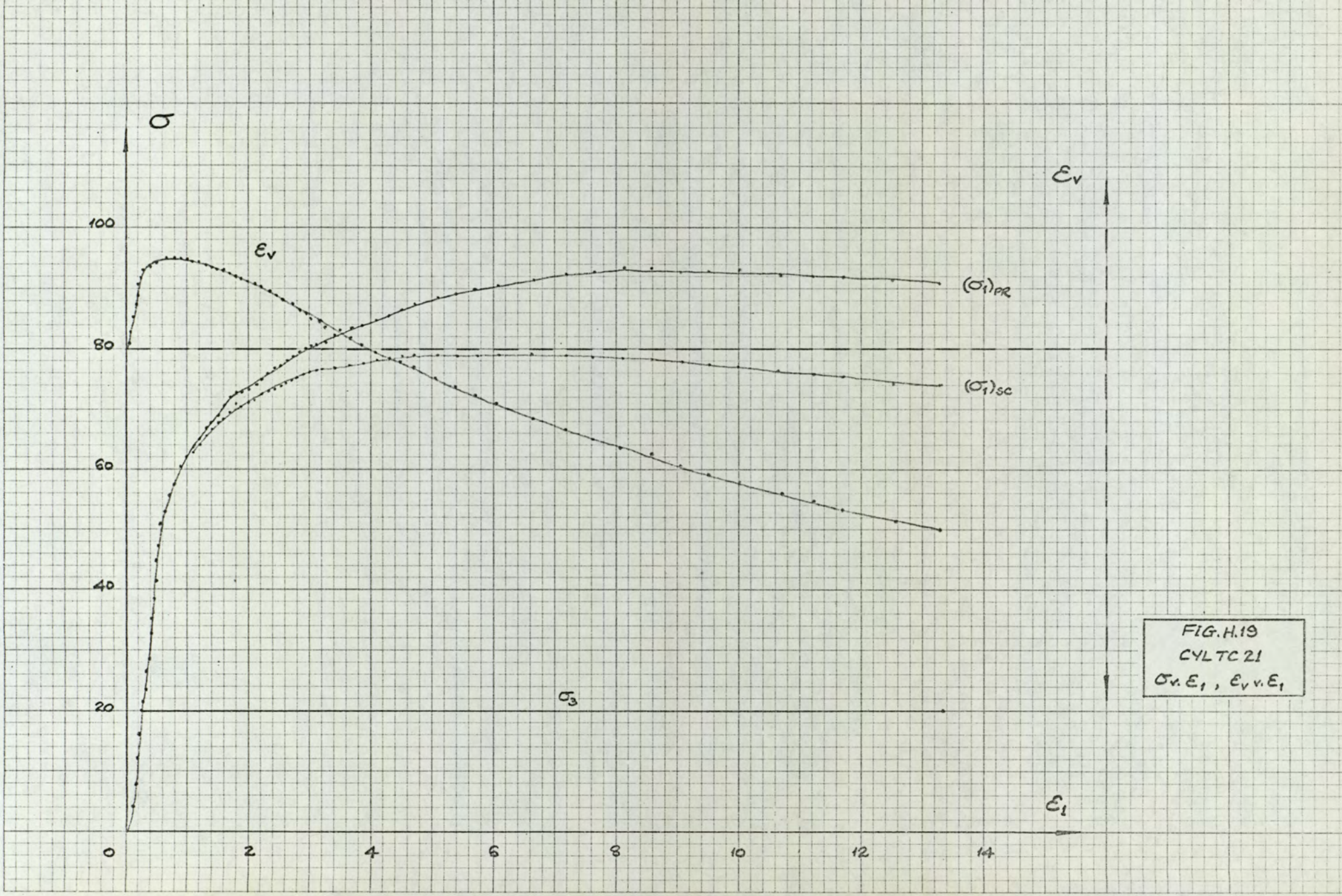

FIG. H.19
CYLTC 21
σ_v v. ε_1 , ε_v v. ε_1

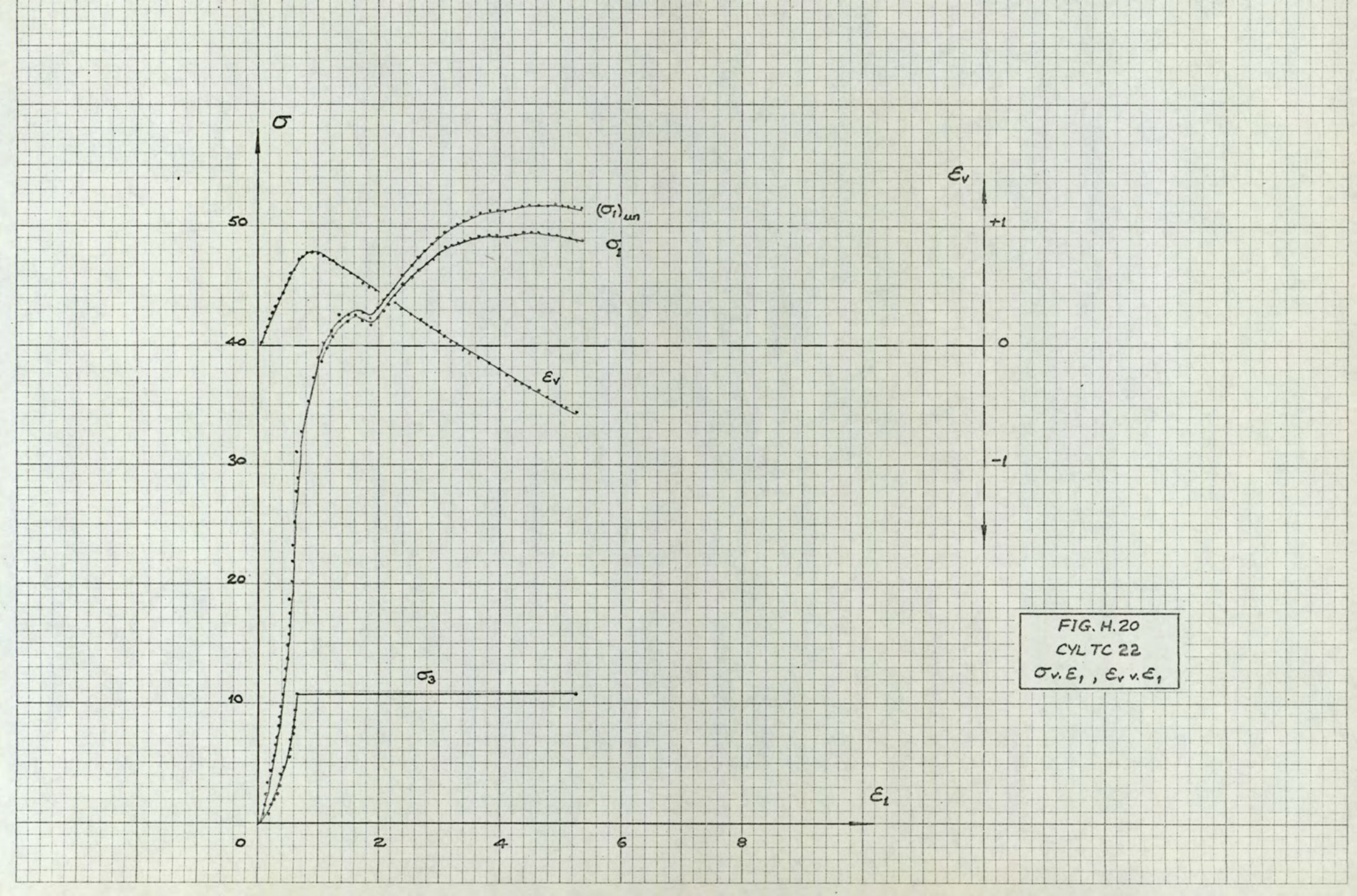

FIG. H.20
CYL TC 22
$\sigma_v . \varepsilon_1$, ε_v v. ε_1

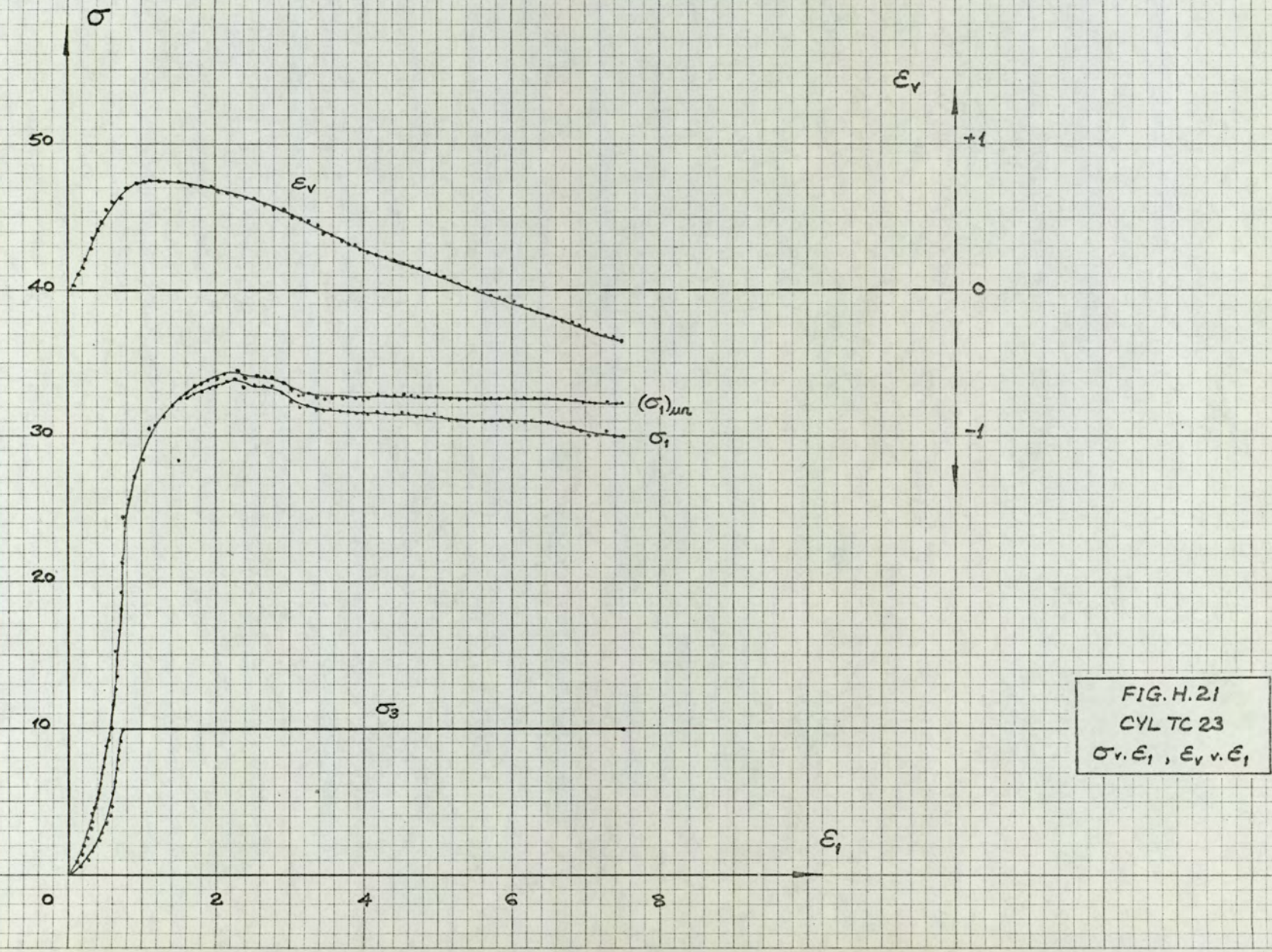

FIG. H.21
CYL TC 23
σ_v. ε_1 , ε_v v. ε_1

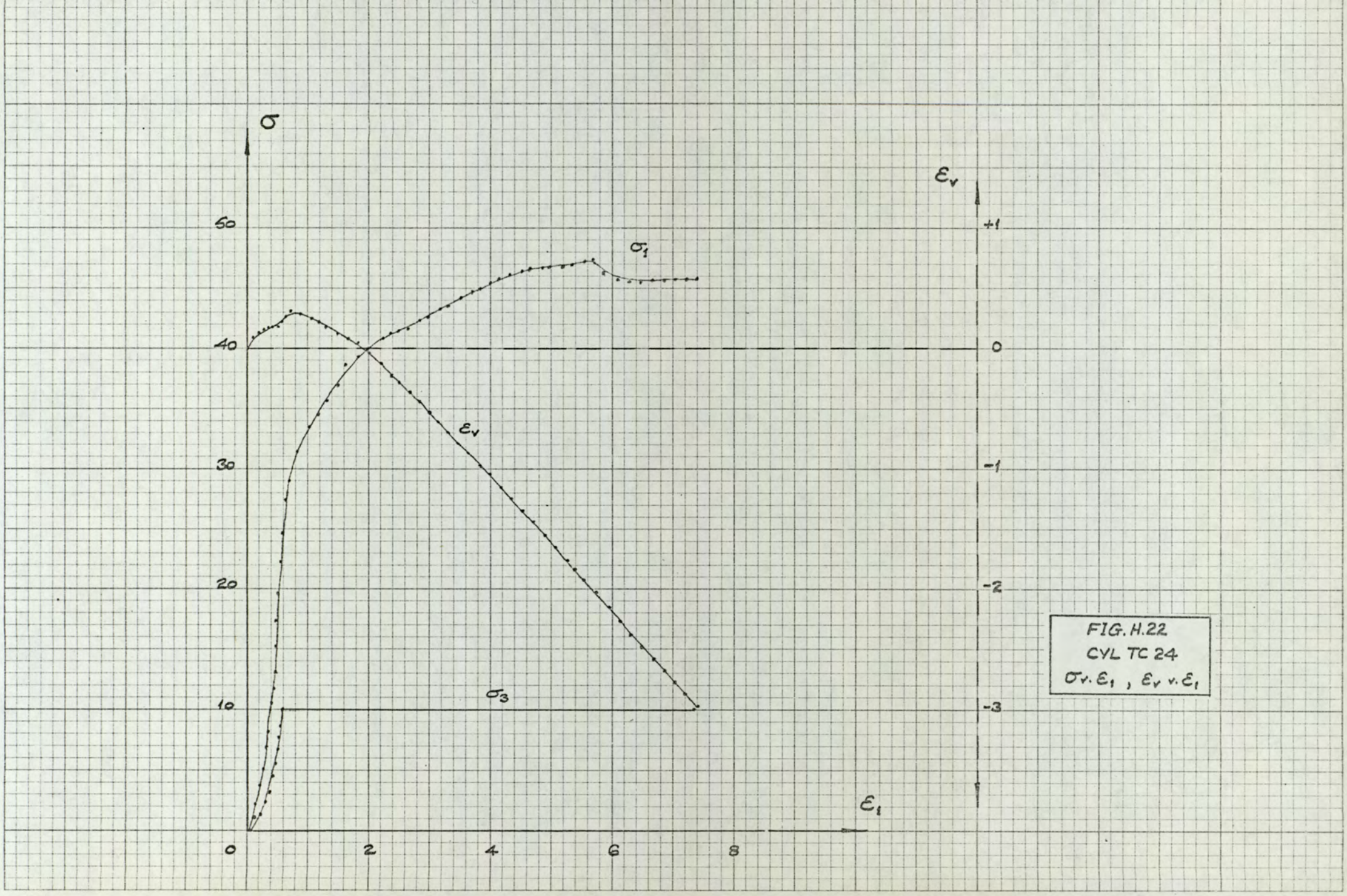

FIG. H.22
CYL TC 24
$\sigma_v . \varepsilon_1$, ε_v v. ε_1

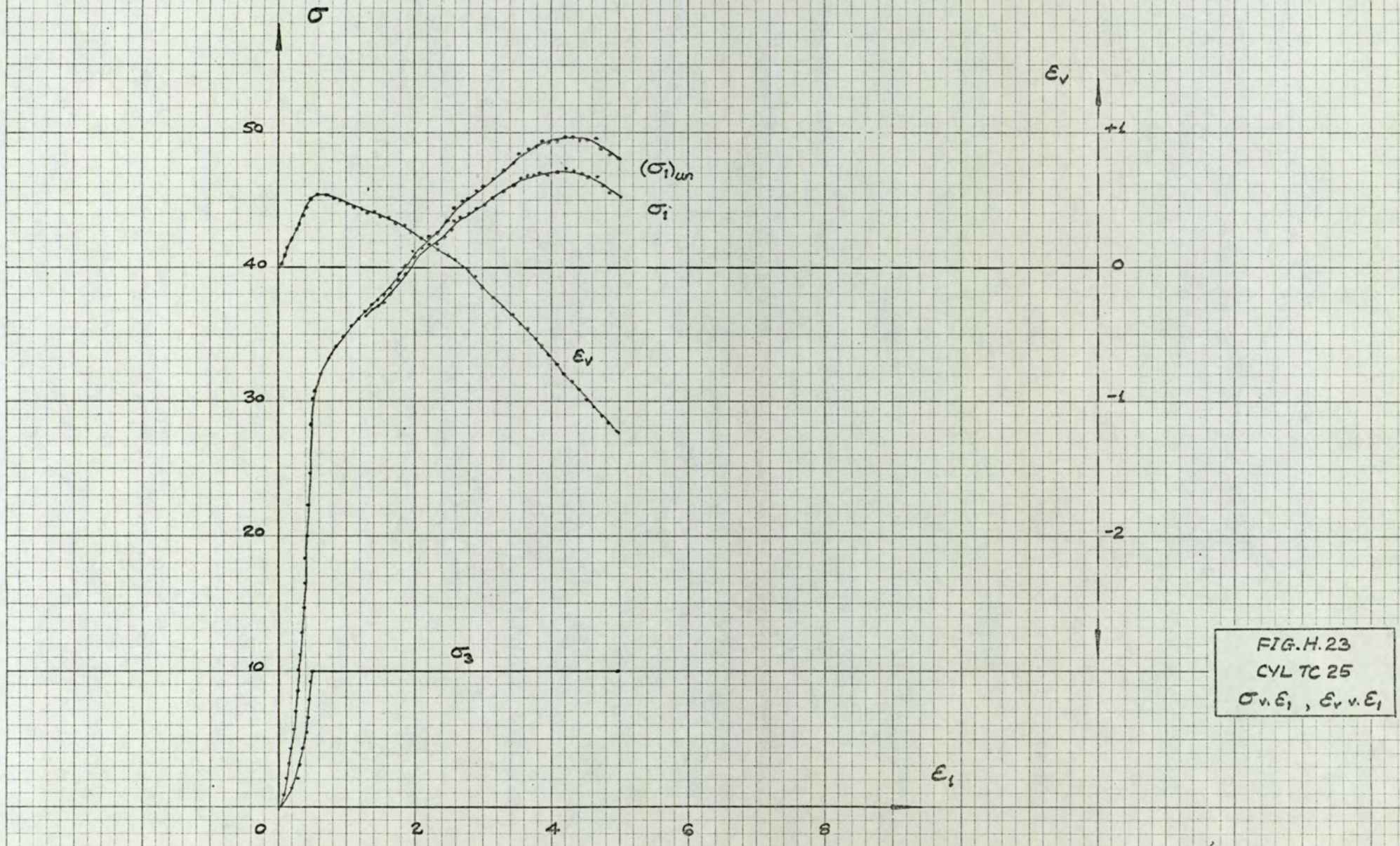

FIG. H. 23
CYL TC 25
σ_v. ε_1 , ε_v v. ε_1

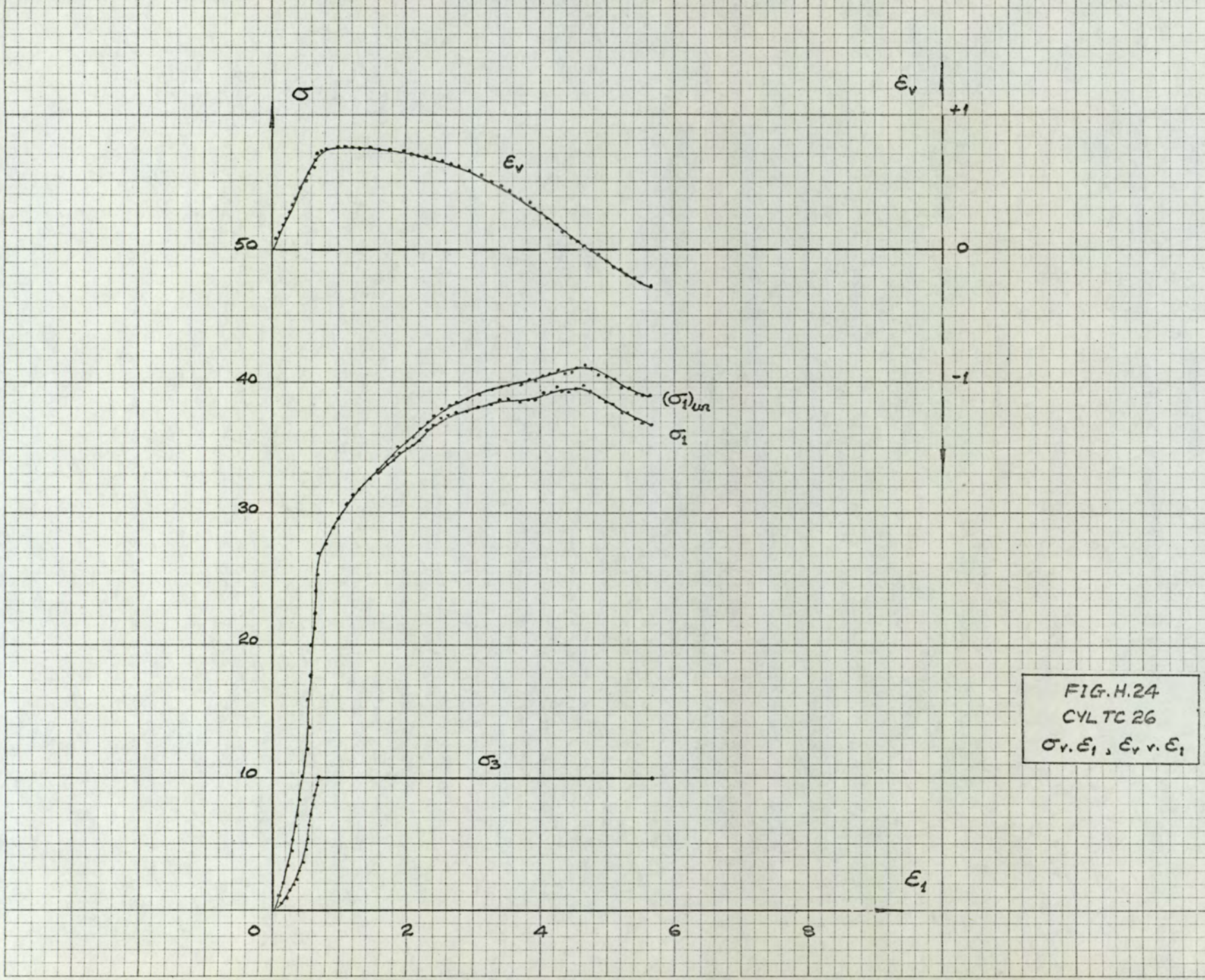

FIG. H.24
CYL TC 26
σ_v v. ε_1 , ε_v v. ε_1

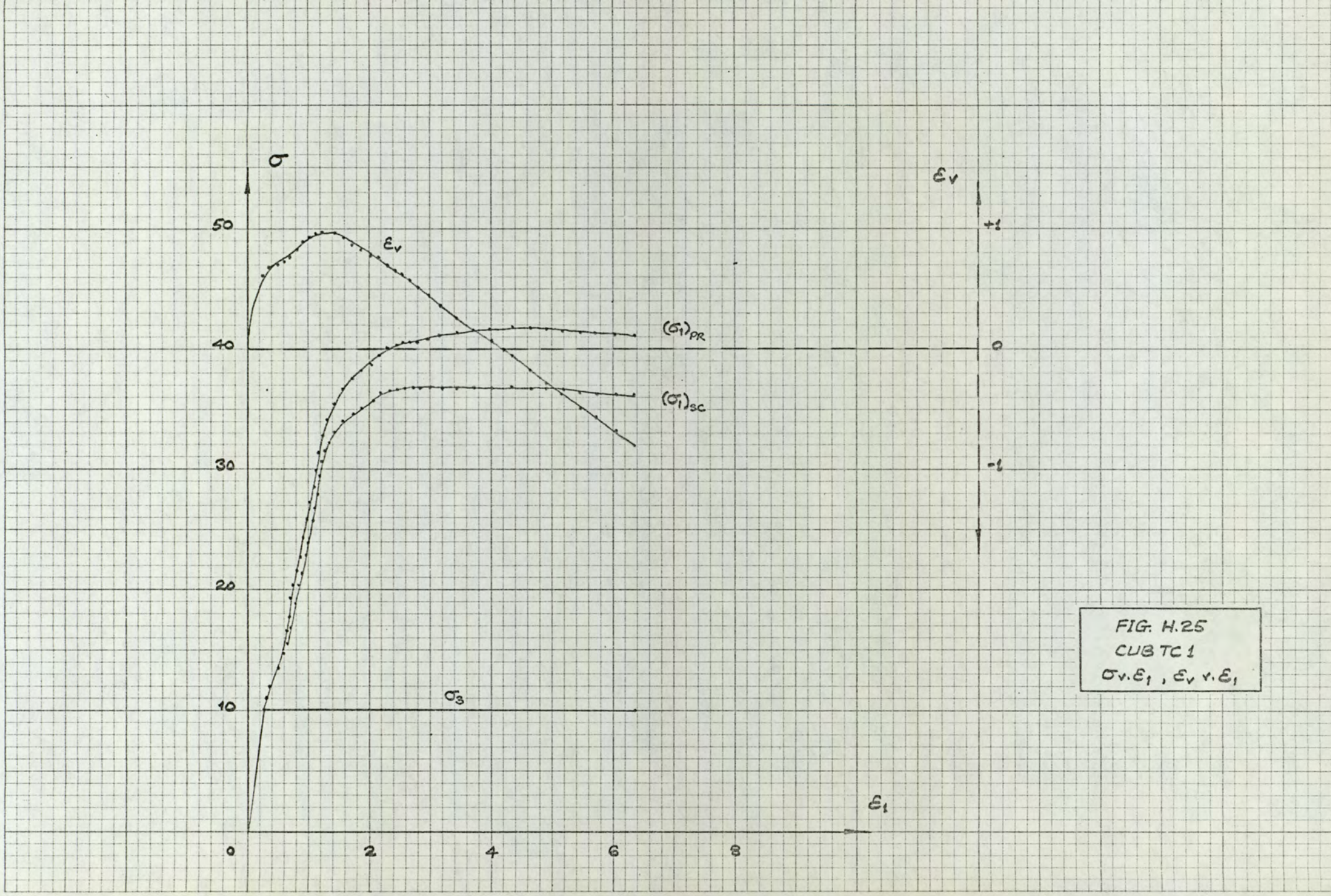

FIG. H.25
CUB TC 1
$\sigma_v . \varepsilon_1$, ε_v v. ε_1

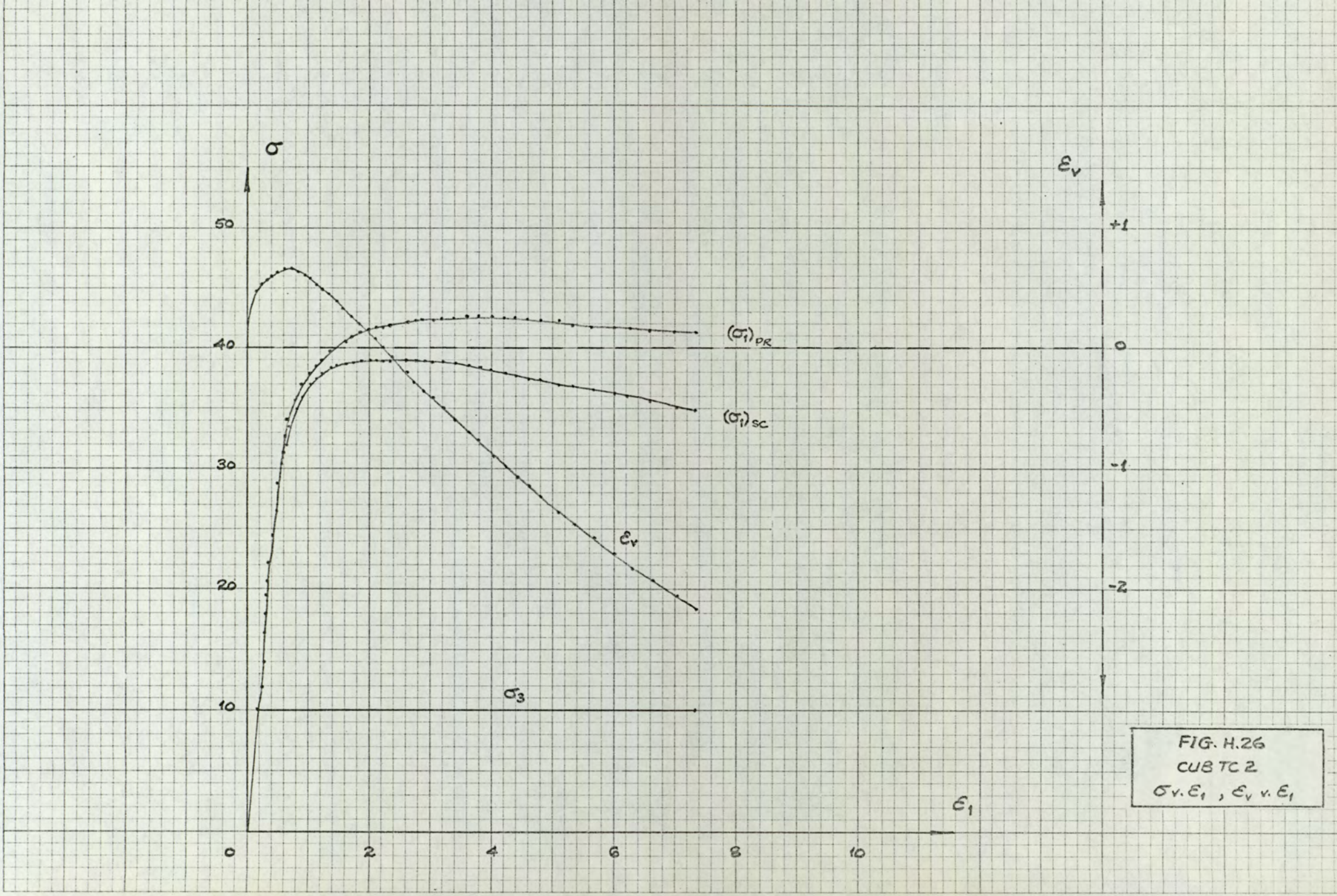

FIG. H.26
CUBTC 2
$\sigma_v . \varepsilon_1$, ε_v v. ε_1

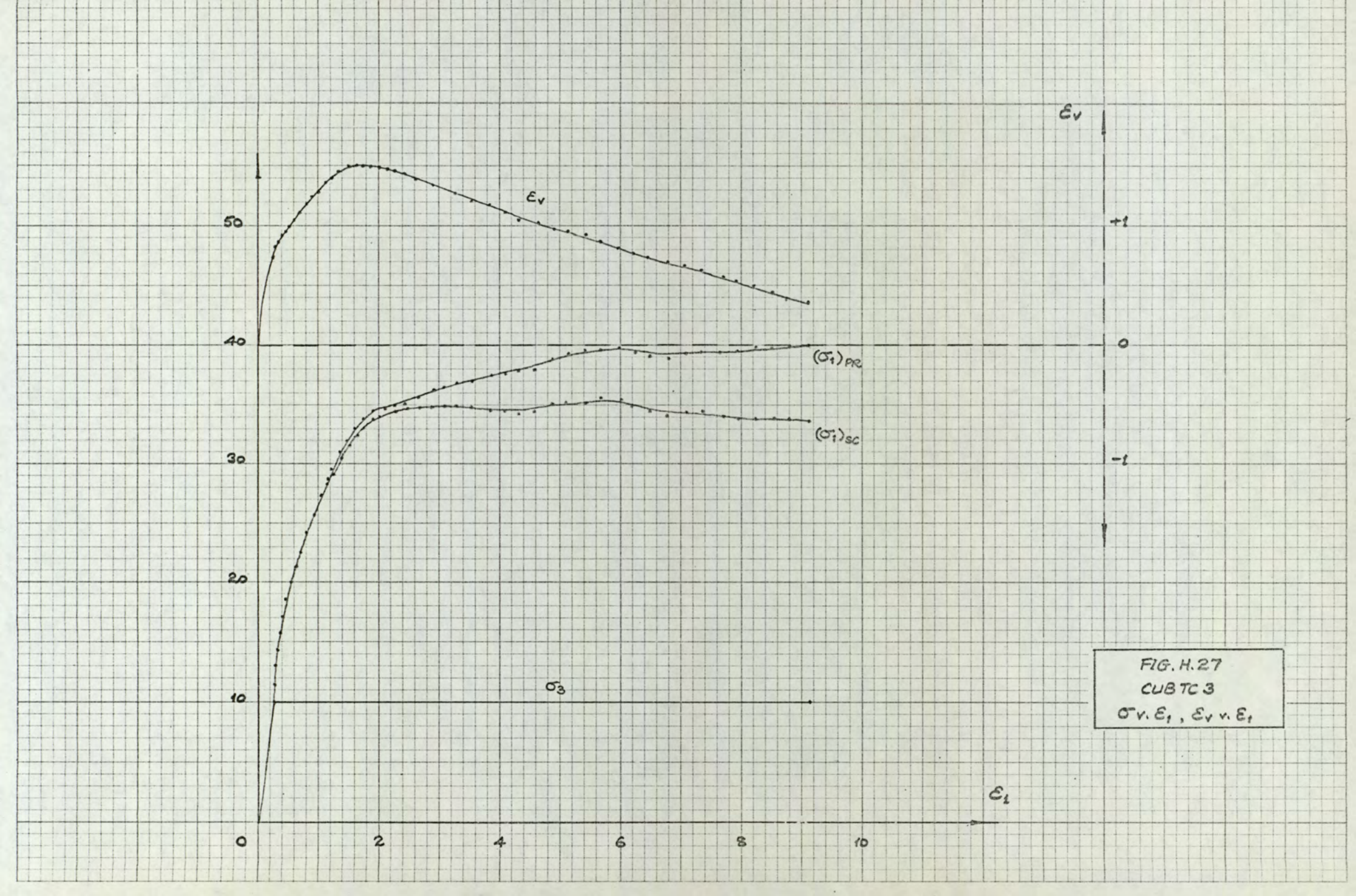

FIG. H.27
CUBTC 3
σ_v v. ε_1 , ε_v v. ε_1

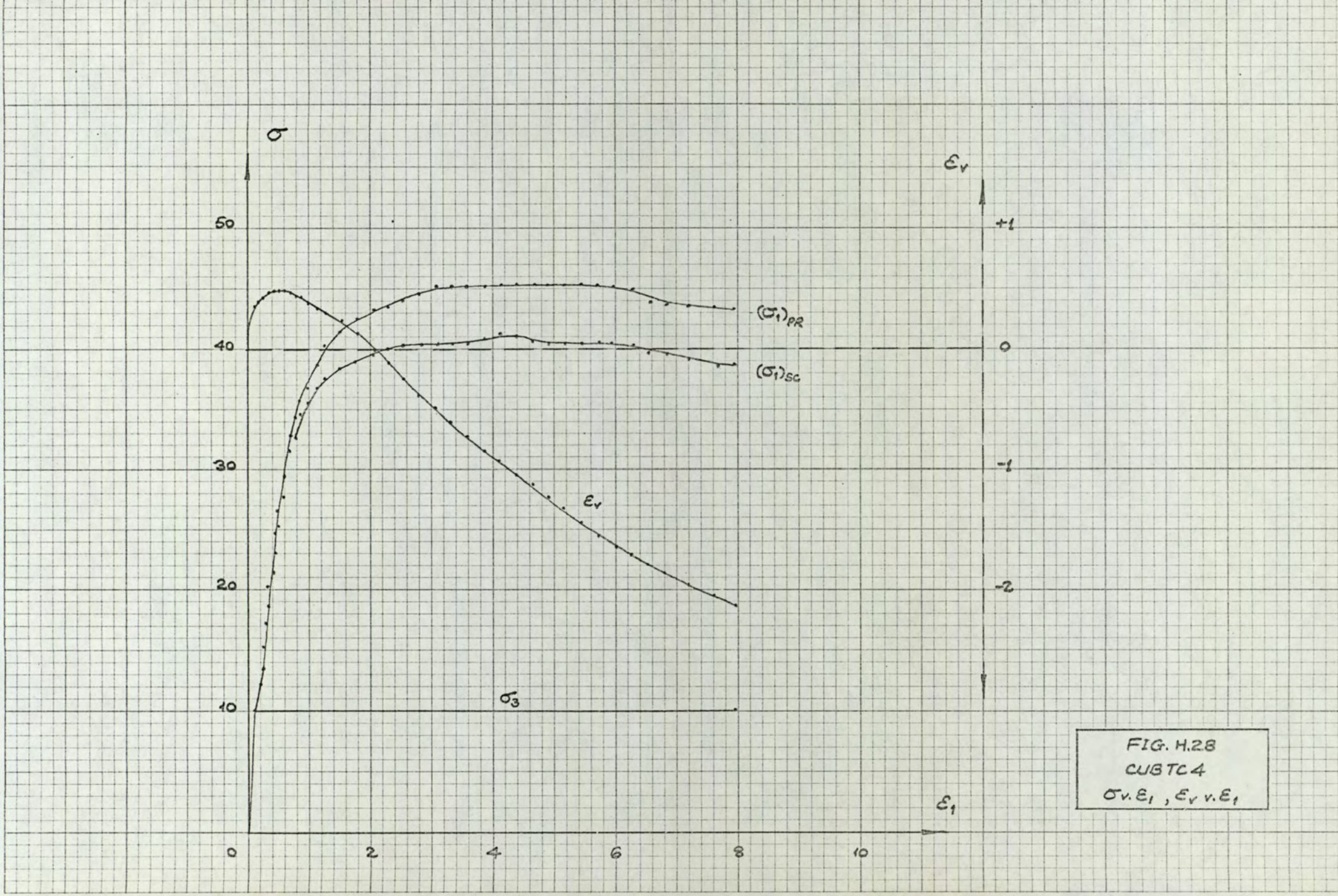

FIG. H.28
CUBTC 4
$\sigma_v . \varepsilon_1$, ε_v v. ε_1

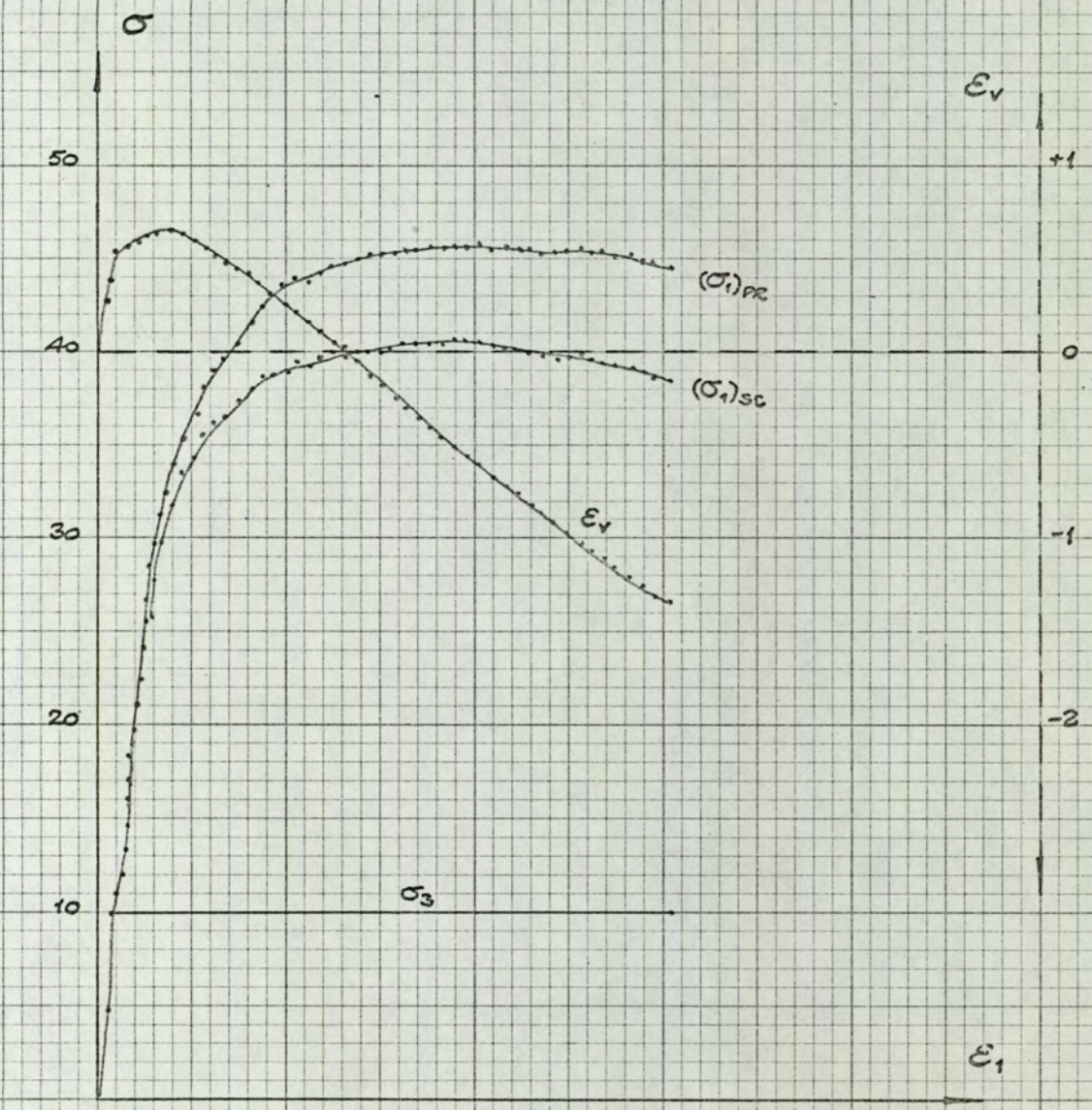

FIG. H.29
CUB TC 5
σ_v. ε_1 , ε_v v. ε_1

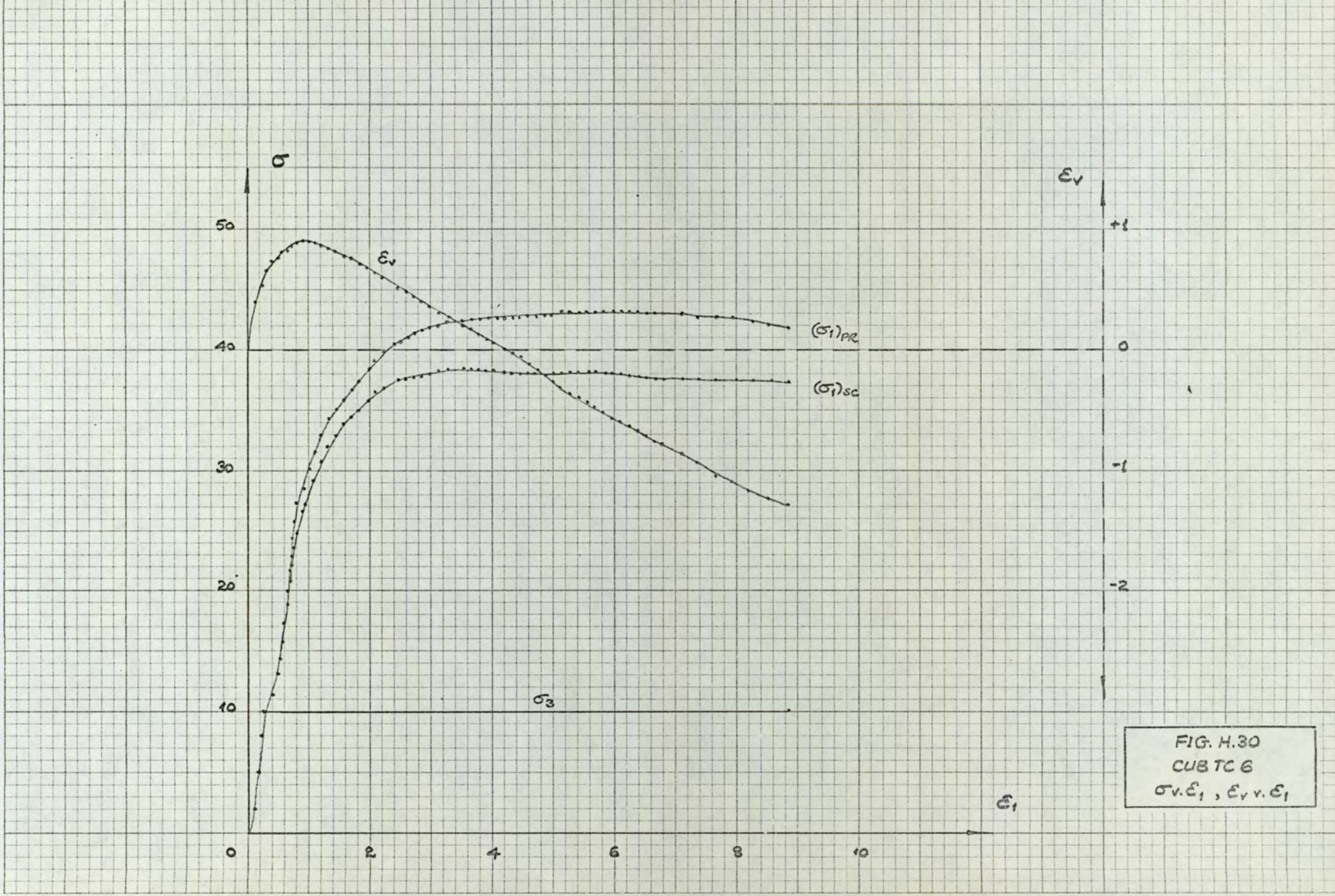

FIG. H.30
CUB TC 6
$\sigma_v . \varepsilon_1$, ε_v v. ε_1

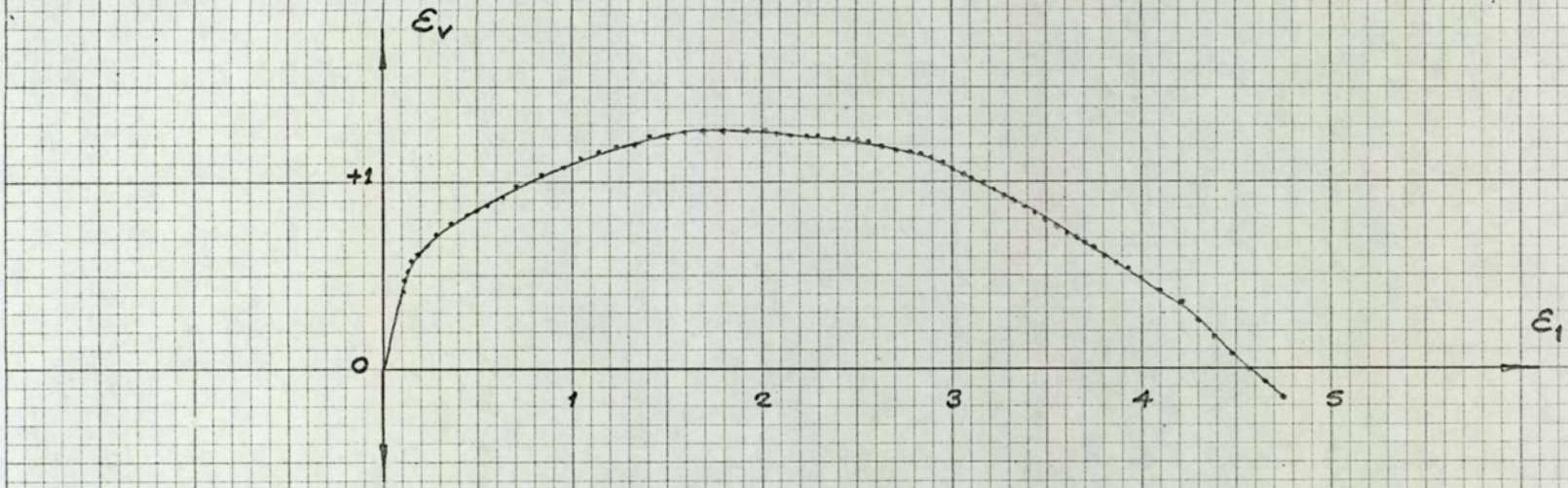

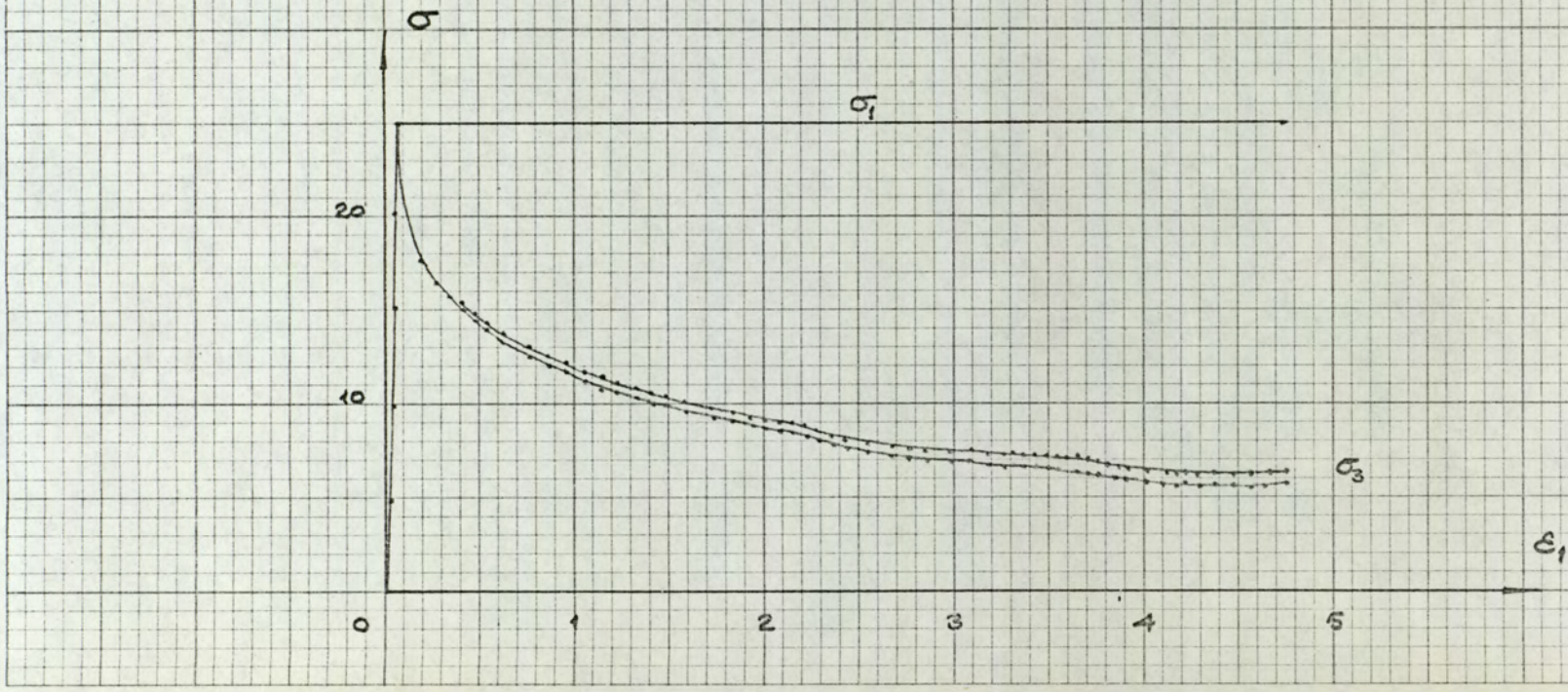

FIG. H.31
CYL TE 1
$\sigma_v . \varepsilon_1$, $\varepsilon_v v . \varepsilon_1$

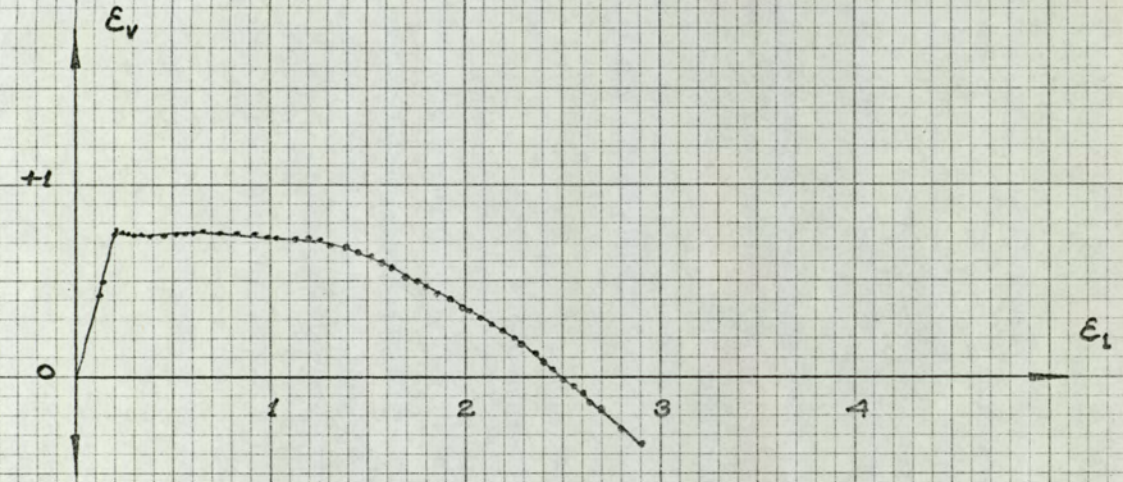

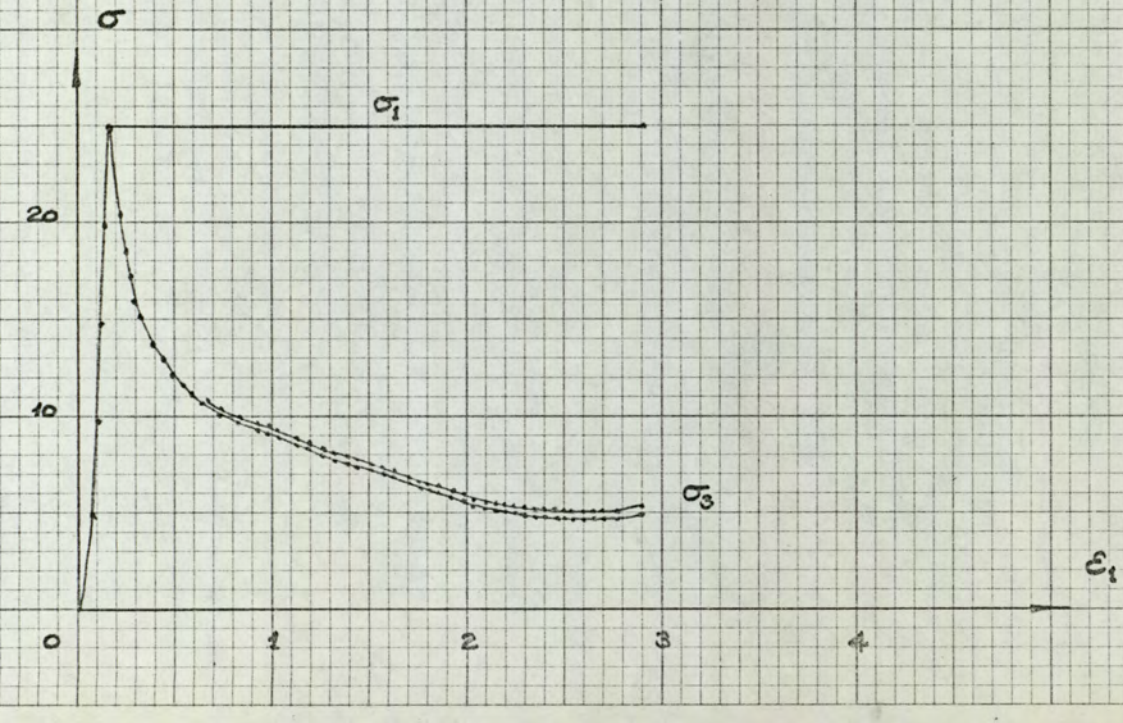

FIG. H.32
CYLTE 2
σ v. ε_1 , ε_v v. ε_1

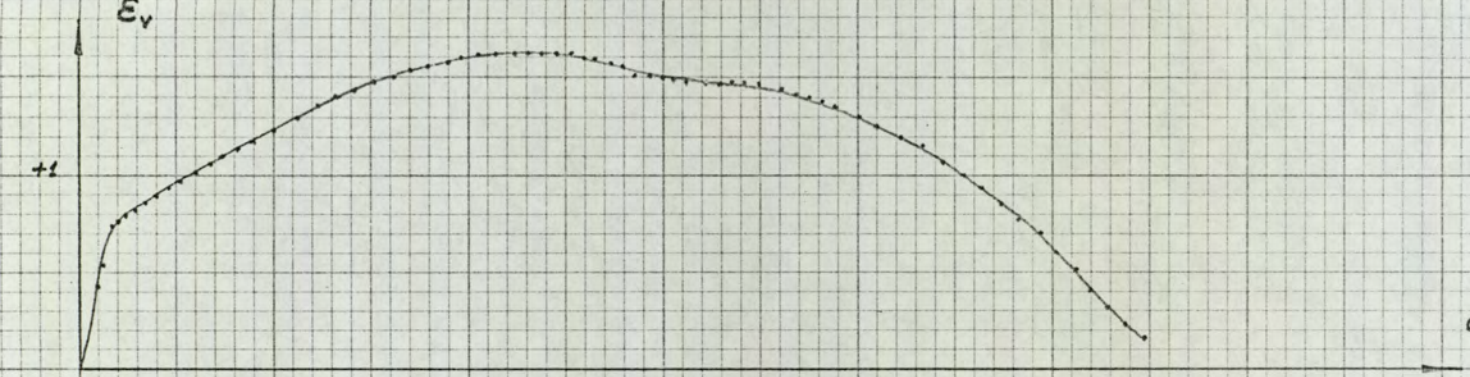

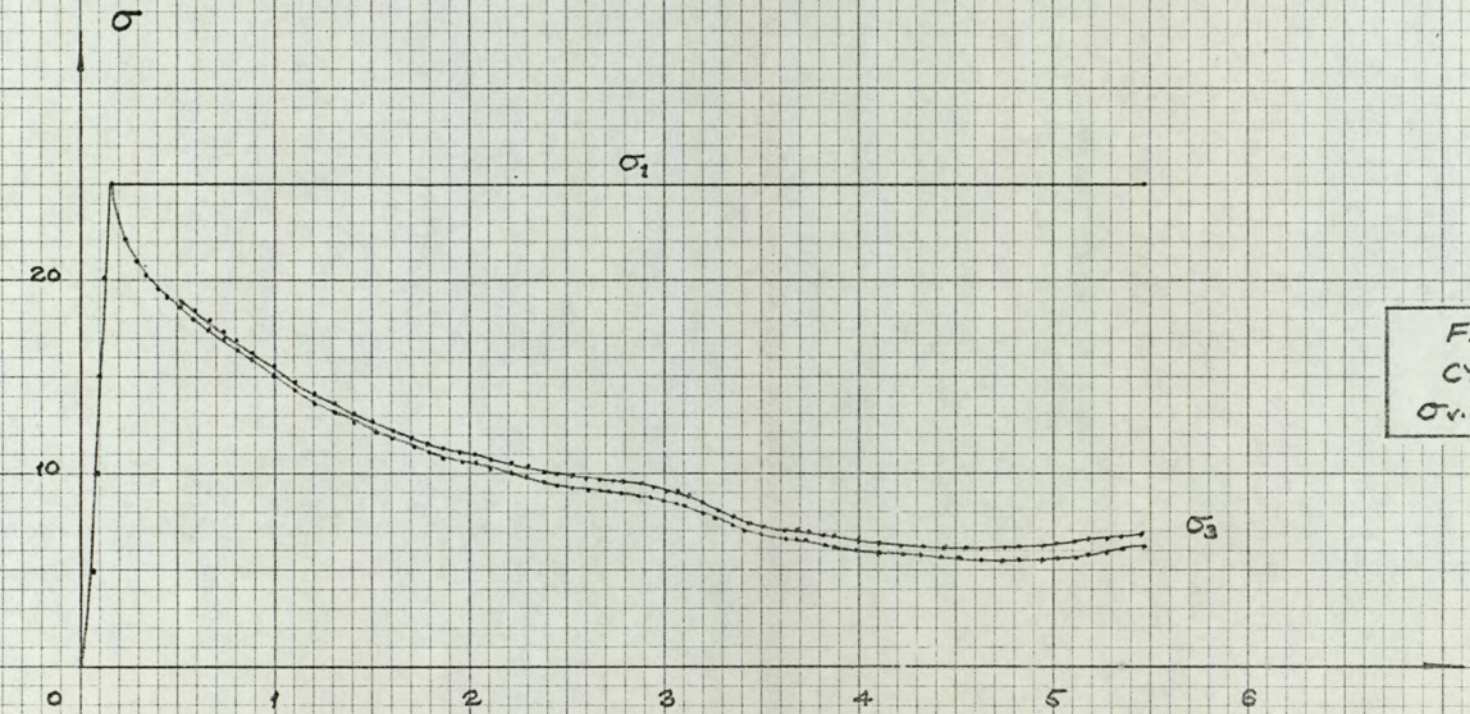

FIG.H.33
CYL TE 3
$\sigma_v . \varepsilon_1$, ε_v v. ε_1

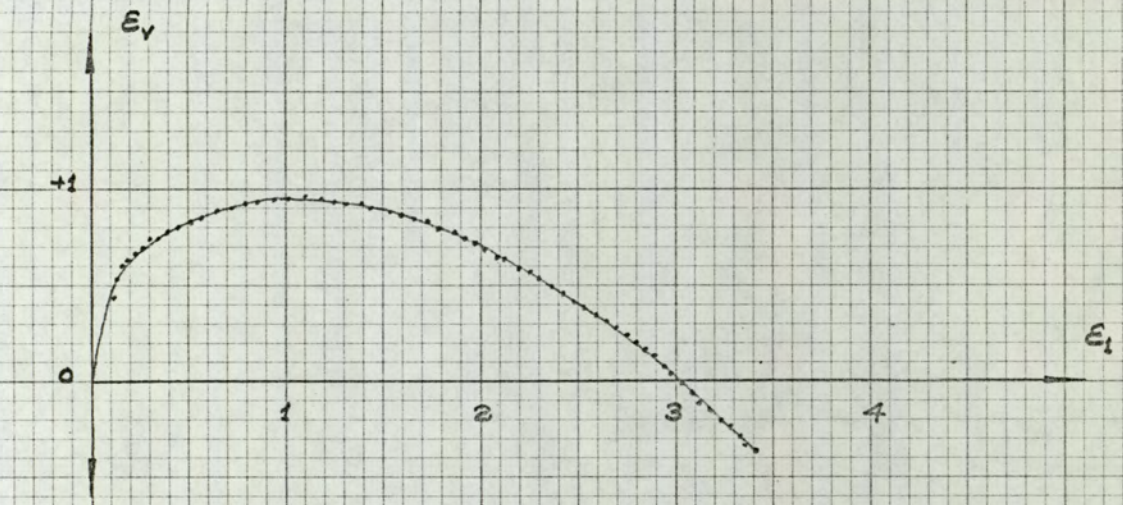

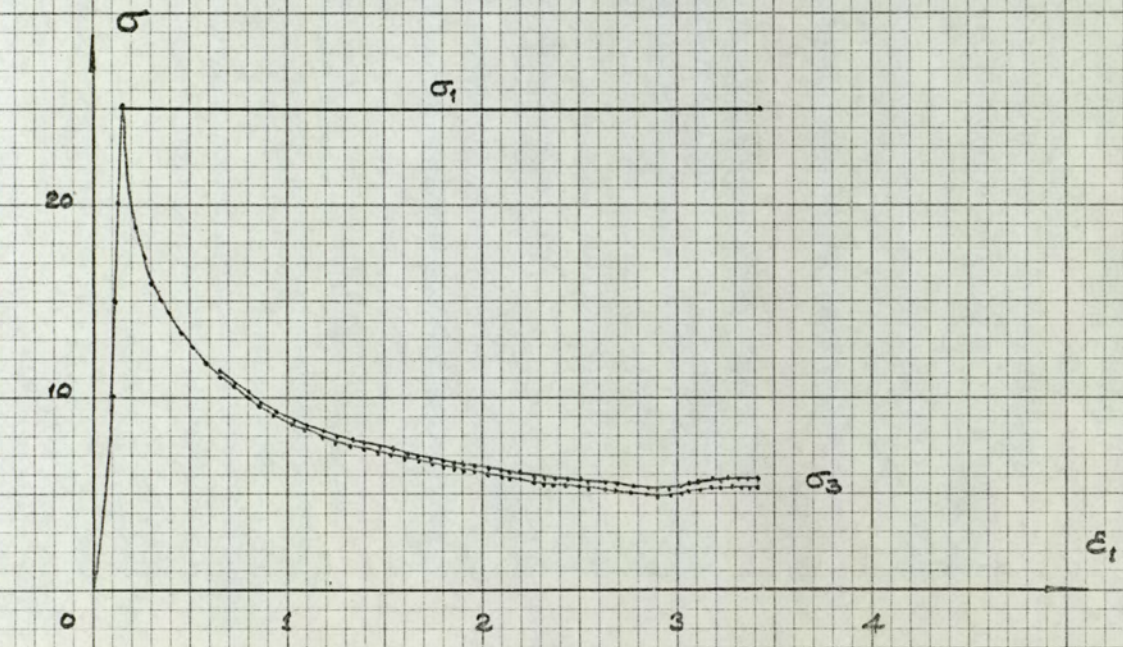

FIG. H. 34
CYL TE 4
σ v. ε_1 , ε_v v. ε_1

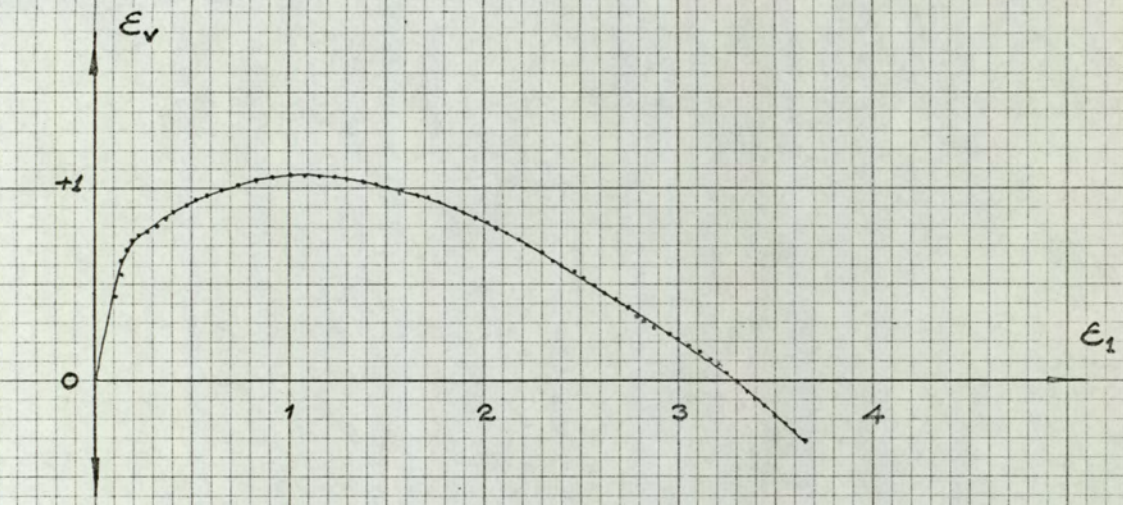

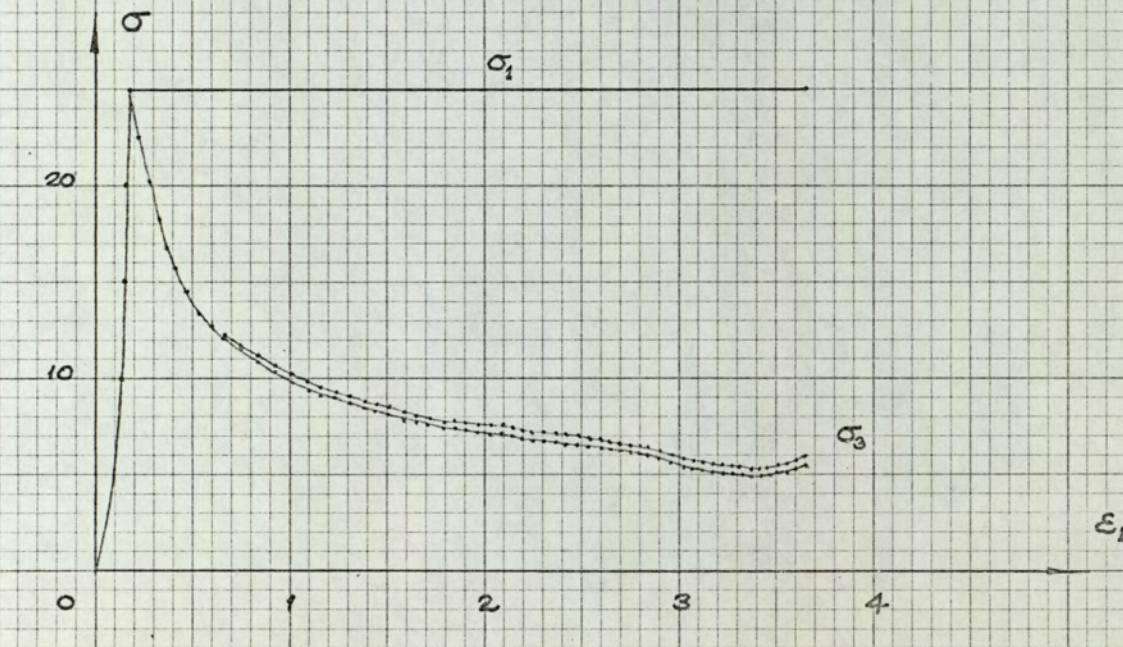

FIG. H.35
CYLTE 5
σ v. ε_1 , ε_v v. ε_1

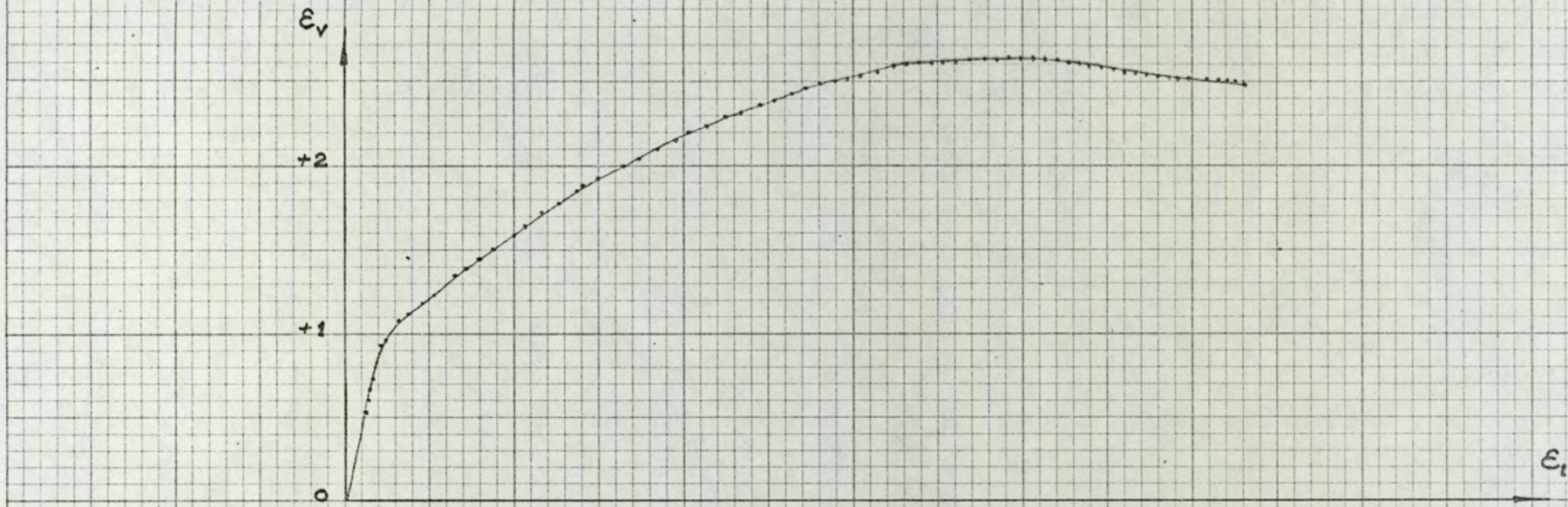

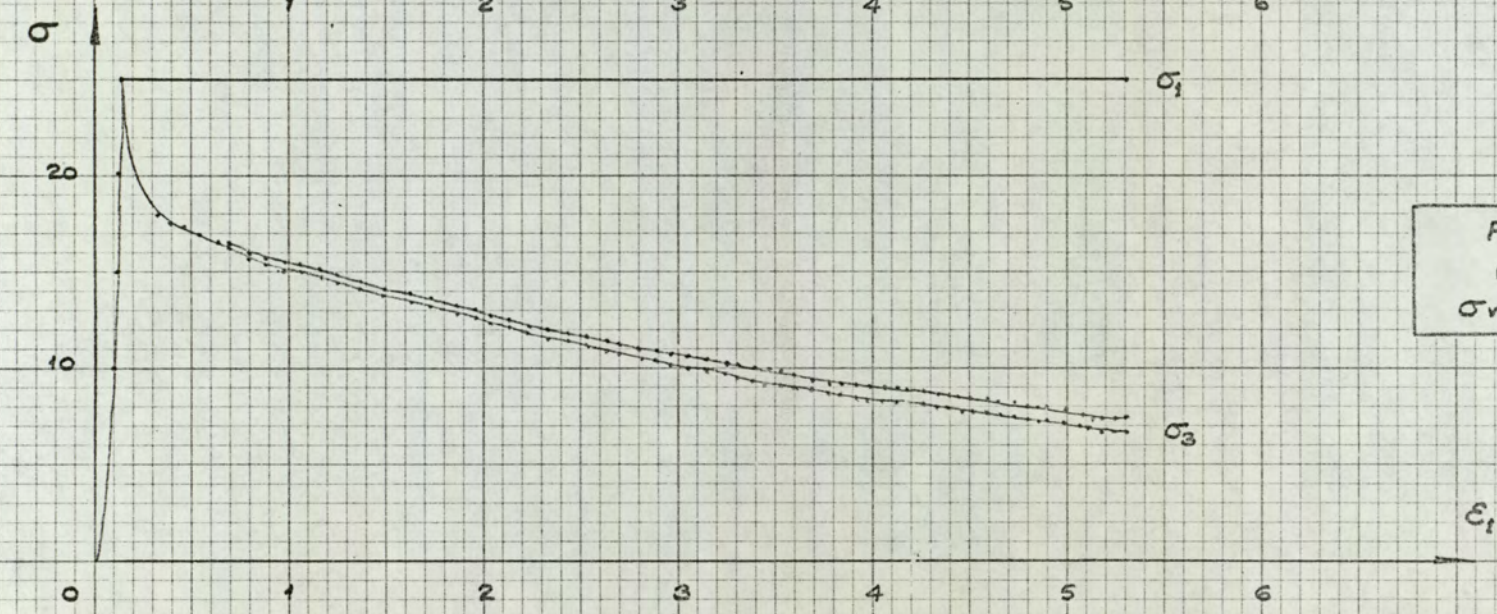

FIG. H.36
CYLTE 6
σ_r v. ε_1 , ε_v v. ε_1

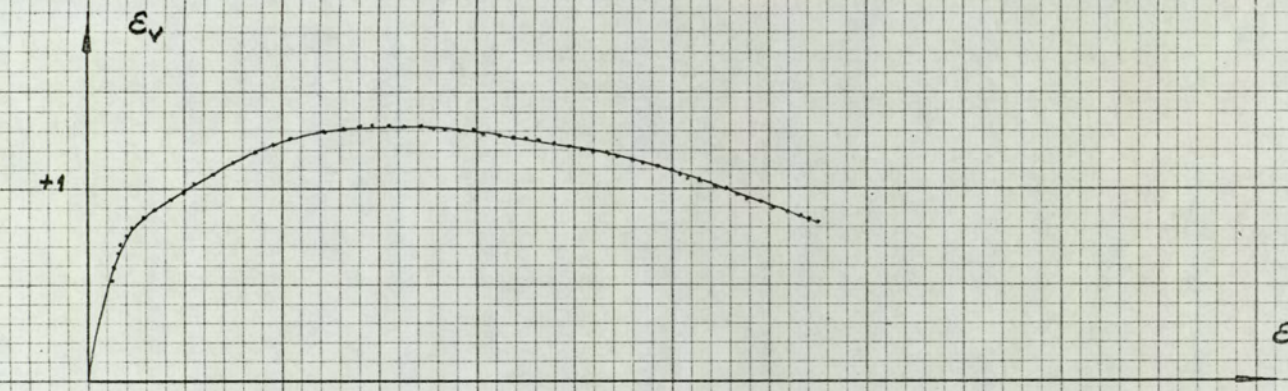

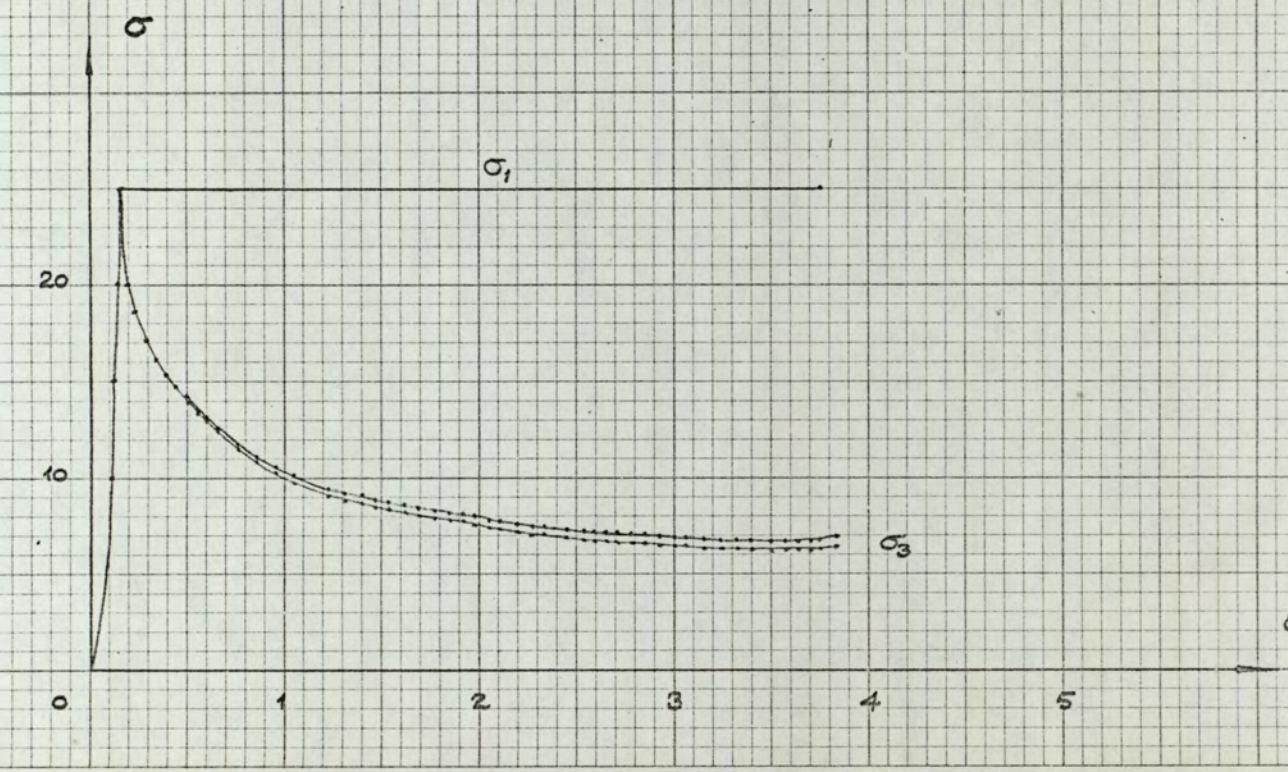

FIG. H.37
CYLTE 7
$\sigma_v . \varepsilon_1$, ε_v v. ε_1

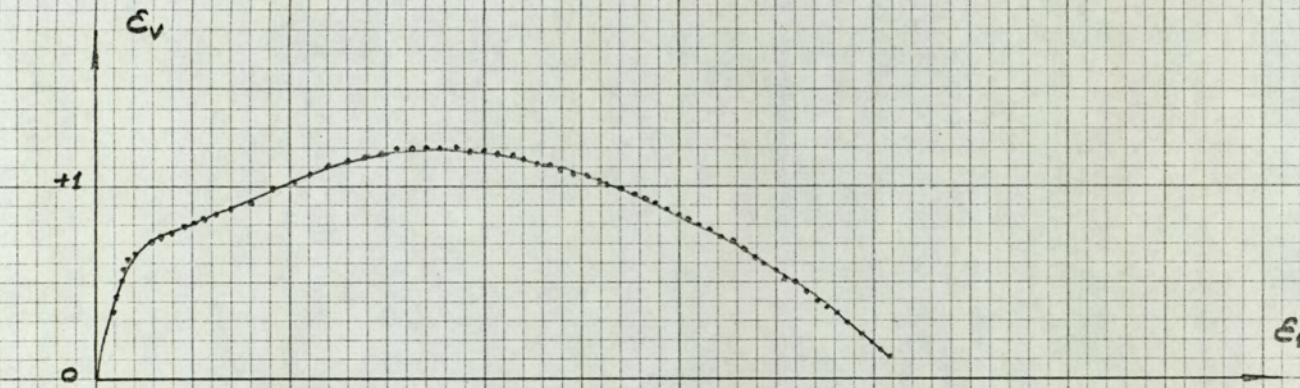

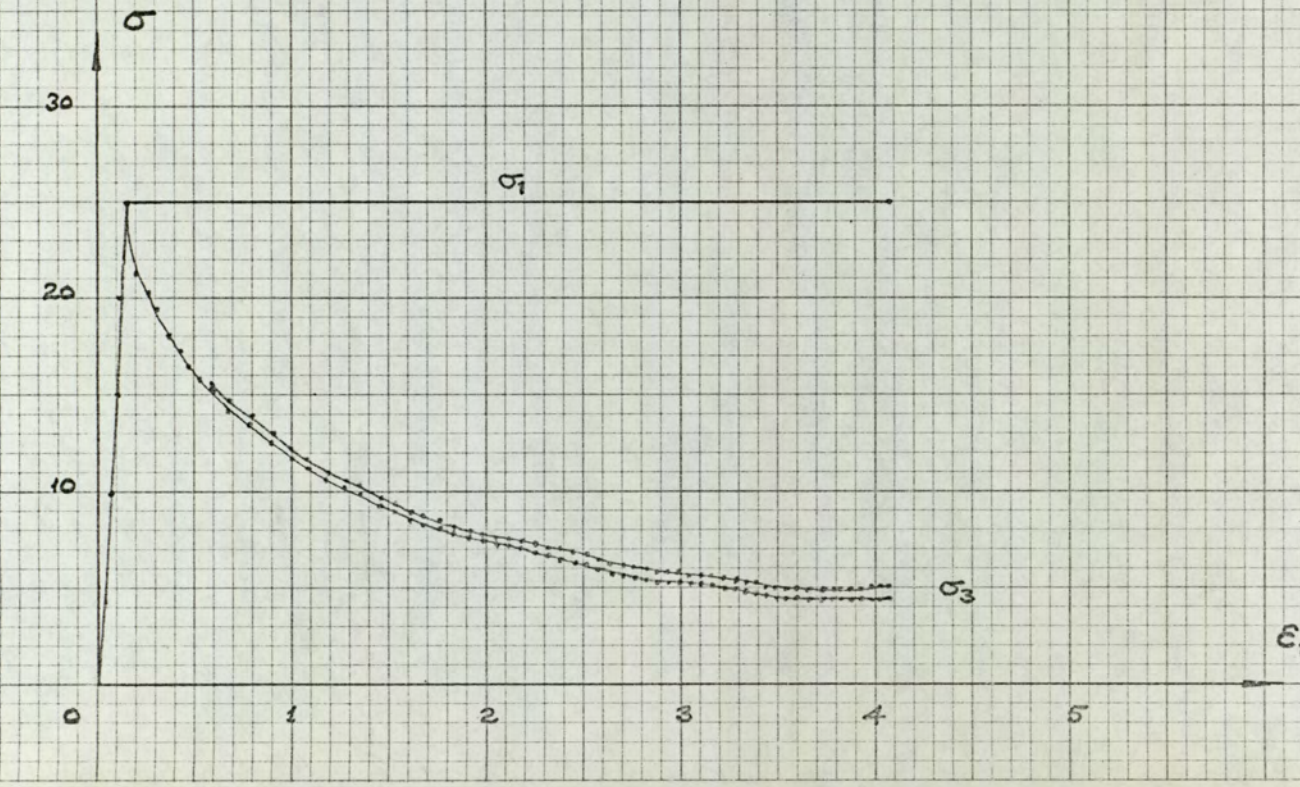

FIG. H.38
CYL TE 8
σ_1 v. ε_1 , ε_v v. ε_1

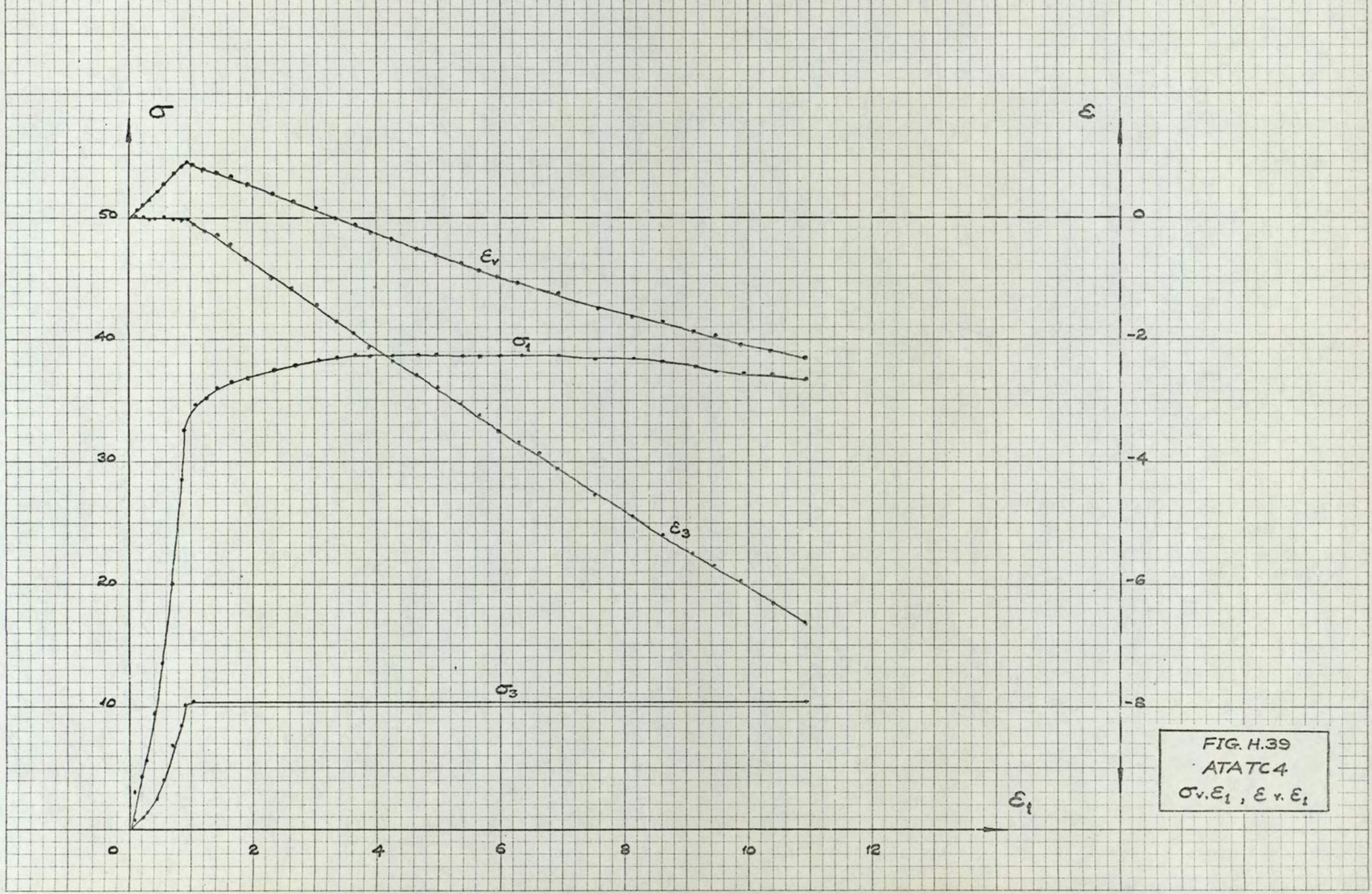

FIG. H.39
ATATC4
$\sigma_v . \varepsilon_1$, $\varepsilon_v . \varepsilon_1$

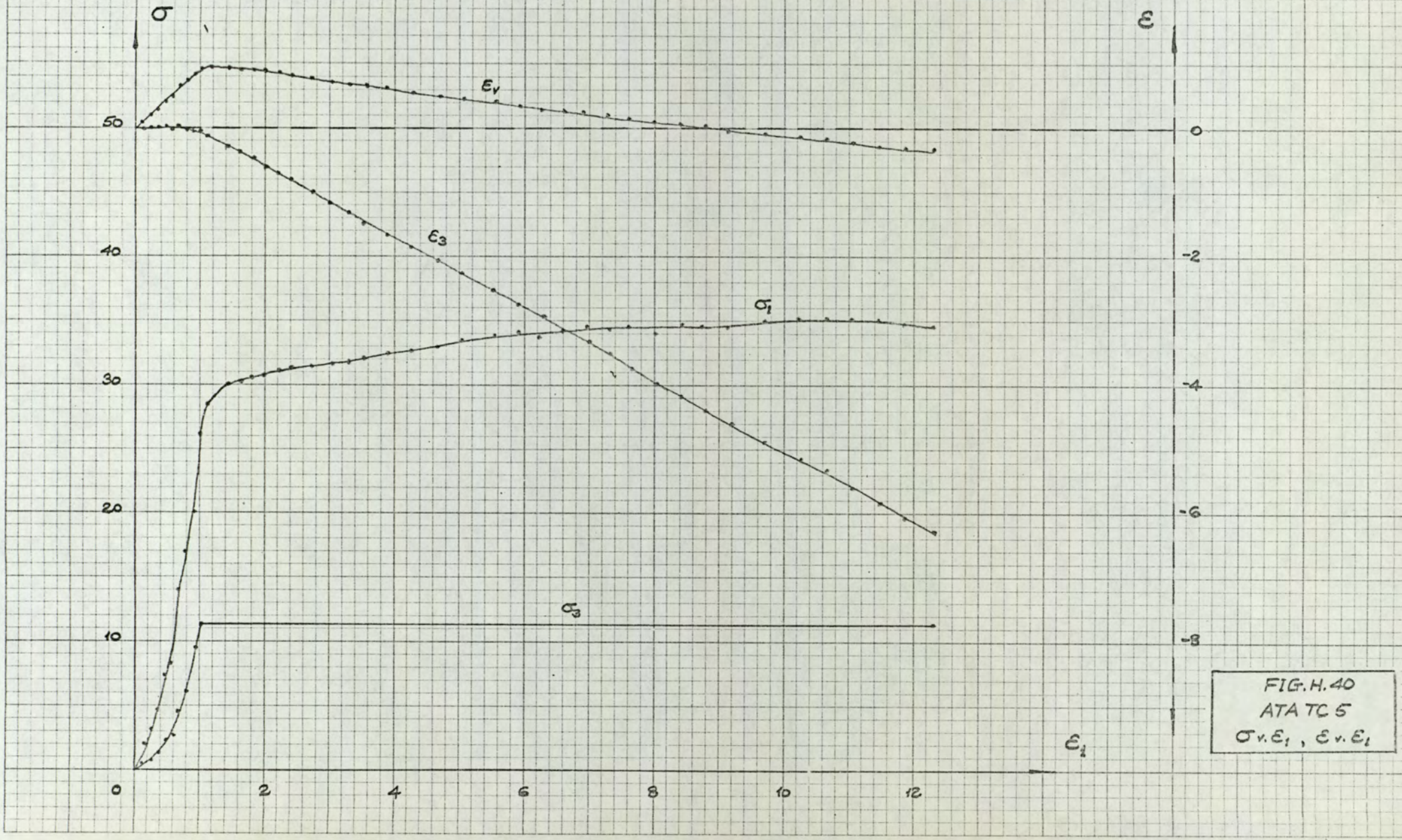

FIG. H. 40
ATA TC 5
σ v. ε_1 , ε v. ε_1

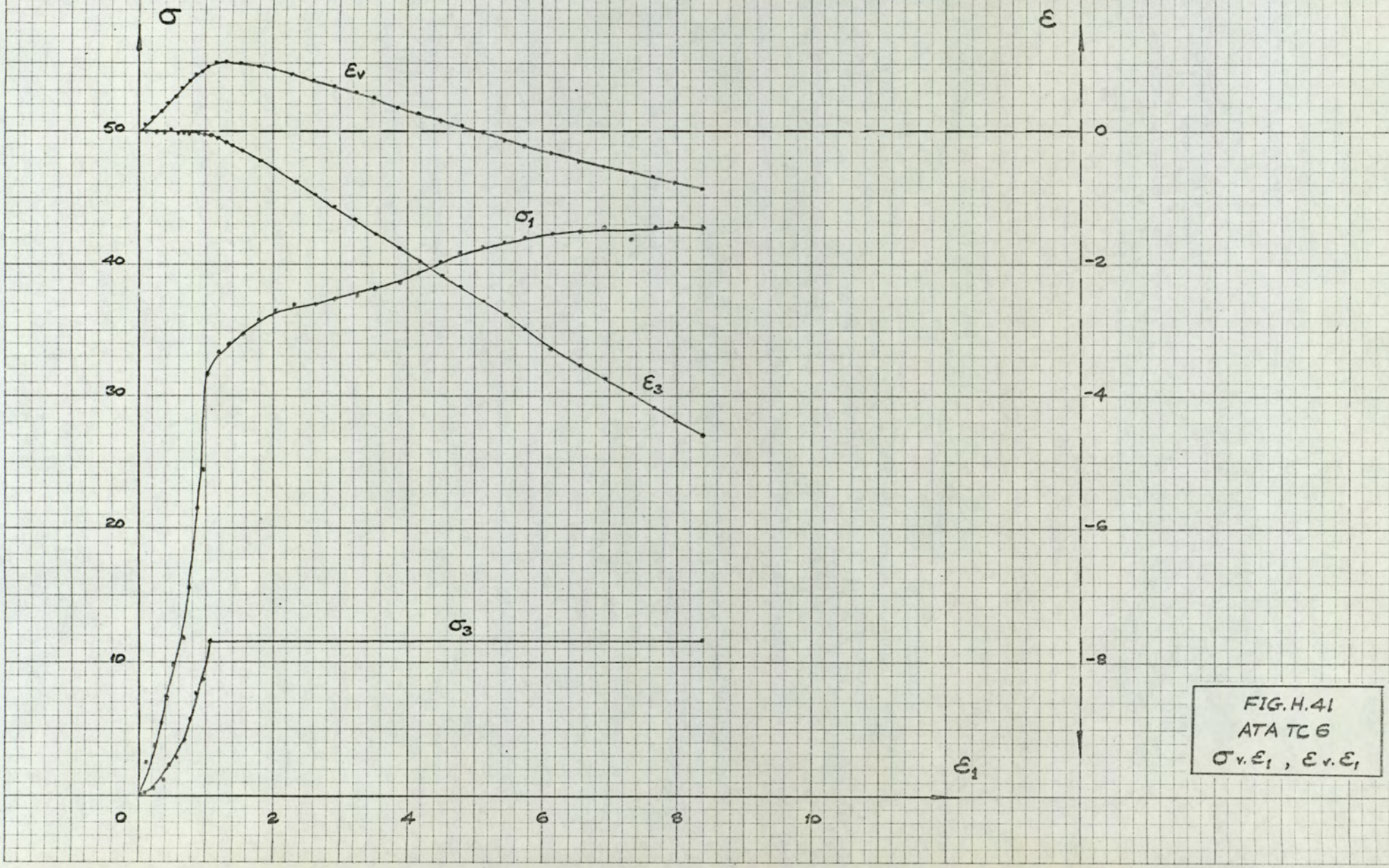

FIG. H.41
ATA TC 6
σ v. ε_1 , ε v. ε_1

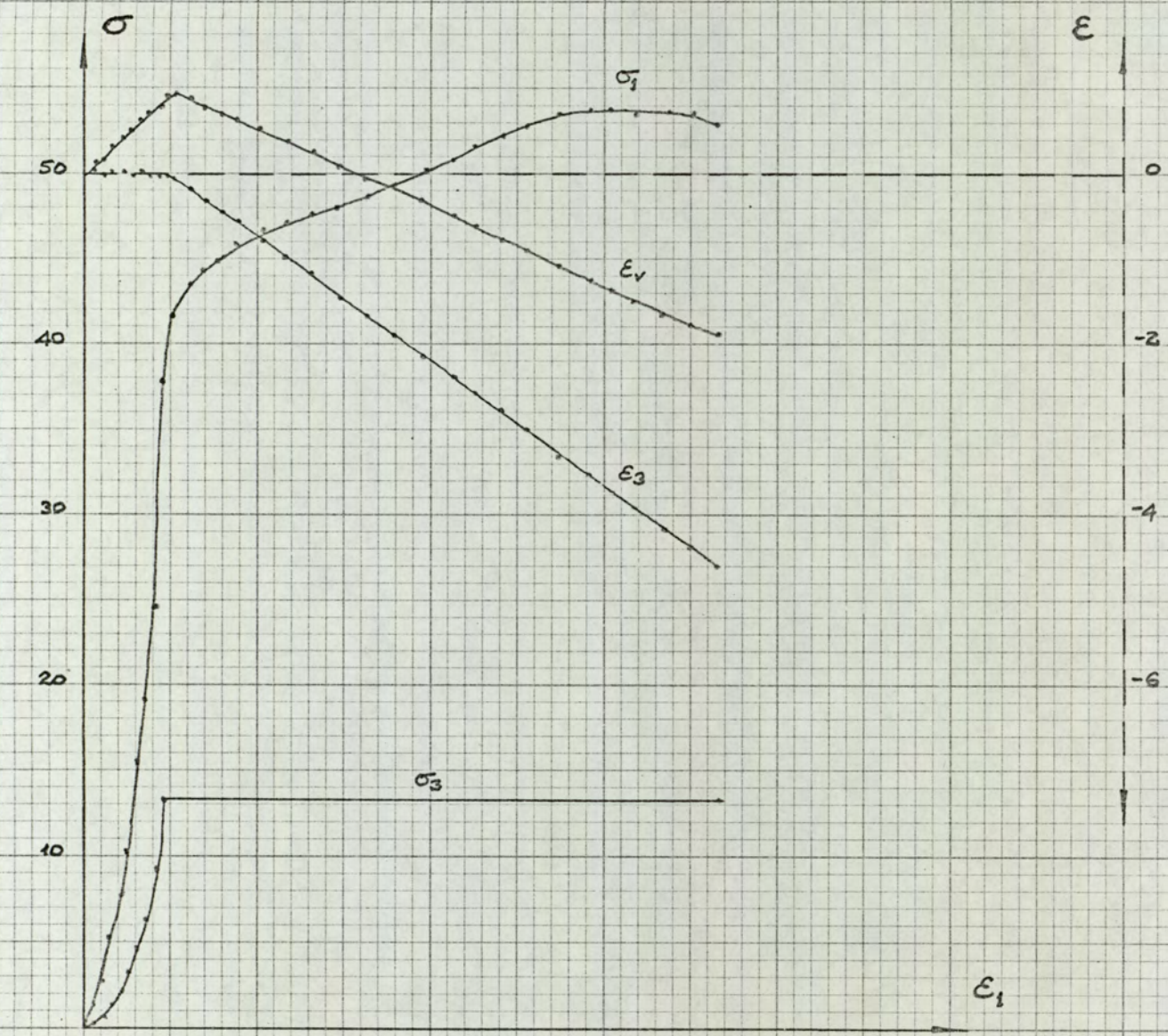

FIG. H.42
ATA TC 9
$\sigma_v . \varepsilon_1$, $\varepsilon_v . \varepsilon_1$

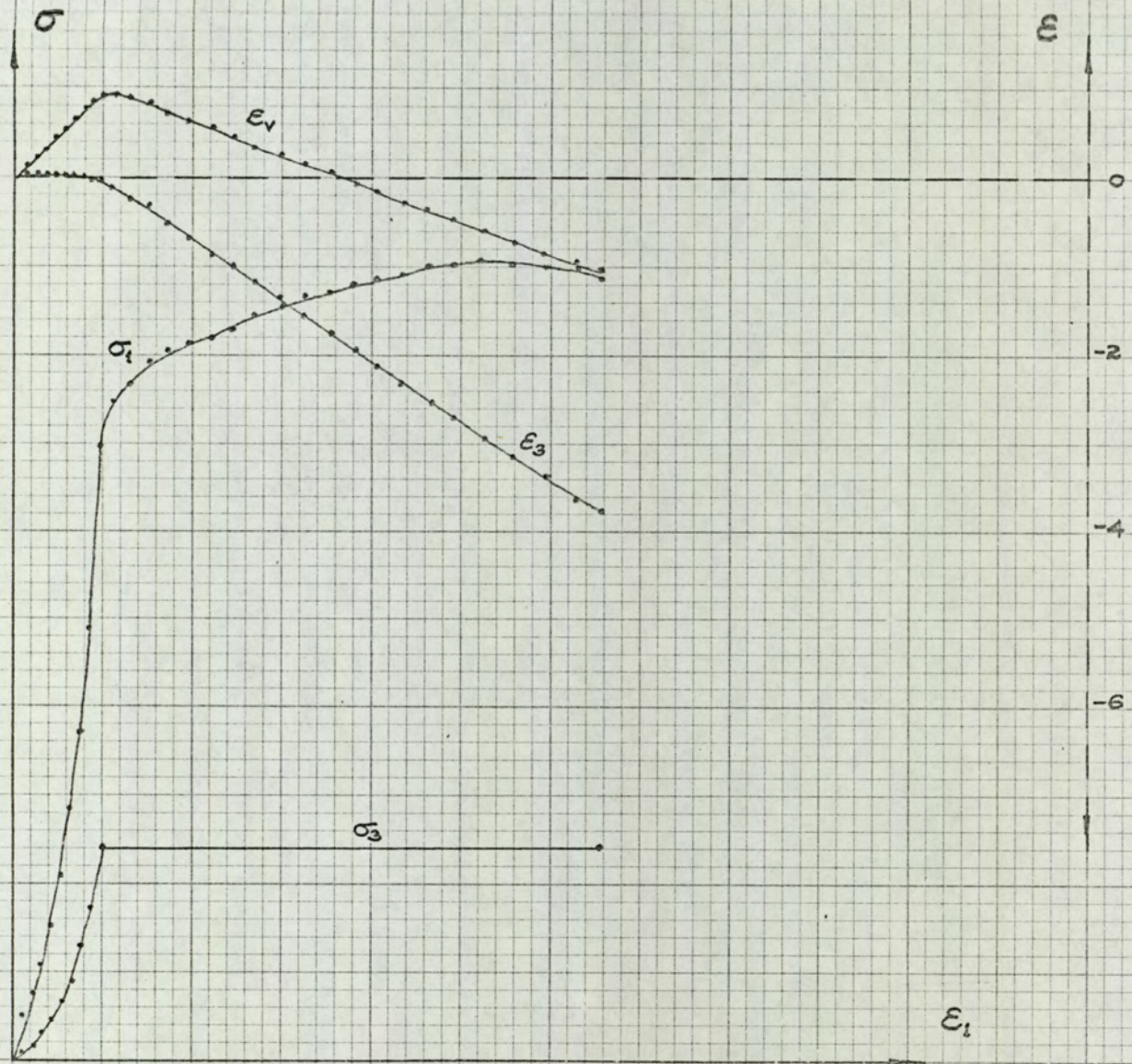

FIG. H.43
ATA TC 10
σ v. ε_1 , ε_v v. ε_1

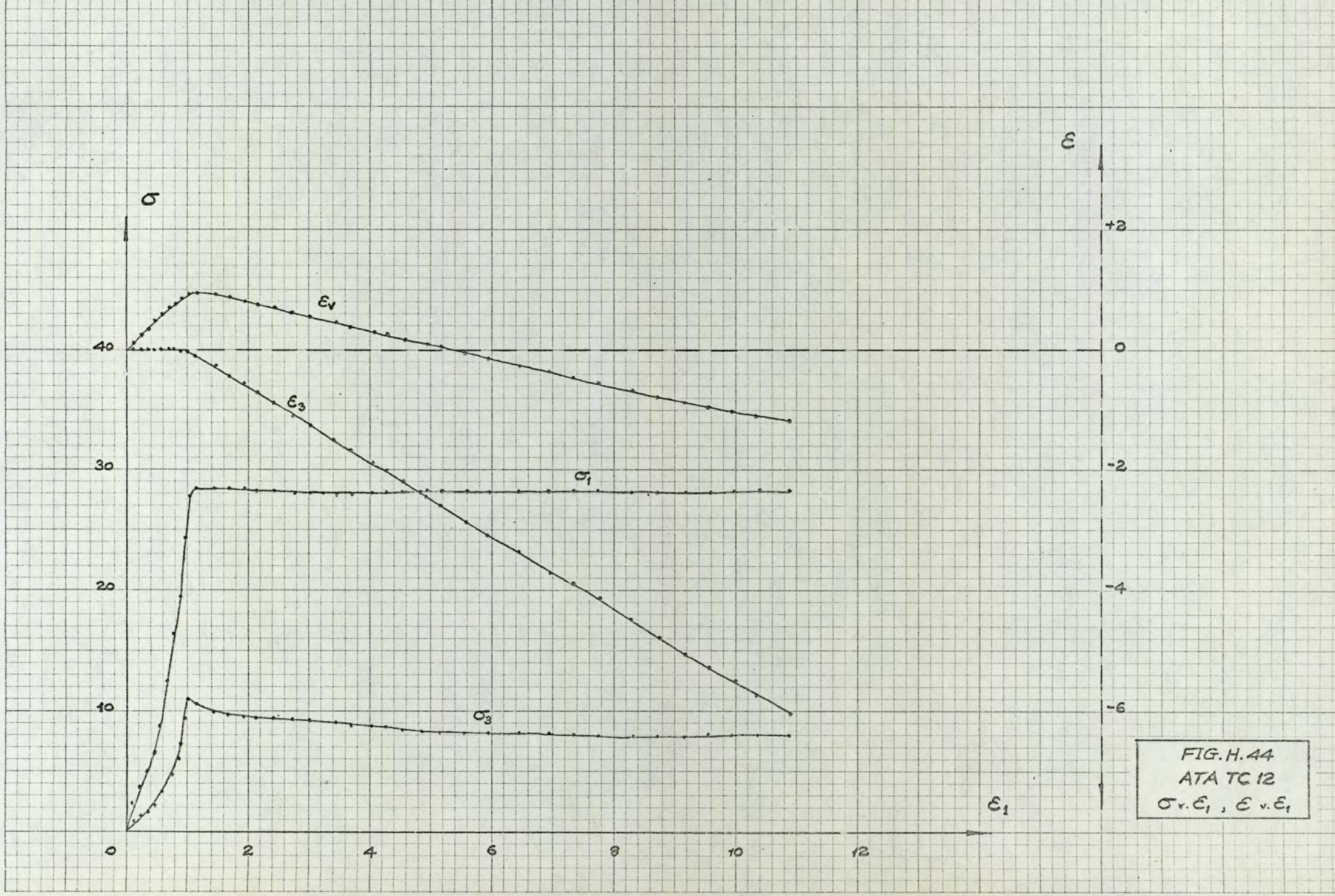

FIG. H. 44
ATA TC 12
σ v. ε_1 , ε v. ε_1

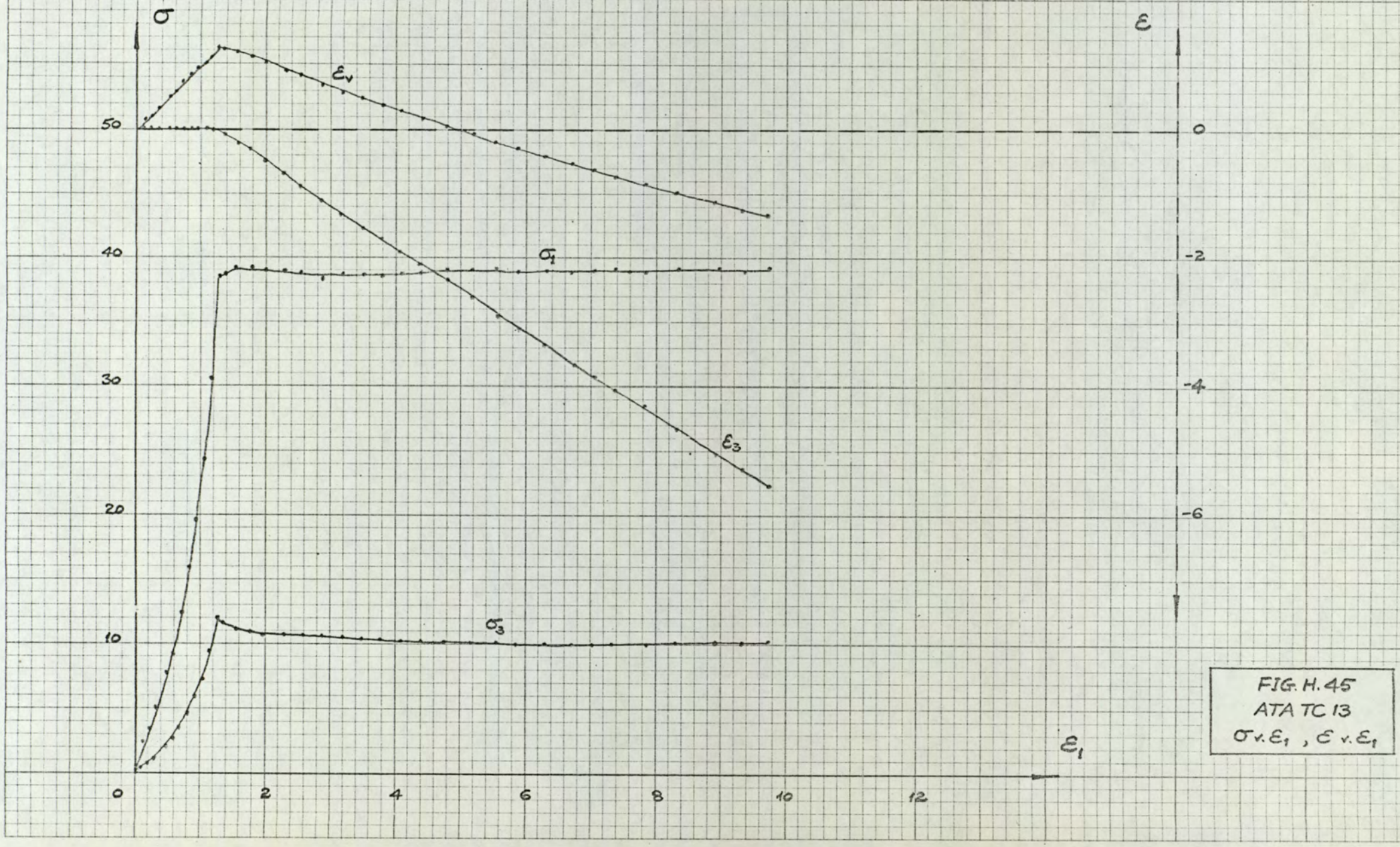

FIG. H. 45
ATA TC 13
σ v. ε_1 , ε v. ε_1

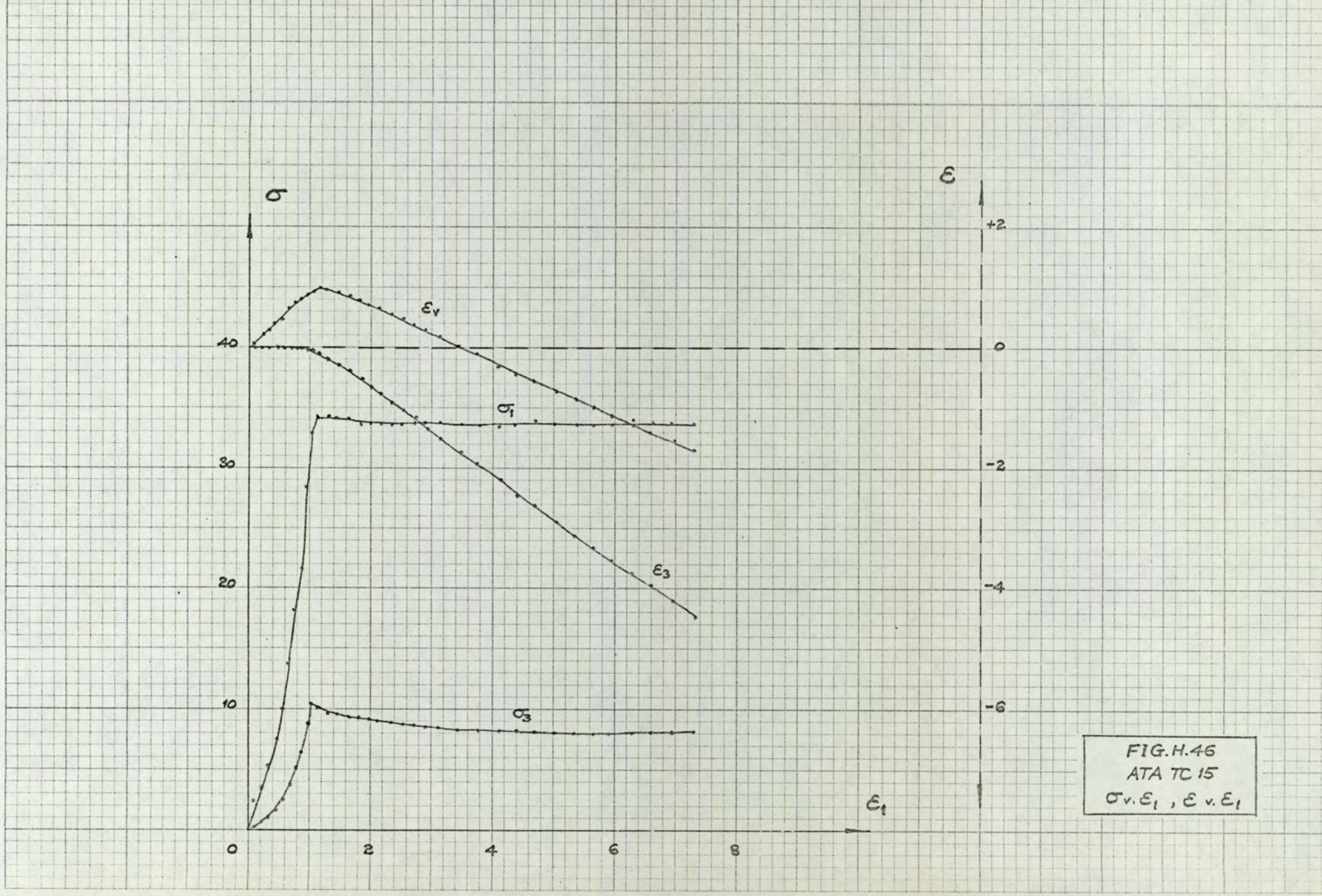

FIG. H.46
ATA TC 15
σ v. ε_1 , ε v. ε_1

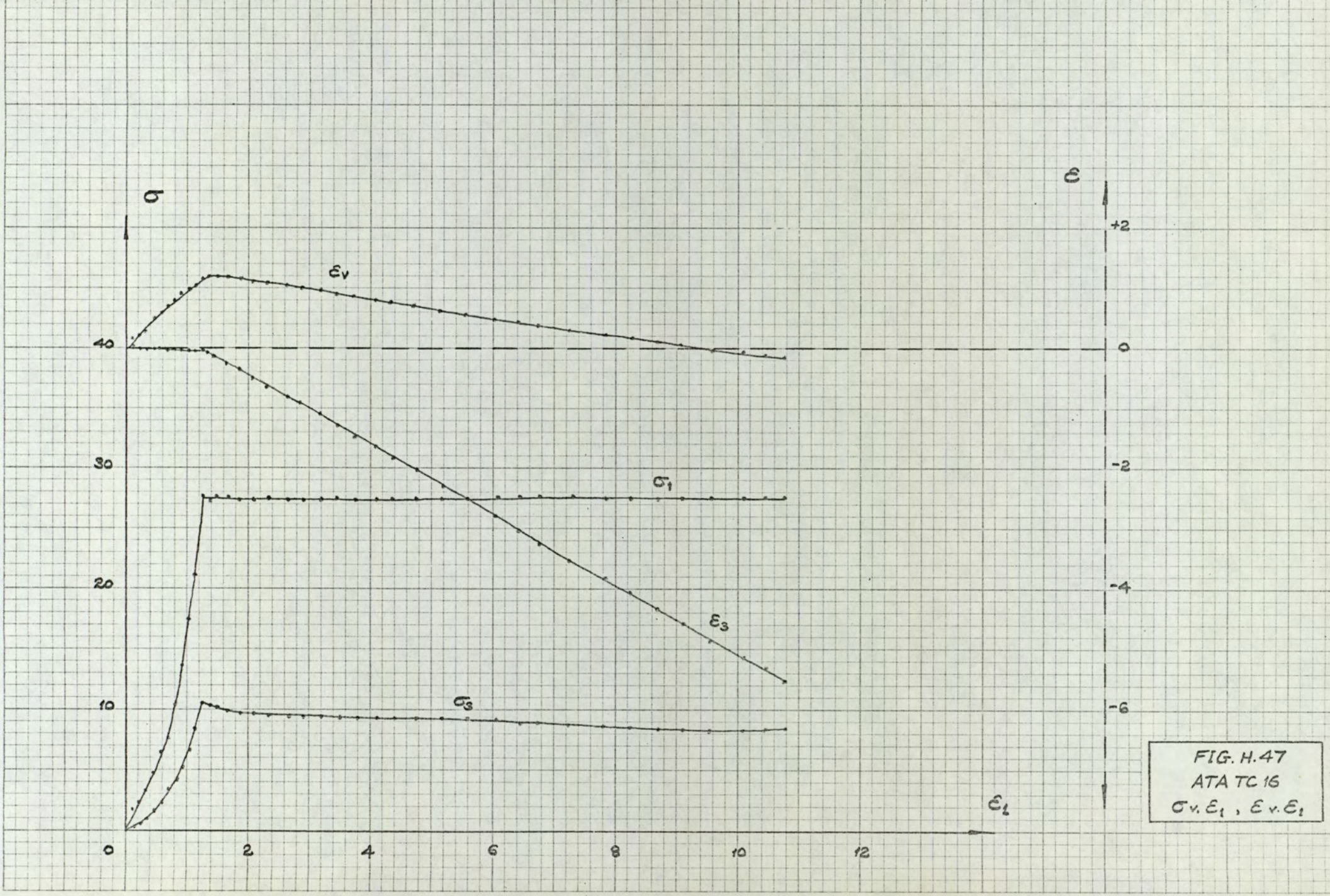

FIG. H.47
ATA TC 16
σ v. ε_1 , ε v. ε_1

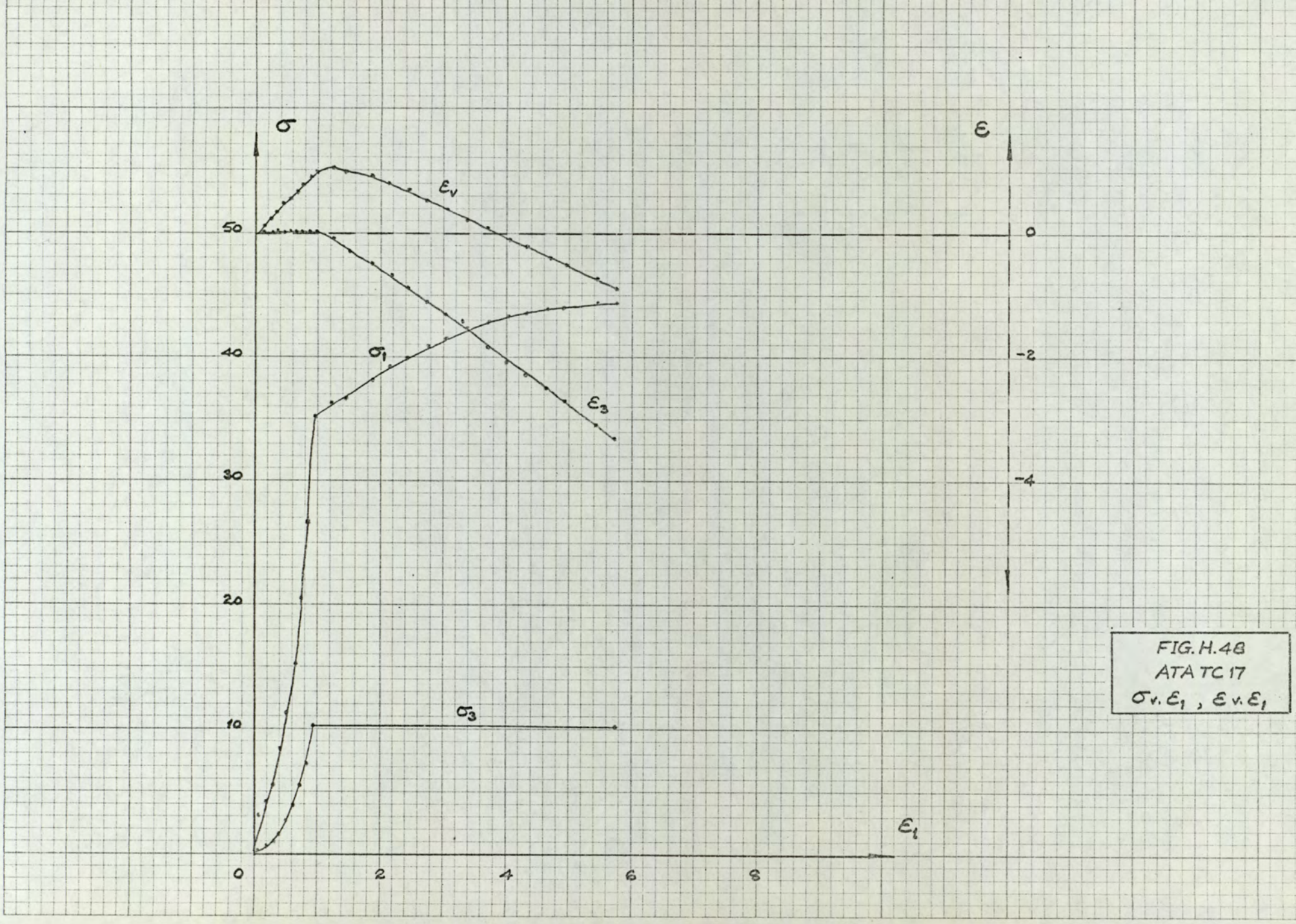

FIG. H.48
ATA TC 17
σ v. ε_1 , ε v. ε_1

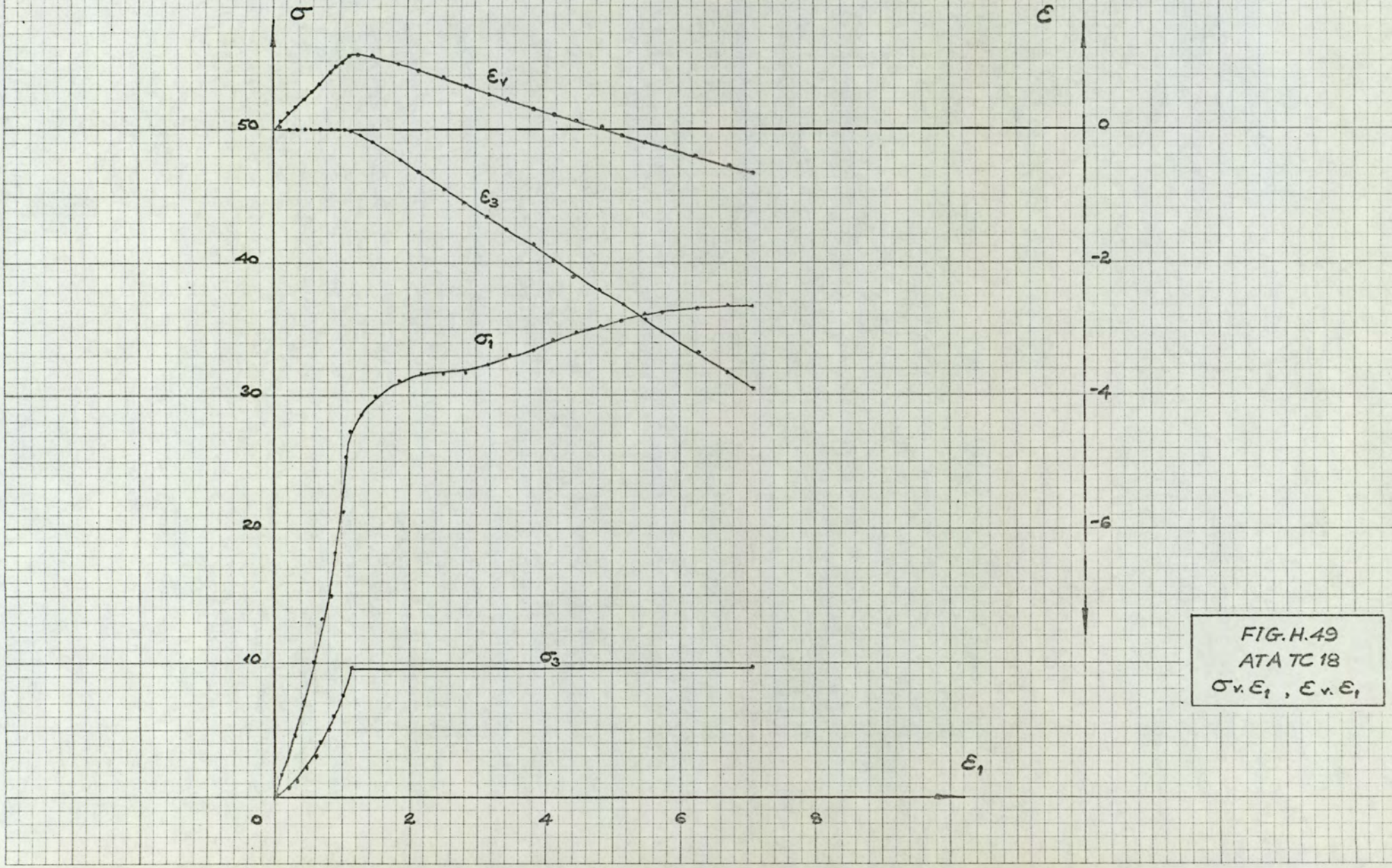

FIG. H.49
ATA TC 18
σ v. ε_1 , ε v. ε_1

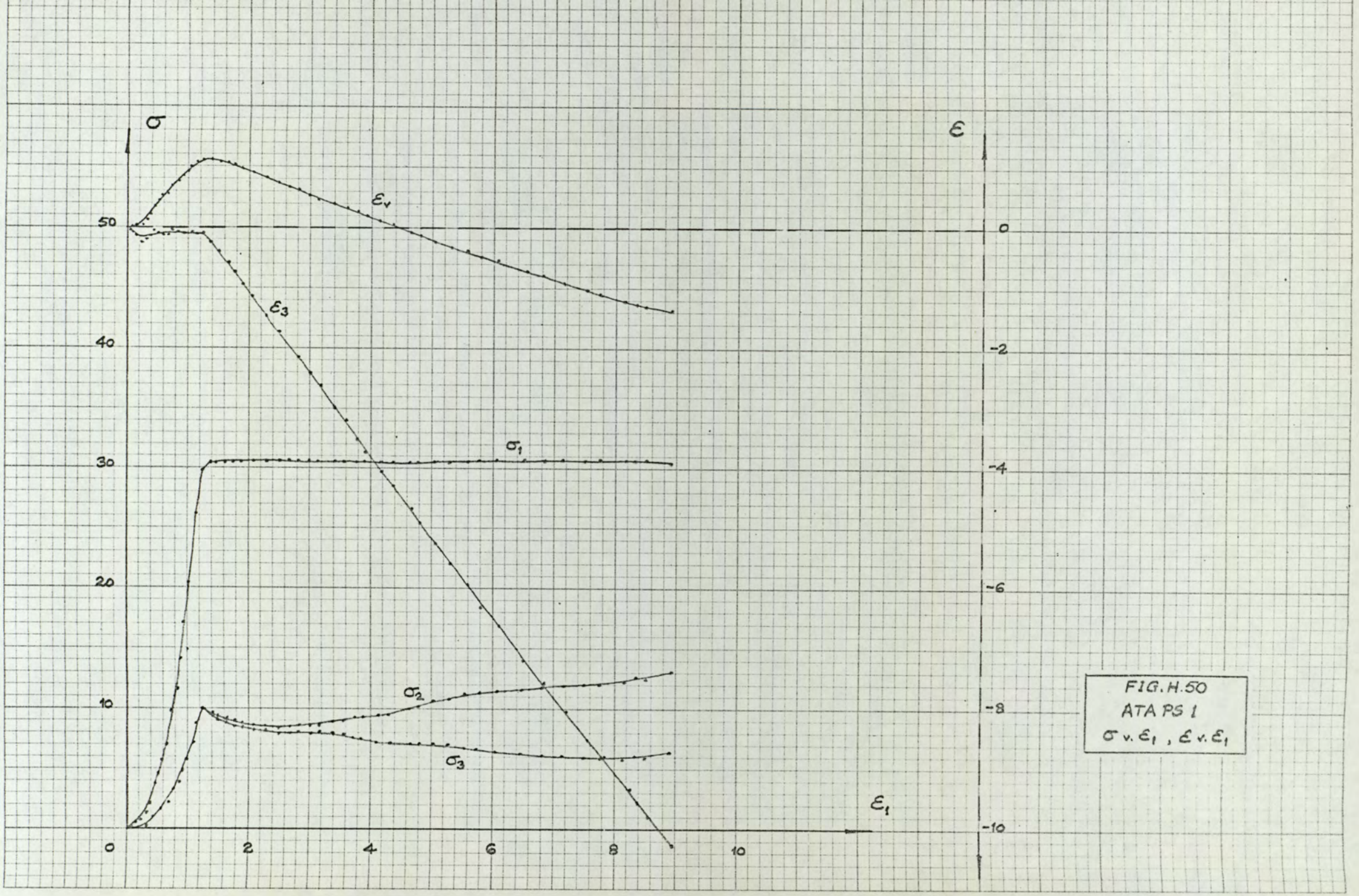

FIG. H.50
ATA PS 1
σ v. ε_1 , ε v. ε_1

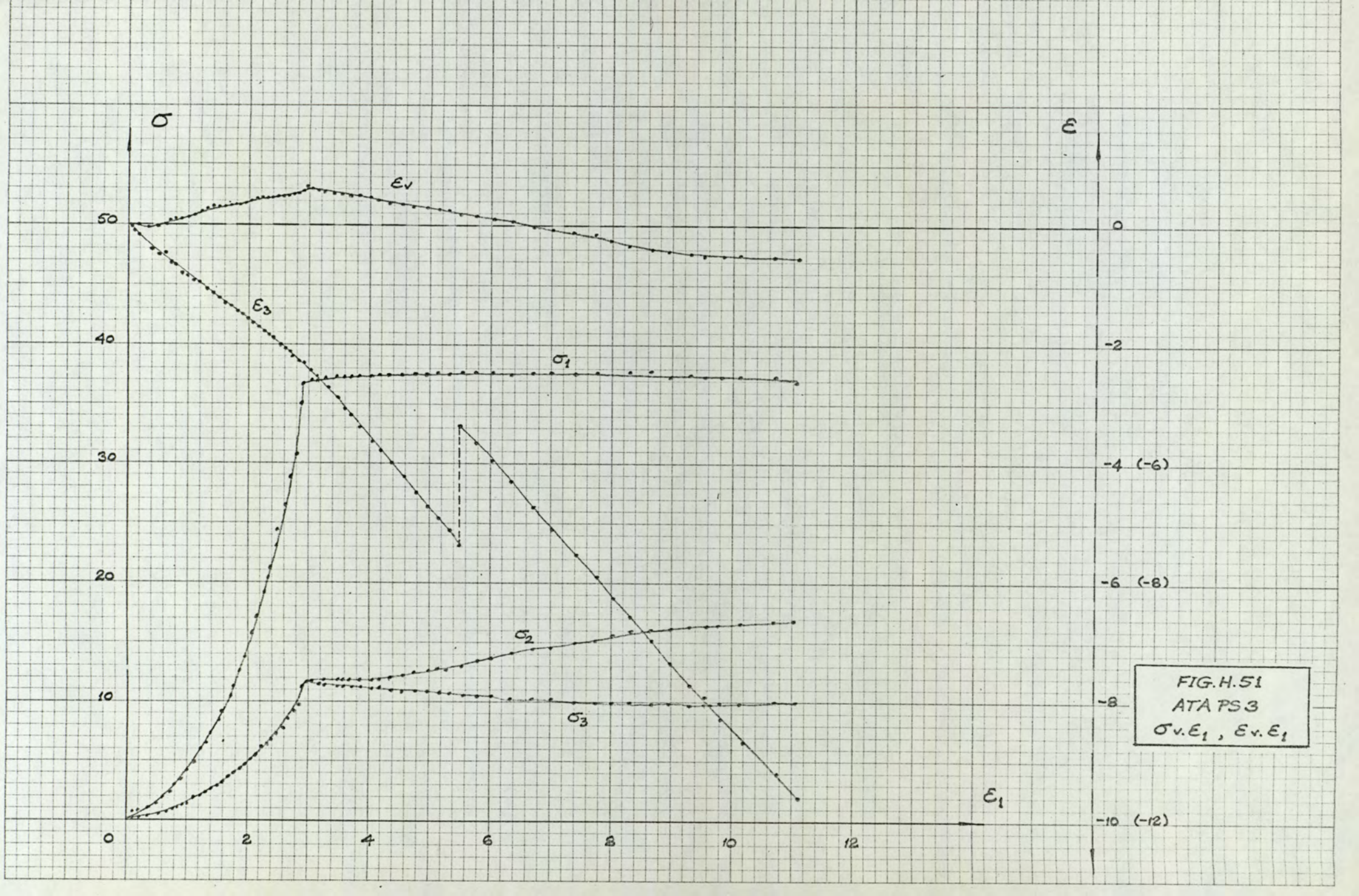

FIG. H.51
ATA PS 3
$\sigma_v . \varepsilon_1$, $\varepsilon_v . \varepsilon_1$

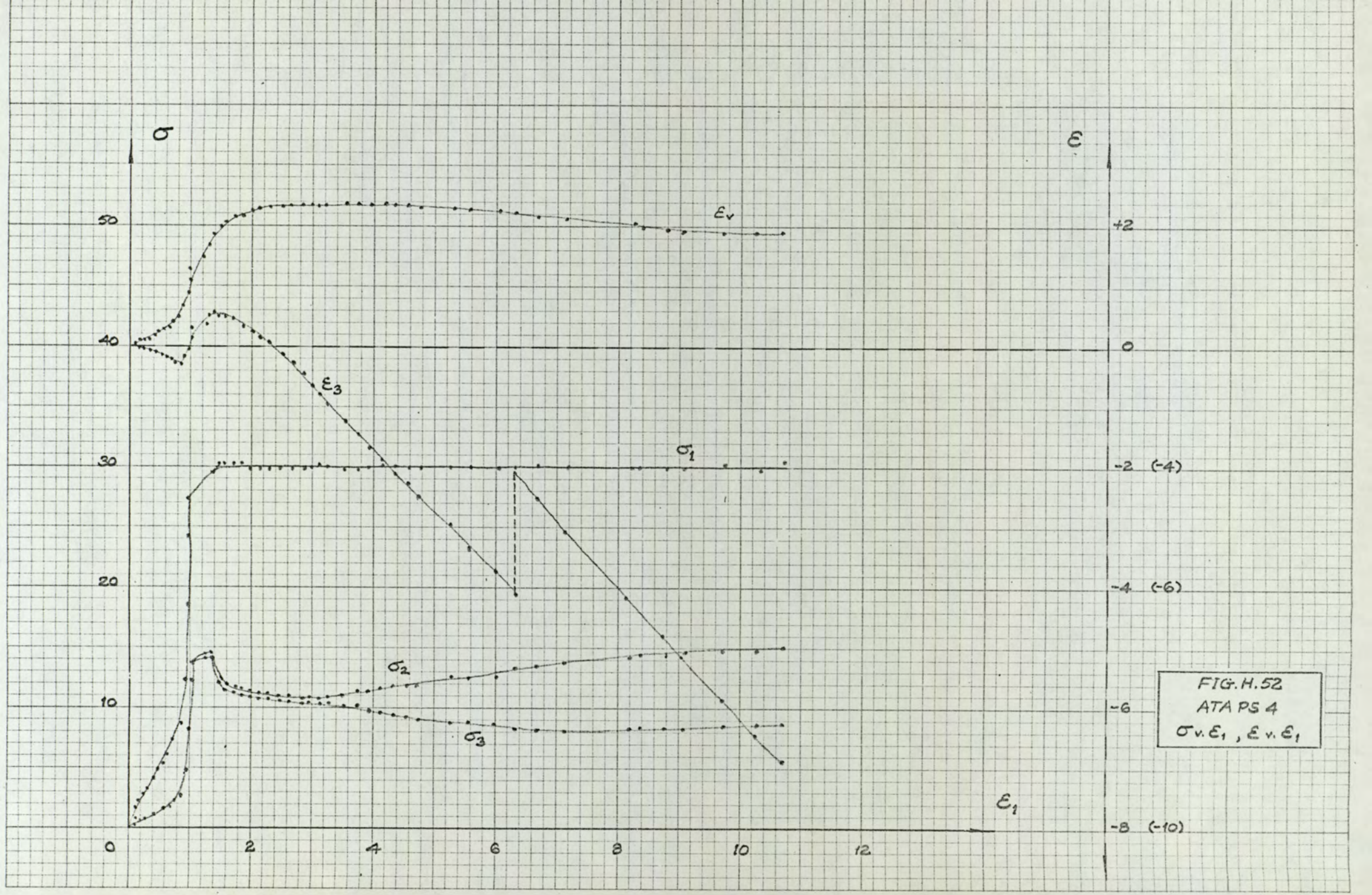

FIG. H.52
ATA PS 4
σ v. ε_1 , ε v. ε_1

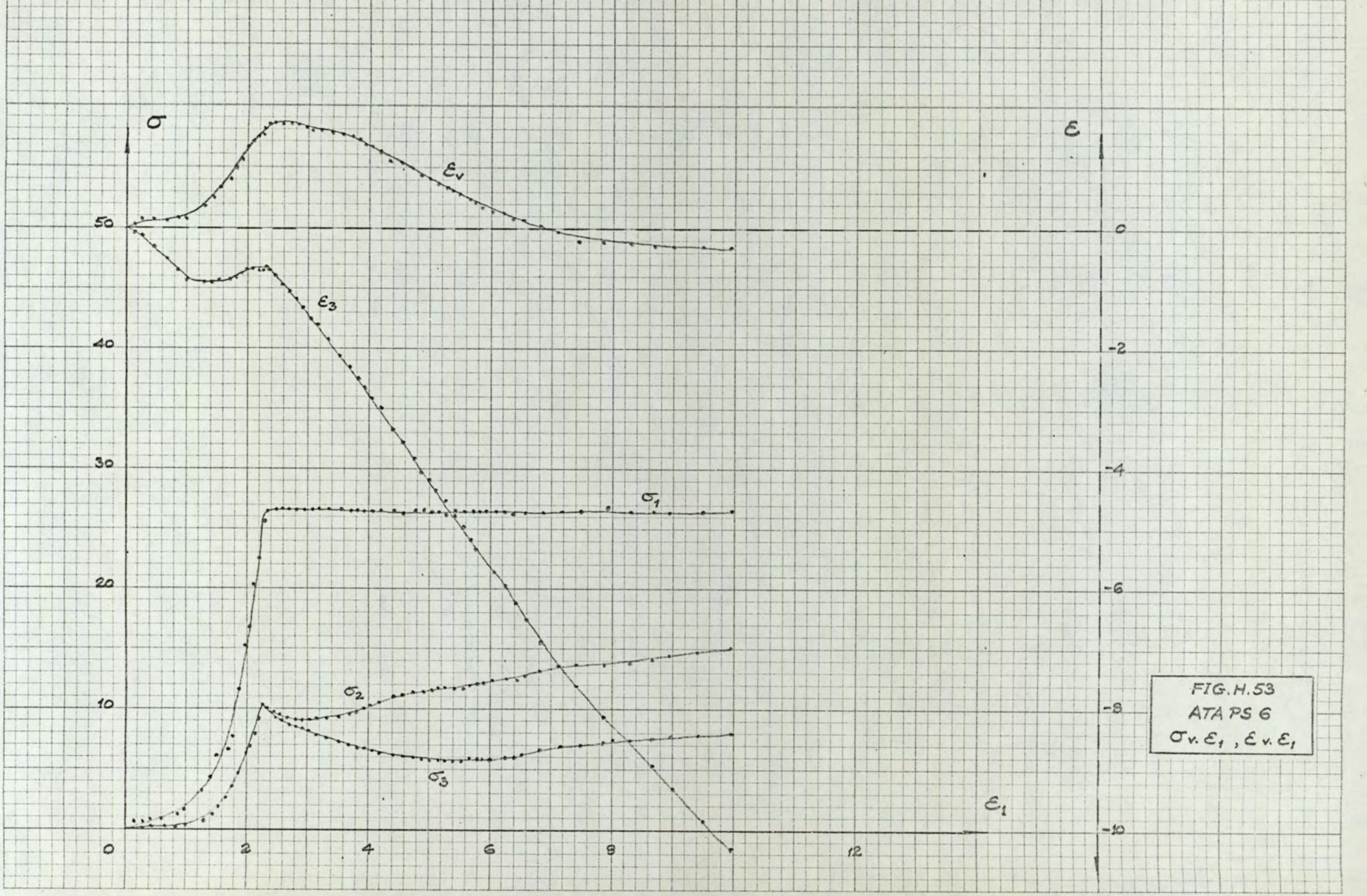

FIG. H.53
ATA PS 6
σ v. ε_1 , ε v. ε_1

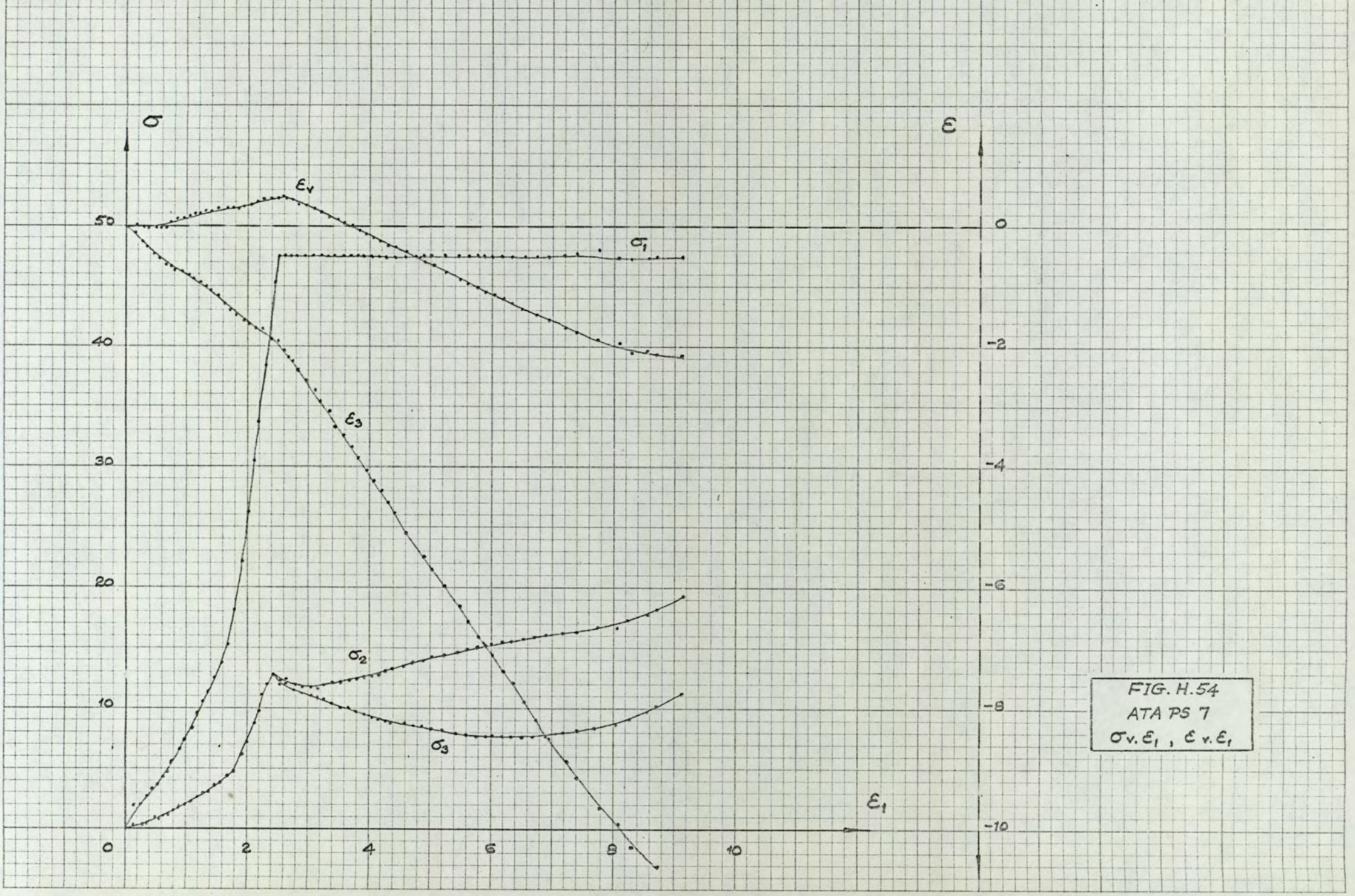

FIG. H.54
ATA PS 7
σ v. ε_1 , ε v. ε_1

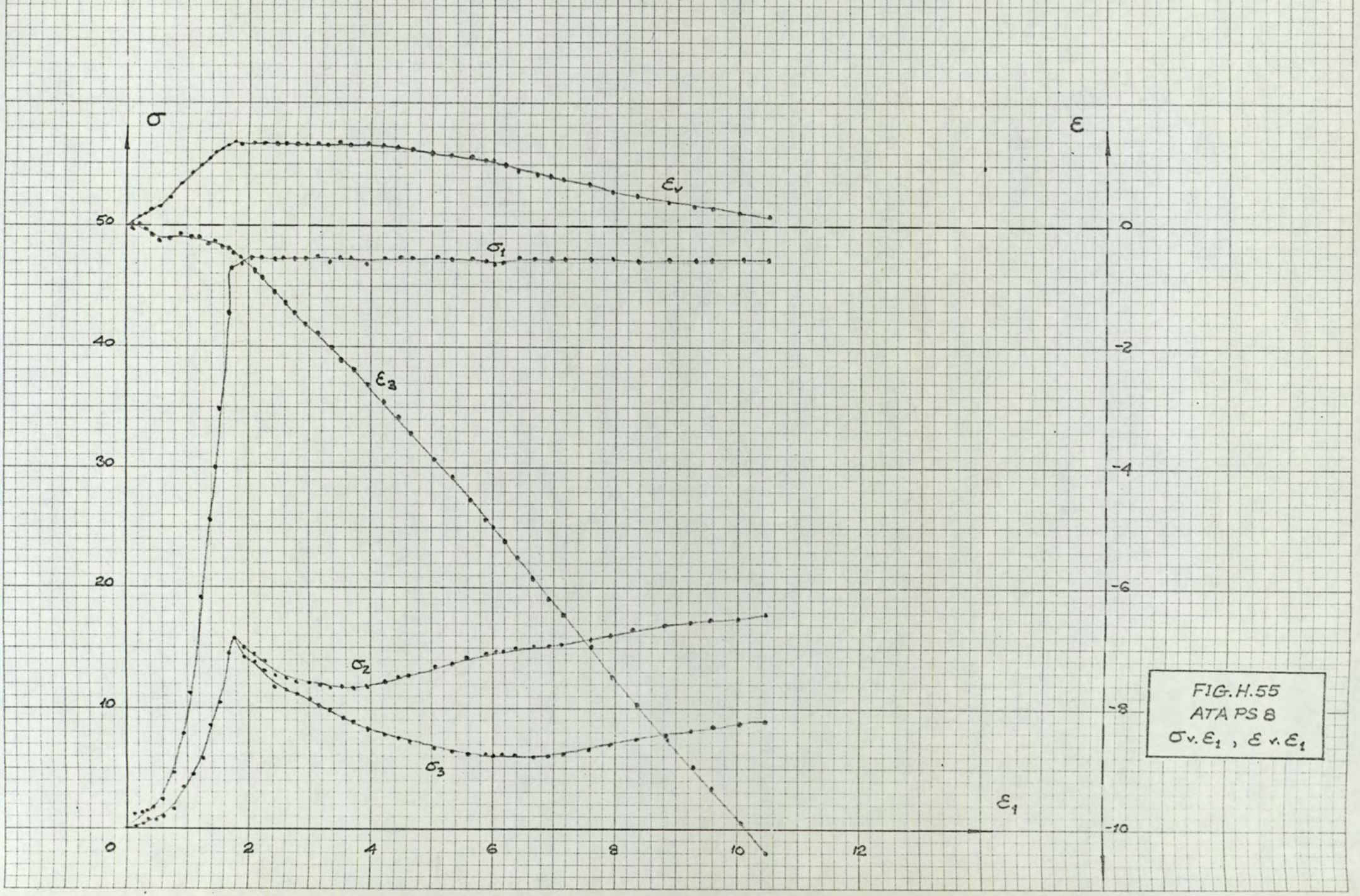

FIG. H.55
ATA PS 8
σ v. ε_1 , ε v. ε_1

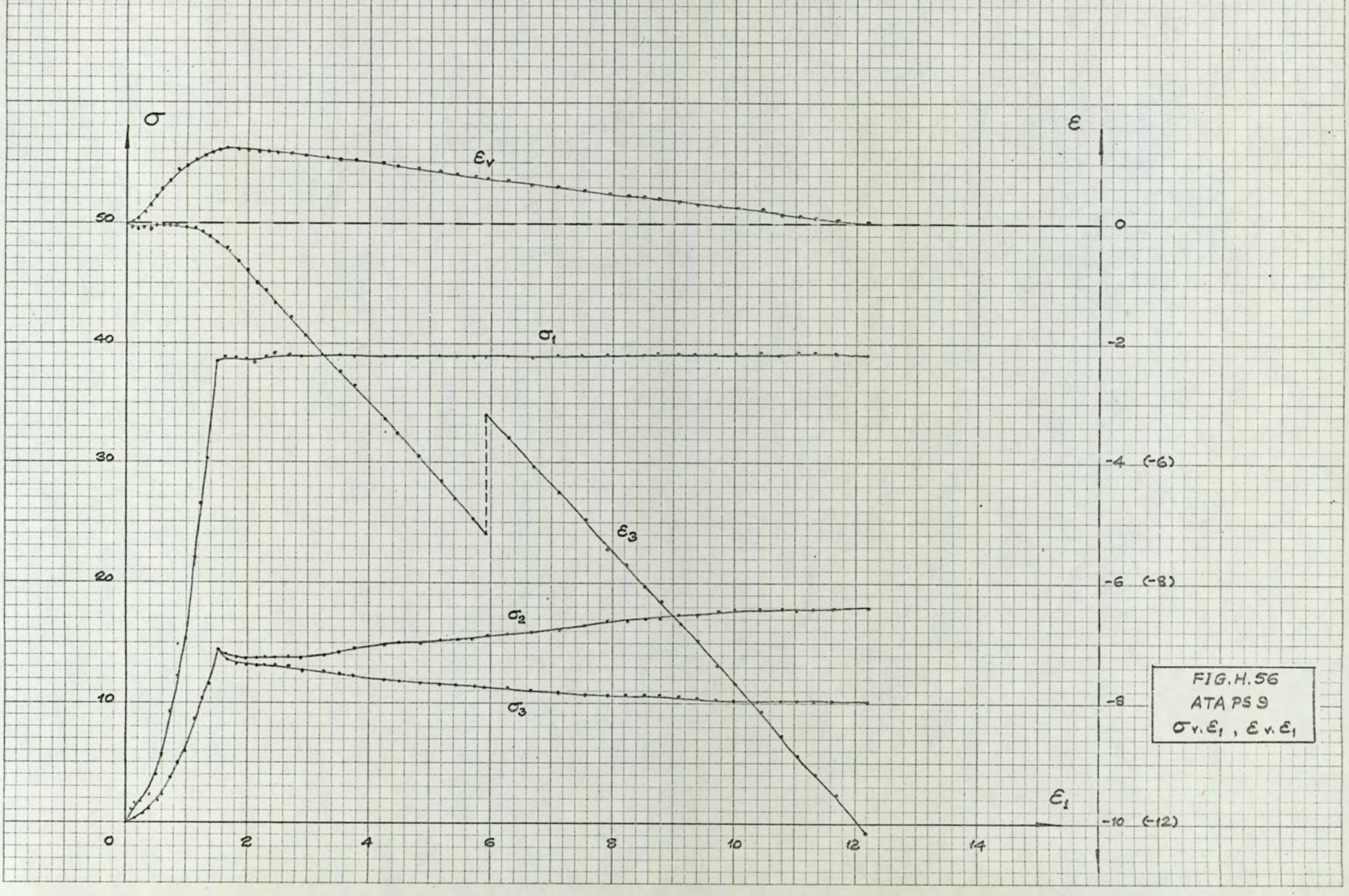

FIG. H. 56
ATA PS 9
σ_v, ε_1 , $\varepsilon_v, \varepsilon_1$

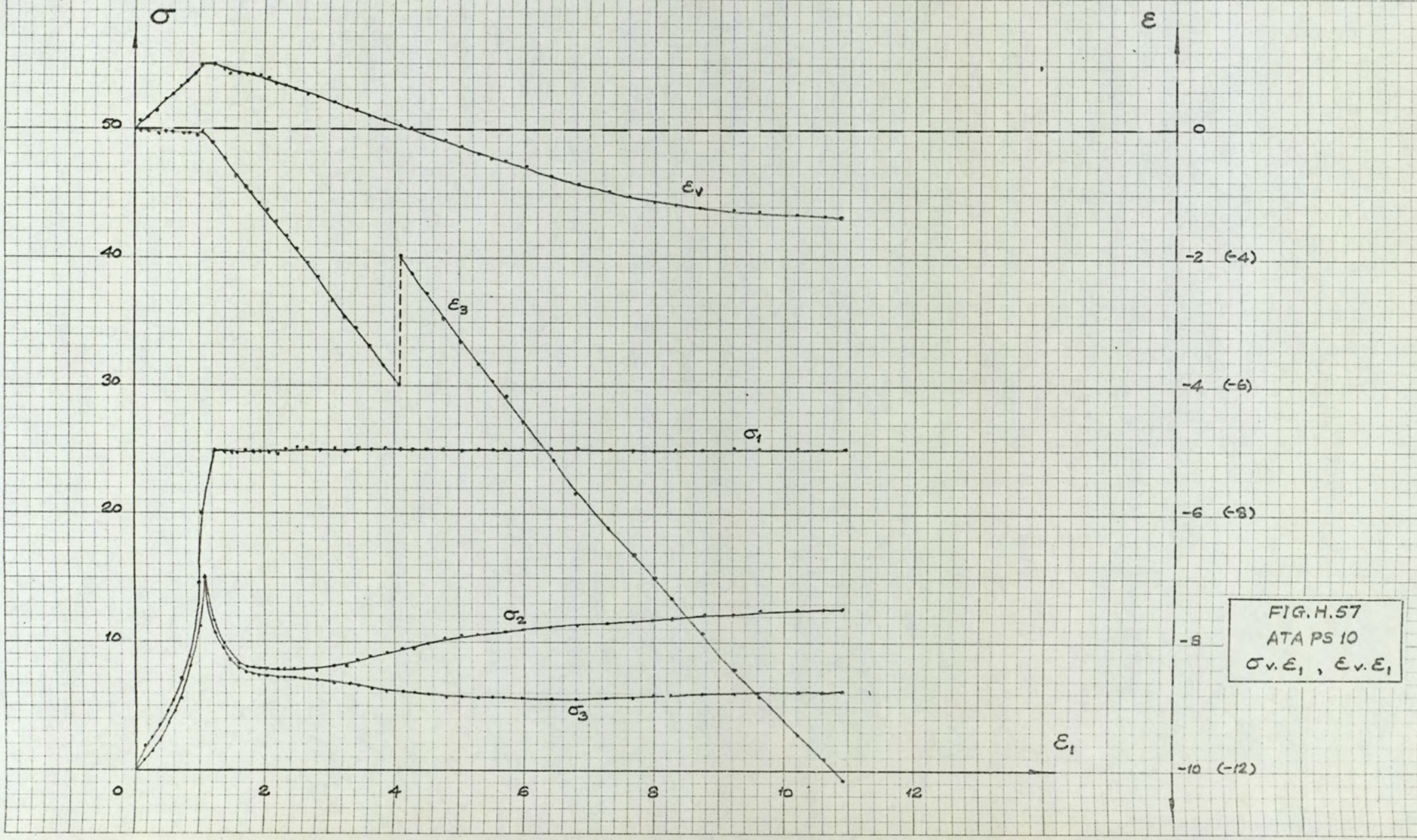

FIG. H.57
ATA PS 10
$\sigma_v . \varepsilon_1$, $\varepsilon_v . \varepsilon_1$

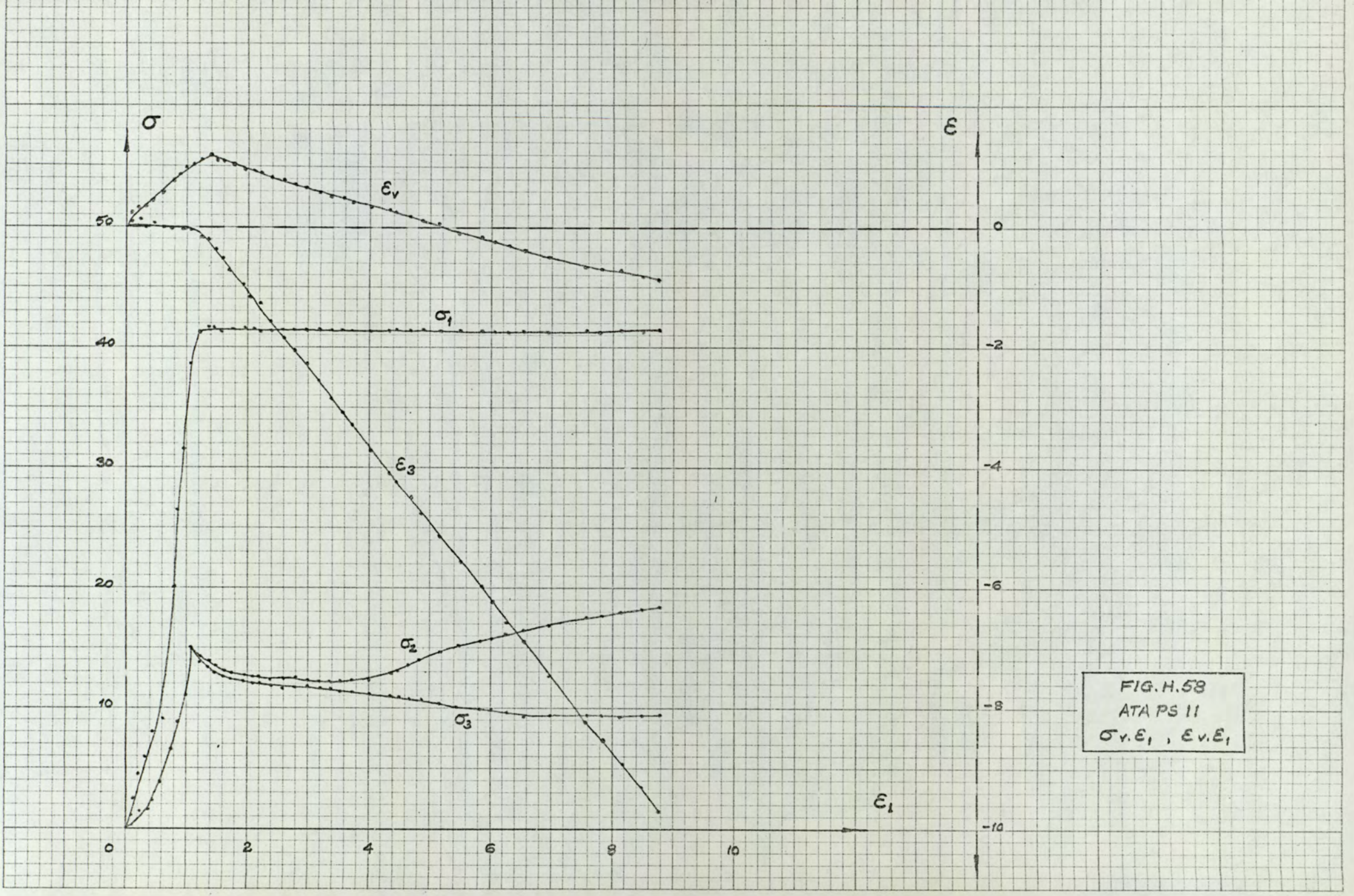

FIG. H.58
ATA PS 11
σ v. ε_1 , ε v. ε_1

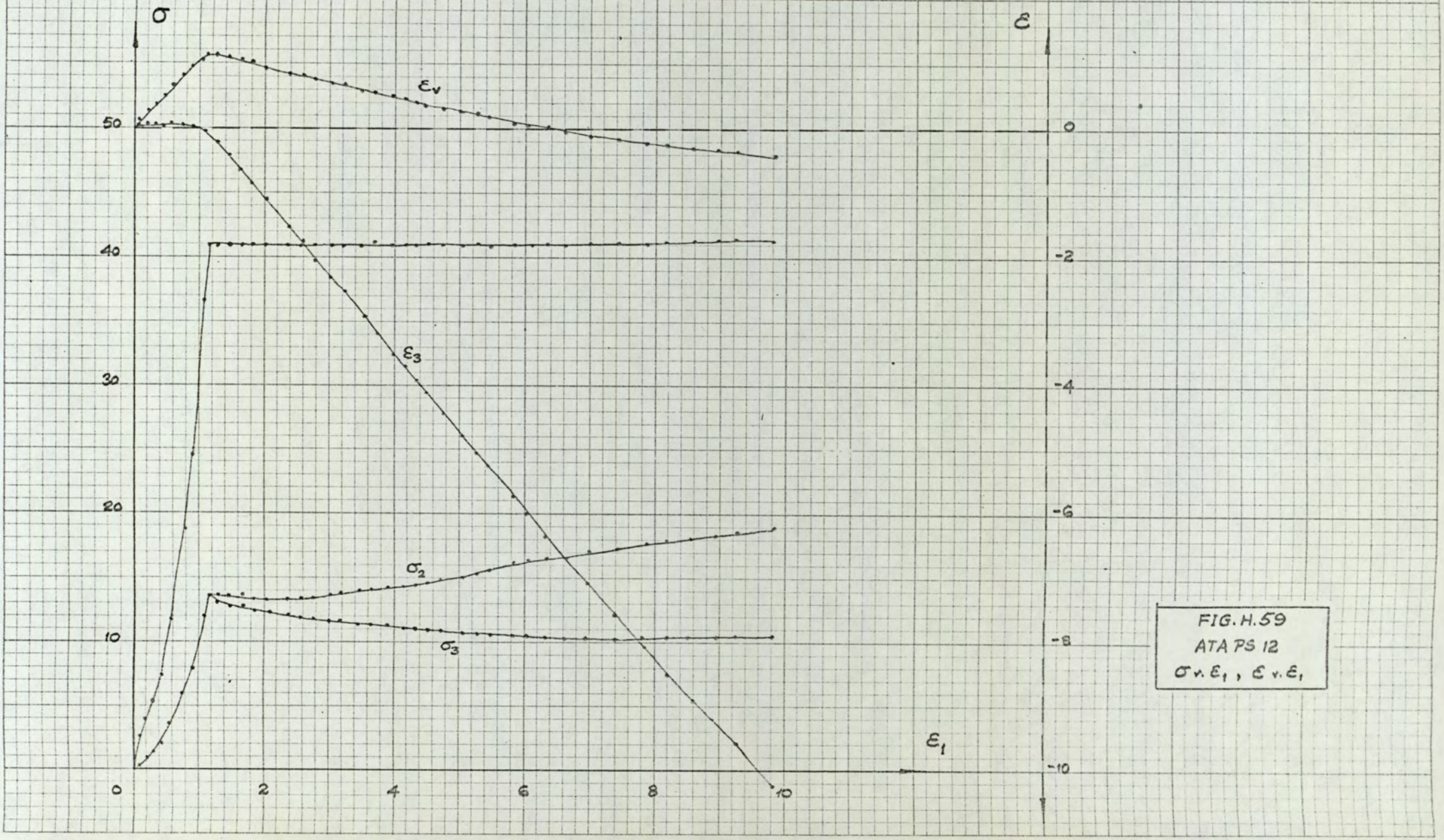

FIG. H.59
ATA PS 12
σ v. ε_1 , ε v. ε_1

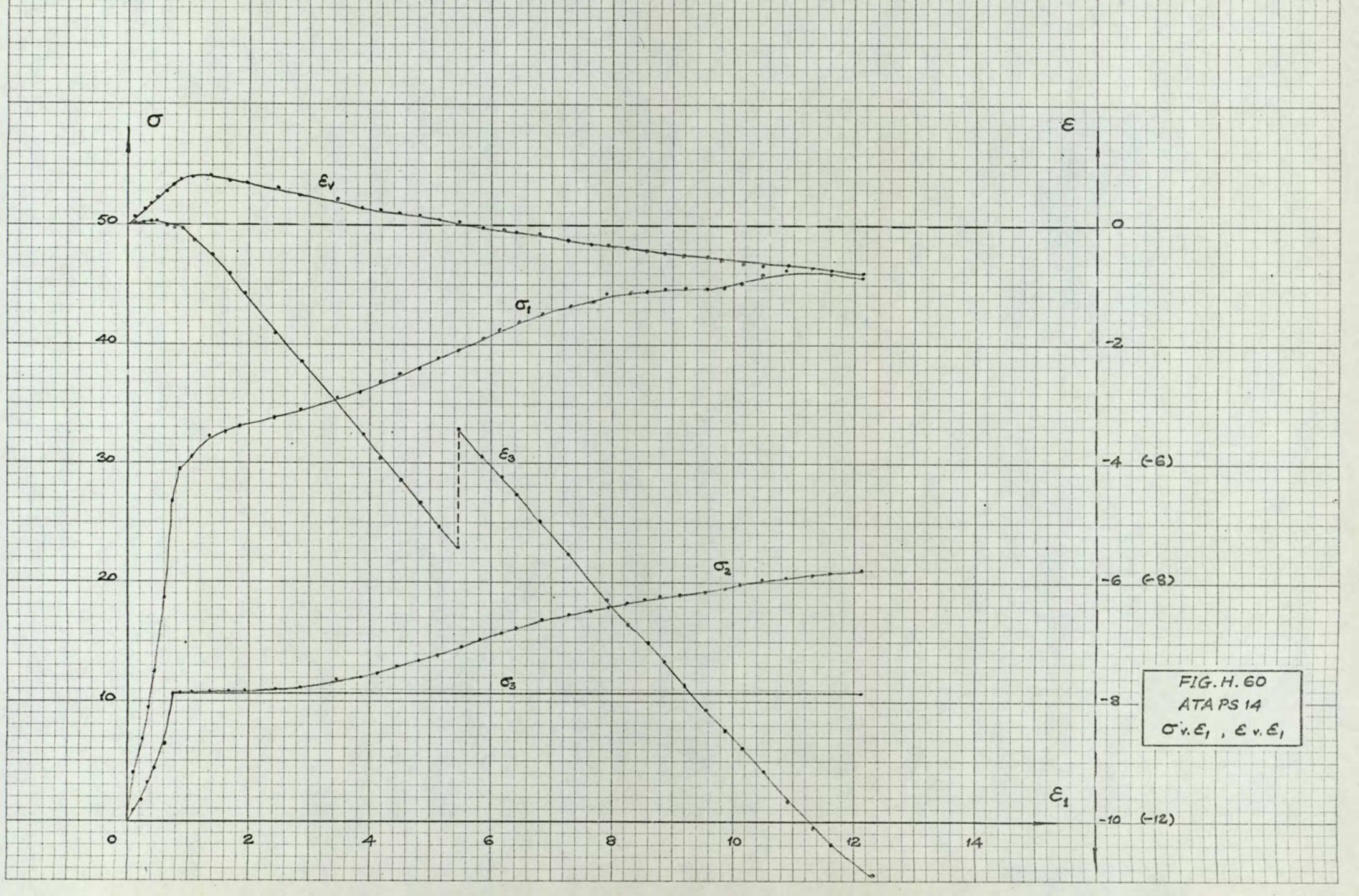

FIG. H. 60
ATA PS 14
σ v. ε_1 , ε v. ε_1

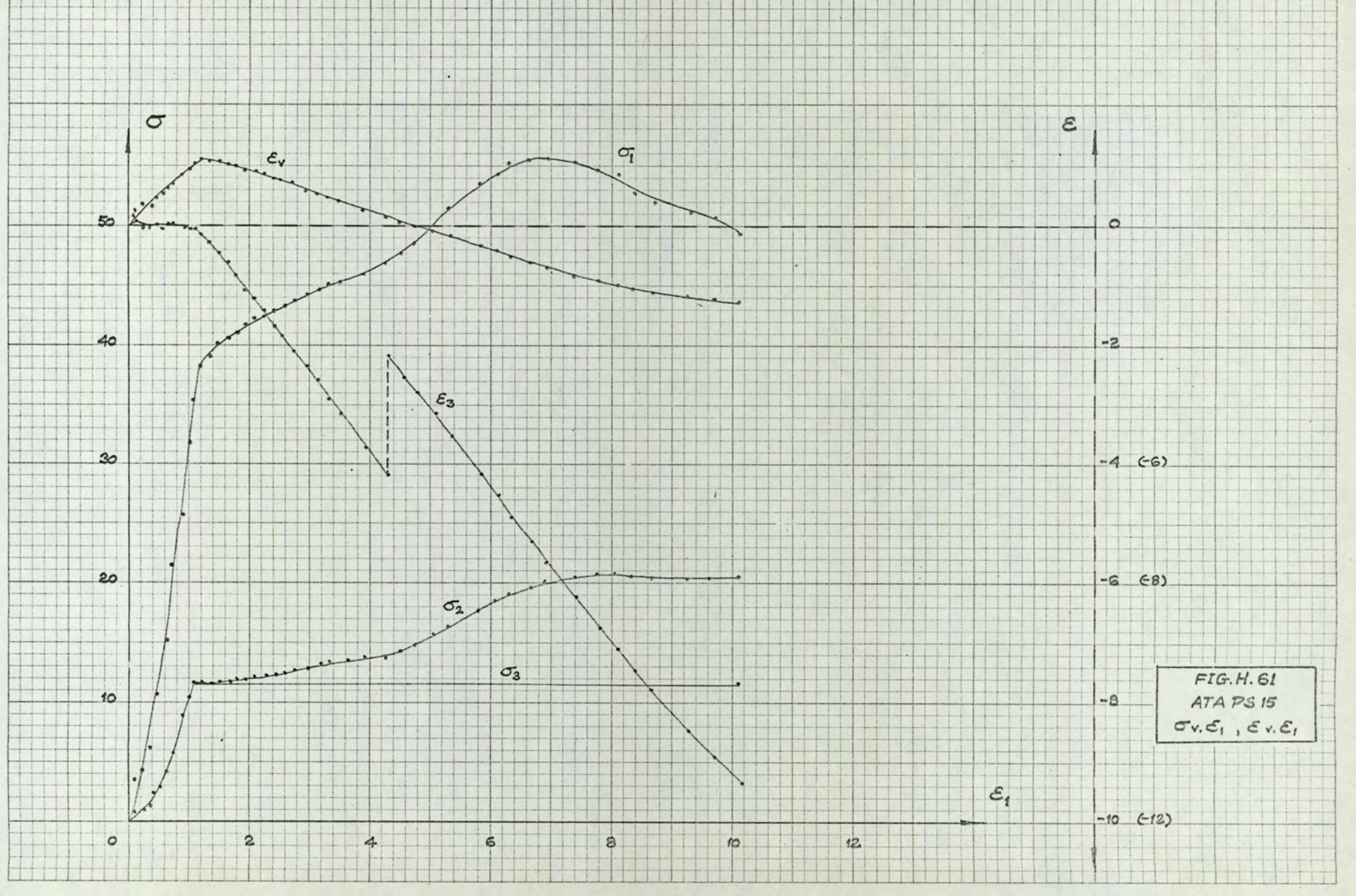

FIG. H. 61
ATA PS 15
σ v. ε_1 , ε v. ε_1

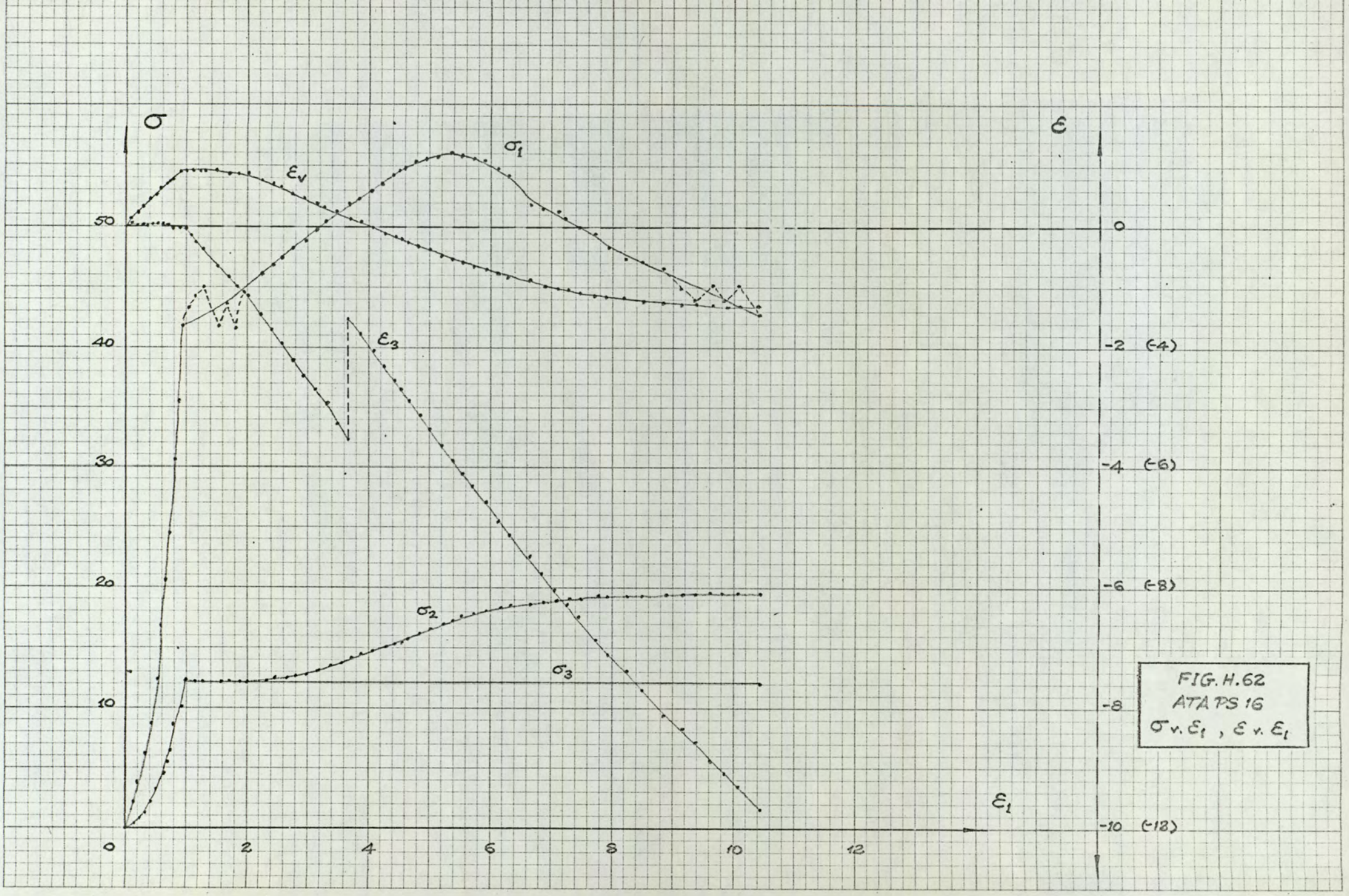

FIG. H.62
ATAPS 16
σ v. ε_1 , ε v. ε_1

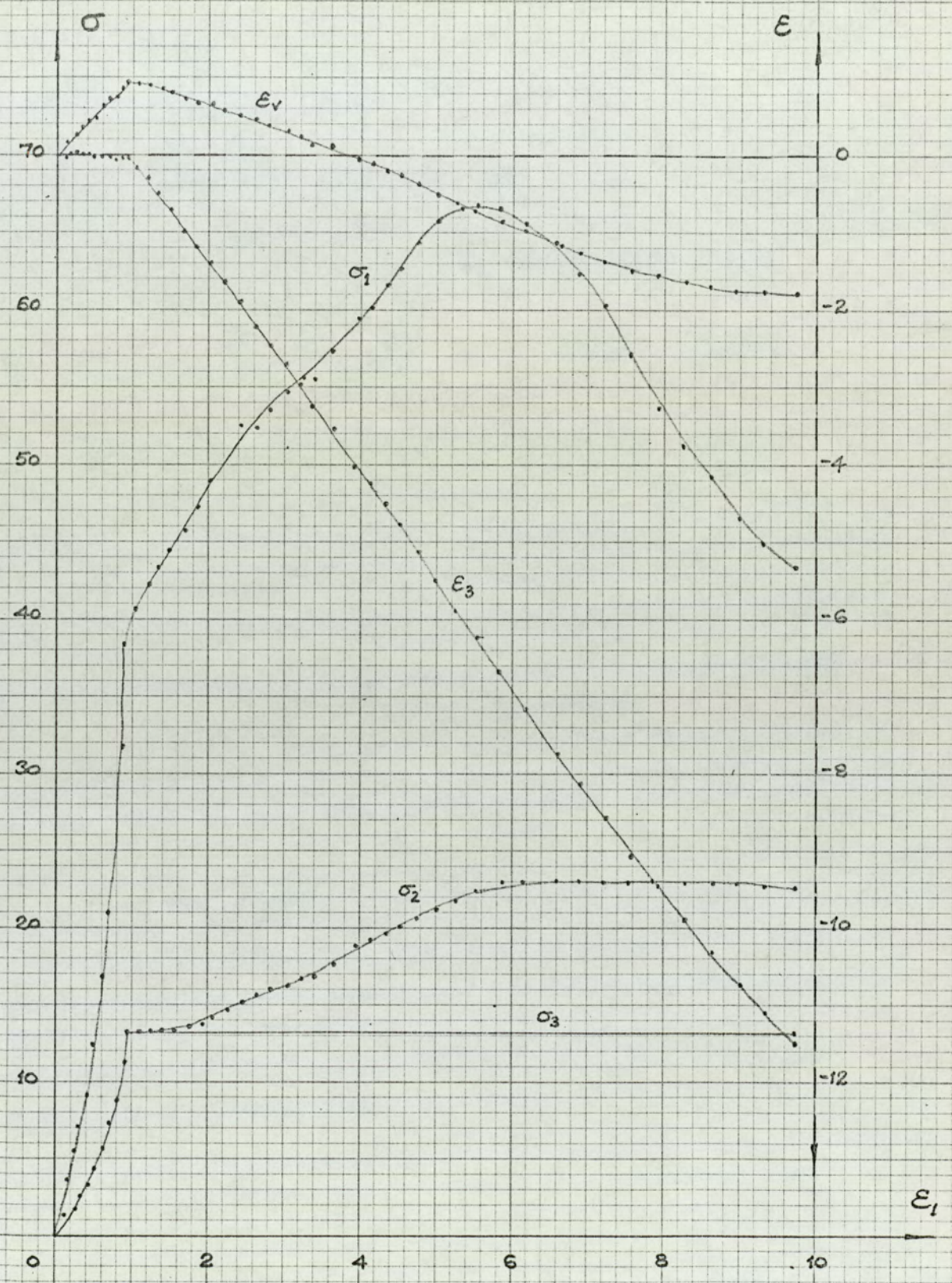

FIG. H. 63
ATA PS 17
$\sigma_v . \varepsilon_1$, $\varepsilon_v . \varepsilon_1$

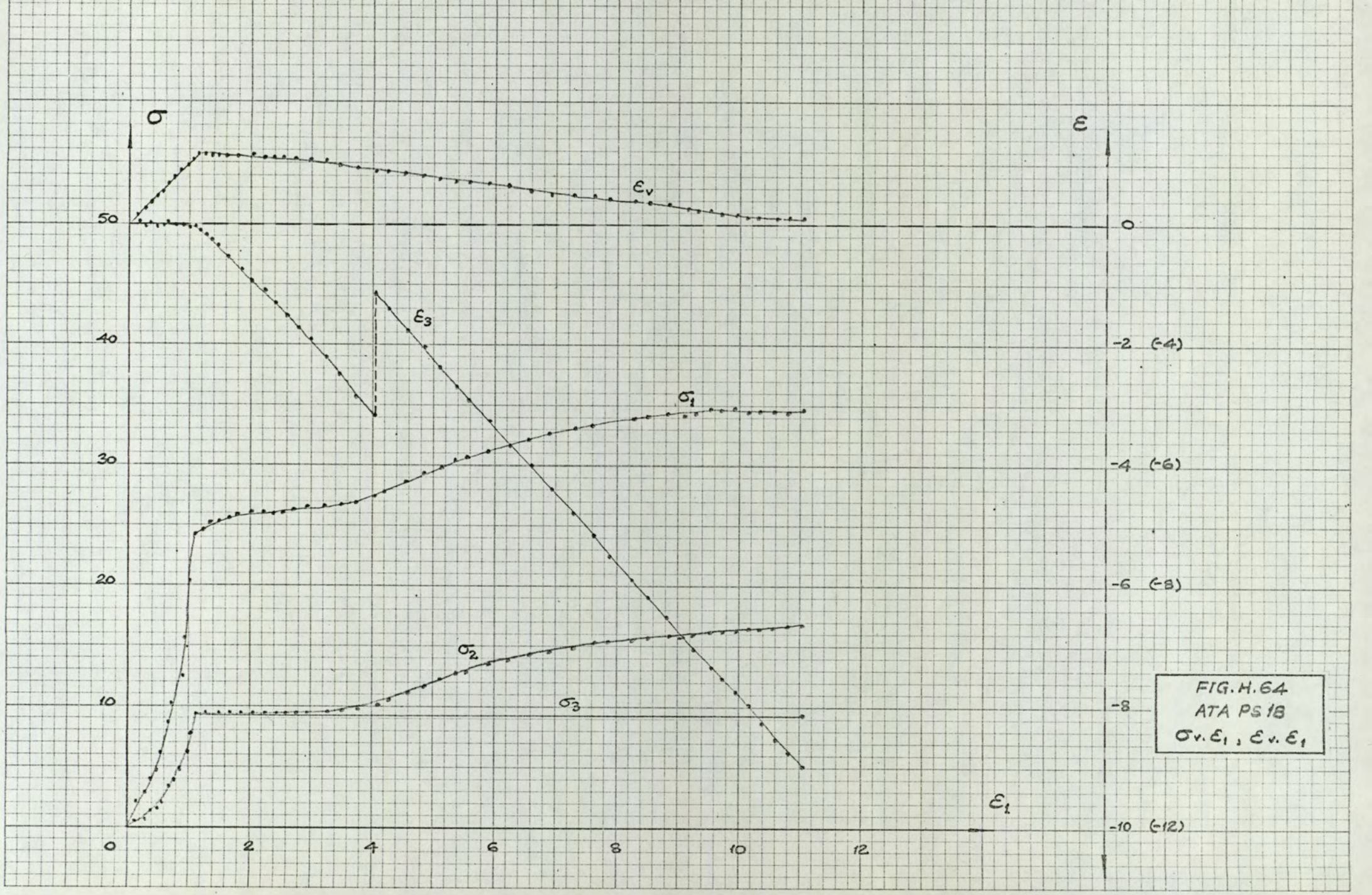

FIG. H. 64
ATA PS 18
$\sigma_v . \varepsilon_1$, $\varepsilon_v . \varepsilon_1$

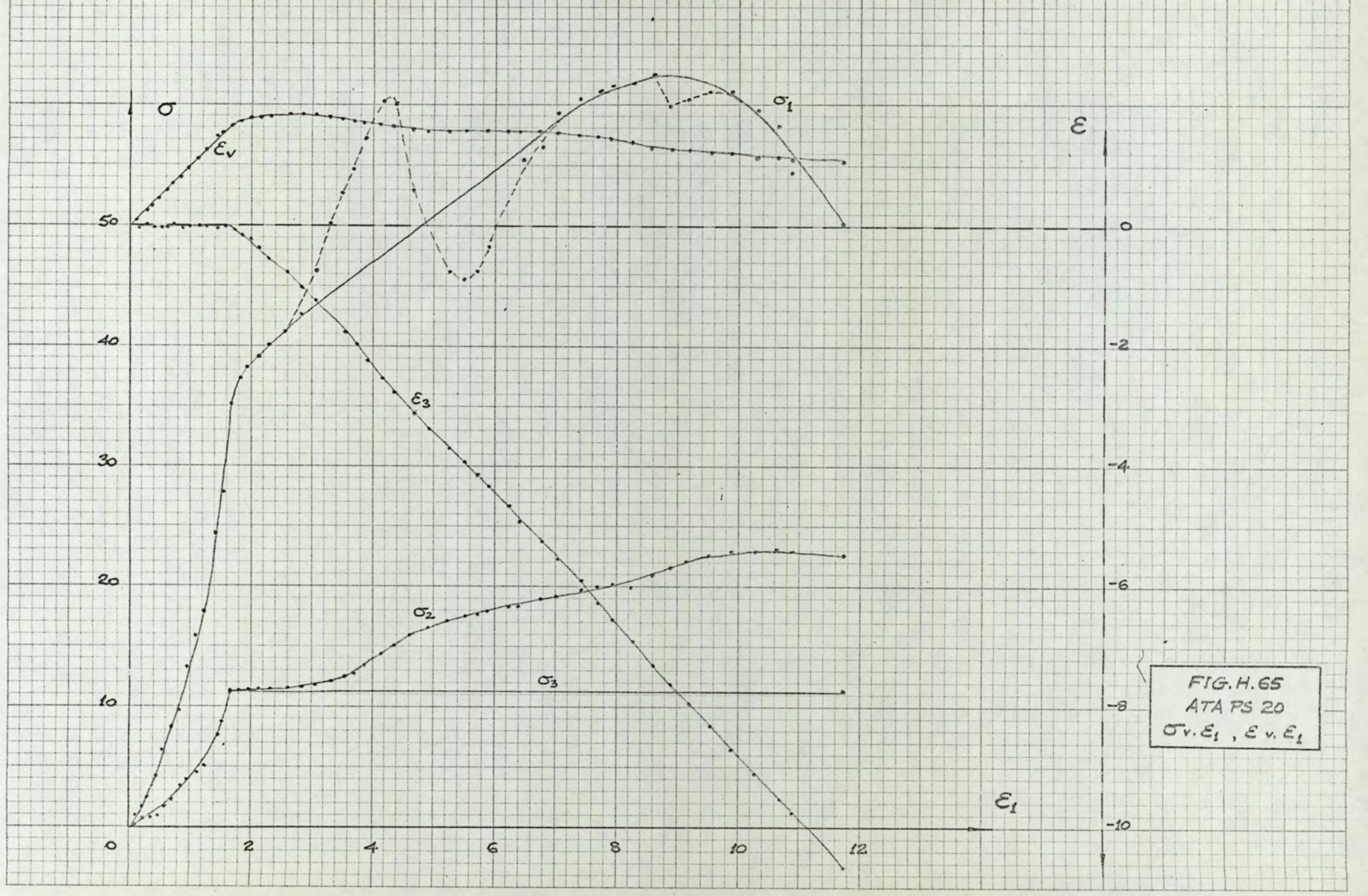

FIG. H. 65
ATA PS 20
σ v. ε_1 , ε v. ε_1

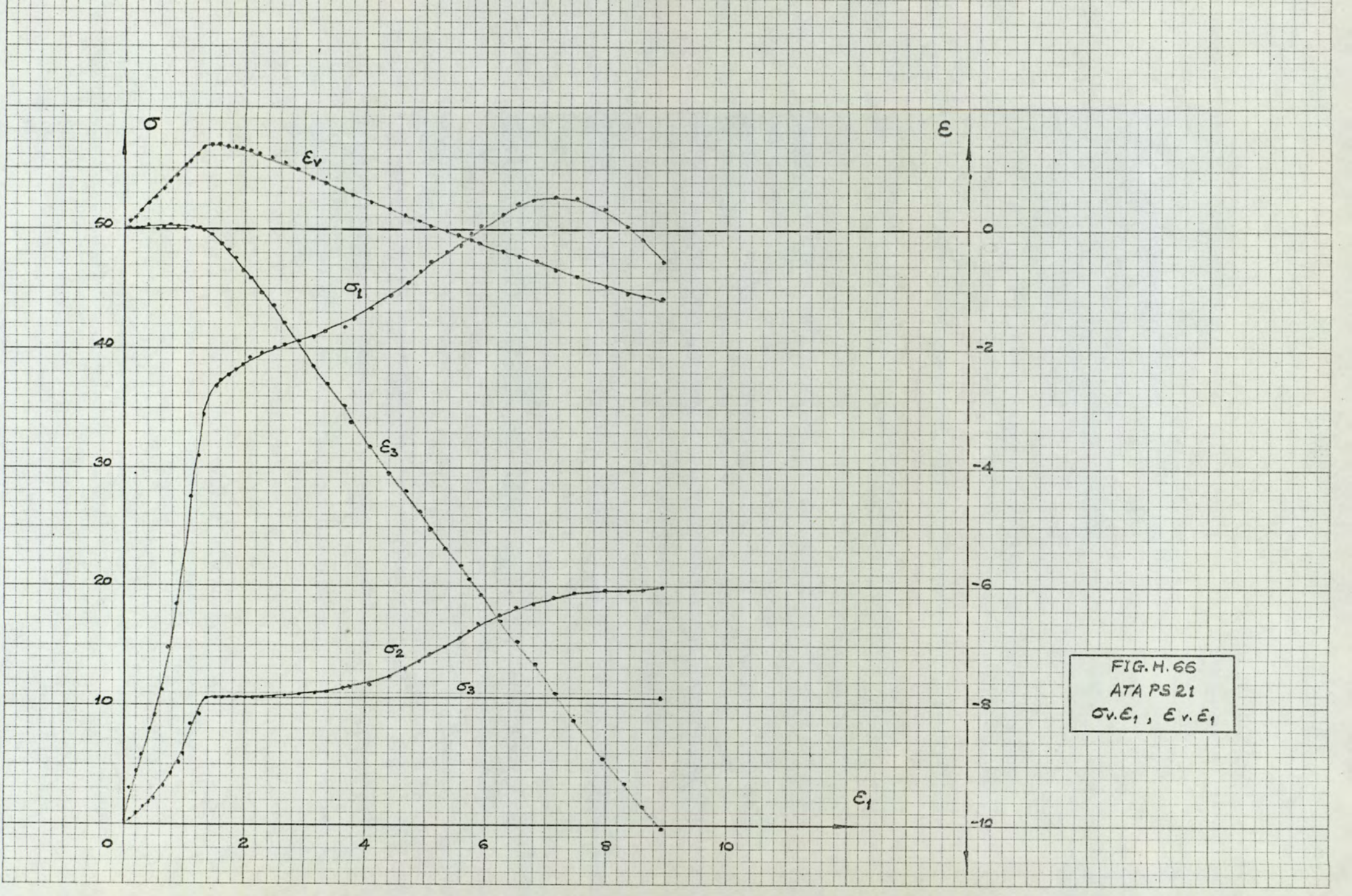

FIG. H. 66
ATA PS 21
$\sigma_v . \varepsilon_1$, $\varepsilon_v . \varepsilon_1$

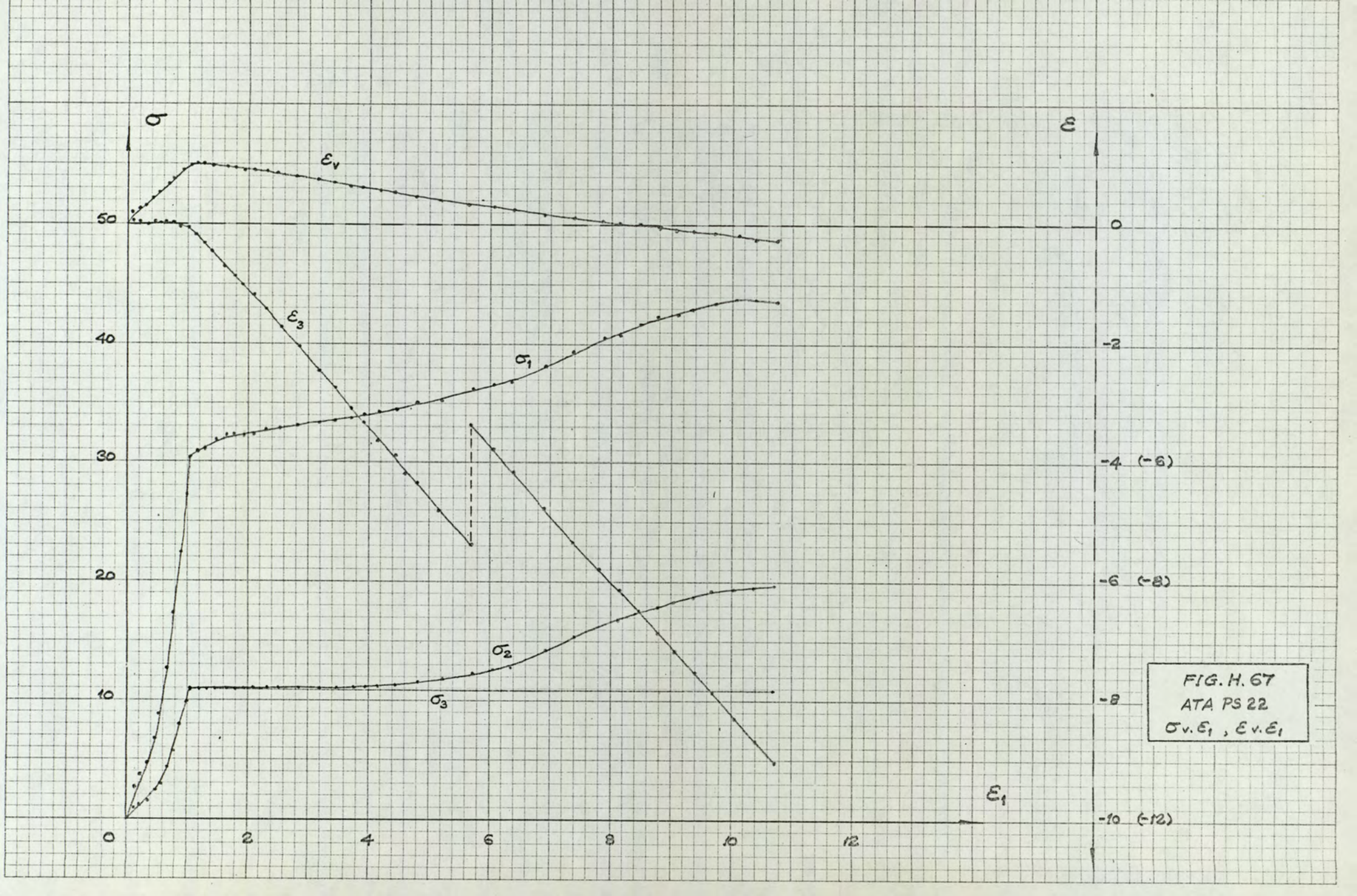

FIG. H. 67
ATA PS 22
σ v. ε_1 , ε v. ε_1

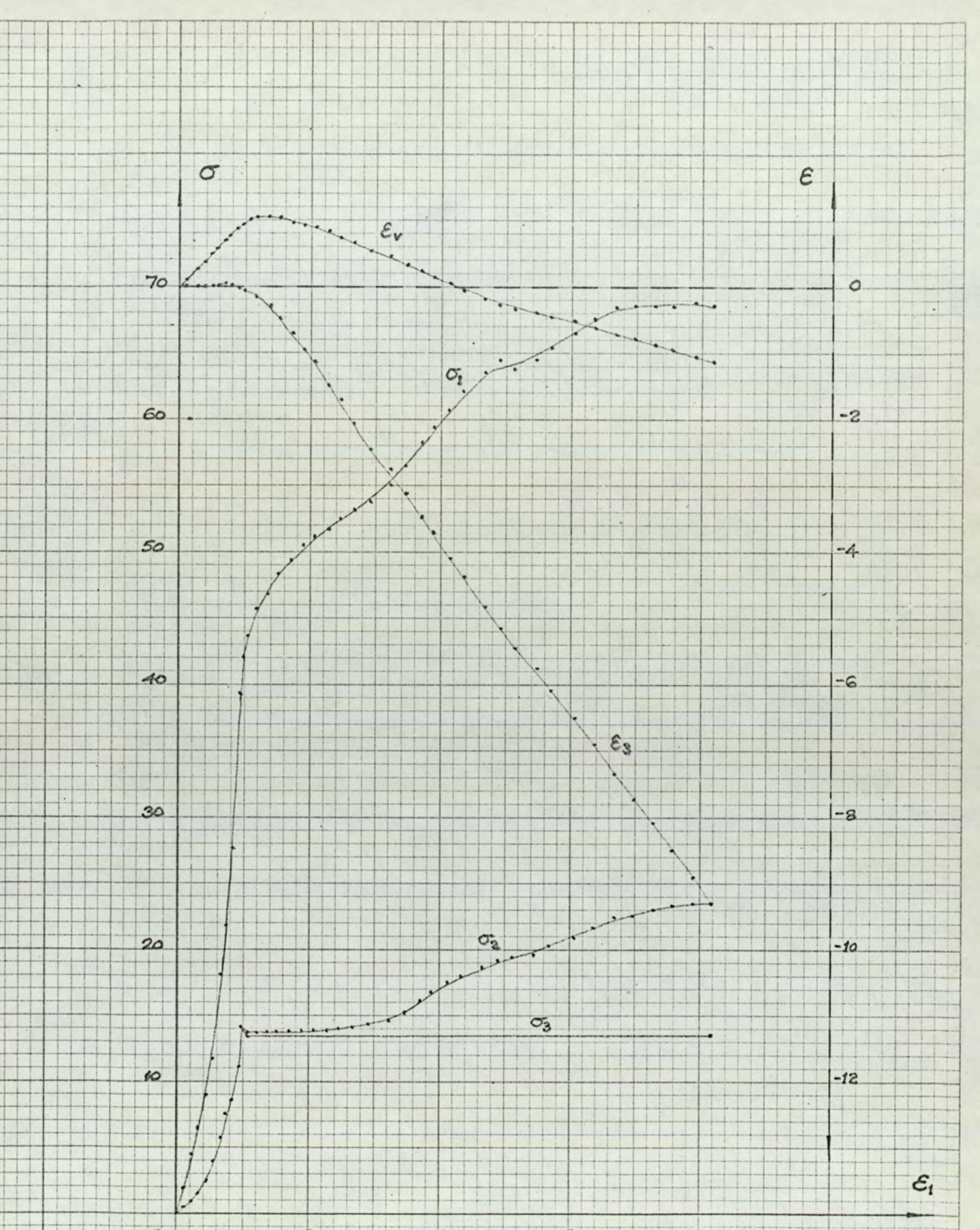

FIG. H. 68
ATA PS 23
σ_v. ε_1 , ε_v. ε_1

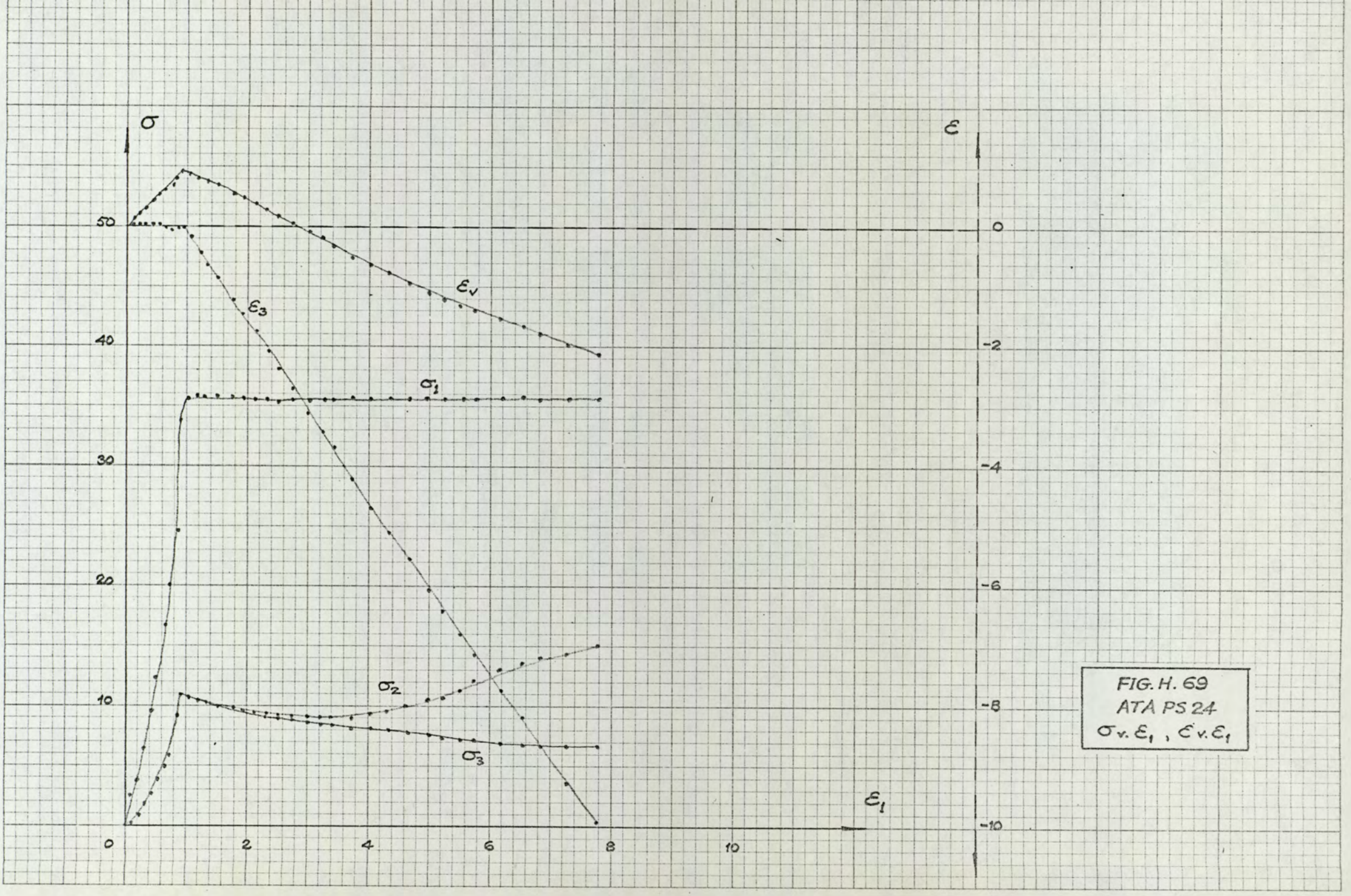

FIG. H. 69
ATA PS 24
σ v. ε_1 , ε v. ε_1

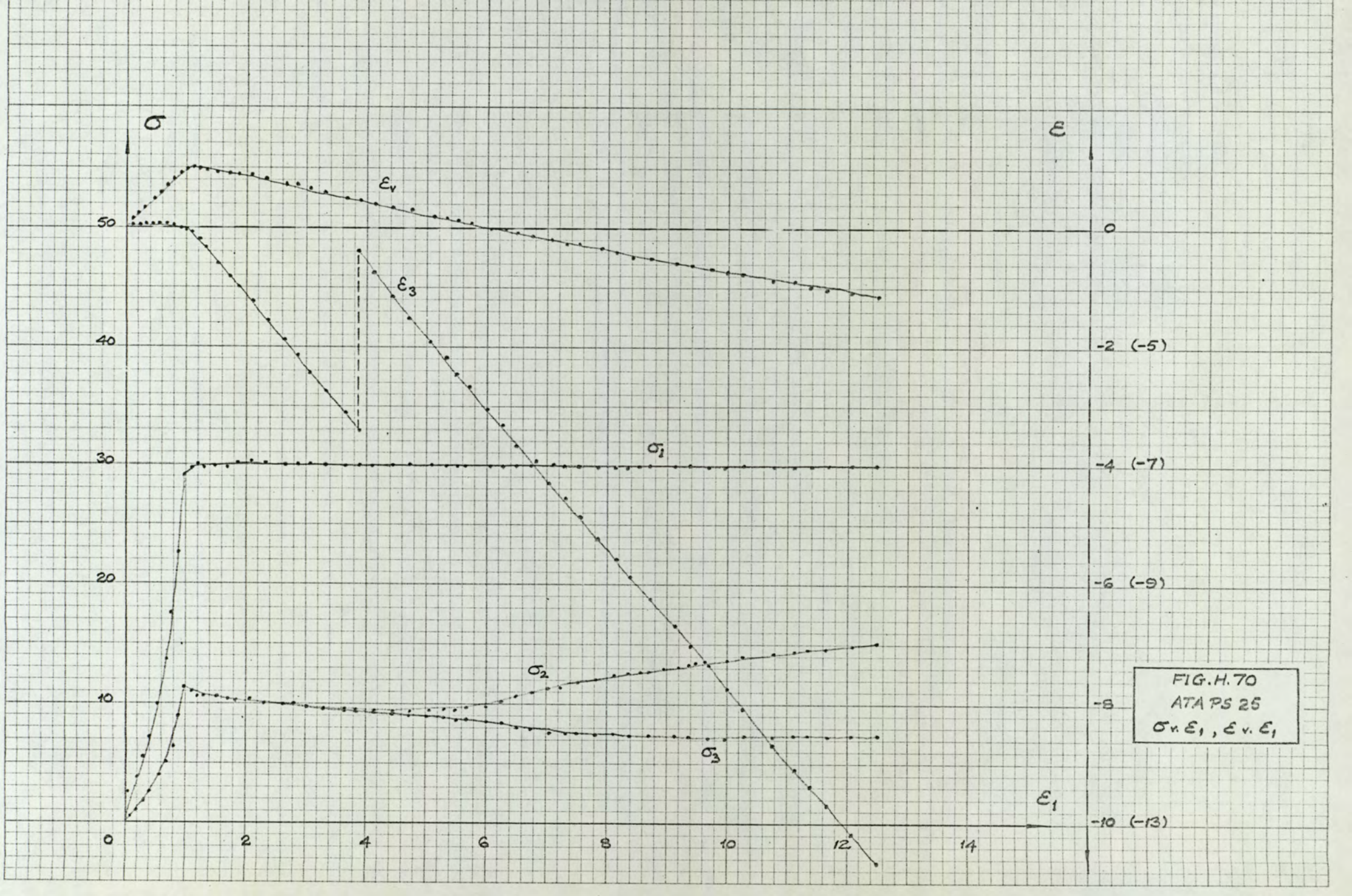

FIG. H. 70
ATA PS 25
σ v. ε_1 , ε v. ε_1

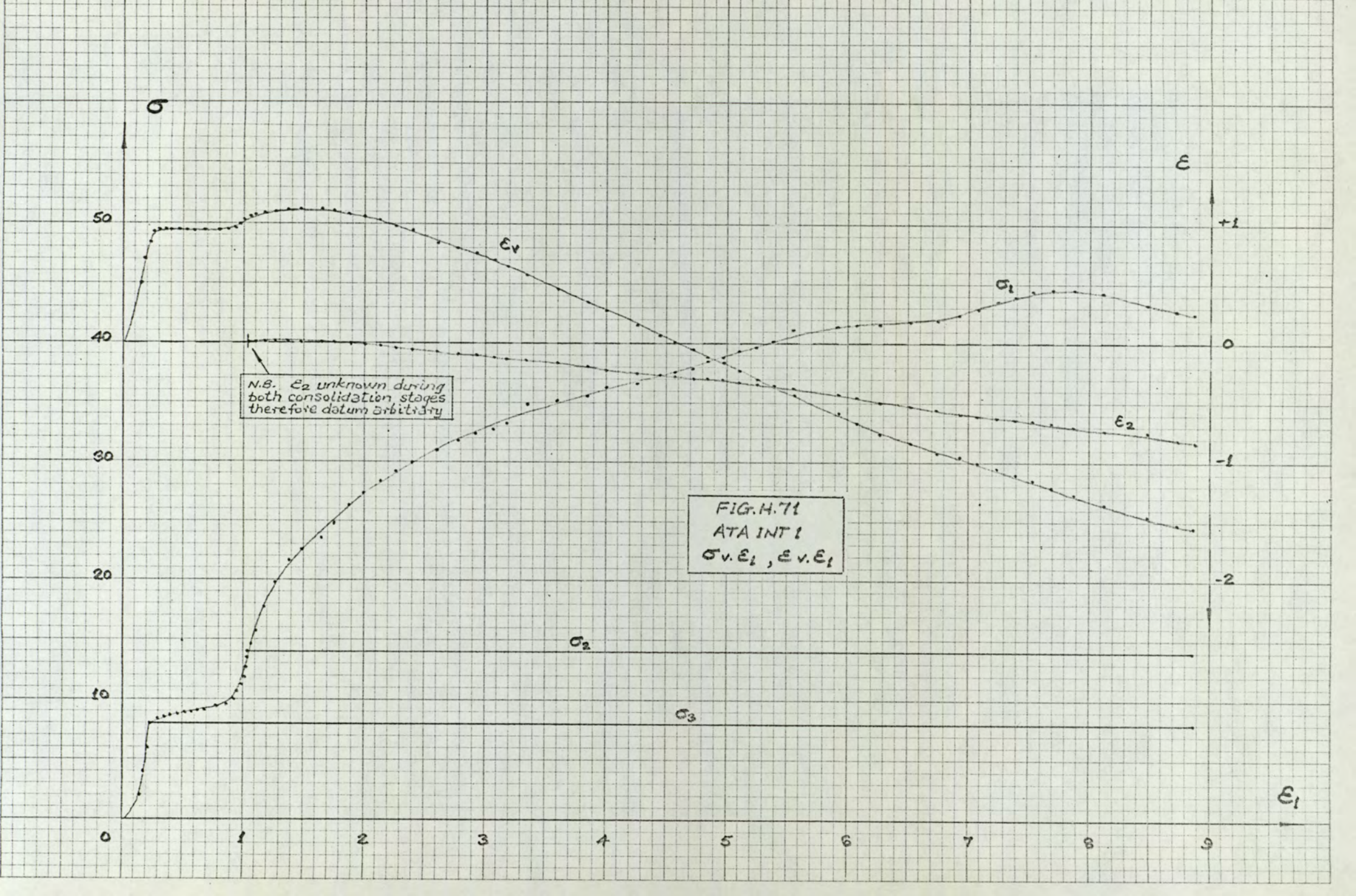

FIG. H.71
ATA INT 1
$\sigma_v . \varepsilon_1$, $\varepsilon_v . \varepsilon_1$

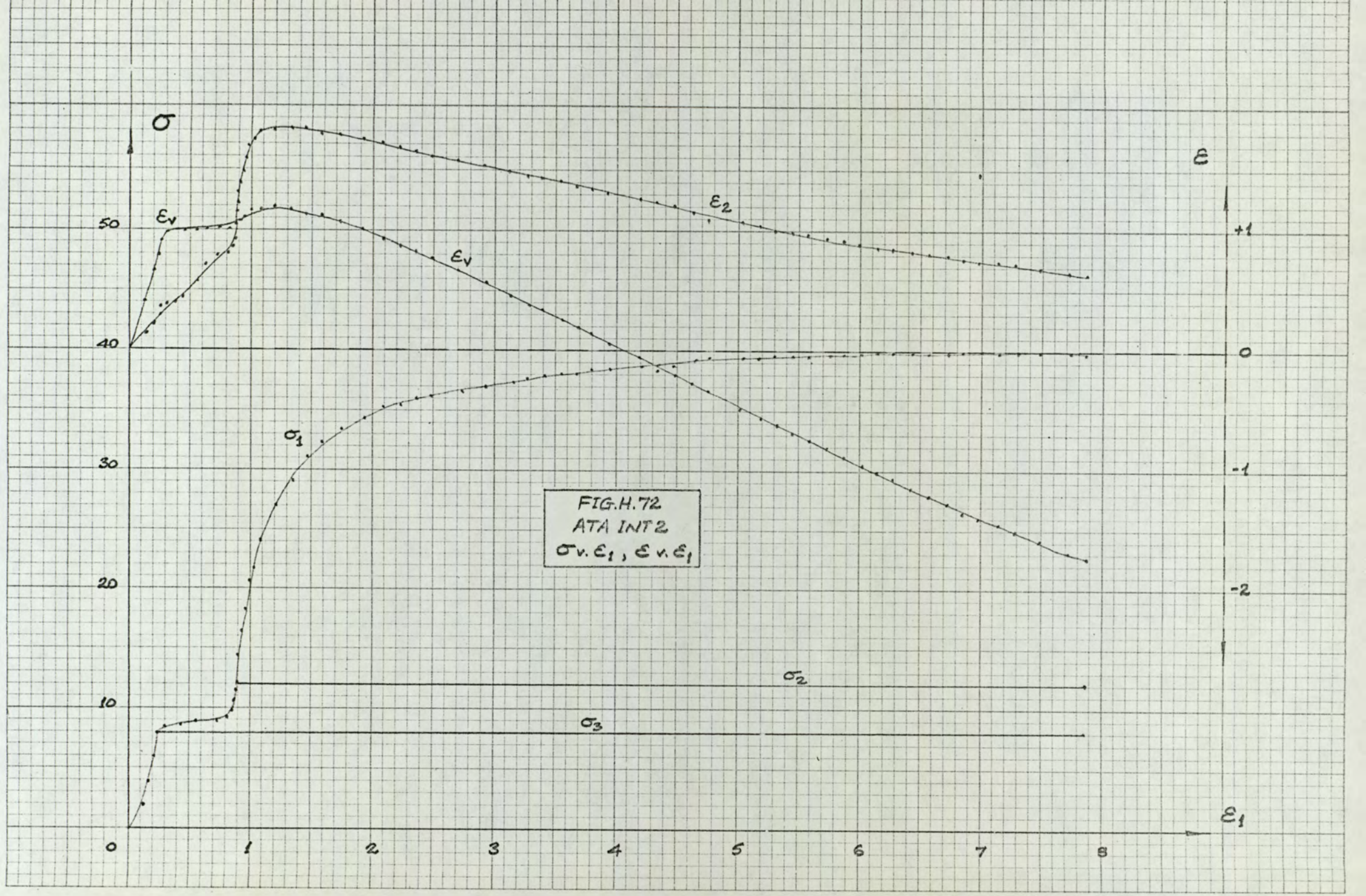

FIG.H.72
ATA INT 2
$\sigma_v . \varepsilon_1$, $\varepsilon_v . \varepsilon_1$

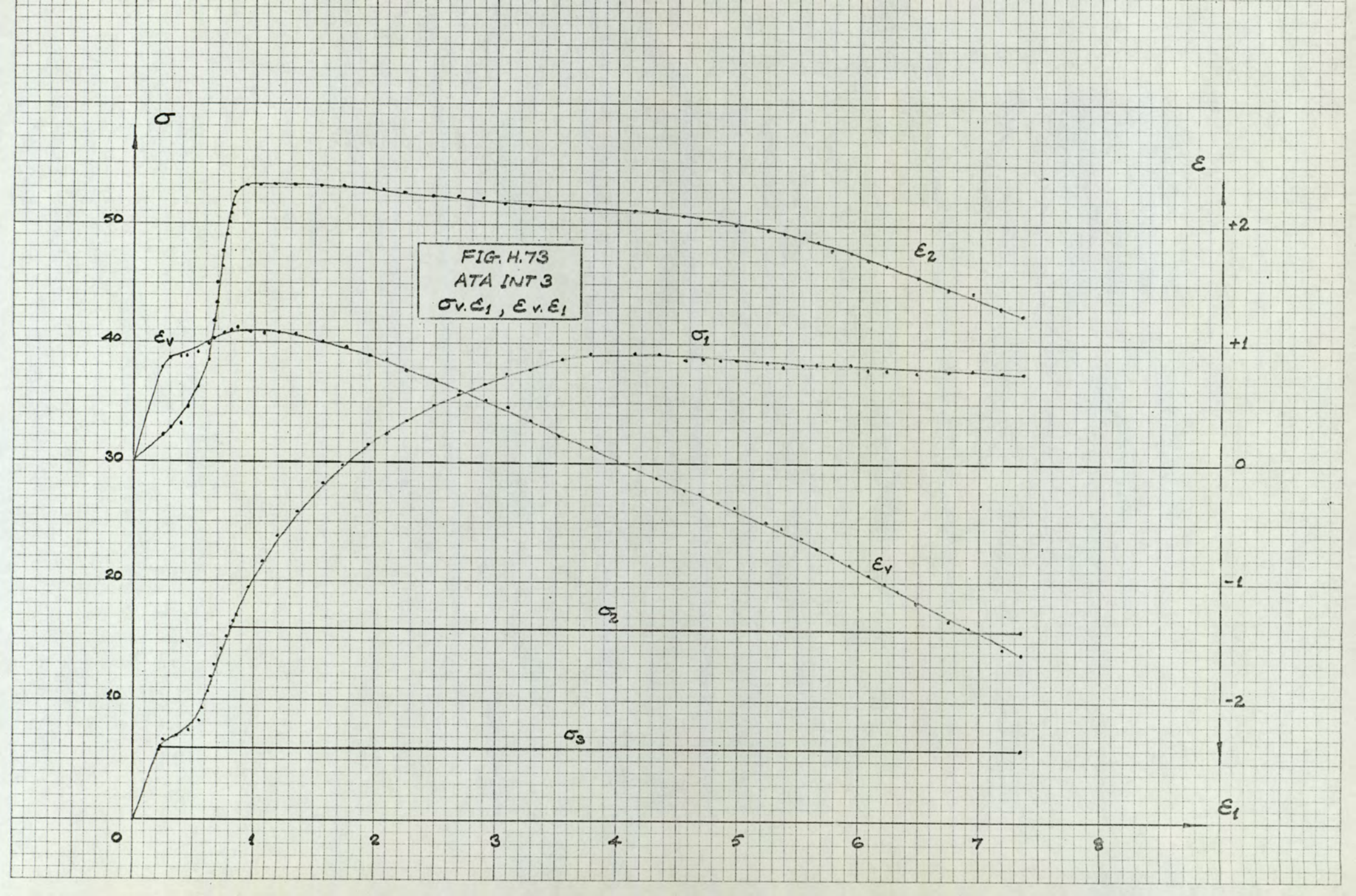
σ
ε
50
40
30
20
10
0
+2
+1
0
-1
-2
1
2
3
4
5
6
7
8
ε_2
ε_v
σ_1
ε_v
σ_2
σ_3
ε_1
FIG. H.73
ATA INT 3
$\sigma_v . \varepsilon_1$, $\varepsilon_v . \varepsilon_1$

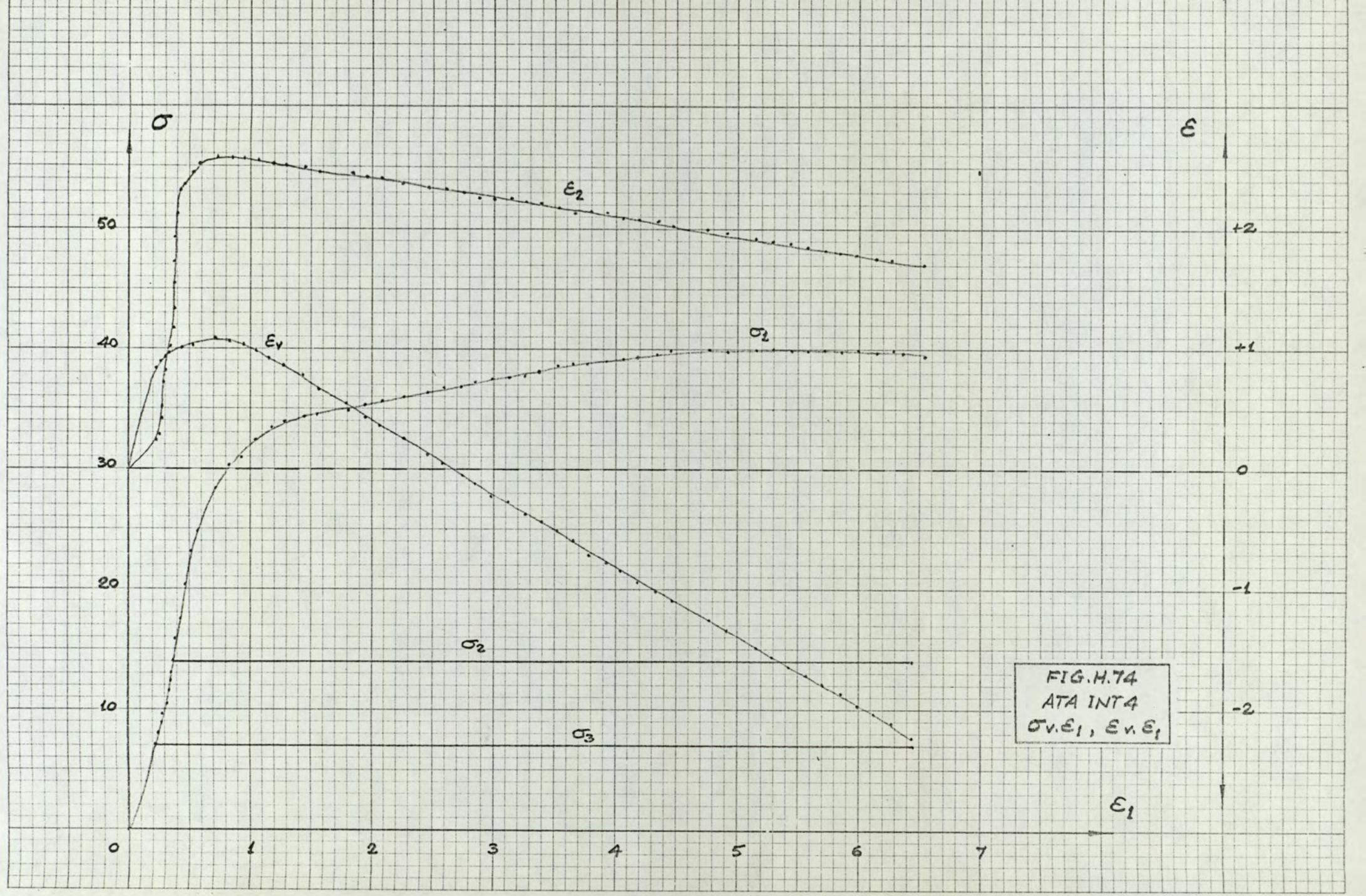

FIG.H.74
ATA INT4
$\sigma_v . \varepsilon_1$, $\varepsilon_v . \varepsilon_1$

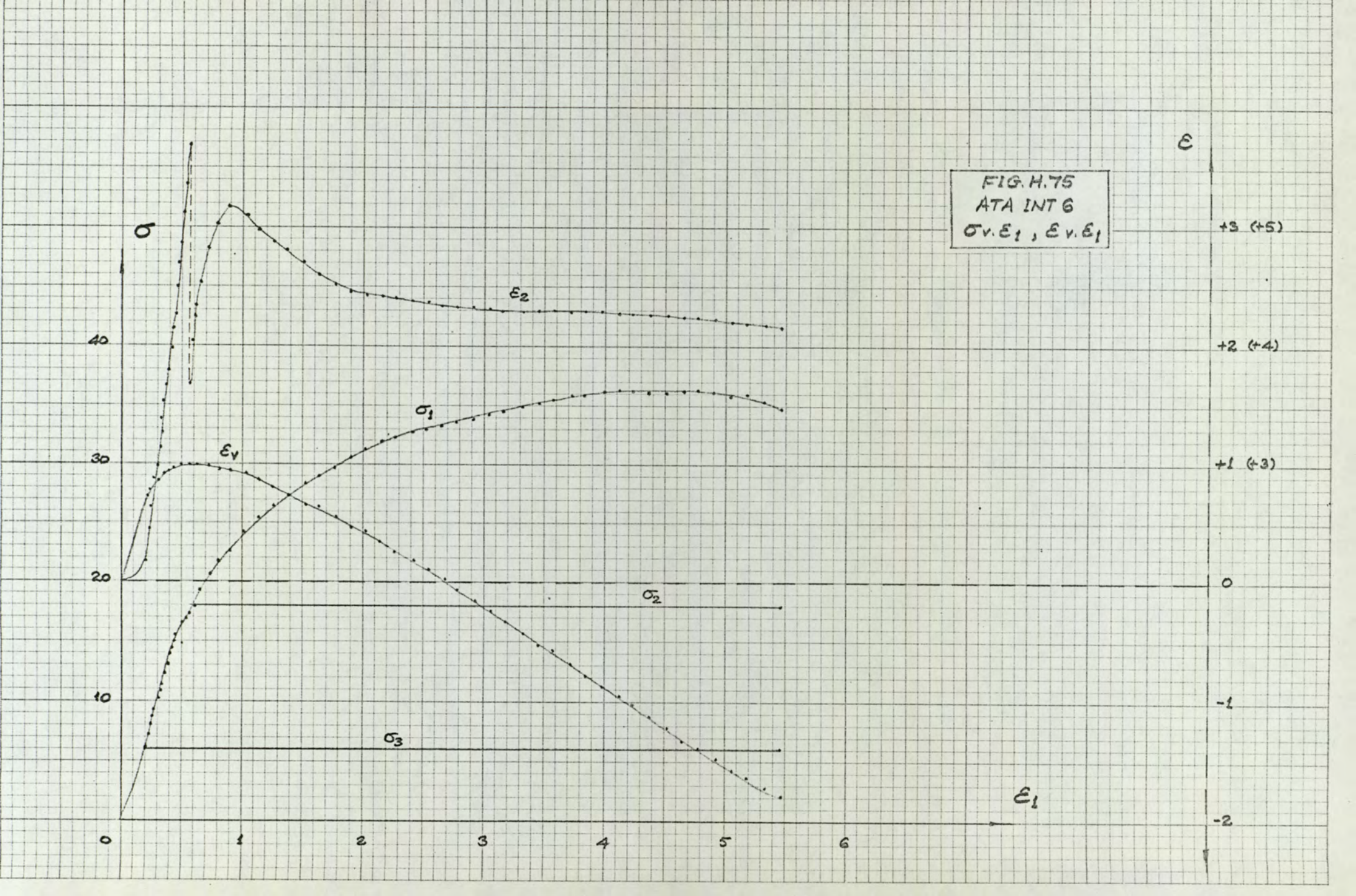
FIG. H.75
ATA INT 6
σ v. ε1 , ε v. ε1
σ
ε
ε2
σ1
ε1
σ2
σ3
ε1
40
30
20
10
0
1
2
3
4
5
6
+3 (+5)
+2 (+4)
+1 (+3)
0
-1
-2

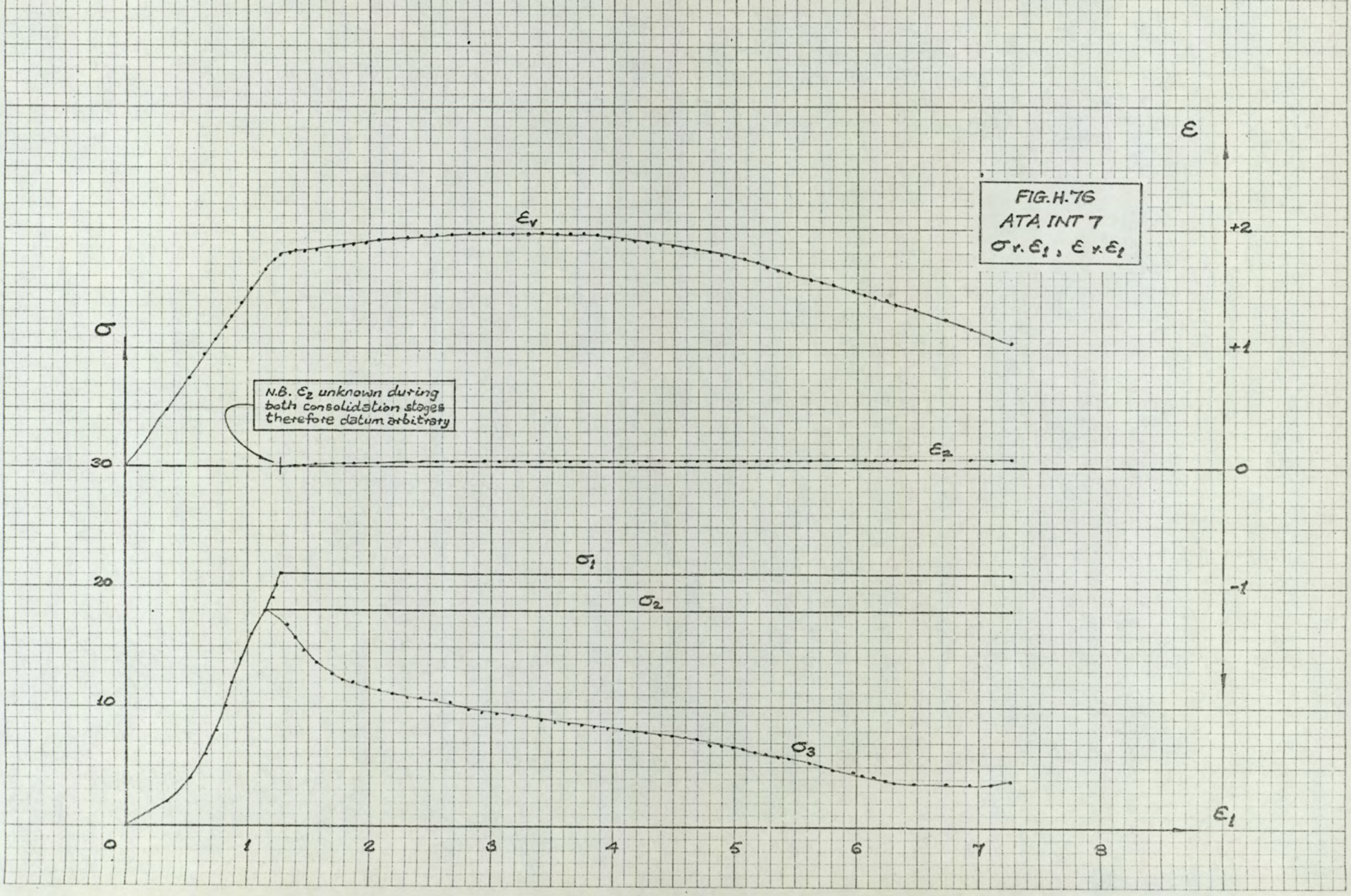
FIG. H. 76
ATA INT 7
σ v. ε1 , ε v. ε1
ε
σ
εv
ε2
σ1
σ2
σ3
ε1
N.B. ε2 unknown during both consolidation stages therefore datum arbitrary
30
20
10
0
1
2
3
4
5
6
7
8
+2
+1
0
-1

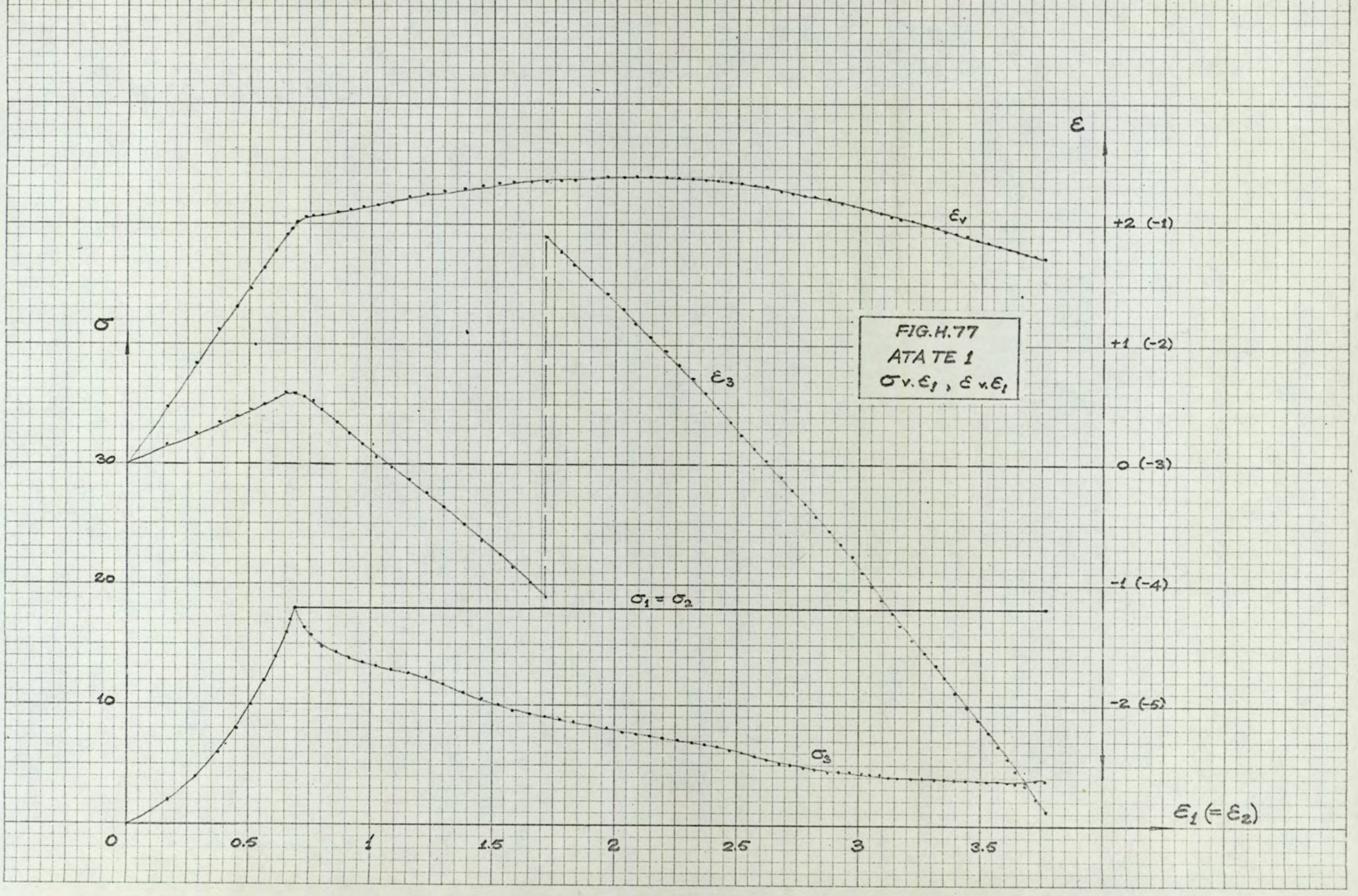

FIG. H. 77
ATA TE 1
$\sigma_v . \varepsilon_1$, $\varepsilon_v . \varepsilon_1$

ACKNOWLEDGEMENTS

I wish to acknowledge the help and enthusiastic encouragement given by my supervisor D. H. Bennett[2], B.Sc.(Eng.), C.Eng., M.I.C.E., A.M.I.E. (Aust.), F.G.S., and the interest shown by Professor M. Holmes[1], B.Sc., Ph.D., C.Eng., F.I.C.E., F.I.Struct.E., F.I.Mun.E.

In much of the experimental work M. Lyons[3] provided valuable assistance, and also developed the membrane manufacturing process. C. Thornton[4], B.Sc., performed the friction-slider tests and a few of those in the conventional triaxial apparatus. C. P. Thomas[5], B.Sc., kindly allowed his precise volume change device to be used in the intermediate stress tests. I wish to thank each of the above and also K. Starzewski[6], B.Sc., Ph.D., C.Eng., M.I.C.E., and R. Gisbourne[8], B.Sc., for their contributions to this project.

I am indebted to Miss C. L. Horton for her expertise in typing the manuscript, and to Miss P. C. Sage who skilfully traced the engineering drawings.

Many components of the new apparatus were manufactured in the Department, and I am grateful to W. C. Parsons[7] and his staff for their willing co-operation. I wish also to acknowledge the assistance of the staff of the Computer Centre in the processing of all the test data.

Finally, I am thankful for the understanding shown by my wife, particularly during the latter stages of this work, and also for her efforts in tracing many of the graphs and assembling the finished material.

S. Dyson

[1] Head of Department of Civil Engineering

[2] Senior Lecturer in civil engineering

[3] Senior Technician

[4] Research student

[5 6] Lecturers in civil engineering

[7] Chief Technician

[8] Senior Engineer, Geotechnical Engineering Limited, (formerly research student, University of Aston in Birmingham).

LIST OF REFERENCES

Arthur, James and Roscoe (1964) -

"The determination of stress fields during plane strain of a sand mass";

Geotechnique, Vol. 14, No. 4.

Arthur and Shamash (1967) -

"A note on the accuracy of displacement measurements in soils using an X-ray method";

Civil Eng. and Public Works Review, Apr. 1967.

Arthur and Menzies (1968) -

Correspondence on: "A new soil testing apparatus";

Geotechnique, Vol. 18, No. 2.

Barden and Khayatt (1966) -

"Incremental strain rate ratios and strength of sand in the triaxial test";

Geotechnique, Vol. 16, No. 4.

Barden and Khayatt (1968) -

"Incremental stress-strain relations for sand";

Univ. of Manchester Res. Report No. 5, March, 1968.

Barden, Ismail and Tong (1969) -

"Plane strain deformation of granular material at low and high pressures";

Geotechnique, Vol. 19, No. 4.

Bell (1965) -

"Stress-strain charactersitics of cohesionless granular materials subject to statically applied homogeneous loads in an open system";

Ph.D. Thesis, California Inst. of Technology.

Bell (1968) -

Correspondense on: "A new soil testing apparatus";

Geotechnique, Vol. 18, No. 2.

Bishop (1950) -

Discussion on: "Measurement of shear strength of soils";

Geotechnique, Vol. 2, No. 2.

Bishop (1954) -

Correspondence on: "Shear characteristics of a saturated silt in triaxial compression";

Geotechnique, Vol. 4, No. 1.

Bishop (1966) -

"The strength of soils as engineering materials";

Geotechnique, Vol. 16, No. 2.

Bishop and Henkel (1953) -

"A constant-pressure control for the triaxial compression test";

Geotechnique, Vol. 3, No. 3.

Bishop and Henkel (1957) -

"The measurement of soil properties in the triaxial test";

Edward Arnold, London.

Bishop and Donald (1961) -

"The experimental study of partly saturated soils in the triaxial apparatus";

Proc., 5th Int. Conf., Vol. 1.

Bishop and Green (1965) -

"The influence of end restraint on the compression strength of a cohesionless soil";

Geotechnique, Vol. 15, No. 3.

Bishop and Green (1969) -

"A note on the drained strength of sand under generalised strain conditions";

Geotechnique, Technical Note Section, Vol. 19, No. 1.

Bishop and Garga (1969) -

"Drained tension tests on London Clay";

Geotechnique, Vol. 19, No. 2.

Bjerrum and Kummeneje (1961) -

"Shearing resistance of sand samples with circular and rectangular cross-sections";

Norwegian Geotechnical Inst., Pub. No. 44.

Bjerrum and Landva (1966)

"Direct simple shear tests on a Norwegian quick clay";

Geotechnique, Vol. 16, No. 1.

Broms and Casbarian (1965) -

"Effects of the rotation of the principal stress axes and of the intermediate stress on the shear strength";

Proc. 6th Int. Conf., Vol. 1.

Buissman (1934) -

"Proefanderuindelyke bepaling van de greas van inwendig evenwient van een grandmassa";

De Ingenieur, Vol. 49, Part B.

Calladine (1963) -

Correspondence on: "The yielding of clays";

Gectechnique, Vol. 13, No. 3.

Casagrande and Shannon (1948) -

"Stress-deformation and strength characteristics of soils under dynamic loads";

Proc., 2nd Int. Conf., Vol. 5.

Chen (1948) -

"An investigation of stress-strain and strength characteristics of cohesionless soils";

Proc. 2nd Int. Conf., Vol. 5.

Cole (1967) -

"Soils in the simple-shear apparatus";

Ph.D. Thesis, Cambridge University.

Coleman (1960) -

Correspondence on: "Suction and the yield and failure surface for soil in principal stress space";

Geotechnique, Vol. 10, No. 4.

Coumoulos (1967) -

"A radiographic study of soils";

Ph.D. Thesis, Cambridge University.

Cornforth (1961) -

"Plane strain characteristics of a saturated sand";

Ph.D. Thesis, University of London.

Cornforth (1964) -

"Some experiments on the influence of strain conditions on the strength of sand";

Geotechnique, Vol. 14, No. 2.

Daniel (1954) -

"A study of the stress-strain characteristics of granular materials";

Ph.D. Thesis, University of London.

Daniel (1957) -

"Stress strain characteristics of a granular material";

Engineering, July 12, 1957.

Dantu (1961) -

"Etude mécanique d'un milieu pulvérulent formé de sphères égales de compacité maxima";

Proc. 5th Int. Conf., Vol. 1.

Dantu (1968) -

"Etude statistique des forces intergranulaires dans un milieu pulvérulent";

Geotechnique, Vol. 18, No. 1.

Davis and Poulos (1963) -

"Triaxial testing and three-dimensional settlement analysis";

Proc., 4th Australia-New Zealand Conf.

De Beer (1950) -

"The cell test";

Geotechnique, Vol. 2 , No. 2.

De Josselin de Jong and Geuze (1957) -

"A capacitive cell apparatus";

Proc., 5th Int. Conf., Vol. 1 .

Drucker (1959) -

"A definition of a stable inelastic material";

Trans., A.S.M.E., Jour. of Appl. Mechs., Vol. 26, No. 1.

Drucker, Gibson and Henkel (1957) -

"Soil mechanics and work-hardening theories of plasticity";

Trans., A.S.C.E., Vol. 122.

Duncan and Seed (1966) -

"Strength variations along failure surfaces in clay";

Jour. Soil Mechs. & Found. Div., A.S.C.E., Vol. 92, No. SM6.

Duncan and Seed (1967) -

"Corrections for strength test data";

Jour. Soil Mechs. & Found. Div., A.S.C.E., Vol. 93, No. SM5.

El Sohby (1964) -

"The behaviour of particulate materials under stress";

Ph.D. Thesis, University of Manchester.

Escario (1961) -

Discussion on: "Soil properties and their measurement";

Proc. 5th Int. Conf., Vol. 3.

Escario and Uriel (1961) -

"Optical methods of measuring the cross section of samples in the tri-axial test";

Proc., 5th Int. Conf., Vol. 1.

Esrig and Bemben (1965) -

Discussion on: "Soil properties - shear strength and consolidation";

Proc. 6th Int. Conf., Vol. 3.

Finn and Mittal (1963) -

"Shear strength of soil in a general stress field";

A.S.T.M., S.T.P. 361: Laboratory shear testing of soils.

Finn, Wade and Lee (1967) -

"Volume changes in triaxial and plane strain tests";

Jour. Soil Mechs. & Found. Div., A.S.C.E., Vol. 93, No. SM6.

Fraser (1957) -

"The influences of stress ratio on compressibility and pore pressure coefficients in compacted soils";

Ph.D. Thesis, University of London.

Geuze (1948) -

"Critical density of some Dutch sands";

2nd Int. Conf., Vol. 3.

Girijavallabhan and Reese (1968) -

"Finite element method for problems in soil mechanics";

Jour. Soil Mechs. & Found. Div., A.S.C.E., Vol. 94, No.SM2.

Graton and Fraser (1935) -

"Systematic packing of spheres with particular attention to porosity and permeability";

Jour. of Geology, Vol. 43.

Green (1967) -

Correspondence on: "A new soil testing apparatus";

Geotechnique, Vol. 17, No. 3.

Green (1969) -

"Strength and compressibility of granular materials under generalised strain conditions";

Ph.D. Thesis, University of London.

Habib (1953) -

"Influence de la variation de la contrainte principale moyenne sur la résistance au cissaillement des sols";

Proc., 3rd Int. Conf., Vol. 1.

Hambly (1969) -

"Plane strain behaviour of soft clay";

Ph.D. Thesis, University of Cambridge.

Hambly and Roscoe (1969) -

"Observations and predictions of stresses and strains during plane strain of wet clay";

Proc. 7th Int. Conf., Vol. 1.

Hansen, Bent (1961) -

"Shear box tests on sand";

Proc., 5th Int. Conf. Vol. 1.

Haythornthwaite (1960) -

"Mechanics of the triaxial test";

Jour. Soil Mechs, & Found. Div., A.S.C.E., Vol. 86, No.SM5.

Haythornthwaite (1960) -

Discussion on: "Failure hypotheses for soils";

Res. Conf. on Shear Strength of Cohesive Soils, Boulder, A.S.C.E., p. 989.

Henkel and Gilbert (1952) -

"The effect of the rubber membrane on the measured triaxial compression strength of clay samples";

Geotechnique, Vol. 3, No. 1.

Henkel and Wade (1966) -

"Plane strain tests on a saturated remoulded clay";

Jour. Soil Mechs. & Found. Div., A.S.C.E., Vol. 92, No.SM6.

Horn and Deere (1962) -

"Frictional characteristics of minerals";

Geotechnique, Vol. 12, No. 4.

Horne (1965) -

"The behaviour of an assembly of rotund, rigid, cohesionless particles, Parts I and II";

Proc., Royal Society, A, Vol. 286.

Horne (1969) -

"The behaviour of an assembly of rotund, rigid, cohesionless particles - Part III";

Proc. Royal Society, A, Vol. 310.

Housel (1936) -

"Internal stability of granular materials";

Proc., A.S.T.M., Vol. 36, No. 2.

Hvorslev (1936) -

"A ring shear apparatus for the determination of the shearing resistance and plastic flow of soils";

Proc., 1st Int. Conf., Vol. 1.

Jakobson (1957) -

"Some fundamental properties of sand";

Proc. 4th Int. Conf., Vol. 1.

Jaky (1944) -

"A nyugalmi nyomas tenyezoje";

Magyar Mernok-es Epitesz-Egylet Kozlonye, p. 355.

Januskevicius and Vey (1965) -

"Stresses and strains in triaxial specimens";

A.S.T.M., S.T.P. 392: Instruments and apparatus for soil and rock mechanics.

Karman (1911) -

"Festigkeitsversuche uneter allseitegem druck";

Zeitschrift des Vereines Deutsches Ingenieure, Vol. 55, No. 42.

Kirkpatrick (1957) -

"The condition of failure for sands";

Proc., 4th Int. Conf., Vol. 1.

Kirkpatrick and Belshaw (1968) -

"On the interpretation of the triaxial test";

Geotechnique, Vol. 18, No. 3.

Kjellman (1936) -

"Report on an apparatus for the consummate investigation of the mechanical properties of soils";

Proc., 1st Int. Conf., Vol. 2 .

Kjellman (1951) -

"Testing the shear strength of clay in Sweden";

Geotechnique, Vol. 2, No. 3.

Ko and Scott (1967) -

"A new soil testing apparatus";

Geotechnique, Vol. 17, No. 1.

Ko and Scott (1967) -

"Deformation of sand in hydrostatic compression";

Jour. Soil Mechs. & Founds. Civ., A.S.C.E., Vol. 93, No. SM3.

Ko and Scott (1967) -

"Deformation of sand in shear";

Jour. Soil Mechs. Founds. Div., A.S.C.E., Vol. 93, No. SM5.

Lee (1970) -

"Comparison of plane strain and triaxial tests on sand";

Jour. Soil Mechs. & Found. Div., A.S.C.E., Vol. 96, No. SM3.

Lee and Seed (1964) -

Discussion on: "The importance of free ends in triaxial testing";

Jour. Soil Mechs. & Founds. Div., A.S.C.E., Vol. 90, No. SM6.

Lee, Seed and Dunlop (1969) -

"Effect of transient loading on the strength of sand";

Proc., 7th Int. Conf., Vol. 1.

Lenoe (1966) -

"Deformation and failure of granular media under three-dimensional stresses";

Experimental Mechanics, Feb. 1966.

Leussink and Wittke (1963) -

"Difference in triaxial and plane strain shear strength";

A.S.T.M., S.T.P. 361: Laboratory shear testing of soils.

Lewin and Burland (1970) -

"Stress-probe experiments on saturated normally-consolidated clay";

Geotechnique, Vol. 20, No. 1.

Lomize and Kryzhanovsky (1967) -

"On the strength of sand";

Proc. Geotechnical Conf., Oslo, Vol. 1.

Lomize, Kryzhanovsky, Vorontsov and Goldin (1969) -

"Study of deformation and strength of soil under three dimensional states of stress";

Proc., 7th Int. Conf., Vol. 1.

Lorenz, Neumeuer and Gudehus (1965) -

"Tests concerning compaction and displacements performed on samples of sand in the state of plane deformation".

Proc. 6th Int. Conf., Vol. 1.

Lundgren and Mitchell (1968) -

"Effect of loading method on triaxial test results";

Jour. Soil Mech. & Found. Div., A.S.C.E., Vol. 94, No. SM1.

Marsal (1965) -

Panel discussion;

Proc., 6th Int. Conf., Vol. 3, pp. 310-316.

McMurdie and Day (1958) -

"Compression of soil by isotropic stress";

Proc., American Soil Science Society, Vol. 22.

Nakase (1960) -

"A device for triaxial compression testing of sand";

Soil and Foundation, Vol. 1, No. 1.

Nash and Dixon (1960) -

"The measurement of pore pressure in sand under rapid loading triaxial test";

Conf. on Pore Pressure and Suction in Soils, London.

Newland and Allely (1957) -

"Volume changes in drained triaxial tests on granular materials";

Geotechnique, Vol. 7, No. 1.

Newland and Allely (1959) -

"Volume changes during undrained triaxial tests on saturated dilatant granular materials";

Geotechnique, Vol. 9, No. 4.

Olsen and Campbell (1967) -

"Bushing friction in triaxial shear testing";

Materials Research and Standards, Vol. 7, No. 2.

Parikh (1967) -

"The shearing behaviour of a sand under axisymmetric loading";

Ph.D. Thesis, University of Manchester.

Parkin (1965) -

"On the strength of packed spheres";

Jour. Australian Math. Soc., Vol. 5, Part 4.

Peltier (1957) -

"Recherches expérimentales sur la courbe intrinsique de rupture des sols pulvérulents";

Proc. 4th Int. Conf., Vol. I.

Penman (1953) -

"Shear charactersitics of saturated silt, measured in triaxial compression";

Geotechnique, Vol. 3, No. 4.

Poorooshasb and Roscoe (1961) -

"The correlation of the results of shear tests with varying degrees of dilation";

Proc., 5th Int. Conf., Vol. 1.

Poorooshasb, Holubec and Sherbourne (1966) -

"Yielding and flow of sand in triaxial compression";

Canadian Geotechnical Jour., Vol. 3, No. 4.

Prater (1965) -

"A constant deviator stress rheometer for investigating undrained creep in saturated clay soil";

Civil Eng. and Public Works Review, Vol. 60, No. 706, May.

Procter (1967) -

"The stress-dilatancy behaviour of dense sand in the hollow cylinder test";

M.Sc. Thesis, University of Manchester.

Rennie (1959) -

"On the strength of sand";

Jour. Aust. Math. Soc., Vol. 1.

Rendulic (1936) -

"Relation between voids ratio and effective principal stresses for a remoulded clay";

Proc., 1st Int. Conf., Vol. 3.

Rendulic (1937) -

"Ein grundgesetz der Ton-mechanik und sein experimentaller beweis";

Bauingenieur, Vol. 18.

Rittenhouse (1943) -

"A visual method of estimating two-dimensional sphericity";

Jour. of Sedimentary Petrology, Vol. 13, No. 2.

Roscoe (1953) -

"An apparatus for the application of simple shear to soil samples";

Proc. 3rd Int. Conf., Vol. 1 .

Roscoe (1967) -

Contribution to panel discussion: "Shear strength of soil other than clay";

Proc., Geotechnical Conf., Oslo, Vol. 2 .

Roscoe (1970) -

"The influence of strains in soil mechanics";

Geotechnique, Vol. 20, No. 2.

Roscoe, Schofield and Wroth (1958) -

"On the yielding of soils";

Geotechnique, Vol. 8, No. 1.

Roscoe and Schofield (1963a) -

"Mechanical behaviour of an idealised wet clay";

Proc., 2nd European Conf. Soil Mech., Wiesbaden, Vol. 1 .

Roscoe, Schofield and Thurairajah (1963b) -

"An evaluation of test data for selecting a yield criterion for soils";

A.S.T.M., S.T.P. 361: Laboratory shear testing of soils.

Roscoe and Poorooshasb (1963c) -

"A theoretical and experimental study of strains in triaxial compression tests on normally consolidated clays";

Geotechnique, Vol. 13, No. 1.

Roscoe, Arthur and James (1963d) -

"The determination of strains in soils by an X-ray method";

Civil Eng. & Public Works Review, Vol. 58.

Roscoe, Bassett and Cole (1967) -

"Principal axes observed during simple shear of a sand";

Proc., Geotechnical Conf., Oslo, Vol. 1.

Roscoe and Burland (1968) -

"On the generalised stress-strain behaviour of wet clay";

Engineering Plasticity, Cambridge Univ. Press.

Rowe (1962) -

"The stress-dilatancy relation for static equilibrium of an assembly of particles in contact";

Proc., Roy. Soc. A, Vol. 269, pp 500-527.

Rowe and Barden (1964) -

"Importance of free ends in triaxial testing";

Jour. Soil Mechs. & Found. Div., A.S.C.E., Vol. 90, No. SM1.

Rowe, Barden and Lee (1964) -

"Energy components during the triaxial cell and direct shear tests";

Geotechnique, Vol. 14, No. 3.

Rowe and Peaker (1965) -

"Passive earth pressure measurements";

Geotechnique, Vol. 15, No. 1.

Saada (1967) -

"Stress-controlled apparatus for triaxial testing";

Jour., Soil Mech. and Found. Div., A.S.C.E., V.93, No. SM6.

Schofield and Wroth (1968) -

"Critical state soil mechanics";

McGraw-Hill, London.

Schraerer, Schaad, and Haefeli (1948) -

"Contribution to the shearing theory";

Proc., 2nd Int. Conf., Vol. 5.

Seiffert (1933) -

"Untersuchungsmethod um festzustellen ob sich ein gegebenes baumaterial für den bau eines erddammes eignet";

Les Congrès, des Grands Barrages, Vol. 3.

Shibata and Karube (1965) -

"Influence of the variation of the intermediate principal effective stress on the mechanical properties of normally consolidated clays";

Proc. 6th Int. Conf., Vol.1 .

Shibata and Karube (1967) -

Discussion on: "Plane strain tests on a saturated remoulded clay";

Jour. Soil Mechs. & Found. Div., A.S.C.E., Vol. 93, No. SM5.

Shockley and Ahlvin (1960) -

"Nonuniform conditions in triaxial test specimens";

Proc., Research Conf. on Shear Strength of Cohesive Soils, Boulder, A.S.C.E.

Skinner (1969) -

"A note on the influence of interparticle friction on the shearing strength of a random assembly of spherical particles";

Geotechnique, Vol. 19, No. 1.

Smith, Foote and Busang (1929) -

"Packing of homogeneous spheres";

Phy. Review, Vol. 34, p.1271.

Stanton and Hveem (1934) -

"Role of the laboratory in the preliminary investigation and control of materials for low cost bituminous pavements";

Proc. 14th Annual Meeting, Highway Research Board, Vol. 2.

Sultan and Seed (1967) -

"Stability of sloping core earth dams";

Jour. Soil Mechs. & Found. Div., A.S.C.E., Vol. 93, No. SM4.

Sutherland and Mesdary (1969) -

"The influence of the intermediate principal stress on the strength of sand";

Proc., 7th Int. Conf., Vol. 1 .

Taylor (1942) -
"Research on consolidation of clays";
Dept. of Civil and Sanitary Eng., M.I.T., Cambridge.

Taylor (1948) -
"Shearing strength determinations by undrained cylindrical compression tests with pore pressure measurements";
Proc., 2nd Int. Conf., Vol. 5.

Terzaghi (1936) -
"Stress distribution in dry sand and in saturated sand above a yielding trap door";
Proc., 1st Int. Conf., Vol. 1.

Thomas (1970) -
Unpublished research into the mechanical properties of Lias Clay;
University of Aston in Birmingham.

Thurston and Deresiewicz (1959) -
"Analysis of a compression test of a face-centered cubic array of elastic spheres";
Trans., A.S.M.E., Jour. Appl. Mechs.

Timoshenko and Goodier (1951) -
"Theory of Plasticity";
McGraw-Hill, New York.

Trollope and Currie (1957) -
"Small embedded earth pressure cells - their design and calibration";
Proc., 3rd Australia-New Zealand Conf. Soil Mechs.

Tschebotarioff (1953) -
"The tensile strength of disturbed and recompacted clay";
Proc., 3rd Int. Conf., Vol. 1.

U.S. Waterways Experiment Station (1944) -
"Soil pressure-cell investigation";
Technical Memo, No. 210-1.

Whitman and Luscher (1962) -

"Basic experiments into soil-structure interaction";

Jour. Soil Mechs. & Found. Div., A.S.C.E., Vol. 88, No. SM6.

Wightman (1967) -

"The stress-dilatancy of sands during plane strain compression";

M.Sc. Thesis, University of Manchester.

Wood (1958) -

"Shear strength and volume change characteristics of compacted soil under conditions of plane strain";

Ph.D. Thesis, University of London.

Wroth and Bassett (1965) -

"A stress-strain relationship for the shearing behaviour of a sand";

Geotechnique, Vol. 15, No. 1.

Wu, Loh and Malvern (1963) -

"Study of failure envelopes of soils";

Jour. Soil Mechs. & Found. Div., A.S.C.E., Vol. 89, No. SM1.